

Water Quality Monitoring in Lake Abaya and Lake Chamo Region

A Research Based on Water Resources of the Abaya-Chamo Basin - South
Ethiopia

Ph.D. THESIS

For attainment of the degree

Dr. rer. nat. (Ph.D.)

Submitted by

Ababu Teklemariam Tiruneh

Department 8 (Chemistry – Biology)

University of Siegen

Siegen 2005

urn:nbn:de:hbz:467-1040

TABLE OF CONTENTS

S.NO	CONTENTS	PAGE
I	Abstract	I
II	Acknowledgement	II
III	Preface	III
IV	List of Abbreviations	IV
Chapter 1	Introduction	1-15
Chapter 2	Description of the Abaya – Chamo Water Resources Basin	16-34
Chapter 3	Methods, Procedures and Method Validation	35-111
Chapter 4	Water Quality Analysis Results and Evaluation of Data	112-191
Chapter 5	Design of Water Quality Monitoring System	192-238
Chapter 6	Integrating Water Quality Management with Monitoring	239-261
Chapter 7	Water Quality Modelling	262-294
Chapter 8	Summary Discussion	295-307
Chapter 9	Conclusion	308-310
10	Literature	311-319
11	Appendix	320-359
12	Curriculum Vitae	360-362

Abstract

This study is based on water quality monitoring work of water resources within the Abaya-Chamo basin. The methods, method validation and analysis results have been presented and discussed. Seasonal variation and trends as well as associated water quality management issues are discussed. A water quality monitoring system based on an integrated partial physical orthogonal model has been designed based on data generated within the water resources of the Abaya – Chamo drainage basin. Abstract common factors were extracted by the application of principal component and factor analysis. By overlaying real factors with abstract common factors the underlying causes for the water quality variations have been explained. Surface flow factors, sub surface flow factors, leaching flow factors, effects of soil matrix, rainfall magnitude and intensity, discharge, catchment area and slope, in stream pollution and point sources of pollution, evaporative storage and precipitation chemistry all showed up in such integrated model. This model can be extended by including further physical factors as well as natural and anthropogenic pollution sources and factors. This model can be extended to lakes and ground water sources as well. Design of water quality monitoring intervals was accomplished with the help of spectral analysis. Spatial monitoring spacing for lake water quality was determined after hierarchical cluster analysis. The possibility of modelling the various water quality parameters was investigated. Auto regressive modelling fits well variables that have seasonally evened variation. Variables with short-term fluctuation were modelled with spectral level regression. State-space method was satisfactorily applied for relating the time series between two sampling points located on different rivers. Discharge- base contaminant modelling was modified to compensate for error by establishing a pattern of relationship between calculated and observed contaminant loads.

Key Words: Water Quality Monitoring, Water Quality modelling, Water Quality management.

Acknowledgement

The financial support of this work was obtained from the German Technical Development cooperation (GTZ) through its support programme made available to the Arbaminch University. This support is gratefully acknowledged. Thanks are also due to the German Academic Exchange Service (DAAD) through which I was able to obtain the scholarship support throughout the duration of undertaking my thesis work.

I am grateful to my supervisor, Professor Dr. Bernd Wenclawiak, of the University of Siegen for offering me helpful advice and support as supervisor to my work. I am also much grateful to Professor Dr. Ing. Gerd Foerch, Professor Dr. Briggita Schutt and Professor Dr. Ing. Jürgen Jensen as they have provided me with invaluable advice and support to my effort.

The Arbaminch University has provided me with supports including transport vehicle, chemicals and the usage of laboratory facilities mainly from the department of water and environmental engineering. In this connection, I extend my thanks to Dr. Seleshi Bekele for authorising and facilitating the provision of this assistance through his capacity as Dean. Thanks are also due to Ato Fikre Assefa and Ato Kinfe Kassa as they helped me a lot in the organisation of my laboratory work at Arbaminch. Dr. Mekonen Ayana has, as head of the research section of the Arbaminch University, helped me in facilitating the provision of data, maps, GPS as well as the GTZ research fund for which I am thankful. I am grateful to Thorsten Schmeck and Ulrike Koch from the analytical chemistry group of Siegen University for reading the draft of my thesis and for offering to me helpful suggestions. I am also thankful to Thorsten Schmeck and Ulrike Koch once again and to Henning Beer, Sandra Bohn, Sylvia Wilnewisky and Daniela Krieb all of whom were students in the Analytical Chemistry Group of Siegen University for offering me their kind help and advice in my laboratory work at Siegen University. At the start of my fieldwork in Ethiopia two students from Siegen University, namely, Tobias Humberg and Heiko Stotzel undertook their Diploma – thesis work in water quality monitoring on the rivers Hare and Kulfo in Ethiopia. While thanking them for taking interest in this research I feel obliged to express my appreciation of their work ethic and dedication in doing the research and contribute to what is perhaps the first hand information on river water quality data base for the rivers.

Ababu Teklemariam Tiruneh. University of Siegen. January 2005

PREFACE

This thesis is sub divided in to 9 main chapters including the introductory part and the final conclusion. The chapters are arranged in logical sequence beginning with background and statement of the problem and the methodology employed in the research (Chapter 1). Relevant features of the study area have been discussed in Chapter 2. Water quality analysis, procedures, method validation and quality control features are discussed in chapter 3. Interpretation of the results, design of monitoring system and integration of monitoring and management follow in sequence as chapters 4, 5 and 6 respectively. Modeling aspects are included in chapter 7 and summary of the important findings are discussed in Chapter 8. Finally the conclusion part is given in chapter 9.

The content page numbers at the beginning of the document refers to the main chapters. In addition each chapter begins with a page listing the sub-topics within the chapter in sequence. Page numbers are identified in sequence. Figures, equations and graphs within chapters are likewise independently numbered in sequence as Figure 4.1, Table 4.1, etc. List of Figures and tables have been supplied at the beginning of each chapter to which they belong. Wherever abbreviations have been used in the document, their meaning is listed in the list of abbreviations included at the beginning of the document. An appendix chapter is included at the end, and where data and calculations as well as tables and graphs have been included in the appendix, they are referred to by the chapter number – sequence number. For example the first appendix of chapter 5 is referred to as Appendix 5-1, etc.

A list of cited literature is attached at the end of this thesis and where the literature has been referred to in the document it is identified by a number in the literature list, for example, as [1] for the literature listed first. An acknowledgement page is included at the beginning and the author owes a sincere gratitude to all persons and organizations enlisted in that page for offering their support and in addition also owe the same to others who he may have missed out of ignorance but were nonetheless helpful to his research undertaking.

Ababu Teklemariam Tiruneh. University of Siegen, Germany. January 2005.

LIST OF ABBREVIATIONS

ARIMA	Auto Regressive Integrated with Moving Average
$\mu\text{S.cm}^{-1}$	Micro Siemens per centimeter
Abs	Absorption
ACB	Abaya – Chamo Drainage Basin
AIC	Akaik's Information Criterion
ANC	Acid Neutralising Capacity
ASTM	American Society for Testing Materials
AWTI	Arabminch Water Technology Institute (Ethiopia)
BC	Base Cation
BOD	Biochemical Oxygen Demand
COD	Chemical Oxygen Demand
CSA	Central Statistical Authority Ethiopia
DFT	Discrete Fourier Transform
DIN	Deutsches Institut für Normung
DO	Dissolved Oxygen
DSI	Sodium Dominance Index
EDTA	Ethylene Diamine Tetraacetic Acid
EPA	Environmental Protection Agency
FCA	Factor Analysis
FFT	Fast Fourier Transform
GIS	Geographic Information System
GPS	Geographic Positioning System
ITCZ	Inter Tropical Convergence Zone
LED	Light Illumination Device
MDL	Method Detection Limit
me.L^{-1}	Milli equivalent per Liter
mg.L^{-1}	Milligram per Liter
NA	Not Available
NC	Not Calculated
NTU	Nephelometric Turbidity Unit
PCA	Principal Components Analysis
ppm	Parts per million
Redox	Reduction Oxidation Reaction
RSD	Relative Standard Deviation
SNNPR	Southern Nations, Nationalities and Peoples Region (Ethiopia)
SPSS	Statistical Package for Social Sciences
SRP	Soluble Reactive Phosphorous
TAN	Total Ammoniac Nitrogen
TDS	Total Dissolved Solids
TFS	Total Fixed Solids
TOC	Total Organic Carbon
TVS	Total Volatile Solids
UTM	Universal Transverse Mercator Coordinate System
WHO	World Health Organisation

CHAPTER ONE**INTRODUCTION**

S.No	CONTENTS	PAGE
1.1	Background and Statement of the Problem	2
1.2	Research Objective	2
1.3	Research Methodology	3
1.4	Background of Monitoring Network Experiences	6
	1.4.1 Surface Water Quality Monitoring	6
	1.4.1.1 River Water Quality monitoring	6
	1.4.1.1.1 Standardization	7
	1.4.1.1.2 River Sampling Space and Frequency.	7
	1.4.1.1.3 River Flow Measurement	7
	1.4.1.2 Lakes Water Quality Monitoring.	7
	1.4.1.2.1 Lake Variables Monitored	8
	1.4.2 Ground Water Quality Monitoring	8
	1.4.2.1 Ground Water Quantity Monitoring	9
	1.4.2.2 Ground Water Sampling Frequency And Density.	9
1.5	Design Of Water Quality Monitoring System	9
	1.5.1 Background	9
	1.5.2. Detection of Trend	10
	1.5.3 Determination of Periodic Fluctuations	12
	1.5.4 Estimation of Mean Values	12
	1.5.6 Criteria for Analysis of Sampling Frequency	13
	1.5.7 Determination of Underlying Factors for Water Quality Variations	13
	1.5.7.1 Principal Component Analysis	13
	1.5.7.2 Factor Analysis	14
	1.5.7.2 Cluster Analysis	14

List of Figure

Fig. 1.5.1 Schematics of Water Quality Monitoring and Management.....Page 10

List of Table

Table 1.5.1 Determination of Sampling Frequencies.....Page 13

1.1 BACKGROUND AND STATEMENT OF THE PROBLEM

The ultimate objective of employing water quality management and monitoring is the exploitation of water resources without leading to unrecoverable damage to the environment. The key objective should relate to sustainable exploitation [1]. In Ethiopia water quality monitoring is not an institutionalized regular undertaking with obviously little integration if at all to watershed management [2]. Monitoring is carried out mainly for project decision by consultants/contractors and compliance monitoring in relation to public health concern on major water supplies by the Ministry of health and some environmental monitoring activities entrusted to the Ethiopian Environmental Protection Authority. All these activities are uncoordinated, limited, irregular and not broad based.

Water quality monitoring guidelines (WHO,) are general specifications, which do not take the specific catchment hydrochemistry, climate and anthropogenic influences in to account and offer only information of limited value of interpretation [3]. Such specifications tend to be too broad and too global to be of use in a specific setting.

While there have been a widespread emphasis and attention to specifying monitoring objectives ranging from establishing data base, pollution regulation, law enforcement, decision making, ecological monitoring and research purposes, there has been few emphasis on holistic approach to monitoring design that takes account of interaction among pollutants and common factors for variations [8].

1.2 RESEARCH OBJECTIVE

This research was aimed at systematizing the design of water quality monitoring and management networks based on the water resources within the Abaya –Chamo drainage basin. It tries to take a 'holistic monitoring' approach emphasizing the importance of group interaction of water quality variables as well as contributing factors and the interdependence between the various parts rather than dealing with monitoring in parts. This approach has the real ground support as naturally common factors including geology and climate as well as interaction by human activities determine the water quality status of water resources.

1.3. RESEARCH METHODOLOGY

The methodology of designing a group monitoring system incorporates the application of principal components and factor analysis and the overlapping of real factors concurrently monitored with the abstract common factor derived from the analysis. The application of principal component analysis indicates to what extent the data dimensionality can be reduced and the subsequent common factor analysis tries to find the latent underlying common factors for the data variation based on selected few components from the PCA analysis. Such approach takes account of the interconnection and interaction among the atmosphere, land and water. Therefore, the resulting factor group is explained in terms of the atmospheric, land and water hydro-geo-chemical processes. By taking a time series of measurements of water quality variables as well as real factors, the relative influence of these common factors over the seasons is assessed.

It is understood that pollutants of concern to health and the environment such as pathogenic organisms, nutrients such as ammonia, nitrate, phosphate, heavy metals and other pollutants are not only arising out of point sources but also out of distributed sources [4]. This is particularly so in areas (such as the one on which this study is based), where waste disposal and management system is lacking and that wastes are distributed over space rather than arising as an effluent point source of treated or untreated waste. Because the same physico-chemical factors govern most of the transport of these pollutants despite the large number of variables to monitor it makes every sense to relate these variables in terms of co-occurrences and common factors. Therefore, the application of this common factor approach extends to surface water sources, rivers, lakes, shallow springs and ground water sources.

Once the association between water quality variables and component factors (real, abstract) is established then a monitoring group is established consisting of the variables and the associated factors responsible for the variation. The spectrum of peaks defines the monitoring interval in this group, which is determined from spectral analysis of continuous time-series data. The amount of information produced by monitoring is proportional to the frequency of monitoring. The periodogram, which is the area under the spectral density curve, defines the information contained at a given level of monitoring since the periodogram is the auto covariance of the data ($\tau = 0$) defined by the frequency level. A maximum frequency of $f = 0.5$, designated as

the Nyquist frequency is assumed to contain 100% of the information (variance) which is the total information contained in the time series data. There is often an optimum frequency between 0 and 0.5 indicating the point at which any further increase in frequency of monitoring results in only a moderate gain of information.

The choice of monitoring interval is dictated primarily by intended use of the water quality information and by economic considerations. The methodology employed and demonstrated in this research shows the relevance and adequacy of each frequency of monitoring with respect to interpretation of the data by association with common factors. As an example if four major factors account for 2/3 of the data variation, monitoring frequency should be chosen as to obtain this level of variance in order to enable interpretation of the data variation with respect to these common factors. Therefore, a link is provided between the application of principal component /Factor analysis and the choice of monitoring frequency.

Water quality monitoring will have an increased impact and justification in terms socio-economic values if it's integrated with watershed management [5]. The integration of water quality monitoring with watershed management is demonstrated in this research through a case of ammonia monitoring, its occurrence, health and environmental implication, land and lake dynamics, and implication on water quality management.

A model provides a mathematical basis for relating the auto variance and cross variance among the water quality data in time and space. Such models, apart from providing a "structure" to the data variation, use can be made of the capability of these water quality models to forecast future changes. Water quality data are 'ordered' in time and space. Therefore, there exists auto-correlation as well as cross-correlation among the data values in both time and space. In addition, trends and persistence occur in the data. This means that models have to account for all these components of the data variation. A typical water quality auto regressive model contains a trend component, a periodic component and a persistent component often referred to as the stationary series. The trend component is modeled through statistical trend analysis. The periodic and persistent components are modeled through a combined auto-regressive Moving average model (ARIMA). Direct regression among water quality variables is often not valid since the independent variable is not random in nature but rather ordered which violates the assumption of regression between a dependent variable and independent variable. For this reason

relating variables is done through 1) regression between residuals of the autoregressive models of the respective variables 2) spectral level regression or 3) principal Component Regression. The application of these models to the water quality data collected in this research has been demonstrated and is described in this report.

Discharge based contaminant modeling is a suitable model for estimating river contaminant load. Many water quality variables display a power relationship of increasing or decreasing order with discharge. Estimation based on such power rating curve equation that takes account of bias in the mean load estimate has been developed [82]. In this research it will be shown that since logarithmic discharge and contaminant transformation do not eliminate the bias (because of the nature of the distribution of discharge and pollutants in the study area are not log-normal) and since the rating curve equation is only approximate, the aggregate error due to these two factors has been accounted for by a transfer function which is derived from a definite pattern of relationship between actual contaminant load and the theoretically calculated load.

Regionalization involves (1) transferring information to stream flow sites with little or no information at a flow point located between sampling stations or located in drainage basin with similar lithology and other environmental factors affecting water quality, and (2) extrapolating short term records gathered by the aerial synthesis network to obtain water quality average and extreme characteristics over a variety of flow conditions. It is anticipated that water quality of rivers, lakes and under ground sources display regional similarity. This regional pattern has been demonstrated in this research by comparative analysis of water quality of the rivers, lakes and under ground water sources within the Abaya –Chamo drainage basin. The qualities from all the water sources display, for example, a strong correlation with elevation above mean sea level, which is the resultant of the interplay between climate and hydro-geology both of which vary with elevation in the region. A state-space model between river water quality variables display a close fit to the actual data which suggests a basis for establishing such model basin wide.

1.4 Background of Monitoring Network Experiences

1.4.1 Surface Water Quality monitoring

The experiences of surface water quality monitoring mainly in Europe are briefly described below [6]. Surface water quality monitoring is divided into parts based on the flow characteristics, i.e., surface water quality monitoring (river water quality monitoring and lake water quality monitoring) and ground water quality monitoring.

1.4.1.1 River Water quality monitoring

Surface water quality monitoring may have one or several purposes including: general characterization of rivers and streams, monitoring for assessment of leaching from agricultural fields, monitoring for the purpose of estimating pollutant and nutrient loading from catchment into lakes, or on trans-boundary rivers from one country into another. Integrated river water quality monitoring and catchment for studying the detail interaction between catchment, soil and water bodies, local lake monitoring for environmental purposes with state local standards and settings, Multi purpose monitoring handle a combination of objectives such as the above ones [6].

In the Nordic countries, Denmark, Finland, Norway and Sweden, there are monitoring networks with the purpose of monitoring water quality and loading from specific catchments. These monitoring networks generally consist of up to 20 relatively small stream catchments and involve detailed integrated studies of both river water quality and of the catchment (for example, land use, soil type). The main purposes of these networks are to monitor reference areas, loadings from agricultural land or the impact of acid precipitation.

The number of variables measured varies from 4 to 120, but all programmes generally include the determination of basic variables (e.g. pH, conductivity, water temperature), organic pollution indicators (e.g. dissolved oxygen, BOD), nutrients and suspended solids. Many programmes also include determination of specific ions (e.g. chloride, sulphate, calcium) and heavy metals. Additionally, the determination of more specific contaminants such as organic micro pollutants and radionuclide is included in some monitoring programmes.

The aerial density of sampling sites varies from one sampling site per 10,000 km² to more than five sampling sites per 1,000 km², with 1 to 2 sampling sites per 2,000

km² generally being found. The density of sampling sites in relation to population varies from 2 to 500 sites per million inhabitants [6].

1.4.1.1.1. Standardization

In Europe, for example many countries organize water quality monitoring at national level at the same time ensuring standard monitoring practices. Local monitoring, however, do exist as well. In Germany for example The German Federal States monitor the environmental state of lakes in their respective areas. Local lake monitoring activities are generally not standardized at a national level, and the variables and sampling frequency vary [6].

1.4.1.1.2 River Sampling Space and Frequency.

In Europe for example on major rivers river sampling frequencies range from 4 to 30 per year. Sampling frequencies depend on the objective of the monitoring and the rivers seasonal characteristics.

1.4.1.1.3 River Flow Measurement

River flow monitoring is an inseparable part of the river water quality-monitoring program. Estimation of pollutant loads and study of weathering and nutrient transport, etc would be difficult without concurrent measurement of river discharge. The drawbacks of many existing river flow measurement is their location mostly confined downstream in the low land. While this practice helps in assessing the river chemical input to lakes, there is a need to locate gauging station upstream as well to make comparative evaluations [6].

1.4.1.2 LAKE WATER QUALITY MONITORING.

Some countries make inventory of lake water quality done locally and the summary produced at national level after the data collected at local levels were gathered. Some countries traditionally monitor nationally important lakes (Austria). There are countries that make lake monitoring as part of in land (river and land) monitoring (Netherlands, Portugal) [6].

1.4.1.2.1 Lake Variables Monitored

For Lake waters the number of determinants measured is generally in the order of 20 to 30. Most programmes include determination of basic variables (temperature, pH, conductivity, dissolved oxygen), organic pollution indicators (total organic carbon, biochemical oxygen demand, chemical oxygen demand), eutrophication indicators (nitrogen and phosphorus species, chlorophyll-a, Secchi depth) and major specific ions (Ca, Mg, Na, K, etc.). Some countries also include determination of heavy metals (Finland, Sweden) and persistent organics. . Some monitoring programmes also include measurements of total phosphorus, total nitrogen and ammoniacal nitrogen. The extent of acidification is also assessed using of various biological indicators such as zoobenthos, phytoplankton, and fish [7].

1.4.2 GROUND WATER QUALITY MONITORING

The objectives of ground water quality monitoring in general include surveillance purpose monitoring and 'monitoring for water quality trend identification, assessment of compliance with national or continental legislation Examples include the European commission control of drinking water quality, or monitoring for compliance with the EU Nitrates directive. Other objectives include evaluation of saline water intrusion, assessment of the effects on the ground water quality of air borne pollutants and of anthropogenic pollutant inputs over a catchment. (Human and animal wastes, agricultural activities).

The ground water quality variables to be monitored include: descriptive parameters (e.g. conductivity, pH, turbidity, odor); Major ions (e.g., Ca, Mg, Na, K, NO_3 , NO_2 , NH_4 , Cl, SO_4 , HCO_3); Additional parameters also include DOC, boron, fluorine, cyanide, hydrocarbon benzene), Heavy metals (e.g. Cr, Pb, Cd, Hg, Ni), Organic substances including chlorinated solvents (e.g. trichloroethene; tetrachloroethene; 1,1,1 trichloroethane; 1,1-dichloroethene); and Pesticides (herbicides, insecticides).

The lowest sampling frequency for basic ground water quality monitoring programmes is once every 2 years compared to the highest frequency of 12 times per year. These differences are due to differences in monitoring purpose or objectives (e.g. specific networks with small number of sampling sites, high sampling frequency and small number of variables). Little useful information was received on

the limits of detection achieved for the determinands. In some cases values above detection limit are only given as an order of magnitude value (mainly in monitoring systems for drinking water), If there are no exact values, statistical evaluations for example analysis of time series, are difficult.

1.4.2.1 Ground Water Quantity Monitoring

The objectives of ground water quantity monitoring include collection of basic data, for management purposes (ex. Piezometric monitoring for compliance with national legislation) and for scientific research. (Ex. Piezometric network for mathematical modeling).

1.4.2. 2 Ground Water Sampling Frequency and Density

Density of monitoring sites is very variable ranging from 0.1 to 1000 per 100 Sq. Km. Some sites are evenly distributed over the aquifer space. Others are mainly concentrated around drinking water wells. Sampling frequencies range from continuous monitoring to only 2-3 times per year. The hydrogeological conditions dictate the water quality seasonal variation and hence the frequency of sampling.

1.5 DESIGN OF WATER QUALITY MONITORING SYSTEM

1.5.1 Background

Design of a water quality-monitoring network is an iterative process. It evolves in time in response to changing data needs, objectives of monitoring, economic vagaries, changing force functions and so on. The design must reflect the societal need. In this sense, one might even say the design process is a state of mind.

When designing or redesigning a water quality monitoring network system, it is often necessary to gain a clear understanding of the dynamic behavior of the water quality process involved. The design process can be shown in the following framework (figure 1.5.1)

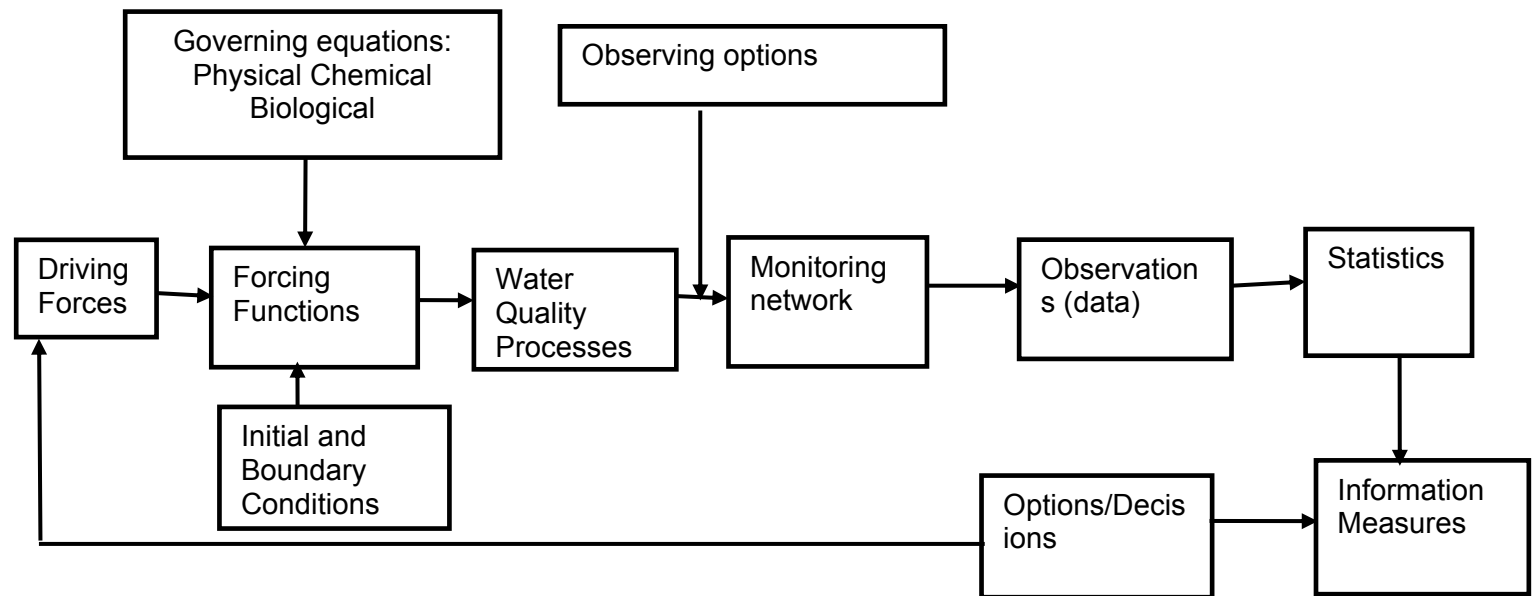


Fig. 1.5.1 Schematics of Water Quality Monitoring and Management [8]

Each component of the design process is expressed in terms of numbers and / or equations, and statistics are used to express data in summary form. When the information is magnitudes in the form of plots or tabulated data, etc., one says it is of non-parametric form.

1.5.2 Detection of Trend

One of the objectives of a water quality-monitoring network is to monitor the actual state of water quality. This is accomplished through (1) detection of trends, (2) determination of periodic fluctuations, and estimation of mean values of the stationary component. Indeed the sampling frequency will be dictated by the trend detectability, the accuracy of estimation of the mean values. Each of these components will have its own frequency and the sampling frequency will be the highest of these three magnitudes.

The power of the student's t-test is used as a quantitative criterion for detection of a linear or step trend. The power of the test is the probability of trend detection, i.e., trend delectability. For a sample size of N independent observations, the power of the trend detection can be calculated by:

$$P_w = 1 - \beta = F(n_T - t_{\alpha/2}) \dots\dots\dots (1.1)$$

Where F is the cumulative distribution function (CDF) of the student's t-statistic, β is the probability of making a type II error, $t_{\alpha/2}$ is the quantile of the student's t – distribution with N-2 degrees of freedom at a probability level of α and n_T is the trend number defined as:

$$n_T = \frac{T_r}{2S/\sqrt{N}} \text{ For a step trend and} \dots\dots\dots (1.2)$$

$$n_T = \frac{T_r^*}{\sqrt{12} s / \sqrt{N(N+1)(N-1)}} \dots\dots\dots (1.3)$$

For a linear trend, where T_r and T_r^* are the magnitudes of step and linear trends, respectively, and s is the sample standard deviation.

For water quality observations that are serially correlated, the effective number is used. The effective number is defined as the number of independent observations that gives the variance of the estimation of the mean equal to that of the number of serially correlated observations. The relation between N_e and N is expressed as

$$N_e = \left[\frac{1}{N} + \frac{2}{N^2} \sum_{i=1}^{N-1} (N-i)\rho(i\Delta t) \right]^{-1} \dots\dots\dots (1.4)$$

The number of samples when replaced with T/Δ will give a relation between the sampling interval and the power of observation.

Where Δt is the sampling interval and ρ is the correlation coefficient. At a given location, the standard deviation and the correlation structure are estimated from the sample of observations. The trend magnitude and the length of time must be estimated from observations. The power of observation and the frequency of sampling f_T for detection are then specified [8].

1.5.3 Determination of Periodic Fluctuations

Due to seasonal variations in climate, ex. Rainfall, water quality parameters may exhibit periodic fluctuations. These fluctuations may be determined using Fourier series analysis. The spectral analysis reveals the highest frequency of significant periodic fluctuations in the real time series. Let this frequency be f_s . Then the sampling frequency f_p should be more than twice f_s , i.e., $f_p \geq 2f_s$ in order to capture the significant frequent fluctuation. For determining the exact sampling frequency, the half width R_h of confidence intervals of the estimation of the spectral density can be constructed for a serially correlated water quality time series as:

$$R_h = \frac{2st_{\alpha/2}}{\sqrt{N_e}} \dots\dots\dots (1.5)$$

R_h can be employed as a criterion for estimation of periodic fluctuations and then the sampling frequency f_p for pre-specified length of time [8].

1.5.4 Estimation of Mean Values

The water quality is reduced to one that is trend free and non-periodic. The reduced time series is hopefully stationary. The half width of the confidence interval of the mean can be used for estimation of mean value of the stationary series. The half width of the confidence interval R_m may be constructed as:

$$R_m = \frac{St_{\alpha/2}}{\sqrt{N_e}} \dots\dots\dots (1.6)$$

The sampling frequency for estimation of the mean can be determined by specifying the threshold value of the half-width.

1.5.6. Criteria For analysis of Sampling Frequency

For determination of sampling frequency, a quantitative measure of network effectiveness is needed, which in turn is related to, among other things, monitoring objectives. The sampling frequency is suggested to be the highest of f_T , f_p and f_m .

Table 1.5.1 Determination of Sampling Frequencies [8]

Technical Objectives	Quantitative criterion	Characteristics of Time Series	Sampling Frequency
Detection of trend	Trend Detectability	Type of trend, magnitude of trend, Standard deviation, Autocorrelation	F_T
Determination of Periodic Fluctuation	Nyquist Frequency and Accuracy of parameter estimation	Periodicity, Standard deviation, Autocorrelation	F_p
Estimation of Mean	Accuracy of estimation, Information content of mean	Standard deviation, Autocorrelation	F_m
Monitoring actual state			$F = \max(f_T, f_p, f_m)$

1.5.7. Determination of Underlying Physical Factors for Water Quality Variation

While the water quality parameters to be monitored may be large, the underlying factors responsible for the space and time distribution of these parameters are often few. In this research the application of principal components and factor analysis has been employed in order to find the underlying common factors for the water quality variations from which the design of monitoring follows. The detail of the procedure and results are described below.

1.5.7.1 Principal Component analysis

In order to examine a relationship among a set of p -correlated variables, it may be useful to transform the original set of variables to a new set of uncorrelated variables called the principal components [9, 10]. These principal components are linear combination of the original variables and are derived in decreasing order of importance so that for example the first principal component accounts for as much of the variation in the original data. The transformation is in fact an orthogonal rotation in p – space. Water Quality Monitoring Design Using Principal Components can be

employed if the transformation leads to adequate reduction of data dimensionality [11]

1.5.7.2 Factor Analysis

The p components of the principal model may be viewed as p common factors explaining the dependence structure of the p response variables, while the $m < p$ common factors of the factor model explain most of the dependence structure with the residuals accounted for by the specific factors. In other words, the principal component model attributed all of the total variance to the P common factors, while the factor model splits the variance of each response variable in to two parts - the variance due to the common factors (the communality) and the variance due to the sampling variation of each response variable (the specificity) [9, 10].

The techniques of each factor analysis concern itself with estimating the factor loadings λ_{ij} and the specific variances ζ_i , $i = 1, \dots, p$, $j = 1, \dots, m$. It is also concerned with the methods for evaluating the common factors for an individual as a function of its responses. These values are called factor scores.

Once the factor loadings have been obtained, the major burden of the analysis is to make the best interpretation of the common factors. This involves the technique of factor rotation, which due to its subjectivity, is the most controversial part of factor analysis.

1.5.7.3 Cluster Analysis

Clustering is a means of searching for groups of similar objects or similar variables. Clustering could be by samples (objects) or by variables [12]. Clustering is achieved by means of similarity between objects and variables. Measures of similarity are defined in terms of correlation coefficients when proportional objects are very similar or otherwise in terms of Euclidean distance in N dimensional space (for N variables or objects). Mahalanobis distance is used when some variables are highly correlated to avoid giving too much emphasis to the same information. After deciding how the distances are to be measured, the similarity between two objects I and j is calculated from [12]:

$$S_{ij} = 1 - \frac{d_{ij}}{d_{\max}} \dots \dots \dots (1.7)$$

Where S_{ij} is the similarity between objects i and j , d_{ij} is the distance between them and d_{\max} is the maximum distance among the objects in a data set. The similarity of an object with itself is 1 and the similarity with the two most distant objects is 0.

There are many clustering techniques, the major ones being classified as hierarchical and non-hierarchical. The agglomerative hierarchical method, which is used in this research, is a technique whereby clusters are progressively linked to form bigger clusters until a single big cluster of all the objects is obtained [12].

CHAPTER 2

DESCRIPTION OF THE ABAYA – CHAMO WATER RESOURCES BASIN

S.NO.	CONTENTS	PAGE
2.1	Background	18
2.2	Geology	21
2.3	Hydro-Climatological Conditions	22
	2.3.1 Climate	22
	2.3.2 Tributary Rivers within The Abaya – Chamo Basin	23
	2.3.2.1 Hare River Water	24
	2.3.2.2 Kulfo River	25
	2.3.2.3 Sile River	26
	2.3.2.4 Other Rivers in the Abaya – Chamo Drainage Basin	27
2.4	Settlement, Population Growth and Land use	28
2.5	Water Supply	29
2.6	Sanitation	31
2.7	Industrial and Irrigation Development	32
2.8	Previous Water Quality Studies	33

S.No.	LIST OF TABLES	PAGE
Table 2.3.2.4.1	Rivers draining in to the Abaya and Chamo Lakes	27
Table 2.5.1	Water Supply sources in the SNNPR, Ethiopia	29
Table 2.5.2	Distribution of Safe and Unsafe Sources of Water Supply in the SNNPR	31
Table 2.5.3	Sanitation Coverage in the SNNPR, Ethiopia	31
Table 2.5.4	Distribution of Sanitation facilities in the SNNPR, Ethiopia	32
Table 2.7.1	Irrigation Schemes and Sizes on major River Tributaries of the Abaya-Chamo Basin	32
Table 2.8.1	Summary of Water Qualities of Rift valley lakes (Kebede E., Zinabu G.Mariam, etal, 1994)	34

S.No.	LIST OF FIGURES	PAGE
Fig. 2.1.1	The Rift Valley Lakes Drainage Basin	19
Fig. 2.1.2	The Lake Abaya Chamo Catchment Basin	20
Figure 2.1.3	The location of water quality sampling sites	21
Fig. 2.3.1.1	Daily Precipitation Data for the year 2003(Arbaminch Weather Station).	23
Fig. 2.3.2.1.1	The Lower Part of the Hare River and its Surrounding Catchment	24
Fig. 2.3.2.1.2	Daily variation of Flow (Hare River)	25
Fig. 2.3.2.2.1	. The Lower Part of the Kulfo River and its Surrounding Catchment	26
Fig. 2.3.2.2.2	Daily Flow variation (Kulfo River)	26
Fig. 2.4.1	Settlement and land use in the Arbaminch Town Area – adjoining Lake Abaya and showing Rivers Hare and Kulfo	30

2.1 BACKGROUND

The Abaya Chamo drainage basin is a sub basin of the rift valley that crosses through Ethiopia midway in the north south direction. The basin comprises mainly the two lower lying lakes. Lake Abaya and lake Chamo and rivers like Gelana, Bilate, etc the drain in to Lake Abaya. The rivers kulfo and Sile enter in to Lake Chamo and the overflow from Lake Chamo drains in to the Sagan River, which in turn drains finally to the Chew Bahir. The main rivers draining in to Lake Abaya are listed as: Gelana, Milate, Gidabo, Hare, Baso, and Amesa. In addition a number of small brooks and ephemeral rivers enter the Abaya Lake. The rivers draining in to Lake Chamo are listed as: Sile, Argoba, Wezeka, Sego, in addition to the over flow from Lake Abaya which confluences with river kulfo and eventually drains to Lake Chamo. The Abaya and Chamo Lakes are hydrologically interconnected. An overflow from Lake Abaya flows in to Kulfo River that in turn ends up in to the Chamo Lake. The level difference between the two lakes is 62 meters, Abaya Lake being higher than Chamo Lake. The altitude of the region varies between 4200 m above sea level, (Mount Guge) and 1108 m above sea level (at the outflow from the Chamo Lake). The region is located in the range 37 – 38 ° in eastern longitude and 5 – 8 ° in the northern latitude. The two lakes have been used for transport (Lake Abaya), fishery and tourism. The lakes have not been used for irrigation. However, the tributaries (rivers Bilate, Kulfo, etc) have been used intensively for irrigation [50].

There have been some studies done in the past about the limnology of the two lakes and the influence of increased upper catchment activities and increased utilization of the tributaries to the two lakes. There had been isolated cases of observation in which wild lives were seen to have died, may be due to the consumption of toxic substances produce by the blue green algae [95].

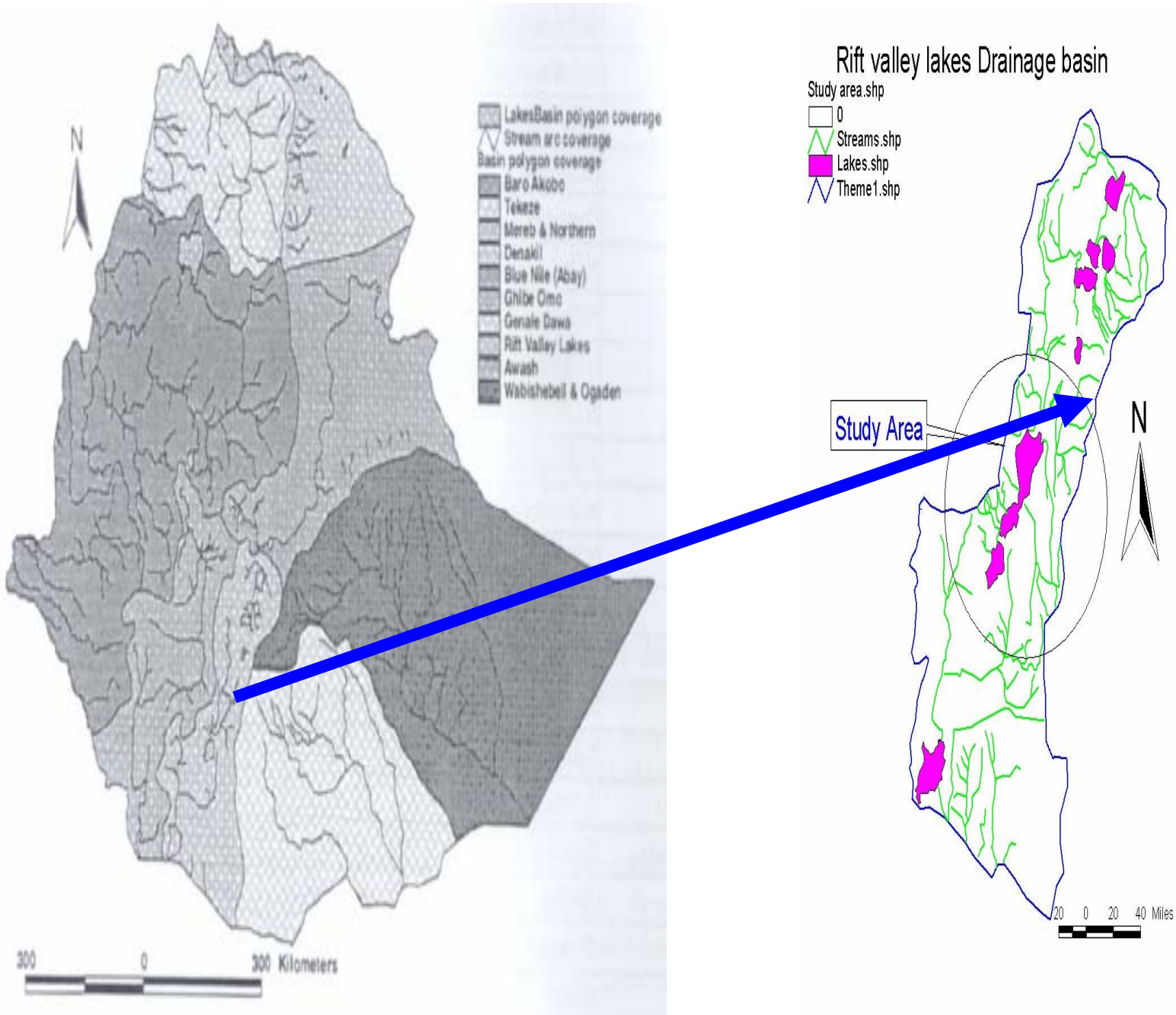


Figure 2.1.1: The rift valley lakes drainage basin in which the Abaya-Chamo basin is a part is shown in relation to the Ethiopian drainage map. The lakes which are part of this rift valley basin include Lake Abaya, Lake Chamo, Lakes Langano, Abiyata, Zway, Shala. The Abaya – Chamo Lakes basin is shown on the right diagram as a study area with a circle.

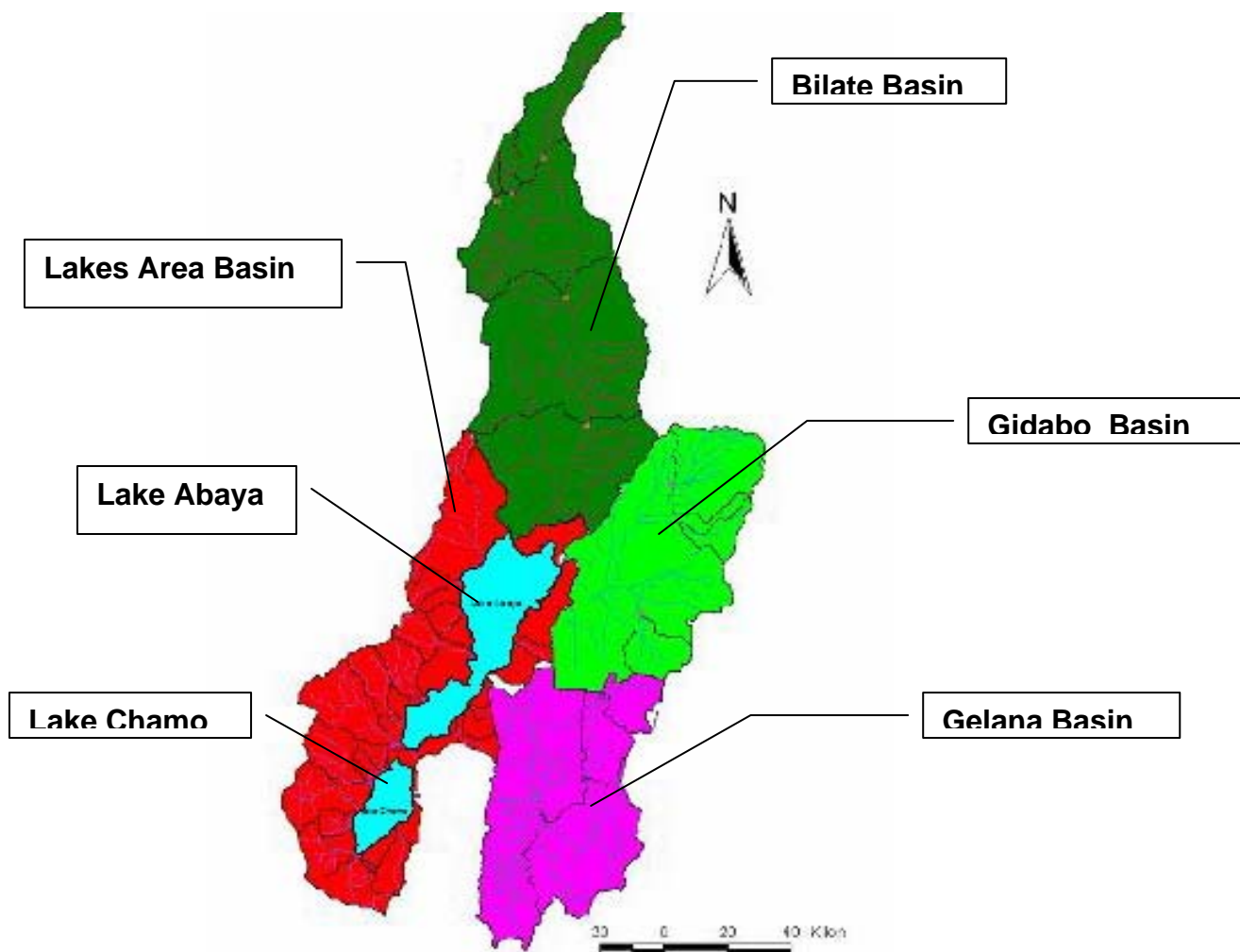


Figure 2.1.2 The Lake Abaya Chamo Catchment Basins identified by the names of the major rivers that flow from the catchment in to the lakes.

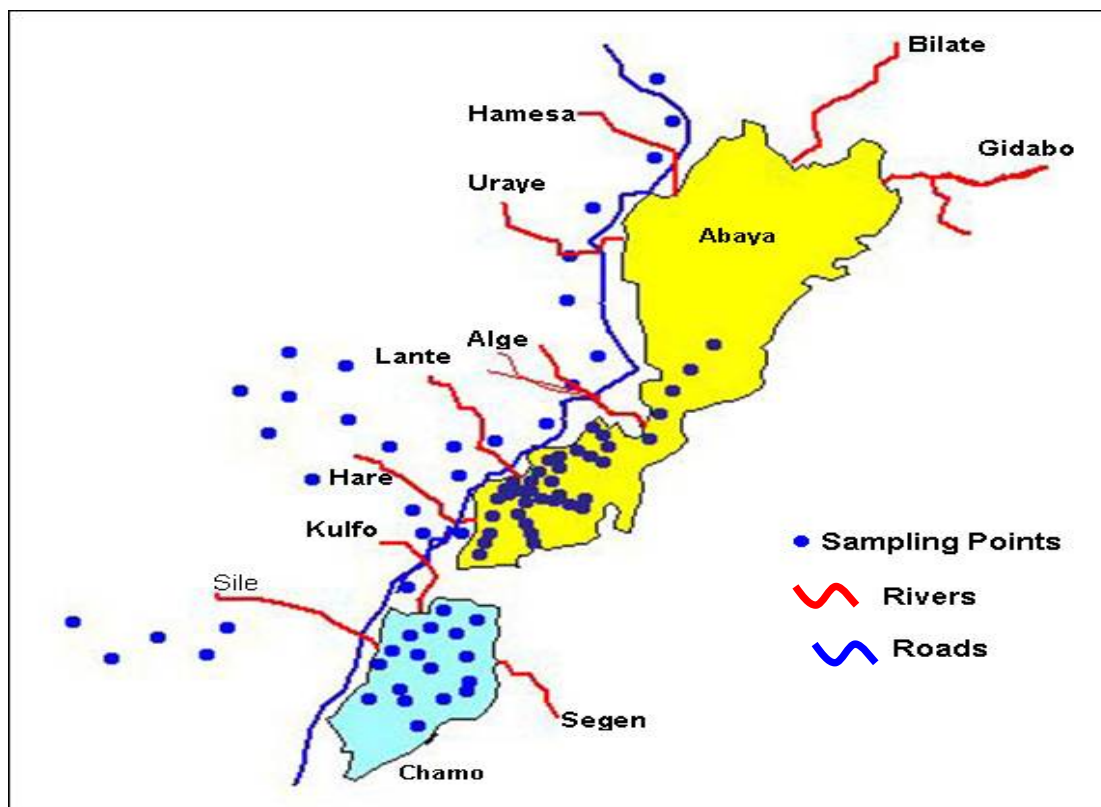


Figure 2.1.3: The location of water quality sampling sites within the study area which is the Abaya-Chamo Lakes basin. The blue circle dots indicate the sampling points. The lines in red locate the major rivers that are tributary to the lakes. The blue line locates the major road connecting the cities.

2.2 GEOLOGY

The Abaya – Chamo basin being part of the rift valley was formed by volcanic activities in the Rift Valley during the period of Pliocene and Holocene. Accordingly, it is believed that ancient basement rocks lie under the whole Rift Valley. They consist of gneisses, which transform into granites and gneissosities [47]. The latest layers are consolidated ash flows of volcanic activities transformed into basalts and ignimbrites (tuffs). The area is, therefore, mainly characterized by volcanic rocks of tertiary and quaternary periods as well as with quaternary period alluvium deposits. In the northern part of the Abaya Chamo basin, most of the area is covered with Pliocene ignimbrites, which are mostly acidic and inter-bedded with tuff and pumice. In the low land part of the Abaya Chamo Basin most part of the upper land is covered with recent quaternary period Aden series, basaltic flows and related spatter cones. Some parts of the upper reach, all of the middle reach and upper half of the lower land area are characterized by tertiary period trap series alkali basalt and trachyte

generally known as Oligocene basalt flows. The remaining half of the lower reach, at the flat area around the lakes, is covered with quaternary period alluvium deposits.

2.3 HYDRO-CLIMATOLOGICAL CONDITIONS

2.3.1 Climate

The climate in the basin varies from tropical to alpine. The inter-tropical convergence zone (ITCZ) is responsible for the bimodal rainfall system bringing humid wind from the Indian Ocean. Apart from the ITCZ, the rainfall distribution in the area is affected by the effects of altitude. The climate sub division given below is based on altitude, which according to this classification places the area falls in the hot to moderately hot- humid climate (Kolla-Weine Dega region) with humid character as well as higher temperature [47].

Hot Regions (Kolla):	up to 1.500 m
Moderately hot and humid (Weyna Dega):	1.500 m – 2.300 m
Moderately cold (Dega):	2.300 m – 3.200 m
Cold (Wurch):	3.200 m – 3.700 m

The wet rainy seasons for Chamo and Southern Abaya are March-May and September-October. The wet and rainy Seasons for Northern and North Abaya (Bilate) includes months of July -October, and for the other parts of the catchment is April-May and October [47].

The Abaya – Chamo Basin climate is further characterised by high rate of evaporation (about 2300 mm per year on average) and the precipitation average of about 600 mm. The area in the past has been affected by global climatic change with a shift to a decrease in precipitation peaks and with consequent impact on the lakes. Climatic phenomenon such as the Elnino has resulted in rise in precipitation and consequent increase in lake levels at some periods in the past.

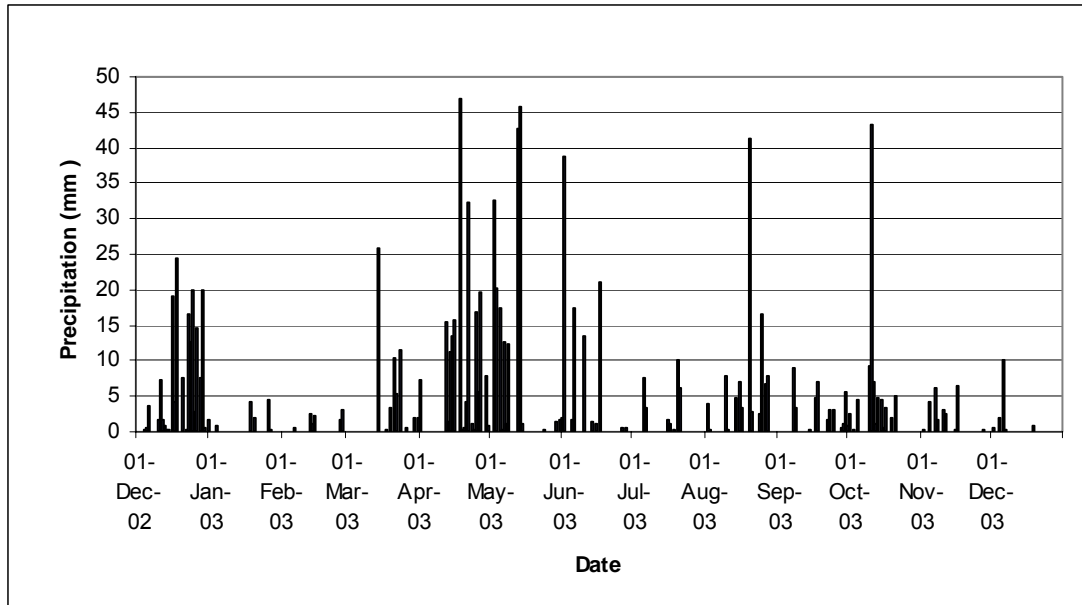


Fig. 2.3.1.1 Daily Precipitation Data for the year 2003 (Arbaminch Weather Station (Total Annual Precipitation = 881 mm)

Fig. 2.3.1.1 shows the precipitation measurement data from a near by meteorological station at Arbaminch University (south of Lake Abaya and North West from Lake Chamo). The precipitation shown has a bi-modal seasonal variation with peaks in the periods March – May and August – October. The annual precipitation for this year totals to 881 mm. The rivers in the basin mostly display a wide range of flow (Maximum-Minimum flow) and enter the lakes as flash flows. The sudden flood flow exhibits very quick rise and fall of water level that resulted in very steep flood hydrograph. The flashy nature resulted in high sediment load that in the future will lead to a decrease in the capacities of the lakes.

The average temperature in the lowland areas recorded in the Arbaminch weather station lies between 22°C to 24°C yearly. The variation between day and night temperatures is about 12°C. In the highland areas on an altitude of 2.700 m a.s.l. The temperature is much lower. In Chench, the temperature varies between 12°C and 14°C.

2.3.2 TRIBUTARY RIVERS WITHIN THE ABAYA – CHAMO BASIN

The three rivers where more frequent water quality sampling and testing has been carried out lie in the vicinity of the town of Arbaminch and are described below in detail. The remaining rivers where scattered sampling and testing were done within the basin are briefly listed.

2.3.2.1 Hare River Water

The Hare River catchment area is placed in the western part of the Abaya-Chamo-Basin in the southern region of Ethiopia. The linear distance to the capital city of Ethiopia, Addis Ababa, is 350 km to the north. It is situated on the geographical coordinates between 37° 27' and 37°37' eastern longitude, and 6° 03' and 6° 18' northern latitude (Figure 4). The area is about 169 km square and ends at the western boundary of the Lake Abaya. Arbaminch is the actual administrative capital of the Gamu Gofa zone, 5 km away from the catchment of Hare River,

Hare River is a small river but extensively used by the farmers to irrigate their crops, in the villages Chano Dorga and Chano Mille areas. A diversion weir has been constructed with the objective of irrigating a command area of 1300 hectares of land. The mean annual flow of Hare is estimated around $2.1 \text{ m}^3 \cdot \text{Sec}^{-1}$



Fig. 2.3.2.1.1. The Lower Part of the Hare River and its Surrounding Catchment

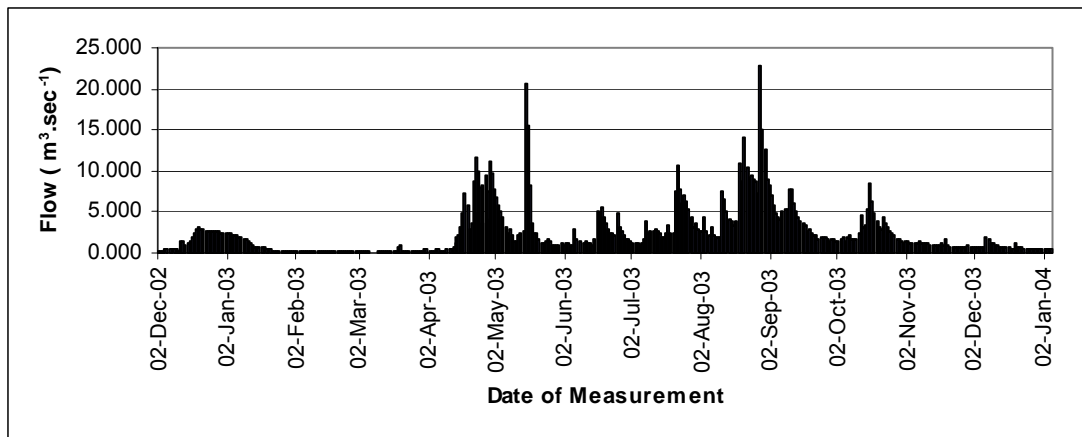


Fig. 2.3.2.1.2 Daily variation of Flow (Hare River)

2.3.2.2 Kulfo River

Kulfo catchment area is defined by the geographical coordinates between $5^{\circ} 55'$ and $6^{\circ} 15'$ North latitude and $37^{\circ} 18'$ and $37^{\circ} 36'$ East longitude. The elevation of the catchment area varies from 3600 m above sea level at the peak of Wishu Ridge to 1100 m at the entrance to Lake Chamo. The whole catchment area is bounded by different Ridges of different altitude. The Rift Valley flat area with the two lakes (Abaya and Chamo) stretched from north-east to south-west.

The Kulfo River is being used for irrigation and for domestic consumption by scattered settlement of the rural population who also grow sugar cane plantation and use the Kulfo River to irrigate the plants. The main irrigation consumption of Kulfo River is by the Arbaminch State Farm that owns 100 hectares of land. The flow diverted by this scheme is so high that during the dry season the river is completely diverted towards the state farm leaving the downstream without any water. The downstream section is a wetland area whose ecosystem has been reportedly affected by the dry up.



Fig. 2.3.2.2.1. The Lower Part of the Kulfo River and its Surrounding Catchment

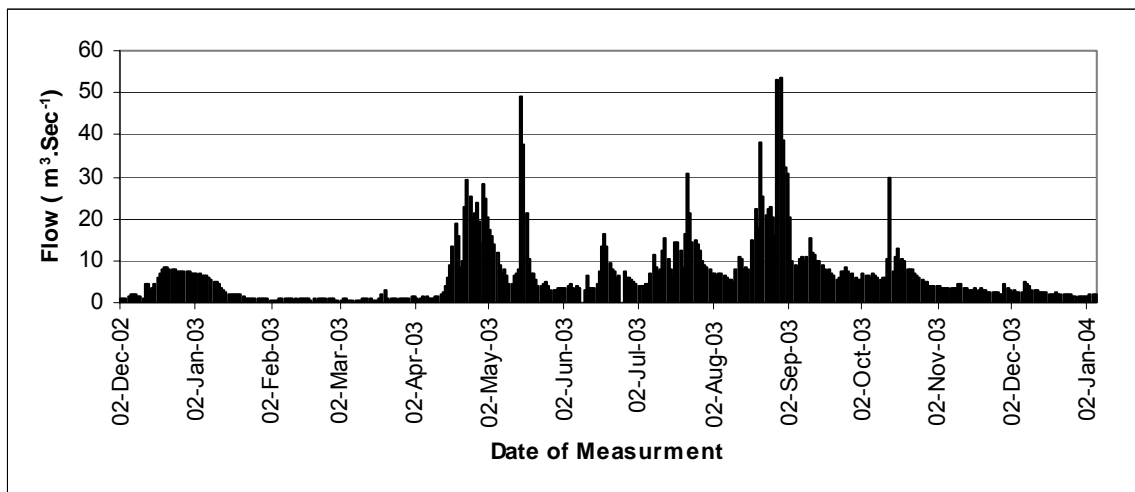


Fig. 2.3.2.2.2 Daily Flow variation (Kulfo River)

2.3.2.3 Sile River

The Sile river drains from the near by highland area of Bonke-Beza such as Kenchame, Gerbensa, Kershe, Zegite Merche and Gobo Beke. The draining seasonal streams are Chile, Holpe, Omile and Oslo that form the small river Sile.

The river drains in to Lake Chamo. The total catchment area of Sile River is 237.05 square kilometres. The Sile River is utilised for irrigating the Sile state farm. There is no recorded flow data for the Sile River.

2.3.2.4 Other Rivers in the Abaya – Chamo Drainage Basin

The Rivers tributary to the Abaya Chamo Lakes and their drainage areas are given in the table 2.3.2.4.1.

Table 2.3.2.4.1 Rivers draining in to the Abaya and Chamo Lakes [50].

Serial number	River name	Draining in to lake	Drainage area (Square kilometres)
1	Bilate	Abaya Sub Basin	5756.9
2	Gidabo		3446.62
3	Iyaye		47.76
4	Tuta, Kubi; buchise, Fato		280.06
5	Wallo, Tora		97.06
6	Haro		24.54
7	Odo Haro oda		67.06
8	Dimo		58.13
9	Deda Muke Guracha Dade		71
10	Geda Bonke – Abaya side		4.12
11	Arbaminch Ersha Limat		39.78
12	Hare		183.29
13	Lante		54.14
14	Basso		180.57
15	Shope		161.9
16	Abae		59.49
17	Dekursa		71.93
18	Udula		60.1
19	Irae		105.38
20	Amessa		506.75
21	Abela Mereko Mutate		244.52
22	Abaya lake		1108.9
		Chamo Sub Basin	
1	Kulfo		455.13
2	Geda Okolo		30.75
3	Genta Kenchema		15.56
4	Sile		237.05
5	Sego		61.1
6	Arguba-Wezeka		151.4
7	Walesa		47.62
8	Waneta		4.51
9	Wezeka		225.34
10	Doyso		140.89
11	Abulo, Olfecho		56.1
12	Geda Bonke		57.8
13	Chamo Lake		328.63

2.4 SETTLEMENT, POPULATION GROWTH AND LAND USE

The basin is found mainly in the Southern Nations, Nationalities and Peoples Region (SNNPR) of Federal Republic of Ethiopia and a small portion of it in the neighbouring Oromia region. The population is from a diverse multi ethnic group with over 30 different languages spoken in the various localities. According to the 1994 census, the basin population is estimated as 3.62 Million. The current population estimate is around 4.5 Million in the basin area accounting for about 2.4% of population growth. Most of the inhabitants live nomadic life to peasants mainly in the high land settlements while there are major cities and towns along the main road.

The Abaya Chamo drainage basin as a sub basin of the rift valley lakes system has been an area of rapid population growth and settlement due partly to its water resource potential. Concomitant to this is the increasing land use and degradation of the natural ecosystem because of deforestation caused by increasing fire wood demand and clearing of lands for agriculture and burning of forests and bushes for livestock and grazing purposes. Because of the sustained dry period and lack of soil moisture, land irrigation with river waters is under a steadily increasing practice in the area. As a result there is an ever increase utilisation of the rivers for drinking and irrigation uses. Recently the Ethiopian Government has stepped up soil conservation and water harvesting practices in the area as a short-term strategy for combating drought and ensuring food security. Ponds and rainwater storage tanks are being constructed to meet the demand of water for irrigation and domestic water use.

Ethiopia has, in the recent past three decades, been subjected to drought and famine and soil erosion and deforestation. The increase in the settlement and population as well as agricultural and irrigation activities in the Abaya – Chamo drainage basin has been large in the recent past with inevitable changes on the water qualities of the surrounding resources [17]. The Lakes Abaya and Chamo, which are interconnected by over flow, have in the past been affected by water quality changes as a result of this multitude of factors [15]. Decreased water level and increasing salinity has been observed in the past as well as deteriorating of the lakes ecology due possibly to changes in the water quality.

Because of the drought problem, population settlement is being planned and implemented in the area where water accessibility and use is simultaneously considered in the process. The increasing population and increase in water demand

and water use, and the need for environmental protection call for a systematic management of resources of which the river water qualities are an integral and essential part.

2.5 WATER SUPPLY

Water supply coverage in the region is far from complete while the performance of existing supplies in several cases unsatisfactory. The percentage of urban population with relatively safe potable water supply coverage is estimated to be around 70% with the remaining 30 % using unsafe sources for part or whole of their water demand (i.e. rivers, ponds, lakes, unprotected well). Rural areas water supply coverage is poor with only about 24% considered as relatively safe supplies and a vast 76% of the remaining population using unsafe sources of supply. Due to much poorer sanitation coverage many water sources are polluted and this is the cause for many water borne illnesses among the population, child mortality and morbidity cases. Table 2.5.1 below indicates the sources of supply in the SNNPR[13, 14].

Table 2.5.1 Water Supply sources in the SNNPR, Ethiopia [13, 14]

Population	Sources of Water (%)					Total
	Tap	Protected well/Spring	Unprotected well/spring	River/Lake/pond	Not stated	
Urban	55.5%	15.5%	13.3%	15%	0.7%	100%
Rural	4.6%	10.9%	31.7%	52.6%	0.2%	100%
Total	8%	11.2%	30.4%	50.1%	0.3%	100%

The population in the Abaya -Chamo basin covered with supply from either sources considered unsafe or safe is given in table 2.5.2 for rural and urban settlements [50].

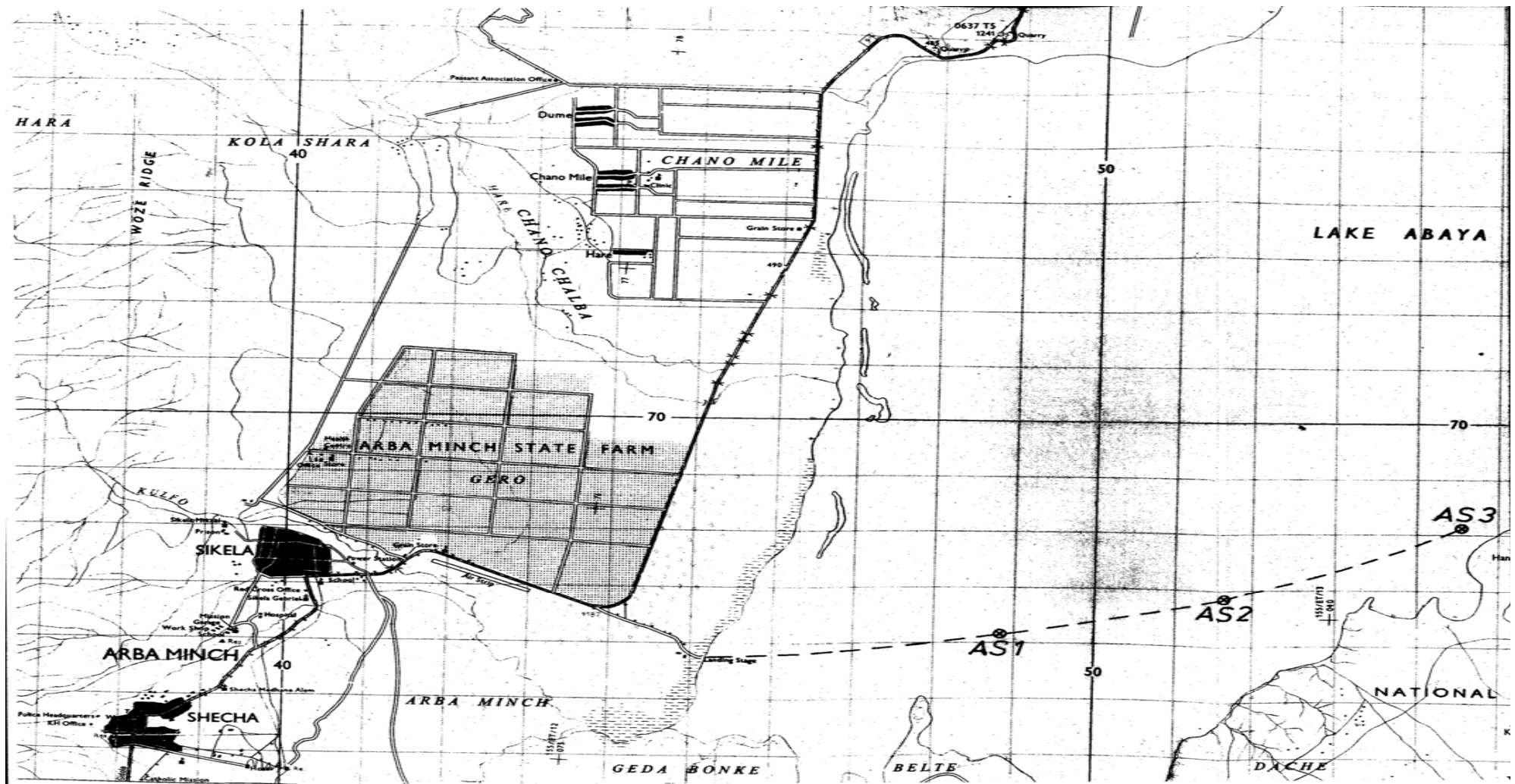


Fig. 2.4.1 Settlement and land use in the Arbaminch Town Area – adjoining Lake Abaya and showing Rivers Hare and Kulfo [47]

Table 2.5.2 Distribution of Safe and Unsafe Sources of Water Supply in the SNNPR
[13, 14]

Population	Total Population	Supply Status			
		Safe Supply		Unsafe Supply	
		Population	Percent	Population	Percent
Urban	34,1402	208,529	61.1%	132873	38.9%
Rural	3,276,770	631,537	19.3%	2,645,233	80.7%
Total	3,618,172	840,066	23.2%	2,778,106	76.8%

2.6 SANITATION

The percentage of the population having proper sanitation facility is very low [13, 14]. The form of sanitation is largely confined to onsite facilities with sewerage facilities confined to government institutions and dwellings in such premises. Table 2.5.3 shows the percentage of urban and rural population with and without toilet facilities.

Table 2.5.3 Sanitation Coverage in the SNNPR, Ethiopia

Population	With Toilet (%)	Without Toilet (%)	Not Stated (%)
Urban	62.9%	35.9%	1.2%
Rural	9.2%	90.4%	0.4%
Total	12.8%	86.8%	0.4%

Toilet facilities are either of flush toilets, pour flush and pit latrines with the later covering by far the greatest portion of the population. The flush toilet (cistern or pour flush) cover 2% of the population. 94% of the town population and almost all of the rural population have no bathing facilities. Table 2.5.4 shows the population in the ACB region with various levels of sanitation facilities.

Table 2.5.4 Distribution of Sanitation facilities in the SNNPR, Ethiopia

Population	Size of population	Presence of Toilet Facilities				No Toilet
		Flush Toilet	Percent(%)	Dry Toilet Facilities	Percent	Percent
Urban	341402	7638	2.2%	223021	65.3%	34.7%
Rural	3276770	0	0.0%	401575	12.3%	87.7%
Total	3618172	7638	0.2%	624596	17.3%	82.7%

2.7 INDUSTRIAL AND IRRIGATION DEVELOPMENT

The existing industrial development is very low with the textile factory located in Arbaminch city as a major industrial facility. Small-scale cottages exist such as tannery, cereal mill plants, coffee processing plants, quarry, etc.

Several of the tributaries of the Abaya and Chamo lakes are being used for irrigation. Crops grown by state irrigation farm establishments include tobacco (North of Lake Abaya), Cereals (Irba Lola, Bilate), Banana ((Arbaminch, Sile), and Cotton (Arbaminch, Sile). Table 2.7.1 provides the major tributaries of the lakes Abaya and Chamo and the associated irrigation schemes and areas irrigated [50].

Table 2.7.1 Irrigation Schemes and Sizes on major River Tributaries of the Abaya-Chamo Basin [50].

S. No	River	Sizable Irrigation Scheme	Irrigated Area (ha)
1	Bilate	Tobacco farm	1000
		- Chericho	1300
2	Gidabo	Gidabo Diversion	400
		Wamole	50
3	Hare	Hare Farmers irrigation	1200
4	Baso	Baso Project	
5	Wajifo	Wajifo Project	400
		Shafe Project	
6	Amesa	Humbo – Amesa Irrigation	Not available

	River	Sizable Irrigation Scheme	Irrigated Area (ha)
7	Alluvial Fans of Abaya	Abaya State farm	700
8	Kulfo	Arbaminch State Farm	1200
9	Sile	Sile state farm	1300
10	Argoba (Wezeka)	Argoba Irrigation	80
Total	Total		7,630 + unaccounted

2.8 Previous Water Quality Studies

There is a scattered and limited amount of information available about water quality study in the area. Records of water quality intended for potable water uses are available at the time of project preparation. These data are scattered and have not been stocked in to a central data system. A number of investigations have been carried out on the qualities of Lakes Abaya and Chamo. Wood and Talling [95] have reviewed available records of 1960, 1970s relating hydrology chemical characteristics and algal distribution of the rift valley lakes in which the two Lake Abaya and Chamo have been included. A more recent assessment has been done by Kebede [46] as well as Zinabu [15, 16]. This study attempts to connect with these earlier studies by presenting seasonal water quality measurements for the two lakes and some of the contributing rivers and relate these measurements with long term variation of the water qualities of the two lakes. It also attempts to give explanation to the possible increase in salinity from the assessment of the water balance model proposed earlier by Seleshi Bekele [50] and river water quality data obtained in this study. Table 2.8.1 shows a summary of the water quality data of the Ethiopian Rift valley lakes reported by Dr. Zenabu Gebermariam in 1994 [47].

Table 2.8.1 Summary of Water Qualities of Rift valley lakes [47]

Lake	Sampling Date	Depth (m)	K25 μS Cm ⁻¹	Salinity g L ⁻¹	Sum Cations me L ⁻¹	Sum Anions me L ⁻¹	Na+ me L ⁻¹	K+ me L ⁻¹	Ca+ me L ⁻¹	Mg++ me L ⁻¹	HCO3- +HCO32- me L ⁻¹	Cl- me L ⁻¹	SO42- me L ⁻¹	SiO2 mg L ⁻¹	PO4-P μg L ⁻¹	Total Phosphorus μg L ⁻¹	NO2- +NO3- μg L ⁻¹	NH3 - N μg L ⁻¹	pH pH units	Chlorophyll a μg L ⁻¹
Koka	10.5.91	0	286			2.97					2.5	0.18	0.29	14.6	9.5		1.4	bd		13.5
		0-0.6	286	0.2	3.08	3.02	1.35	0.14	1.16	0.43	2.6	0.22	0.2	12.5	bd	224	bd	bd	8.2	15.6
Zway	27.3.91	0-2	410	0.4	4.38	4.64	2.87	0.31	0.56	0.64	4	0.32	0.32	37	bd	2190	3.9	36.3	8.5	154.2
Awassa	12.3.91	0												37.9	12.4	30	58.3			48.3
		0-3	830	0.8	7.56	9.37	5.96	0.69	0.43	0.48	8.25	0.39	0.73	42.6	12.4	36.2	34.9	5.7	8.75	16.2
Abaya	16.3.91	0-2	925	0.9	10.34	11.37	9.13	0.44	0.45	0.32	9.37	1.11	0.89	20.3	147	237	180	13.2	8.65	5
		5-6			10.01		8.91	0.41	0.42	0.27				21.4	149	216	256	14.4		3.3
Chamo	15.3.91	0-2	1320	1	9.06	14.56	7.26	0.78	0.32	0.7	12	1.71	0.85	0.4	25.5	135	18.6	11.8	8.9	44.2
		4-5	1260		14.14	15.37	12.61	0.49	0.35	0.69	12.25	2.02	1.1	0.6	29.4	165	25.7	27.9		34.6
Langano	8.3.91	0			15.28		14.35	0.51	0.23	0.19		3.28	1.16		20	99.4		10		5.9
		0-2	1770	2.4	16.8	17.32	15.78	0.54	0.25	0.23	12.5	3.66	1.16	27.6	20	70.4	44.9	50	8.95	2.4
		15			15.65		14.7	0.51	0.24	0.2										
Metehara	12.5.91	0	7155	5.3		69.6					44	12.8	12.8	106.8	1295		88.7	<1	9.4	26.7
		0-12	7441		80.43	71.2	78.56	1.72	0.11	0.04	46.5	12.6	12.1	105.8	1302	1850	94.6	6.2	9.4	12.9
Shalla	20.3.91	0-4	21940	18.1	277	288	272	4.56	0.16	0.07	218	54.4	16.3	56	809	860	bd	4.3	9.65	15.8
		16-17			253	268	249	3.51	0.21	0.07	215	40.4	13.1	59	818	928	bd	3.8		6.1
Abijata	20.3.91	0									349			122	115	511			9.85	135.3
		0-2	28130	26.4	426	437	416	9.72	0.12	0.02	325	88.3	24	114	98	435	bd	88.1	9.85	14.7
		3-4			415	417	397	18.33	0.13	0.02	324	73.2	20.2	111	115	413	bd	122.9		10.6
Chitu	22.3.91	0									581			189	2011	2190	bd	bd	10.2	145.5
		0-1.5	49100	44.9	895	693	864	31.2	0.16	0.05	573	99	21.1	222	1985	2300	bd	bd	10.15	224
		8			709	737	684	23.69	0.12	0.04	576	140.2	20.6	217.5	2347	2492	bd	35	10.1	182

Salinity values were calculated by summing the concentration of the individual components. bd= below detection.

CHAPTER THREE

METHODS, PROCEDURES AND METHODS VALIDATION

S.No.	CONTENTS	PAGE
3.1	Quality Control and Method Validation of Analytical Methods	39
3.2	Description of Method Validation	40
	3.2.1 Reproducibility	40
	3.2.2 Calibration of Photometric Measurements	41
	3.2.3 Outlier Detection	41
	3.2.4 Check for Matrix Effects (Standard Addition)	42
	3.2.5 Method Detection Limit	43
	3.2.6 Comparison of Slopes and Intercepts of Calibration Lines	44
3.3	Procedures and Method Validation Results by Parameters	45
	3.3.1 Absorption Data	45
	3.3.2 Air Pressure, Air Temperature and Water temperature	49
	3.3.3 Alkalinity	50
	3.3.4 Ammonia	54
	3.3.5 Biochemical Oxygen Demand (BOD)	59
	3.3.6 Calcium	64
	3.3.7 Chemical Oxygen Demand (COD)	66
	3.3.8 Chloride	68
	3.3.9 Chlorophyll a and b	70
	3.3.10 Conductivity	72
	3.3.11 Dissolved Oxygen	74
	3.3.12 Hardness	75
	3.3.13 Nitrate	76
	3.3.14 Nitrite	83
	3.3.15 PH	86
	3.3.16 Phosphate	87
	3.3.17 Potassium	89
	3.3.18 River Discharge	91
	3.3.19 Silica	93
	3.3.20 Sodium	95
	3.3.21 Sulfate	96
	3.3.22 Sulphide	98
	3.3.23 Total Residue	99
	3.3.24 Total Volatile and fixed residue	100
	3.3.25 Turbidity	102
	3.3.26. Indicator Bacteria (Coliforms)	103
3.4	Summary of Water Quality Parameters Relative Standard Deviation and Method Detection Limit Attained in the Tests	109

S.NO.	LIST OF FIGURES	PAGE
Figure 3.1.1	Instruments used for sample filtration, weighing of reagents, distillation and reagent bottles	40
Figure 3.3.1.1	Spectrophotometer for Absorption Measurement	46
Fig. 3.3.1.2	95% confidence Limits of Absorption Measurement	48
Fig. 3.3.1.3	Linearity Fit of Absorption Measurement	48
Fig. 3.3.1.4	Linearity Fit of Absorption Measurement	49
Figure 3.3.3.1	Burette and magnetic Stirring Device Used for Titration	51
Fig. 3.3.3.2	95% Confidence Limits of Alkalinity Measurement of Samples	52
Fig. 3.3.3.3	Method Detection Limit Variation with Concentration for Alkalinity	53
Fig. 3.3.3.4	Method Detection Limit Used as Quality Control for Alkalinity	53
Fig. 3.3.4.1	Calibration Line with 95 % Confidence Limits for Ammonia Absorption	55
Fig. 3.3.4.2	Variation of Relative Standard deviation for Ammonia With Concentration	56
Fig. 3.3.4.3	Calibration Line for Ammonia At Different Times	59
Fig. 3.3.5.1	Incubator used for the BOD Determination	61
Fig. 3.3.5.2	Variation of Relative Standard Deviation with concentration for BOD	61
Fig. 3.3.5.3	Variation of Method detection Limit with Concentration for BOD	62
Fig. 3.3.6.1	Method Detection Limit for Calcium Determination	66
Fig. 3.3.7.1	COD Digestion Apparatus	67
Fig. 3.3.8.1	95% confidence Limits of Chloride Determination	70
Fig. 3.3.13.1	Water Bath used for Sample Digestion in the Determination of Nitrate	76
Fig. 3.3.13.2	Line of Best Fit for Nitrate Standards	78
Fig. 3.3.13.3	Line Fit Plot (Nitrate) for Standards containing Chamo Lake Sample	79
Fig. 3.3.13.4	Nitrate Calibration Performed at Different Times	81
Fig. 3.3.14.1	Best line of Fit for Nitrite Standards	84
Figure 3.3.15.1	pH Meter used for the pH Determination	86
Fig. 3.3.16.1	Variation of Relative Standard Deviation with Concentration for Phosphorous	88
Fig. 3.3.17.1	Flame Photometer Used for Potassium and Sodium Determination	90
Fig. 3.3.18.1	Stream Cross Section and Current Meter Positions	91
Fig. 3.3.19.1	Best Line of Fit for Silica Absorption of Standards (Spectrophotometric Determination with Methylene Blue at 650 nm)	94
Fig. 3.3.19.2	Variation of Relative Standard Deviation with Concentration for Silica	94
Fig. 3.3.21.1	Calibration Line for Sulfate Absorption Spectrophotometric at 425 nm	97
Figure 3.3.23.1	Drying Oven Used for the Total Solids Determination	100
Figure 3.3.24.1	Drying Furnace For Volatile Solids Determination	101

S.NO.	LIST OF FIGURES	PAGE
Figure 3.3.25.1	Turbidimeter used for the Determination of Turbidity	103
Figure 3.3.26.1	Incubator used for Coliform growth and Determination	106

S.NO.	LIST OF TABLES	PAGE
Table 3.2.5.1	Upper critical values of Student's t distribution with ν degrees of freedom	44
Table 3.3.1.1	Calculation of mean, SD, and RSD for Absorption Data	47
Table 3.3.1.2	Relative standard deviation and method detection limits for absorption measurements.	48
Table 3.3.4.1	Standard Solution Volumes added and Concentrations in Ammonia Determination	54
Table 3.3.4.2	Absorption Data for Ammonia Standard Solutions	55
Table 3.3.4.3	Calculation of Method Detection Limit for Ammonia Determination	57
Table 3.3.5.3.1	Statistics of the BOD Determination for Lake Chamo	63
Table 3.3.5.4.1	Outlier Test for BOD Test Data (Q-Test)	64
Table 3.3.5.4.2	Outlier (Test) for BOD Test Data (ASTM Method)	64
Table 3.3.7.1	COD TEST Result and Calculation	68
Table 3.3.9.1	Calculation of chlorophyll a values for Lakes Abaya and Chamo	72
Table 3.3.10.1	Conductivity Measurement of Standard Solutions	73
Table 3.3.13.1	Nitrate Absorption of Standards and calculation of MDL Values	77
Table 3.3.13.2	Nitrate Absorption using the Method of Standard Additions	78
Table 3.3.13.3	Coincidence of Lines Test for Nitrate Calibration Lines	79
Table 3.3.13.4	Comparison of calibration Lines for Nitrate made at Different Times	81
Table 3.3.13.5	Categorical Variables assigned for the four Calibration lines of Nitrate	82
Table 3.3.14.1	Data for Nitrite Absorption of Standards	83
Table 3.3.14.2	Determination of the Nitrite Content of Chamo Samples	85
Table 3.3.14.3	Determination of the Nitrite Content of Abaya Samples	85
Table 3.3.14.4	MDL calculation for Nitrite from Lake Chamo Low absorption Sample	85
Table 3.3.16.1	Absorption of Phosphate Standard Solutions and MDL Calculation	89
Table 3.3.17.1	Potassium Standard Solutions Volume Added and concentration	89
Table 3.3.19.1	Absorption Data for silica standards and MDL Calculation	93
Table 3.3.20.1	Sodium Standard Solutions – Volume added and concentrations.	95
Table 3.3.21.1	Sulphate Standard Solutions – Volume added and Concentrations	96
Table 3.3.21.2	Absorption Data for Sulphate Standards and RSD Values	97
Table 3.3.21.3	Method Detection Limit Calculation from Sulphate Standard Absorption data	98
Table 3.3.26.1	Preparation of Lauryl Tryptose Broth	105
Table 3.3.26.2	MPN Index For Serial Dilutions Of Sample	108
Table 3.4.1	Summary of Water Quality Parameters Relative Standard Deviation and Method Detection Limit Attained in the Tests	109

3.1 QUALITY CONTROL AND METHOD VALIDATION OF ANALYTICAL METHODS

The procedures for the majority of the parameters have been referred to from the standard Methods for the Examination of Water and Waste Water (19th edition, American Public Health Association, American Water Works Association and Water Environment Federation, Washington, D.C.) [18]. The determination of nitrite has been referred to from the German Standard Code (*DIN 38405 Teil 10: Deutsche Einheitsverfahren zur Wasser-, Abwasser- und Schlamm –Untersuchung, (Gruppe D, Anionen)*) [19]. For the photometric absorption measurement which is used for indirect assessment of suspended solids in water the reference literature used is: *Ausgewählte Methoden der Wasser Untersuchung. Bd. I. Jena: VEB Gustav Fischer Verlag 1976. pp 58-59* [20]. All chemicals and reagents used for the determinations are of analytical reagent grade type unless where they were specified to be different in the stated procedures. Laboratory distilled water has been used for blank and for dilution of reagents and rinsing purposes. The protocols stated in the procedures with respect to sampling, sample pretreatment and sample determinations have been followed in the determinations [21]. A minimum of three repetitions has been carried out for each sample measurement included in this report. The relative standard deviation for most measurements falls below 5%. Method detection limits where applicable were determined by running blank determinations using the same procedures as the sample procedure. The calculated values of method detection limits for each of the determination are provided in the table at the end of this chapter. Flame photometric and Spectrophotometric determinations were calibrated by running a minimum of six calibration standards where at least three solutions were prepared for each of the standards. Few determinations such as Nitrate required more than three standards repetitions. Standardization for titrants in titration measurements was carried out using primary reference standards. Turbidity and absorption measurements for water clarity assessment were carried out by single dilution for absorption measurements and multiple dilutions for turbidity measurements. The pH meter has been calibrated between each measurement by a laboratory prepared buffer. The stability of conductivity meter reading has been checked with the help of a standard 3M KCl solution. The analytical balance instrument has been calibrated with the standard weights supplied with the instrument.

**Analytical Balance****Reagent Bottles****Filtration Apparatus****Distillation Apparatus**

Figure 3.1.1 Instruments used for sample filtration, weighing of reagents, distillation and reagent bottles

3.2 DESCRIPTION OF METHOD VALIDATION

3.2.1 Reproducibility

The precision of analytical determination of samples and standards was determined by analyzing a minimum of three repetitions for each of the samples and standards in a set. The mean value is taken to be the average of these measurements after outliers have been removed. The standard deviation is likewise calculated from the same set of data. The relative standard deviation was calculated as the ratio of the standard deviation to mean values expressed in percentage [22].

3.2.2 Calibration of Photometric Measurements

Correlation of absorption intensity (in the case of spectrophotometric absorption measurements) or emission intensity (in the case of flame photometric determination) with the concentration of the analyte in the test forms the basis of quantitative evaluation. Measurements must be performed in the linear range where the response and analyte concentration are uniquely related, expressed by Beer's law. This is performed by preparing a set of standards for the analyte of increasing concentration in the range in which the absorption or emission is linearly correlated with the analyte concentration. The calibration equation is determined by regression of the line over these set of points plotted by analyte concentration versus absorption/emission. The analysis has been performed by the use of EXCEL 2000 spreadsheet.

3.2.3 Outlier Detection

Two tests have been employed for comparison of the sensitivity of the methods over the outliers. The first method called the Q-test is a simple statistical test to determine if a data point that appears to be very different from the rest of the data points in a set may be discarded. Only one data point in a set may be rejected using the Q-test. The Q-test is:

$$Q = \frac{|\text{Suspected Outlier} - \text{Closest Value}|}{|\text{Maximum Value} - \text{Minimum Value}|} \dots\dots\dots (3.1)$$

The value of Q is compared to a critical value, Q_c . If Q is larger than Q_c the outlier can be discarded with 90% confidence [22].

In the second method called the ASTM method, assuming that $x_1, x_2 \dots x_n$ constitutes a group of observations of a normally distributed sample, where $x_1 \leq x_2 \leq \dots \leq x_n$, and that the population standard deviation s is known (or the external information about s is available). In the ASTM Standard Practice for Dealing with Outlying Observation (E 178-94) an outlier rejection procedure is recommended for known s , whose null distribution has been deduced by Nair; the criterion is also called Nair's statistic. Let x_1 or x_n be the doubtful value. If the sample statistic

$$\begin{aligned}
 T_1 &= \frac{|\bar{X} - X_1|}{\sigma} > T_{1\infty} \\
 T_n &= \frac{|X_n - \bar{X}|}{\sigma} > T_{n\infty}
 \end{aligned}
 \tag{3.2}$$

Where

- T_1, T_n = sample statistics of x_1 and x_n , respectively,
- X_n, x_1 = maximum and minimum values of the observations, respectively,
- \bar{X} = Arithmetic average of all n values,
- σ = The population standard deviation, and
- $T_{1\infty}$ and $T_{n\infty}$ critical values for T_1 and T_n at the significance level α ,

Then x_1 or x_n can be justified as an outlier at the significance level α .

ASTM E – 178 outlier rejection generally recommends using a low significance level such as 1% and those significance levels greater than 5% should not be common practice.

The equation above can be rewritten as:

$$T_n = \frac{|X_m - \bar{X}|}{\sigma} > T(n, \alpha) \tag{3.3}$$

Where T_n is the sample statistic, X_m is the doubtful value (either X_1 or X_n) and $T(n, \alpha)$ is the critical value for T_n at the significance level α , either one sided or two sided.

An example of the outlier test results using both the Q-test and ASTM method is given in section 3.3.5.4 for the BOD determination.

3.2.4 Check for Matrix Effects (Standard Addition)

The term matrix refers to components other than the analyte. If the sample matrix is different from the matrix of the standard, the slope of the calibration curve (sensitivity) may change causing an error in the estimated concentration. The method of standard addition has been employed for the absorption measurements of lake samples in particular in order to check for the matrix effect, namely the effect of co-absorption by interfering substances or the effect of salinity on the intensity of absorption measurement. The method of standard additions consists of adding different amounts of standard to the same volume of the unknown and dilute to a fixed

volume. The x-intercept of the line measured from the y-axis gives the analyte concentration. Comparison of slopes from standard addition of samples and the one with only standards has been made. For example the statistical slope comparison test (described below) for nitrate showed that the slopes are different which suggests that standard addition techniques have to be employed for the determination of nitrate in the lake samples.

3.2.5 METHOD DETECTION LIMIT

(Remark: The following procedure taken from the EPA method is also related to the section 15 entitled "Schnellschätzung der Nachweisgrenze" of the DIN 32645 Nachweis, Erfassung and Bestimmungsgrenze) [23, 24].

The method detection limit is taken as the minimum concentration of a substance that can be measured and reported with 99% confidence that the analyte concentration is greater than zero and is determined from analysis of a sample in a given matrix containing the analyte [23].

The MDL is computed as the product of the standard deviation and the critical t-value:

$$\text{MDL} = t_{\nu, \alpha} \times S \dots \dots \dots (3.4)$$

For the blank method of determination from a series of N blank samples the standard deviation is determined from the formula

$$s^2 = \frac{1}{n-1} \left[\sum_{i=1}^N (X_i - \bar{X})^2 \right] \dots \dots \dots (3.5)$$

For the determination involving calibration line having a calibration equation $Y = a + bx$, the values of S is determined from

$$S = \frac{1}{b} * \sqrt{\frac{\sum_{i=1}^N (Y_{L,i} - \bar{Y}_L)^2}{N-1}} \dots \dots \dots (3.6)$$

Which is simply the standard deviation of the response Y for the N blank samples divided by the slope of the calibration line.

The critical t-value is looked up using reference tables such as the one shown in Table 3.2.5.1:

$$t_{\nu, \alpha} = (\text{Look up Value}) \dots \dots \dots (3.7)$$

Table 3.2.5.1: Upper critical values of Student's t distribution with ν degrees of freedom [23]

Degrees of Freedom	Probability of exceeding the critical value (α)					
	0.1	0.05	0.025	0.01	0.005	0.001
ν	0.1	0.05	0.025	0.01	0.005	0.001
1	3.078	6.314	12.706	31.821	63.657	318.313
2	1.886	2.920	4.303	6.965	9.925	22.327
3	1.638	2.353	3.182	4.541	5.841	10.215
4	1.533	2.132	2.776	3.747	4.604	7.173
5	1.476	2.015	2.571	3.365	4.032	5.893
6	1.440	1.943	2.447	3.143	3.707	5.208
7	1.415	1.895	2.365	2.998	3.499	4.782
8	1.397	1.860	2.306	2.896	3.355	4.499
9	1.383	1.833	2.262	2.821	3.250	4.296
10	1.372	1.812	2.228	2.764	3.169	4.143

3.2.6 Comparison of Slopes and Intercepts of Calibration Lines

To test for the “robustness” of the calibration procedures the slopes and intercepts determined at different times of test were compared by employing the statistical slope comparison procedure. Another situation where this test has been employed (as was mentioned above under matrix effects) was to see if the method of standard addition procedure gives results different from the normal procedure there by stating the need for accounting for matrix effects [22].

In order to statistically test if two lines are identical in terms of their slopes, a categorical variable Z was introduced identifying the samples source (Z = 1 for standards without sample and Z = 0 for standards with the sample). The general equation becomes:

$$Y_i = \beta_0 + \beta_1 * X_i + \beta_2 * Z_i + \beta_3 * X_i * Z_i + \epsilon_i, \dots \dots \dots (3.8)$$

Where Y is the absorption, X the concentrations and ε is the residual. The test for coincidence is accepted if β₂ = β₃ = 0. The test for equality of slopes is accepted if β₃ alone is zero. The test can easily be extended to more than two lines. For example to compare the slopes and intercepts of four lines (as was done for nitrate determination) the general equation becomes:

$$Y_i = \beta_0 + \beta_1 * X_i + \beta_2 * Z_{1i} + \beta_3 * Z_{2i} + \beta_4 * Z_{3i} + \beta_5 * Z_{1i} * X_i + \beta_6 * Z_{2i} * X_i + \beta_7 * Z_{3i} * X_i + \epsilon_i$$

Using the lines designated in the graphs above, the equation for each line in terms of X and the categorical variable Z (either 0 or 1 substituted accordingly) becomes:

Line 1: $Y = \beta_0 + (\beta_1 + \beta_5) X + \beta_2$

Line 2: $Y = \beta_0 + (\beta_1 + \beta_6) X + \beta_3$

Line 3: $Y = \beta_0 + (\beta_1 + \beta_7) X + \beta_4$

Line 4: $Y = \beta_0 + (\beta_1) X$

3.3 PROCEDURES AND METHOD VALIDATION RESULTS BY PARAMETERS

The detail of method procedures, standard calibration, precision and method detection limit calculations are given below for each parameters analyzed.

3.3.1 Absorption Data

(Reference: Ausgewählte Methoden der Wasser Untersuchung. Bd. I. Jena: VEB Gustav Fischer Verlag 1976. pp 58-59)

The absorption of sample was measured against blank (distilled water) in a spectrophotometer. The difference in absorption between unfiltered and filtered

samples gives a measure of the suspended solids and turbidity of the water. A wavelength range of 400 – 700 nm was used for measurement, the 500 nm being selected as the regular point of measurement for repeated samples taken from the rivers and lakes.

The sample in the sampling bottling was vigorously shaken to ensure that a homogenous suspension was transferred to the Erlenmeyer flasks for further stirring and homogenisation. For better accuracy of measurement, the spectrophotometric absorption readings should lie in the range 0 – 1. If the sample absorption reading happened to be greater than 1, dilution of the sample with distilled water was carried out. Commonly a dilution giving 5% and 10% sample concentration was prepared by pipetting respectively 5 and 10 mL volumes of the sample in to a 100 mL volumetric flask diluting this sample up to the mark with filtered portion of the same sample. The filtered portion should contain no turbidity or suspended solids. The sample from the sampling bottle or a dilution of it (as outlined in step 2 above) was transferred to 250 mL Erlenmeyer flasks and the sample stirred further with magnetic stirrer to provide a homogenous sample. The samples were then transferred to cuvettes and the spectrophotometer absorption reading of the sample was taken immediately at a wavelength of 500 nm. Likewise a portion of the sample was filtered with Glass fibre filter and its absorption reading noted at the same wavelength of 500 nm. The spectrophotometric absorption of the sample solids is taken as the difference between the unfiltered and filtered sample absorption readings. A typical calculation of absorption mean, standard deviation and relative standard deviation is given in table 3.3.1.1



Figure 3.3.1.1 Spectrophotometer for Absorption Measurement

Table 3.3.1.1 Calculation of mean, SD, and RSD for Absorption Data

Date	Sample	Dilution	Absorption values				Mean Abs	Standard Deviation (Abs)	Relative Standard Deviation
			Sample 1 (Abs)	Sample 2 (Abs)	Sample 3 (Abs)	Sample 4 (Abs)			
17-Jun-03	Hare	10	0.038	0.044	0.042	0.044	0.42*	0.00	0.67%
17-Jun-03	Kulfo	20	0.443	0.450	0.441	0.441	8.875*	0.00	0.05%
21-Jul-03	Sile	10	0.138	0.135	0.14	0.138	1.377*	0.00	0.15%
17-Jun-03	Abaya	1	0.162	0.161	0.161	0.161	0.162*	0.00	0.31%
17-Jun-03	Chamo	1	0.377	0.378	0.375	0.368	0.374*	0.00	1.20%

*The mean absorption values stated in this column have been multiplied by the dilution factor (3rd column) since the samples have been diluted to enable measurement in the linear ranges.

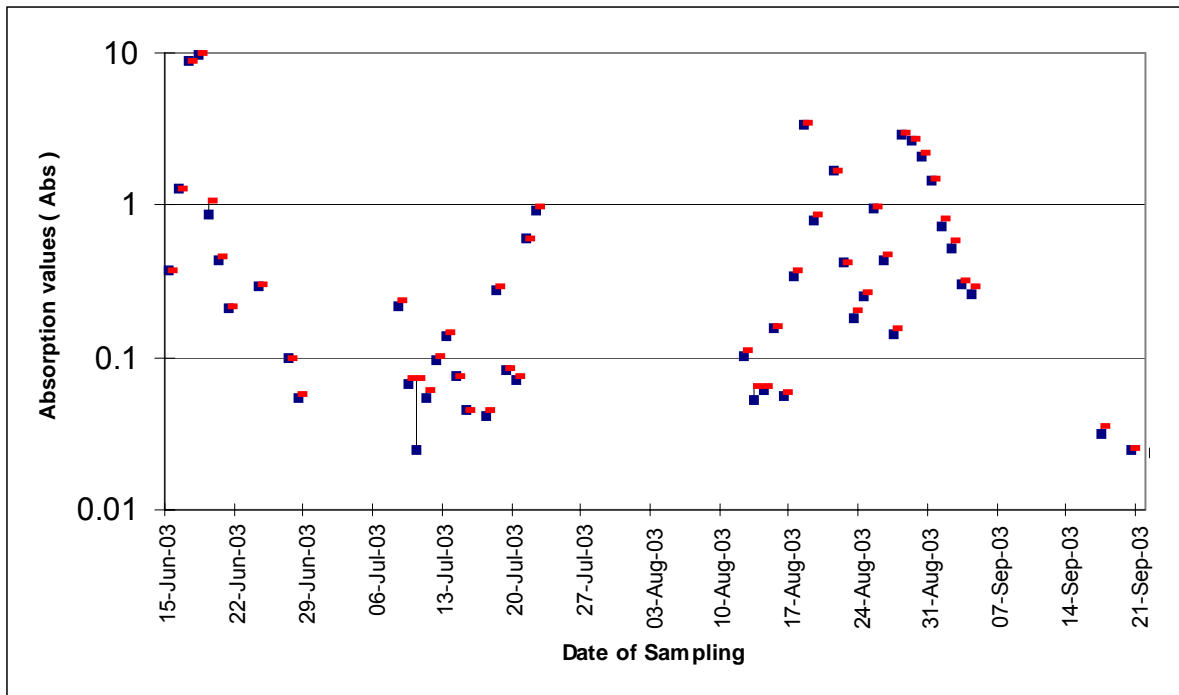


Fig. 3.3.1.2 Absorption measurement. The top and bottom bars indicate the 95% Confidence Limits of Absorption Measurement while the thin vertical bar Indicates the separation of the confidence limits. Since the standard deviation is low the upper and lower 95% confidence intervals show very close to each other.

The average relative standard deviation is 2.2% with 95% of the samples analysed having less than 5% relative standard deviations (Figure 3.3.1.2). The method detection limit – worked out for samples containing low absorption values is 0.005. The calculated values of the mean, standard deviation and method detection limits for some of the samples is given in table 3.3.1.2

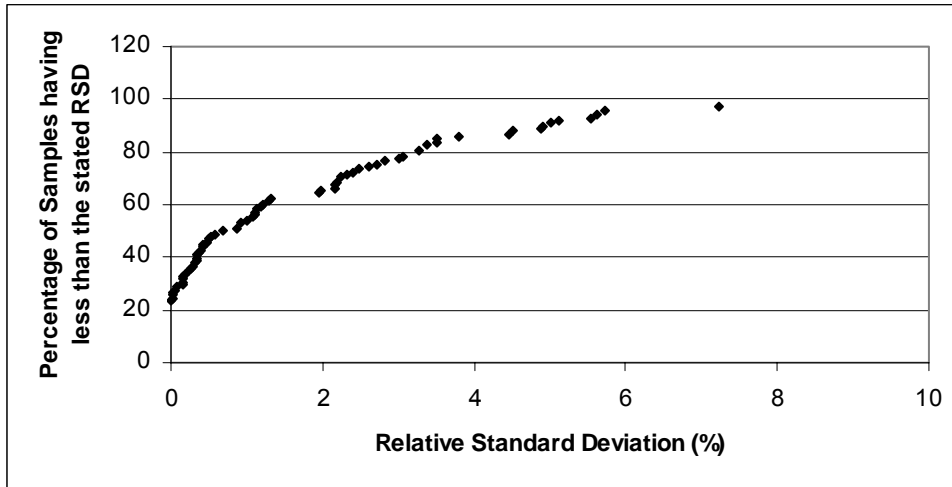


Figure 3.3.1.3 Variation percentage of relative standard deviation with the cumulative number of samples analysed. Over 95% of the samples analysed have RSD value less than 6% showing the good precision of this procedure.

Table 3.3.1.2 Relative standard deviation and method detection limits for absorption measurements.

Sample	Dilution	Absorption	Absorption	Absorption	Absorption	Mean	Stddev	Rlstdev	Student t	MDL (mg/L)
Hare	1	0.252	0.214	0.193	0.184	0.21075	0.0302	14.35%	3.747	0.113
Kulfo	1	0.375	0.38	0.371	0.369	0.37375	0.0049	1.30%	3.747	0.018
Hare	10	0.058	0.062	0.061	0.06	0.6025	0.0017	0.28%	3.747	0.006
Kulfo	20	0.065	0.064	0.064	0.064	1.285	0.0005	0.04%	3.747	0.002
Hare	10	0.038	0.044	0.042	0.044	0.42	0.0028	0.67%	3.747	0.011
Kulfo	20	0.443	0.45	0.441	0.441	8.875	0.0043	0.05%	3.747	0.016
Abaya	1	0.162	0.161	0.161	0.161	0.16125	0.0005	0.31%	3.747	0.002
Chamo	1	0.377	0.378	0.375	0.368	0.3745	0.0045	1.20%	3.747	0.017
Hare	10	0.05	0.049	0.052	0.05	0.5025	0.0013	0.25%	3.747	0.005
Kulfo	20	0.491	0.493	0.495	0.495	9.87	0.0019	0.02%	3.747	0.007
Hare	10	0.076	0.077	0.076	0.074	0.7575	0.0013	0.17%	3.747	0.005
Kulfo	20	0.051	0.05	0.051	0.041	0.965	0.0049	0.50%	3.747	0.018
Kulfo	10	0.044	0.044	0.046	0.046	0.45	0.0012	0.26%	3.747	0.004
Hare	1	0.09	0.09	0.088	0.089	0.08925	0.0010	1.07%	3.747	0.004
Kulfo	1	0.216	0.215	0.216	0.212	0.21475	0.0019	0.88%	3.747	0.007
Hare	10	0.055	0.056	0.057	0.0575	0.56375	0.0011	0.20%	3.747	0.004
Kulfo	1	0.31	0.295	0.298	0.296	0.29975	0.0069	2.32%	3.747	0.026
Hare	10	0.065	0.07	0.07	0.07	0.6875	0.0025	0.36%	3.747	0.009

3.3.1.1. Linearity of Absorption Measurement:

Since the error of measurement increases at high absorption values such as when the sample contains high suspended solids, dilution is necessary to bring the sample

to low absorption ranges for measurement. Unlike turbidity measurements, spectrophotometric absorption measurement displays linearity over a wide range of absorption values. Fig. 3.3.1.2 was obtained by measuring absorption at various levels of dilution of high absorption sample.

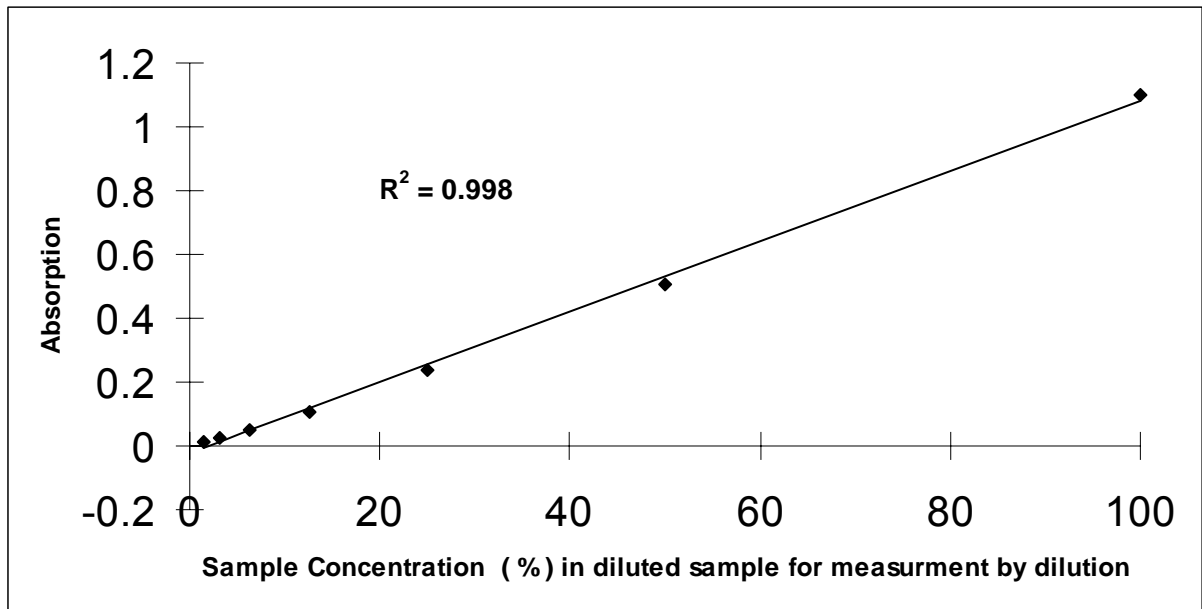


Fig. 3.3.1.4 Linearity Fit of Absorption Measurement. The sample concentration (%) is the percentage by volume of sample present in sample volume diluted with distilled water. The graph shows that the response of absorption with respect to different levels of dilution is linear. This is in contrast to turbidity measurement where the response is non-linear at high sample concentration (Turbidity exceeding 100 NTU).

Absorption measurements hence display linearity over a wider range of sample dilution, which makes calculation of absorption easy obtained by multiplication of the diluted absorption readings by the dilution factors.

3.3.2 AIR PRESSURE, AIR TEMPERATURE AND WATER TEMPERATURE

These parameters were measured on site with Field-testing equipment. Air pressure was measured with a barometer calibrated to the nearest 1 millibar. Air and water temperatures were measured with digital thermometers whose readings are periodically checked against manual mercury thermometer.

3.3.3 ALKALINITY

(Reference Eaton, A.D., L.S. Clesceri and A.E. Greenberg (1995) Standard Methods for the Examination of Water and Wastewater, 19th edition, American Public health Association, American Water Works Association and Water Environment Federation, Washington, D.C.)

The alkalinities of the samples were determined by titration with 0.1N and 0.02 N HCl solutions. The phenolphthalein alkalinity was determined with the help of phenolphthalein indicator. The total alkalinity end point was determined with the addition of a mixture solution of bromcresol green and methyl red indicators. 40 mL of the 0.05 N Sodium carbonate solution was mixed with 60 mL water in a 300 mL Erlenmeyer flask. A drop (0.05 mL) of the mixed indicator was added and this sample was titrated with the 0.1N HCl. Three titrations were repeated and titration was done up to the first perceptible color change. The Normality of the HCl acid titrant was determined with the following formula:

$$\text{Normality of HCl} = \frac{A(\text{g}) * B(\text{mL})}{53.00(\text{g mol}^{-1} \text{L}) * C(\text{mL})} \dots\dots\dots (3.9)$$

The factor 53 is the equivalent weight of Sodium Carbonate in g per (mol per L). A = gm of Na₂CO₃ weighed in 1 liter of flask. B = mL of Na₂CO₃ Solution taken for titration. C = mL of HCl acid used for titration (Average of the three valid repetitions). For all the samples tested 10 - 100 mL of sample was taken in to a 300 mL Erlenmeyer flask and first a drop of the phenolphthalein solution was added. If the solution appeared colorless there is no carbonate alkalinity. If the solution turned pink, there was carbonate alkalinity and the sample was titrated until the color changed from pink to colorless. The reading was recorded. Next the colorless solution was treated with a drop of the mixed Bromcresol green – Methyl Red indicator and titrated to a color change from green to approximately light pink gray (pH 4.8). The reading was recorded.

The Total, alkalinity was calculated from the following formulas:

$$\text{Total Alkalinity (as CaCO}_3) = \frac{A(\text{mL}) * N(\text{mol.L}^{-1}) * (50000 \text{ mg mol}^{-1})}{\text{mL of Sample}} \dots\dots\dots (3.10)$$

The factor 50000 is the equivalent weight of CaCO_3 in mg mol^{-1} . A = the total mL of HCl acid used in titration up to the mixed indicator color change end point. N = The Normality of HCl acid as calculated in step 2 above (mol L^{-1}). The mean, standard deviation, relative standard deviation and confidence limit for the mean were determined from the statistical data generated with five independent repetitions per sample of the above test procedure.

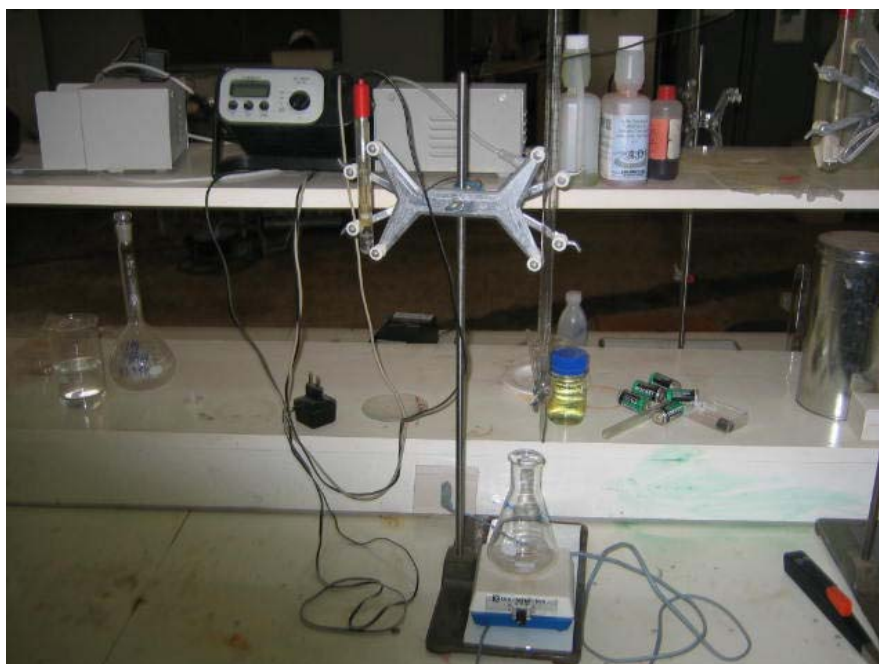


Figure 3.3.3.1 Burette and magnetic Stirring Device Used for Titration

3.3.4.4. Precision of Alkalinity Measurement

The range of relative standard deviation obtained with alkalinity determination is 0 - 11.4 %. The mean relative standard deviation is 4.3% with the 95% confidence limit as 10%. The precision depends on the pH range and the amount of alkalinity present. Blank samples have low precision with RSD values around 10%.

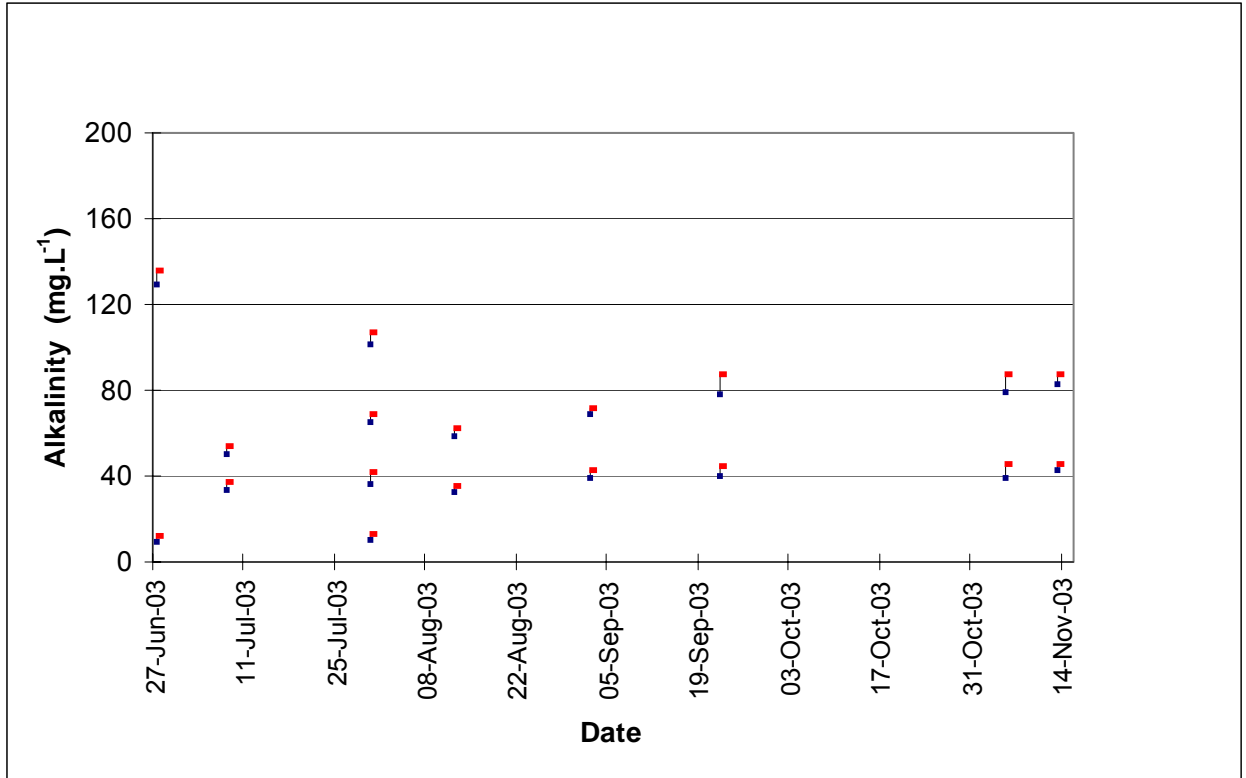


Fig. 3.3.3.2 95% Confidence Limits of Alkalinity Measurement of Samples. The top and bottom bars indicate the 95% confidence Limits of Alkalinity Measurement while the thin vertical bar indicates the separation of the confidence limits. Some of the samples show large confidence intervals (up to 10%).

The 95% confidence limits of measurement for some of the measurements are displayed in Fig. 3.3.3.1 above for comparison with the magnitude of alkalinity measurements.

3.3.4.4. Method Detection Limit (Alkalinity)

The alkalinity has a linear response for method detection limit in the pH range 6.9 to 8.5, i.e. the MDL increases with increasing pH within this range. The regression line is produced from the following data from samples having pH within this range (i.e. blank distilled water, river Hare, Kulfo and River Sile).

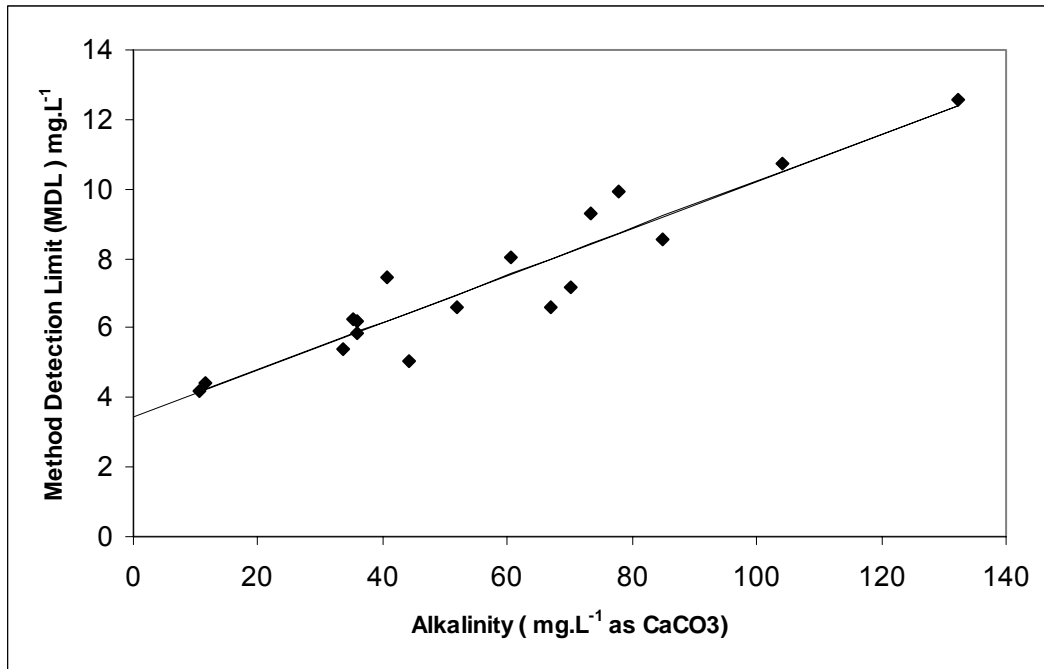


Fig. 3.3.3.3 Method Detection Limit Variation with Concentration for Alkalinity. The value of $S^*t(\nu, \alpha)$ was plotted for samples containing different values of alkalinity. The points plot on straight line. The y-intercept of this line can be taken as the method detection limit.

The calculated method detection limit at 99% confidence limit is about 3.54 mg L^{-1} which is the intercept of the line above on the y-axis. This line can be used as a quality control check where excessive deviation from this line can be considered as an outlier as Fig. 3.3.3.3 shows.

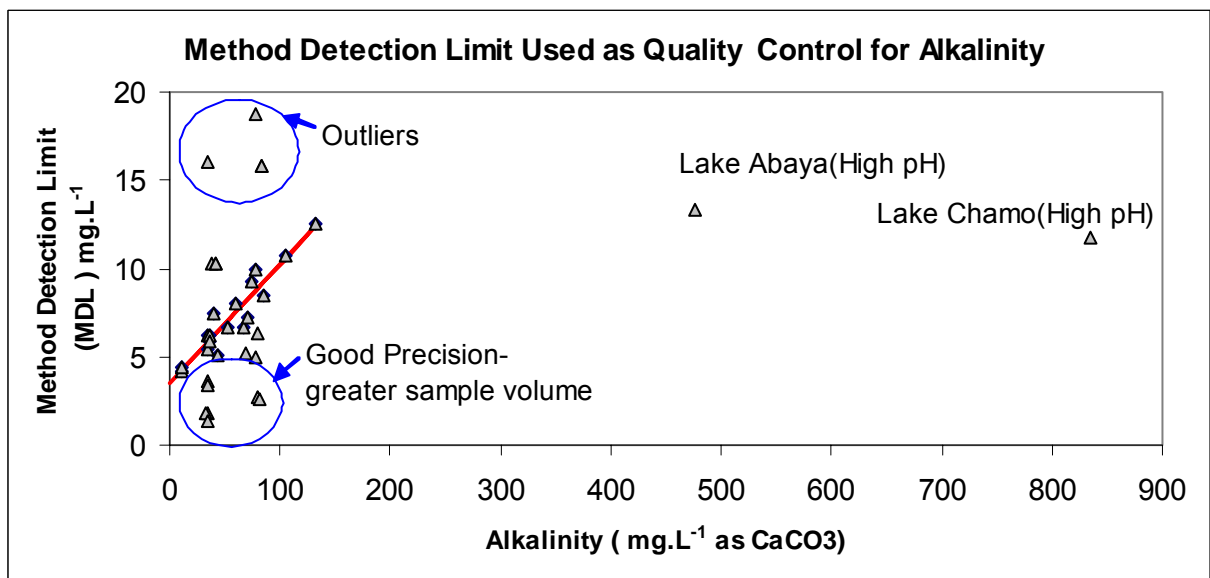


Fig. 3.3.3.4 Method Detection Limit Used as Quality Control for Alkalinity. Points to the right of the red line are of acceptable precision. The points to the right nearer the red line were obtained by increased sample volume. Those further to the right were for lakes Abaya and Chamo, samples which are at pH values of above 9.0. The points on the left above the red

line are possibly outliers as they possess greater standard deviation than those of the majority of samples falling along the red line.

3.3.4 AMMONIA

(Reference Eaton, A.D., L.S. Clesceri and A.E. Greenberg (1995) *Standard Methods for the Examination of Water and Wastewater*, 19th edition, American Public health Association, American Water Works Association and Water Environment Federation, Washington, D.C.)

Ammonia was determined Spectrophotometrically with Nessler's Reagent at a wavelength of 425 nm. The following standard solutions were prepared from the standard ammonium solution. Three solutions were prepared for each standard (See Table 3.3.4.1 below).

Table 3.3.4.1 Standard Solution Volumes added and Concentrations in Ammonia Determination

Standard Label	1	2	3	4	5	6	7
mL of Standard added in a 50 mL Volumetric Flask	0	5	10	20	25	35	40
mg L ⁻¹ of N – Ammonia	0	1	2	4	5	7	8

One drop of EDTA Stabilizer reagent was added to each of the standards and the solutions were mixed well. 2 mL of Nessler Reagent was added. The 50 mL flasks were then each filled up to the mark with water and mixed by inverting the flasks several times. A period of 30 minutes was allowed, as the ammonia concentration in the samples was low. There after the standards absorption was measured with the 6100 Jenway Spectrophotometer at 425 nm wavelength. Between 20 and 40 mL of the sample was pipetted in to a 50 mL flask and treated with reagents in the same way as the standards. The absorption was measured afterwards. A minimum of three independent solutions was prepared for each sample tested.

3.3.4.4. Calibration plot of the standards.

Table 3.3.4.2 shows the absorption of ammonia standards used for the determination. Three repetitions were done at each standard. The calibration plot shown in Figure 3.3.4.1 below was done using the EXCEL regression program.

Table 3.3.4.2 Absorption Data for Ammonia Standard Solutions

Standard Label	St0	St1	St2	St3	St4	St5	St6
mg L ⁻¹ of Ammonia Nitrogen	0	1	2	4	5	7	8
Absorption1	-0.011	0.168	0.180	0.644	0.761	0.906	1.133
Absorption2	-0.015	0.095	0.291	0.637	0.651	1.062	1.171
Absorption3	-0.011	0.131	0.316	0.607	0.715	1.033	1.120
Mean Absorption	-0.012	0.131	0.304	0.629	0.709	1.048	1.141
Standard Deviation	0.0023	0.0365	0.0724	0.0197	0.0552	0.0830	0.0265
Relative Standard Deviation	18%	27%	23%	3%	7%	7%	2%

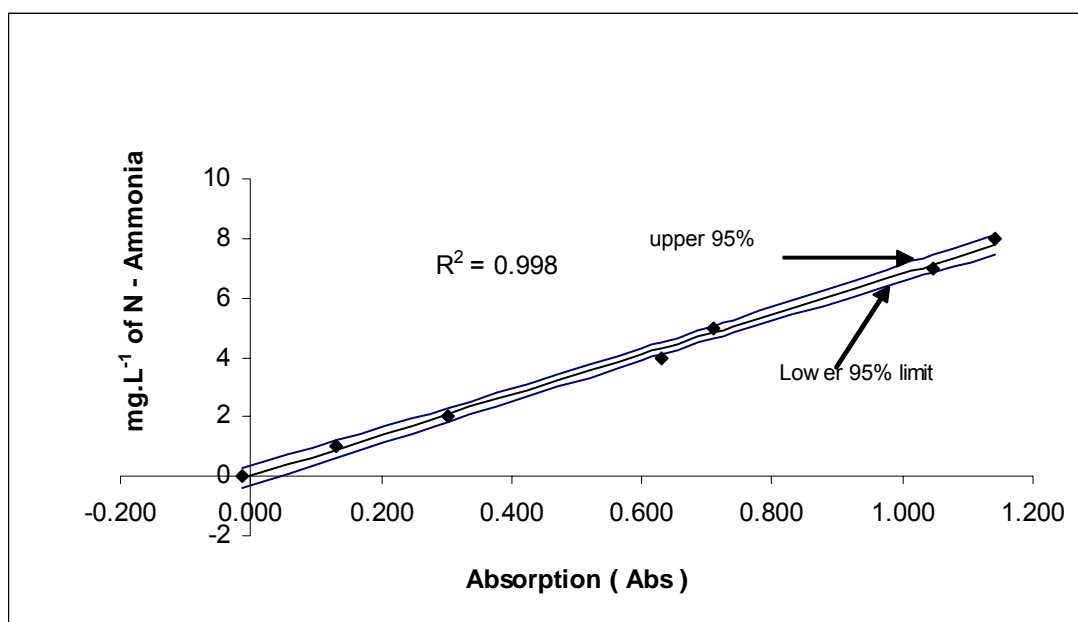


Fig. 3.3.4.1 Calibration Line with 95 % Confidence Limits for Ammonia Absorption. The middle line indicates the mean absorption. The upper and lower lines are for the 95% confidence limits.

3.3.4.2 Linearity of Measurement

The ammonia absorption maintains linearity up to about 10 mg L⁻¹ measured as Nitrogen (N). Therefore, the sample volume shall be adjusted to give measured ammonia in this range.

3.3.4.4. Precision of Ammonia Determination

Spectrophotometric absorption measurements have characteristically decreasing Standard deviation with increasing concentration (or absorption). The instrument has less sensitivity at low absorption values. Figure 3.3.4.2 shows the variation of relative standard deviation with sample ammonia concentration. As it can be seen for samples with low ammonia values greater number of repetition is necessary to arrive at statistically acceptable values [25].

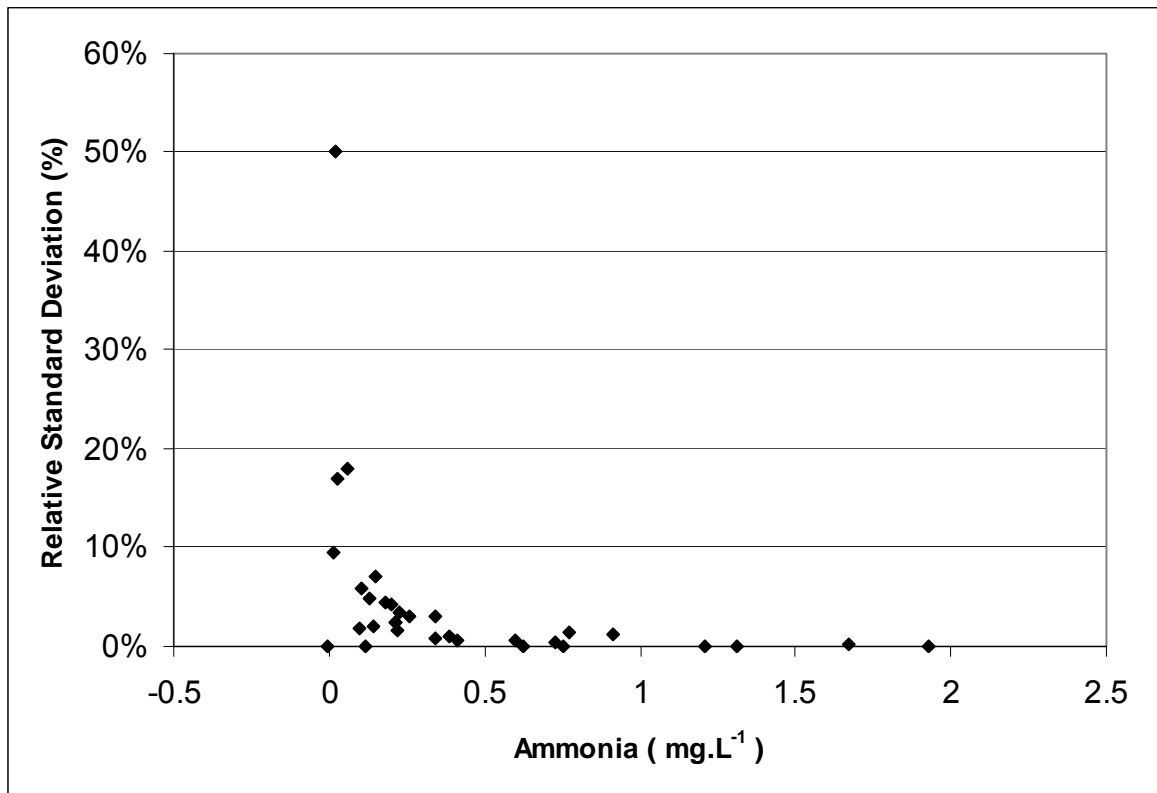


Fig. 3.3.4.2 Variation of Relative Standard deviation for Ammonia with Concentration. The RSD valued increases when the sample contains low ammonia. Greater number of samples would be necessary to achieve better precision at low ammonia values.

Analysis of the relative standard deviation shows that the mean RSD value is 2.1 % and the 95% cutoff limit is around 6%. Samples should therefore be determined with a maximum of 6% relative standard deviation within the range of ammonia values similar to the ones determined in this research. To explain this further, 95% of the samples analyzed have a relative standard deviation of 6% and below. On the other hand the mean of the samples RSD is 2.1 %. The 95% confidence limit of 6% can, therefore, be used as quality control. Figure 3.3.4.3 graphically illustrates this point.

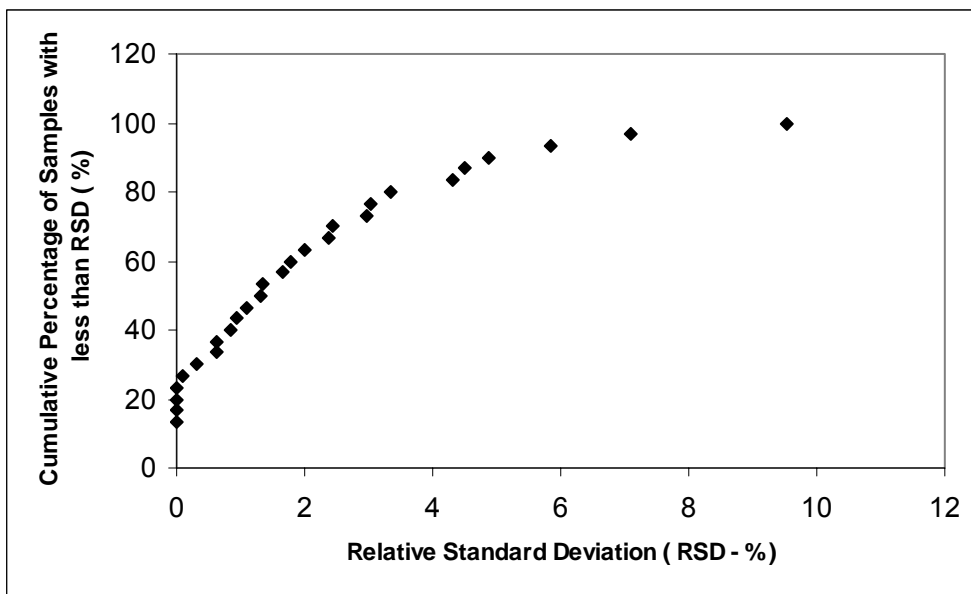


Figure 3.3.4.3 Cumulative Percentage Graph for Relative Standard Deviation – Ammonia. 95% of the samples analyzed have RSD values of 6% and below. Such curve can be used as quality control for the precision of the determination of ammonia in future samples.

3.3.4.4. Method Detection Limit of Ammonia determination

The absorption, standard deviation and the student t value for the given number of samples have been used to calculate the MDL value at various concentrations. Table 3.3.4.3 shows this calculation. The concentrations are worked out using the regression equation: **Absorption (Abs) = Concentration (mg L⁻¹) * 0.146 – 0.00033**

$$\text{Ammonia(N - NH}_3 \text{ mg/L)} = \frac{50 \text{ mL}}{\text{mL added}} \left(\frac{\text{Absorption(Abs)} + 0.00033}{0.146369} \right) \dots\dots\dots (3.11)$$

Table 3.3.4.3 Calculation of Method Detection Limit for Ammonia Determination. The MDL value is determined as S*t where S is the standard deviation of the blank absorption divided by the slope of the calibration line and t is the critical value of the student’s distribution determined from Table 3.2.5.1

Concentration (mg L ⁻¹)	Mean Absorption (Abs)	Standard Deviation	Student t	MDL (mg L ⁻¹)
0	- 0.012	0.002	4.541	(0.002/0.146)*4.541 = 0.062
1	0.131	0.036	4.541	
2	0.303	0.072	4.541	
4	0.629	0.0196	4.541	

Concentration (mg L ⁻¹)	Mean Absorption (Abs)	Standard Deviation	Student t	MDL (mg L ⁻¹)
5	0.709	0.055	4.541	
7	1.047	0.082	4.541	
8	1.141	0.026	4.541	

The method detection limit of ammonia determination is set at 0.062 mg L⁻¹.

3.3.4.5 Check of the Matrix Effects of the Lake Water Quality by Standard Addition Methods

In order to study the effect of the lakes water quality on the absorption of ammonia a method of standard addition was employed where by the standards were prepared in 50 mL volumetric flasks containing 40 mL of the Chamo lake sample. The slope of the line determined from the standard addition method is the same as the line determined above without standard addition. The matrix effect is minimum and the procedure can be followed without standard additions. Since the standard addition involves extrapolation to the x-axis (instead of interpolation), greater number of samples are required for precision which increases the time and cost of measurement.

3.3.4.6 Robustness of Calibration Measurement for Ammonia

The calibration line for ammonia differs from time to time as Fig. 3.3.4.3 shows. The lines refer to calibration done using two different photometers and for each photometer measurements were taken at different times. The lines for photometer 1 differ substantially while for photometer2 there is a measurable difference. Measurements have to be done with fresh standards for ammonia determination.

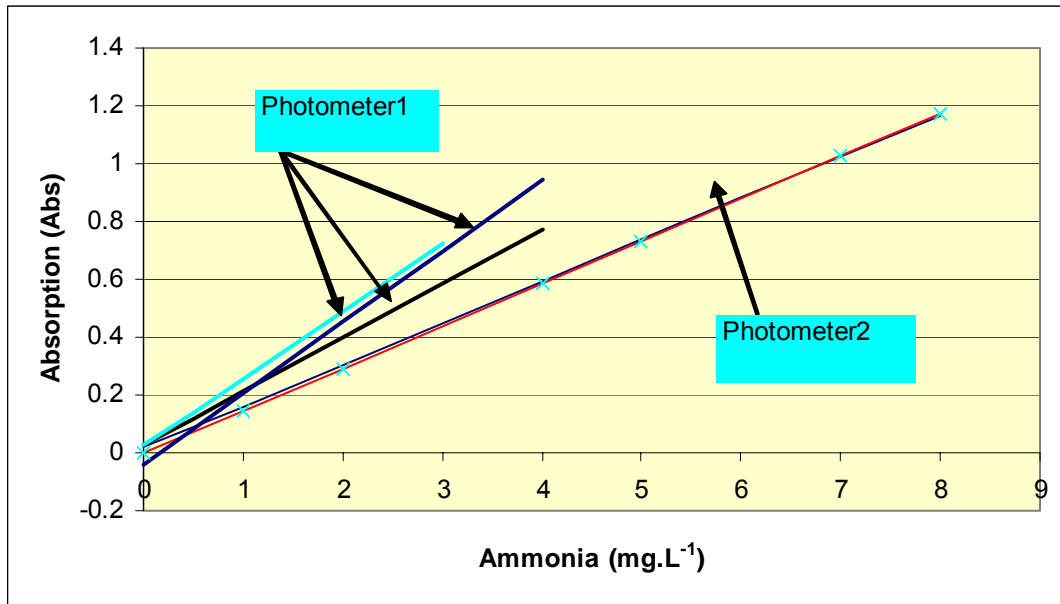


Fig. 3.3.4.3 Calibration Line for Ammonia at Different Times with different photometers. The molar absorptivity which is measured by the slope of the line is variable and should always be determined precisely at the time of the sample determination and using the same photometer as the one used for the sample determination.

For routine field monitoring where standards are taken few from the lab, the variation of the calibration line with time and temperature of monitoring needs to be observed.

3.3.5 BIOCHEMICAL OXYGEN DEMAND (BOD)

(With Winkler's Method for Dissolved Oxygen Determination)

(Reference Eaton, A.D., L.S. Clesceri and A.E. Greenberg (1995) *Standard Methods for the Examination of Water and Wastewater*, 19th edition, American Public Health Association, American Water Works Association and Water Environment Federation, Washington, D.C.)

The method employed consists of filling with sample, to overflowing, an airtight bottle of the specified size and incubating it at the specified temperature for 5 d. Dissolved oxygen was measured initially and after incubation, and the BOD was computed from the difference between initial and final DO. Because the initial DO is determined shortly after the dilution is made, all oxygen uptakes occurring after this measurement is included in the BOD measurement. **A. Preparation of dilution water:** In a 5 Liter plastic container 1 mL each of phosphate buffer, MgSO₄, CaCl₂, and FeCl₃ solutions.L⁻¹ of water were added. Seeding was found to be unnecessary based on prior study of BOD consumption with seeding and without seeding. The dilution water was saturated with DO by aerating with organic-free filtered air. **B) Glucose-Glutamic acid check:** The dilution water quality, seed effectiveness, and analytical technique were checked by making BOD measurements on a mixture of

150 mg glucose.L⁻¹ and 150 mg glutamic acid.L⁻¹. Glucose has an exceptionally high and variable oxidation rate but when it is used with glutamic acid, the oxidation rate is stabilized and is similar to that obtained with many municipal wastes. C) Sample pretreatment: The pH of all samples before testing were checked samples from lakes Abaya and Chamo needed adjustment to pH 7-7.5 with 1N HCl solution. Nitrification inhibition— 3 mg 2-chloro-6- (trichloro methyl) pyridine (TCMP) to each 300-mL bottle were added before capping. D) Dilution technique: The AWTI waste water sample necessitated dilution. Dilution was made so that at least dissolved oxygen of 1 mg L⁻¹ remains after 5 days incubation. Dilutions were prepared directly in BOD bottles—using a wide-tip volumetric pipette, the desired sample volume was added to individual 300 mL BOD bottles of known capacity. The Fill bottles were filled with enough dilution water, so that insertion of stopper will displace all air, leaving no bubbles. Since the titrimetric iodometric methods were used for DO measurement, two bottles were prepared at each dilution. Determine initial DO was determined on one bottle. The other bottle was stoppered tightly, water-sealed, and incubated for 5 d at 20°C. The dissolved oxygen was determined using the azide modification of the iodometric method e). Dilution water blank: Dilution water blank was used as a rough check on quality of unseeded dilution water and cleanliness of incubation bottles. F) Incubation: The bottles were incubated at 20°C ± 1°C G) Determination of final DO: After 5 d incubation DO was determined in sample dilutions and blanks,

Calculation:

For each test bottle meeting the 2.0- mg L⁻¹ minimums DO depletion and the 1.0- mg L⁻¹ residual DO, The BOD was calculated as follows:

$$\text{BOD (mg L}^{-1}\text{)} = \frac{(D_1 - D_2)(\text{mg L}^{-1}) - (B_1 - B_2)(\text{mg L}^{-1}) * f}{P} \dots\dots\dots (3.12)$$

Where D1 = DO of diluted sample immediately after preparation, mg L⁻¹, D2 = DO of diluted sample after 5 d incubation at 20°C, mg L⁻¹, P = decimal volumetric fraction of sample used, B1 = DO of seed control before incubation, mg L⁻¹, B2 = DO of seed control after incubation mg L⁻¹, and f = ratio of seed in diluted sample to seed in seed control = (% seed in diluted sample)/(% seed in seed control). If seed material is added directly to sample or to seed control bottles: f = (volume of seed in diluted sample)/ (volume of seed in seed control)



Figure 3.3.5.1 Incubator used for the BOD Determination

3.3.5.1 Precision of BOD Measurement

The BOD measurement shows considerable scatter and is less reproducible particularly at low BOD values. Fig. 3.3.5.1 shows such a scatter.

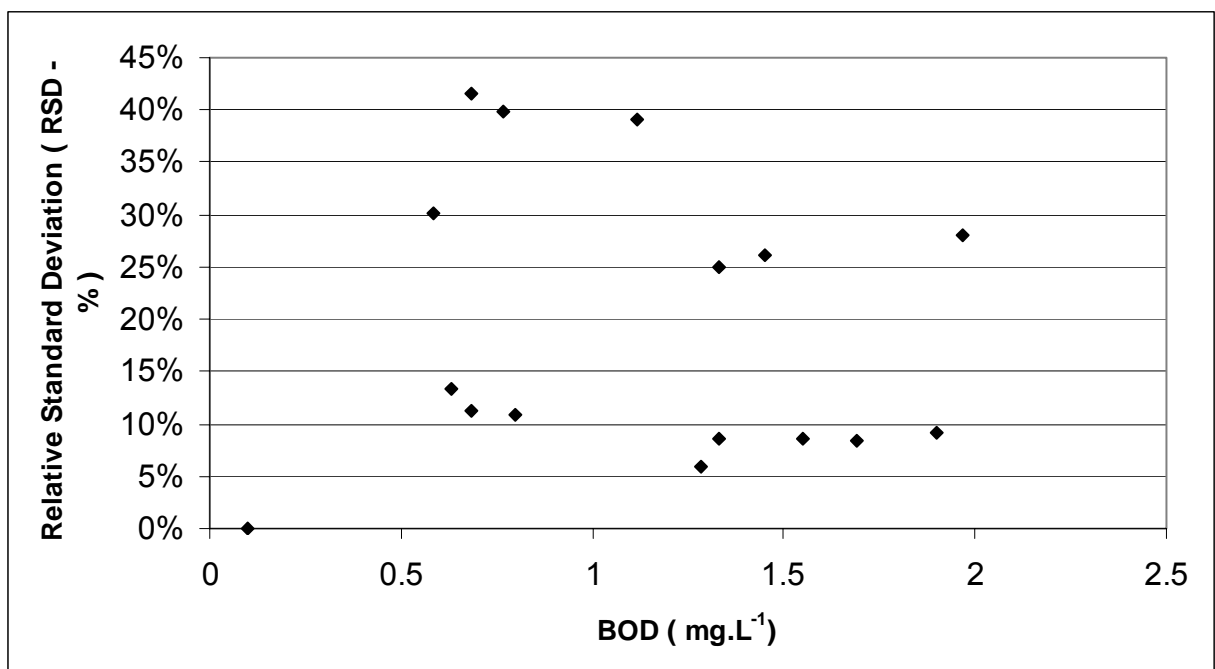


Fig. 3.3.5.2 Variation of Relative Standard Deviation with concentration BOD. The scatter points show higher standard deviation at lower concentrations of BOD. The BOD is not a reliable parameter at the small ranges of values expected for the lake and river waters analyzed.

The mean relative standard deviation is 20 % while the 95% limit is about 38%. If at least 20% precision is required from the BOD determinations, samples having BOD greater than 1.5 mg L⁻¹ may have to be rejected according to figure 3.3.5.1.

3.3.5.2 Method Detection Limit for BOD Determination

The scatter of method detection limit for BOD is given figure 3.3.5.2. The low values of BOD can be used to determine the method detection limit, which stands around 0.7 mg L⁻¹ of dissolved Oxygen.

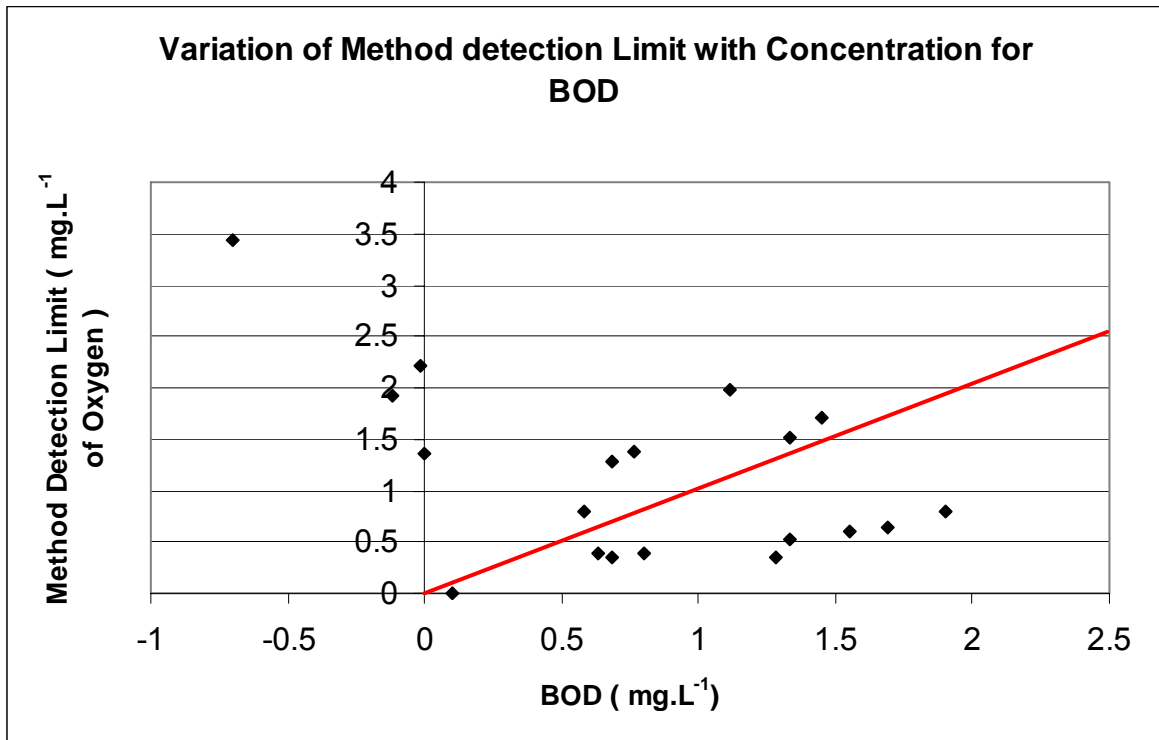


Fig. 3.3.5.3 Variation of Method detection Limit with Concentration for BOD. The method detection limit was calculated as $S \cdot t$ where S is the standard deviation of the blank sample and t is the critical value of the students distribution. The red line indicates the determined BOD value as being equal to the MDL calculated. Samples with BOD less than 1.5 mg L⁻¹ can be considered below detection limit.

The average value for the method detection limit is 0.68 mg L⁻¹ while the 95% limit is 1.3 mg L⁻¹ of dissolve oxygen. This value is close to the relative standard deviation of less than 20%, i.e. 1.5 mg L⁻¹ BOD minimum consumption required for analytical precision.

3.3.5.3 Effect of Increased Number of Samples on BOD Determination Precision

Six samples were taken for analysis of BOD for Lake Chamo samples. The results of BOD determination are summarized in table 3.3.5.3.1. It is clear that the relative standard deviation is not much different from the mean value obtained for earlier measurements using three repetitions only.

Table 3.3.5.3.1 Statistics of the BOD Determination for Lake Chamo. By taking six samples the relative standard deviation that could be attained was only 25%. Therefore, increasing the number of samples has low impact on the precision of the BOD determination

Sample	S1	S2	S3	S4	S5	S6
Initial DO	3.3	3.3	3.3	3.3	3.3	3.3
Dilution	300/300	300/300	300/300	300/300	300/300	300/300
Final DO	2	1.3	2.2	1.7	2.05	2.15
BOD (mg L ⁻¹)	1.3	2	1.1	1.6	1.25	1.15
Average BOD = 1.4 mg L ⁻¹						
Standard Deviation = 0.342	95% confidence Limit = [1.5 - 1.29]					
Relative Standard Deviation = 24.43 %						

3.3.5.4 OUTLIER TEST FOR BOD

The data were examined for outliers, as it appears on surface that the higher values, i.e. 1.6 and 2 look to be an outlier. Two alternative tests were employed for the outlier: the Q-test and Nair's adopted by the ASTM standards. The results of the tests are summarized in Tables 3.3.5.4.1 and 3.3.5.4.2. Both tests confirm that the data are not statistical outliers. It appears that the statistical tests mentioned above are somewhat less sensitive to the suspected outliers present in many of the parameters analyzed in this report.

3.3.5.4.1 Outlier Test using the Q – TEST

Table 3.3.5.4.1 Outlier Test for BOD Test Data. Outlier test was applied to determine if the precision was affected by outliers. The Q-test was applied. It appears that there are no outliers to the data and the RSD value can not be improved further.

Values	Suspected Value	Value Nearest	Minimum Value	Maximum Value	Q	90%	Reject??
						Qcritical	
1.1	2	1.6	1.1	2	0.444	0.56	No
1.15	1.6	1.3	1.1	1.6	0.6	0.642	No
1.25							
1.3							
1.6							
2							

3.3.5.4.2 Outlier Test for BOD (T – Test (Nair’s Test from ASTM Standards))

Table 3.3.5.4.2 Outlier (T - test) for BOD Test. Outlier test was applied to determine if the precision was affected by outliers. The ASTM test was applied. It appears that there are no outliers to the data and the RSD value can not be improved further.

Values	Suspected Value	Mean	Stdev	T	90%	95%	99%	Reject??
					T(Critical)	T(Critical)	T(Critical)	
1.1	2	1.4	0.342	1.754	1.939	2.184	2.408	No
1.15	1.6	1.28	0.195	1.636	1.835	2.08	2.304	No
1.25								
1.3								
1.6								
2								

3.3.6 CALCIUM

(Reference Eaton, A.D., L.S. Clesceri and A.E. Greenberg (1995) *Standard Methods for the Examination of Water and Wastewater*, 19th edition, American Public Health Association, American Water Works Association and Water Environment Federation, Washington, D.C.)

Calcium was determined by the EDTA titrimetric method. When EDTA is added to water it reacts with Calcium before Magnesium. Eriochrome Blue - black R indicator gives a color change when all the Calcium has been complexed at the test pH of 12-13.

Standardization of the EDTA standard. The Molarity of the EDTA standard was determined by titrating 10 mL of the calcium carbonate standard with the EDTA. The value of B was calculated as:

$$B = \frac{10}{A} \dots\dots\dots(3.13)$$

Where A = mL of EDTA required for titration of the 10 mL Calcium Carbonate. B = mg of CaCO₃ equivalent to 1 mL of EDTA titrant.

Sample Titration 100 mL of the sample was taken in to each of the five 300mL capacity Erlenmeyer flasks. 2.0 mL of 1N NaOH was added followed by the addition of about 0.2 gm of the Eriochrome Blue-black + Sodium chloride mixture dye. Indicator The sample was then titrated with the EDTA from a burette slowly until the color changes from red through purple to pure blue with no trace of reddish tint

The calcium Concentration was calculated using the formula:

$$\text{mg Ca .Lit}^{-1} = \frac{A(\text{mL}) * B * 400.8 \text{ mg(Ca) L}^{-1}}{\text{mL of Sample}}$$

The factor 400.8 is the mg of Calcium in 1 liter solution containing 1 gm of Calcium carbonate. A = mL of EDTA, which is the average of the three/five titrations and B = mg of CaCO₃ equivalent to 1 mL of EDTA titrant determined from the procedure 1 above. The sample standard deviation, relative standard deviation and 95 % confidence limit were also worked out.

3.3.6.1 Precision of Calcium Determinations

The relative standard deviations of the whole set of measurements were analysed for calcium determinations. The average relative standard deviation obtained was 6 mg L⁻¹ with 95% of the samples determinations having RSD value less than 11%.

3.3.6.2 Method Detection Limit for Calcium Determination

The MDL was worked out for samples having low values of calcium and the cumulative distribution is shown in Figure3.3.6.1. At the 95% confidence level, the method detection limit is around 1.99 mg L⁻¹ for Calcium determination.

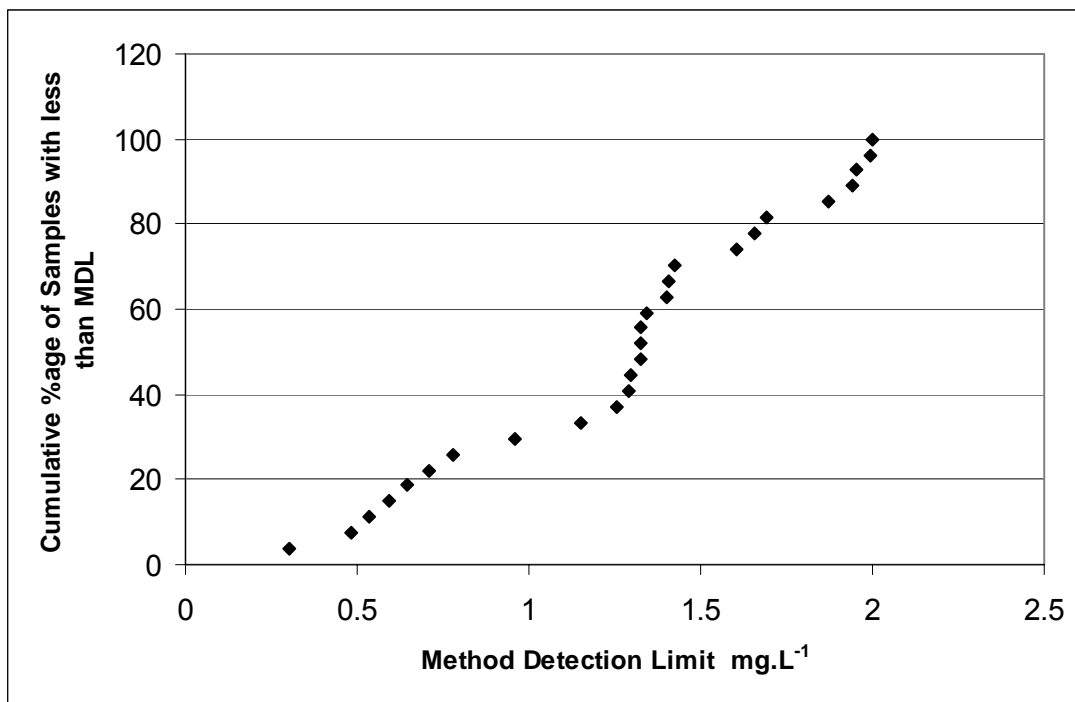


Fig. 3.3.6.1 Method Detection Limit for Calcium Determination. Calcium could be determined with relatively good precision. The graph shows that over 95% of the samples analyzed have RSD values less than or equal to 2 mg L⁻¹.

3.3.7 CHEMICAL OXYGEN DEMAND (COD)

(Reference Eaton, A.D., L.S. Clesceri and A.E. Greenberg (1995) *Standard Methods for the Examination of Water and Wastewater*, 19th edition, American Public health Association, American Water Works Association and Water Environment Federation, Washington, D.C.)

The dichromate method has been selected as a reference method for the COD determination. The sample is boiled under reflux with potassium dichromate and silver sulphate catalyst in strong sulphuric acid. Part of the dichromate is reduced by organic matter and the remainder is titrated with ferrous ammonium sulphate. In an Erlenmeyer flask 20.0 ml of the sample or an aliquot diluted to 20.0 ml with distilled water was placed. 10.0 ml of standard potassium dichromate solution, 0.0417 mol L⁻¹, and a few anti-bumping granules were added and mixed well. Carefully, 30 mL of concentrated H₂SO₄ containing silver sulphate was added, mixing thoroughly by swirling while adding the acid. If H₂SO₄ containing silver sulphate was not used, 0.15 g of dry silver sulphate was added and then, slowly, 30 mL of concentrated H₂SO₄. If the liquid has not been well mixed local heating may occur on the bottom of the flask

and the mixture may be blown out of the flask. The condenser to the flask was attached and the mixture refluxed for 2 hours. After allowing cooling, the condenser was washed with distilled water. The mixture was diluted to about 150 mL with distilled water, cooled to room temperature, and the excess dichromate was titrated with standard ammonium ferrous sulphate using 2-3 drops of ferroin indicator. The end-point is when the color changes sharply from blue-green to reddish-brown, even though the blue-green may reappear within several minutes was noted. In the same manner a blank was refluxed consisting of 20 mL of distilled water together with the reagents and titrated as in the sample above.



Figure 3.3.7.1 COD Digestion Apparatus

Calculation

The COD was calculated using the formula:

$$\text{Concentration of COD} = \frac{(a - b) \times c \times 8000}{V} \text{ mg L}^{-1} \dots\dots\dots (3.14)$$

Where:

- a = ferrous ammonium sulphate (mL) used for blank
 b = ferrous ammonium sulphate (mL) used for sample
 c = molarity (mol L^{-1}) of ferrous ammonium sulphate
 v = volume of sample (mL)

The COD was used for test assessment of the amount of organic matter present in Lake Chamo as well as the raw wastewater from Arbaminch University's waste Influent to the waste stabilisation pond. The result of the tests is given in Table 3.3.7.1.

Table 3.3.7.1 COD TEST Result and Calculation. The blank mL value is the average of three blank titrations. As the COD determination for all the samples given in the table above is determined at the same time, the same blank determination applies to all the samples.

Sample	ml Taken	ml Titrant (b)	Blank mL (a)	Consumption (mL) (a-b)	COD ((mg L^{-1})	Average COD (mg L^{-1})	Standard Deviation	Relative Standard Deviation
Lake Chamo	100	8.5	10.1*	1.613	32.26	29.06	3.8	13.08%
Lake Chamo	100	8.61	10.1	1.503	30.06			
Lake Chamo	100	8.87	10.1	1.243	24.86			
Awti Raw Waste Water	20	9.04	10.1	1.073	107.3	97.97	11.3	11.61%
Awti Raw Waste Water	20	9.26	10.1	0.853	85.3			
Awti Raw Waste Water	20	9.1	10.1	1.013	101.3			

The method gave a relative standard deviation between 11% and 13% for a COD measurement lying between 24 and 107 mg L^{-1} measured as O_2 .

3.3.8 CHLORIDE

(Reference Eaton, A.D., L.S. Clesceri and A.E. Greenberg (1995) Standard Methods for the Examination of Water and Wastewater, 19th edition, American Public health Association, American Water Works Association and Water Environment Federation, Washington, D.C.)

The Argentometric titration with Silver Nitrate method was used in this research for chloride determination. In a neutral or slightly alkaline solution (with pH range between 7 and 9), Potassium chromate can indicate the end point of a silver nitrate titration of Chloride. Silver Chloride is precipitated quantitatively before a red-brown silver chromate is formed. A 100 mL sample volume for the rivers and 25 mL sample volumes for the lake samples were taken in to 300 mL Erlenmeyer flasks with the help of volumetric pipettes. 1.0 mL of potassium Chromate

indicator was added to each sample flask. The pH was adjusted to lie between 7 and 10 mostly with the 1N NaOH. The samples were then titrated to a pinkish yellow end point. The AgNO₃ titrant was titrated in the same manner using the 0.014 N Sodium Chloride as the primary standard and the normality of the silver Nitrate standard was determined. The Chloride Concentration was calculated using the formula:

$$\text{mg Cl L}^{-1} = \frac{(A - B)(\text{mL}) * N(\text{mol.L}^{-1}) * 35450 \text{ mg Cl}/(\text{molL}^{-1})}{\text{mL of Sample}} \dots\dots\dots$$

(3.15)

Where the factor 35450 is the equivalent mg of Chloride present in mol per liter solution. A = mL of titration of the AgNO₃ titrant, which is the average of the three/five titrations and B = mL of titration for the blank. And N = Normality of the AgNO₃ used.

3.3.8.2 Precision of Chloride Determination

95% of the samples analyzed had a relative standard deviation (RSD) value less than 18 % while the median RSD value stands around 8% for chloride determination. The chloride determination is difficult with respect to locating precisely the end-point color change from yellow to brownish yellow of the silver chromate end point color. This is particularly so if very low normality silver nitrate titrants are being used. Turbid samples have to be filtered.

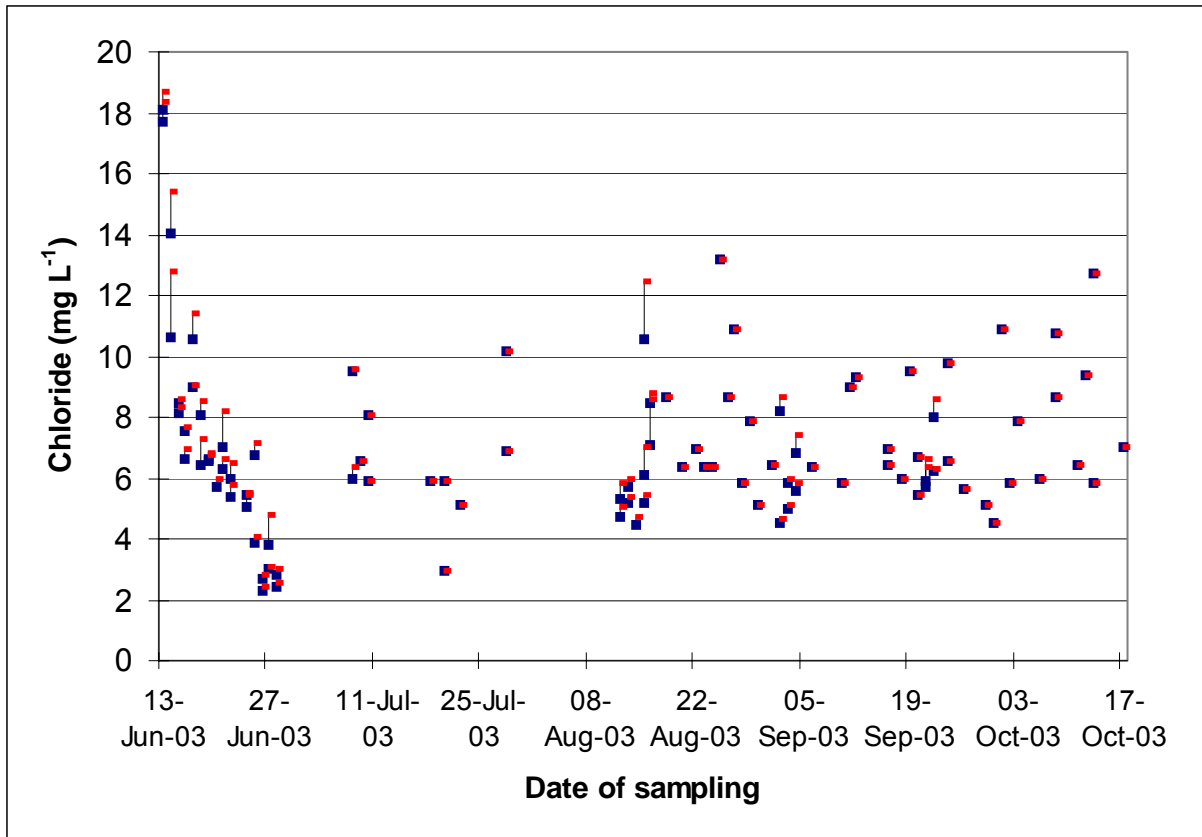


Fig. 3.3.8.1 95% confidence Limits of Chloride Determination. The upper and lower thick marks indicate the upper and lower 95% limits. Chloride has a high standard deviation particularly at low chloride values. The end point colour change is difficult to detect at this low value.

3.3.8.2 Method Detection Limit of Chloride Determination:

The chloride determination for samples containing small amount of chloride was carried out. The method detection limit stands at around 1.25 mg L^{-1} of chloride.

3.3.9 CHLOROPHYLL A AND B

(Reference Eaton, A.D., L.S. Clesceri and A.E. Greenberg (1995) *Standard Methods for the Examination of Water and Wastewater*, 19th edition, American Public health Association, American Water Works Association and Water Environment Federation, Washington, D.C.)

Chlorophyll a was determined Spectrophotometrically with Acetone Extraction. A 100-500 mL volume of the sample was filtered continuously by not allowing the filter to dry during filtration of a single sample. As filtration ends, 0.2 ml of MgCO_3 suspension to the final few milliliters of water in the filter cup was added. If extraction was delayed at this point, filters were placed in individual labeled bags or plastic Petri dishes and stored at $-20 \text{ }^\circ\text{C}$ in darkness. The filter was then placed in the tissue-

grinder, 2-3 ml of 90 per cent acetone was added, and grinding until the filter fibers was separated. The acetone and ground filter were placed into a centrifuge tube rinsing out the grinding tube with another 2 ml of 90 per cent acetone and adding this to the centrifuge tube. The total volume in the centrifuge tube was adjusted to 10 ml with 90 per cent acetone. The top was placed on tube, labeled, and stored in darkness at 4 °C for 10-12 hours. The closed tubes were then centrifuged for 15 minutes at 3,000 rev.min⁻¹ to clarify samples. The clear supernatant was decanted into a clean centrifuge tube and the volume was recorded. A cuvette was filled with 90 per cent acetone. The absorbance on the spectrophotometer at 750 nm and 663 nm were recorded. Zero was made on this blank. The sample was placed in the cuvette and absorbances at 750 nm and 663 nm (750a and 663a) were recorded. Two drops of 1 mol l⁻¹ HCl to sample in 1-cm cuvette (increase acid in proportion to volume for larger cuvettes) were added. The cuvette was agitated gently for 1 minute and the absorbances were recorded at 750 nm and 665 nm (750b and 665b). The procedure was repeated at least three times for all samples.

Calculation: Calculation of the Chlorophyll a content was based on the equation:

$$\text{Chlorophyll a (} \mu\text{g.L}^{-1}\text{)} = \frac{13.9 * [E_{665b} - E_{750b}] - [E_{665a} - E_{750a}] * V_c}{V_s * Z} \dots (3.16)$$

Where:

$E_{665b} - E_{750b}$ = Optical density (absorbance) before acidification.

$E_{665a} - E_{750a}$ = Optical density (absorbance) after acidification.

V_c = the volume of extract in mL

V = the volume of water filtered in liters.

Z = the cuvette path length in cm.

13.9 = an absorption coefficient (constant) for Chlorophyll a.

3.3.9.1 Precision of the Chlorophyll a determination.

The chlorophyll a values determined for Lakes Abaya and Chamo are given in table 3.3.9.1. The relative standard deviation varies from the highest 30% at chlorophyll average of 3.9 $\mu\text{g L}^{-1}$ to 3.7% at value of 47 $\mu\text{g L}^{-1}$.

Table 3.3.9.1 Calculation of chlorophyll a values for Lakes Abaya and Chamo. For Lake Abaya the chlorophyll a value is low and the standard deviation is quite high. Because of the clarity of Lake Chamo and the seasonality of Chlorophyll production there is a variation in the Chlorophyll a value of Lake Chamo at different times of the year (approximately between 15 and 50).

Sample	Volume of Sample Filtered	Volume of Extract (mL)	Absorbance Reading Before Acidification			Absorbance Reading After Acidification			Chlorophyll a ($\mu\text{g.L}^{-1}$)	Mean Chlorophyll a ($\mu\text{g.L}^{-1}$)	Standard Deviation ($\mu\text{g.L}^{-1}$)	Relative Standard deviation (%)	
			E (663 nm) (A)	E (750 nm) (B)	E (663 nm) (C)	E (750 nm) (D)	(A - B) (α)	(C - D) (β)					$\alpha - \beta$
	100	10	0.04	0.01	0.03	0.009	0.03	0.021	0.009	12.51	13.63	1.271	9.32%
Lake Chamo	500	10	0.16	0.006	0.106	0.006	0.154	0.1	0.054	15.01			
	200	7.4	0.06	-0.0025	0.002	-0.04	0.063	0.037	0.026	13.37			
	500	10	0.54	0.013	0.36	0.009	0.527	0.351	0.176	48.93	47.54	1.736	3.65%
Lake Chamo	500	10	0.53	0.012	0.35	0.005	0.518	0.345	0.173	48.09			
	500	10	0.53	0.012	0.36	0.006	0.518	0.354	0.164	45.59			
	500	10	0.071	0.002	0.053	0.003	0.069	0.05	0.019	5.282	3.89	1.274	32.73%
Lake Abaya	500	10	0.05	0.001	0.04	0.001	0.049	0.039	0.01	2.78			
	500	10	0.06	0.003	0.049	0.005	0.057	0.044	0.013	3.614			

3.3.10 CONDUCTIVITY

Electrical Conductivity Method was used for conductivity measurement. The conductivity meter (LF 191) was connected to the power source and the meter was warmed up to about 15 minutes. The following standards were prepared mean while from the standard KCl solution S_0 ($1413 \mu\text{mho cm}^{-1}$) with 50 mL flasks filled up to the mark with distilled water after the indicated mL of KCl was added in each flask.

Table 3.3.10.1 Conductivity Measurement of Standard Solutions. The stability of the conductivity meter was checked every time a sample conductivity is determined by measuring one of the standards in the table which has a conductivity nearer to that of the sample being measured.

Label	S1	S2	S3	S4	S5	S6	S ₀
mL of KCl added in 50 mL Flask	0	1	2	5	10	25	50
Conductivity at 25 °C ($\mu\text{S Cm}^{-1}$)	0	28.3	56.5	141.3	282.6	706.5	1413

The conductivity of each of the above standards were measured with three repetitions by immersing the conductivity probe in to 100 mL beakers containing the standards and stirring for a while. The sequence of measurement was from the most dilute standard S₁ to the most concentrated standard S₀. The probe was rinsed with distilled water in between the measurement. This round of measurement is repeated three times and the measurements were recorded. The sample of water to be tested was brought forward and the sample bottle was shaken. The sample was transferred to an Erlenmeyer flask of 300 mL capacity. The probe was inserted in to this sample and the measurement was noted. The probe was taken out of the sample and rinsed with distilled water and inserted in to the standard, which is nearer to the conductivity being measured. The reading was noted and the probe was once again immersed in the sample after being rinsed with distilled water. This repetition was carried out at least three times. The mean standard deviation and relative standard deviations were computed from the recorded measurements.

3.3.10.1 Precision and Method Detection Limits of Conductivity Measurements

For 95% of the samples analysed the relative standard deviation as was found from these set of experiments is less than 1.8 %. The average is 0.9%. This value indicates that conductivity can be determined with relatively better precision.

3.3.11 DISSOLVED OXYGEN

(Reference Eaton, A.D., L.S. Clesceri and A.E. Greenberg (1995) Standard Methods for the Examination of Water and Wastewater, 19th edition, American Public health Association, American Water Works Association and Water Environment Federation, Washington, D.C.)

The azide modification of the iodometric test was used in this research. To the sample collected in a 250- to 300-mL bottle, 1 mL MnSO₄ solution was added, followed by 1 mL alkali-iodide-azide reagent. If pipettes were dipped into sample, they were rinsed before returning them to reagent bottles. Alternatively, the pipette tips were held just above liquid surface when adding reagents. The bottle was stoppered carefully to exclude air bubbles and mixed by inverting bottle a few times. When precipitate has settled sufficiently (to approximately half the bottle volume) to leave clear supernatant above the manganese hydroxide floc, 1.0 mL concentrated H₂SO₄ was added. The bottle was re-stoppered and mixed by inverting several times until dissolution is complete. A volume corresponding to 200 mL original sample was titrated after correction for sample loss by displacement with reagents. Thus, for a total of 2 mL (1 mL each) of MnSO₄ and alkali-iodide-azide reagents in a 300-mL bottle, $200 \times 300 / (300 - 2) = 201$ mL was titrated. The titration was done with 0.025M Na₂S₂O₃ solution to a pale straw color. A few drops of starch solution were added and the titration continued to first disappearance of blue color. If end point is overrun, back-titration was done with 0.0021M bi-iodate solution added drop wise, or by adding a measured volume of treated sample. Correction was done for amount of bi-iodate solution or sample.

Calculation: For a titration of 200 mL sample 1 mL of 0.0021 M of Na₂S₂O₃ is equivalent to 1 mg L⁻¹ of dissolved oxygen.

3.3.11.1 Precision and Method Detection Limit of DO Measurement.

The RSD value is affected not only by titration but also by sample handling, thus showing some scatters. The distribution of relative standard deviation among the data set shows a mean value of 2.7 % and a 95 % limit of around 9%. Since the sample blank determination is not applicable in dissolved oxygen measurement, a limit corresponding to 0.05 mL of Sodium thiosulphate titrant is taken which is equivalent to 0.05 mg L⁻¹ of dissolved Oxygen for this test.

3.3.12 HARDNESS

(Reference Eaton, A.D., L.S. Clesceri and A.E. Greenberg (1995) Standard Methods for the Examination of Water and Wastewater, 19th edition, American Public health Association, American Water Works Association and Water Environment Federation, Washington, D.C.)

Hardness was determined by titration with EDTA.

1) Standardization of the EDTA standard. The Molarity of the EDTA standard was determined by titrating 10 mL of the calcium carbonate standard with the EDTA. The

value of B is calculated as: $B = \frac{10}{A}$ Where A = mL of EDTA required for titration of

the 10 mL Calcium Carbonate B = mg of CaCO₃ equivalent to 1 mL of EDTA titrant.

2. Sample Titration 2.1) 100 mL of the sample was taken in to each of the five 300mL capacity Erlenmeyer flasks. 2.2) Then 2.0 mL of the buffer solution was added so that the pH stays at 10 ±0.1 2.3) Next about 0.2 gm of the indicator Eriochrome Black T – Sodium Chloride mixture was added a rate of about 0.2 gm per sample. 2.4) The sample was then titrated with the EDTA from a burette slowly until the color changed from purple red to pure blue with no trace of reddish tint 3) The Hardness Concentration was calculated using the formula:

$$\text{Hardness (mg L}^{-1}\text{)} = \frac{A(\text{mL}) * B(\text{mL}) * 1000\text{mg L}^{-1}\text{CaCO}_3 / (\text{mL of 0.01 mol EDTA})}{\text{mL of Sample}} \dots\dots\dots (3.17)$$

Where the factor 1000 is the mg of CaCO₃ equivalent to 1 mL of 0.01 mol of EDTA. A = mL of EDTA, which is the average of the three-five titrations and B = mg of CaCO₃ equivalent to 1 mL of EDTA titrant determined from the procedure 1 above. The sample standard deviation, relative standard deviation and 95 % confidence limit were also worked out.

3.3.12.1 Precision and Method Detection Limits of Hardness Measurement

The 95 % confidence level of hardness determination is 11.9 % while the median value lies at 4.7 %. Therefore, the maximum limit expected is 11.9 % and on average a relative standard deviation of 4.7 % must be attained. There is a slight linear increase in the MDL with concentration. Taking the lower limit of concentrations as

the appropriate range for method detection limit, the Method Detection Limit for Hardness lies around 5 mg L^{-1} .

3.3.13 NITRATE

(Reference: *Ausgewählte Methoden der Wasser Untersuchung. Bd. I. Jena: VEB Gustav Fischer Verlag 1976.*)

Spectrophotometric determination with Sodium Salicylate was employed for the determination of Nitrate. Nitrate ions and Sodium Salicylate together form yellow Sodium Nitrosalicylate, which can be determined spectrophotometrically at 420 nm. 2 mL of Sodium salicylate was added to standards and the sample in a porcelain dish and the solution was evaporated in steam bath at 100 degree Celsius. The residue was dried at 100 degree Celsius and cooled in a desiccator. The solution was allowed to stand for 10 minutes and then 15 mL of distilled water and 7.5 mL of Sodium Hydroxide solution was added, cooling constantly the solution was transferred to a 50 mL volumetric flask and made up to the mark with distilled water. The solution was shaken and the measurement taken against blank solution treated in the same way as the sample and standards after 10 minutes at 420 nm with a spectrophotometer. The method of standard addition was employed to examine if there are sample matrix influences to the determination. The nitrate values were determined from the calibration line prepared from the known standards.



Figure 3.3.13.1 Water Bath used for Sample Digestion in the Determination of Nitrate

3.3.13.1 Determination of Calibration Line for Nitrate

The following result (table 3.3.13.1) was obtained after standards were prepared and run through photometric determination.

Table 3.3.13.1 Nitrate Absorption of Standards and calculation of MDL Values. The MDL value is determined as $S \cdot t$ where S is the standard deviation of the blank absorption divided by the slope of the calibration line and t is the critical value of the student's distribution determined from Table 3.2.5.1

Standard	mL of Standard Added	mg L ⁻¹ of NO ₃ ⁻	Absorption Measurements			Mean (Abs)	Standard Deviation	Relative Standard Deviation	Student t	MDL (mg L ⁻¹)
			Sample 1 (Abs)	Sample 2 (Abs)	Sample 3 (Abs)					
S0	0	0	0	0	0.035	0	0.02	173%	4.541	0.09
S1	1	0.2	0.025	0.03	0.033	0.025	0.004	16.17%	4.541	
S2	5	1	0.09	0.095	0.08	0.095	0.007	8.04%	4.541	
S3	10	2	0.23	0.23	0.235	0.2325	0.002	1.24%	4.541	
S4	20	4	0.4	0.415	0.417	0.416	0.009	2.23%	4.541	

Except for the blank, which may naturally have greater standard deviations, the remaining standard show lower standard deviation.

3.3.13.2 Calibration Equation for Nitrate Determination

The calibration line equation was established by the principle of linear regression using the above set of data. The line of best fit is shown in the Fig. 3.3.13.1 displayed below. The coefficient of determination (R^2) value is 0.994.

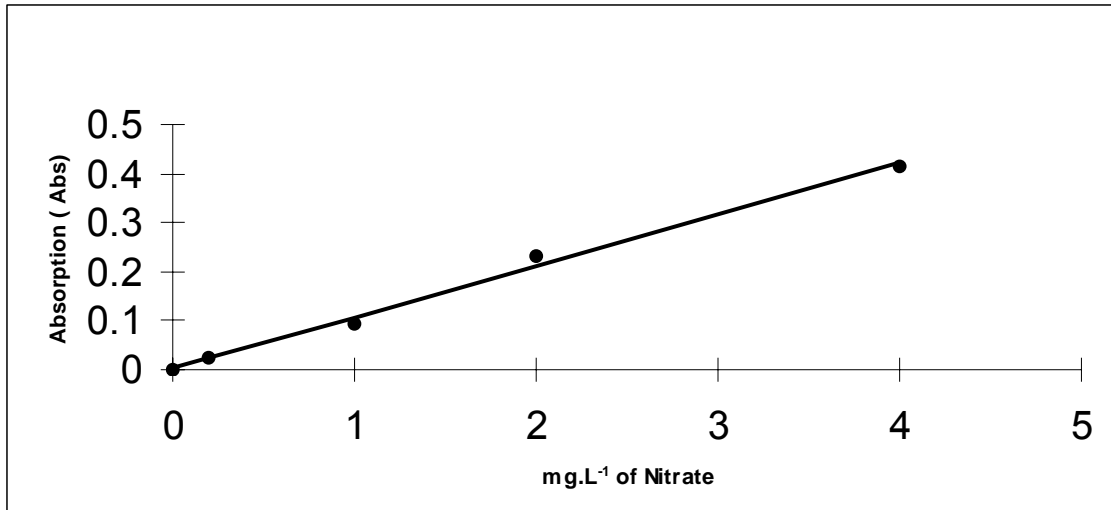


Fig. 3.3.13.2 Line of Best Fit for Nitrate Standards determined from photometric absorption of Standards. Nitrate determination displays linearity over the ranges of nitrate values expected in the samples analyzed.

3.3.13.3 Precision and Method Detection Limit for Nitrate

The relative standard deviation varies between 5 and 20 % for the samples and standards. The method detection limit (see table 3.3.13.1 above) is around 0.16 mg L⁻¹ measured as nitrate.

3.3.13.4 Comparison of Nitrate Values with the Method of Standard Addition

The possible matrix effect of the lake water composition was checked by the method of standard additions. 40 mL of the Lake Chamo sample was added to each of the standards. Table 3.3.13.2 below shows the absorption data obtained with this method of standard addition.

Table 3.3.13.2 Nitrate Absorption using the Method of Standard Additions in order to check for the matrix effect of lake samples. 40mL of Lake Chamo samples was added to each of the standards.

mg L ⁻¹ of Nitrate	Absorption Measurements				Mean (Abs)	Standard Deviation (Abs)	Relative Standard Deviation
	Sample 1 (Abs)	Sample 2 (Abs)	Sample 3 (Abs)	Sample 4 (Abs)			
0	0.1	0.15	0.16	0.126	0.134	0.026	19%
0.2	0.19	0.17	0.1	0.15	0.19	0.038	20%
1	0.27	0.29	0.26	0.27	0.27	0.012	4%
2	0.45	0.4	0.36	0.46	0.45	0.046	10%
4	0.255	0.254	0.25	0.2	0.255	0.026	10%

Fig. 3.3.13.2 below shows the regression line obtained with the method of standard addition after outlier points have been removed.

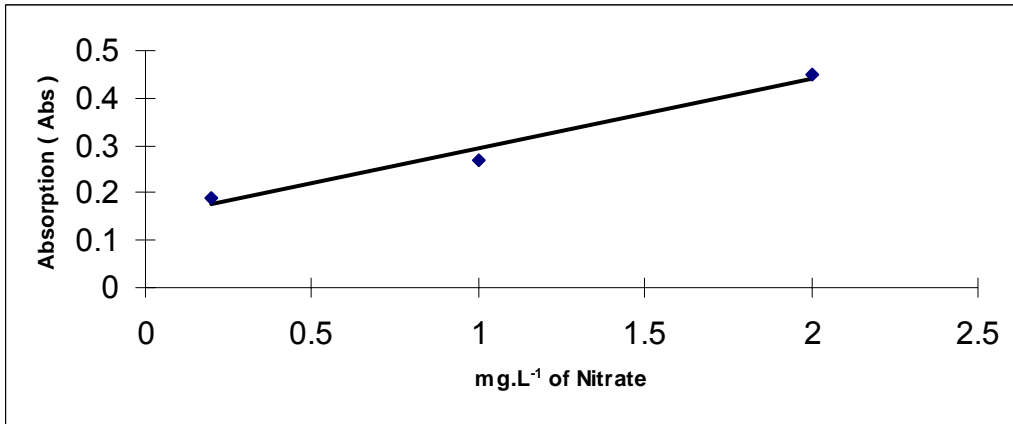


Fig. 3.3.13.3 Line Fit Plot for Standards containing Chamo Lake Sample. This line was determined to check for matrix effects. Comparison with the slope of the line containing the standards only shows a significant difference.

The calculation of the nitrate concentration is given Table 3.3.13.5. Comparison with the data obtained with out standard addition shows a 20 % variation. This percentage is significant and the method of standard addition should be preferred for nitrate determination.

3.3.13.5 Calculation of Nitrate for Lake Chamo Using the Data from Standard Additions

Regression Variables	Conc = a*absorption + b
Intercept (b) =	0.1477
Slope (a) =	0.1459
Sample Concentration =	1.27 mg L ⁻¹

Cross Check with Data from previous Calibration Line	
Raw Sample Absorption =	0.134
Concentration =	1.57 mg L ⁻¹
Percentage Error =	19%

3.3.13.6 Comparison of the Coincidence of the Two Lines of Determination of Nitrate

In order to statistically test if the two lines are identical in terms of their slopes, a categorical variable Z was introduced identifying the samples source ($Z = 1$ for standards without sample and $Z = 0$ for standards with the sample). The intercept obviously is different for the two lines due to the addition of sample in the second case. Therefore, only the slope comparison has to be made. The general equation then becomes:

$$Y_i = \beta_0 + \beta_1 * X_i + \beta_2 * Z_i + \beta_3 * X_i * Z_i + \varepsilon_i, \dots \dots \dots (3.18)$$

Where Y is the absorption, X the concentrations and ε is the residual. The result of multiple regressions testing for the significance of the coefficients is given in table 3.3.13.3 below. The test for coincidence is accepted if $\beta_2 = \beta_3 = 0$. The test for equality of slopes is accepted if β_3 alone is zero.

Table 3.3.13.3 Coincidence of Lines Test for Nitrate Calibration Lines. Both β_2 and β_3 are significant shown by the significance test ($P \leq 0.001$). Therefore the two lines are different confirming the presence of matrix effects in lake samples for nitrate determination.

Coefficient Symbol	Coefficient Estimate	Standard Error	Student t calculated	Significance	P(T<=t(cal))	Lower 95%	Upper 95%
β_0	0.1423	0.0101	14.0550	(P<=0.001)	8.09E-06	0.1175	0.1670
$\beta_1:X_1$	0.1477	0.0049	29.9349	(P<=0.001)	9.22E-08	0.1356	0.1598
$\beta_2:X_2$	-0.1400	0.01431	-9.7807	(P<=0.001)	6.57E-05	-0.1750	-0.1050
$\beta_3:X_3$	-0.0425	0.0069	-6.1001	(P<=0.001)	0.0008	-0.0596	-0.0255

From the results given in Table 3.3.13.3 above it is seen that both coefficients are significant at the 99% confidence level ($t(n-p-1, 0.05) = 2.447$). Therefore, the two lines are neither coincident nor have equal slopes. The matrix effect is not negligible and the method of standard addition has to be followed.

3.3.13.7 Comparison of Calibration Lines Measured at Different Times

The calibration lines for nitrate determined at different times have been plotted in Fig. 3.3.13.3. It is clearly seen that the measurements gave a widely differing slopes. A statistical test was carried out using categorical variables for the four lines and the results of the tests have been summarized in table 3.3.13.4.

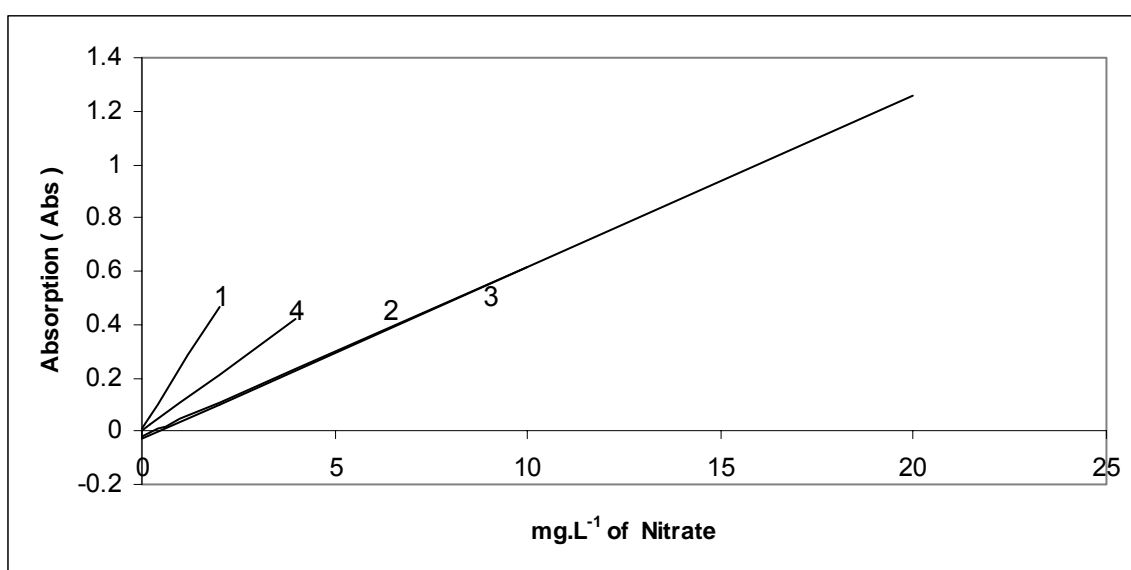


Fig. 3.3.13.4 Nitrate Calibration Performed at Different Times. The lines show that the photometric determination of nitrate gives very different calibration lines. Some of the samples also give erratic results. Therefore, close control of the experiment and greater number of samples is required for Nitrate determination.

Table 3.3.13.4 Comparison of calibration Lines for Nitrate made at Different Times. Similar statistical test for coincidence of the calibration lines indicate that lines 2 and 3 only coincide. The rest of the lines are different from each other

Coefficient Designation	Coefficient Estimate	Standard Error	Student t (calculated)	Significance Test	P(T<=t(cal))	Lower 95%	Upper 95%
β_0	0.0022	0.0041	0.5460	N.S. * (P>0.05)	0.5936	-0.0066	0.0111
$\beta_1:X_1$	0.1051	0.0020	52.1900	(P<=0.001)	1.92E-17	0.10084	0.1094
$\beta_2:X_2$	0.0053	0.0059	0.9080	N.S. (P>0.05)	0.3792	-0.0073	0.0180
$\beta_3:X_3$	-0.0212	0.0050	-4.2181	(P<=0.001)	0.0008	-0.03201	-0.0104
$\beta_4:X_4$	-0.0298	0.0062	-4.7779	(P<=0.001)	0.0002	-0.0432	-0.0164
$\beta_5:X_5$	0.1250	0.0044	28.1022	(P<=0.001)	1.03E-13	0.1155	0.1346

Coefficient Designation	Coefficient Estimate	Standard Error	Student t (calculated)	Significance Test	P(T<=t(cal))	Lower 95%	Upper 95%
$\beta_6:X_6$	-0.0420	0.0021	-19.5794	(P<=0.001)	1.43E-11	-0.0466	-0.0374
$\beta_7:X_7$	-0.0409	0.0020	-19.8905	(P<=0.001)	1.16E-11	-0.0453	-0.0365

N.S. = Not Significant

Using the lines designated in the Fig. 3.3.13.3, the equation for each line in terms of X and the categorical variable Z (either 0 or 1 substituted accordingly) becomes:

$$\text{Line 1: } Y = \beta_0 + (\beta_1 + \beta_5) X + \beta_2$$

$$\text{Line 2: } Y = \beta_0 + (\beta_1 + \beta_6) X + \beta_3$$

$$\text{Line 3: } Y = \beta_0 + (\beta_1 + \beta_7) X + \beta_4$$

$$\text{Line 4: } Y = \beta_0 + (\beta_1) X$$

From the table it is clear that line 1 has slope widely differing from the rest. Calibration lines 2 and 3 have more or less similar slopes and are nearer to line 4. Therefore, lines 2, 3 and 4 are considered as close while line 1 is too far away and possibly an outlier line.

Table 3.3.13.5 Categorical Variables assigned for the four Calibration lines of Nitrate. The Z values are the categorical variables classifying the data by its source. For example for data number 1 (Line 1), the z1 values is equal to one and z2 and z3 are zero.

X	Z1	Z2	Z3	Z1X	Z2X	Z3X	Absorption
0	1	0	0	0	0	0	0.007618
0.2	1	0	0	0.2	0	0	0.053666
0.4	1	0	0	0.4	0	0	0.099714
1.2	1	0	0	1.2	0	0	0.283906
2	1	0	0	2	0	0	0.468097
0	0	1	0	0	0	0	-0.01896
0.2	0	1	0	0	0.2	0	-0.00633
0.4	0	1	0	0	0.4	0	0.006307
0.6	0	1	0	0	0.6	0	0.018941
1	0	1	0	0	1	0	0.044209
2	0	1	0	0	2	0	0.107378
4	0	1	0	0	4	0	0.233717
10	0	1	0	0	10	0	0.612734
0	0	0	1	0	0	0	-0.02762
2	0	0	1	0	0	2	0.100847
10	0	0	1	0	0	10	0.614718

X	Z1	Z2	Z3	Z1X	Z2X	Z3X	Absorption
20	0	0	1	0	0	20	1.257056
0	0	0	0	0	0	0	0
0.2	0	0	0	0	0	0	0.025
1	0	0	0	0	0	0	0.095
2	0	0	0	0	0	0	0.2325
4	0	0	0	0	0	0	0.416

3.3.14 NITRITE

(Reference: DIN 38405 Teil 10: Deutsche Einheitsverfahren zur Wasser-, Abwasser- und Schlamm –Untersuchung, (Gruppe D, Anionen) Bestimmung des Nitrit Ions (Februar 1981).

Nitrite was determined spectrophotometrically with Aminobenzoicsulfonamid. Standards ranging from 0-10 mg L⁻¹ of nitrite were transferred to 50 mL from a burette. The volume was adjusted to 40 ± 2 mL using distilled water. 1 mL of the color reagent was added and the solution was filled with distilled water up to the mark. The pH value must come to 1.9± 0.1 pH units. When the sample was strongly alkaline (Example Lake Abaya and Chamo samples), before filling to 40 mL volume, phosphoric acid was added until this pH was reached (usually 1.5 – 2 mL was enough). The samples were treated in the same manner as the standards. The solution was measured for absorption against similarly prepared blank after 20 minutes at a wavelength of 540 nm. The Nitrite was determined from the calibration equation prepared using the standards.

3.3.14.1 Absorption of Standards:

The following result shown in Table 3.3.14.1 was obtained after standards were prepared and run through a photometric determination.

Table 3.3.14.1 Data for Nitrite Absorption of Standards. Except for the blank, the remaining samples show low standard deviation. Nitrite, therefore, can be determined for low nitrite samples with good precision.

Standard Label	mL Added	mg L ⁻¹ of Nitrite	Absorption Measurements			Mean (Abs)	Standard Deviation (Abs)	Relative Standard Deviation
			Sample 1 (Abs9)	Sample 2 (Abs)	Sample 3 (Abs)			
S0	0	0	0.005	0.002	0.001	0.0026	0.0020	78%
S1	0.5	0.1	0.31	0.33	0.32	0.3200	0.0100	3%
S2	1.5	0.3	0.94	0.98	0.94	0.9533	0.0230	2%
S3	2.5	0.5	1.6	1.7	1.7	1.6666	0.0577	3%

Except for the blank, which may naturally have greater standard deviations, the remaining standard show lower standard deviation.

3.3.14.2 Calibration for Nitrite Determination

The calibration line equation was established by the principle of linear regression using the above set of data. The line of best fit is shown in Figure 3.3.14.1. The coefficient of determination (R^2) value is 0.999.

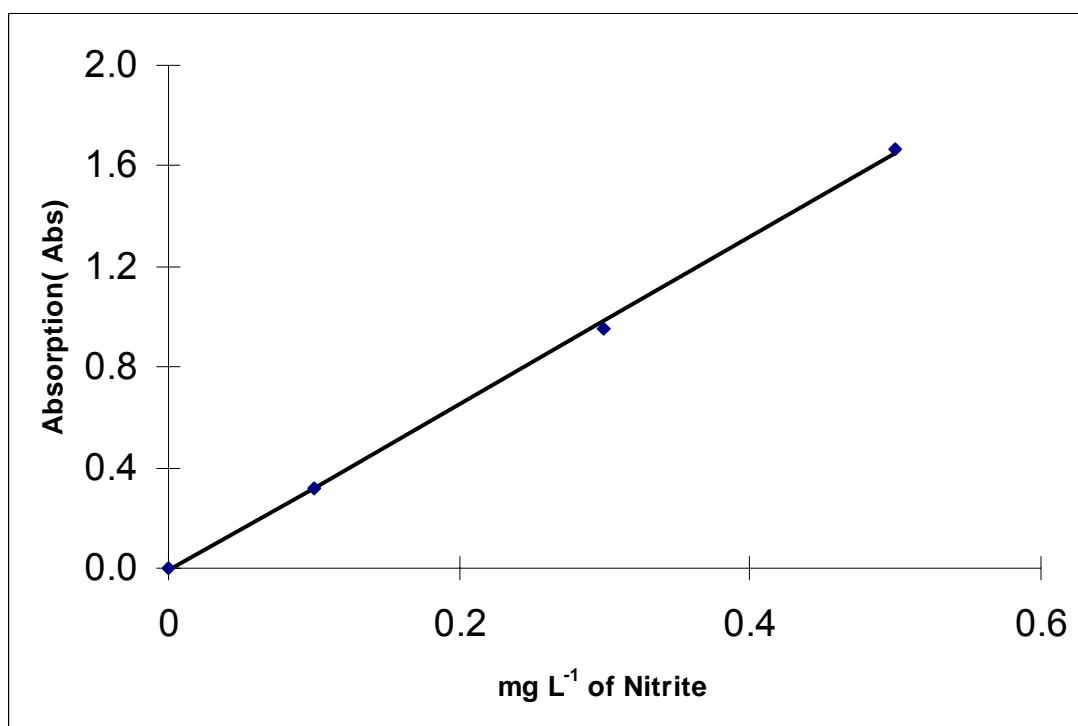


Fig. 3.3.14.1 Best line of Fit for Nitrite Standards. For the ranges of nitrite values expected in the samples analyzed, the nitrite absorption shows linearity (absorption is proportional to concentration).

3.3.14.3. Determination of the Nitrite Content of Samples from Lakes Abaya and Chamo

Five repetitions were carried through for each of the samples from Lakes Abaya and Chamo. The nitrite value was calculated using the calibration equation determined above. Table 3.3.14.2 below summarises the calculation.

Table 3.3.14.2. Determination of the Nitrite Content of Chamo Samples

Sample Label	mL Added per 50mL	Absorption (Abs)	Nitrite (mg L ⁻¹)	Mean (mg L ⁻¹)	Standard Deviation (mg L ⁻¹)	Relative Standard Deviation	Student t	MDL (mg L ⁻¹)
C1	40	0.022	0.012	0.013	0.00088	6.43%	3.365	0.002961
C2	40	0.026	0.013					
C3	40	0.029	0.014					
C4	40	0.026	0.013					
C5	40	0.025	0.013					

Table 3.3.14.3 Determination of the Nitrite Content of Abaya Samples

Sample Label	mL Added per 50mL	Absorption	Nitrite (mg L ⁻¹)	Mean (mg L ⁻¹)	Standard Deviation (mg L ⁻¹)	Relative Standard Deviation	Student t	MDL (mg L ⁻¹)
A1	40	0.04319	0.0203	0.0208	0.001008	4.84%	3.365	0.0034
A2	40	0.041	0.0195					
A3	40	0.048	0.0221					
A4	40	0.045	0.0210					
A5	40	0.046	0.0213					

3.3.14.4 Relative Standard Deviation of Measurement of Nitrite

For the two lakes measurement, the relative standard deviation falls below 7%, which gives an acceptable precision.

3.3.14.5 Detection Limit of the Nitrite Measurement

Taking the blank samples, the calculation of method detection limit is shown in Table 3.3.14.4.

Table 3.3.14. 4 MDL calculation. The calculated MDL value is quite low indicating that small values of nitrite in samples can be detected with this procedure. This is useful as Nitrite can be an indicator of fresh pollution of water samples by animal wastes.

Sample	Absorption (Abs)	Nitrite (mg L ⁻¹)	Mean (mg L ⁻¹)	Standard Deviation (mg L ⁻¹)	Relative Standard Deviation	Student t	MDL (mg L ⁻¹)
Chamo	0.022	0.012	0.014	0.0009	6.4%	3.365	0.003
	0.026	0.013					
	0.029	0.015					
	0.026	0.014					
	0.025	0.013					

The calculations give a method detection limit of 0.003 mg L⁻¹. The detection limit can be taken as 0.003 mg L⁻¹.

3.3.15 PH

(Reference Eaton, A.D., L.S. Clesceri and A.E. Greenberg (1995) Standard Methods for the Examination of Water and Wastewater, 19th edition, American Public health Association, American Water Works Association and Water Environment Federation, Washington, D.C.)

A pH meter was used that employs potentiometric measurement with glass electrode. The equipment used here was the pH 191 WTW (Wissenschaftlich – Technische Werkstaten) model with a temperature compensator. The pH instrument was calibrated with buffer solutions prepared in the laboratory with pH values of 4.01, 7.43 and 10.06 at 20 Degree Celsius. The pH meter was turned on to read the pH directly. The two buffer solutions (pH = 7.43 and pH = 10.06) were brought forward. The pH electrode together with the temperature electrode were rinsed with distilled water and first immersed in the pH 7.43 buffer. The pH value was adjusted to read 7.43 using the Δ pH control. The electrode and temperature probe were then taken out of the pH buffer rinsed with distilled water and immersed in the pH = 10.06 buffer. The measurement is adjusted to read 10.06 using the mV/pH control. The sample of water to be tested was brought forward and filled in to a 300 mL Erlenmeyer flask. The pH electrode and temperature probe were immersed in to the sample and stirred slowly and the reading was noted after it has stabilized. The electrode and probe were taken out rinsed with distilled water and put in to the pH = 7.43 buffer or pH = 10.06 buffer whichever is nearer to the pH measurement of the sample. The reading was adjusted using the Δ pH or mV/pH controls accordingly. The electrodes were again immersed in the sample and the measurement noted again. This sequence is repeated three times at least.

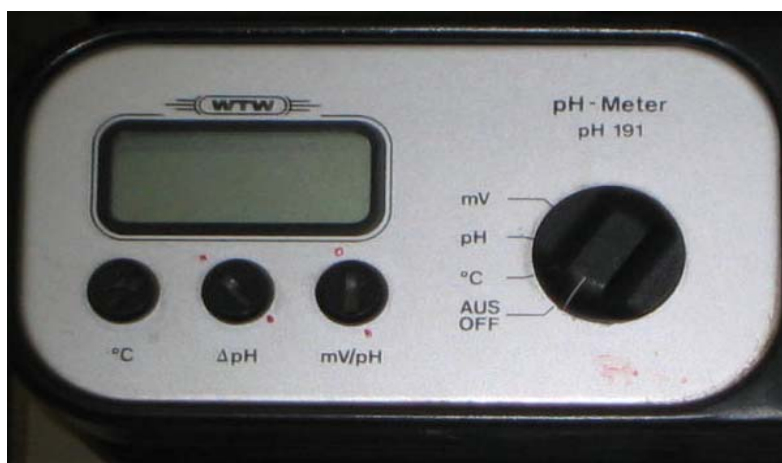


Figure 3.3.15.1 pH Meter used for the pH Determination

3.3.15.1 Precision and Method Detection Limit of pH Determination

The pH data were analysed for the relative standard deviation. It was found out that the mean RSD is 0.17 % while the median value stands at 0.11 %. The 95% cut-off limit is 0.58%. With a pH maximum measured at pH = 10.0, this limit gives a deviation of ± 0.06 pH units as the acceptable deviation. Visual inspection shows a pH of 0.1 units as the method detection limit for pH. PH differences over 0.1 units can be considered as significant. Analysis of the whole data shown in the graph below reveals that the 95% cut-off limit for method detection limit is around 0.15 pH units.

3.3.16 PHOSPHATE

(Reference Eaton, A.D., L.S. Clesceri and A.E. Greenberg (1995) Standard Methods for the Examination of Water and Wastewater, 19th edition, American Public health Association, American Water Works Association and Water Environment Federation, Washington, D.C.)

Soluble reactive phosphorous (SRP) was determined spectrophotometrically with Molybdate Reagent at a wavelength of 380 nm. A yellow color develops when excess Molybdate solution is added to an acidic solution of orthophosphate ions. The resultant color is due to the formation of molybdophosphoric acid, $H_3P Mo_{12}O_{40}$. The optimum condition for the development of the heteropoly complex consists of having a final Molybdate concentration of 0.04 M and a final acidity of 0.257 m in respect of Nitric or Perchloric Acid. Standard solutions ranging in concentrations from 0-0.2 mg L^{-1} of PO_4 measured as P (Phosphorous) were pipetted in to each of 50 mL volumetric flasks from the standard phosphate solution. Three independent solutions were prepared for each standard. 15 mL of water was added to each. Then 5 mL of the 2.5 Nitric Acid was added. Then 5 mL of the Molybdate solution was added. The 50 mL flasks were then each filled up to the mark with water and mixed by inverting the flask several times. A period of 20 minutes was allowed. Thereafter the standards absorption was measured with the Jenway 6100 Spectrophotometer at 380 nm wavelength. Between 20 and 40 mL of the sample was pipetted in to a 50 mL flask and treated with reagents in the same way as the standards. The absorption was measured afterwards. A minimum of three independent repetitions was prepared for each sample tested. The Phosphate values were determined from the sample absorption using the calibration line prepared from the known standards.

3.3.16.2 Precision of Phosphate Measurement

Spectrophotometric absorption measurements have characteristically decreasing Standard deviation with increasing concentration (or absorption). The instrument has less sensitivity at low absorption values. Figure 3.3.16.1 shows the variation of relative standard deviation with sample phosphate concentration. As it can be seen for samples with low phosphate values, greater number of repetition is necessary to arrive at statistically acceptable values.

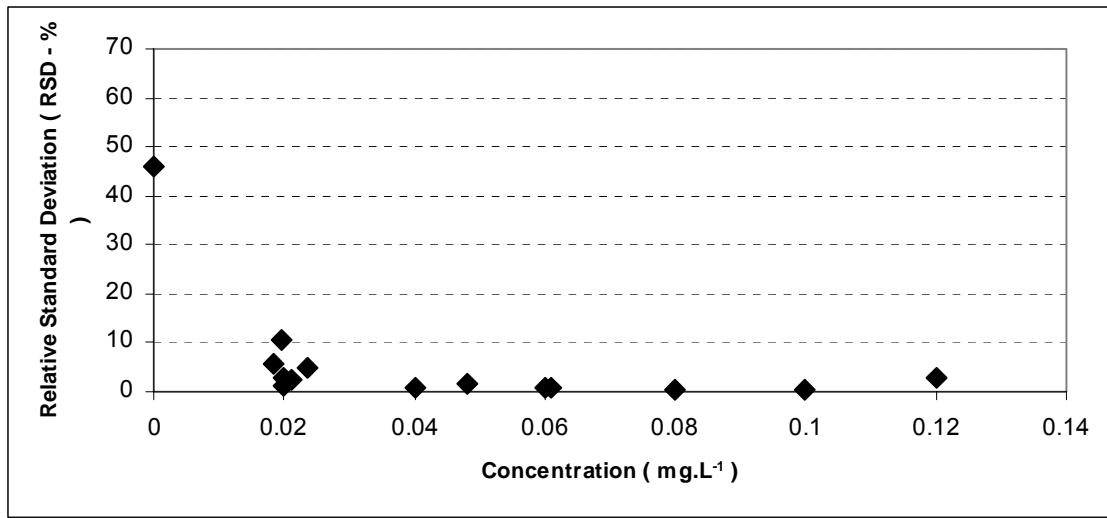


Fig. 3.3.16.1 Variation of Relative Standard Deviation with Concentration for Phosphorous. As is typical with photometric absorption, the standard deviation increases at low sample concentrations. The number of samples has to increase at low phosphate values in order to increase the precision of measurement.

Analysis of the relative standard deviation shown in Fig. 3.3.16.1 above indicated that the mean RSD value is 2.7 % and the 95% cutoff limit is around 6%. Samples should therefore be determined with 6% relative standard deviation within the range of phosphate values similar to the ones determined in this research. Small values require greater number of repetitions.

3.3.16.2 Method Detection Limit for SRP Measurement

The absorption, standard deviation and the student t value for the given number of samples have been used to calculate the MDL value at various concentrations. Table 3.3.16.1 shows this calculation. The concentrations are worked out using the regression equation.

$$P - \text{Phosphate (mg/L)} = \frac{50 \text{ mL}}{\text{mL added}} \left(\frac{\text{Absorption (Abs)}}{13.134} \right) \dots\dots\dots (3.19)$$

Table 3.3.16.1 Absorption of Phosphate Standard Solutions and MDL Calculation. The MDL value is determined as $S \cdot t$ where S is the standard deviation of the blank absorption divided by the slope of the calibration line and t is the critical value of the student's distribution determined from Table 3.2.5.1

Standard Label	mg/L of Phosphate as P	Abs1	Abs2	Abs3	Mean Absorption	Standard Deviation	Relative Standard Deviation	student t	MDL Mg L ⁻¹
St0	0	-0.004	-0.006	-0.01	-0.00667	0.003055	0.458258	4.541	0.00105

3.3.17 POTASSIUM

(Reference Eaton, A.D., L.S. Clesceri and A.E. Greenberg (1995) Standard Methods for the Examination of Water and Wastewater, 19th edition, American Public health Association, American Water Works Association and Water Environment Federation, Washington, D.C.)

The Measurement Method used in this research was the Flame Emission Photometric Method. A sample is sprayed in to a gas flame and excitation is carried out under controlled conditions. The intensity of light at a wavelength of 766.5 nm is measured by a phototube potentiometer. The intensity reading is approximately proportional to the concentration of potassium. The samples of water to be tested were all filtered through glass fiber filter. The first few milliliters filtered were thrown to waste and filtration was continued for few minutes after the water has been filtered out of the glass tube. 2. The following blank and standard solutions were pipetted in to each of 50 mL volumetric flasks from the intermediate Potassium solution. Three independent solutions were prepared for each standard (Table 3.3.17.1).

Table 3.3.17.1 Potassium Standard Solutions – Volumes Added and Concentrations for determination by flame photometric method.

Standard Label	S0	S1	S2	S3	S4	S5	S6
mL of Standard added in a 50 mL Volumetric Flask	0	1	2	3	4	5	6
mg L ⁻¹ of Potassium (K)	0	2	4	6	8	10	12

Each of the 50 mL flasks was filled up to the mark with distilled water. The emission concentration of each standard was determined using the Corning 410 C Flame Photometer operating procedure, which is listed below. The sample of water to be tested was brought and diluted with distilled water so that the emission of the diluted sample falls in the 1 – 12 mg L⁻¹ measurement range. For both Lakes Abaya and Chamo the dilution ratio was 1:5. The rivers Hare and Kulfo did not need dilution. The

emission concentration of the sample was determined again with three independent sample preparation per sample tested for statistical precision. Operation of the Corning 410 Flame Photometer as Followed in this Test. The fuel supply was turned on at the source. The power switch was depressed. The LED was illuminated and the air compressor ignition cycle started. The filter selector was set to the K (Potassium) position. The nebulizer inlet tube was inserted in a beaker containing approximately 100 mL of diluent and 15 minutes was allowed for the operating temperature to stabilize. During the warm up period the set of calibration standard solutions were prepared. The blank solution was aspirated and the “Blank” control was adjusted until the display read zero. The 12 mg L⁻¹ K standard was aspirated for about 20 seconds. Then the “Coarse” and “Fine” controls were adjusted until the reading is set to 12.0. The standard solutions were aspirated and the measurements were read. The blank solution was aspirated and reset to zero before each standard was tested. The standards were measured proceeding from the most dilute to the highest concentration standard. The samples of water were aspirated similarly and the emission readings were recorded.



Figure 3.3.17.1 Flame Photometer Used for Potassium and Sodium Determination

3.3.18 Precision and Detection Limit of Potassium Determination

The relative standard deviation decreases with concentration. The deviation is mostly less than 10 %. Due to the low values, the 95 % cut-off limit is RSD of 9%. The mean value is 2.82 %. It appears that 0.28 mg L⁻¹ is the limiting value for

potassium determination in these data. The statistical cumulative analysis shows 0.26 mg L^{-1} as the cut-off method detection Limit with a mean value of 0.11 mg L^{-1} .

3.3.18 RIVER DISCHARGE

Two measurement methods were used simultaneously 1) the Velocity – Area Method Using current meter and 2) velocity – area method employing the floating technique. Operating Procedure as Followed in this Test. Equipment Used in the Measurements: 1. OSK 1043 Hiroi's Electric Current Meter. 2. Staff gauge for measuring depth. 3. Stopwatch. Procedure: 1) All measurements were made to the nearest centimeter. 2) Two pegs were driven across the river width and a graduated string was tied at each end so that the string is orientated at right angle to the river flow direction. 3) The “zero” mark from one end of the string was adjusted to coincide with river shore so that measurements starts from it ($b_0 = 0$ in figure 3.3.18.1 below). 4) The next horizontal distance b_1 was measured from this end. 5) the channel depth at this point was measured with a staff gauge and the measurement was recorded. 6) The current meter was held at $0.6 * d$ measured from the water surface, where d is the measured depth of the river. The counter was set to the “ON” position after 15 seconds and at the same time the stopwatch was started. 7) At the 50th second on the stop watch the counter was set concurrently to the “OFF” position. The reading on the counter was recoded. 8) The next measurement was repeated at point b_2 and this continued up to the other end of the river section.

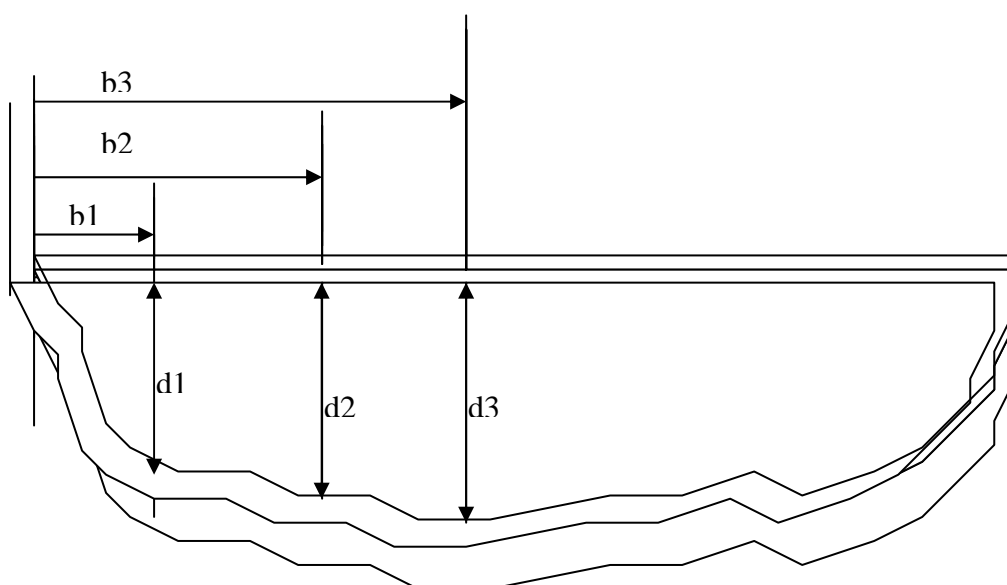


Fig. 3.3.18.1 Stream Cross – Section and Current Meter Positions

Calculation

The discharge through each section was calculated as

$$\begin{aligned}
 Q_1 &= \frac{b_2 - b_0}{2} * d_1 * \bar{v}_1 \\
 Q_2 &= \frac{b_3 - b_1}{2} * d_2 * \bar{v}_2 \\
 &\cdot \dots\dots\dots (3.20) \\
 &\cdot \\
 Q_N &= \frac{b_{N+1} - b_{N-1}}{2} * d_N * \bar{v}_N
 \end{aligned}$$

Where \bar{v} is the mean velocity in meters per second determined from the current meter reading by the following calibration equation:

$$\bar{v} \text{ (m/Sec)} = 0.120 * N + 0.001 \dots\dots\dots (3.21)$$

Where N is the number of revolutions of the current meter propeller per second. The b and d values are the width and depth measurements respectively as shown in the above figure in meters.

The total discharge was then summed as:

$$Q_{TOTAL} = Q_1 + Q_2 + Q_3 + Q_4 + \dots\dots + Q_N + \dots\dots\dots (3.22)$$

2) Floating Technique: In this method the surface velocity was determined by observing the movement of a suitable floating object over a distance of about 40 meters. The velocity was calculated as the average of three observations in which the distance of 40 meters was divided by the observed time in seconds. This velocity was multiplied by the cross sectional area determined above for the current meter to give the discharge. A correction factor of 0.8 was applied to convert the surface velocity to the average velocity. This factor however is variable [26, 27].

3.3.19 SILICA

(Reference Eaton, A.D., L.S. Clesceri and A.E. Greenberg (1995) *Standard Methods for the Examination of Water and Wastewater*, 19th edition, American Public health Association, American Water Works Association and Water Environment Federation, Washington, D.C.)

Silica was determined spectrophotometrically by the hetero-poly blue method using ammonium Molybdate as the colour-forming reagent. 1) Equal volumes (by dilution) of Standards and samples were pipetted in to 50 mL plastic beakers. 2) To each beaker 1.0 mL of 1+1 HCl was added. 3) This was followed immediately by the addition of 2.0 mL of Ammonium Molybdate reagent. The solution was mixed and left to stand for 5-10 minutes. 4) 2.0 mL of Oxalic acid was added and the solution mixed thoroughly. 5) After at least 2 minutes has elapsed 2.0 mL of the reducing reagent was added and the solution mixed well. 6) After 5 minutes the blue colour was measured spectrophotometrically at 815 nm against similarly prepared blank solution. The Silica concentration was determined from the calibration line prepared from the known standards.

3.3.19.1 Determination of Absorption of Standards

. The absorption of silica standards using the hetero-poly blue method employed for determining silica spectrophotometrically is given in table 3.3.19.1.

Table 3.3.19.1 Absorption Data for silica standards with photometric determination by heteropoly blue method at 815 nm. The precision at low silica concentration is quite low (see the first four rows). Therefore, low silica concentrations require greater number of samples to improve the precision.

Label	mL added/50 mL	mg L ⁻¹ of Silica (as SiO ₂)	Absorption Measurements			Mean (Abs)	Standard Deviation (Abs)	Relative Standard Deviation
			Sample 1 (Abs)	Sample 2 (Abs)	Sample 3 (Abs)			
S0	0	0	0	0.006	0.005	0.0037	0.0032	87%
S1	0.5	0.01	0.006	0.007	0.015	0.0065	0.0049	75%
S2	1	0.02	0.003	0.01	0.005	0.0075	0.0036	48%
S3	2	0.04	0.006	0.006	0.011	0.0077	0.0028	37%
S4	5	0.1	0.018	0.018	0.014	0.0167	0.0023	13%
S5	10	0.2	0.03	0.04	0.036	0.0353	0.0050	14%
S6	50	1	0.12	0.13	0.13	0.1267	0.0057	4%

3.3.19.2 Scatter Plot and Calibration of Standards

Fig. 3.3.19.1 shows the line of fit for silica absorption of standards.

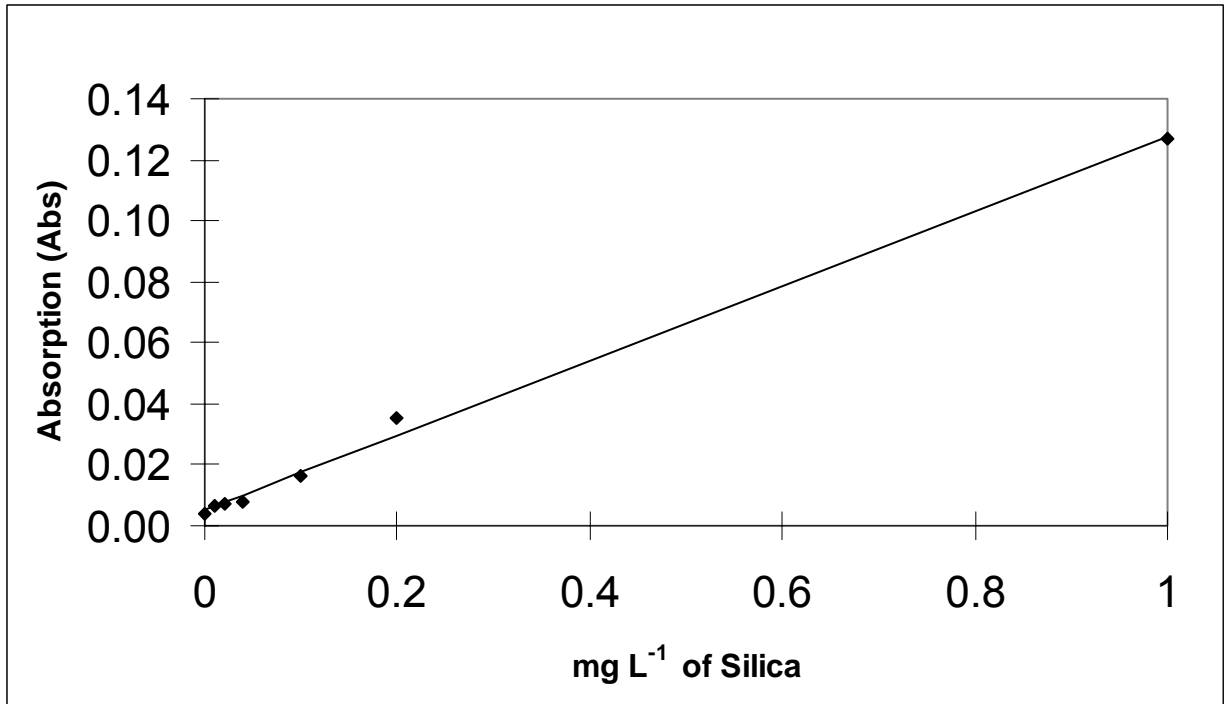


Fig. 3.3.19.1 Best Line of Fit for Silica Absorption of Standards (Spectrophotometric Determination with Methylene Blue at 650 nm) displaying linearity over smaller range of values. Almost all of the samples need to be diluted in order to bring the absorption to the linear range.

3.3.19.2 Precision and Method Detection Limit

The variation of relative standard deviation with absorption is given in Fig.3.3.19.2. The RSD value falls below 10% for concentration of silica above 0.2 mg L⁻¹ only. The method detection limit calculated for the blank samples is 0.015 mg L⁻¹ of silica measured as SiO₂.

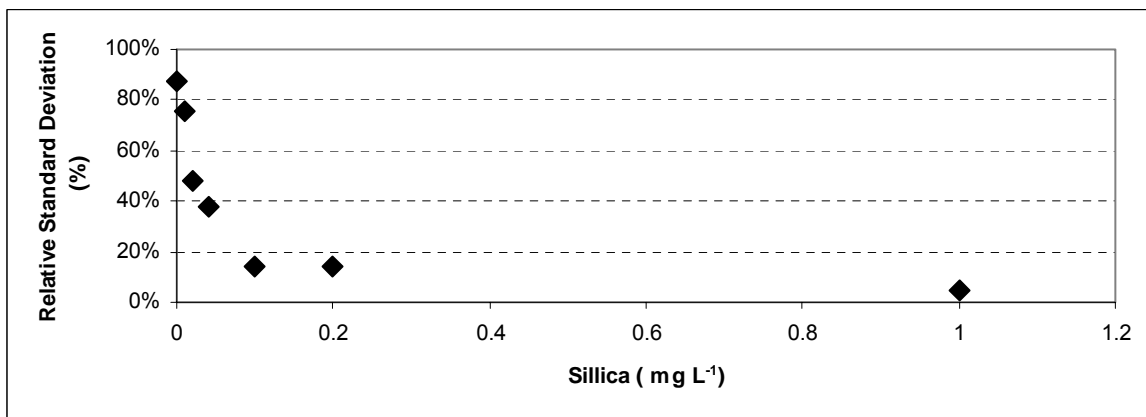


Fig. 3.3.19.2 Variation of Relative Standard Deviation with Concentration for Silica. The precision is low at low concentration of silica. Sample dilution must not bring the concentrations so low as to reduce the precision of determination shown above.

3.3.20 SODIUM

(Reference Eaton, A.D., L.S. Clesceri and A.E. Greenberg (1995) Standard Methods for the Examination of Water and Wastewater, 19th edition, American Public Health Association, American Water Works Association and Water Environment Federation, Washington, D.C.)

Flame Emission Photometric Method was used in this research. The samples of water to be tested were all filtered through glass fiber filter. The first few milliliters filtered were thrown to waste and filtration was continued for few minutes after the water has been filtered out of the glass tube. The following blank and standard solutions were pipetted in to each of 50 mL volumetric flasks from the intermediate Sodium solution. Three independent solutions were prepared for each standard (See Table 3.3.20.1 below).

Table 3.3.20.1 Sodium Standard Solutions – Volume added and concentrations for determination by flame photometric procedure.

Standard Label	S0	S1	S2	S3	S4	S5	S6
mL of Standard added in a 50 mL Volumetric Flask	0	1	2	3	4	5	6
mg L ⁻¹ of Sodium (Na)	0	2	4	6	8	10	12

Each of the 50 mL flasks was filled up to the mark with distilled water. The emission concentration of each standard was determined using the Corning 410 C Flame Photometer operating procedure, which is listed below. The sample of water to be tested was brought and diluted with distilled water so that the emission of the diluted sample falls in the 1 – 12 mg L⁻¹ measurement range. For Lake Abaya a dilution ratio of 1:50 was used and for Lake Chamo the dilution ratio was 1:100. The rivers Hare and Kulfo did not need dilution for Sodium determination. The emission concentration of the sample was determined again with three independent sample preparation per sample tested for statistical precision.

3.3.20.1 Precision and Detection Limit of Sodium Measurement

The analysis of RSD data for sodium show a mean RSD value of 0.73 and median 0.73%. The 95% cut-off point was 1.90%. Therefore, the maximum limit of relative standard deviation is considered to be 1.9% for these data. The scatter of method detection limit is shown below. 0.3 mg L⁻¹ is the probable method detection limit for sodium determination

3.3.21 SULFATE

(Reference Eaton, A.D., L.S. Clesceri and A.E. Greenberg (1995) *Standard Methods for the Examination of Water and Wastewater*, 19th edition, American Public health Association, American Water Works Association and Water Environment Federation, Washington, D.C.)

Spectrophotometer determination of Barium Sulphate Turbidity Formation at a wavelength of 420 nm. The following standard solutions were prepared from the standard sulphate solution to each of the three 100 mL volumetric flasks. Three solutions were prepared for each standard (See Table 3.3.21.1).

Table 3.3.21.1 Sulphate Standard Solutions – Volume added and Concentrations.

Standard	S0	S1	S2	S3	S4	S5
mL Added	0	3	5	10	20	25
mg L ⁻¹ of Sulphate	0	6	10	20	40	50

10 mL of the electrolyte solution was added. Then after 20 mL of the stabiliser solution was added. The mixture was diluted to the 100 mL mark with distilled water. About 0.3 gm of Barium Sulphate powder was added and inverting for about 2 minutes mixed the contents. Between 10 and 50 mL of the sample was taken in to 100 mL volumetric flasks as appropriate and the procedure above is also repeated for the samples as well. The solutions were measured within 5 minutes of reaction time for absorption at a wavelength of 420 nm against a reagent blank as reference.

Operation of the Jenway 6100 Spectrophotometer.

- 1) The unit was connected to the mains power supply and a period of 15 – 30 minutes was allowed for warming up to stabilize the readings.
- 2) After warming up period, the wavelength of measurement was selected by turning the wavelength adjustment knob until the desired wavelength is displayed.
- 3) The %T was selected by the use of the MODE keypad.
- 4) The chamber lid was opened. With the blank cuvette in position, the shutter was moved to the closed position. The chamber lid was closed thereafter. The CAL keypad was pressed and the display updated to zero.
- 5) A cuvette was filled with distilled water and inserted in to the cell holder. The shutter was located in to the open position. The CAL keypad was pressed. The display adjusted to 100 %.
- 6) The MODE keypad was pressed to display the ABS mode while the blank cuvette was in position. The display updated to zero.
- 7) The cuvette was filled with the standards and the sample in a series and placed in to the cell holder and the chamber lid closed. The absorption reading was in each case was noted.

3.3.21.1 Sulphate Standards Absorption

The following values were obtained for the absorption of sulphate standards by the Barium Sulphate Turbidimetric method (Table 3.3.21.2 below).

Table 3.3.21.2 Absorption Data for Sulphate Standards and RSD Values. The Barium Sulphate turbidimetric method gives stable absorption as displayed by the low relative standard deviation except for the blank samples. Three sample repetitions are adequate in most cases.

Standard	mL Added	mg L ⁻¹ of Sulphate	Absorption Measurement			Mean (Abs)	Standard Deviation (Abs)	Relative Standard Deviation (%)
			Sample 1 (Abs)	Sample 2 (Abs)	Sample 3 (Abs)			
S0	0	0	0.005	0.010	0.010	0.008	0.002	34%
S1	3	6	0.030	0.032	0.030	0.030	0.001	4%
S2	5	10	0.035	0.040	0.040	0.038	0.002	7%
S3	10	20	0.075	0.070	0.072	0.072	0.002	3%
S4	20	40	0.140	0.100	0.130	0.135	0.020	15%
S5	25	50	0.150	0.155	0.170	0.158	0.010	6%

The calibration line for sulphate absorption was determined using the absorption data given in table 3.3.2.1.2 above and the concentrations of sulphate for the standards as (y-x) variables in linear regression. Fig. 3.3.21.2 shows the regression line.

3.3.21.2 Calibration line of Absorption of Sulphate Standards

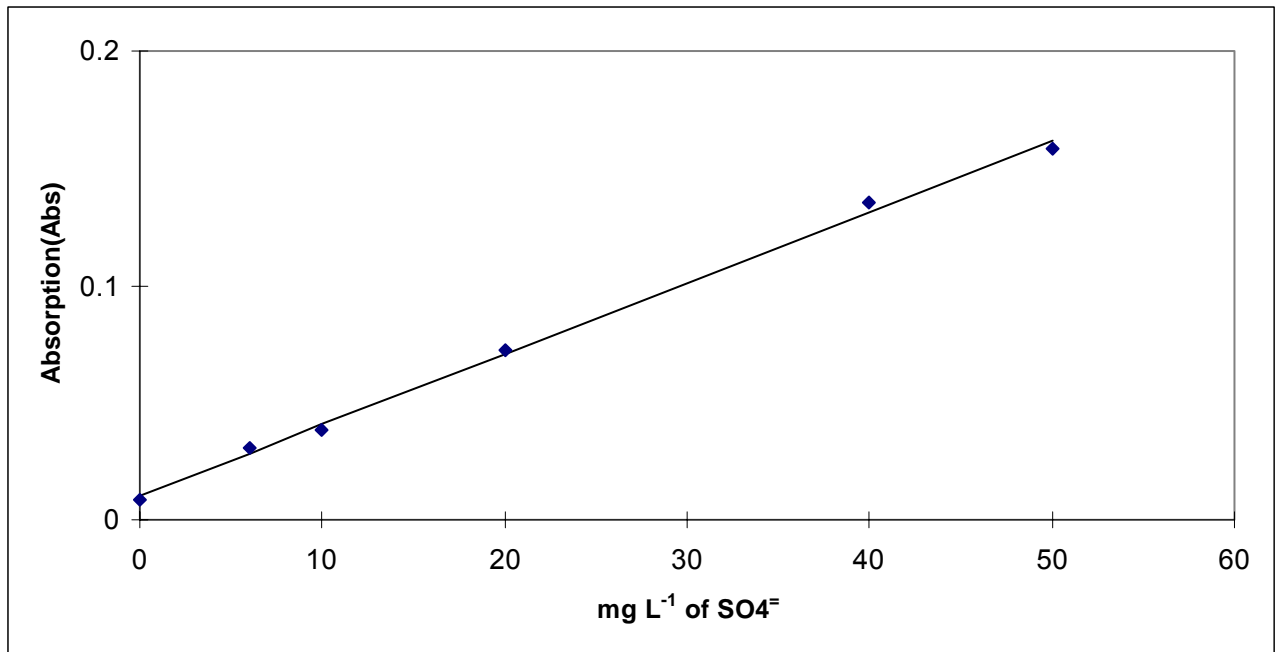


Fig. 3.3.21.1 Calibration Line for Sulfate Absorption Spectrophotometric at 425 nm. The photometric absorption displays linearity over a wider range of sulphate concentration as shown in the graph above.

3.3.21.3 Precision and Method Detection Limits

The relative standard deviation varies from 0-15 % for the non-blank absorption of samples taking three repetitions for the standards. The measurement range gives 0-50 mg L⁻¹ of sulphate over which there is a linear response of absorption over concentration. The method detection limit calculation is given in Table 3.3.21.3. The value corresponding to the blank absorption is taken as the method detection limit. This value is around 1.0 mg L⁻¹ of Sulphate.

Table 3.3.21.3 Method Detection Limit Calculation from Sulphate Standard Absorption data. The MDL value is determined as $S \cdot t$ where S is the standard deviation of the blank absorption divided by the slope of the calibration line and t is the critical value of the student's distribution determined from Table 3.2.5.1

Standard	mL Added	mg L ⁻¹	Absorption Measurements			Mean (Abs)	Standard Deviation (Abs)	Relative Standard Deviation (%)	Student t	MDL mg L ⁻¹
			Sample 1 (Abs)	Sample 2 (Abs)	Sample 3 (Abs)					
S0	0	0	0.005	0.01	0.01	0.008	0.002	34%	4.541	1.01
S1	3	6	0.03	0.0325	0.03	0.030	0.001	4%	4.541	
S2	5	10	0.035	0.04	0.04	0.038	0.002	7%	4.541	
S3	10	20	0.075	0.07	0.072	0.072	0.002	3%	4.541	
S4	20	40	0.14	0.1	0.13	0.135	0.020	15%	4.541	
S5	25	50	0.15	0.155	0.17	0.158	0.010	6%	4.541	

3.3.22 SULFIDE

(Reference Eaton, A.D., L.S. Clesceri and A.E. Greenberg (1995) *Standard Methods for the Examination of Water and Wastewater*, 19th edition, American Public Health Association, American Water Works Association and Water Environment Federation, Washington, D.C.)

Sulfide in this research was determined using the Iodometric Method. Iodine reacts with Sulfide oxidizing it to sulfur. Reducing substances such as thiosulphate, sulfite and organic compounds may interfere. Interferences may be eliminated by precipitating sulfide as Zinc sulphate, removing the supernatant and replacing it with distilled water. A 200 mL sample was pipetted in to 300 mL Erlenmeyer flask. 0.15 mL (about 3 drops) of the 2N Zinc Acetate solution was added. 0.1 mL (2 drops) of 6N NaOH was added. The solution was stoppered and mixed. The precipitate was settled and later filtered with glass fiber filter. The precipitate was returned to the original 300 mL Erlenmeyer flask and about 100 mL water was added. Iodine solution was measured in to the 300 mL Erlenmeyer flask from a burette in excess of the sulphide present. 2 mL of the 6N HCl was added. The entire solution was back

titrated with 0.025 N Na₂S₂O₃ solution using starch as indicator to the disappearance of the blue color.

Calculation: The sulphide was calculated using the following formula:

$$\text{mg S}^{2-} / \text{L} = \frac{[(A(\text{mL}) - B(\text{mol.L}^{-1})) - (C(\text{mL}) - D(\text{mol.L}^{-1}))] * 16000}{\text{mL Sample}} \dots\dots\dots (3.23)$$

Where A = mL of Iodine solution added. B = Normality of Iodine Solution. C = mL of Na₂S₂O₃ titrated and D = normality of Na₂S₂O₃ solution.

3.3.23 TOTAL RESIDUE

(Reference Eaton, A.D., L.S. Clesceri and A.E. Greenberg (1995) Standard Methods for the Examination of Water and Wastewater, 19th edition, American Public health Association, American Water Works Association and Water Environment Federation, Washington, D.C.)

The Measurement Method used in this research was the Gravimetric Method with Sample drying in an Oven. A well-mixed sample is evaporated in a weighed dish and dried to constant weight in an oven at 103 – 105 °c. The increase in weight over that of the empty dish represents the total solids. The evaporating dishes were washed with water and chlorine rinsed with distilled water and kept in the oven at 103 – 105 degrees for 1 hour. Prior to weighing, the dishes were taken out of the oven and kept in a dessicator to balance the temperature. When the temperature was stabilized, the dishes were weighed with a balance and the empty weight was recorded. The sample bottle was thoroughly shaken and a 100 mL volume was pipetted using a measuring pipette on to the dishes. Four dishes were prepared for each sample. The dishes with the sample were dried in the oven at a temperature of 103 – 105 degrees for 24 hours and then cooled in a dessicator. The measurement of weight was taken after the dishes temperature has stabilized and the measurements were recorded.

Calculation

The total Solids was calculated using the formula:

$$\text{mg Total Solids. L}^{-1} = \frac{(B(\text{mg}) - A(\text{mg})) * 1000}{\text{Sample Volume , mL}} \dots\dots\dots (3.24)$$

Where A = Weight of dish, mg And B = Weight of dried residue + dish, mg,



Figure 3.3.23.1 Drying Oven Used for the Total Solids Determination

3.3.23.1 Precision and Method Detection Limit for Total Residue

The whole range of determination of total solids was analyzed for the relative standard deviation. The sample set has a median RSD of 7.5 % and a mean of 8.6. The 95% limit of rejection is 20 %, which is considered the highest limit for a relative standard deviation. It is believed that with better precision of the instrument, a lesser amount of RSD can be arrived at. The method detection limit is calculated as 10 mg L⁻¹.

3.3.24 TOTAL VOLATILE AND FIXED RESIDUE

(Reference Eaton, A.D., L.S. Clesceri and A.E. Greenberg (1995) Standard Methods for the Examination of Water and Wastewater, 19th edition, American Public health Association, American Water Works Association and Water Environment Federation, Washington, D.C.)

The procedure used was gravimetric with ignition of sample at 550 °C. The residue obtained from the determination of total solids is ignited at 550 °C in a muffle furnace. The loss of weight on ignition is reported as mg L⁻¹ total volatile solids (TVS) and that which is remaining is total fixed solids (TFS). The clean evaporating dish was heated to 550 °C for one hour to remove organic matter that may be adhering to the dish. The dishes were cooled in a dessicator until they were used. The procedure for Total solids was followed. After Total Solids has been calculated, the porcelain was placed

in the muffle furnace at 550 °C for one hour. The dishes were reweighed until constant weight was obtained.



Figure 3.3.24.1 Drying Furnace used for Volatile Solids Determination

The total fixed solid and volatile solids were calculated as:

$$\text{Total Fixed Solids mg L}^{-1} = \frac{(C(\text{mg}) - A(\text{mg})) * 1000}{\text{Sample Volume , mL}} \dots\dots\dots (3.25)$$

$$\text{Total Volatile Solids mg L}^{-1} = \frac{(B(\text{mg}) - C(\text{mg})) * 1000}{\text{Sample Volume , mL}} \dots\dots\dots (3.26)$$

Where A = Weight of empty dish, mg

B = Weight of dried residue + dish, mg at (103-105)⁰C and

C = Weight of dish + dried residue at 550⁰C.

3.3.24.1 Precision and method Detection Limit for Volatile and Fixed Residue

The relative standard deviation is 20% and the method detection limit is calculated as 15 mg L⁻¹.

3.3.25 TURBIDITY

(Reference Eaton, A.D., L.S. Clesceri and A.E. Greenberg (1995) Standard Methods for the Examination of Water and Wastewater, 19th edition, American Public health Association, American Water Works Association and Water Environment Federation, Washington, D.C.)

The Nephelometric Turbidimetric method has been used in this research. The instrument used was the HACH Model 2100A Turbidimeter. Standards supplied with this equipment were available in the ranges of 0.1, 1, 10, 100 and 1000 NTU. The cell was dried with a tissue paper that would not leave water film on the cell surface. Standard cells supplied with the instrument (0.1, 1, 10, 100 and 1000 NTU) were cleaned on their outer surface and made ready. Before turning on, the needle was checked to read zero. The power switch was turned on. The instrument was allowed to warm up for 15 minutes. Samples were vigorously shaken and transferred to each of Five 300 mL Erlenmeyer Flasks. The sample in these flasks was stirred further with magnetic stirrer at 200 Revolutions per minute. The calibration was started by selecting measuring range starting from 1000. The cell riser was placed in the sample cell compartment followed by the standard cell 1000. The light shield was placed over the standard cell. If the reading was not 1000, it was adjusted to read this value by turning the right STANDARDISE control knob forward and backward accordingly. The sample was transferred from the flask to the sample cell while the sample is being in mixed form. A minute or so was waited for until the air bubble from the sample cell disappeared. The standard in the cell compartment was then replaced with the sample cell. The reading was noted while the light shield was on place. If the reading was less than 100, the trial was repeated using the 100 NTU standard. If the reading further falls below 100, the cell riser was removed and the test was carried out using, successively the lower standards of 10, 1 or 0.1 NTU. The sample test was continued for the five sample repetitions and the readings were recorded. For high turbidity water, usually well over 100 NTU, several dilutions of the sample were prepared using distilled water and the readings were taken for these dilutions.



Figure 3.3.25.1 Turbidimeter used for the Determination of Turbidity

3.3.25.1 Precision and Method Detection Limits for Turbidity Measurement

The relative standard deviation of measurement varies between 0 and 7% for the entire data. With multiple dilution procedure it is possible to arrive at better precision for turbidity measurements. The 95% cut-off limit for turbidity relative standard deviation is about 5% from the cumulative percentage graph. The mean value is 1.7%. For the method detection limit, the limit is 1 NTU with respect to the measured values.

3.3.26 WASTE POLLUTION INDICATOR BACTERIA (COLIFORMS)

(Reference Eaton, A.D., L.S. Clesceri and A.E. Greenberg (1995) Standard Methods for the Examination of Water and Wastewater, 19th edition, American Public Health Association, American Water Works Association and Water Environment Federation, Washington, D.C.)

The multiple-tube fermentation technique for members of the coliform group (MPN – Most Probable Number method) was used. The definition and procedure as well as method of estimating the MPN using tables is elaborated below.

3.3.26.1 Introduction and Background

Traditionally, indicator bacteria have been used to determine the possible presence and to estimate the amount of faecal contamination in water samples. The detection of indicator bacteria is preferred over direct pathogen detection because the former are considered to be normal, non-pathogenic intestinal inhabitants that are present in faeces and wastewater in much higher numbers than pathogenic micro organisms and because they are technically easier to detect and quantify than pathogens. Present standards for the sanitary quality of water with respect to faecal contamination, are expressed in terms of concentrations of indicator bacteria. The word "coliform" has been used to describe various genera of the family *Enterobacteriaceae* that ferment lactose. It should be emphasized that "coliforms" are actually defined in operational or functional terms that are based upon the media and incubation conditions used for their isolation and quantification. None of these operational definitions detects all members of the family *Enterobacteriaceae* and some include members of other families.

3.3.26.2 Objective: The objective of the MPN test was to estimate the total and faecal coliform and *E. coli* concentrations of samples water within the Abaya – Chamo Basin and thereby examine the extent of bacterial contamination of the various water sources.

3.3.26.3 Method of Determination: The Multiple-Tube Fermentation Technique

The Multiple-Tube Fermentation Technique defines coliforms as "all facultative anaerobic, gram-negative, non-spore-forming, rod-shaped bacteria that ferment lactose with gas formation within 48 hr. at 35°C." In this method the coliform bacteria are detected and quantified by their ability to grow and produce gas in lactose-containing liquid medium under specified incubation conditions. This technique actually consists of three successive steps or tests: Presumptive, Confirmed and Completed. For the Presumptive Test, dilutions of the sample are inoculated into fermentation tubes of lactose or lauryl tryptose broth and incubated at 35°C for 48 hr. For the Confirmed Test, organisms from all positive fermentation tubes (those with growth plus gas) of the Presumptive Test are transferred to fermentation tubes of brilliant green lactose bile broth and incubated at 35°C for 48 hr. Tubes showing both growth and gas are considered positive Confirmed tubes. For the Completed Test, organisms from positive Confirmed tubes are isolated in pure culture on agar plates of differential/selective media (Endo or eosin methylene blue agar) and then tested

for: (1) growth and gas production in fermentation tubes of lactose or lauryl tryptose broth incubated at 35°C for 48 hr.; and a negative reaction in the Gram stain. For a positive Completed Test, the organisms must show growth plus gas production in the fermentation tubes and be Gram negative.

Growth Media1. Presumptive Phase

- a. Lauryl tryptose broth was used in the presumptive portion of the multiple-tube test. Since the medium has been refrigerated after sterilization, it was incubated overnight at room temperature (20°C) before use. The dehydrated ingredients was added to water and mixed thoroughly, and heated to dissolve. The pH was checked to be 6.8 ± 0.2 after sterilization. Sufficient medium was dispensed before sterilization in fermentation tubes with an inverted vial, to cover inverted vial at least one-half to two-thirds after sterilization. The tubes were capped with metal caps.

Table 3.3.26.1 Preparation of Lauryl Tryptose Broth

Inoculum <i>mL</i>	Amount of Medium in Tube <i>mL</i>	Volume of Medium + Inoculum <i>mL</i>	Dehydrated Lauryl Tryptose Broth Required <i>g/L</i>
1	10 or more	11 or more	35.6
10	10	20	71.2
10	20	30	53.4
20	10	30	106.8
100	50	150	106.8
100	35	135	137.1
100	20	120	213.6

2. Confirmed Phase

Culture medium: Brilliant green lactose bile broth was used in fermentation tubes for the confirmed phase. The dehydrated ingredients were added to water, mixed thoroughly, and heated to dissolve. pH was checked to be around 7.2 ± 0.2 after sterilization. Before sterilization, the media was dispensed in fermentation tubes

with an inverted vial, sufficient medium to cover inverted vial at least one-half to two-thirds after sterilization. The tubes were capped with metal caps.



Figure 3.3.26.1 Incubator used for Coliform growth and Determination

3.3.26.4 PROCEDURE:

A. Sample Dilution: Sample(s) were diluted serially 10-fold. Mixing of sample was carried out by shaking the sample 25 times before diluting. To make 10-fold dilutions, 1 ml of sample was pipetted into a 99-ml dilution blank. The top of the dilution container was sealed and mixed vigorously 25 times.

B. Two-Step-Tube Fermentation Technique for Total and Faecal Coliforms (5 tubes per dilution):

1: Inoculation of tubes for presumptive test: 25 fermentation tubes were placed in a test tube rack as groups of 5 dilutions, and marked as to their dilutions. Using a 5- or 10-ml pipet, 1-ml volumes of each sample dilution to be tested was inoculated into the 5 replicate tubes. The tubes were incubated at 35°C in an incubator. Observation of presumptive tubes and inoculation of tubes for Confirmed Total and Faecal Coliform Tests and for *E. coli* was carried out after 24 and 48 hours. 2. Reading Presumptive Tubes: After incubation period, the

rack of tubes was gently shaken back and forth several times to release gas in positive tubes. All tubes were examined for the presence of growth (turbidity or cloudiness) and gas in the inverted tube. Tubes showing both were recorded as presumptive positive. All lactose broth fermentation tubes that are Presumptive positive at about 24 hr and all additional Presumptive positive tubes at 48 +/- 3 hr were submitted to the confirmed tests. A sterile wood applicator was inserted into the broth of the positive tubes to a depth of >2 cm to wet the end. The organisms on the wet end of the applicator were transferred to a fermentation tube of brilliant green lactose bile (BGLB) broth by briefly immersing the wet end of the applicator into the BGLB broth. The same applicator and same procedure were used to transfer material from the same Presumptive positive tube to a fermentation tube of EC medium containing MUG. The applicator was discarded. A fresh applicator stick was used for each positive Presumptive tube. The BGLB broth tubes were inoculated in a 35°C incubator and the EC tubes a in 44.5°C water bath. 3. Reading Confirmed Tubes. The EC tubes were examined at 24 +/- 2 hr for growth plus gas. Tubes showing both were scored as Confirmed positive for faecal coliforms. The BGLB tubes were examined at 48 +/- 3 hr for growth plus gas. Tubes showing both were scored as Confirmed positive for total coliforms.

Calculation of Most Probable Number

The total and faecal coliform and *E. coli* densities of the sample were calculated from the number of positive and negative tubes of three sample dilutions according to the procedures described in Standard Methods for the Examination of Water and Wastewater and using the tables provided below. The Most Probable Number of total and faecal coliforms per 100 ml was computed and recorded using the data from the confirmed tubes (BGLB and EC). Also the upper and lower 95% confidence limits for these MPN values were recorded. The MPN values and confidence limits are found in the same table for three dilutions and five tubes per dilution (source: Standard Methods for the Examination of Water and Wastewater). The coliform density is stated as most probable Number per 100 mL of sample. Dilution factors were applied in the calculation of MPN for dilution sets smaller than the standard set (10, 1, and 0.1) to which the tables apply.

Table 3.3.26.2: MPN Index for Serial Dilutions of Sample

Number of Tubes Giving Positive Reaction out of			MPN Index per 100 mL	95% Confidence Limit (Lower)	95% Confidence Limit (Upper)
5 of 10 mL each	5 of 1 mL each	5 of 0.1 mL each			
0	0	0	<2		
0	0	1	2	<0.5	7
0	1	0	2	<0.5	7
0	2	0	4	<0.5	11
1	0	0	2	<0.5	7
1	0	1	4	<0.5	11
1	1	0	4	<0.5	11
1	1	1	6	<0.5	15
1	2	0	6	<0.5	15
2	0	0	5	<0.5	13
2	0	1	7	1	17
2	1	0	7	1	17
2	1	1	9	2	21
2	2	0	9	2	21
2	3	0	12	3	28
3	0	0	8	1	19
3	0	1	11	2	25
3	1	0	11	2	25
3	1	1	14	4	34
3	2	0	14	4	34
3	2	1	17	5	46
3	3	0	17	5	46
4	0	0	13	3	31
4	0	1	17	5	46
4	1	0	17	5	46
4	1	1	21	7	63
4	1	2	26	9	78
4	2	0	22	7	67
4	2	1	26	9	78
4	3	0	27	9	80
4	3	1	33	11	93
4	4	0	34	12	93
5	0	0	23	7	70
5	0	1	31	11	89
5	0	2	43	15	110
5	1	0	33	11	93
5	1	1	46	16	120
5	1	2	63	21	150
5	2	0	49	17	130
5	2	1	70	23	170
5	2	2	94	28	220
5	3	0	79	25	190
5	3	1	110	31	250
5	3	2	140	37	340
5	3	3	180	44	500
5	4	0	130	35	300
5	4	1	170	43	490
5	4	2	220	57	700

Number of Tubes Giving Positive Reaction out of					
5 of 10 mL each	5 of 1 mL each	5 of 0.1 mL each	MPN Index per 100 mL	95% Confidence Limit (Lower)	95% Confidence Limit (Upper)
5	4	3	280	90	850
5	4	4	350	120	1000
5	5	0	240	68	750
5	5	1	350	12	1000
5	5	2	540	180	1400
5	5	3	920	300	3200
5	5	4	1600	640	5800
5	5	5	>2400		

3.4 SUMMARY OF WATER QUALITY PARAMETERS RELATIVE STANDARD DEVIATION AND METHOD DETECTION LIMIT ATTAINED IN THE TESTS

The methods, relative standard deviation and method detection limits for the parameters described in this chapter are given in summary form in Table 3.4.1 shown below.

Table 3.4.1 Summary of Water Quality Parameters, Methods of Determination Relative Standard Deviation and Method Detection Limit Attained in the Tests.

S.No.	Parameter	Method of Determination	Relative Standard Deviation	Method Detection Limit
1	Absorption Data	Spectrophotometer at 400 – 700 nm	2.2 %	0.005 abs
2	Air Pressure	Using Barometer (Field Kit)	NC*	0.5 Bar
3	Air Temperature	Using Thermometer	NC*	0.1°C
4	Alkalinity	By Titration with Hydrochloric Acid	4.4%	3.5 mg L ⁻¹
5	Ammonia	Spectrophotometric Method (425 – 500 nm) with Nessler Reagent	2.1%	0.074 mg L ⁻¹
6	BOD (Winkler)	Measurement of Oxygen uptake of Aerobic Microorganisms by Incubating a Sample plenty in	24%	0.68 mg L ⁻¹

S.No.	Parameter	Method of Determination	Relative Standard Deviation	Method Detection Limit
		Oxygen for 5 days at a temperature of 20 °C.		
7	Calcium	EDTA Titrimetric Method	5 %	1.4 mg L ⁻¹
8	COD	Oxidation with Potassium Dichromate in a reflux	10%	0.9 mg L ⁻¹
9	Chloride	Argentometric Titration	8%	1.5 mg L ⁻¹
10	Chlorophyll a and b	Spectrophotometer with aqueous Acetone Extraction	10%	2 µg L ⁻¹
11	Conductivity	Measurement through a conductivity meter.	2%	0.1µS Cm ⁻¹
12	Dissolved Oxygen	1) The Azide Modification of Iodometric Method (Winkler's Method) 2) Membrane Electrode Technique	2.7%	0.05 mg L ⁻¹
13	Hardness	EDTA Titrimetric Method	4.7 %	2.5 mg L ⁻¹
14	Nitrate	Spectrophotometric determination with Sodium Salicylate (Measurement at 420 nm)	5%	0.05 mg L ⁻¹
15	Nitrite	Spectrophotometric Determination with Aminobenzoic Sulfonamid (absorption measured at 540 nm).	7%	0.004 mg L ⁻¹
16	pH	Potentiometric Measurement with a Glass Electrode	0.2%	0.1 pH units
17	Phosphate	Spectrophotometric with Molybdophosphoric Acid (Absorption measured at 380 nm).	2.7%	1µg L ⁻¹
18	Potassium	Flame Emission Spectrophotometric (Emission measured at a wave length of 766.5 nm).	2.8%	0.1 mg L ⁻¹
19	River Discharge	Using Current Meter and Floating Technique	NA	NA
20	Silica	Spectrophotometric Heteropoly Blue Method (Absorption measured at 650 or 815 nm).	5%	0.015 mg L ⁻¹
21	Sodium	Flame Emission Spectrophotometric (Emission measured at 589 nm)	0.7%	0.1 mg L ⁻¹
22	Sulfate	Turbidimetric Method	1 %	5 mg L ⁻¹
23	Sulfide	Titrimetric	5%	0.5 mg L ⁻¹
24	TDS	Potentiometric Measurement (For field use)	5%	1mg L ⁻¹
25	Total Filterable Residue	Gravimetric with evaporating of sample in an oven at 103 – 105 ⁰ c.	8%	10 mg L ⁻¹
26	Total Residue	Gravimetric with evaporating of sample in an oven at 103 – 105 ⁰ c	8%	10 mg L ⁻¹
27	Total Non-Filterable Residue	Gravimetric with filtration and evaporating of sample in an oven at 103 – 105 ⁰ c	8%	10 mg L ⁻¹
28	Total Volatile and fixed residue	Gravimetric with evaporating of sample in a furnace at 5500c	15%	15 mg L ⁻¹

S.No.	Parameter	Method of Determination	Relative Standard Deviation	Method Detection Limit
29	Turbidity	Nephelometric method.	2%	1 NTU
	<i>*Not Calculated</i>			

CHAPTER FOUR

WATER QUALITY MONITORING RESULTS AND EVALUATION OF DATA

S.No.	CONTENTS	PAGE
4.1	River Water Quality Monitoring Results and Evaluation of Data	116
	4.1.1 Conceptual Basis of Water Quality Change Models	116
	4.1.2 Modelling Water Quality Changes:	116
	4.1.3 Major Ion Concentrations	118
	4.1.4 River Water Quality Response as a Result of Catchment Changes	122
	4.1.5 Nutrient Transport	123
	4.1.6 Seasonal Variation in Water Quality	125
	4.1.7 The Influence of Sodium Dominance on Alkalinity and Buffering Capacity	134
	4.1.8 Relating Pollutant Loading to the Catchment Area and Flow	135
	4.1.9 Influence of Rain Water Quality on the Rivers	136
	4.1.10 Regional Similarity in Water Quality Variation.	137
	4.1.10.1 Intra-River Principal Component analysis	137
	4.1.11 Global Climatic Change Effects	141
	4.1.12 Basis for Future Monitoring	141
	4.1.13 Discussion	142
4.2	Lake Water Quality Monitoring Results and Evaluation	144
	4.2.1 Seasonal Variation	146
	4.2.1.1 Major Ions seasonal Variations	146
	4.2.1.2 PH and Buffering Capacity Seasonal Variation	157
	4.2.2 Long term variation – Conductivity, ionic compositions and Salinity	158
	4.2.3 Silicate, Nitrate Ammonia and Phosphate	165
	4.2.4 Chlorophyll a Concentration	165
	4.2.5 Dissolved Oxygen	166
	4.2.6 Discussion	166
4.3	Investigation of the Water Qualities of Under Ground Water Sources Within the Abaya - Chamo basin	167
	4.3.1 Background to Ground Water Chemical Composition and Variation	167
	4.3.2 Chemical Composition of ground Water Sources in the Abaya – Chamo Basin	170
	4.3.2.1 Variation of chemical Composition with Altitude	170
	4.3.2.2 Chloride Variation	
	4.3.2.3 Conductivity versus TDS Lines of Surface and Ground Water Sources	172
	4.3.2.4 Alkalinity versus Hardness Variation	173
	4.3.2.5 Piper Tri - linear Plots of Ground and Surface Water Samples	175
	4.3.2.6 Seasonal Variation of Under Ground Water Sources	180
	4.3.3 Investigation of Ground Water Pollution	181
	4.3.3.1 Analysis of Ground Water Samples for Common Pollution Factors	185

S.No.	LIST OF FIGURES	PAGE
Fig. 4.1.3.1	River Hare Major Ions (mg L^{-1})	120
Fig. 4.1.3.2	River Kulfo Major Ions (mg L^{-1})	120
Fig. 4.1.3.3	River Sile Major Ions (mg L^{-1})	121
Fig. 4.1.5.1	BOD Variation for the River Water Samples	123
Fig. 4.1.5.2	Ammonia Increase with River Flow (Hare River)	124
Fig. 4.1.5.3	Ammonia Increase with River Flow (Kulfo River)	125
Fig. 4.1.6.1	Alkalinity Time Series for Hare River	126
Fig. 4.1.6.2	Alkalinity Time Series for Kulfo River	126
Fig. 4.1.6.3	River Kulfo Conductivity Time Series	127
Fig. 4.1.6.4	River Hare Conductivity Time Series	127
Fig. 4.1.6.5	Sodium River Hare	127
Fig. 4.1.6.6	Sodium River Kulfo	128
Fig. 4.1.6.7	Turbidity Time Series Data Hare River	128
Fig. 4.1.6.8	Turbidity Time Series Data Kulfo River	128
Fig. 4.1.6.9	PH Variation of River Kulfo	129
Fig. 4.1.6.10	PH Variation of River Hare	129
Fig. 4.1.6.11	Total Solids River	129
Fig. 4.1.6.12	Total Solids River Hare	130
Fig. 4.1.6.13	Potassium River Hare	130
Fig. 4.1.6.14	Potassium River Kulfo	131
Fig. 4.1.6.15	Spectrophotometric Absorption Data for Kulfo River	131
Fig. 4.1.6.16	Spectrophotometric Absorption Data For Hare River (500 Nm)	132
Fig. 4.1.6.17	Calcium Hare River	132
Fig. 4.1.6.18	Calcium Kulfo River	132
Fig. 4.1.6.19	Hardness River Kulfo	133
Fig. 4.1.6.20	Hardness River Hare	133
Fig. 4.1.6.21	Chloride Hare River	133
Fig. 4.1.6.22	Chloride Kulfo River	134
Fig. 4.1.7.1	Variation Of Rivers Alkalinity With Sodium Dominance Index	134
Fig. 4.1.8.1	Comparison Of Weathering Rates For Hare And Kulfo Catchment	135
Fig. 4.1.10.1.1	Scree Plot For River Data Combined	138
Fig. 4.1.10.1.2	Sodium Ions Relationships For Hare-Kulfo Rivers	138
Fig. 4.1.10.1.3	Alkalinity Relationships Between Hare And Kulfo Rivers	139
Fig. 4.1.10.1.4	River Discharge Relationship Between Hare And Kulfo Rivers	139
Fig. 4.1.10.1.5	Turbidity Relationship Between Hare And Kulfo Rivers	140
Fig. 4.1.10.1.6	Chloride Relationship Between Hare And Kulfo Rivers	140
Fig. 4.2.1	Lake Abaya Major Ions (mg L^{-1})	145
Fig. 4.2.2	Lake Chamo Major Ions (mg L^{-1})	145
Figure 4.2.3	Comparison of rainfall and lake Chamo conductivity	146
Fig. 4.2.1.1	Alkalinity Time Series For Lake Chamo	147
Fig. 4.2.1.2	Alkalinity Time Series For Lake Abaya	147
Fig. 4.2.1.3	Hardness Lake Abaya	148
Fig. 4.2.1.4	Hardness Lake Chamo	148
Fig. 4.2.1.5	Lake Abaya Conductivity Time Series	149
Fig. 4.2.1.6	Lake Chamo Conductivity Time Series	149
Fig. 4.2.1.7	Chloride Lake Abaya	150
Fig. 4.2.1.8	Chloride Lake Chamo	150
Fig. 4.2.1.9	PH Variation Of Lake Abaya	151
Fig. 4.2.1.10	PH Variation Of Lake Chamo	151
Fig. 4.2.1.11	Sodium Lake Abaya	152
Fig. 4.2.1.12	Sodium Lake Chamo	152
Fig. 4.2.1.13	Potassium Lake Abaya	153
Fig. 4.2.1.14	Potassium Lake Chamo	153

S.No.	LIST OF FIGURES	PAGE
Fig. 4.2.1.15	Total Solids Lake Chamo	154
Fig. 4.2.1.16	Total Solids Lake Abaya	154
Fig. 4.2.1.17	Volatile Solids Lake Abaya	154
Fig. 4.2.1.18	Volatile Solids Lake Chamo	155
Fig. 4.2.1.19	Turbidity Time Series Data Lake Abaya	155
Fig. 4.2.1.20	Turbidity Time Series Data Lake Chamo	155
Fig. 4.2.1.21	Spectrophotometric absorption Data For Lake Abaya (500 Nm)	156
Fig. 4.2.1.22	Spectrophotometric Absorption Data For Lake Chamo (500 Nm)	156
Fig. 4.2.1.23	Comparison Of Turbidity Variation For Lakes Abaya And Chamo	157
Fig. 4.2.2.1	Trends In Major Ion Concentration For Lake Chamo	159
Fig. 4.2.2.2	Trends In Salinity Of Lake Chamo	160
Fig. 4.2.2.3	Trends In Salinity Of Lake Abaya	160
Fig. 4.2.2.4	Chloride And Sodium Co variation For Lake Chamo Over Years 1970 – 2003	161
Fig. 4.2.2.5	Inflow Reduction To Lake Chamo Since 1970	162
Fig. 4.2.2.6	Average Yearly Abaya Lake Level	164
Fig. 4.3.2.1.1	Variation of TDS with altitude in the Ground Water Sources (Arbaminch - Sodo)	170
Fig. 4.3.2.2.1	Chloride Variation (Sodo - Arbaminch Route)	171
Figure 4.3.2.2.2	The location of water quality samples within the study area	172
Fig. 4.3.2.3.1	Conductivity vs. TDS Lines for Surface and Ground Water Sources in the Abaya Chamo Basin	173
Fig. 4.3.2.4.1	Hardness Versus Alkalinity variation for Ground Water samples	174
Fig. 4.3.2.4.2	Hardness Versus Alkalinity Variation for Surface and Ground Water samples	174
Fig. 4.3.2.5.1	Piper Trilinear Plot of Surface And Subsurface Water Samples From Abaya-Chamo	177
Fig. 4.3.2.5.2	Piper Trilinear Plot of Springs And Ground Water Samples From Arbaminch – Sodo Area	178
Fig. 4.3.2.5.3	Piper Trilinear Plot Of Surface And Subsurface Water Samples From Arbaminch Area	179
Fig. 4.3.2.6.1	Conductivity Time Series Arbaminch Spring Supply	180
Fig. 4.3.2.6.2	Conductivity time Series AWTI Ground Water supply	180
Fig. 4.3.3.1	Plot of Phosphate against Nitrate for Ground Water samples	182
Fig. 4.3.3.1.1	Eigen value Plot for Ground Water Samples	186
Fig. 4.3.3.1.2	Factor Analysis Results of Ground Water Pollution investigation	188
Fig. 4.3.3.1.3	Factor Loading Plots for Ground Water Pollution Investigation Data	191

S.NO.	LIST OF TABLES	PAGE
Table 4.1.3.1	Ranges of Variation of Chemical Concentrations of Rivers and Lakes	119
Table 4.1.9.1	Comparison of Precipitation Chemistry with that of Kulfo River	136
Table 4.2.1	Ranges of Variation of Chemical Concentrations Lakes	144
Table 4.2.2.1	Trends in Major Chemical Concentrations for Lake Abaya	158
Table 4.2.2.2	Trends in Major Chemical Concentrations for Lake Chamo	159
Table 4.2.2.3	Water balance Model Results for Lakes Abaya and Chamo	163
Table 4.3.1.1	Chemical Compositions of Surface and Ground Water Sources within the Abaya – Chamo Basin	168
Table 4.3.3.1	Results of Coliform Test and Associated Water Quality Analysis	183

4.1 RIVER WATER QUALITY ANALYSIS RESULTS AND EVALUATION OF DATA

4.1.1 Conceptual Basis of Water Quality Change Models

Biological and chemical processes in the soils of catchments are keys to the responses of surface water quality to catchment changes, pollution and atmospheric inputs. These processes include [28]:

- Anion retention by catchment soils (e.g. sulphate (SO₄) adsorption);
- Weathering of minerals in catchment soils as a source of base cations (calcium (Ca), magnesium (Mg), sodium (Na), potassium (K));
- Adsorption and exchange of base cations and Al by catchment soils;
- Buffering of soil solution pH by weak organic acids (e.g. humic and fulvic acids) and by weak inorganic acids (e.g. Al hydroxides and carbonic acid);
- Formation of Al complexes with fluoride (F) and sulphate ions and with organic compounds;
- Biologically mediated transformations and uptake of cations and anions (particularly base cations and both oxidized and reduced N species) ;
- Generation of acid neutralising capacity (ANC) by dissociation of carbonic acid with subsequent exchange of hydrogen (H) ions for base cations.

Water chemistry changes in response to changed deposition occur over time scales of years to decades in natural systems [30].

4.1.2 Modelling Water Quality Changes:

The conceptual approach of river water quality model is based on its interaction with the catchment. A wide range of observed catchment responses can be theoretically produced by a rather simple system of soil reactions [29, 31]. The Acid neutralising capacity is defined as the sum of base cation concentrations minus the sum of strong acid anion concentrations [28]:

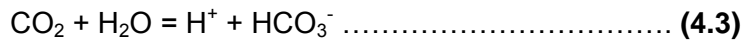
$$\text{ANC} = 2(\text{Ca}^{2+}) + 2(\text{Mg}^{2+}) + (\text{Na}^{+}) + (\text{K}^{+}) + (\text{NH}_4^{+}) - 2(\text{SO}_4^{2-}) - (\text{Cl}^{-}) - (\text{NO}_3^{-}) \dots \dots \text{(4.1)}$$

Where all concentrations are in moles per litre. Considering the dominant ions in fresh surface waters, and applying charge balance considerations, the definition of ANC above.

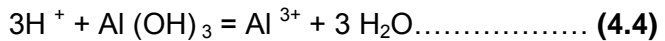
The above equation is equivalent to:

$$ANC = 2(\text{CO}_3^{2-}) + (\text{HCO}_3^-) + (\text{OH}^-) + m (\text{A}^{m-}) - (\text{H}^+) - n (\text{Al}^{n+}) \dots \dots \dots (4.2)$$

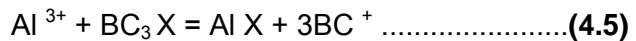
Where $n (\text{Al}^{n+})$ represents the net charge on the species of inorganic Al present and $m (\text{A}^{m-})$ represents the net charge on the species of organic anion present. While numerically equivalent, the former definition. The first equation is commonly referred to as the “charge balance ANC”, while the latter equation is the familiar definition of bicarbonate–carbonate alkalinity. The CO_2 dissolves in soil water to form carbonic acid, which then dissociates to H^+ ion and bicarbonate (HCO_3^-) and carbonate (CO_3^{2-}) ions [28]:



Hydrogen ions in soil solution react with these Al solids to produce inorganic Al in the soil solution:



The trivalent Al in solution will undergo a number of hydrolysis and complexation reactions to produce the array of Al species represented as $n (\text{Al}^{n+})$ and $m (\text{A}^{m-})$ in the ANC definition above. Mineral and organic solids in soils have distributed surface charges that provide a substrate for cation adsorption and exchange. Generally, the cation exchange sites on the soil matrix have a higher affinity for the trivalent Al cation than for di- or monovalent base cations. An exchange of cations between dissolved and adsorbed phases results:



Where BC^+ represents a base cation and X represents the soil exchange complex. Combining the definitions of ANC with a consideration of these general soil processes, the following conclusions can be reached: (1) any process that produces strong base cations increases the ANC of the soil solution; (2) any process that

produces strong acid anions decreases the ANC of the soil solution; (3) if ANC decreases, pH will decrease and inorganic Al will increase; and (4) a large strong base cation exchange pool provides a buffer against ANC change. The converse statements are also true [28].

The river water quality therefore can be modelled as an input – out put process of the catchment where by the input information is provided through atmospheric inputs (rain water quality), anthropogenic input (point and non-point sources of pollution). The catchment processes are modelled by biological production and removal and transformation of ions according to studies of the soil ion exchange processes.

Time series modelling is possible where the time steps are monthly or yearly. Time series inputs to the model include annual or monthly estimates of: (1) deposition of ions from the atmosphere (wet plus dry deposition); (2) discharge volumes and flow routing within the catchment; (3) biological production, removal and transformation of ions; (4) internal sources and sinks of ions from weathering or precipitation reactions; and (5) climate data. Constant parameters in the model include physical and chemical characteristics of the soils and surface waters, and thermodynamic constants. The model is calibrated using observed values of surface water and soil chemistry for a specified period [32].

4.1.3 Major Ion Concentrations

The results of data analysis of rivers (and lakes) of major compounds for the period of measurement (December 2002 – January 2004) are presented in table 4.1.3.1. Figures 4.1.3.1 – 4.1.3.3 show the relative dominance of the ions for the three rivers.

Table 4.1.3.1 Ranges of Variation of Chemical Concentrations of Rivers and Lakes. Most of the parameters were determined by taking samples during the different season of the year.

Ion	Chemical formula	Unit	Lake Abaya	Lake Chamo	River Hare	River Kulfo	River Sile
pH		PH Units	8.4 - 8.98	9.0 - 9.23	6.0 – 8.7	6.48 – 9.48	7.4 – 8.5
Conductivity		$\mu\text{S.Cm}^{-1}$	1030-1110	1810 - 1960	40 - 90	80 - 200	115 - 533
Turbidity		NTU	64 - 90	40-100	10-750	7-1950	9-389
Spectrophotometric absorption (500 nm)		Abs	0.08 – 0.14	0.08 – 0.135	0.003 – 1.5	0.01 - 11	0-1.3
Total Solids		mg L^{-1}	700-975	1200-1500	40 -2725	65-5620	215-660
Volatile Solids		mg L^{-1}	165-380	360 -478	14-257	6-564	15-170
Suspended Solids		mg L^{-1}	60-250	50-350	5 - 2660	5 - 5500	5 - 310
Dissolved Solids		mg L^{-1}	911.10	1522.45	25 - 60	53 - 132	76 - 350
Alkalinity	CaCO_3	mg L^{-1} as CaCO_3	450 - 540	765 - 910	20 - 90	40 -160	60 - 380
Calcium	Ca^{2+}	mg L^{-1}	15-24	12-20	4-15	5-20	5-25
Magnesium	Mg^{2+}	mg L^{-1}	2-5	7-12	1-7	2-13	3-40
Sodium	Na^+	mg L^{-1}	213 - 250	375 - 440	2-7	3-9	5-20
Potassium	K^+	mg L^{-1}	15-19	22-28	0.5 – 1.40	0.5 –2.0	1.1 – 3.2
Ammonia	NH_3	mg L^{-1}	0.16-0.58	0.03-0.45	0-019	0.006-0.35	0.005-0.23
Ammonium	NH_4^+	mg L^{-1}	0.6-0.7	0.07-0.3	0-1.74	0.014-0.95	0.005-0.87
Carbonate	CO_3^{2-}	mg L^{-1}	30- 55.24	60- 117	0-0.7	0-2.5	0- 3.32
Bicarbonate	HCO_3^-	mg L^{-1}	400-500	750-850	20-120	40-190	60- 337
Chloride	Cl^-	mg L^{-1}	64-78	127-160	2-14	3-12	7-42
Sulphate	SO_4^{2-}	mg L^{-1}	25-34	12-26	1-9	1-8	1-13
Nitrate	NO_3^-	mg L^{-1}	0.6-1.8	0.7-3	0-1	0.5-1.8	0.5-2.1
Nitrite	NO_2^-	mg L^{-1}	0-0.05	0-0.02	0-0.03	0-0.05	0-0.06
Phosphate	PO_4^{3-}	mg L^{-1}	0-0.19	0-0.03	0-0.06	0-0.06	0- 0.07
Silicacid	H_2SiO_3	mg L^{-1}	44.29	3.14	22.26	21.42	28.97
H-Sillica	HSiO_3^-	mg L^{-1}	6.04	0.76	0.10	0.92	1.25
Siliciumion	SiO_3^{2-}	mg L^{-1}	0.00	0.00	0.00	0.00	0.00

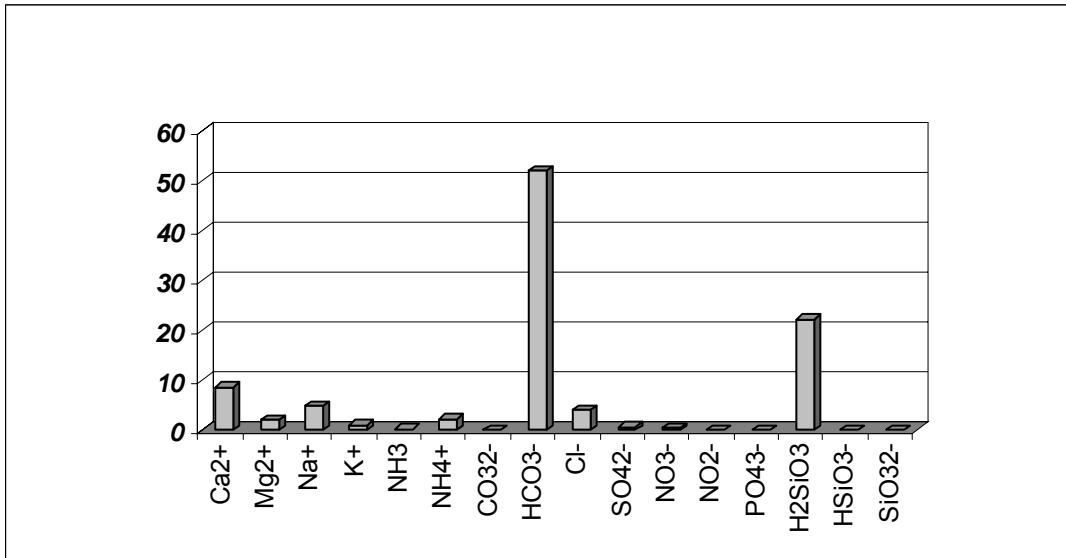


Fig. 4.1.3.1 River Hare Major Ions (mg L⁻¹). The river water is dominated by calcium, as well as bicarbonate ions.

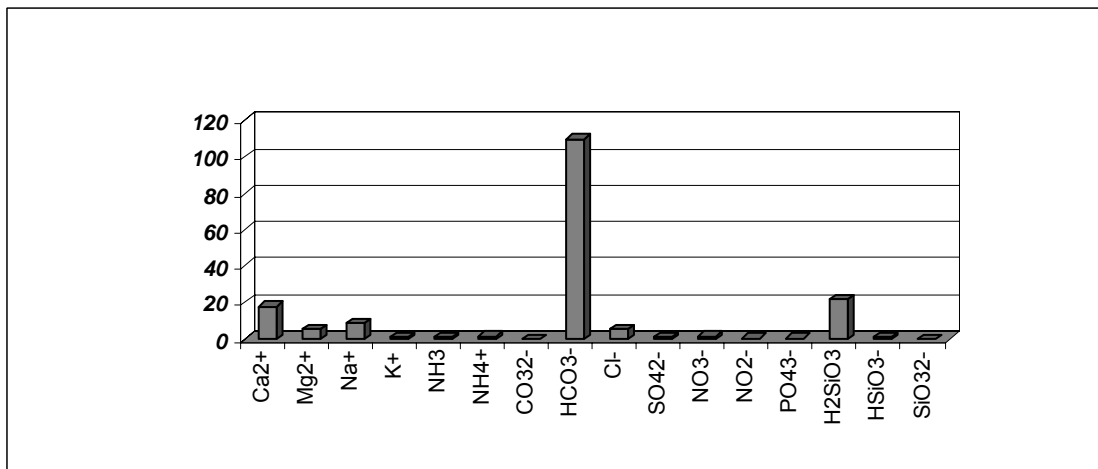


Fig. 4.1.3.2 River Kulfo Major Ions (mg L⁻¹). The river water is dominated by calcium, and bicarbonate ions.

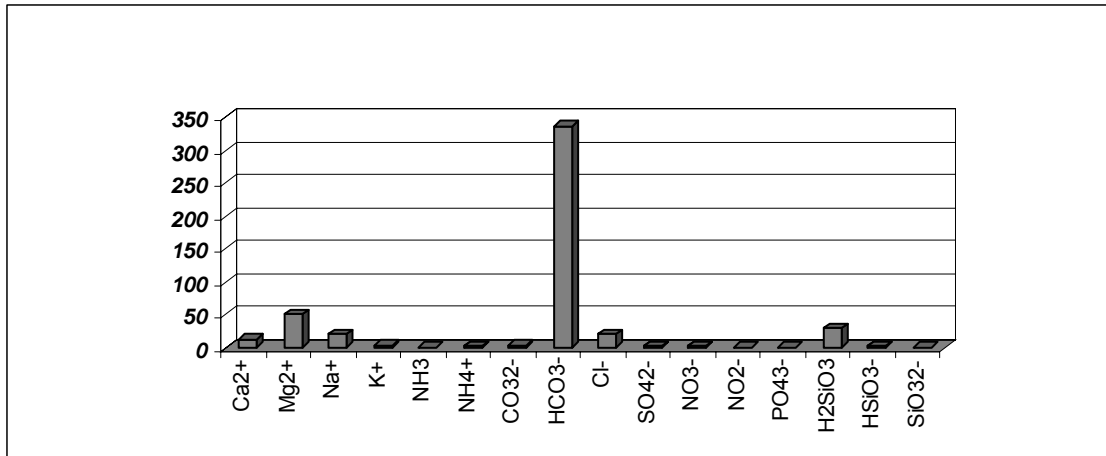


Fig. 4.1.3.3 River Sile Major Ions (mg L⁻¹). The river water is dominated by magnesium and bicarbonate ions.

All the rivers chemistry is dominated by the Calcium-Magnesium-Bicarbonate compounds, which is characteristic of the basaltic formation of the parent rock in the region. The Chloride content of rivers at lower elevation such as Sile River is higher. This is probably due to the evaporative influence and longer residence time in the lower elevations. Bicarbonate and other ions are also greater in these rivers due probably to the same influence.

The water qualities of the rivers Hare, Kulfo and Sile are influenced by the capacities of the respective catchments to retain the H⁺ ions and in return exchange it for Calcium, Magnesium and Sodium. The rivers contain higher concentrations of bicarbonate and the equivalent divalent Calcium and Magnesium ions followed by Sodium and Potassium. The concentrations of chloride, sulphate and nitrate are relatively low. Looking at silica concentrations, all the rivers contain higher silica concentrations, which is again characteristic of the parent rock formation. The rate of Silica weathering appears to be of the same order of magnitude for the rivers because of the close pH range in which the dissolved silica (mainly Silicic acid) appears constant.

It is worth noting that sodium concentrations are of equal orders of magnitude as calcium and magnesium concentrations for both rivers Hare and Kulfo. This implies that the hardness is only a part of the alkalinity concentrations.

Strong correlations between pH and alkalinity for Kulfo River imply the dominant effect of higher bicarbonate concentration for Kulfo River. For Hare River its alkalinity

is less strongly correlated with pH. The same can be said for Sile River where the bicarbonate concentration is 150% higher than that of Hare River. For Sile River, the pH varies slowly due to the increased dependence of the pH on the bicarbonate concentrations and the increased buffering capacity of the water with increasing bicarbonate concentrations.

The Chloride concentration is the highest for Sile River. As this river drains a low land plain the increased rate of evaporation might lead to increased storage of chloride which is leached down the soil and appears as an inter-flow. The dry weather concentration of Chloride for Sile River is 20 mg L⁻¹ compared to 4 and 5 mg L⁻¹ for rivers Hare and Kulfo.

Since Lake Chamo receives most of the inflows from the lower lying tributaries, Kulfo, Sile and even lower lying rivers with increased evaporation storage (i.e. Wezeka, Doyaso, Sego Rivers) they contribute to the increased concentration of salts (salinity) of Lake Chamo as compared to Lake Abaya which receives rivers from the upper highland catchment (i.e. Bilate, Gidabo, Gelana, Hare, Hamesa, Baso, Shefie, Wajifo, Wogeba, Bishan Guracha, Humbo Tebela, etc.)

Because of the higher bicarbonate concentrations of the low lying rivers as a result of the increased exchange of Cations (Sodium, Calcium and Magnesium mainly), the alkalinity of Lake Chamo is much higher than that of Lake Abaya (520 mg L⁻¹ as CaCO₃ for Lake Abaya as compared to 850 mg L⁻¹ for Lake Chamo).

4.1.4 River Water Quality Response as a Result of Catchment Changes

Catchment changes directly affect dissolved nutrients and solids transport. One would anticipate a higher sediment load on Hare and Kulfo rivers over time as a result of land degradation that has transformed the catchment and resulted in increased soil loss [33]. The same can be said of nutrients in the form of organic carbon and organic nitrogen as well as ammonia.

Stream pH change over longer period as implied in continental and European stream water quality studies may not be anticipated as the occurrence of acid rains is not a likely phenomenon. However, burning of grasses and bushes for livestock grazing may contribute to increase in sulphate and nitrate concentrations and the resulting

acidification followed by release of hydrogen and aluminium ions (in the form of H^+ and Al^{n+}) in to the stream waters.

Catchment based experiments have provided important insights into the magnitude of the effects of forest management activities on water quality. Characteristics most affected are sediment load, dissolved nutrient concentrations, and temperature. Changes in stream water nutrient concentrations following cutting vary substantially between localities. In some studies only marginal increases in concentrations of NO_3^- , K^+ , and other constituents have been observed following cutting. In contrast, clear cutting of forests in other areas has resulted in large increases in concentrations of some nutrients.

4.1.5 Nutrient Transport

The extent of nutrient transport was assessed by measuring the transport of nitrate, sulphate, phosphate, ammonium, BOD and the extent of volatile solids mass in the river water samples. BOD measurements are normally low for both the rivers Hare, Kulfo and Sile and this parameter is not practical as an assessment of the organic matter content of the water. COD or TOC measurement provides a better assessment although both are expensive for a routine measurement.

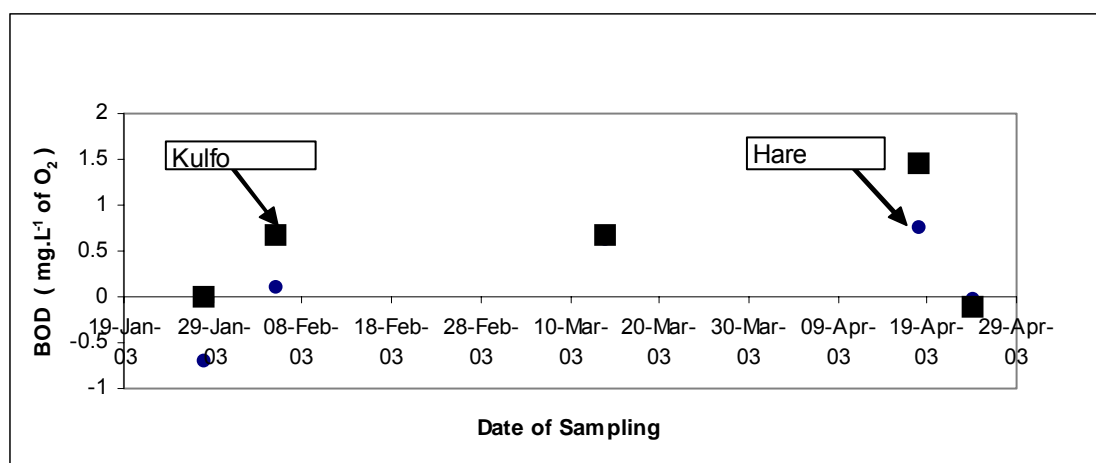


Fig. 4.1.5.1 BOD variation for the River Water Samples between months of January and April. The BOD slightly increases during the rainy periods (January –February and Late April) and decreases during the dry seasons (February-March)

Examination of the graph of BOD variation shown in Fig. 4.1.5.1 shows that the BOD value gradually decreases during the summer dry period and shows an increase on the onset of the rainy season.

Sulphate and nitrate values are normally recorded low (between 0 and 1 mg L⁻¹). The inputs associated with these chemicals, such as domestic waste pollution and fertilizer application are thought to be low for the upstream catchment area. Acid rain effect normally that results in higher levels of sulphate and nitrate in the water is not expected in this catchment. Precipitation water quality analysis shows higher pH and low values of these nutrients.

A strong retention of the catchment for H⁺ and NH₄⁺ is observed by the steady increase in pH during the dry season and the consequent depletion of ammonium concentration measurements taken during this time.

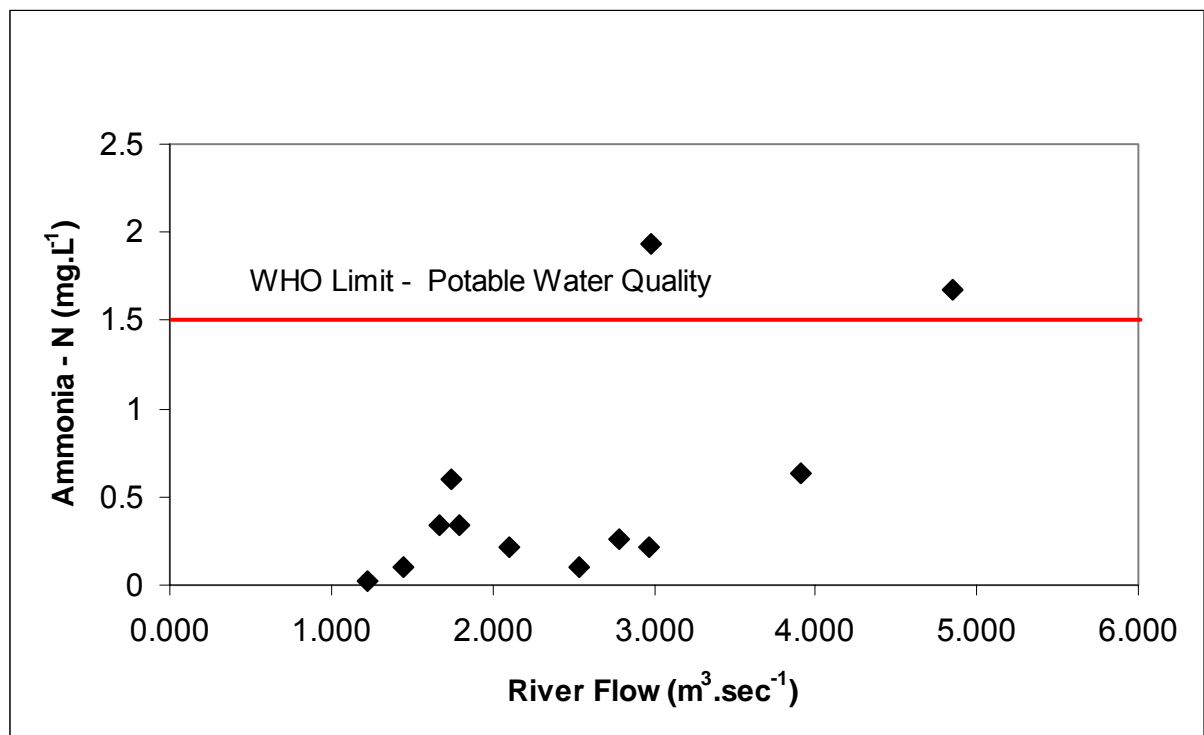


Fig. 4.1.5.2 Ammonia Variation with River Flow (Hare River). The ammonia concentration shows a general increasing trend with the river discharge (flow).

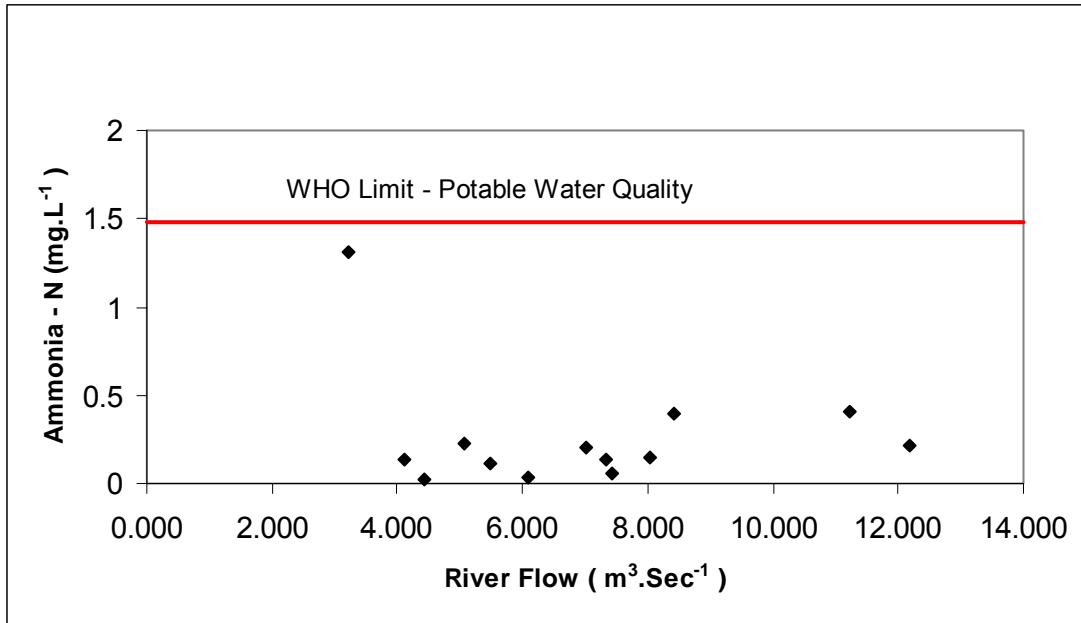


Fig. 4.1.5.3 Ammonia variation with River Flow (Kulfo River). There is a slight increase of ammonia with river flow. However, this effect is barely noticeable in the above figure.

The influence of the soil buffering capacity is apparent by the seasonal measurement of ammonium ion concentrations. Kulfo catchment has a stronger retention for ammonium with increased flow the release rate is moderate (see Figure 4.1.5.3 above). For river Hare the ammonium concentration increases more than that of Kulfo River with increase in flow. The x- axis values for the two graphs above are comparable when the discharges are normalized to the catchment areas (as the catchment area of Kulfo is 360 sq Km twice that of Hare 180 sq-Km.). The red line in the figures indicates the WHO limit on ammonia in drinking water [34].

4.1.6 Seasonal Variation in Water Quality

The alkalinity of Hare River varies between a season minimum of around 20 mg L⁻¹ and dry season maximum 100 mg L⁻¹. The variation of Kulfo alkalinity is between 30 and 160 mg L⁻¹. There is an even greater variation in conductivity because of the aggregate effect of the constituent ions. The conductivity of Kulfo varies between 80 and 200 $\mu\text{S.Cm}^{-1}$. For river Hare, the conductivity varies between 40 and 100 $\mu\text{S.Cm}^{-1}$. The remaining ions follow similar seasonal increase and decrease but with less pronounced effect as individuals ions are being measured. The pH of Hare River varies between 6.9 and 8.5. The pH for river Kulfo varies between 7.2 and 9. The solids concentrations, turbidity and absorption measurements are all high for river Kulfo compared with that of river Hare. During the rainy season the solids content of

river Kulfo can be as high as 6000 mg L⁻¹ while that of Hare River is around 3000 mg L⁻¹. The turbidity and spectrophotometric absorption also vary with similar orders of magnitude. Alkalinity and conductivity display distinct long term seasonal variation and low short frequency runoff induced variation. This similar variability is followed by calcium and hardness and to a lesser degree sodium and potassium. On the other hand Chloride, Solids, turbidity all display short-term variation mainly caused by surface flow runoff episodes.

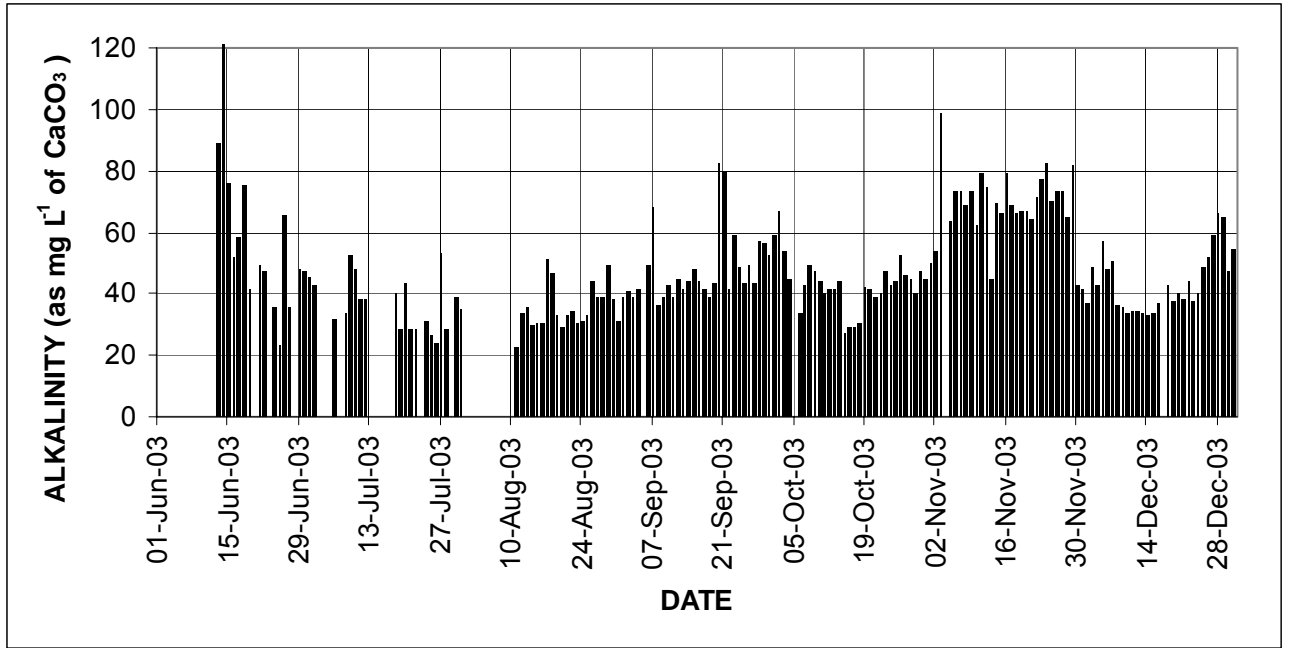


Fig. 4.1.6.1 Alkalinity Time Series for Hare River

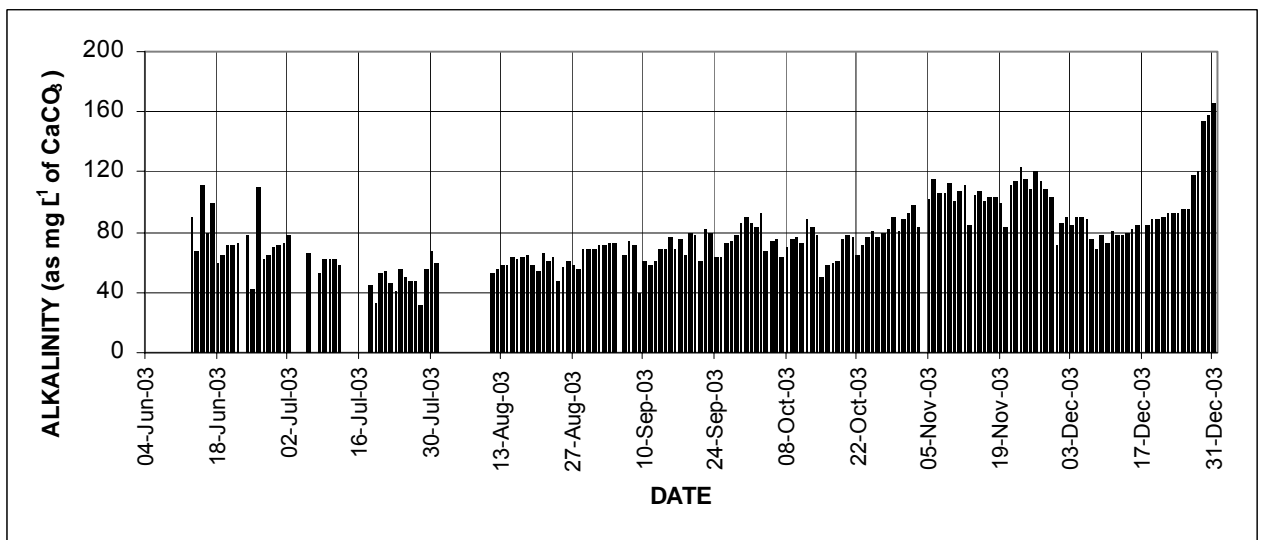


Fig. 4.1.6.2 Alkalinity Time Series for Kulfo River

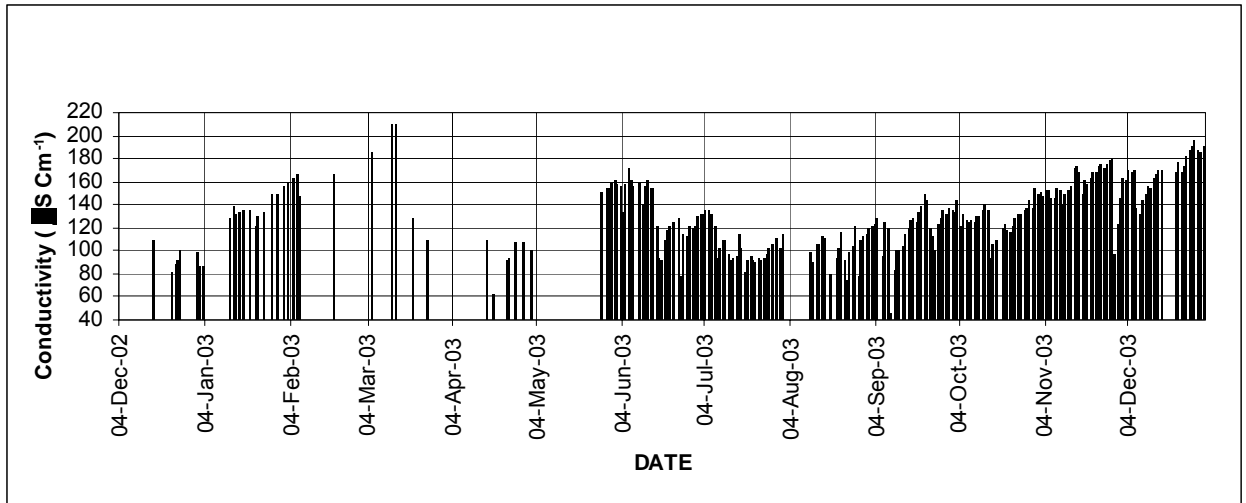


Fig. 4.1.6.3 River Kulfo Conductivity Time Series

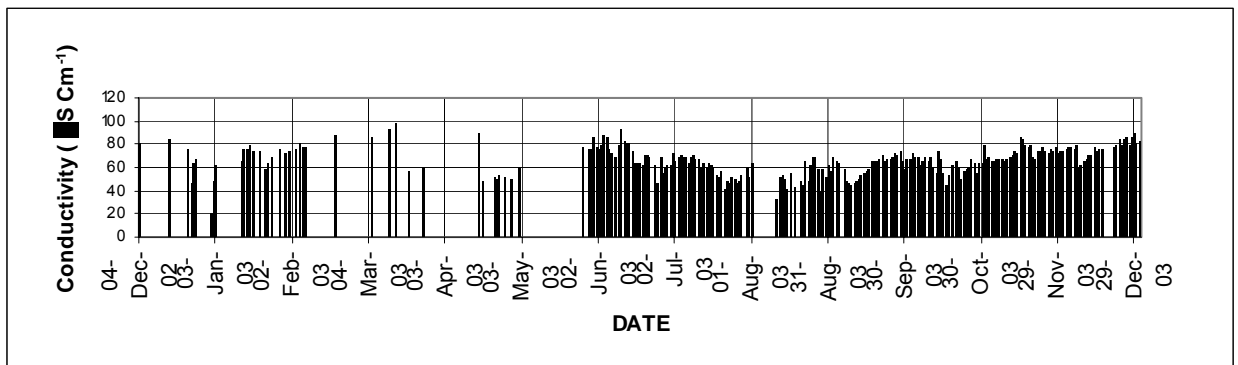


Fig. 4.1.6.4 River Hare Conductivity Time Series

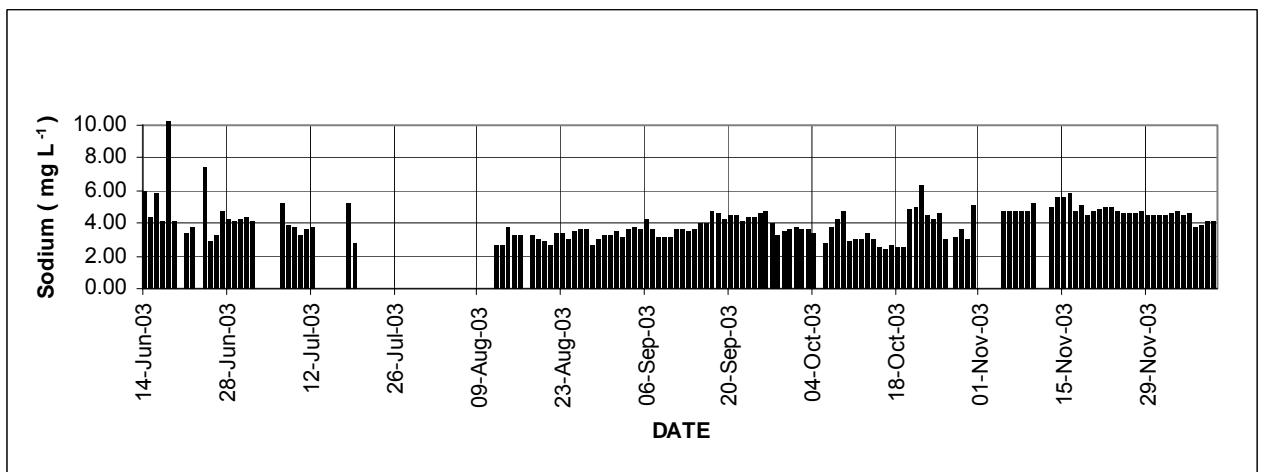


Fig. 4.1.6.5 Sodium River Hare

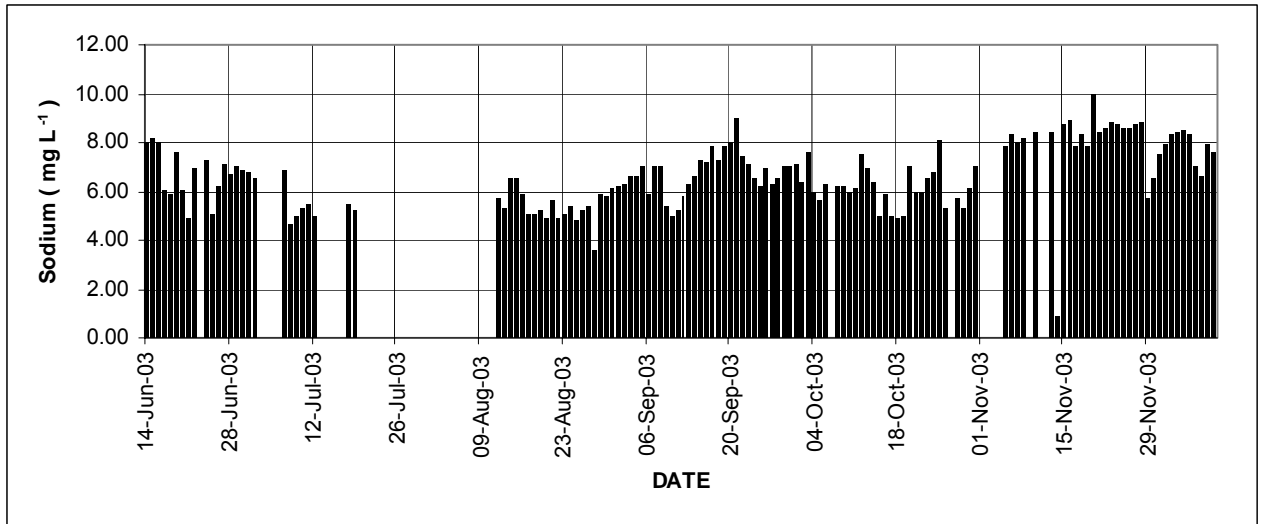


Fig. 4.1.6.6 Sodium River Kulfo

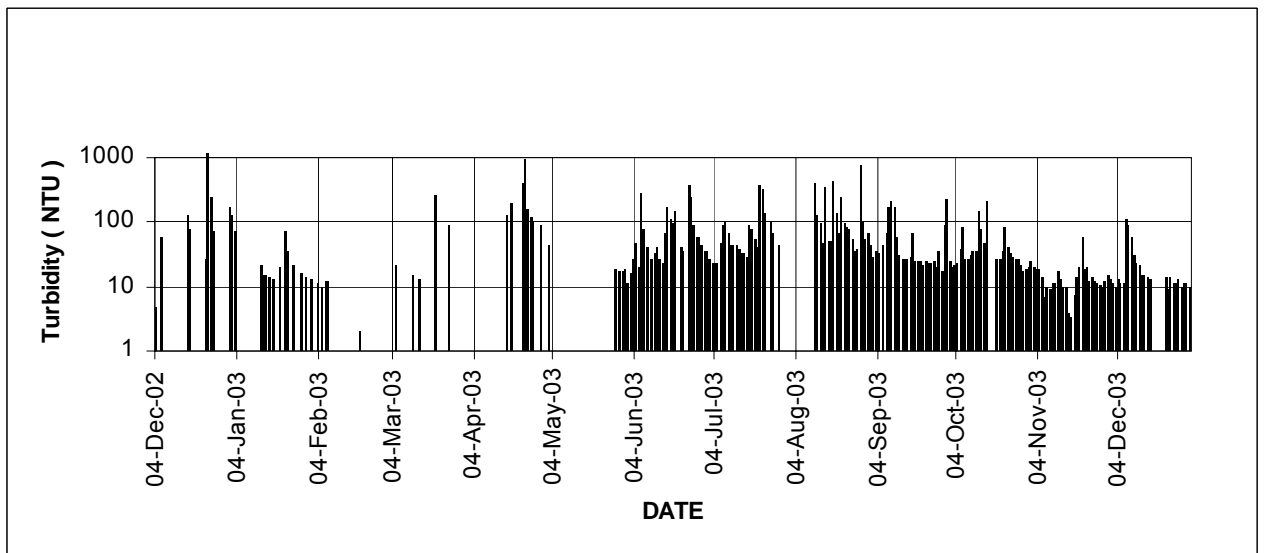


Fig. 4.1.6.7 Turbidity Time Series Data Hare River

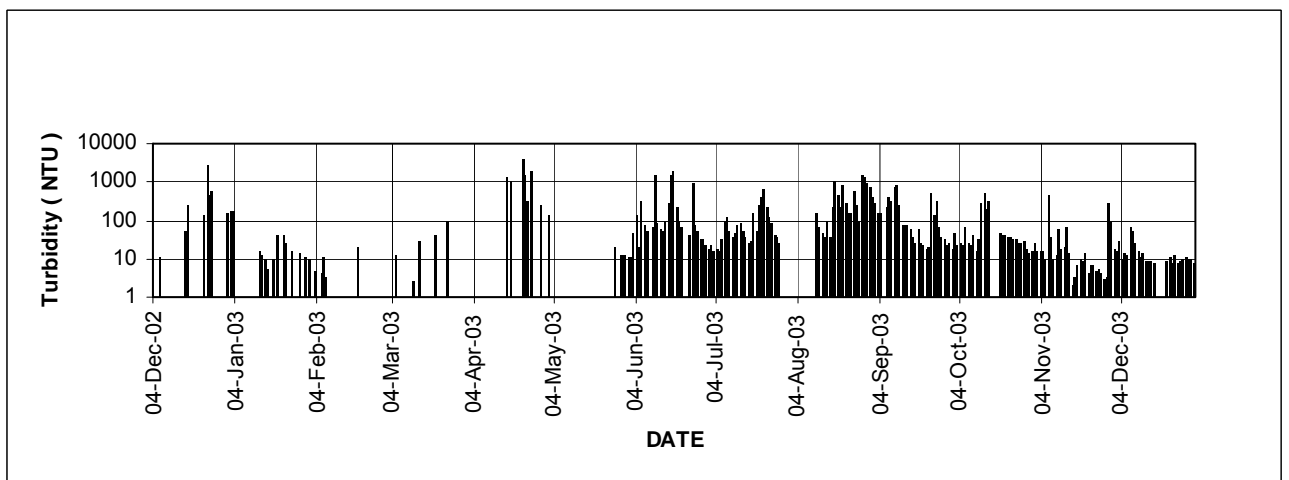


Fig. 4.1.6.8 Turbidity Time Series Data Kulfo River

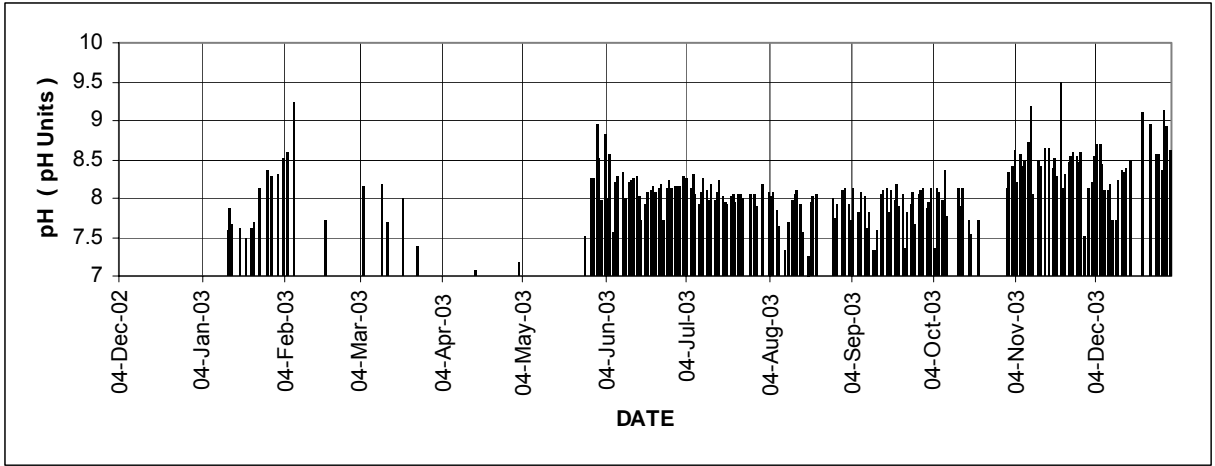


Fig. 4.1.6.9 pH Variation of River Kulfo

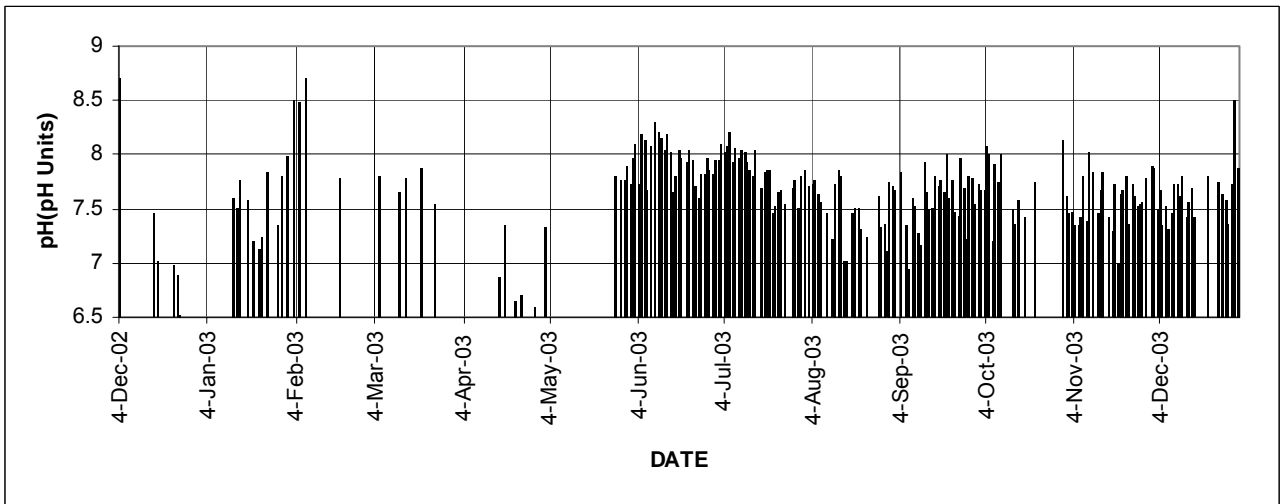


Fig. 4.1.6.10 pH Variation of River Hare

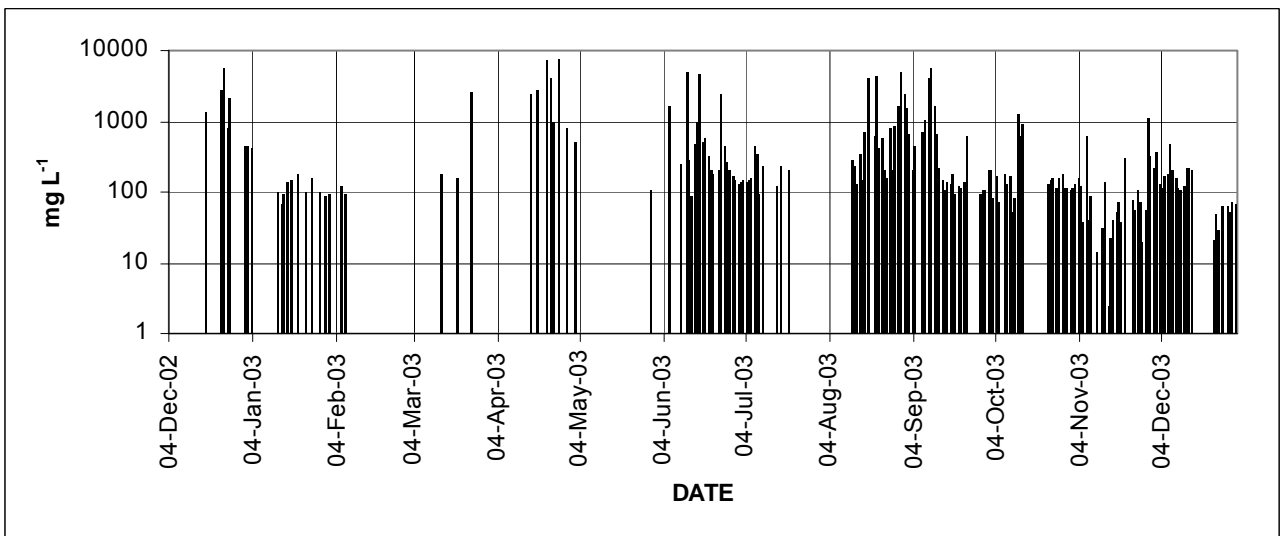


Fig. 4.1.6.11 Total Solids River Kulfo

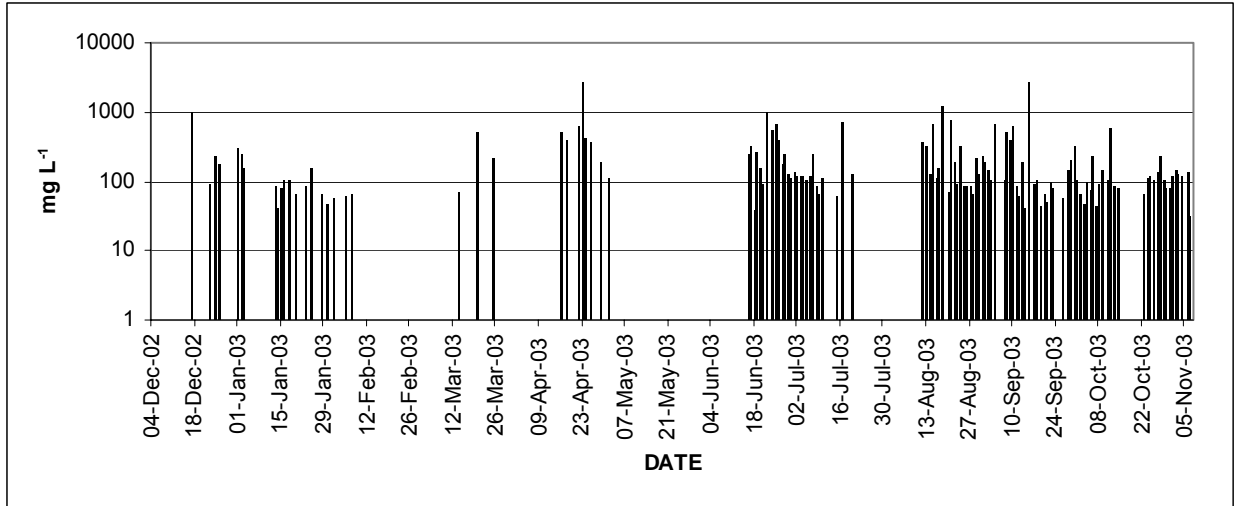


Fig. 4.1.6.12 Total Solids River Hare

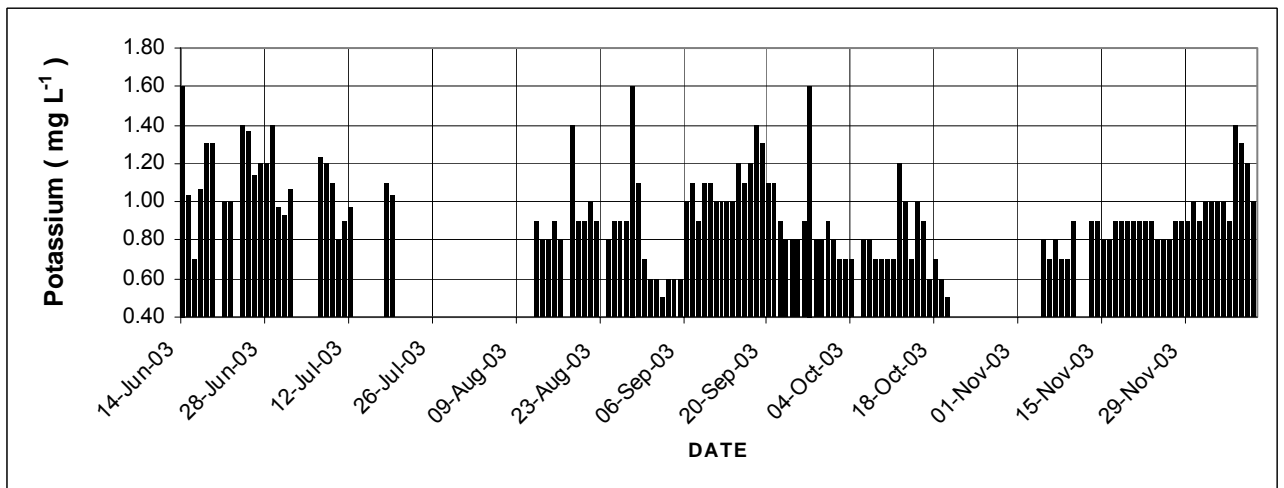


Fig. 4.1.6.13 Potassium River Hare

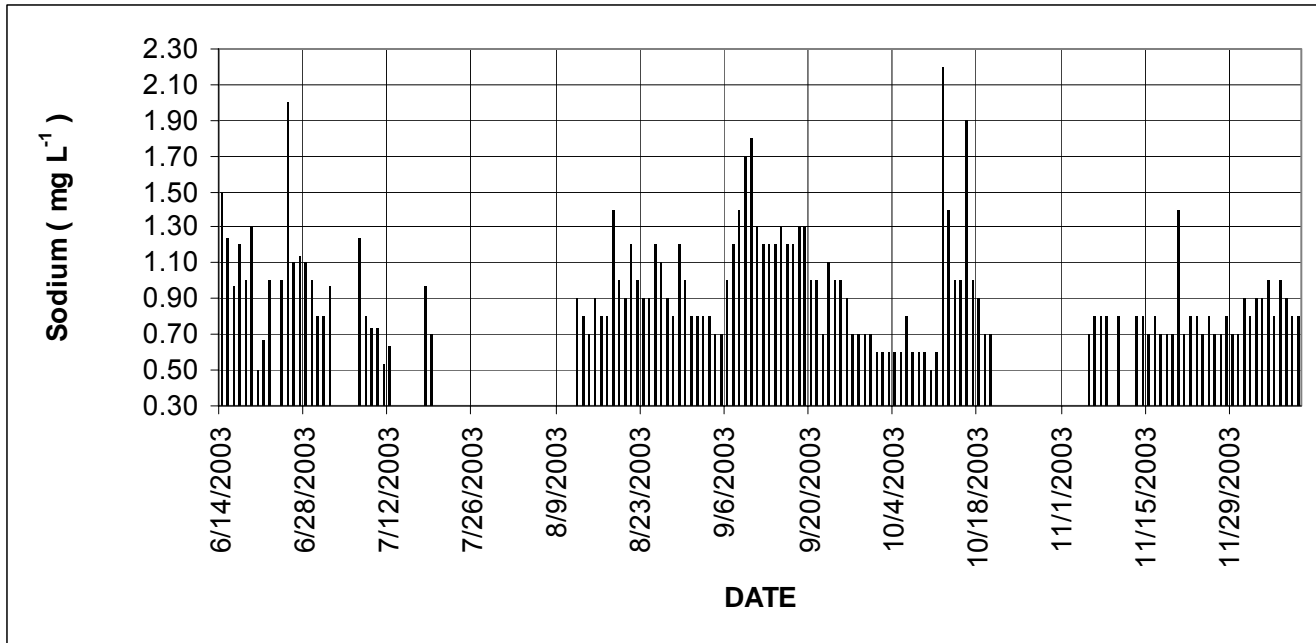


Fig. 4.1.6.14 Potassium River Kulfo

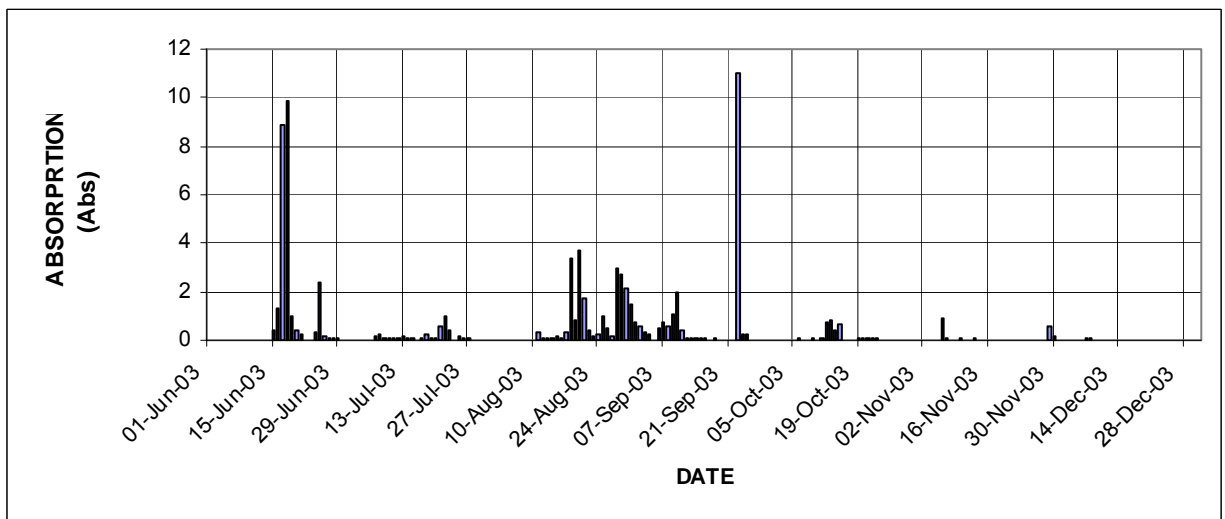


Fig. 4.1.6.15 Spectrophotometric Absorption Data for Kulfo River

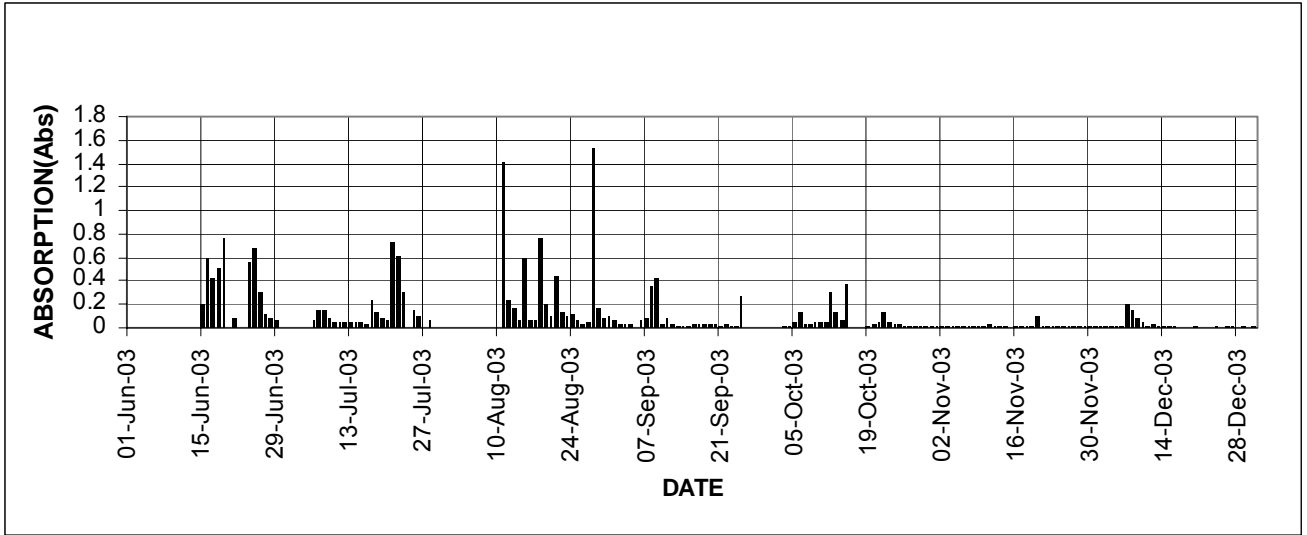


Fig. 4.1.6.16 Spectrophotometric Absorption Data for Hare River (500 Nm)

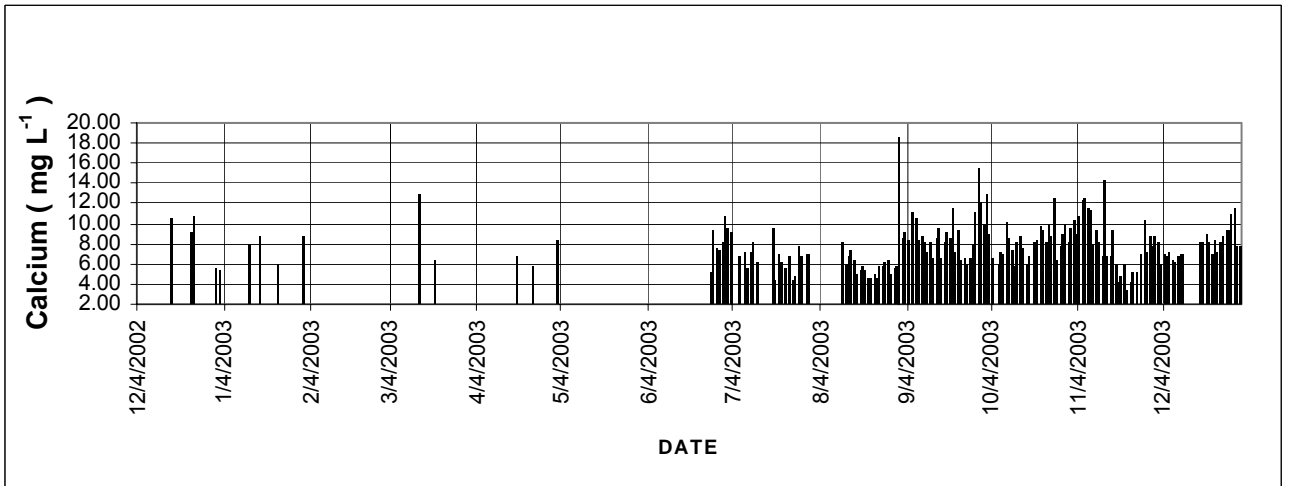


Fig. 4.1.6.17 Calcium Hare River

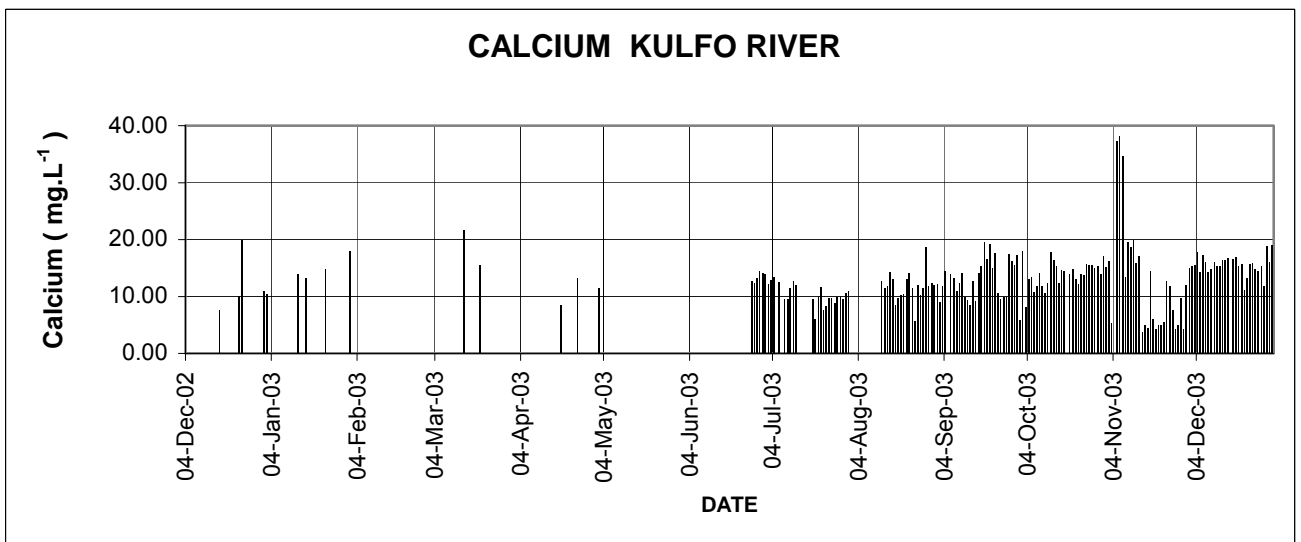


Fig. 4.1.6.18 Calcium Kulfo River

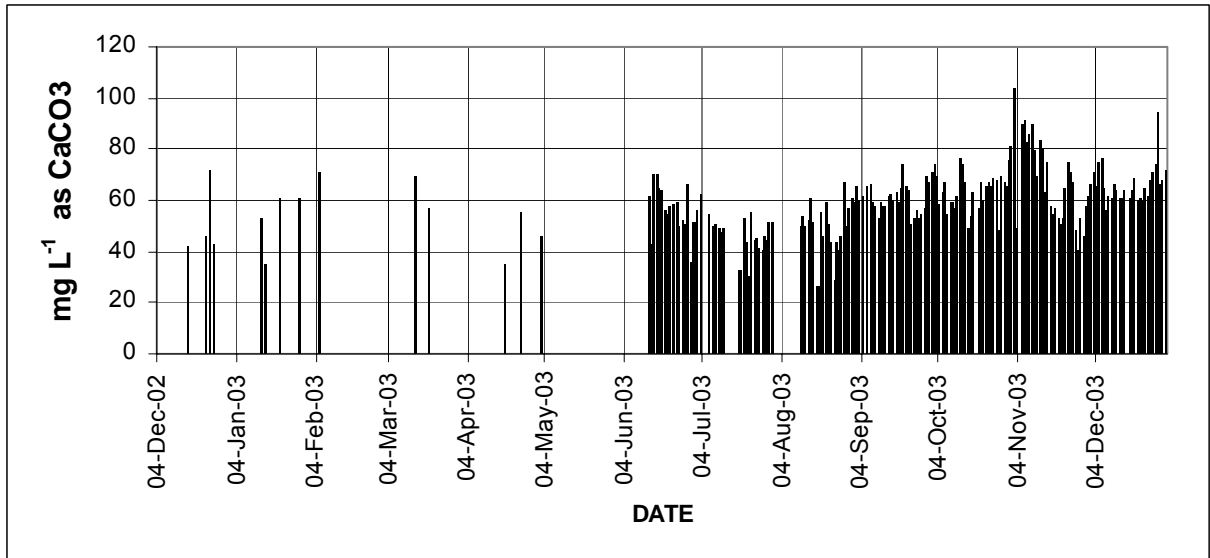


Fig. 4.1.6.19 Hardness River Kulfo

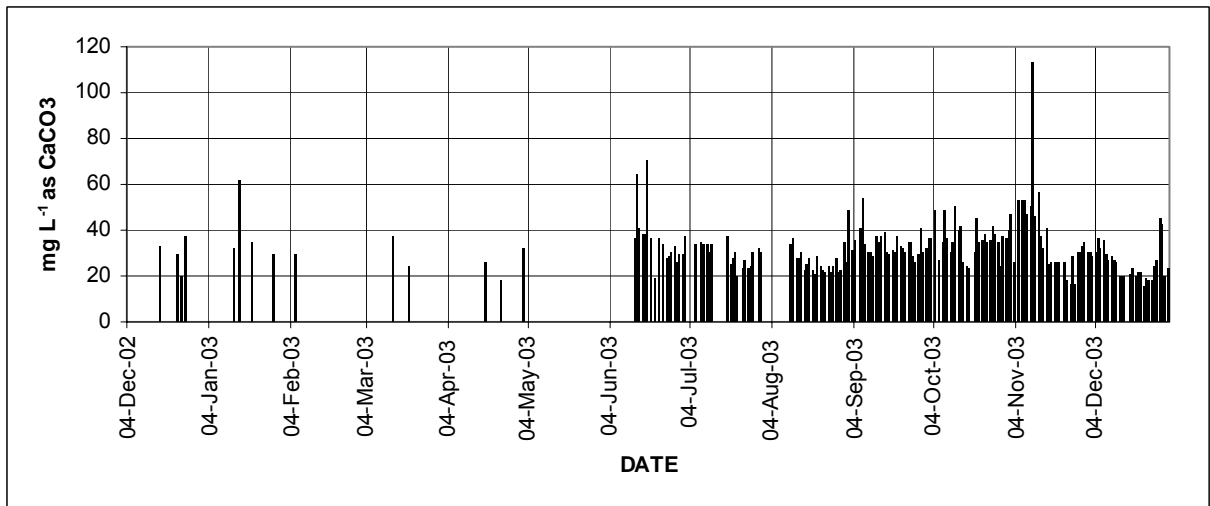


Fig. 4.1.6.20 Hardness River Hare

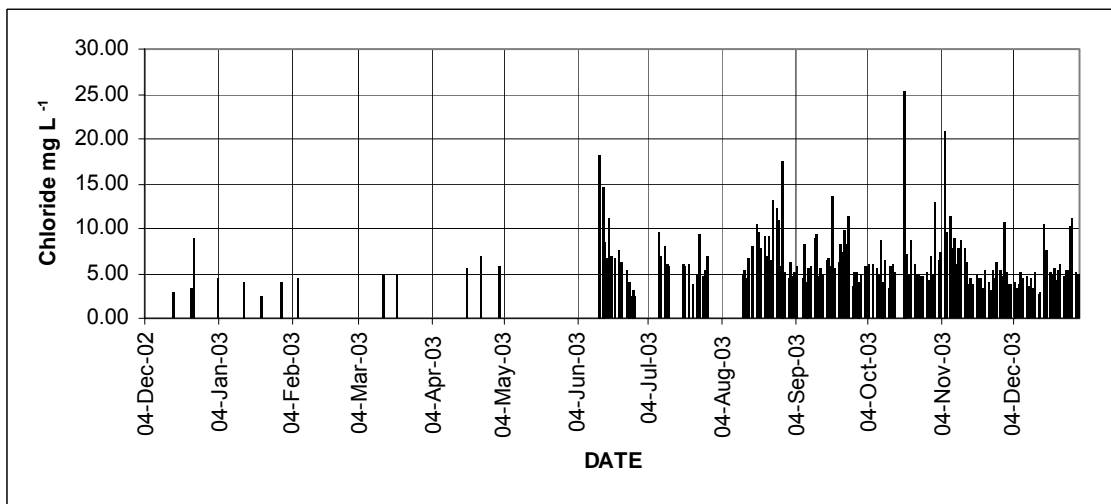


Fig. 4.1.6.21 Chloride Hare River

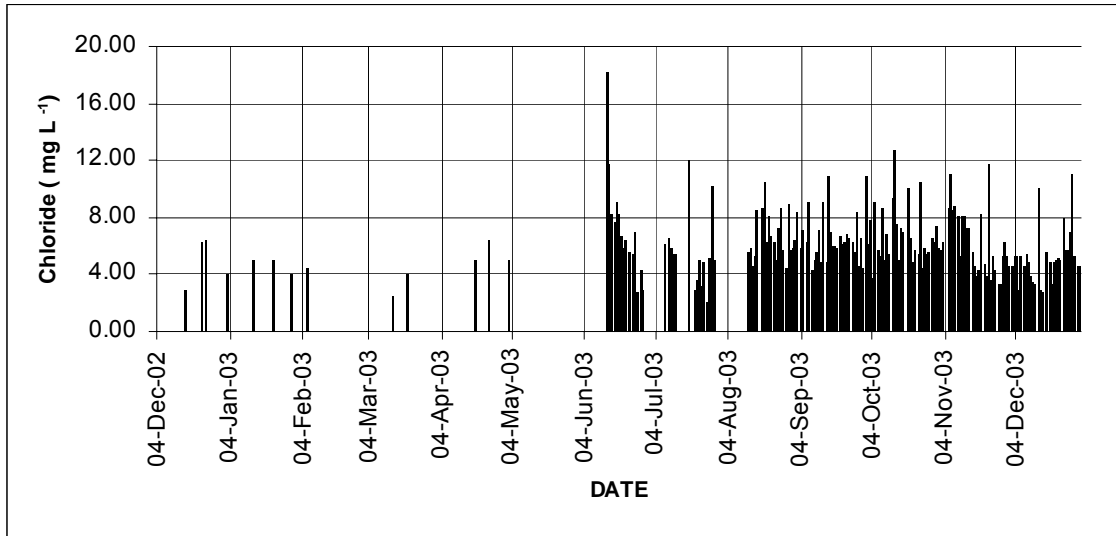


Fig. 4.1.6.22 Chloride Kulfo River

4.1.7 The Influence of Sodium Dominance on Alkalinity and Buffering Capacity

The effect of sodium dominance on pH and alkalinity can be evaluated in terms of the Sodium fraction present in the water. It is seen that generally the alkalinity increases with decreasing sodium percentage present in the water. This implies that catchments with greater sodium fraction have less buffering capacity and hence are more sensitive to pH variation than do catchments with greater sodium fraction.

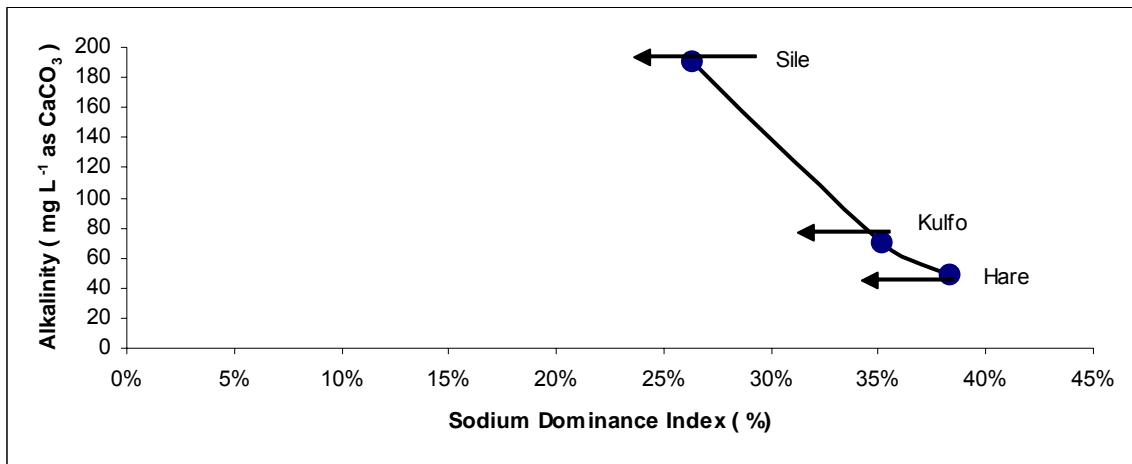


fig. 4.1.7.1 Variation of rivers alkalinity with sodium dominance index. Catchments with greater sodium fraction have less buffering capacity and hence are more sensitive to pH variation than do catchments with greater sodium fraction.

The Sodium dominance Index is calculated as the ratio in milli-equivalent per liter of sodium concentration to the total cation concentration also expressed in milli-equivalent per liter. This index was calculated for the rivers and plotted in Fig. 4.1.7.1. River Hare has lower alkalinity and the higher sodium dominance index and its catchment is considered to be more sensitive to change such as soil acidification than rivers Kulfo and Hare.

4.1.8 Relating Pollutant Loading to the Catchment Area and Flow

The solids mass transported per unit of the catchment area can be used as an indication of the rate of soil weathering within the catchment [35, 37]. This rate of weathering for both solids and solutes is either transport limited (lack of sufficient flow to transport the substance) or surface limited (there is enough flow available but the weathering rate attains saturation levels) [36]. Surface controlled weathering attains a plateau with increased flow while transport controlled weathering has increasing weathering rate with increasing flow/mass ratios [36, 38].

Figure 4.1.8.1 shows, the weathering rates for Hare and Kulfo catchments. It is apparent that the weathering rates are of comparable magnitude. However, Hare River seems to have greater rate of weathering than Kulfo River particularly at low flows.

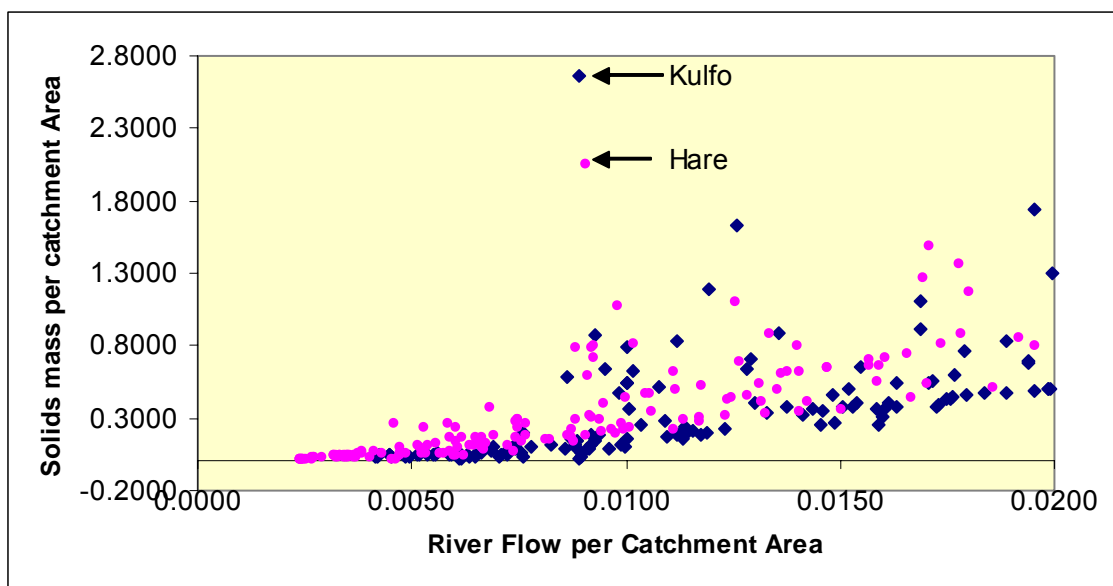


Fig. 4.1.8.1 Comparison of Weathering Rates for Hare and Kulfo Catchment. This rate of weathering for both solids and solutes is either transport limited. Catchment of river Hare seems to yield more solids than that of Kulfo River. Both the solids load as well as the river flow was normalized over the respective catchment areas.

The weathering rate of both catchments is not surface controlled. In fact weathering appears to increase with increase in flow for both rivers.

4.1.9 Influence of Rain Water Quality on the Rivers

In order to compare the river water quality at different season with the quality of the river water, the rain water quality (precipitation chemistry) was analysed. This analysis also qualitatively evaluates the relative atmospheric contribution to the river water quality. The average values of a number of repeated samples is calculated and given in Table 4.1.9.1.

Table 4.1.9.1 Comparison of Precipitation Chemistry with that of Kulfo River. This comparison helps in evaluating to what extent the river water resembles the rain water at the different times of the year.

Parameter	Unit	Rain Water (AWTI)	Kulfo River (Base Flow Chemistry)
pH	pH Units	7.43	8.69
Conductivity	$\mu\text{S.Cm}^{-1}$	62	169
Turbidity	NTU	0	10
Alkalinity	mg L^{-1} as CaCO_3	26.42	70
Hardness	mg L^{-1} as CaCO_3	20	65
Calcium	mg L^{-1}	9.35	17.83
Magnesium	mg L^{-1}	0	5
Chloride	mg L^{-1}	16.62	5.3
Sodium	mg L^{-1}	0.65	8.4
Potassium	mg L^{-1}	0.52	0.9
Ammonium	mg L^{-1}	0.69	1.219
Nitrate	mg L^{-1}	1.53	1.28

It can be seen that the influence of rain is of comparable order of magnitude with the river base flow for chloride, sodium, potassium, ammonium and nitrate. For chloride, the rainwater content has a higher concentration than that of the base flow. Therefore, it is not surprising that the variability of chloride concentration occurs with the rain. Principal component analysis of the river water quality data with precipitation data included showed that chloride and precipitation lie on the same side of the same principal component.

It is apparent, therefore, that river water quality modelling has to consider the atmospheric precipitation chemistry [39]. It has to be mentioned that the precipitation chemistry was not done by the use of a standard collection apparatus as this was not

available and the location of collection which is within the premise of Arbaminch University certainly not representative (but may be indicative) of the overall precipitation of the Kulfo catchment [39].

4.1.10 Regional Similarity in Water Quality Variation.

Relating the water quality variables on a regional scale helps in establishing inter-regional water quality models and in evaluating the relative catchment response of one river with respect to another such as for example the transport of solids by runoff processes [40].

In order to simplify the prediction of relationship among the variables within the region, variable aggregation and principal component analysis were carried out on the data, which is explained in detail below.

4.1.10.1 Intra-River Principal Component analysis

The water quality variation similarity between the rivers lying in the same hydrological regimes such as the ones in the Abaya- Chamo drainage basin is supported by the results of the principal component analysis carried out by aggregating the monitored variables of the rivers Hare and Kulfo and analysing the aggregate for principal components. The results of the analysis suggested the following:

The principal components are about 5, which means little new information is added by aggregating the data from the two rivers Hare and Kulfo since the individual principal components are five for both rivers.

1. River Discharges are regionally related. There is a strong correlation of river discharges between Hare and Kulfo rivers.
2. Conductivity, alkalinity and sodium concentrations share a common principal component both within an individual river as well as between rivers. These are variables heavily influenced by subsurface flow and might indicate similar subsurface flow characteristics.
3. Variables influence by surface flow characteristics such as discharge (the result of overland flow) and suspended solids share a common principal component.
4. Chloride between the two rivers fall in the same principal components so also Calcium and Hardness in to another components

Scree Plot For River data Combined

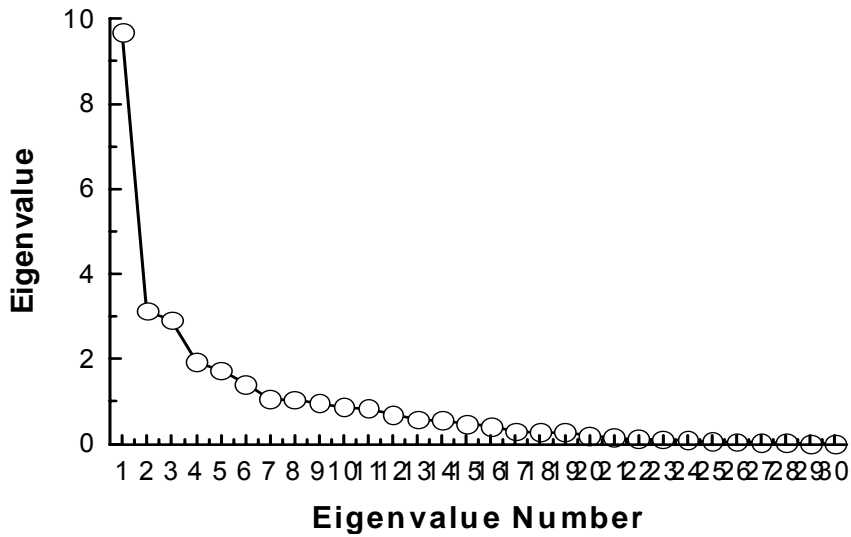


Fig. 4.1.10.1.1 Scree Plot for River Data Combined. The scree plot is the plot of the eigen values from the principal component analysis of the water quality data. The eigen values are obtained by orthogonal transformation of the water quality correlation matrix in to a matrix of independent components (a diagonal matrix). The eigen values are proportional to the data variance and the total variance of the data remains constant during the transformation. For example in the above figure the first Eigen value accounts for a great portion of the data variance.

The above variable clustering by principal components simplifies regional relationship in to few variables, which is reduced to river discharges, alkalinity, and conductivity and sodium concentrations between Hare and Kulfo rivers.

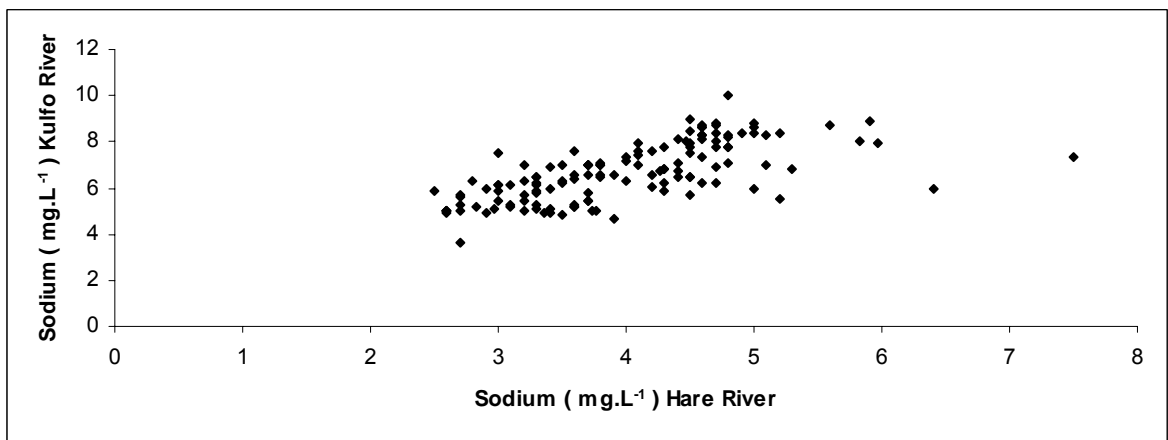


Fig. 4.1.10.1.2 Sodium Ions relationships for Hare-Kulfo Rivers indicating identical seasonal variation over rivers lying in proximity to each other. This strengthens the concept of regional similarity in water quality.

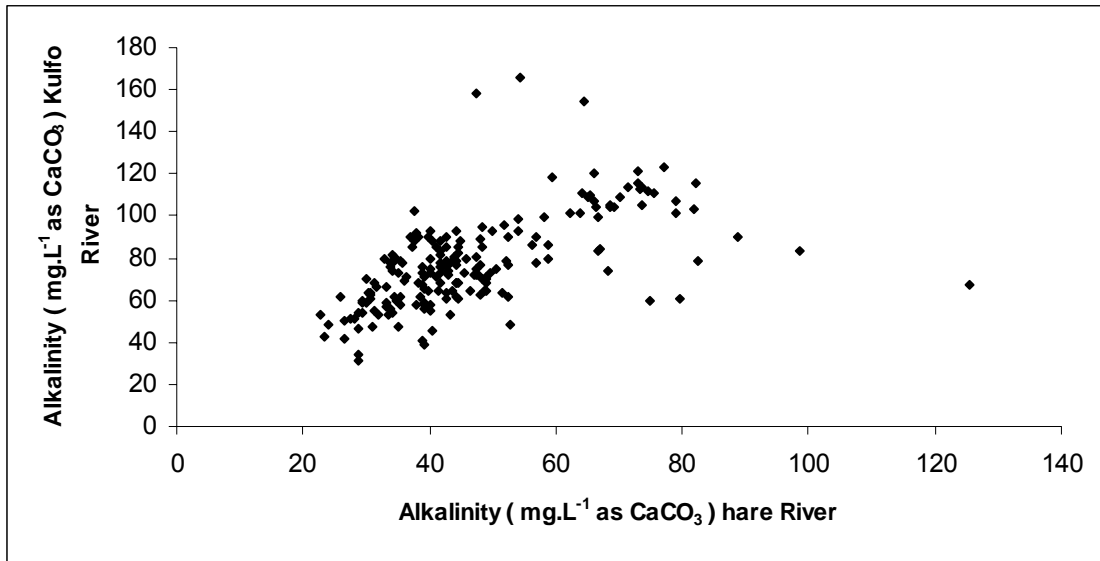


Fig. 4.1.10.1.3 Alkalinity Relationships between Hare and Kulfo Rivers

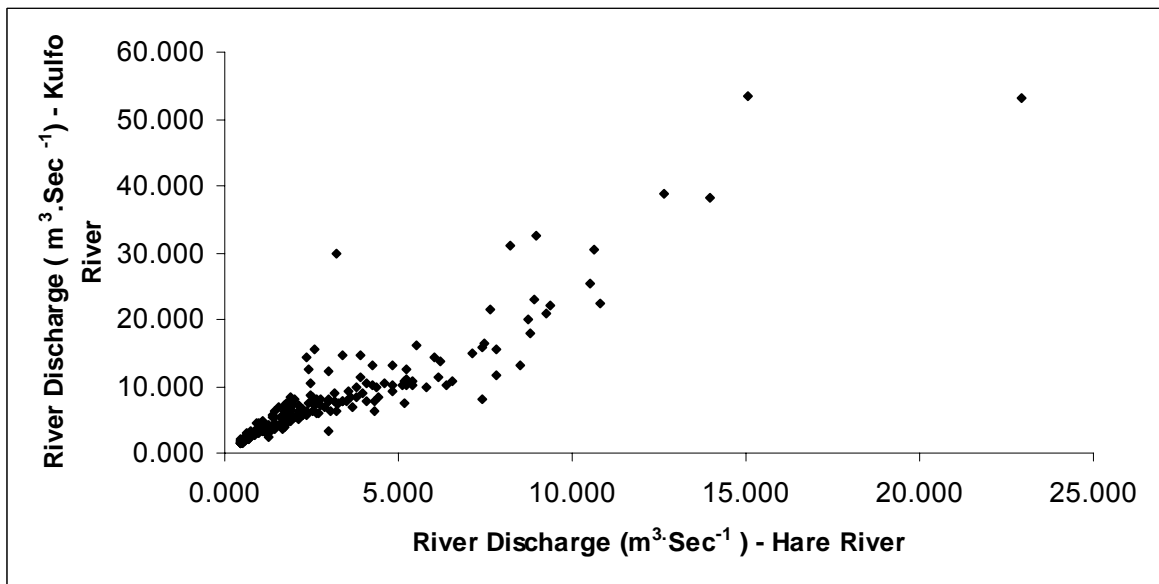


Fig. 4.1.10.1.4 River Discharge Relationship between Hare and Kulfo Rivers

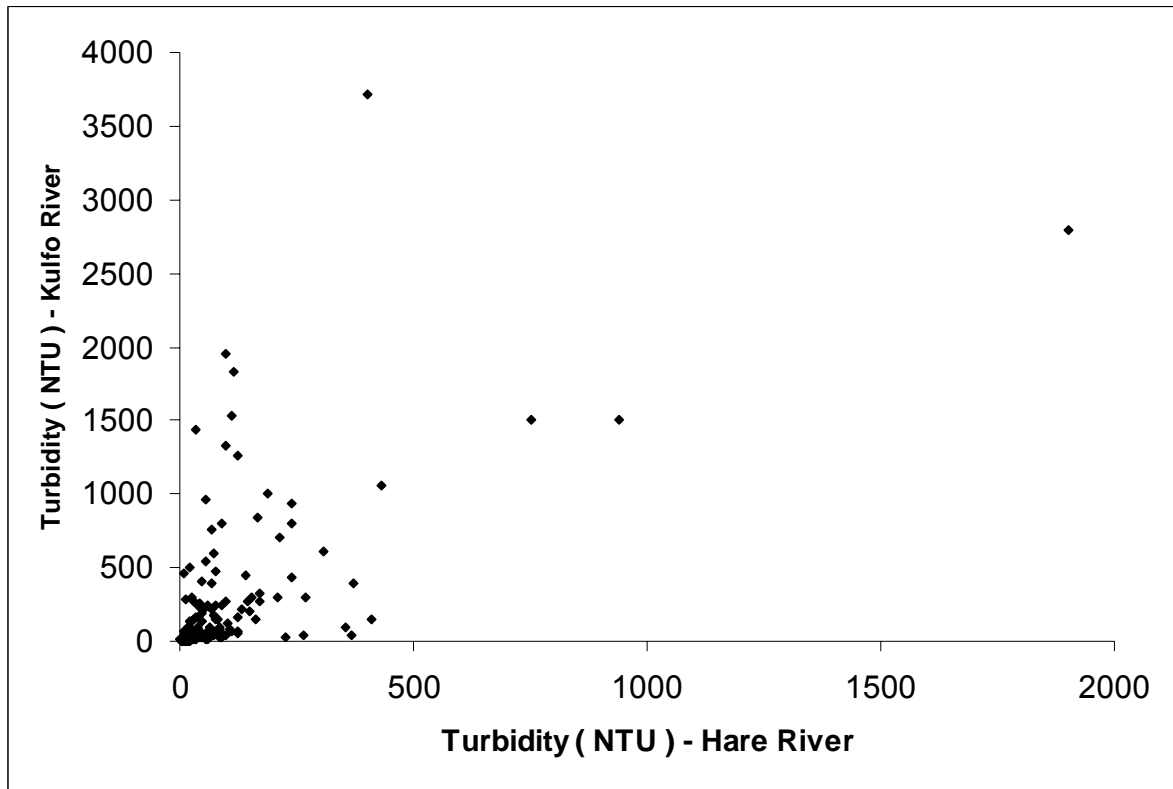


Fig. 4.1.10.1.5 Turbidity Relationship between Hare and Kulfo Rivers

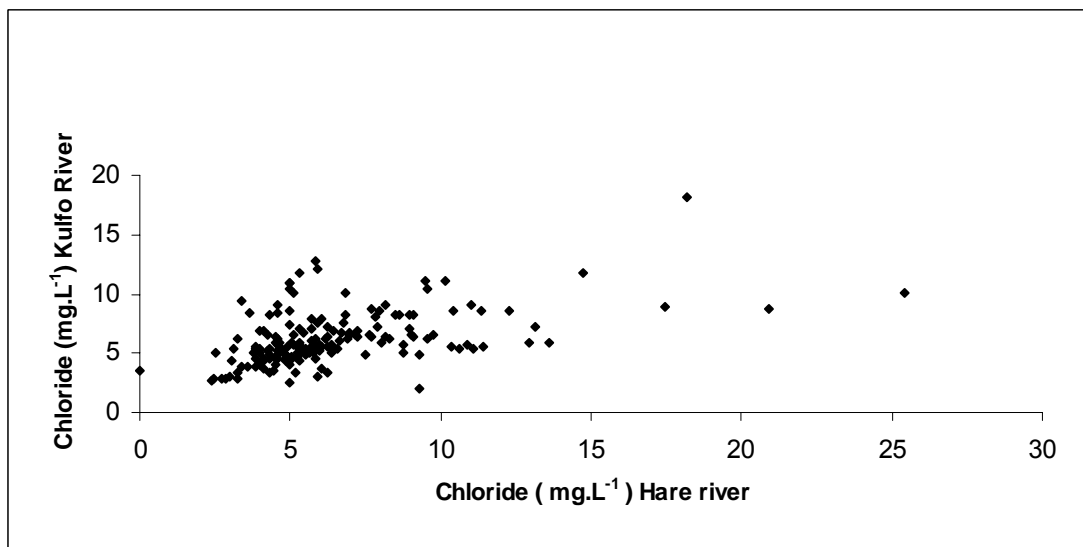


Fig. 4.1.10.1.6 Chloride Relationship between Hare and Kulfo Rivers

Figure 4.1.4.1.10 shows a linear trend for the discharge between the two rivers with the slope changing between different flow ranges. Three slope ranges can be seen in the graph. For the alkalinity and conductivity relationships somewhat good linear

trend is observable. This indicates long time subsurface catchment processes are similar. On the other hand, as the graphs above for turbidities show, there is a poor linear relationship between the turbidities of the two rivers. The surface processes, which result in turbidity formation, are governed by catchment area, slope. Soil type and other factors, which introduce heterogeneity in to the variable relationship. An attempt has been made by the author to account for the statistical variation using a time –series analysis described in the reference literature.

It can be concluded that the principal components for the two rivers are more or less of same order of magnitude and are strongly related. This is indicated by the fact that the variables falling in to the aggregate principal components are simply equal to the sum of the variables falling in to the individual principal components.

4.1.11 Global Climatic Change Effects

Changes due to climate change (temperature and precipitation) are expected to be relatively well buffered by the mineral composition (higher pH), the organic matter content or the structural stability of many soils [41]. The catchment area is not thought to be acid sensitive [42]. However, decreases in cover by vegetation or annual or perennial crops, caused by any locally major declines in rainfall not compensated by CO₂ effects, could lead to soil structure degradation and decreased porosity, as well as increased runoff and erosion on sloping sites and by the concomitant more extensive and rapid sedimentation. Changes in options available to land users because of climate change may have similar effects.

4.1.12 Basis for Future Monitoring

This time series monitoring of water quality can serve as a basis of future sampling and monitoring design where by the curve that fits the long term seasonal variation defines the degree of freedom and the sampling interval can be decided from the number of points required to define the curve [43].

Parameters whose values in greater percentage fit in to this model include conductivity, alkalinity, Hardness Calcium and Sodium. These parameters have their greater percentage explained by long-term seasonal variation. This is not surprising as the parameters are heavily influenced by subsurface processes.

On the other hand Turbidity and solids, chloride have higher short term runoff based variation which can be modelled as periodic functions of runoff and rain where as the long term seasonal component monitoring interval is decided from the fitting curve used for seasonal de-trending. Higher frequency components can only be picked if continuous monitoring is available. However, major events have lower frequency and a compromise can be reached for the sampling interval required for identifying the short-term periodic components.

4.1.13 Discussion

Water quality monitoring data for rivers Hare, Kulfo and Sile - which are part of the tributaries of the Abaya-Chamo Lake Basin in Southern Ethiopia - has been presented and the variability discussed. The water quality parameters are a function of the geo-chemistry of the catchments, hydrological events including atmospheric inputs and the catchment morphology where land use is a factor. The lower lying Sile River is characterised by increased alkalinity and salinity than the upper lying Hare and Kulfo rivers. The seasonal variation of the water quality parameters can be classified as mainly long-term seasonal variability or short-term rain induces surface flow based variability. Alkalinity and conductivity display distinct long term seasonal variation and low short frequency runoff induced variation. This similar variability is followed by calcium and hardness and to a lesser degree sodium and potassium. On the other hand Chloride, Solids, turbidity all display short-term variation mainly caused by surface flow runoff episodes.

The buffering capacity of the rivers and their alkalinity is negatively correlated with the sodium dominance ratio. Catchments with fewer ratios of Sodium ion release in to rivers retain more H^+ ion and nutrients such as NH_4^+ than catchments with lower ratio. The weathering rate for Rivers Hare and Kulfo were computed by normalising the river discharges and solids load to their respective catchment areas. A plot of this normalised solids load against normalised discharge shows Hare river has greater rate of weathering than Kulfo River. Regional similarity between the water quality variables was tested by applying principal component analysis to the aggregate data of all rivers. It was found out that the principal components stay the same, which implies no new information has been added. Therefore, variables belonging to the same principal components were related. For example Chloride of Kulfo River

belongs to the same principal component as Hare River and they are linearly related. Therefore, regional correlation among water quality variables is strongly suggested as part of monitoring optimisation.

This time series monitoring of water quality can serve as a basis of future sampling and monitoring design where by the curve that fits the long term seasonal variation defines the degree of freedom and the sampling interval can be decided from the number of points required to define the curve. Parameters whose values in greater percentage fit in to this model include conductivity, alkalinity, Hardness Calcium and Sodium. On the other hand Turbidity, solids and chloride have higher short term runoff based variation which can be modelled as periodic functions of runoff and rain where as the long term seasonal component monitoring interval is decided from the fitting curve used for seasonal de-trending.

4.2 LAKE WATER QUALITY MONITORING RESULTS AND EVALUATION

The summary of ranges of variation of the water qualities of the lakes as well as some of the tributary rivers is given in table 4.2.1 again. Both lakes are characterised as alkaline – saline lakes with dominant ions of sodium, bicarbonate and chloride. Lake Chamo possesses greater concentration of these ions than Lake Abaya because of Lake Chamo's tributary rivers increasingly Saline water quality, the longer retention time of the lakes and the higher rate of evaporation in the lake as well as on the catchment at the lower elevations in which Lake Chamo and its catchment are situated.

Table 4.2.1 Ranges of variation of Chemical Concentrations Lakes

Ion	Chemical formula	Unit	Lake Abaya	Lake Chamo	River Hare	River Kulfo	River Sile
pH		PH Units	8.4 - 8.98	9.0 - 9.23	6.0 – 8.7	6.48 – 9.48	7.4 – 8.5
Conductivity		$\mu\text{S}\cdot\text{Cm}^{-1}$	1030-1110	1810 - 1960	40 - 90	80 - 200	115 - 533
Turbidity		NTU	64 - 90	40-100	10-750	7-1950	9-389
Spectrophotometric absorption (500 nm)		Abs	0.08 – 0.14	0.08 – 0.135	0.003 – 1.5	0.01 - 11	0-1.3
Total Solids		mg L^{-1}	700-975	1200-1500	40 -2725	65-5620	215-660
Volatile Solids		mg L^{-1}	165-380	360 -478	14-257	6-564	15-170
Suspended Solids		mg L^{-1}	60-250	50-350	5 - 2660	5 - 5500	5 - 310
Dissolved Solids		mg L^{-1}	911.10	1522.45	25 - 60	53 - 132	76 - 350
Alkalinity	CaCO_3	mg L^{-1} as CaCO_3	450 - 540	765 - 910	20 - 90	40 -160	60 - 380
Calcium	Ca^{2+}	mg L^{-1}	15-24	12-20	4-15	5-20	5-25
Magnesium	Mg^{2+}	mg L^{-1}	2-5	7-12	1-7	2-13	3-40
Sodium	Na^+	mg L^{-1}	213 - 250	375 - 440	2-7	3-9	5-20
Potassium	K^+	mg L^{-1}	15-19	22-28	0.5 – 1.40	0.5 –2.0	1.1 – 3.2
Ammonia	NH_3	mg L^{-1}	0.16-0.58	0.03-0.45	0-019	0.006-0.35	0.005-0.23
Ammonium	NH_4^+	mg L^{-1}	0.6-0.7	0.07-0.3	0-1.74	0.014-0.95	0.005-0.87

Ion	Chemical formula	Unit	Lake Abaya	Lake Chamo	River Hare	River Kulfo	River Sile
Carbonate	CO ₃ ²⁻	mg L ⁻¹	30- 55.24	60- 117	0-0.7	0-2.5	0- 3.32
Bicarbonate	HCO ₃ ⁻	mg L ⁻¹	400-500	750-850	20-120	40-190	60- 337
Chloride	Cl ⁻	mg L ⁻¹	64-78	127-160	2-14	3-12	7-42
Sulphate	SO ₄ ²⁻	mg L ⁻¹	25-34	12-26	1-9	1-8	1-13
Nitrate	NO ₃ ⁻	mg L ⁻¹	0.6-1.8	0.7-3	0-1	0.5-1.8	0.5-2.1
Nitrite	NO ₂ ⁻	mg L ⁻¹	0-0.05	0-0.02	0-0.03	0-0.05	0-0.06
Phosphate	PO ₄ ³⁻	mg L ⁻¹	0-0.19	0-0.03	0-0.06	0-0.06	0- 0.07
Silicacid	H ₂ SiO ₃	mg L ⁻¹	44.29	3.14	22.26	21.42	28.97
H-Sillica	HSiO ₃ ⁻	mg L ⁻¹	6.04	0.76	0.10	0.92	1.25
Siliciumion	SiO ₃ ²⁻	mg L ⁻¹	0.00	0.00	0.00	0.00	0.00

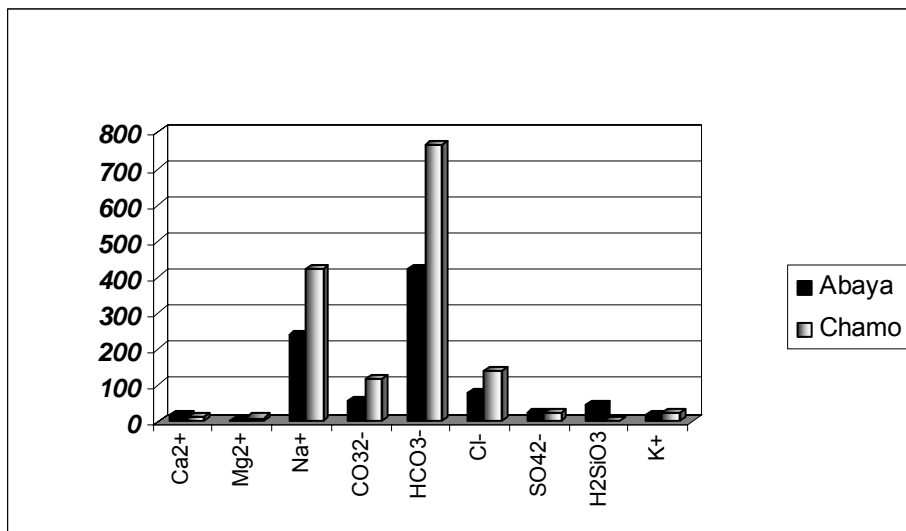


Fig. 4.2.1 Lake Major Ions (mg L⁻¹). Both lakes chemistry is dominated by Bicarbonate, Sodium and chloride ions. These dominances are a combination of river inflows from the catchment, evaporative concentration and loss of ions because of biological deposition.

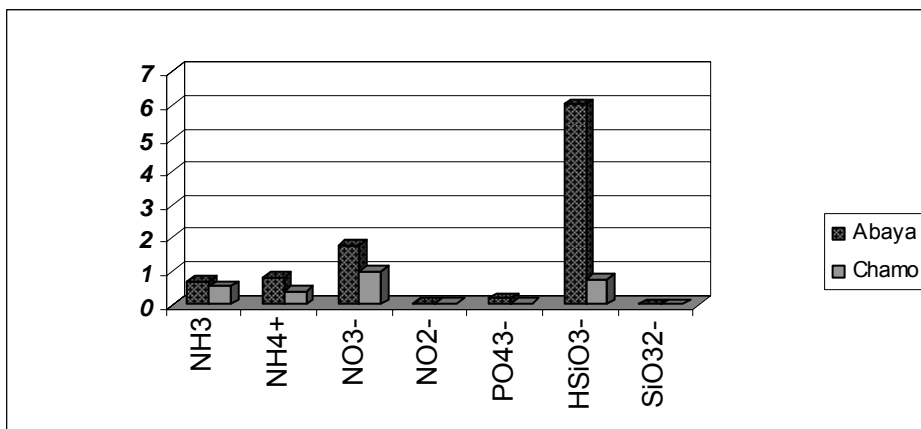


Fig. 4.2.2 Lake Nutrient Ions (mg L⁻¹). Silica is low in lake Chamo due possible to diatom growth as compared with that of Lake Abaya.

4.2.1 Seasonal Variation

4.2.1.1 Major Ions seasonal Variations

The results of the laboratory and field measurements have been plotted below as a time series for the two lakes. The variation of most of the analytes generally follows the seasonal precipitation pattern as expected [44]. The change in concentration is generally greater for Lake Chamo then it is for Lake Abaya. This also implies that dilution is important for alleviating stressed conditions in Lake Chamo than in Lake Abaya where the dilution influence seems to be minimum.

Chloride concentration graph as well as conductivity and many of the other cations and anions follow similar pattern with peaks coinciding with one another. It is worth noting that there is an increasing trend of conductivity and chloride concentration for Lake Abaya throughout the season and this part of increase may be part of the long-term salinity increase of Lake Abaya.

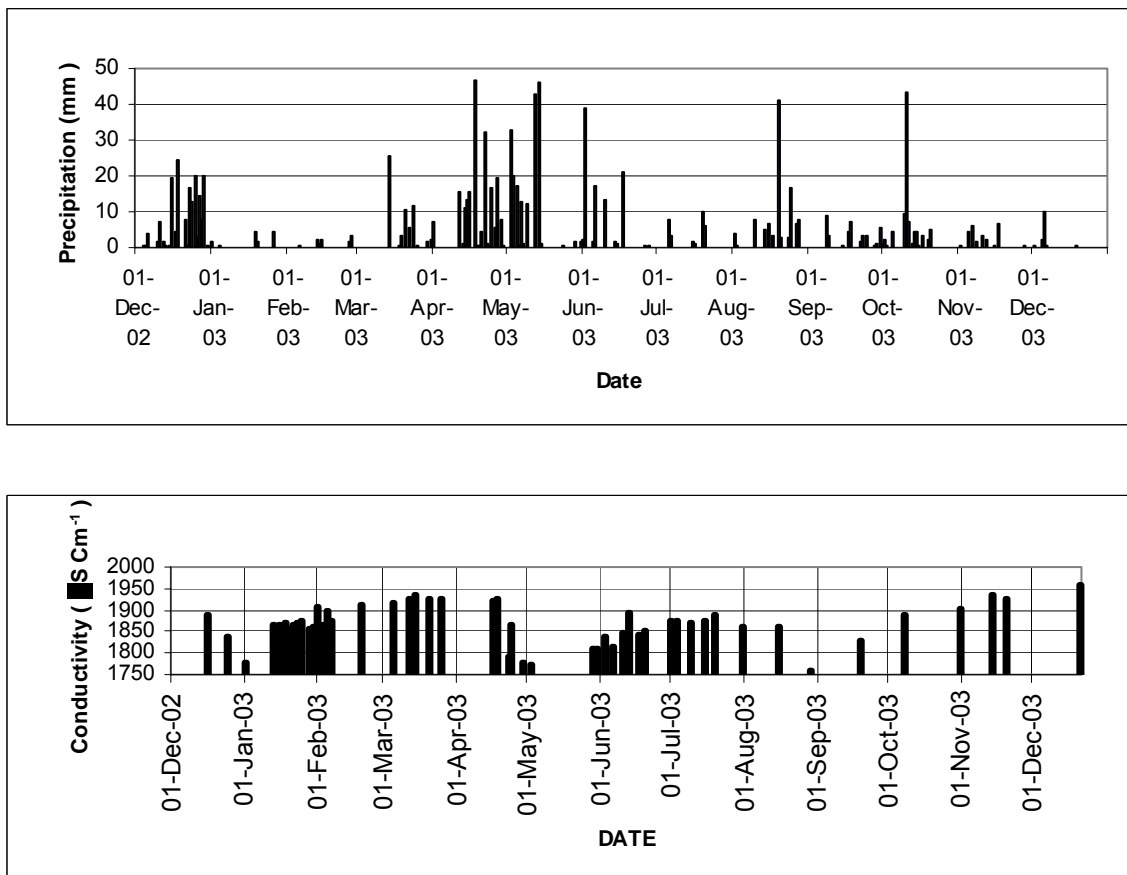


Figure 4.2.3 Comparison of rainfall and Lake Chamo conductivity. Generally the conductivity decreases during the rainfall seasons and increases during the dry seasons.

The residence time of water in Lake Chamo is greater than that of Lake Abaya and as such Lake Abaya should have shown greater and rapid change in concentration in response to the precipitation and runoff inflow in to the lakes. However, the greater length and area of the lake precludes fast mixing and the response is lowered. This is more so since Lake Abaya has ceased to overflow and the flow pattern is more localised.

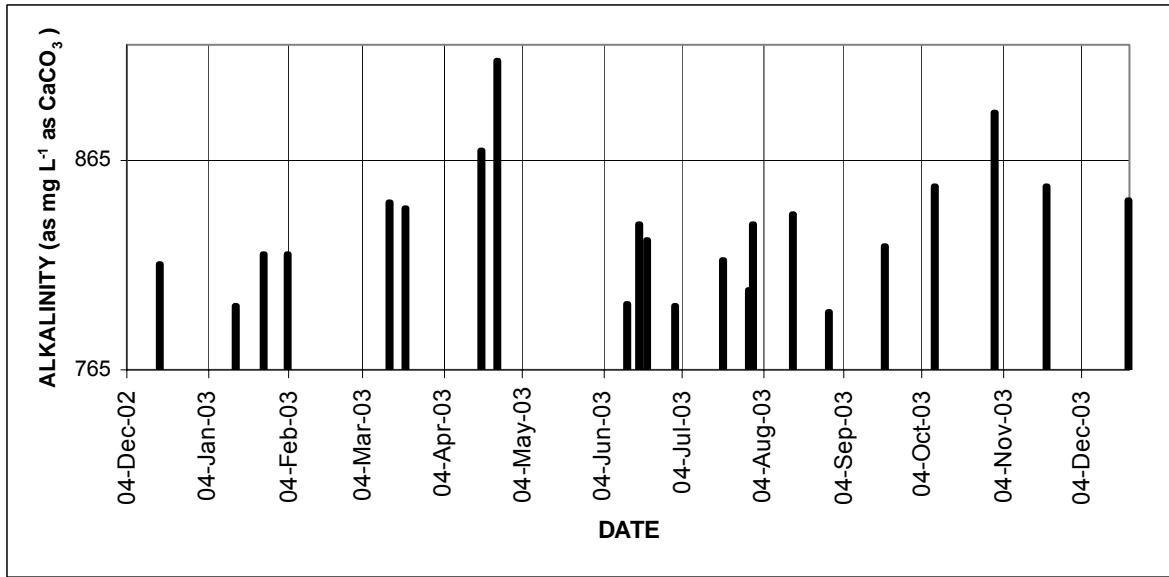


Fig. 4.2.1.1 Alkalinity Time Series for Lake Chamo

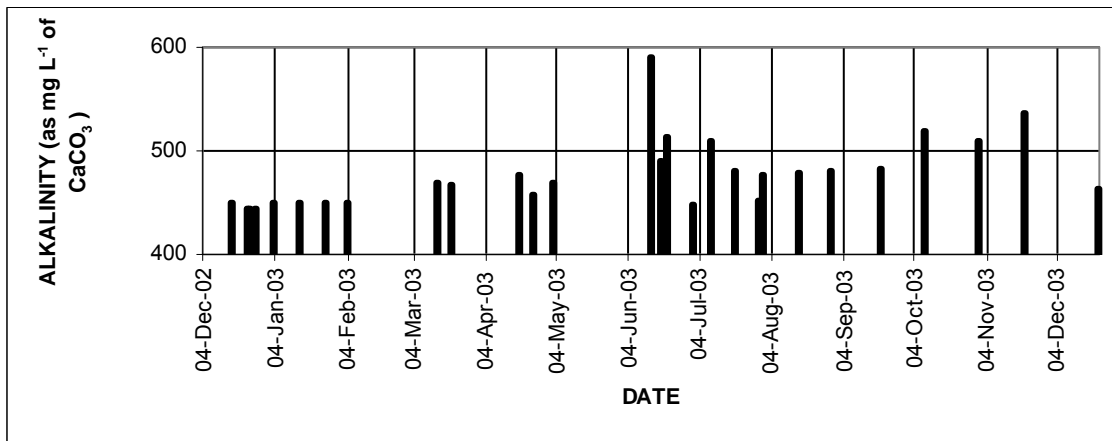


Fig. 4.2.1.2 Alkalinity Time Series for Lake Abaya

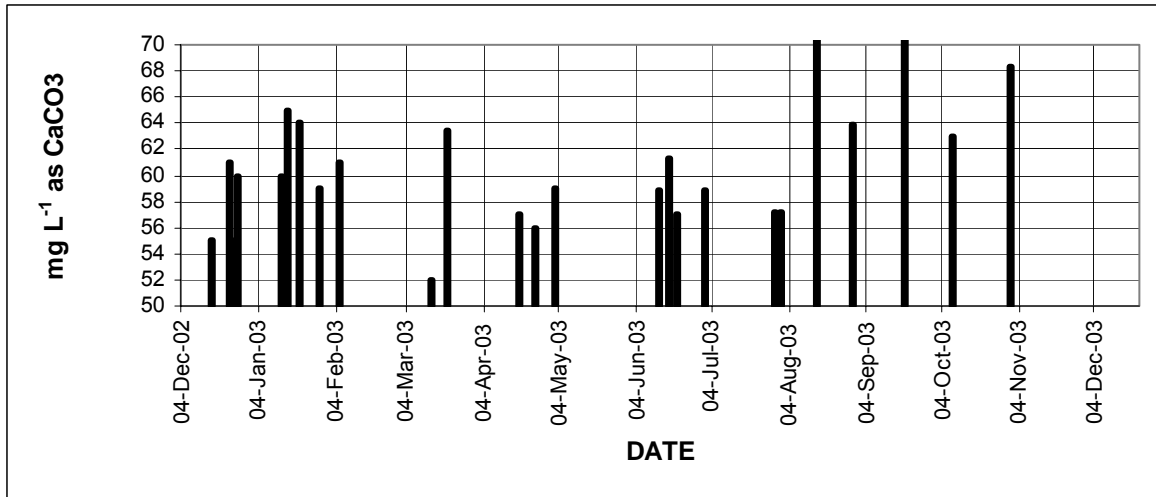


Fig. 4.2.1.3 Hardness Lake Abaya

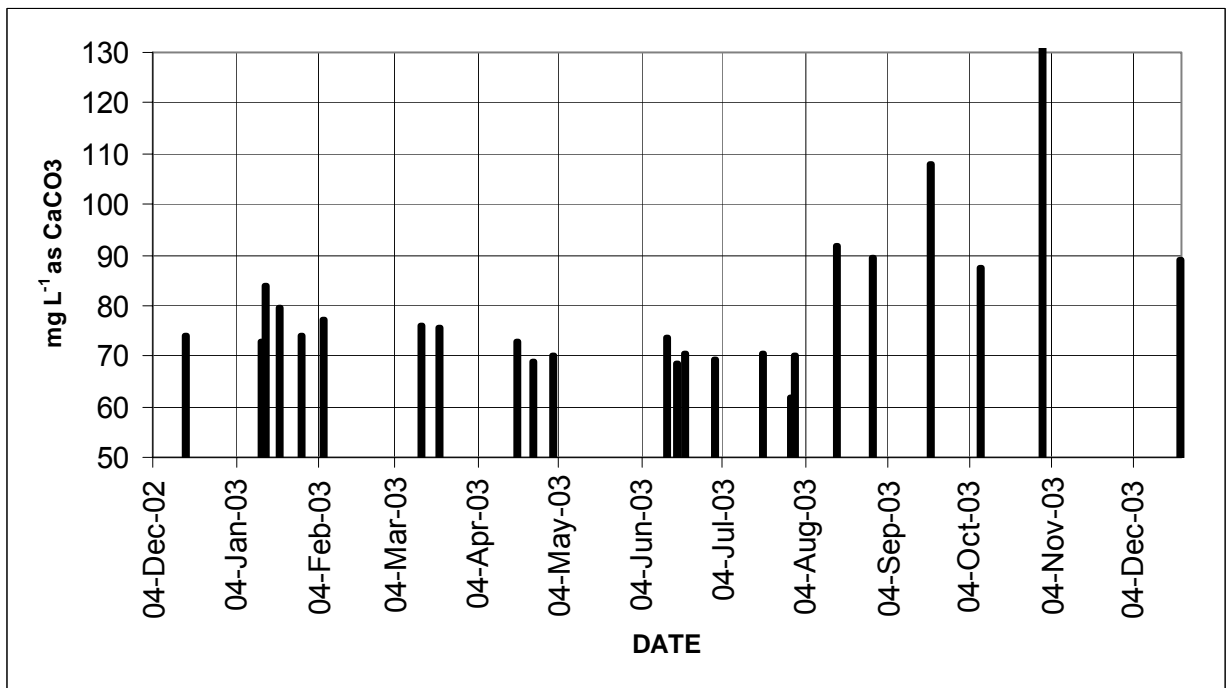


Fig. 4.2.1.4 Hardness Lake Chamo

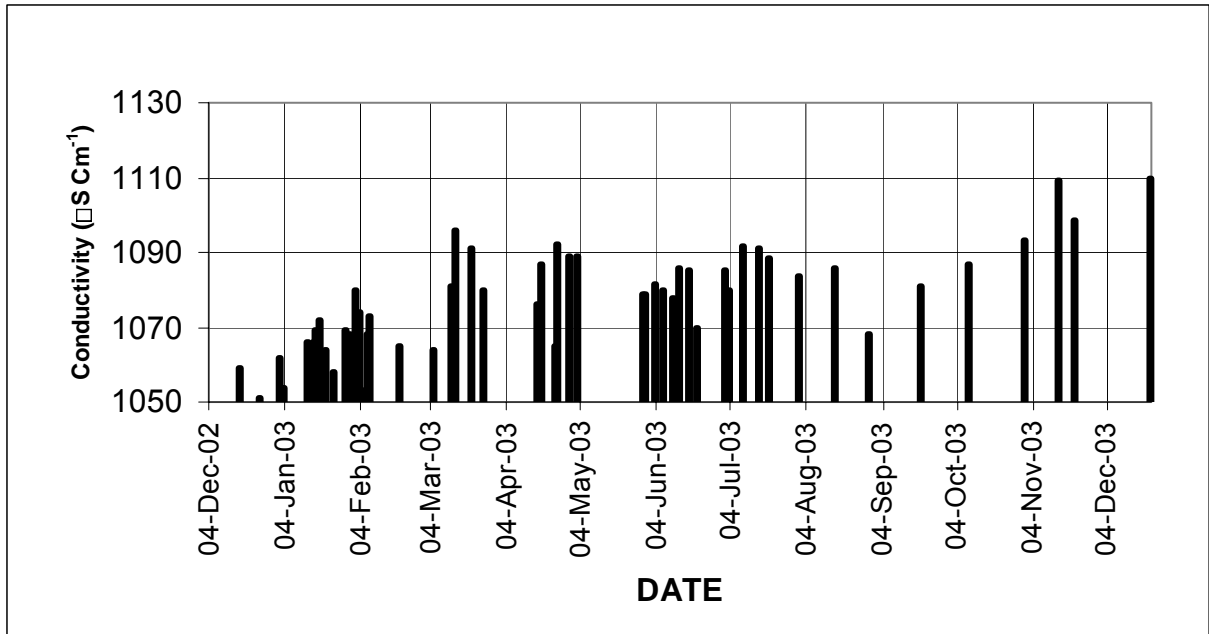


Fig. 4.2.1.5 Lake Abaya Conductivity Time Series

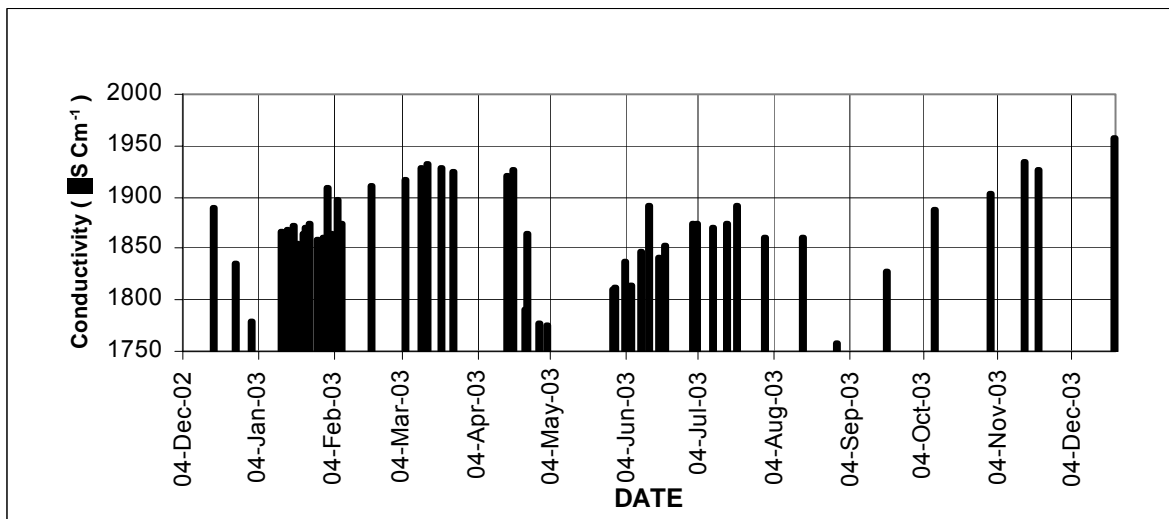


Fig. 4.2.1.6 Lake Chamo Conductivity Time Series

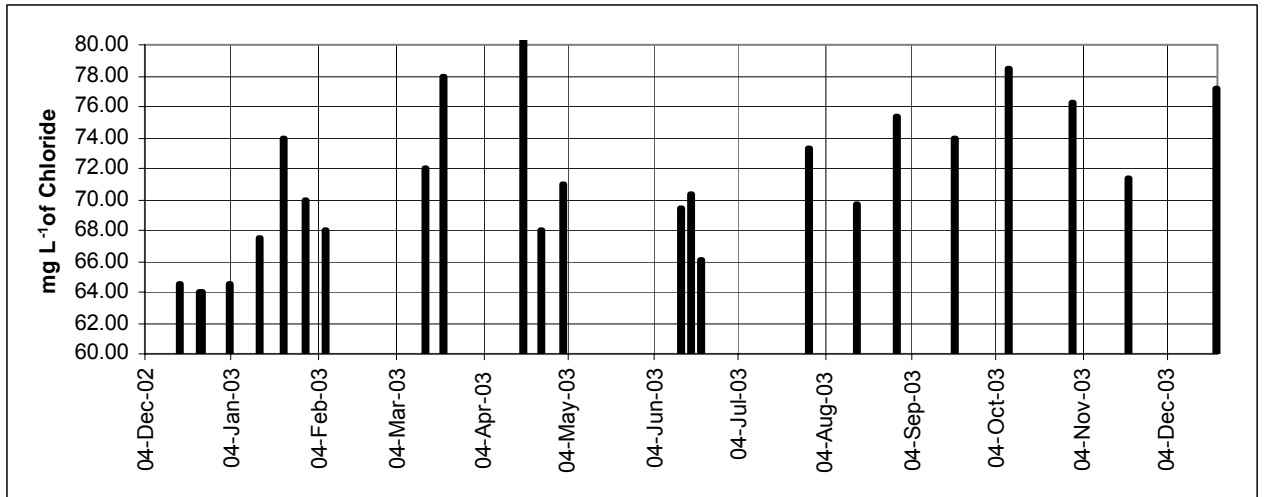


Fig. 4.2.1.7 Chloride Lake Abaya

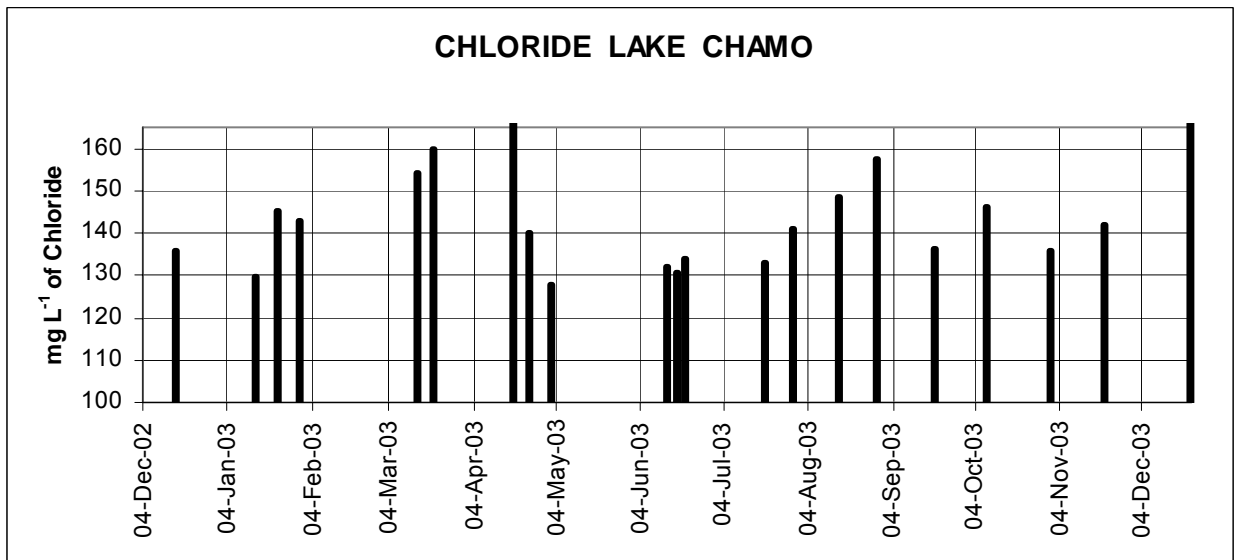


Fig. 4.2.1.8 Chloride Lake Chamo

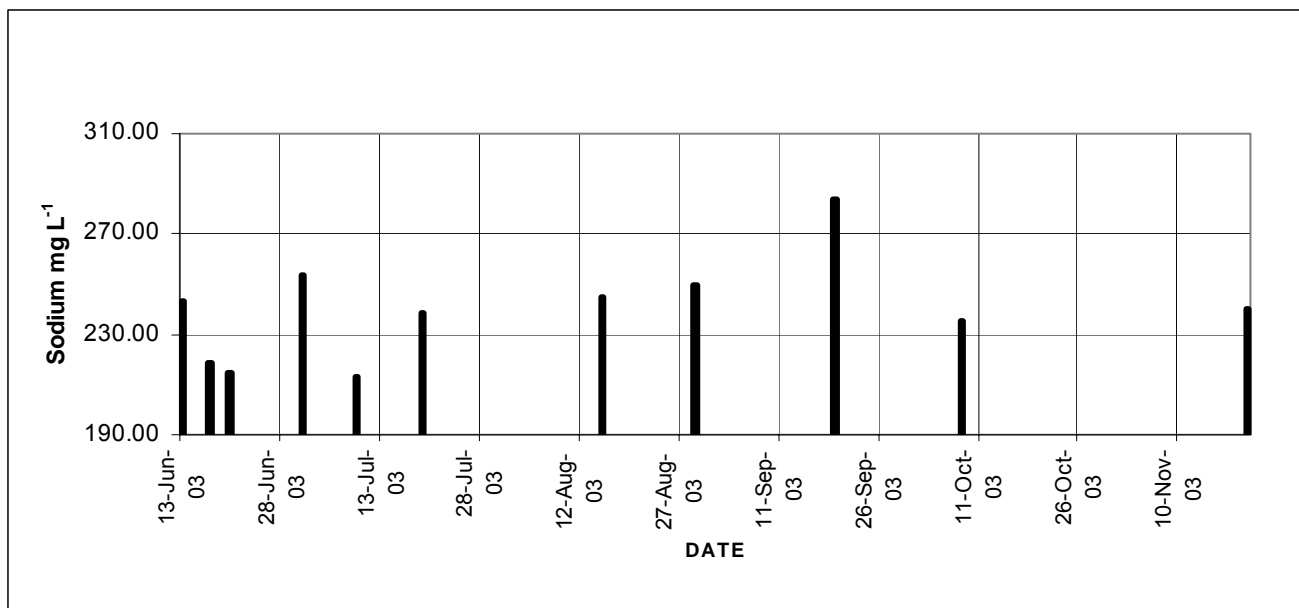


Fig. 4.2.1.11 Sodium Lake Abaya

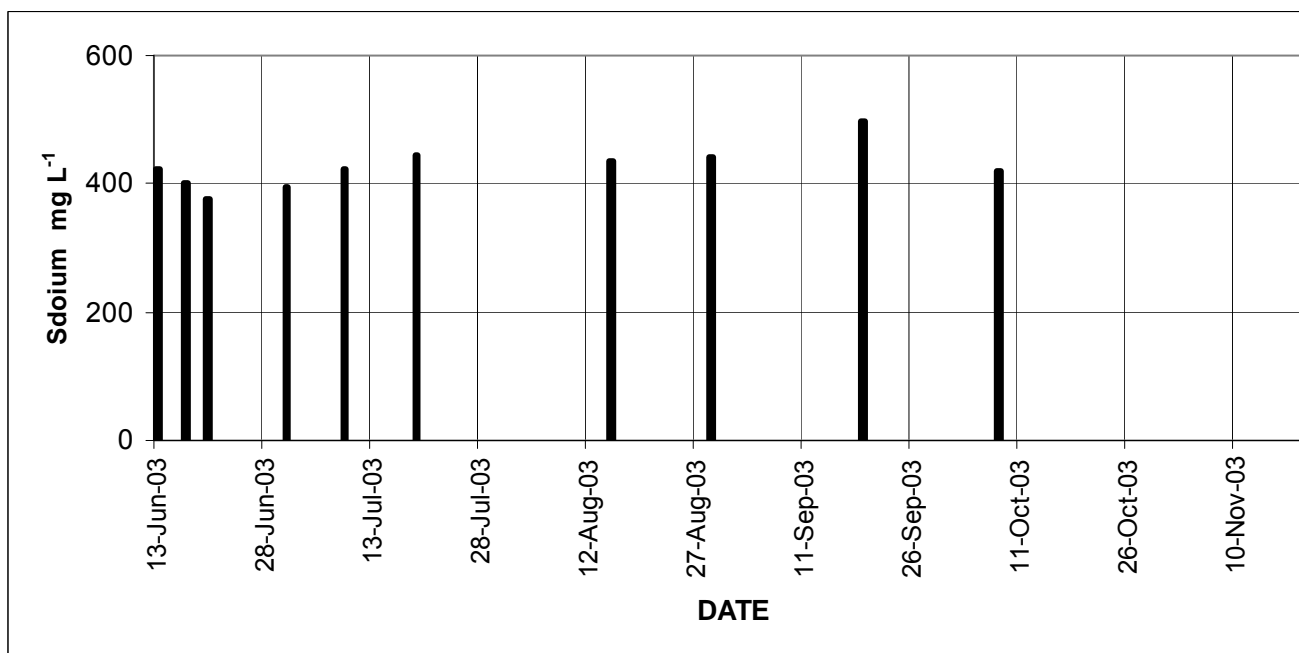


Fig. 4.2.1.12 Sodium Lake Chamo

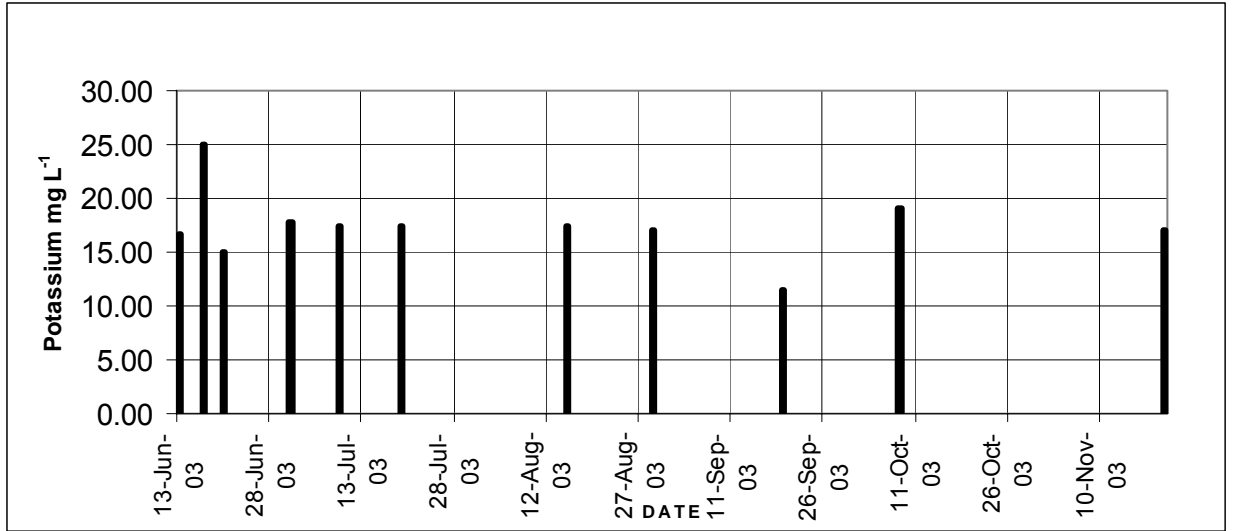


Fig. 4.2.1.13 Potassium Lake Abaya

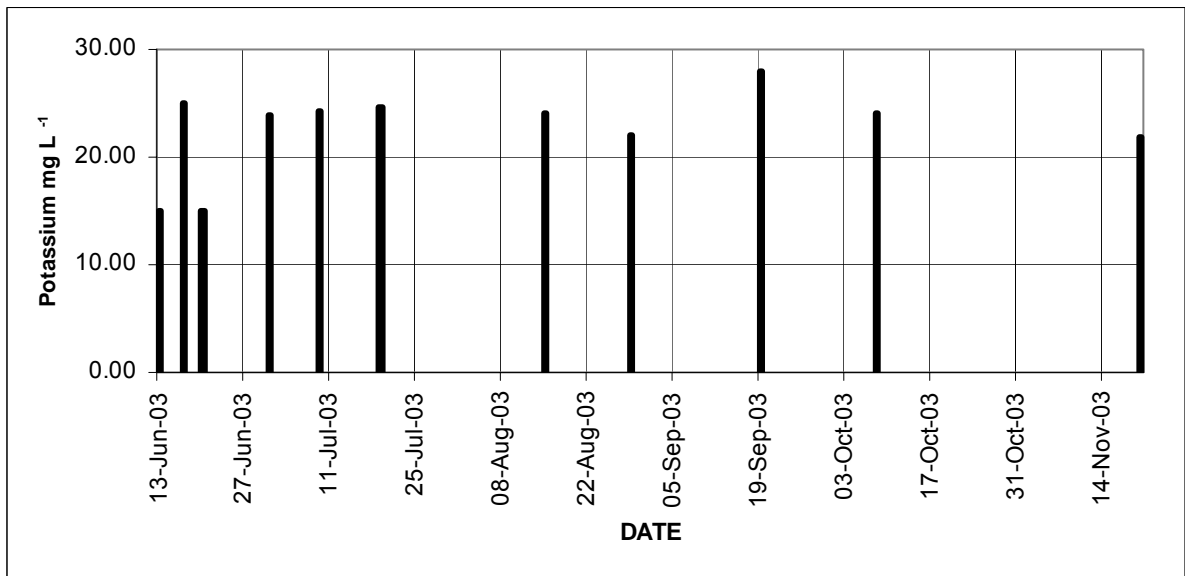


Fig. 4.2.1.14 Potassium Lake Chamo

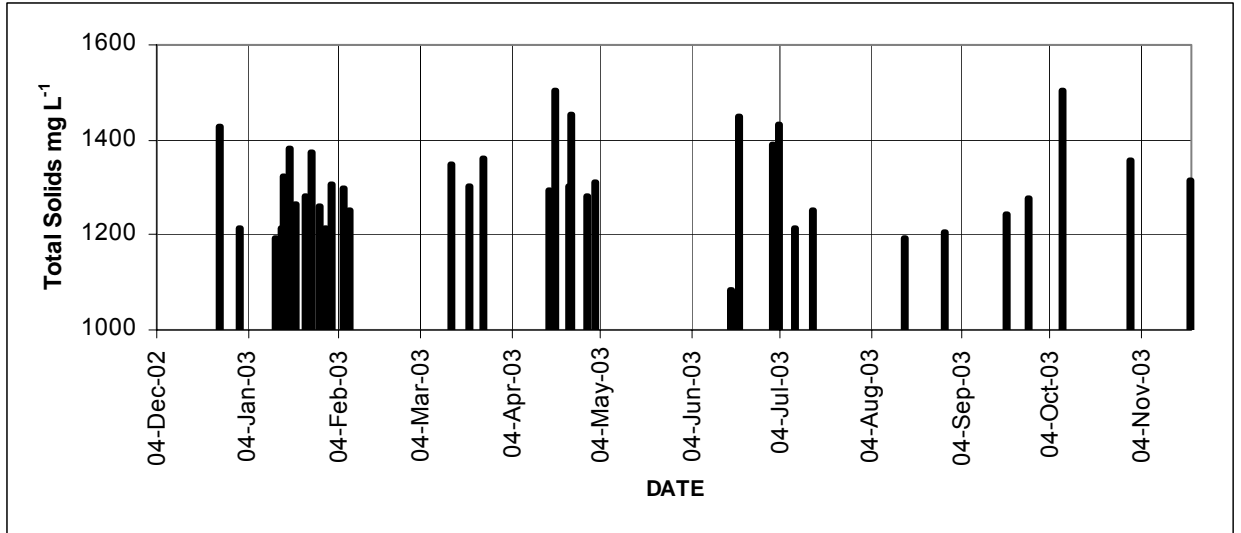


Fig. 4.2.1.15 Total Solids Lake Chamo

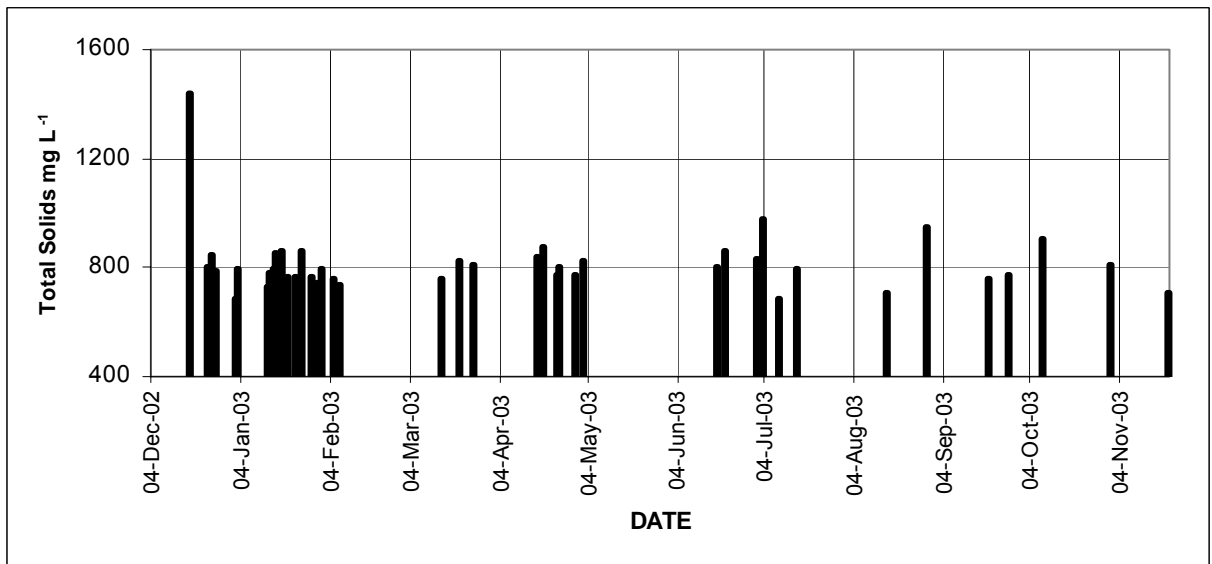


Fig. 4.2.1.16 Total Solids Lake Abaya

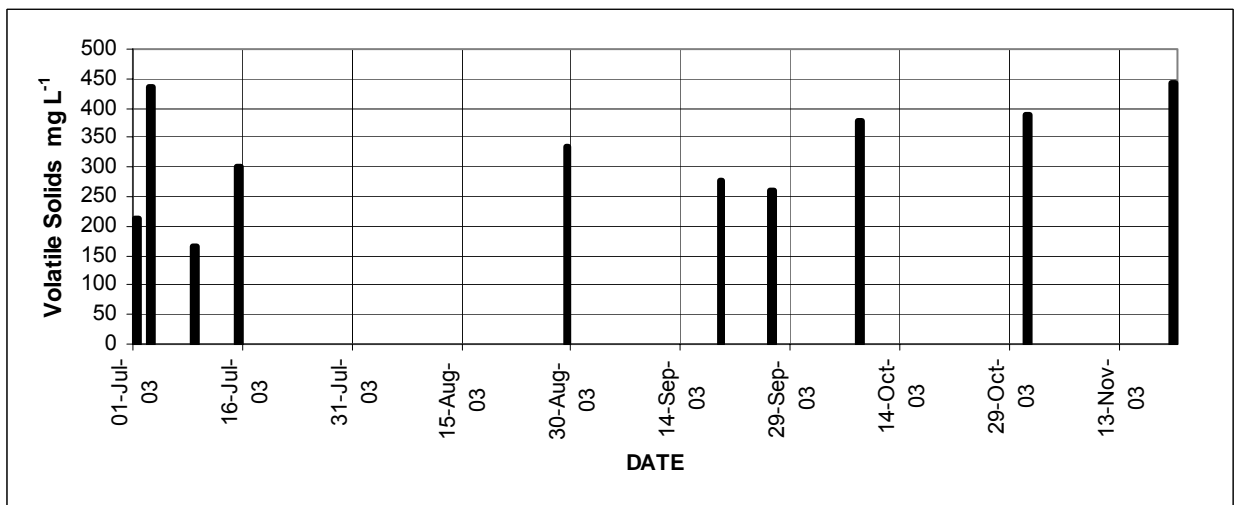


Fig. 4.2.1.17 Volatile Solids Lake Abaya

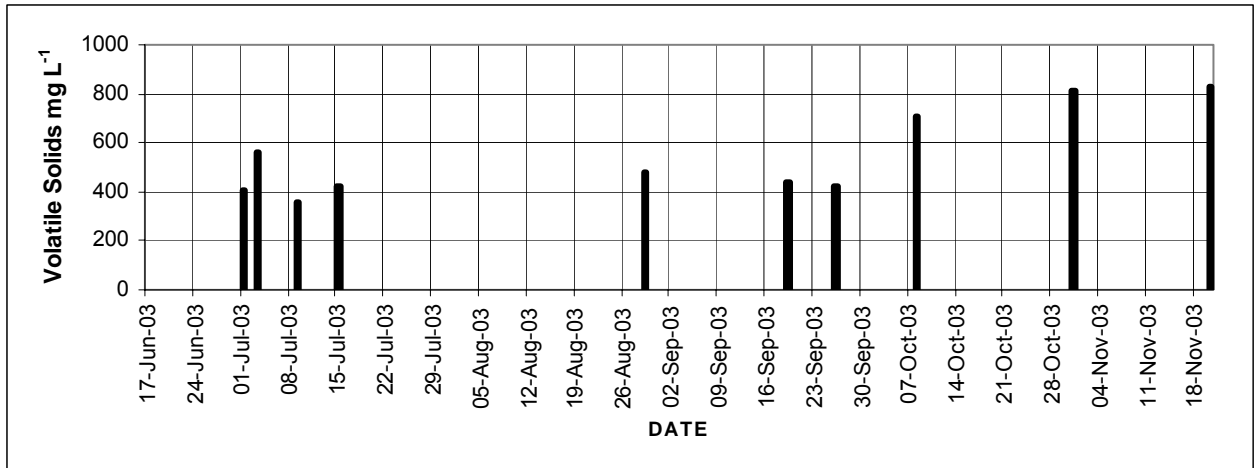


Fig. 4.2.1.18 Volatile Solids Lake Chamo

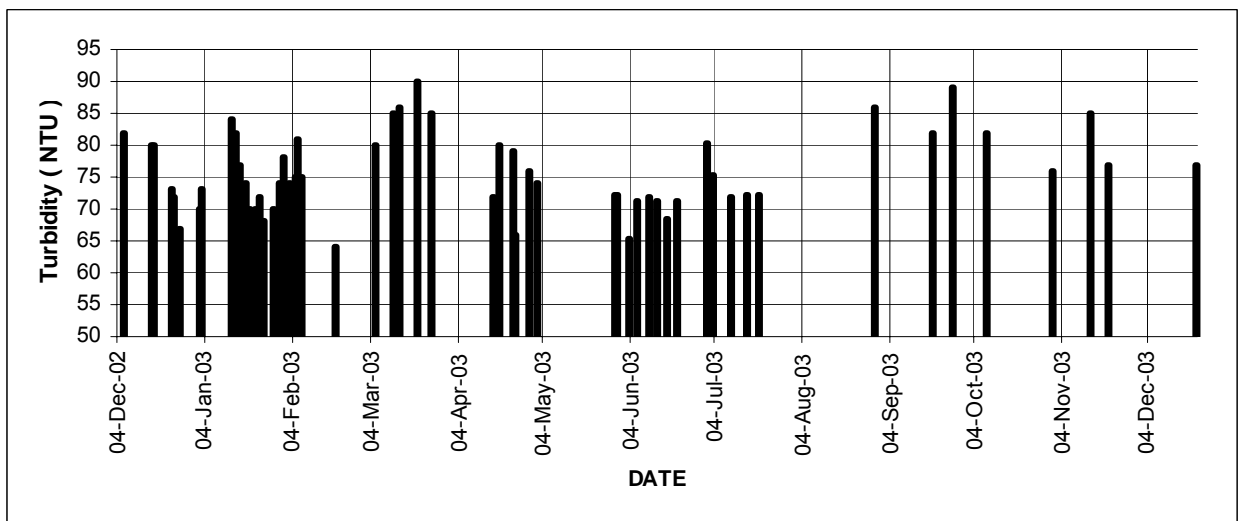


Fig. 4.2.1.19 Turbidity Time Series Data Lake Abaya

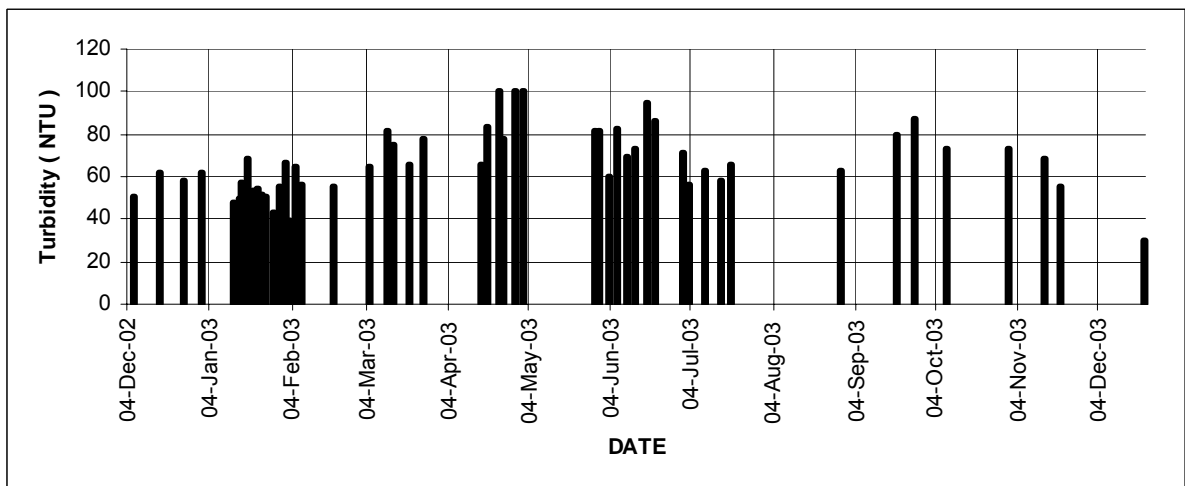


Fig. 4.2.1.20 Turbidity Time Series Data Lake Chamo

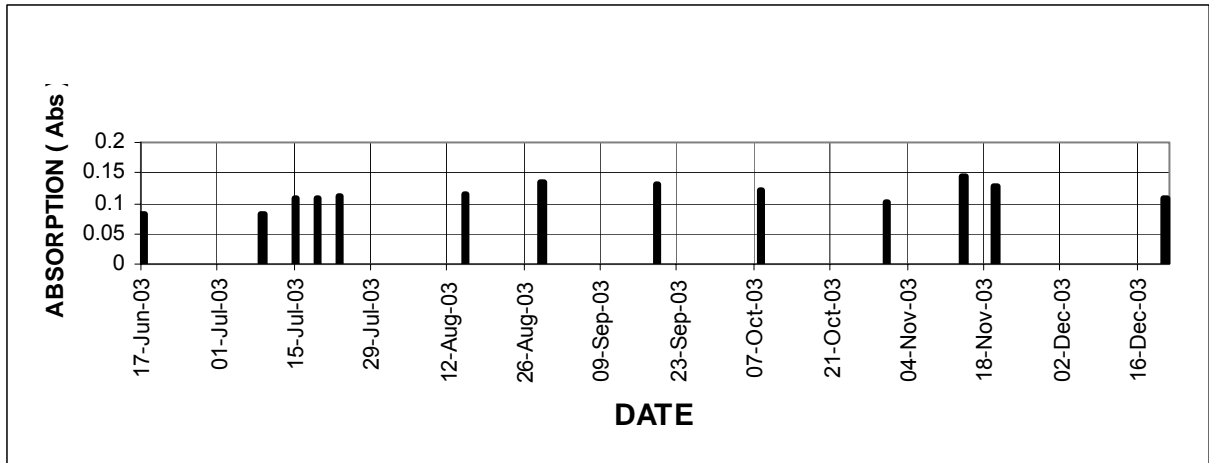


Fig. 4.2.1.21 Spectrophotometric absorption Data for Lake Abaya (500 Nm)

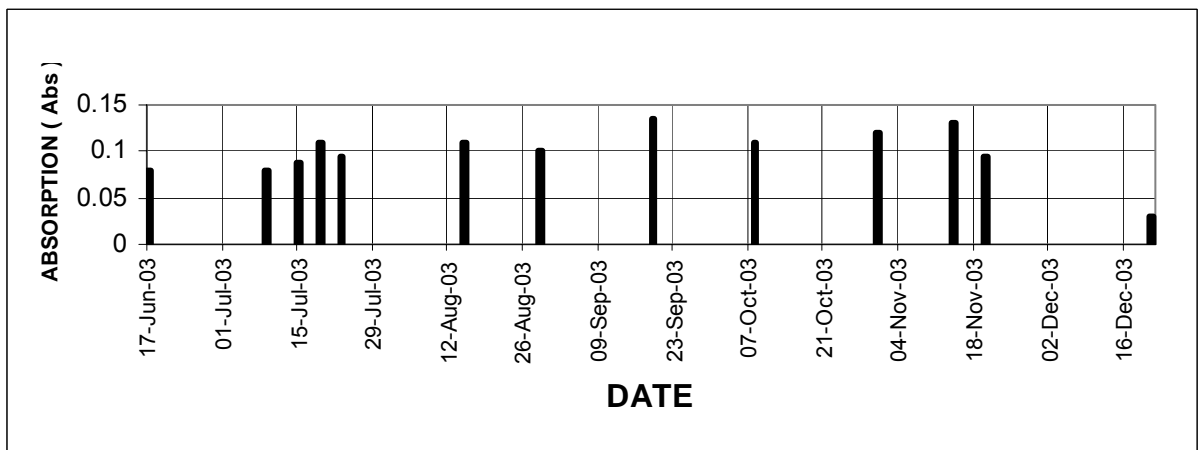


Fig. 4.2.1.22 Spectrophotometric Absorption Data for Lake Chamo (500 Nm)

Turbidity fluctuation is high for Lake Chamo but quickly receding during the drier period thus allowing for more productive conditions in the summer. For Lake Abaya

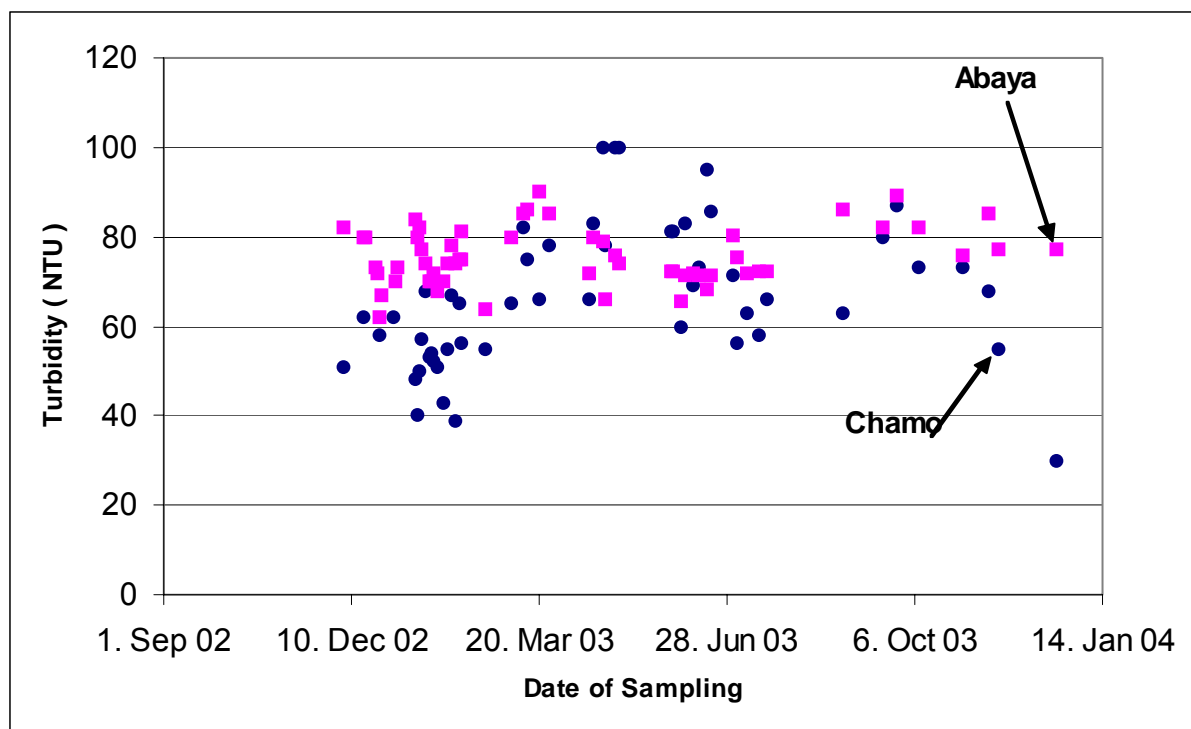


Fig. 4.2.1.23 Comparison of Turbidity Variation for Lakes Abaya and Chamo. Lake Chamo shows greater seasonal variation in turbidity than Lake Abaya. The productivity of the lake is also affected by this seasonal variation.

The turbidity fluctuation is limited staying above that of Lake Chamo for most of the dry season. The location of peaks for the turbidities of the two lakes differs because of the different periods of precipitation of the upper Abaya Catchment.

4.2.1.2 PH and Buffering Capacity Seasonal Variation

Due to the geological characteristics of the area that is underlain by the tertiary and quaternary period basaltic formations and the dominance of the calcium-magnesium-bicarbonate contents of the rivers, the alkalinity and pH of these lakes are normally high. There is a gradual and slight increase of the pH towards the end of the dry season and a decrease as the rainy season progresses. Lake Abaya shows an increase and decrease in pH of about ± 0.1 units. Lake Chamo pH variation follows the same seasonal pattern and because of the seasonal influence the pH change is more discernable. The pH variation is minimum for Lake Abaya in line with what was observed for the other parameters. Lake Chamo has greater pH change largely due to seasonal effect of the rain and dilution [45]. Due to the higher buffering capacity of both lakes endowed with high concentration of carbonates and bicarbonates, short term pH changes are expected to be buffered by the higher alkalinity.

4.2.2 Long term variation – Conductivity, ionic compositions and Salinity

The salinity accumulation of Lake Chamo is greater than that of Lake Abaya owing to an aggregate of contributing factors: less inflow in to the lake, greater salinity of the inflowing rivers, greater evaporation and less precipitation from the lakes and greater retention time in Lake Chamo than in Lake Abaya.

Tables 4.2.2.1 and 4.2.2.2 show the comparison of concentrations of ions for the two lakes sampled at different times starting from 1961. It is apparent at a glance of the data that there is an upwards significant rate of increase in the concentrations of most of the ions for both lakes. Both lakes over recent years face increasing salinity [46]. Lake Chamo faces greater rate of Increase in salinity which amounts to 40% increase over the past 40 years. The trend in salinity increase on Lake Abaya started from after 1976 and is still increasing at a moderate rate.

Table 4.2.2.1 Trends in Major Chemical Concentrations for Lake Abaya [46, 47, 48]

	Year	1961	1964	1966	1975	1976	1988	1991	1995	2001	2003
pH	pH units		8.90	8.90				8.65	8.80	9.0	8.98
Conductivity	$\mu\text{S cm}^{-1}$	1008	698	1068	918			921	1071	1034	1075
Sum (Cations)	meL^{-1}	10.5	9.1	9.8	10.1	10.2		10.34			12.08
Sum (Anions)	me L^{-1}	10.6	9.1	10.5	10.4	9.2		11.37			11.56
Salinity	g L^{-1}	0.84	0.73	0.82	0.70	0.74		0.89	0.92		0.96
Ca^{2+}	me L^{-1}	0.6	0.8	0.8	0.7	0.6		0.45	0.7	0.9	0.9
Mg^{2+}	me L^{-1}	0.5	0.2	0.2	0.3	0.3		0.32	0.3	0.43	0.27
Na^+	me L^{-1}	9	7.7	8.5	8.5	8.8		9.13	9.6		10.42
K^+	me. L^{-1}	0.4	0.4	0.4	0.4	0.4		0.44			0.45
SiO_2	mg L^{-1}	45	40	48				20.5			39
$\text{CO}_3^{2-} + \text{HCO}_3^-$	me L^{-1}	8.5	7.4	8.4	6.3	7.4		9.37	9.9	9.6	9.47
Cl^-	me L^{-1}	1.5	1.1	1.4	1.5	1.3		1.11	1.68	1.74	2.17
SO_4^{2-}	me L^{-1}	0.6	0.6	0.7	0.8	0.1		0.89		0.62	0.52
$\text{NO}_3^- + \text{NO}_2^-$	$\mu\text{g L}^{-1}$							200		361	434
$(\text{NH}_3 + \text{NH}_4^+) - \text{N}$	$\mu\text{g L}^{-1}$							15		470	900
$(\text{PO}_4^{3-}) - \text{P}$	$\mu\text{g L}^{-1}$		128	14				151		110	187
Total - P	$\mu\text{g L}^{-1}$							237			
Chl ^a	$\mu\text{g L}^{-1}$			69			7	5			3.9

Table 4.2.2.2 Trends in Major Chemical Concentrations for Lake Chamo [46, 47, 48]

	Year	1964	1966	1979	1988	1991	1995	2001	2003
pH	pH units	8.9	8.9			9.2	9.32	9.22	9.23
Conductivity	$\mu\text{S Cm}^{-1}$	1232	1120			1568	1570	1743.556	1868
Sum (Cations)	me L^{-1}	13.6	10.8			16.2			20.47
Sum (Anions)	me L^{-1}	13.5	11.7			16.2			20.98
Salinity	g L^{-1}	1.07	0.90			1.30	1.43		1.65
Ca^{2+}	me L^{-1}	0.7	0.7			0.4	0.3	0.62	0.73
Mg^{2+}	me L^{-1}	0.8	0.6			0.6	0.8	1.23	0.84
Na^+	me L^{-1}	11.6	9.1			14.7	15.45		18.3
K^+	me L^{-1}	0.5	0.4			0.6			0.58
SiO_2	mg L^{-1}	28	38			1.5		0.35	3
$\text{CO}_3^{2-} + \text{HCO}_3^-$	me L^{-1}	10.9	9.4			13.3	15	14.8	16.46
Cl^-	me L^{-1}	2	1.7			3.1	2.8	3.32	3.97
SO_4^{2-}	me L^{-1}	0.6	0.6			0.2		0.25	0.52
$\text{NO}_3^- + \text{NO}_2^-$	$\mu\text{g L}^{-1}$							600	280
$(\text{NH}_3 + \text{NH}_4^+) - \text{N}$	$\mu\text{g L}^{-1}$					20		650	300
$(\text{PO}_4^{3-}) - \text{P}$	$\mu\text{g L}^{-1}$		30			29.4		9	28
Total - P	$\mu\text{g L}^{-1}$								
Chla	$\mu\text{g L}^{-1}$		89	73	170	100.3			15- 100

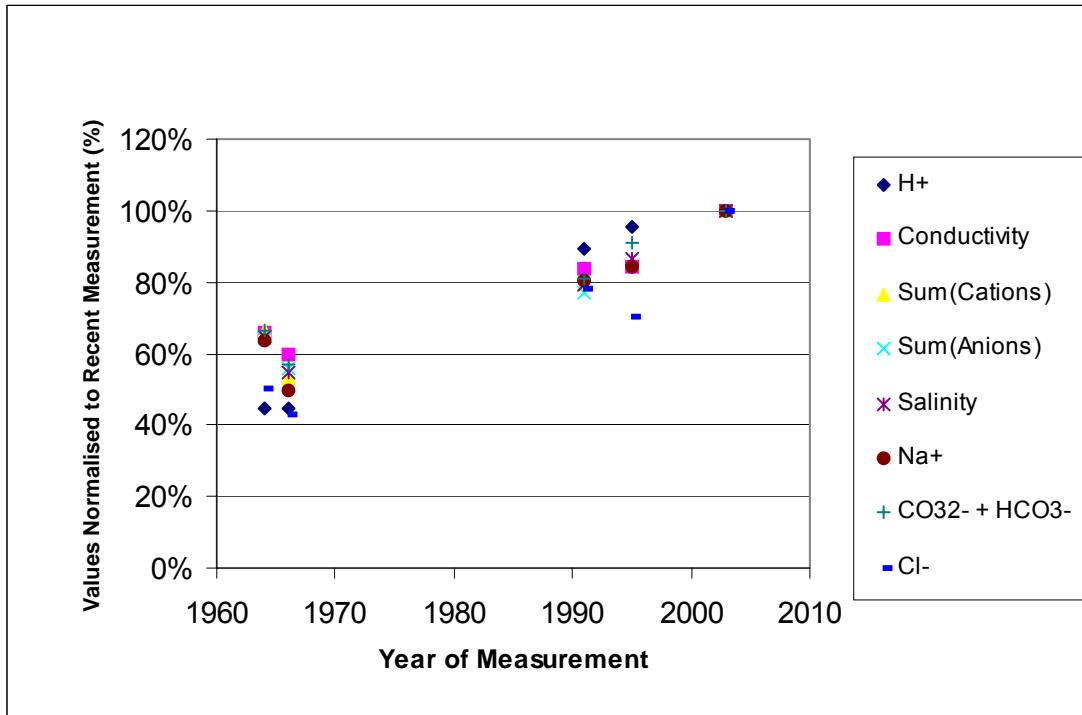


Fig. 4.2.2.1 Trends in Major Ion Concentrations for Lake Chamo. There is a steep increase in the salinity of the lakes over the last 40 years amounting to almost 1% per year. Evaporative concentration is evident as the major ions increase almost in the same proportion.

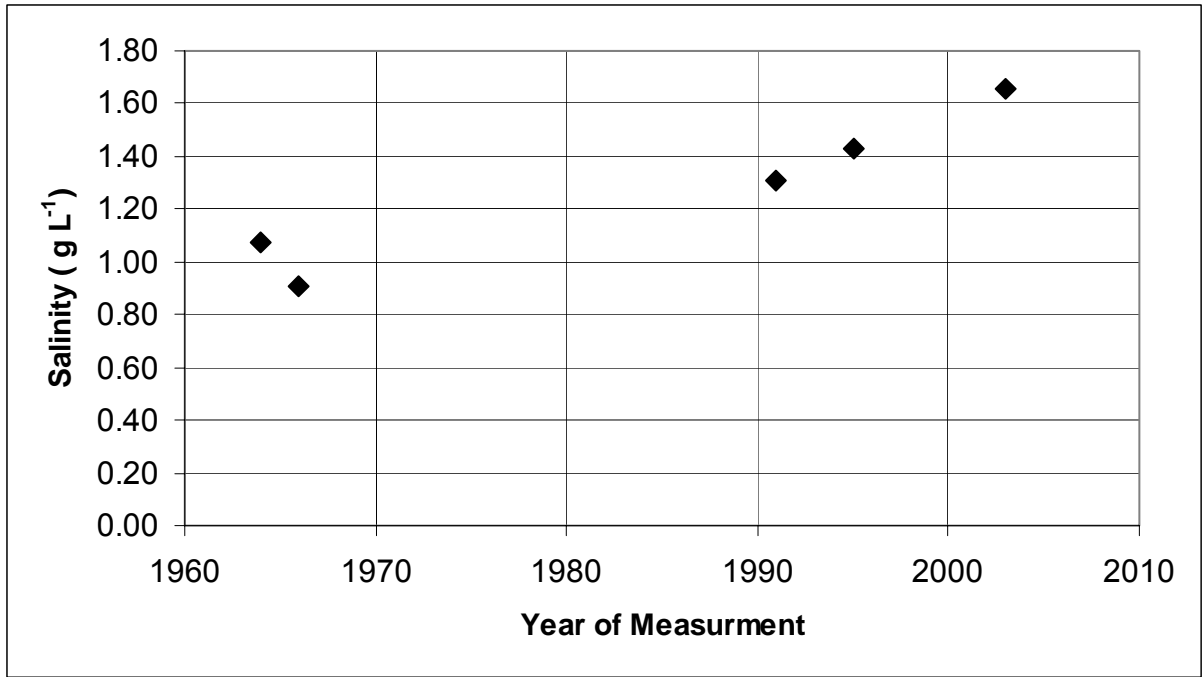


Fig. 4.2.2.2 Trends in Salinity of Lake Chamo

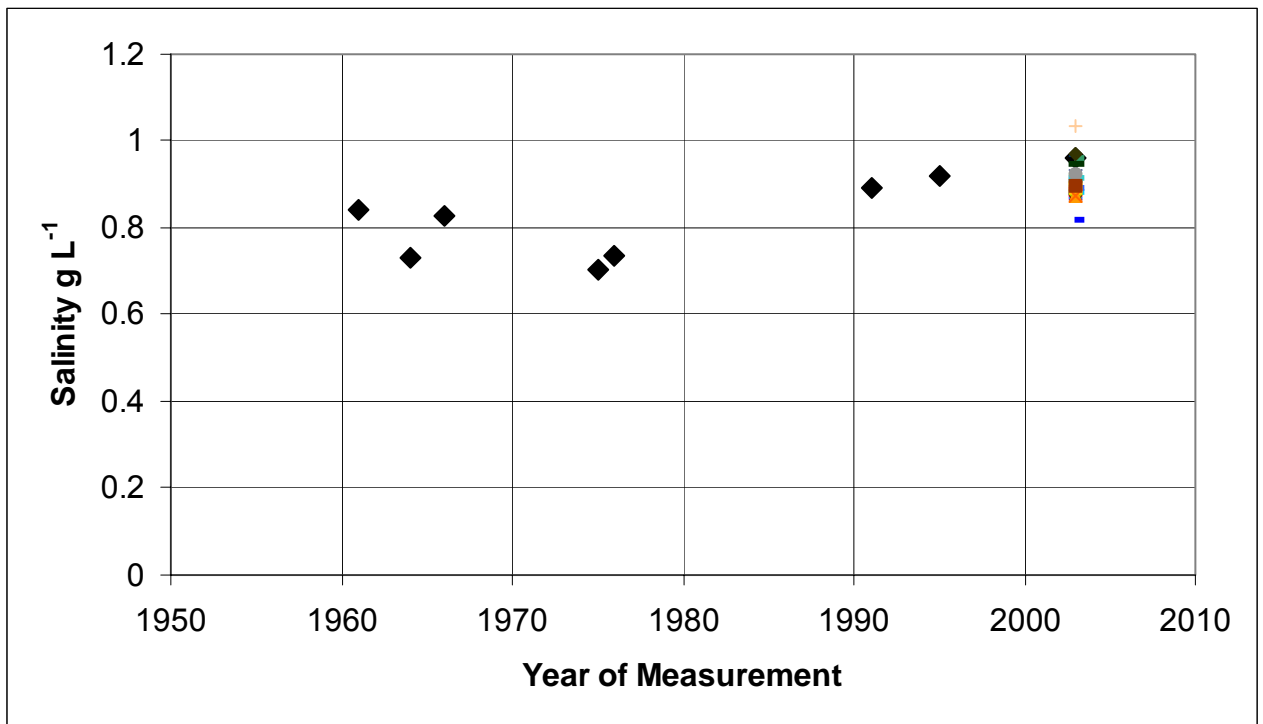


Fig. 4.2.2.3 Trends in Salinity of Lake Abaya. (The Cluster of Points at 2003 represents the seasonal measurements). There has been a general increase in salinity of Lake Abaya since 1979 and still continuing to the present day.

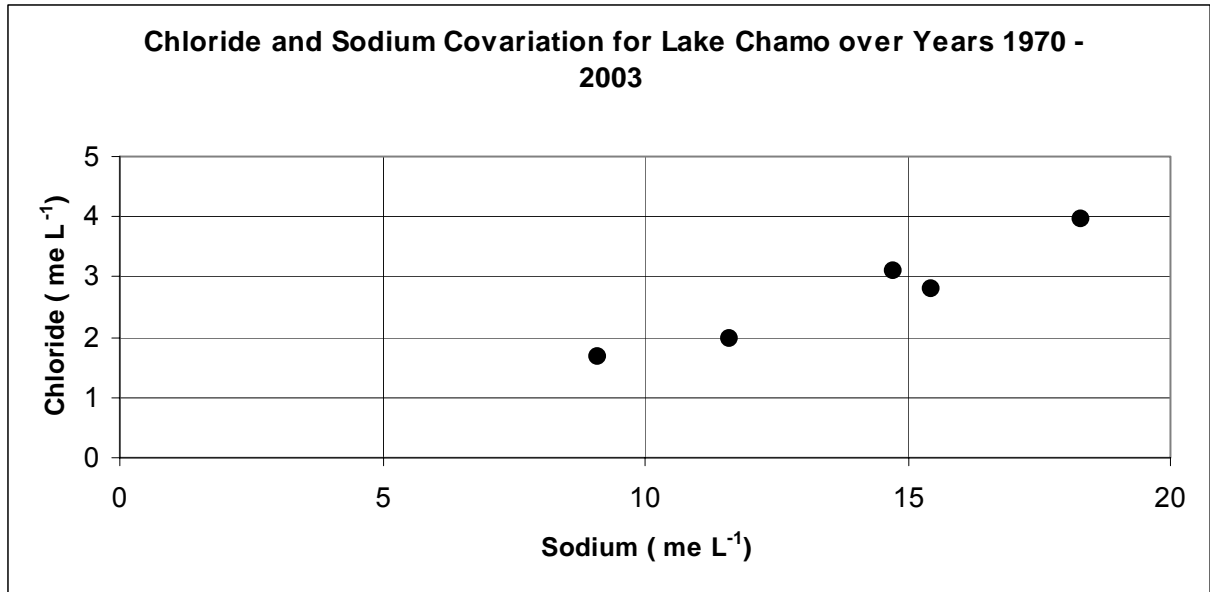


Fig. 4.2.2.4 Chloride and Sodium Co variation for Lake Chamo over Years 1970 – 2003. This co variation suggests that sodium and silicate loss by reverse weathering is minimal or did not happen as was suggested by some researchers

Figures 4.2.2.1 – 4.2.2.4 show the trends in major ions and salinities for lakes Abaya and Chamo. Lake Chamo shows increase in salinity by about 40% in the last 40 years. This trend seems linear and unabated and hence will have damaging consequences to the species distribution and the lakes eco system. Since major change in the ions distribution of the catchment inflow is not anticipated to have an impact on the lake salinity, the major cause of the increase in salinity is probably due to the decrease in the lake inflow and the relative increasing influence in the evapo-transpiration from the lake. As the lake is an economic resource for the area, this trend is a cause for concern.

Seleshi Bekele [50] estimated the decrease in flow from Lake Chamo since 1970 as a result of water use (ground water and river water for irrigation, water supply) as well as inflow reduction due to marshy and inundated areas. Fig. 4.2.2.5 shows the results of his estimate.

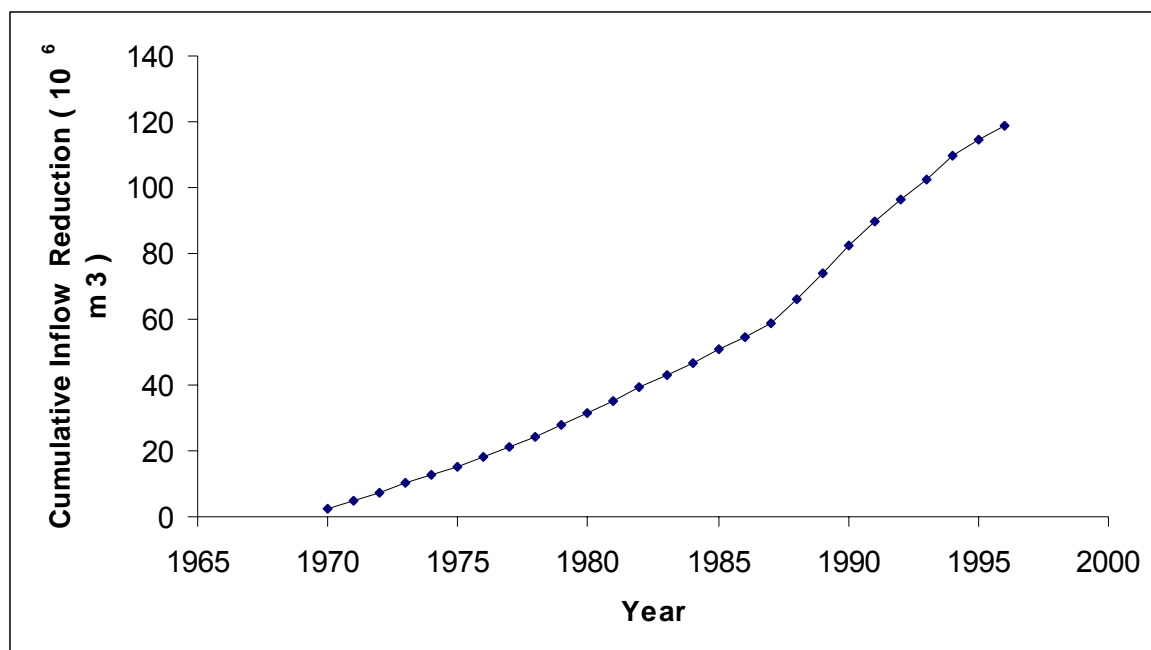


Fig. 4.2.2.5 Inflow Reduction to Lake Chamo since 1970 [50]. This calculated reduction in inflow in to the lake contributes to the loss of the lake volume and the observed increase in salinity. The water balance model of the same author, however, discounts this effect as minimal. This assertion needs further investigation as flow reduction appears a major factor in salinity increase on this lake and the lake volume and lake chemical ion concentration varies greatly during the various seasons.

According to this study this reduction in flow is not considered significant considering the total cumulative inflow in to Lake Chamo. During the period 1970 – 1996, the estimated total cumulative inflow in to Lake Chamo is 10164 Million m³. The flow reduction is a mere 1% at a conservative estimate and is not expected to affect the salinity of Lake Chamo.

Lake Chamo is inter- connected with Lake Abaya through an over flow from Lake Abaya. Lake Chamo's water balance taking in to consideration all factors precipitation, surface and subsurface flow as well as evaporation from the lake shows that Lake Chamo has a deficit which when accumulated leads to increase in salinity. The overflow to lake Chamo in the past was maintained because of the over flow from Lake Abaya which has stopped since December 1980. Since then there has been no outflow from both lakes. The water balance simple model calculation result is summarised in table 4.2.2.3 below for the two lakes.

The simple water balance model for lakes Chamo and Abaya - shown in Table 4.2.2.3 based on inflow in to the lakes, precipitation and evaporation as well as geo-

morphological condition of the lakes - indicates that Lake Chamo possesses no outflow excess, which naturally leads to a more evaporative formation.

Table 4.2.2.3 Water Balance Model Results for Lakes Abaya and Chamo [50]. This water balance model result concludes that Lake Chamo has a net evaporative loss which partly explains the observed increase in salinity over the years.

Lake	Daily Inflow (Million m ³ day ⁻¹)	Evaporation (Million m ³ day ⁻¹)	Precipitation (Million m ³ day ⁻¹)	Outflow (Million m ³ day ⁻¹)
Abaya	5.39	7.02	2.18	+0.55
Chamo	1.33	1.99	0.54	-0.12

Lake Chamo is more sensitive to changes in salinity due to the low inflow relative to the net evaporation-precipitation loss of water from the lake. If the trend in flow reduction continues, this lake will experience an increased level of salinity with adverse impact on the lakes ecosystem.

On the contrary lake Abaya's annual average water balance shows that there is an excess outflow, which assists in reducing the salinity increases. However, contrary to this model's estimate, the salinity of Lake Abaya is also increasing at a moderate rate over recent years. Examination of the salinity trend for Lake Abaya shows that it falls in the period 1960 – 1980 and after which there is a rapid increase in salinity and later evening out to a gradual increase.

This phenomenon may be correlated with the decrease in water level of Lake Abaya in the period 1980 – 1989 mainly caused by a meteorological drought phase leading to reduced peaks and volumes in precipitation [49]. The water level record shown below indicates this trend. The graph also shows the period 1977 – 1980 where the last over flow from Lake Abaya in to Lake Chamo occurred and never happened since then. The occurrence of Elnino may have resulted in partial recovery of the lake salinity.

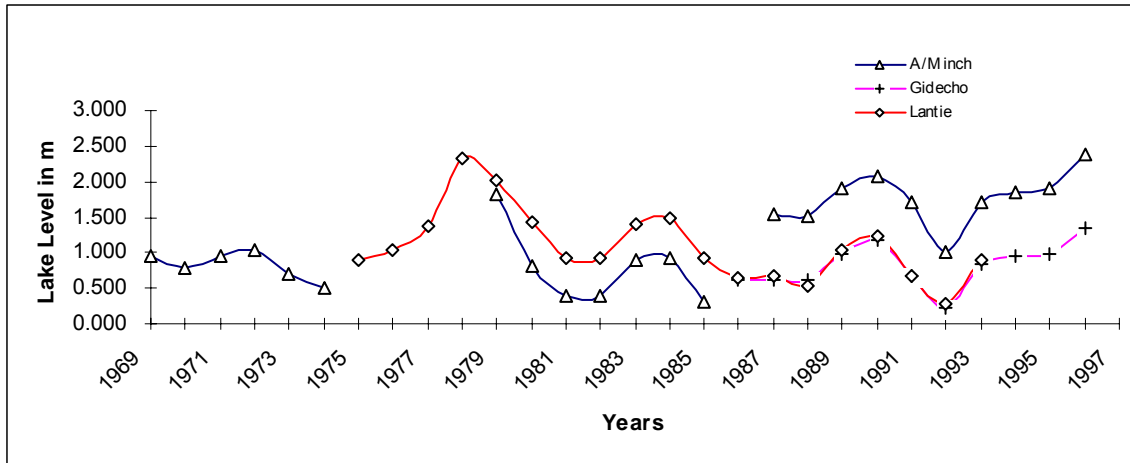


Fig. 4.2.2.6 Average Yearly Abaya Lake Level (Measured from Different Points). There has been a long term decrease in lake level starting from 1979 and continuing up to 1989. This period also exhibited an increase in salinity of Lake Abaya.

Since 1993 there has been a continuous increase in the water level recorded values over Lake Abaya, which apparently does not go with the increase in the lake salinity. As the lake salinity continues to increase, the cause for water level increase is hypothesised to be probably due to bed level rise from tectonic movements or caused by a completely different factor: volume displacement as a result of increase in rate of sediment transport from the catchment [52, 53, and 55]

Part of the water level recovery could be explained by the gradual increase in the precipitation trend in the period 1993 leading up to the El Nino, 1998. The overall precipitation pattern then after is erratic and does not show a major trend that explains the continuing rise in water level.

The increase in salinity for Lake Abaya may be explained similar to Lake Chamo's flow deficit in water balance over the lake. This may happen if precipitation is decreasing and /or evaporation rate is increasing and may be due to increase in consumptive use of water in the Abaya catchment. Similar water consumption estimate by the same author [50] suggested these uses do not have a major impact on the lakes water balance over the near future. The loss of water depth in the lakes under expected increase in irrigation and domestic water consumption is suggested to be 0-2 m in the next 25 years. This leaves one to guess the hydro-meteorological factors mentioned above might have been altered from what is supposed in the model to account for the salinity increase. The global climate change may be the contributing factor in the slow recovery of Lake Abaya from increased salinity and since Lake Chamo is dependent on Lake Abaya's over flow for its water level and

chemical equilibrium it will continue to increase its salinity over time unless the level in Abaya rises due to improved weather events in future.

4.2.3 Silicate, Nitrate Ammonia and Phosphate

Generally the concentration of these nutrients have increased in both lakes Abaya and Chamo except for the soluble reactive phosphorous in Lake Chamo which did not show significant increase. Observing the rapid increase in nitrate concentration in both lakes since 1991, it is possible to anticipate that an increase in nutrient levels has already occurred in the lakes in response to pollution from the tributary catchment [51]. Measurement of Sulphate has increased for Lake Chamo while there is a decrease in value for Lake Abaya. The concentration of Silica is low for Lake Chamo. The generally marked decrease in Silica concentration has earlier been observed for the Ethiopian rift valley lakes [46, 48]. It has been suggested that increase in nitrogen and sulphur may have led to increase in phytoplankton biomass [57]. Lower Silicate concentrations have been related to diatom crop in Lake Chamo [46, 48]). The recent measurement made by this study showed a rise in silica concentrations for both Abaya and Chamo which contradicts the increase In Nitrogen and Sulphur concentration that may have led to the phytoplankton growth.

4.2.4 Chlorophyll a Concentration

Chlorophyll a values have in the past observed to increase in for Lake Chamo while Lake Abaya has a more or less similar measurement. The measurement of Chlorophyll a in this study for Lake Abaya is low and not significantly different from previous measurements. On the other hand Lake Chamo's chlorophyll-a measurement varied between 15 and 50 $\mu\text{g L}^{-1}$ and is some how lower than previous measurements. It was found that phosphate measurement for Lake Chamo fell below detection limit in the summer with a decrease in dissolved oxygen concentration. The depletion of phosphorous may have restricted the chlorophyll a abundance in Lake Chamo.

4.2.5 Dissolved Oxygen

Dissolved oxygen in the summer fell below 3 mg L^{-1} and this condition was observed together with loss of soluble reactive phosphorous. Algal respiration and death of aquatic habitats may have led to a decrease in dissolved oxygen concentration and an increase in the concentration of ammonia observed for Lake Chamo.

4.2.6 Discussion

Monitoring of the variation of water quality of the lakes Abaya and Chamo over the short term follows the seasonal precipitation pattern with Lake Chamo displaying significant variation in response to seasonal changes. Lake Abaya has a more stable concentration with limited response to the seasons. Due to the fact that lake Chamo has been subject to flow reduction and decrease in water level the impact of seasonal water quality changes has become significant and may affect the lake ecology as such [58]. Comparison of seasonal variation with longer-term data records show that both lakes are being subject to increased salinity although Lake Abaya shows only a moderate increase. Examination of the different contributing factors points to flow reduction and the global climate regime change as being the probable cause of the salinity increase. Since Lake Chamo depends on the outflow from Lake Abaya for its water level and chemical balance and since this overflow has ceased to exist, lake Chamo has been subjected to decrease in water level and increase in salinity for a longer period.

The nutrient and chlorophyll measurements characterise both lakes as eutrophic. Dissolved oxygen measurement fall below 3 mg L^{-1} in Lake Chamo with simultaneous loss of phosphorous. This condition may have been caused by algal death and respiration and may lead to increased concentration of ammonia and nutrients through internal recycling. Cynobacteria, species normally abundant in Lake Chamo may find this condition suitable [54]. The increase in nitrogen and sulphate as well as ammonia in both lakes over recent years might be due to pollution from the catchment rather than internal recycling and this cannot be conclusively stated, as past measurements of inflow river water quality measurements are not available. Pollution assessment of the tributary catchment shall be undertaken as part of a water quality-monitoring program for the lakes [56].

4.3 Investigation of the Water Quality of Under Ground Water Sources within the Abaya - Chamo basin

4.3.1 Background to Ground Water Chemical Composition and Variation

Ground water hardness is a measure of all divalent cations, usually dominated by calcium and magnesium. These cations are contributed mainly from dissolution of the carbonate mineral component rocks and sediments. Although maximum concentrations are probably reached quickly as groundwater infiltrates, subsequent cation exchange, as groundwater passes through clay-rich strata, may provide an indication of chemical evolution and groundwater travel [59].

Alkalinity, the capacity of water to neutralize an acid, is derived principally from the bicarbonate anion by dissolution of carbonate rocks. Although hardness and alkalinity are both customarily expressed as the amount of calcium carbonate dissolved that would give the measured value, the two may differ for a given water sample due to processes other than calcium carbonate dissolution. For example, cation exchange may result in divalent cations removed from solution, dissolution of gypsum produces calcium ion, and bicarbonate is a product of reduction-oxidation reactions.

Sulphate is also most likely derived from the dissolution of gypsum or the weathering of pyrite. The tendency of sulphate to be chemically reduced in an evolving reduction-oxidation environment and hence consumed during movement in the subsurface may provide a means of distinguishing flow on different scales. Chloride and nitrate in ground water likely originate from non-natural sources and are indicators of urbanization and agriculture, respectively. They are transported from on or near the ground surface but the distribution of these components in groundwater may be complicated by the uneven distribution of releases and partitioning between surface runoff and infiltration. Chloride has no significant health implications and limits are specified to prevent undesirable taste. However, because of its common association with septic field or landfill leachate, the presence of chloride may imply other contamination. Nitrate is derived from fertilizer or can be associated with livestock and can cause oxygen deprivation to the blood in infants. Sulphate may have a mild laxative effect and hardness is an aesthetic parameter, preventing the lathering of soap and producing calcium deposits in water-heating appliances and fixtures. Alkalinity is a measure of the acid-neutralizing capability of water and usually correlates with hardness [59].

Table 4.3.1.1 Chemical Compositions of Surface and Ground Water Sources within the Abaya – Chamo Basin

Sample Source	UTM-East	UTM North	Altitude (meters) a.s.l	TDS mg L ⁻¹	Condu- ctivity μS Cm ⁻¹	Alkalinity mg L ⁻¹ as CaCO ₃	Bicar- bonate mg L ⁻¹	Hardness mg L ⁻¹	Calcium mg L ⁻¹	Magne- sium mg L ⁻¹	Sodium mg L ⁻¹	Pota- ssium mg L ⁻¹	Sulphate mg L ⁻¹	Chloride mg L ⁻¹
Humbo Hand Pump	3643000	7418000	1580	153.6	131.0	83.3	101.7	65.1	5.3	12.4	10.0	2.7	0.5	21.5
Humbo Hand pump	3643000	7418000	1580	133.9	142.0	75.8	92.4	69.1	7.3	12.2	8.8	2.4	0.1	10.7
Ela Kebela Spring	3653000	7440000	1700	74.1	82.0	32.7	39.9	40.7	6.5	5.8	8.0	2.6	2.1	11.3
Ela Kebela Spring	3653000	7440000	1700	78.9	114.0	26.4	32.2	22.4	6.5	1.4	18.1	6.0	3.0	14.7
Basa Spring Water	3665000	7370000	1440	93.1	111.0	49.0	59.8	63.0	3.4	13.1	7.2	3.6	3.3	6.0
Abela Rain Water	3668000	7378000	1380	24.6	13.0	7.2	8.8	22.4	6.4	1.5	0.2	0.2	1.5	7.5
LashoSolar Pump	3710000	7275000	1260	162.8	442.0	46.0	56.1	128.1	6.7	26.8	43.0	11.5	16.0	18.7
Korga Hand pump	3660000	7213000	1230	266.2	420.0	134.9	164.7	114.9	10.4	21.3	42.2	10.6	6.5	17.0
Ola Mulato hand Pump	3620000	7140000	1240	214.0	345.0	111.7	136.3	53.9	9.1	7.4	50.9	1.8	4.9	8.5
Wajifo Hand Pump	3670000	7220000	1220	353.5	652.0	162.8	198.7	252.2	7.0	56.4	53.0	2.2	15.2	36.2
Mirab Spring Water	3620000	7000000	1295	249.8	463.0	119.6	146.0	228.8	5.5	51.8	28.2	3.4	14.9	15.0
Mira Abaya Borehole	3630000	6970000	1290	276.8	566.0	120.2	146.7	186.5	5.3	41.7	50.1	9.8	15.1	23.2
Mole Borehole	3630000	6950000	1220	229.5	451.0	108.1	131.9	191.4	5.7	42.6	33.0	3.8	13.9	12.5
Farah Gosa Spring Water	3590000	6880000	1206	89.5	157.0	38.8	47.3	87.2	6.5	17.0	8.8	1.3	6.2	8.5
Lante Borehole	3500000	6800000	1190	148.4	293.0	69.6	85.0	140.3	5.7	30.3	17.8	1.6	10.1	8.0
Chano Mile Hand Pump	3448999	6819018	1216	265.6	593.0	121.4	148.1	208.4	7.3	45.7	49.8	1.6	17.3	13.0
KolaShara1	3405334	6814515	1270	516.0	918.0	199.8	243.8	294.0	7.3	66.3	105.3	3.0	19.5	87.5
Kolashara2	3406820	6818348	1270	299.0	498.0	70.2	85.6	139.0	7.3	29.0	88.0	2.4	22.5	20.0
Kolashara3	3408556	6819370	1257	438.0	786.0	152.7	186.3	247.0	7.3	55.0	56.7	1.4	13.2	60.0
Kolashara4	3410982	6821767	1252	333.0	557.0	80.8	98.6	156.0	7.3	33.1	92.7	2.5	22.7	30.0
ChanoDorga1	3434966	6836982	1263	374.0	648.0	135.5	165.4	228.0	7.3	50.4	51.7	2.0	17.3	20.0
Chanodorga2	3433368	6837977	1286	403.0	649.0	135.5	165.4	228.0	7.3	50.4	46.0	4.2	17.2	14.0
Chanodorga3	3433265	6835058	1265	399.0	650.0	135.5	165.4	228.0	7.3	50.4	57.0	2.3	19.2	14.0
Chanodorga4	3436798	6834366	1273	401.0	651.0	128.7	157.0	220.0	7.3	48.5	54.0	2.4	18.5	14.0
Chanomile1	3442511	6823171	1272	408.0	656.0	115.5	141.0	204.0	7.3	44.7	23.0	9.0	13.3	10.0
Chanomile2	3446924	6823691	1195	382.0	649.0	128.7	157.0	220.0	7.3	48.5	20.0	0.7	11.5	14.0
Chanomile3	3452644	6820158	1228	492.0	809.0	135.5	165.4	228.0	7.3	50.4	36.0	2.9	14.8	16.0

Sample Source	UTM-East	UTM North	Altitude (meters) a.s.l	TDS mg L ⁻¹	Condu- ctivity μS Cm ⁻¹	Alkalinity mg L ⁻¹ as CaCO ₃	Bicar bonate mg L ⁻¹	Hardness mg L ⁻¹	Calcium mg L ⁻¹	Magne sium mg L ⁻¹	Sodium mg L ⁻¹	Pota ssium mg L ⁻¹	Sulphate mg L ⁻¹	Chloride mg L ⁻¹
Chanomile4	3451046	6816271	1182	443.0	758.0	153.6	187.4	248.0	7.3	55.2	67.0	2.4	21.3	14.0
Chanomile5	3448999	6819018	1207	377.0	634.0	132.1	161.2	224.0	7.3	49.5	79.0	1.6	23.4	14.0
Lake Abaya	3479320	6768350	1207	898.3	1074.6	520.0	634.6	58.5	18.0	3.1	239.6	17.4	25.4	77.0
Lake Chamo	3377980	6559660	1109	1520.5	1868.4	852.9	1040.8	78.8	14.7	10.1	420.6	22.5	24.9	140.6
River Hare	3408020	6758920	1232	97.5	76.8	49.0	59.8	30.4	8.7	2.1	4.7	1.0	0.7	4.0
River Kulfo	3414840	6674650	1230	176.9	169.3	70.1	85.5	65.3	17.8	4.9	8.4	0.9	0.9	5.3
River Sile				452.2	540.0	190.1	232.0	242.4	12.6	50.7	20.6	3.2	1.1	19.2
ArbaMinch Rain Water				61.6	62.0	26.4	32.2	20.0	9.4	0.0	0.7	0.5	1.4	16.6
AMUniversity Ground water				416.0	723.0	330.0	402.7	227.0	25.0	39.5	78.0	1.0	2.6	34.5
ArbaMinchSprings				209.0	379.0	200.0	244.1	147.0	30.0	17.2	11.0	1.9	2.9	14.0

4.3.2 Chemical Composition of ground Water Sources in the Abaya – Chamo Basin

The result of chemical analysis to determine composition of the ground water sources in the study area is summarized in the Table 4.3.1.1. In general the chemical composition is largely of the bicarbonate-calcium-magnesium type, which is typical of the basaltic parent rock formation of the area. The detail chemical differentiation among the different locations is described in the sections that follow.

4.3.2.1 Variation of chemical Composition with Altitude

There is a general inverse correlation of the dissolved constituents with elevation in the area. This fact has been reported by earlier studies in the area [60]. This observation indicates to the common assumption of low lying areas contain water having long residence time and hence greater extent of dissolving of compounds from the subsurface. The same observation has been noted for river water qualities in the area.

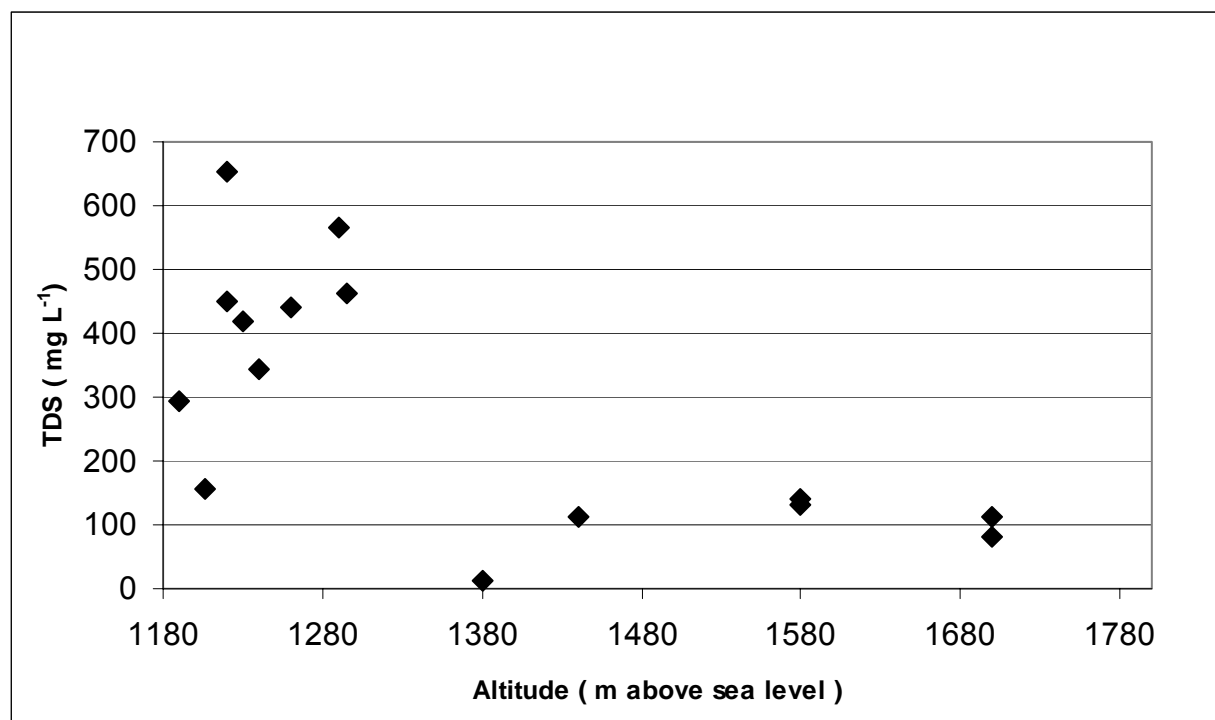


Fig. 4.3.2.1.1 Variation of TDS with altitude in the Ground Water Sources (Arbaminch - Sodo). There is a clear separation in the TDS of samples taken from the higher elevation and those taken from the lower elevation. There is a general increase in TDS over decrease elevation in the area.

4.3.2.2 Chloride Variation

The increase in chloride concentration observed in some of the ground water samples is attributable to surface sources and evaporative conditions since aquifers are believed to contain little chloride material in them. On the other hand the increase in sodium and potassium as well as Calcium at the lower lying deeper wells is expected since base cations generally increase with increase in the extent of ground water dissolution. For the deeper wells chloride content decreases as expected because of dilution of the chloride content as water percolates deeper. Ground water from near surface sources tends to show higher chloride content. The sources of chloride are mostly surface source as explained above [61].

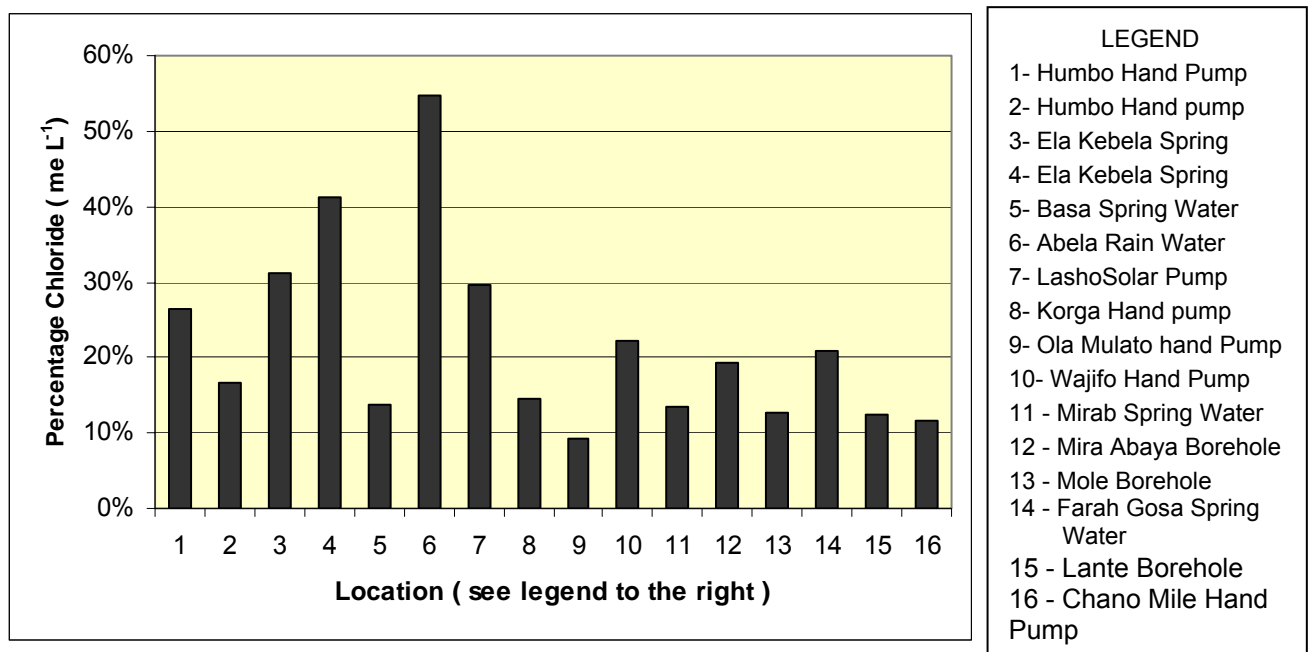


Fig. 4.3.2.2.1 Chloride variation (Sodo - Arbaminch Route). Refer to Figure for the location of the sampling points within the general sampling map of the study area. The upper catchments (1-8) have greater chloride concentration indicating near surface flow conditions.

As Figure 4.3.2.2.1 shows, the percentage of chloride decreases with decreasing elevation as one travels from the high altitude region of Sodo to the low land areas of Arbaminch (from left to right in Figure 4.3.2.2.1). Most of the ground water sources in the upper catchment are from near surface origins.

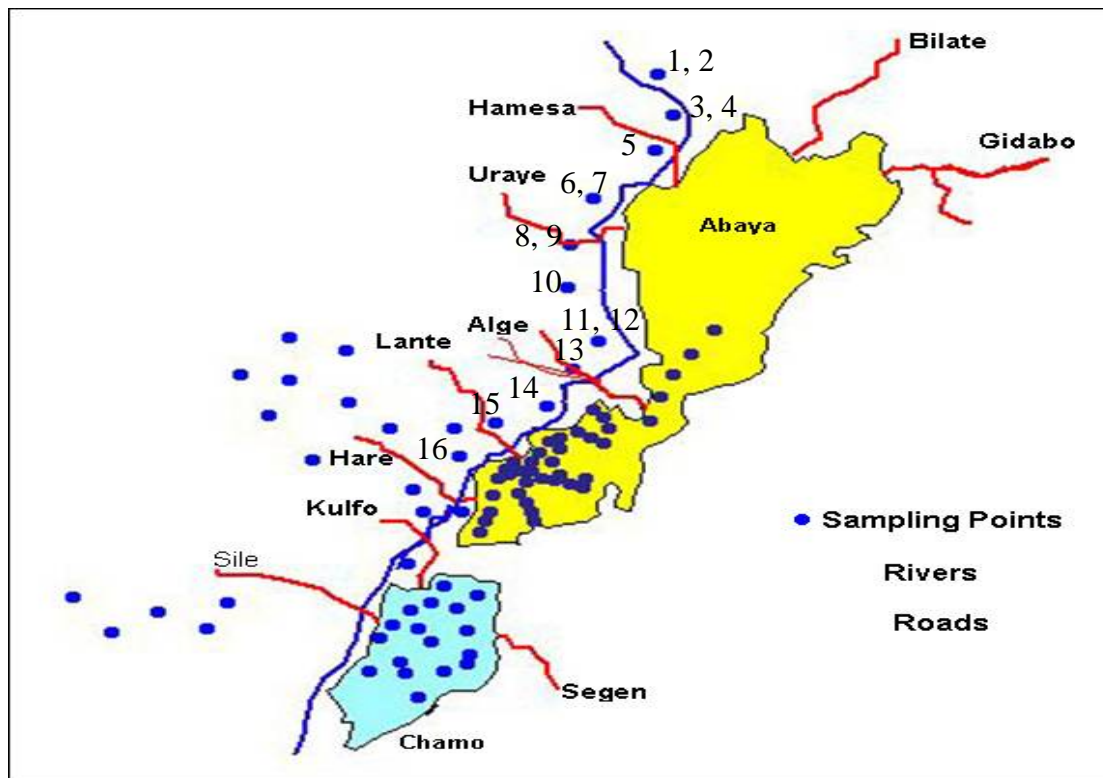


Figure 4.3.2.2: The location of water quality samples within the study area which is the Abaya-Chamo Lakes basin reproduced again here. The numbers indicated in the diagram refer to the ground water sampling points used for the chloride determination (see figure).

4.3.2.3 Conductivity versus TDS Lines of Surface and Ground Water Sources

The similarity in the chemical composition of the water sources drawn from subsurface sources (springs, ground water) is shown by the linear plot of the TDS against conductivity shown in figure 4.3.2.3.1 with minor deviations. The samples have been taken from wide distance ranges but still show more or less similar chemical characteristics. The surface water sources plotted include rainwater, rivers Hare, Kulfo and Sile in addition to Lakes Abaya and Chamo.

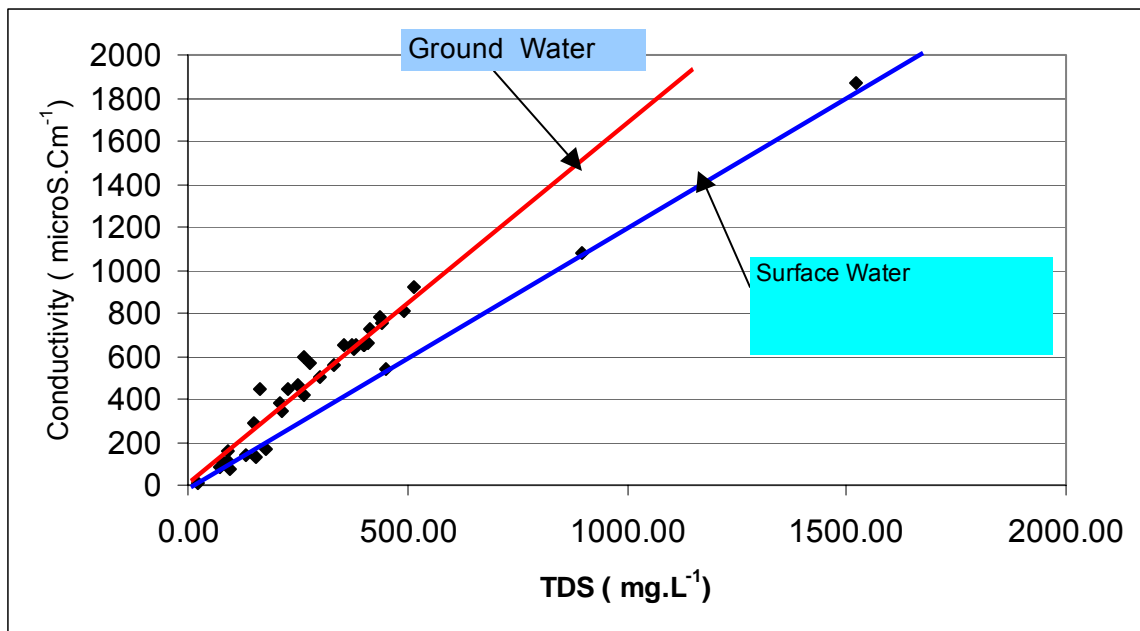
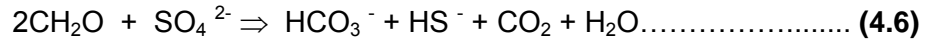


Fig. 4.3.2.3.1 Conductivity vs. TDS Lines for Surface and Ground Water Sources in the Abaya Chamo Basin. Both the surface sources as well as the ground water sources display similar characteristics since the TDS versus conductivity line joins the various sources together. Surface sources have more sodium which has less conductivity than calcium which is dominating subsurface sources.

4.3.2.4 Alkalinity versus Hardness Variation

Hardness of ground water in the region varies between 20 and 280 mg L⁻¹ with increasing hardness values displayed in the lower elevation sources. The Carbon dioxide content of the water samples is high as a result of which the extent of dissolving of Calcium and Magnesium in exchange for dissociated hydrogen ion is high in the area.

When the source of Hardness is only calcium carbonate, the hardness and alkalinity values are expected to be the same. Figures 4.3.2.4.1 and 4.3.2.4.2 show the alkalinity and hardness co-variation for the different ground water sources analysed in the area. Generally the hardness plots above the alkalinity. For samples such as from Arbaminch university ground water, Korga and Ola-Mulato boreholes the alkalinity is greater than the hardness. Since these boreholes are located lowland the cation exchange process resulting in loss of calcium and magnesium for sodium may be the cause. This argument goes well for Korga and Ola-Mulato wells, as they are located in clay rich regions of the upper catchment. The other possibility is for redox reaction resulting in loss of sulphate and increase in bicarbonate values by the reaction shown below.



However, for ground water sample from Arbaminch University the dissolved oxygen content is quite high and the above reaction can only occur under anaerobic condition, which is not the case in this well.

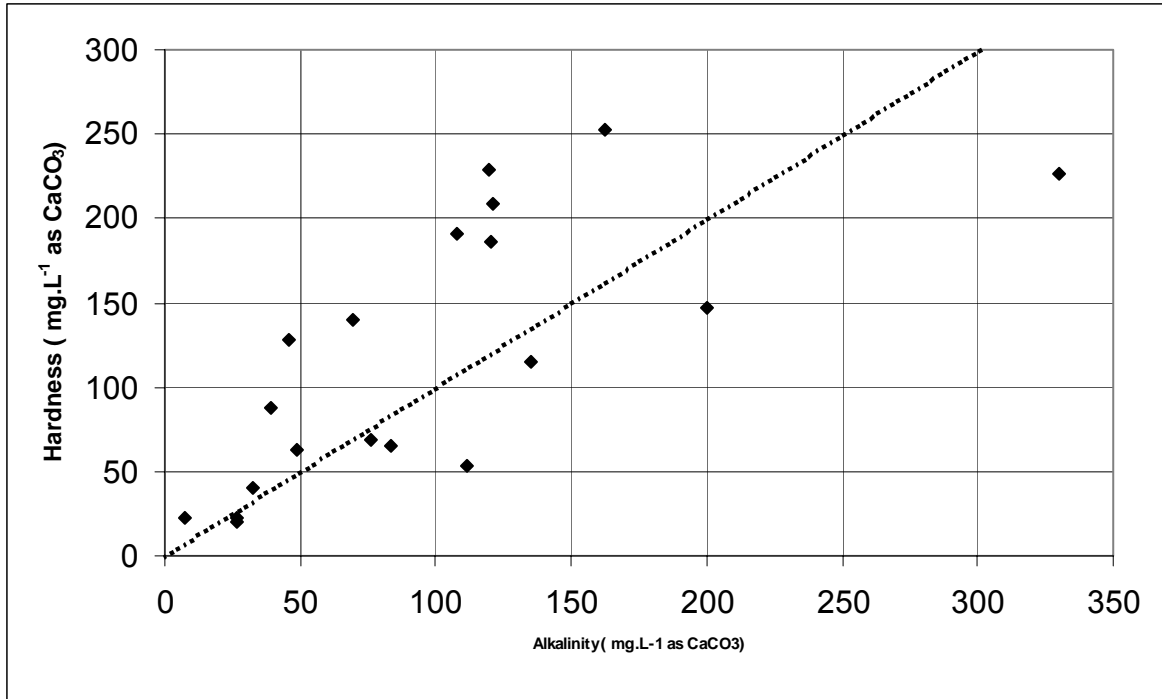


Fig. 4.3.2.4.1 Hardness Versus Alkalinity variation for Ground Water samples. For the samples that plot above the dotted 45 degree slope line, the hardness is greater due to greater calcium carbonate concentration. Samples which plot below this line have loss of calcium in exchange possible for sodium at the deeper depths of ground. Such waters are expected to have long residence times.

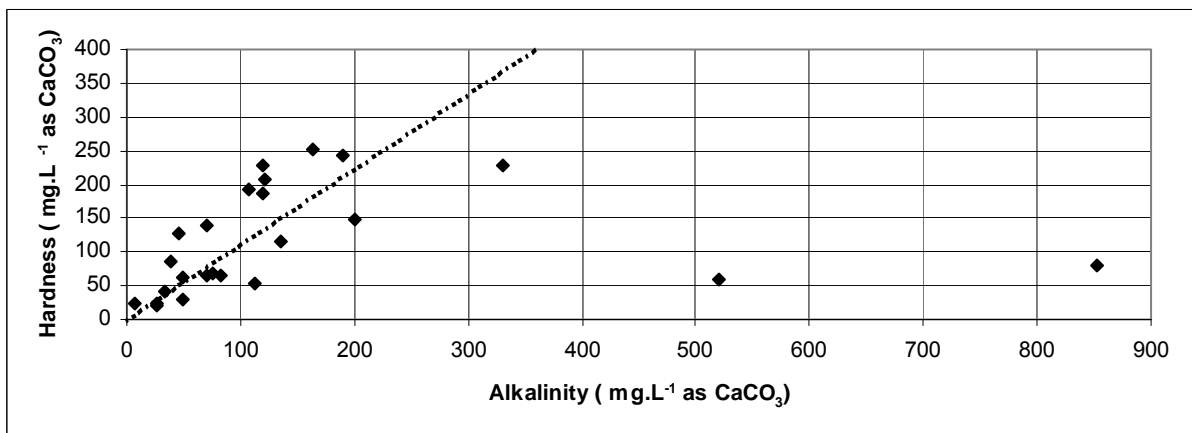


Fig. 4.3.2.4.2 Hardness Versus Alkalinity variation for Surface and Ground Water Samples. The same situation applies here as that of Figure 4.3.2.4.1.

4.3.2.5 Piper Tri - linear Plots of Ground and Surface Water Samples

The piper tri linear diagram is a plot in percentage of ions present to enable one determine the flow characteristics the dominant ions and the spatial relationship of ions among different points in surface and subsurface water. The chemical concentrations in milli-equivalent per liter were converted and plotted on the piper trilinear diagrams shown in Figures 4.3.2.5.1 – 4.3.2.5.3. Samples from rainwater, river water and lakes have been included for comparison. Most of the ground water sources plot in the high bicarbonate – Magnesium – Calcium area, which are characteristics of the basaltic formation of the geology of the area.

The chemical composition of most of the samples from the low land area (Mirab Abaya, Mole, Lante, Chano Mile, Kola Shara, etc) plot in small clustered area indicating similar characteristics of the under ground water. Samples from the high land areas (Humbo, Sodo, Ela Kebela, Basa, Abela, etc) plot in the outer circle to this dense cluster of well-evolved subsurface waters. They are characterised by low dissolved solids (TDS) and possibly low residence times. The spring source from Basa (sample Number 5 in the diagram) appears very turbid during the rainy season, further confirming near surface flow conditions. Samples from Korga and Olamulato plot down with higher percentage of Sodium and potassium.

Samples that represent near surface flow conditions (1 and 2 from Humbo ground water, 5 – Spring water from Basa region) plot nearer the surface water samples (river sources) indicating their surface flow conditions. Their TDS value is intermediate between well-evolved high TDS ground water and unevolved low TDS spring water sources. Rain water from Arbaminch (Elevation =1210m a.s.l) and Abela (Altitude = 1700 m a.s.l), plot in the high Chloride – Calcium- Magnesium area. The spring water sources near Mirab Abaya plot near the rainwater than others indicating chemically unevolved spring that may as well display intermittent flow conditions. This is further confirmed by their lowest Total Dissolved Solids Conditions.

Arbaminch springs plot near to the rivers Kulfo, Sile and Hare. This spring water has its source in the upland catchment and its chemical characteristics resemble that of the base flow river conditions. Therefore, there is a possibility that pollution from the sources may travel in much the same way as such pollution travel as subsurface flow and appear with the rivers base flow.

Ground water samples from Arbaminch University and two samples from Korga and Olamulatto have relatively higher Sodium and Potassium than Calcium and Magnesium. This might have arisen as a result of ion exchange between Sodium and Calcium/Magnesium or precipitation of Calcium carbonate under saturated conditions. Ground water samples near the lakes also have increasingly greater percentage of Sodium/Potassium over Calcium/Magnesium (ChanoMille 1-5). Long residence time and higher total dissolved solids (in comparison with neighbouring sources) may have been the accompanying conditions with such ground water sources.

Fig. 4.3.2.5.1 PIPER TRILINEAR PLOT OF SURFACE AND SUBSURFACE WATER SAMPLES FROM ABAYA-CHAMO

- 1 - Humbo Hand Pump # 1
- 2 - Humbo Hand Pump #2
- 3 - Ela kebela spring #1
- 4 - Ela kebela spring #2
- 5 - Basa spring Water
- 6 - Abela Rain Water
- 7 - Lasho Solar Pump
- 8 - Korga hand Pump
- 9 - Ola Mulato hand Pump
- 10 - Wajifo Hand Pump
- 11 - Mirab Spring Water
- 12 - Mirab Abaya Borehole
- 13 - Mole Borehole
- 14 - Fara Gosa Spring Water
- 15 - Lante Borehole
- 16 - ChanoMile Hand Pump
- 17 - Kolashara #1
- 18 - Kolashara #2
- 19 - Kolashara#3
- 20 - Kolashara #4
- 21 - Chanodorga #1
- 22 - Chanodorga #2
- 23 - Chanodorga #3
- 24 - Chanodorga #4
- 25 - Chanomile #1
- 26 - Chanomile #2
- 27 - Chanomile #3
- 28 - Chanomile #4
- 29 - Chanomile #5
- 30 - Lake Abaya
- 31 - Lake Chamo
- 32 - Hare River
- 33 - Kulfo River
- 34 - Sile River

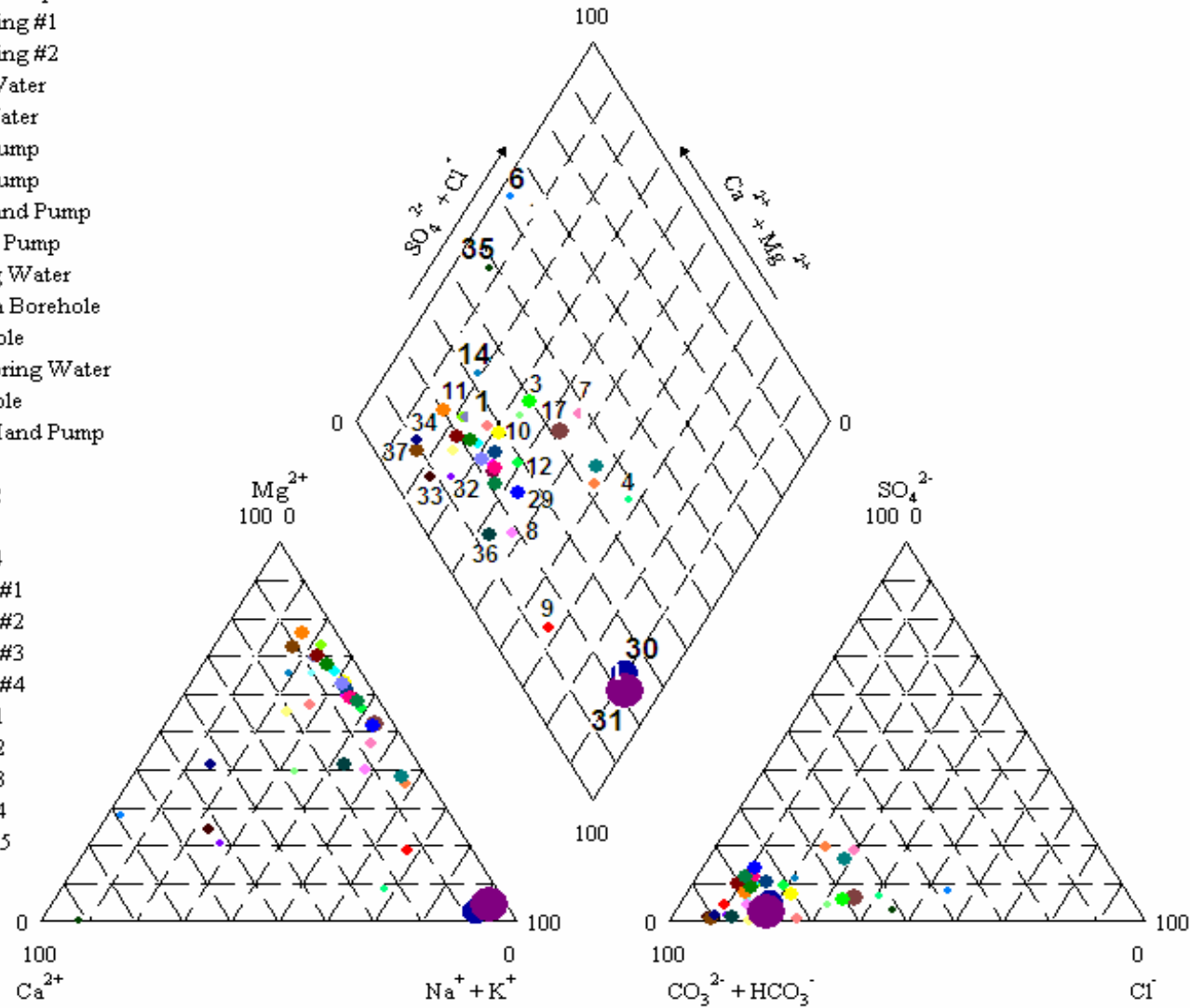


Fig. 4.3.2.5.2 PIPER TRILINEAR PLOT OF SPINGS AND GROUND WATER SAMPLES FROM ARBAMINCH – SODO AREA

EXPLANATION

- 1- Humbo Hand Pump #1
- 2- Humbo Hand Pump #2
- 3- Ela Kebela Spring #1
- 4- Ela kebel Spring #2
- 5- Basa Spring Water
- 6- Abela Rain Water
- 7- Lasho Solar pump
- 8- Korga Hand Pump
- 9- Ola mulat hand Pump
- 10- Wajifo hand Pump
- 11 - Mirab Spring Water
- 12 - Mirab Abaya Boprehole
- 13 - Mole Borehole
- 14 - farah Gosa Spring Water
- 15 - Lante Borehole
- 16 - Chano Mile hand Pump

- 25
- 353

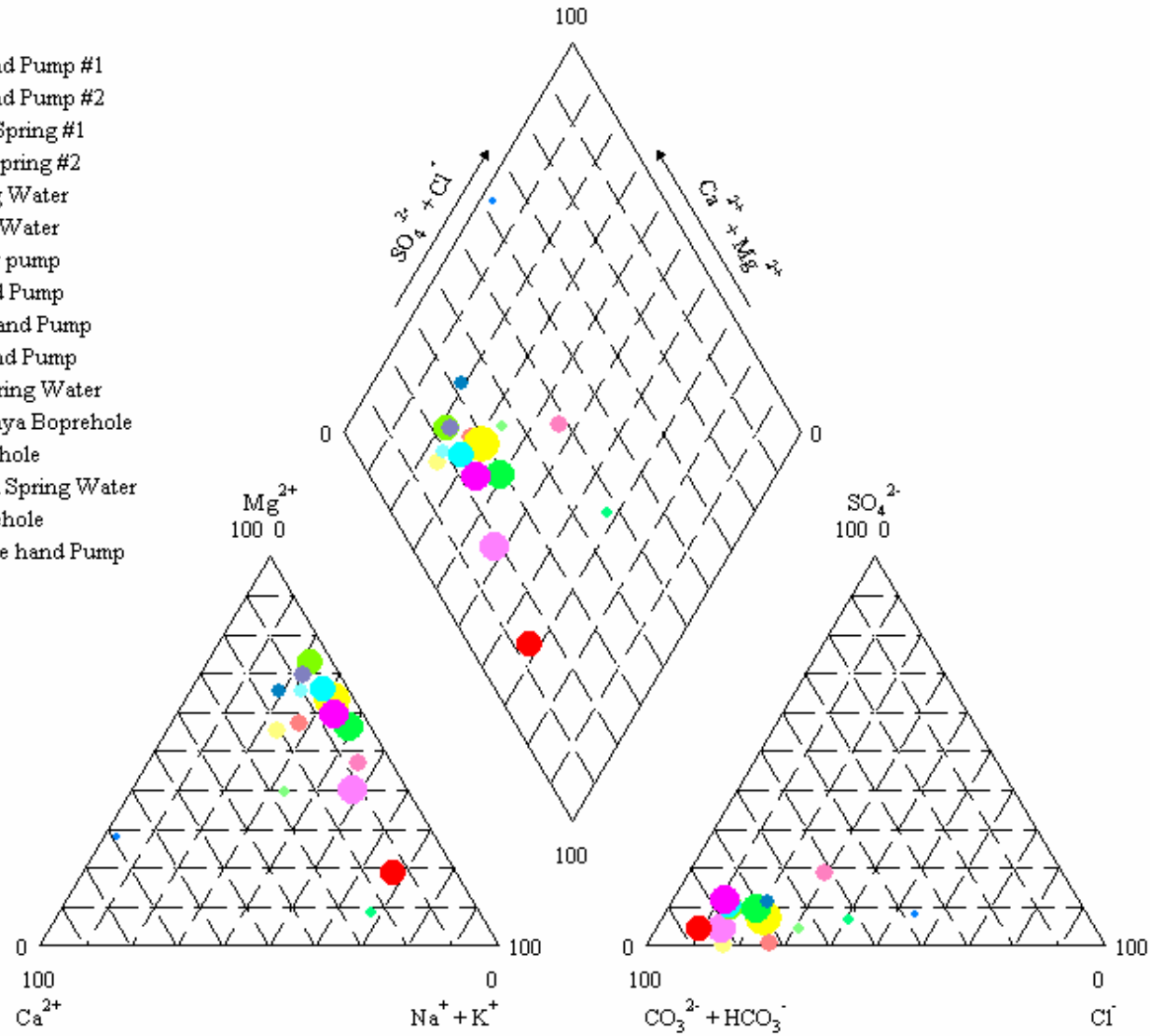
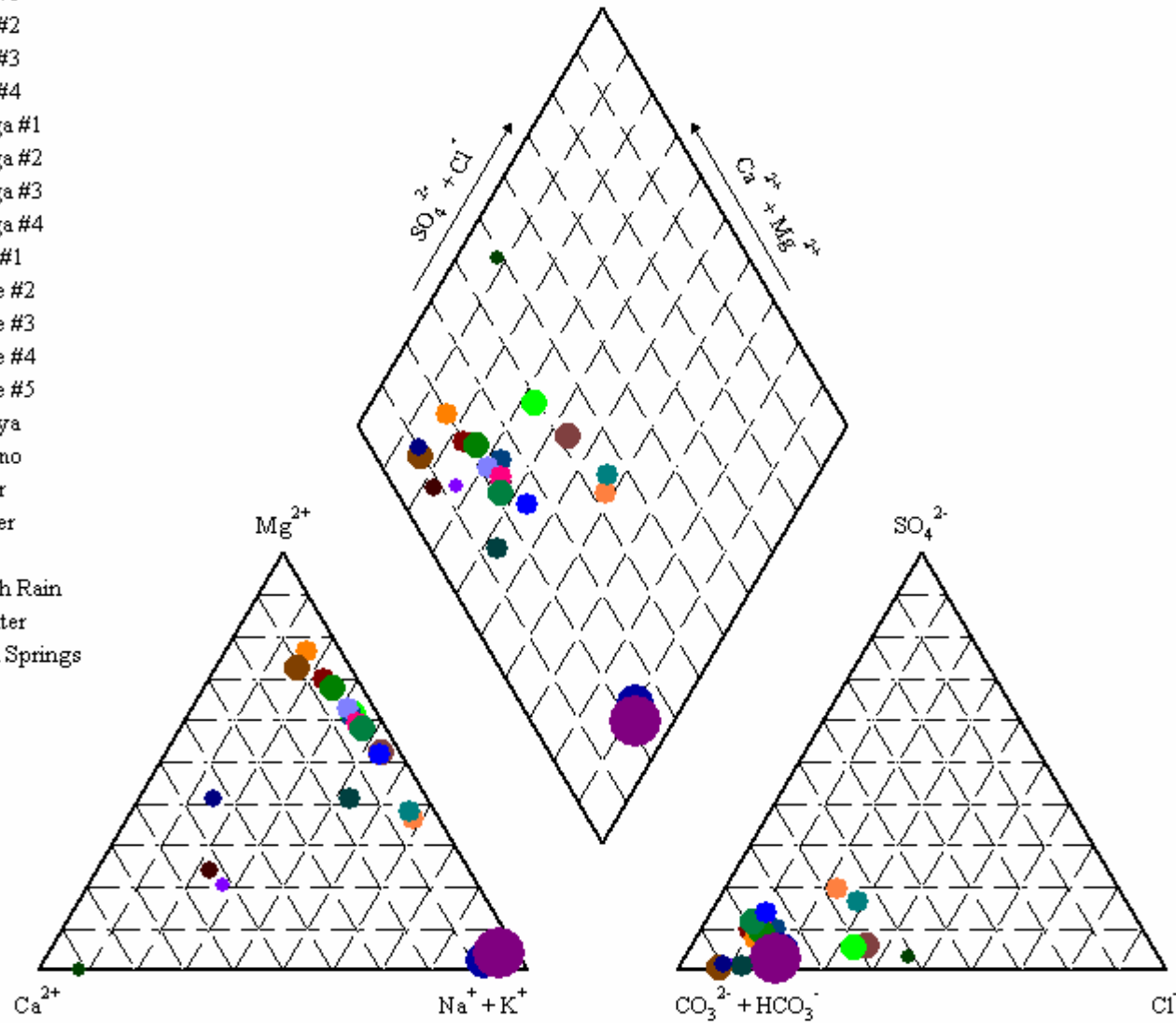


Fig. 4.3.2.5.3 PIPER TRILINEAR PLOT OF SURFACE AND SUBSURFACE WATER SAMPLES FROM ARBAMINCH AREA

EXPLANATION

- 1 - Kolashara #1
- 2 - Kolashara #2
- 3 - Kolashara #3
- 4 - Kolashara #4
- 5 - Chanodorga #1
- 6 - Chanodorga #2
- 7 - Chanodorga #3
- 8 - Chanodorga #4
- 9 - Chanomile #1
- 10 - Chanomile #2
- 11 - Chanomile #3
- 12 - Chanomile #4
- 13 - Chanomile #5
- 14 - Lake Abaya
- 15 - Lake Chamo
- 16 - Hare River
- 17 - Kulfo River
- 18 - Sile River
- 19 - Arbaminch Rain
- 20 - AMU Water
- 21 - Arbminch Springs

- 62
- 1520



4.3.2.6 Seasonal Variation of Under Ground Water Sources

A brief examination of the water quality variation of different ground water sources in the area reveals characteristic variation depending on the extent of connection with seasonal surface flow. Figures 4.3.2.6.1 and 4.3.2.6.2 show the conductivity time series for Arbaminch spring and ground water at Arbaminch University respectively. The spring source indicates a decrease in conductivity because of its closer connection with the upland catchment surface source. On the other hand the ground water at AMU does show a trend, which is apparent due to its remote connection from surface flow [62].

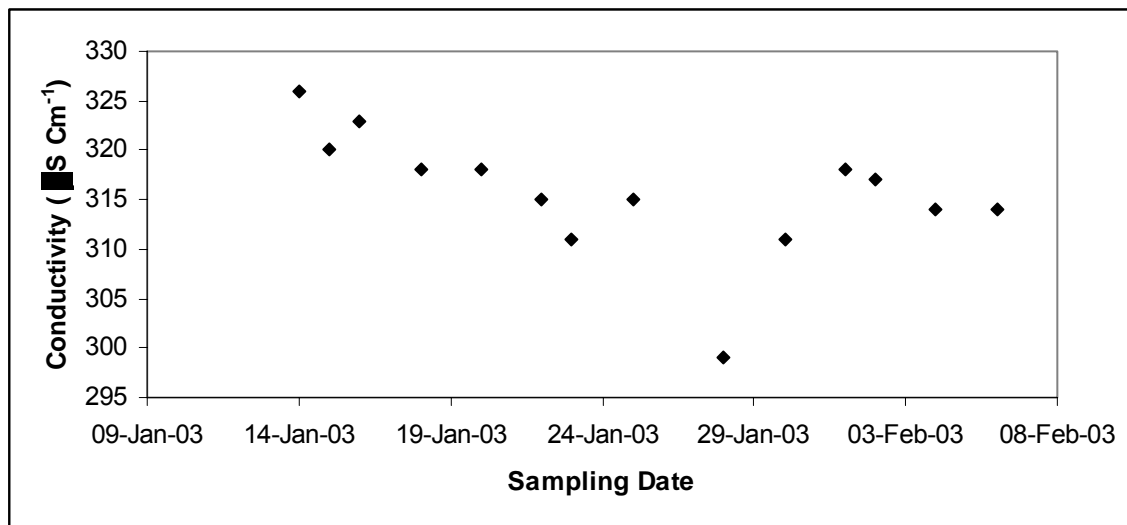


Fig. 4.3.2.6.1 Conductivity Time Series Arbaminch Spring Supply. The Arbaminch spring supply responds rapidly to seasonal changes indicating surface flow augmentation. Some studies also related this surface flow condition with the presence of increased nitrate and phosphate pollutants.

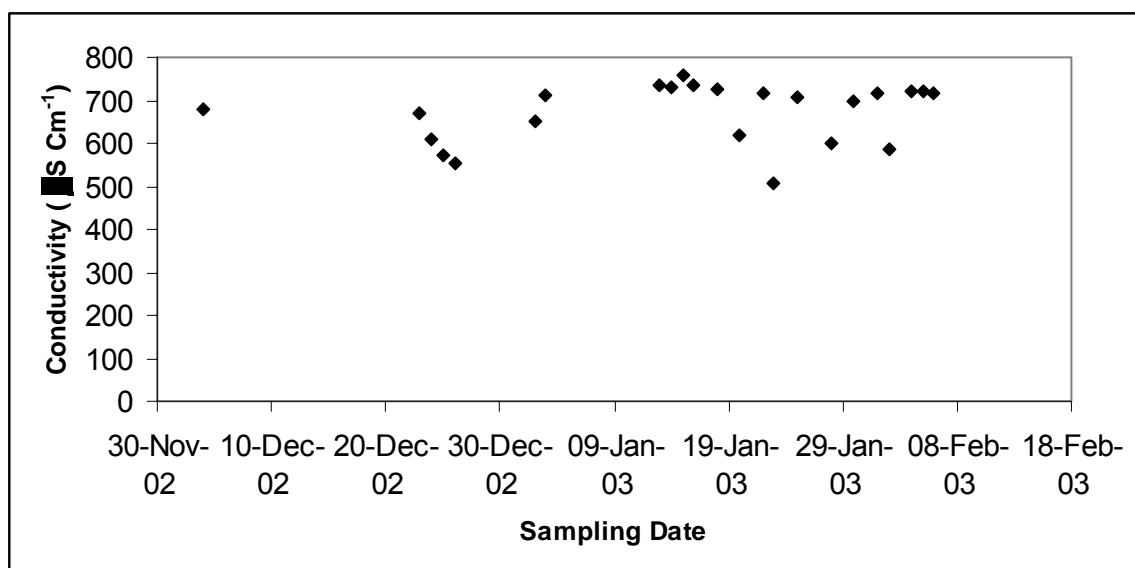


Fig. 4.3.2.6.2 Conductivity time Series AWTI Ground Water supply. The AWTI ground water supply has a more damped variation in water quality over the seasons indicating less surface flow augmentation.

The variability of the chemical composition is therefore dependent on connection with surface water sources. The analysis described above for the geo chemical composition of the groundwater sources analysed in the region classifies the samples with respect to this interconnection. This in turn has an implication on the extent of pollution that may occur and the frequency of monitoring that has to be specified.

4.3.3 Investigation of Ground Water Pollution

About 30 samples from different ground water sources were analysed for coliform bacteria, ammonium, phosphate, nitrate, nitrite, and pH and water temperature. The purpose of this investigation was to identify the extent of pollution of these ground water sources from surface anthropogenic sources and to classify these samples with respect to these sources. Pollution of ground water with human and animal wastes is expected to have high nitrate/phosphate ratio where as fertilizer sources of pollution have lower ratios [60]. As the water percolates deep ammonia, nitrite, organic matter are expected to be removed within the soil as well as bacteria. The presence of these compounds may therefore indicate anaerobic conditions or direct pollution from near surface sources. The simultaneous presence of bacteria and nitrite/ammonia may indicate such direct pollution. On the other hand the absence of bacteria in the presence of these reducing compounds may indicate reducing conditions within the ground water regions. As with chloride, groundwater with the higher nitrate concentrations probably have very short transport routes, either by surface water flow or very shallow groundwater flow.

Table 4.3.3.1 summarises the results of analysis of these samples for the mentioned parameters. The plot of nitrate against phosphate shown in Figure 4.3.3.1 shows that mostly the higher nitrate concentrations are associated with low phosphate concentrations suggesting that pollution sources are largely from human and animal origin rather than fertilizer sources.

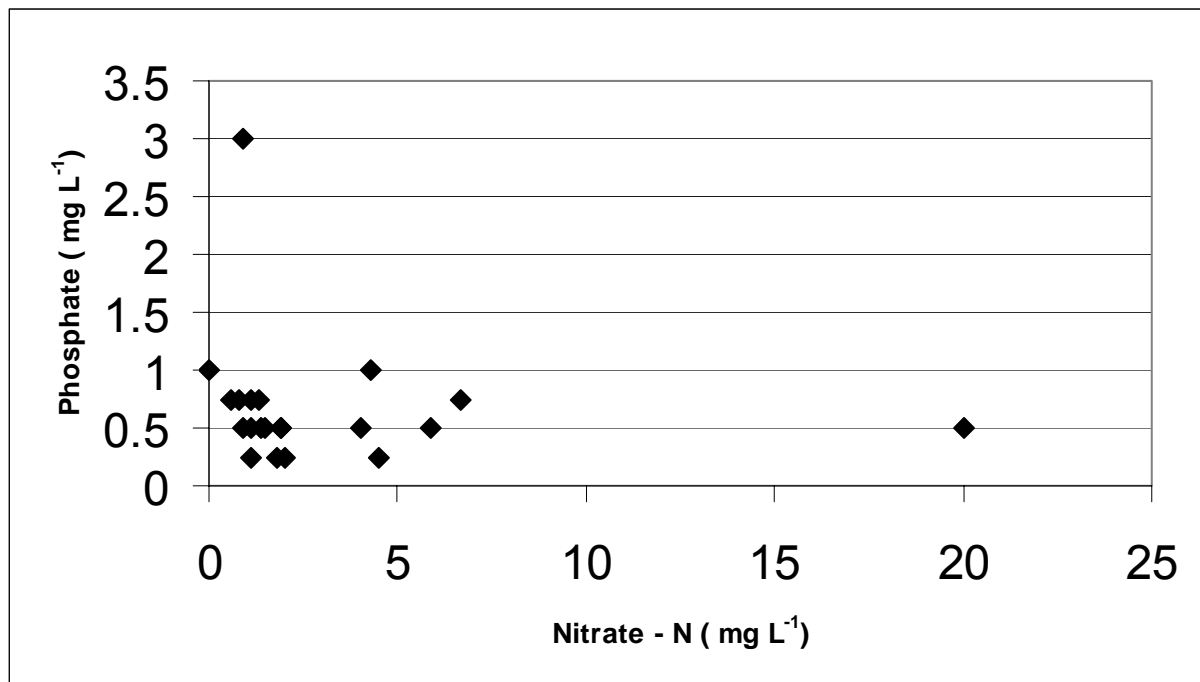


Fig. 4.3.3.1 Plot of Phosphate against Nitrate for Ground Water samples. Except for one sample, the nitrate content is much greater than the phosphate content. This condition indicates that the source of pollution is animal waste rather than fertilizer where DAP (Diammonium phosphate) is used as the fertilizer.

For example the point in the Figure 4.3.3.1 with the highest nitrate concentration (20 mg L⁻¹) which is well above the 10 mg L⁻¹ minimum limit set by the WHO on health grounds has a low phosphate content indicating that the source of pollution is human/animal waste. This source area is observed to be unprotected polluted well environment in the highlands of Chencha town North-West of Arbaminch.

Table 4.3.3.1 Results of Coliform Test and Associated Water Quality Analysis for springs and Ground Water Samples in the Abaya- Chamo Basin. Many of the sources of ground water and springs analyzed show bacterial as well as nitrate pollution both of which are a direct health risk to consumers.

District	Sampling Point	Site Condition	North	East	PH	Water Temp	Nitrite (NO ₂ ⁻)	Ammonia (N-NH ₃)	Nitrate (N-NO ₃ ⁻)	Phosphate (PO ₄ ³⁻)	Faecal Coliforms
			UTM	UTM	(pH units)	(°C)	(mg L ⁻¹)	(mg L ⁻¹)	(mg L ⁻¹)	(mg L ⁻¹)	MPN/100mL
Mirab Abaya	Wajifo Town	Developed Spring, Well protected Distribution Point	360909	713597	7.44	24.5	0.0045	0.22	4.5	0.25	> 2400
Mirab Abaya	Wajifo Bunde #1	Hand Pump, low land, good environment	361241	712982	7.19	29.9	0.004	0.03	6.7	0.75	7
Mirab Abaya	Yayike Kebele	Protected Spring from Near Mountain	361120	707124	7.14	26	0.003	0.07	1.3	0.75	240
Mirab Abaya	Dalbo	Hand Pump, low land, good environment	363213	695131	6.99	30.6	0.004	0.14	4.3	1	11
Mirab Abaya	Mole	Motorized Pump, low land, good environment	364142	692714	7.12	32.2	0.004	0.11	4	0.5	22
Mirab Abaya	Lante School	Hand Pump, low land, good environment	350403	678047	7.2	28.7	0.003	0.09	1.1	0.75	< 2
Arbaminch	Kulfo River	Turbid water	341412	667230	7.86	23.8	0.004	0.29			> 2400
Arbaminch	Crocodile Farm	Borehole, lowland	344949	666108	7.18	26.8	0.006	2.65	0.9	3	< 2
Arbaminch	Arbaminch Springs	Spring Source	340145	663648	7.04	23.5	0.006	0.01	2	0.25	280
Arbaminch	Airport	Borehole, lowland good environment	343626	667785	7.91	27.5	0.26	0	1.1	0.5	170
Arbaminch	Qola shele School	Hand pump, low land, increased agriculture	326178	651342	7.29	24	0.0045	0.4	1.9	0.5	6
Arbaminch	Shelle Becha #1	Protected hand pump, near to irrigation canal	327944	648538	6.99	26	0.009		1.9	0.5	< 2
Arbaminch	Shelle Becha #2	Hand pump, low land, good environment	328185	647768	6.97	26.6	0.006	0.02	1.4	0.5	2
Arbaminch	Elgoluda #1	Hand pump, low land, good environment	329752	645878	7.25	26.6	0.003	0	0.6	0.75	< 2
Arbaminch	Elgoluda #2	Open well, near to toilet polluted environment	329787	645871	7.52	23.8	0.012	0.11	0	1	> 2400
Mirab Abaya	Elgo Dugo	Hand pump, near to farm land	328967	644648	7.01	27.6	0.023	0	5.9	0.5	< 2
Chencha	Doko Gera	Hand pump, good environment, higher elevation	341261	693137	6.93	16.8	0.002	0.02	0.9	0.5	< 2
Chencha	Doko Hyle	Hand pump, good environment, higher elevation	341260	692412	6.95	16.8	0.003	0.01	1.1	0.25	< 2
Chencha	Doko Share	Hand pump, good environment, higher elevation	341043	691898	6.73	17.3	0	0.53	0.8	0.75	< 2
Chencha	03 Kebele	Hand pump, polluted environment, higher elevation	342415	690812	5.48	16.4	0.005	0	20	0.5	8
Chencha	Dorze Town	Spring pipe Distribution, higher elevation	342168	684728	6.83	16.9	0.0045	0	1.8	0.25	> 2400

District	Sampling Point	Site Condition	North	East	PH	Water Temp	Nitrite (NO ₂ ⁻)	Ammonia (N-NH ₃)	Nitrate (N-NO ₃ ⁻)	Phosphate (PO ₄ ³⁻)	Faecal Coliforms
			UTM	UTM	(pH units)	(°C)	(mg L ⁻¹)	(mg L ⁻¹)	(mg L ⁻¹)	(mg L ⁻¹)	MPN/100mL
Chencha	Dorze Town	Hand pump, good environment, higher elevation	342014	684800	6.09	18.1	0.003	0.1	1.5	0.5	< 2
Arbaminch	Qola shele School	Hand pump, protected by fence			7.21	28	0.005				
Arbaminch	Shelle	Hand pump, fenced			7.21	28	0.006				> 2400
Arbaminch	Shelle Becha #1	Shallow depth, protected by fence, hand pump supported			7.21	28	0.014				< 2
Arbaminch	Shelle Becha #2	Shallow depth, protected by fence, hand pump supported			7.21	28	0.014				< 2
Arbaminch	Elgo Luda	Shallow depth, protected by fence, hand pump supported			7.21	28	0.088				130
Arbaminch	Elgo Luda #2	Shallow depth, not protected by fence, hand pump supported			7.21	28	0.01				
Arbaminch	Elgo Gonto Chamo	Shallow depth, not protected by fence, hand pump supported			7.21	28	0.314				130
Arbaminch	Elgo Dugo	Shallow depth, not protected by fence, hand pump supported			7.21	28	0.0125				130

4.3.3.1 Analysis of Ground Water Samples for Common Pollution Factors

Water Quality Parameters Selected

Seven water quality parameters were selected namely Water temperature, pH, Nitrite, Nitrate, ammonia, Phosphate and faecal coliforms. The selection of these parameters is done with the probable sources of pollution in mind. As the use of these sources is for drinking and household purposes it is the health effect of the pollutants that is of major concern. Water temperature is a general hydro-climatic variable. The pH is a variable describing physical and biological chemical changes within the water sources. The nutrients nitrite, ammonia and phosphate arise as a result of pollution from animal and agricultural wastes (fertilizer). Nitrate is a direct health risk on infants causing a disease called methemoglobinemia (blue-babies disease). The ratio of Nitrate to phosphate in the water indicates the sources of pollution, whether it could be from animal waste or possibly from leaching of fertilizers. Nitrite is often an intermediate stage of biological transformation of waste water. It can indicate the presence of a recent pollution from animal wastes. Faecal coliform is an indicator variable. Water sources polluted with excretions from warm blooded animals contain high amounts of these indicator bacteria. Such polluted sources of water are generally considered unsafe for potable uses. The methods of determination for these variables have been described in detail under Chapter Two.

Results of the Water Quality Analysis

The summary of the results of the water quality analysis for the parameters mentioned above is given Table 4.3.3.1

Classification of the Water quality Results in terms of Common Factors

Principal component analysis and factor analysis were carried out using seven of the water quality variables and the samples from the ground water sources mentioned above. Factor analysis with varimax rotation in many cases suggested four factors to be statistically significant at the 95% confidence limit. Number of factors less than four indicates statistically insignificant common factor analysis.

Initial analysis also indicated three samples as outliers (sharing little communality with the rest of the samples). These samples were removed from the analysis. The samples are the two boreholes from crocodile farm and the airport both of which are near the lakes and

contain very high ammonia and phosphate, and, a polluted open well with very high concentration of nitrate.

The remaining data were analysed using common factor analysis. Four factors were suggested by the statistical analysis and also by the eigenvalue plot (Figure 4.3.3.1.1). The samples score plots appear fairly clustered around these factors with no single sample outlier (taking in to account that only a net of 19 samples were analysed finally). Figure 4.3.3.1.2 b shows the factor score plots of the samples for the four factors.

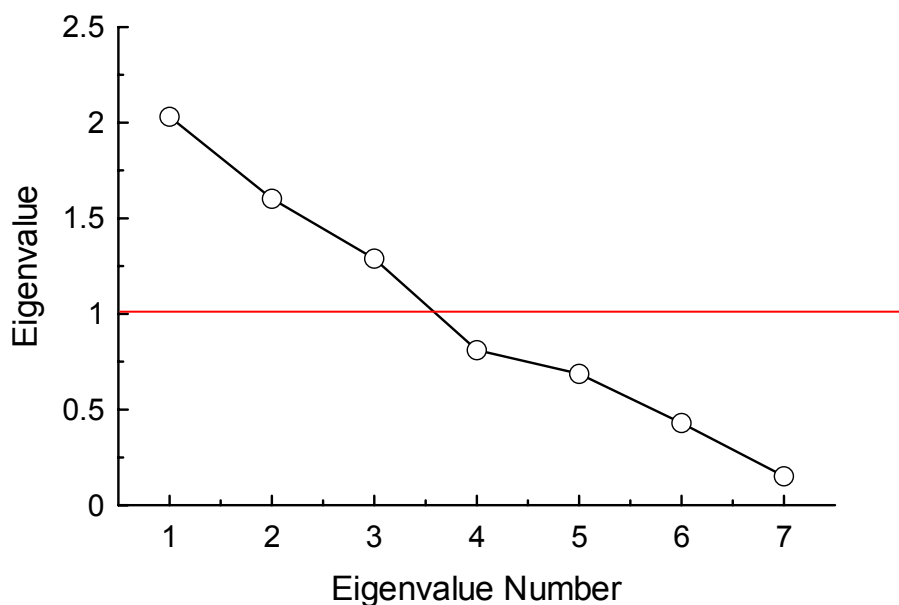
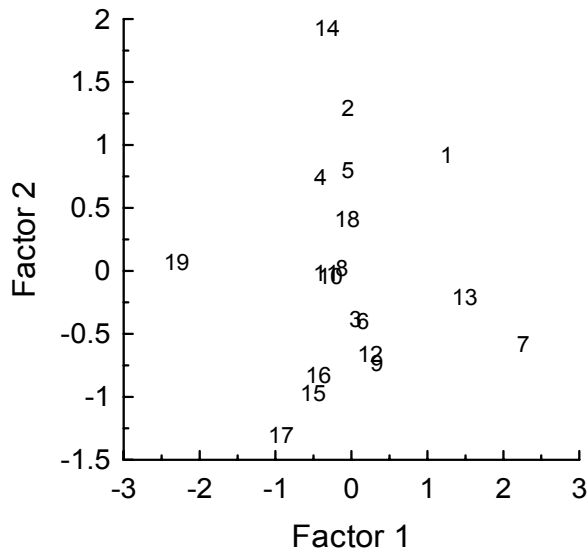
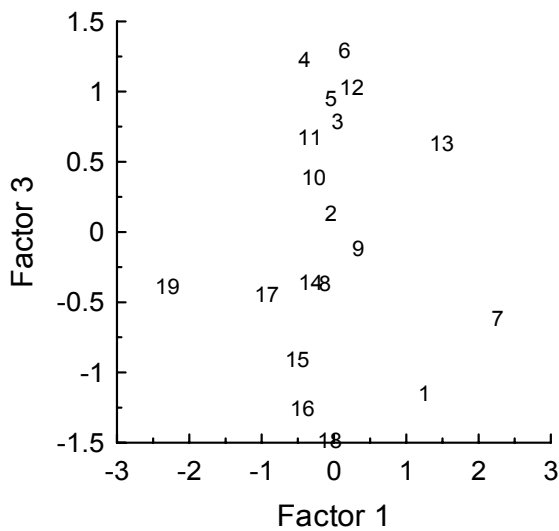


Fig. 4.3.3.1.1 Eigen value Plot for Ground Water Samples. The scree plot is the plot of the Eigen values from the principal component analysis of the water quality data. The Eigen values are obtained by orthogonal transformation of the water quality correlation matrix in to a matrix of independent components (a diagonal matrix). The Eigen values are proportional to the data variance and the total variance of the data remains constant during the transformation. For example in the above figure almost none of the eigen value accounts for a great portion of the data variance which indicates that the data dimensionality is not much reduced by the transformation.

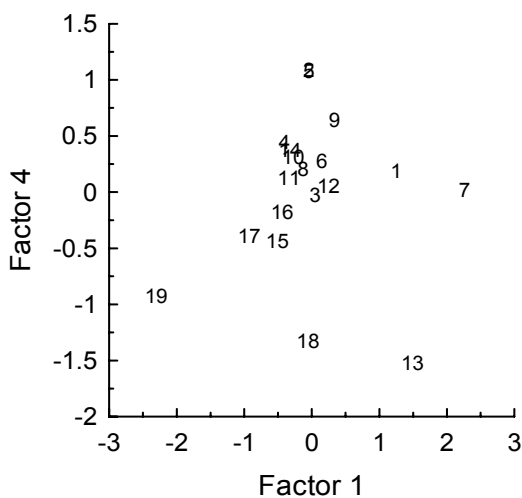
Factor Scores: Factor 1 - Factor 2



Factor Scores: Factor 1 - Factor 3

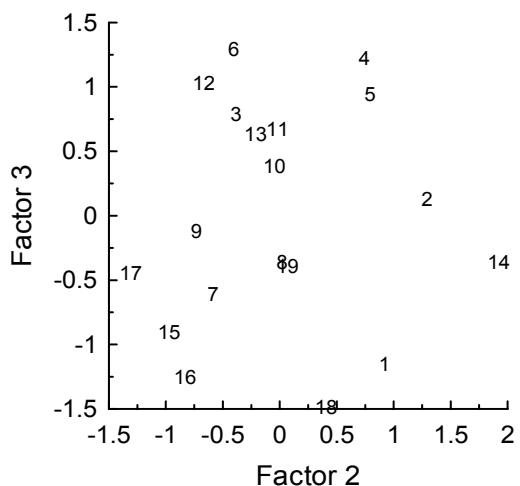


Factor Scores: Factor 1 - Factor 4

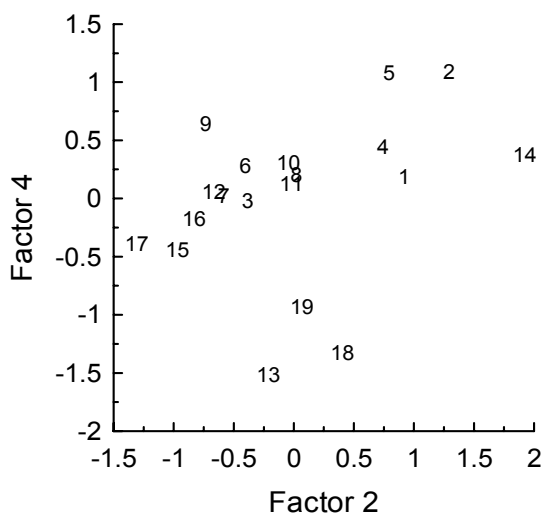


1	Wajifo Town	Developed Spring, Well protected Distribution Point
2	Wajifo Bunde #1	Hand Pump, low land, good environment
3	Yayike Kebele	Protected Spring from Near Mountain
4	Dalbo	Hand Pump, low land, good environment
5	Mole	Motorized Pump, low land, good environment
6	Lante School	Hand Pump, low land, good environment
7	Kulfo River	Turbid water
8	Arbaminch Springs	Spring Source
9	Qola shele School	Hand pump, low land, increased agriculture
10	Shelle Becha #1	protected hand pump, near to irrigation canal
11	Shelle Becha #2	Hand pump, low land, good environment
12	Elgoluda #1	Hand pump, low land, good environment
13	Elgoluda #2	Open well, near to toilet polluted environment
14	Elgo Dugo	Hand pump, near to farm land
15	Doko Gera	Hand pump, good environment, higher elevation
16	Doko Hyle	Hand pump, good environment, higher elevation
17	Doko Share	Hand pump, good environment, higher elevation
18	Dorze Town	Spring pipe Distribution, higher elevation
19	Dorze Town	Hand pump, good environment, higher elevation

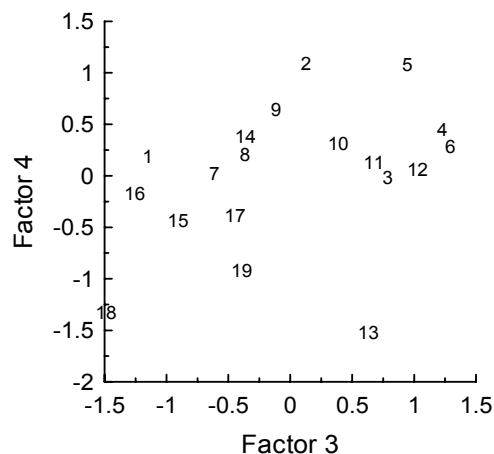
Factor Scores: Factor 2 - Factor 3



Factor Scores: Factor 2 - Factor 4



Factor Scores: Factor 3 - Factor 4



1	Wajifo Town	Developed Spring, Well protected Distribution Point
2	Wajifo Bunde #1	Hand Pump, low land, good environment
3	Yayike Kebele	Protected Spring from Near Mountain
4	Dalbo	Hand Pump, low land, good environment
5	Mole	Motorized Pump, low land, good environment
6	Lante School	Hand Pump, low land, good environment
7	Kulfo River	Turbid water
8	Arbaminch Springs	Spring Source
9	Qola shele School	Hand pump, low land, increased agriculture
10	Shelle Becha #1	protected hand pump, near to irrigation canal
11	Shelle Becha #2	Hand pump, low land, good environment
12	Elgoluda #1	Hand pump, low land, good environment
13	Elgoluda #2	Open well, near to toilet polluted environment
14	Elgo Dugo	Hand pump, near to farm land
15	Doko Gera	Hand pump, good environment, higher elevation
16	Doko Hyle	Hand pump, good environment, higher elevation
17	Doko Share	Hand pump, good environment, higher elevation
18	Dorze Town	Spring pipe Distribution, higher elevation
19	Dorze Town	Hand pump, good environment, higher elevation

Fig. 4.3.3.1.2 Factor Score Plots for Ground Water Pollution investigation Data

The factor loadings plot for the seven variables is given in the Figure 4.3.3.1.3 and the interpretation is given by analysing these loadings with the known sources condition and factor scores as described below.

Factor 1 varies with most with high coliforms (variable 7) and higher pH (variable 1). Samples loaded highly on to this factor are: polluted open well that is near to toilet, turbid river water, spring water from a shallow ground water source. Incidentally all are samples taken from the low lands. Considering the low population density in the high lands this may not be surprising. Nitrite (variable 3) is the closest correlated variable to coliform density in addition to pH (variable 1) and ammonia (variable 4). Nitrate and phosphate appear to have very low co-variation with coliform counts. These samples can be classified as grade one-pollution cases - bacterially most polluted and posing immediate health dangers from water borne illnesses.

Factor 2 is loaded most on nitrate followed by nitrite and low on coliforms. Samples most loaded on this factor are a hand pump near farmland. Phosphate values are low. Direct contamination is ruled out as coliforms are moderately low and the wells appear to be well protected. The high nitrate concentrations measured from these wells range from 4-7 mg L⁻¹ as Nitrogen and one sample at 20 mg L⁻¹. These values are well above the background concentrations arising from geological origins (Frisbie, H.S., 1999) the sources of pollution could be infiltration of animal wastes or organic fertilizer. Nitrate readily leaches from soil. The presence of nitrite may be suggesting fresh contamination. These sources can be classified as grade two pollution cases with high nitrate content and some coliforms both of which pose a health danger.

Factor 3 show slightly higher values of phosphates. Samples loaded are mostly from the highlands. High values of nitrates are also indicated. Phosphates tend to be sorbed by aquifer solids, especially in calcareous systems (Phosphate forms poorly soluble iron, aluminum, calcium, and magnesium compounds that do not readily leach from most soils), and therefore are not transported to any significant extent in ground waters The exception to this is in aquifers consisting of relatively more sandy soils. Sandy soils have limited sorption capacity for phosphate. Therefore, phosphorus associated with human and animal wastes as well as fertilizers discharged to sandy aquifer systems can be readily transported in to ground waters. The high nitrate content may point to non-natural sources mentioned above.

Factor 4 is loaded highly on samples with high nitrate but at the same time relatively low nitrite that made it different from factor 2. Coliforms are indicated but their counts are low. Ground water samples near irrigated agriculture are loaded high on to this factor. The source of nitrate could be fertilizer rather than animal waste. Nonetheless, the high nitrate content makes this source as posing a health danger.

In conclusion the ground water sources investigated show direct pollution from human and animal wastes because of lack of appropriate protection (unprotected wells, open sources, rivers and springs) therefore posing immediate health dangers from water borne illnesses and nitrate interference in blood hemoglobin activity in infants. Such sources are identified by very high coliform counts as well as relatively high values of nitrite. The aquifer characteristics in some ground water favored leaching of wastes from animal and human origins as well as possibly agricultural fertilizers showing high nitrate and phosphate as well as nitrite.

Well protection measures must be taken including walling and capping of open wells, removal of toilets from near wells, fencing of wells and excluding animals and human wastes from around water sources, treatment of river water and even spring water sources with slow sand filters and management of application of fertilizers as well as locating wells away from areas of agricultural activities.

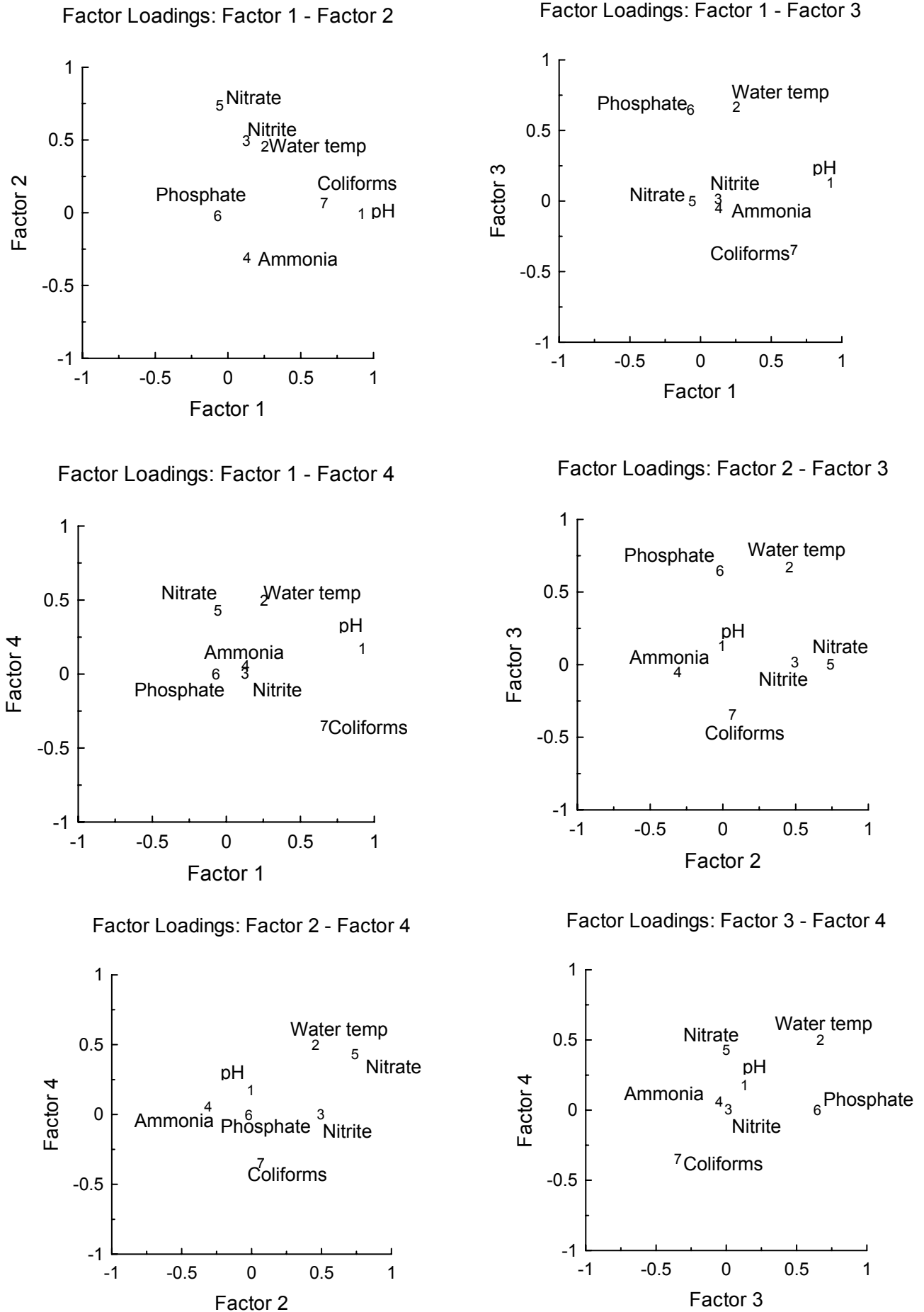


Fig. 4.3.3.1.3 Factor Loading Plots for Ground Water Pollution Investigation Data

CHAPTER FIVE
DESIGN OF WATER QUALITY MONITORING SYSTEM

S.No.	CONTENTS	PAGE
5.1	Introduction	195
5.2	Results of Principal Component Analysis	195
5.3	Factor Analysis Results	196
5.4	Significance and Interpretation of Factors common to the Water Quality Parameters	198
	5.4.1 Factors Common to Kulfo Rivers	198
	5.4.2 Factors Common To Hare River	206
	5.4.3 Factor Score Plots	212
	5.4.4 Importance of Data Integrity and Continuity	212
5.5	Design of River Water Quality Monitoring System	213
	5.5.1 Design Group 1	213
	5.5.2 Design Group 2	214
	5.5.3 Design Group 3	214
	5.5.4 Design Group 4	214
	5.5.5 Determination of Monitoring Intervals	215
	5.5.6 Trend Detection and Elimination	215
	5.5.7 Monitoring Design through Spectral Analysis	215
	5.5.7.1 Group I Monitoring variables	215
	5.5.7.2 Group II Monitoring Variables	217
	5.5.7.3 Group III Monitoring Variables	223
	5.5.7.4 Group IV Monitoring Variables	224
5.6	Design of Lake Water Quality Monitoring System	228
	5.6.1 Temporal Monitoring Interval Design- Lake Abaya	228
	5.6.2 Temporal Monitoring Interval Design- Lake Chamo	230
	5.6.3 Spatial Monitoring Interval Design	233
	5.6.3.1 Comparison of Variable Values Among the Different Clusters.	234
	5.6.3.2 Significance of the Clustering Differences within Lake Abaya	234
	5.6.3.2.1 Variation of pH among the clusters	234
	5.6.3.2.2 Variation of Other Water Quality variables Among the clusters	237
	5.6.3.2.3 Interpretation of Re-Clustering of Lake Area	238

S.No.	LIST OF FIGURES	PAGE
Fig. 5.3.1	Scree Plot Kulfo River	197
Fig. 5.4.1.1	Factor Loadings for Kulfo River Factor 1 - Factor 2	199
Figure 5.4.1.2	Factor Loadings for Kulfo River Factor 1 – Factor 3	200
Figure 5.4.1.3	Factor Loadings for Kulfo River Factor 1 – Factor 4	201
Figure 5.4.1.4	Factor Loadings for Kulfo River Factor 2 – Factor 3	202
Figure 5.4.1.5	Factor Loadings for Kulfo River Factor 2 – Factor 4	202
Figure 5.4.1.6	Factor Loadings for Kulfo River Factor 3 – Factor 4	203
Fig. 5.4.2.1	Scree Plot for Kulfo River Data	204
Figure 5.4.2.2	Factor Loadings for Hare River Factor 1 – Factor 2	206
Figure 5.4.2.3	Factor Loadings for Hare River Factor 1 – Factor 3	207
Fig. 5.4.2.4	Variation of Carbon dioxide in ppm with season (Hare River)	208
Fig. 5.4.2.5	Variation of Carbon dioxide in ppm with season (Kulfo River)	209
Figure 5.4.2.6	Factor Loadings for Hare River Factor 1 – Factor 4	210
Figure 5.4.2.7	Factor Loadings for Hare River Factor 2 – Factor 3	210
Figure 5.4.2.8	Factor Loadings for Hare River Factor 2 – Factor 4	211
Figure 5.4.2.9	Factor Loadings for Hare River Factor 3 – Factor 4	211
Figure 5.4.3.1	Factor Score Plot for Kulfo River Factor 1 - Factor 2	212
Fig. 5.5.7.1.1	Spectrum of Conductivity - Kulfo River	216
Fig. 5.5.7.1.2	Percentage Information against Frequency - Kulfo Conductivity	216
Fig. 5.5.7.2.1	Spectrum of Kulfo River Discharge	218
Fig. 5.5.7.2.2	Percentage Information against Frequency of Monitoring - Kulfo River Discharge	218
Fig. 5.5.7.2.3	Spectrum of Turbidity - Kulfo River	219
Fig. 5.5.7.2.4	Percentage Information versus Frequency - Turbidity Kulfo River	220
Fig. 5.5.7.2.5	Spectrum of Rainfall	220
Fig. 5.5.7.2.6	Percentage Information Versus Frequency - Rainfall Data	221
Fig. 5.5.7.3.1	Spectrum of Air Temperature - Kulfo	223
Fig. 5.5.7.3.2	Spectrum of pH - Kulfo	223
Fig. 5.5.7.4.1	Spectrum of Hardness - Kulfo	225
Fig. 5.5.7.4.2	Spectrum of Calcium Kulfo River	225
Fig. 5.5.7.4.3	Spectrum of Chloride - Kulfo River	226
Fig. 5.6.1.1	Spectrum of pH - Lake Abaya	228
Fig. 5.6.1.2	Spectrum of Turbidity - Lake Abaya	228
Fig. 5.6.1.3	Spectrum of Alkalinity - Lake Abaya	229
Fig. 5.6.1.4	Spectrum of Conductivity - Lake Abaya	229
Fig. 5.6.2.1	Spectrum of pH - Lake Chamo	231
Fig. 5.6.2.2	Spectrum of Alkalinity - Lake Chamo	231
Fig. 5.6.2.3	Spectrum of Conductivity - Lake Chamo	232
Fig. 5.6.2.4	Spectrum of Turbidity - Lake Chamo	232
Fig 5.6.3.1	Plot of the Cluster Analyses Results on the Layout of Lake Abaya using GIS	235

S.NO.	LIST OF TABLES	PAGE
Table 5.2.1	Proportion of Data Accounted by Principal Components	196
Table 5.3.1	Factor Pattern Matrix (Factor Loadings)	197
Table 5.5.7.1.1	Design of monitoring Interval for Group I parameters	217
Table 5.5.7.2.1	Design of Monitoring Interval for Group II Variables - Kulfo River	221
Table 5.5.7.3.1	Design of Monitoring Interval for Group III Variables - Kulfo River	224
Table 5.5.7.4.1	Design of Monitoring Interval for Group IV Variables - Kulfo River	226
Table 5.6.1.1	Lake Abaya Design of Temporal Monitoring Interval	230
Table 5.6.2.1	Lake Chamo Design of Temporal Monitoring Interval	233
Table 5.6.3.1.1	The Average Value of Water Quality Data Within Cluster Groups	234
Table 5.6.3.2.1.1	Statistical Significance Test for pH Difference within Clusters	236
Table 5.6.3.2.1.2	Statistical Significance Test for pH Difference within Clusters	236
Table 5.6.3.2.1.3	Statistical Significance Test for pH Difference within Clusters	236
Table 5.6.3.2.2.1	Regrouping of Clusters by Statistical tests	237

5.1 Introduction

Chapter One introduced the concept of water quality monitoring design. According to the approach adopted in the methodology of this research. This chapter illustrates a water quality monitoring system design based on an integrated partial physical orthogonal model based on data generated within the water resources of the Abaya – Chamo drainage basin. Abstract common factors were first extracted by the application of principal component and factor analysis [63]. By overlaying real factors with abstract common factors the underlying causes for the water quality variations have been explained. Surface flow factors, sub surface flow factors, leaching flow factors, effects of soil matrix, rainfall magnitude and intensity, discharge, catchment area and slope, in stream pollution and point sources of pollution, evaporative storage and precipitation chemistry all showed up in such integrated model. This model can be extended by including further physical factors as well as natural and anthropogenic pollution sources and factors. This model can be extended to lakes and ground water sources as well.

Design of water quality monitoring intervals was accomplished with the help of spectral analysis of the data after trends were diagnosed and removed and within groups of monitoring as defined by the factor model described above. The percentage information for a given frequency of monitoring was derived from the integral of the spectral density plot, which is equivalent to the auto-covariance of the data. Optimum monitoring intervals are indicated in the plot of such integrals. Spatial monitoring spacing for lake water quality was determined after hierarchical cluster analysis. The detail of the design approach is presented below.

5.2 Results of Principal Component Analysis

The application of principal component analysis to fifteen of the water quality data of river Kulfo show the first few components account for the majority of the data variation. 75% of the data variation can be accounted for by the first five factors. Table 5.2.1 shows the proportion of data accounted for by each component.

Table 5.2.1 Proportion of Data Accounted by Principal Components. The principal component analysis performs an orthogonal transformation of the water quality correlation matrix in to a matrix of independent components (a diagonal matrix). The Eigen values are proportional to the data variance and the total variance of the data remains constant during the transformation. For example the first Eigen value accounts for 36% of the data variance.

Component (In Order of magnitude)	Eigen Value	Proportion	Cumulative Proportion
Comp. 1	5.3718	0.358	36%
Comp. 2	2.141	0.143	50%
Comp. 3	1.5343	0.102	60%
Comp. 4	1.1275	0.075	68%
Comp. 5	1.0395	0.069	75%
Comp. 6	0.8588	0.057	80%
Comp. 7	0.7318	0.049	85%
Comp. 8	0.6255	0.042	90%
Comp. 9	0.5246	0.035	93%
Comp. 10	0.3165	0.021	95%
Comp. 11	0.2359	0.016	97%
Comp. 12	0.2102	0.014	98%
Comp. 13	0.1419	0.009	99%
Comp. 14	0.101	0.007	100%
Comp. 15	0.0397	0.003	100%

In order to find the common factors responsible for the water quality variation common factor analysis with varimax rotation was applied using the first four factors. The number of factors was selected by applying the criteria of Eigen values falling above 1. Since the fourth and fifth factors are more or less equal in Eigen values four factors have been applied. Similar results have been obtained for Hare River and the same number of factors has been selected also for factor analysis of Hare river water quality. The detail of the results of factor analysis is given below.

5.3 Factor Analysis Results

The scree plot shown below shows that the intersection of the steeper and milder slope happens at around factor number four. Therefore, the selection of four factors is sufficient for factor analysis. The factor loadings, uniqueness and communalities after varimax rotation are shown in Table 5.3.1.

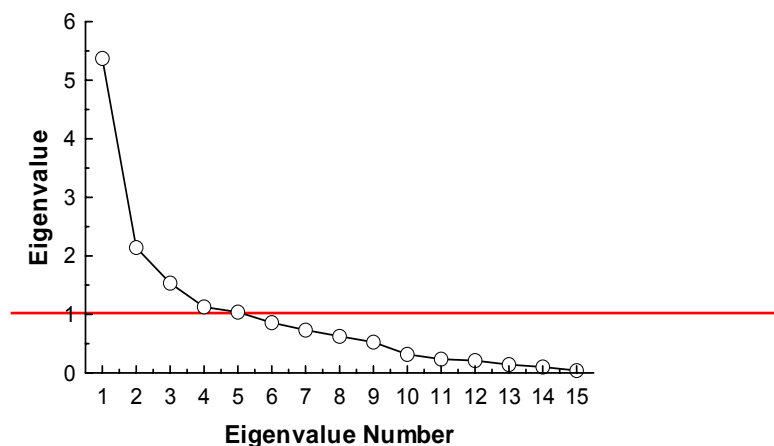


Fig. 5.3.1 Scree Plot Kulfo River. The scree plot is the plot of the Eigen values from the principal component analysis of the water quality data. The Eigen values are obtained by orthogonal transformation of the water quality correlation matrix in to a matrix of independent components (a diagonal matrix). The Eigen values are proportional to the data variance and the total variance of the data remains constant during the transformation. For example in the above figure the first Eigen value accounts for a great portion of the data variance.

Table 5.3.1 Factor Pattern Matrix (Factor Loadings). Factor analysis is further rotation of the principal component matrix that converts m of the principal components in to a set of p common factors. The uniqueness is the proportion of the data variance that is not accounted by the factors. Communality is that proportion which is accounted by the common factors.

Variable	Parameter	Factor1	Factor2	Factor3	Factor4	Uniqueness	Communality
X1	Rainfall	-0.057	0.114	-0.027	0.290	0.899	0.101
X2	River Discharge	-0.221	0.812	-0.303	0.059	0.196	0.804
X3	Air Temperature	0.447	-0.155	0.789	0.093	0.145	0.855
X4	Water Temperature	0.238	-0.146	0.785	-0.109	0.295	0.705
X5	Turbidity	-0.277	0.943	-0.111	0.147	0.000	1.000
X6	Conductivity	0.911	-0.303	0.222	-0.023	0.028	0.972
X7	pH	0.664	-0.127	0.392	0.036	0.388	0.612
X8	Total Solids	-0.475	0.552	0.031	0.017	0.468	0.532
X9	Alkalinity	0.745	-0.141	0.220	0.053	0.373	0.627
X10	Hardness	0.305	-0.122	0.041	0.806	0.241	0.759
X11	Calcium	0.012	-0.031	0.058	0.876	0.228	0.772
X12	Chloride	0.001	0.087	-0.339	0.403	0.715	0.285
X13	Sodium	0.498	-0.207	0.265	0.133	0.622	0.378
X14	Potassium	-0.441	0.232	0.006	0.010	0.752	0.248
X15	Absorption (500 nm)	-0.132	0.516	-0.071	-0.005	0.711	0.289
Proportion		0.199	0.162	0.119	0.115		
Cumulative Proportion		0.199	0.361	0.480	0.596		

5.4 Significance and Interpretation of Factors common to the Water Quality Parameters

All the common factors considered are abstract factors rather than being real factors since the factors have negative loadings as well. In order to enable the interpretation of these factors their alignment with real factors such as river flow variation, weather parameters, air and water temperature as well as rainfall is analysed. Factors that are loaded highly with these real factors are considered to be influenced by these variables or draw a common cause with them.

With this approach the common abstract factors are explained below for the two rivers Hare and Kulfo. In turn the influence of these factors on the water quality variabilities are investigated.

5.4.1 Factors Common to Kulfo Rivers

From the principal component analysis of the water quality data considered four factors have been selected using the scree plot criteria (intersection of the lower milder slope with the upper steeper slope of the Eigen values versus principal component plot).

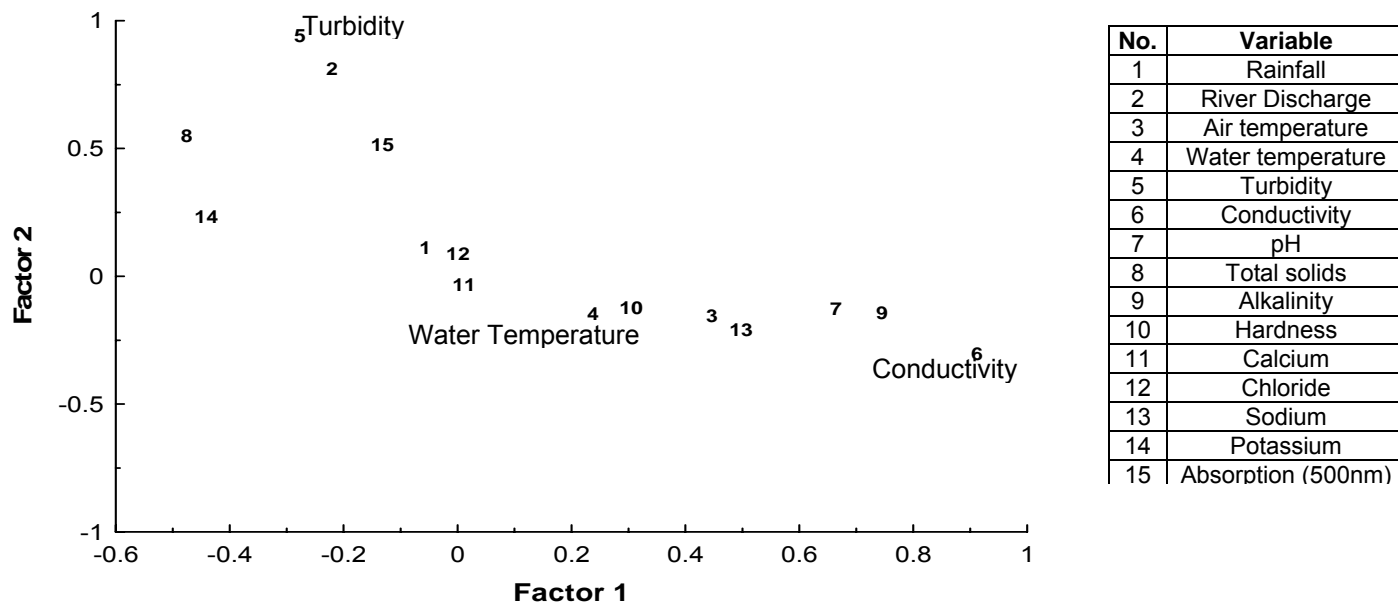


Figure 5.4.1.1 Factor loading: factor1 – factor2. Factor 1 is the long term transition factor where air and water temperature load significantly. Factor 2 is the short term rain induced latent factor. River discharge load significantly.

Factor 1 in the Figure 5.4.1.1 is the long-term transition factor that is accompanied by significant change in weather parameters: air temperature changes significantly. The increase in water temperature is also noticeable. These changes occur over a longer term (see the spectrum plots of air and water temperatures for Kulfo River below). Other real factors are loaded negatively: river discharge decreases significantly. Rainfall regime changes from wet to dry and the river solids load (variables 8, 15, 5) all decrease significantly. Since rainfall has a negative loading this further supports the evidence of long-term variation.

Conductivity is loaded highly on this factor followed by alkalinity. The change in conductivity is largely due to bicarbonate followed by Sodium and Magnesium in that order. Chloride changes little may be due to the lack of evaporative storage at the lower subsurface flow.

The buffering potential of the soil is seen through the high bicarbonate exchange-giving rise to increased alkalinity during the transition to the drier season.

Factor 2 is related with the rising phase of the river flow. Rainfall is positively loaded with this factor that indicates the period of increased precipitation. At the same time river flow has the maximum loading on it. Solids loads increase rapidly (variables 8,

15, 5). Since air and water temperature are negatively loaded with it but only slightly, this factor represents some average period and not a spontaneous high frequency variation. Chloride level increases almost the same as rainfall, which indicates a near surface input from the catchments due to evaporative storage. This increase cannot be considered to be part of atmospheric input as the discharge loading is much higher than chloride loading on the same factor. Potassium increases and in relative terms it indicates the surface-near surface storage input that overshadows any decrease due to dilution. This is because the potassium levels are low during dry seasons. Conductivity decreases the most because it represents the aggregate of ions in solution. All the other ions (except Calcium) decrease due to dilution effects and little surface input. Since particles (silt, clays, etc) dominate in this portion of the flow, pollutants associated with these particles will also show an increase [64].

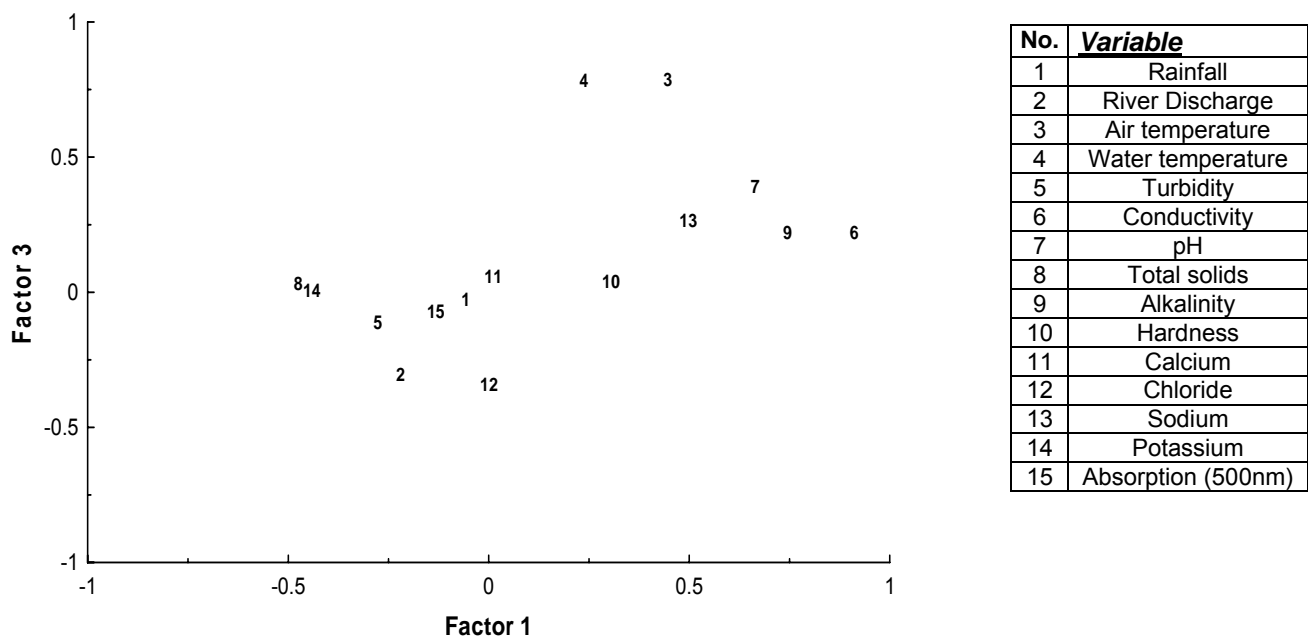


Figure 5.4.1.2 Factor Loadings for Kulfo River Factor 1 – Factor 3. Factor 3 exhibits pH change due to sodium exchange. It is a variation occurring during the drier part of the season.

Factor 3 shows almost zero loading on rainfall, which indicates a drier part of the season. Flow continues to decrease while there is a slow reduction in turbidity. Air and water temperature are equally and highly loaded on this factor. The pH change, which is greater than that of alkalinity, might be due to sodium exchange and the release of more carbon dioxide. Hardness and calcium have almost zero loading, which indicates poor exchange of divalent ions in the drier season subsurface flow.

Chloride has a negative loading which partly indicates the absence of any groundwater intrusion, evaporative storage release or any salt contamination.

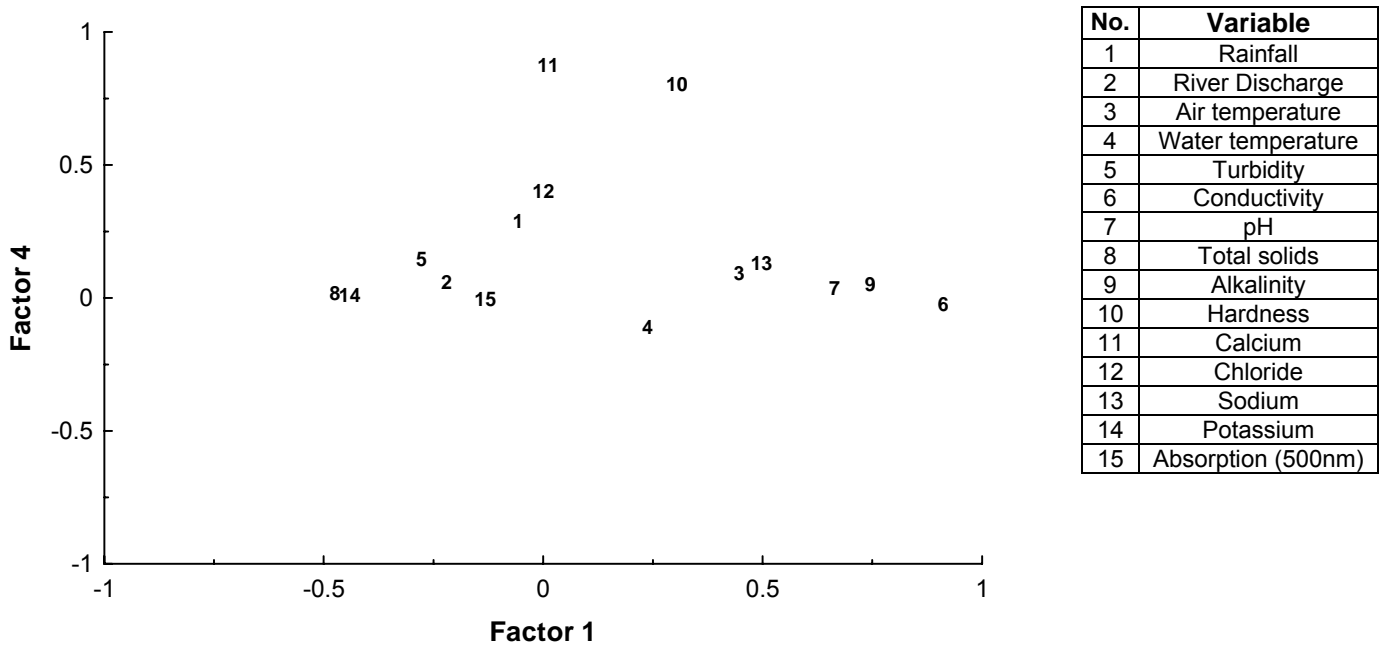


Figure 5.4.1.3 Factor Loadings for Kulfo River Factor 1 – Factor 4. Factor 4 is a variation accounting for a low intensity rainfall. It is a near surface flow factor where chloride, calcium and hardness show increased concentration.

Factor 4 represents the phase where there has been rain of low magnitude and intensity in the station considered but the discharge is decreasing slightly. The solids loads are reducing (see figure 5.4.1.3). The net effect of low intensity rainfall is to increase the water hardness and calcium as well as Chloride. This variation is considered as short term variation because long term weather effects (air temperature and water temperature are poorly loaded on this factor. Air temperature is positively loaded while water temperature is negatively loaded on this factor. Considering the low Eigen value of this factor compared with the first three factors, it is obvious to see that this factor explains only few of the data variation among the set considered. The low communality of Calcium, hardness and chloride as well as rainfall is explained by their association with this factor. If it could be considered as special factor it is associated with low rainfall events with little impact on river discharge.

The rest of the plot of factors combination for Kulfo River is given in the Figures 5.4.1.4 – 5.4.1.6.

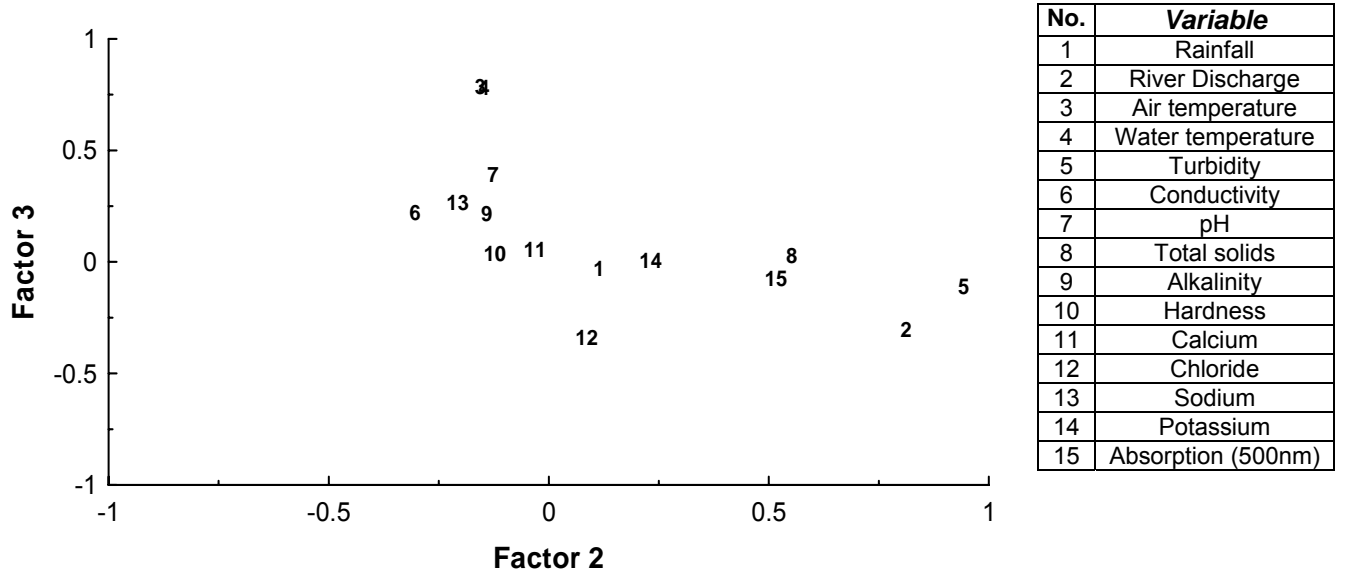


Figure 5.4.1.4 Factor Loadings for Kulfo River Factor 2 – Factor 3

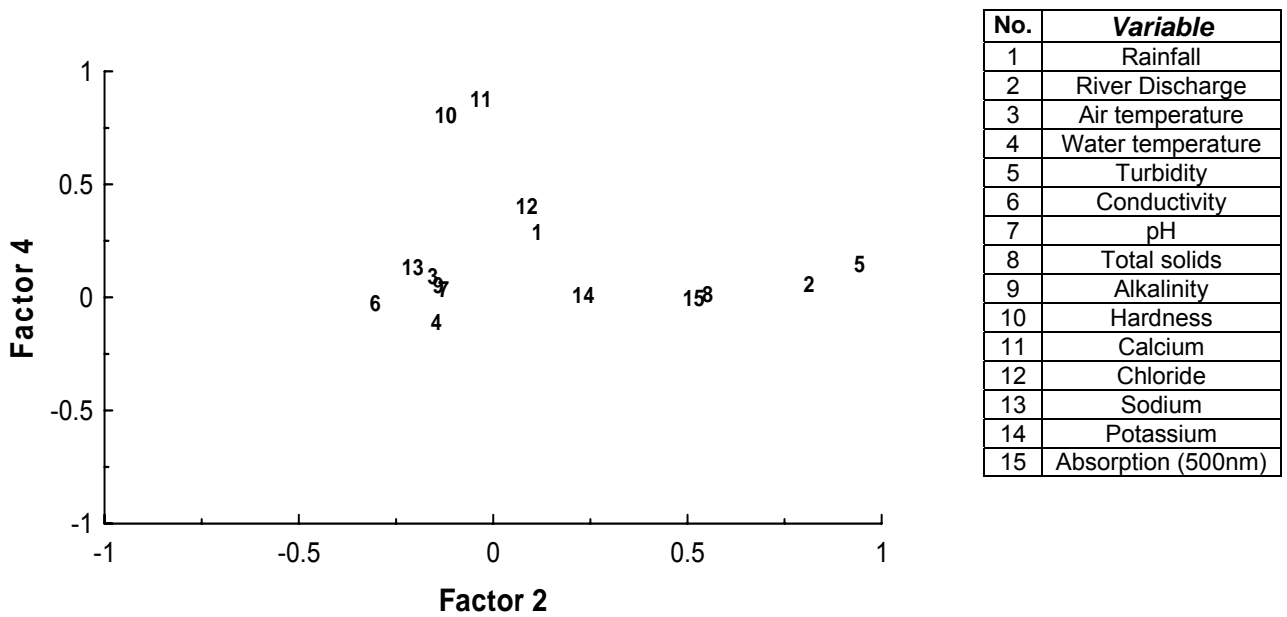


Figure 5.4.1.5 Factor Loadings for Kulfo River Factor 2 – Factor 4

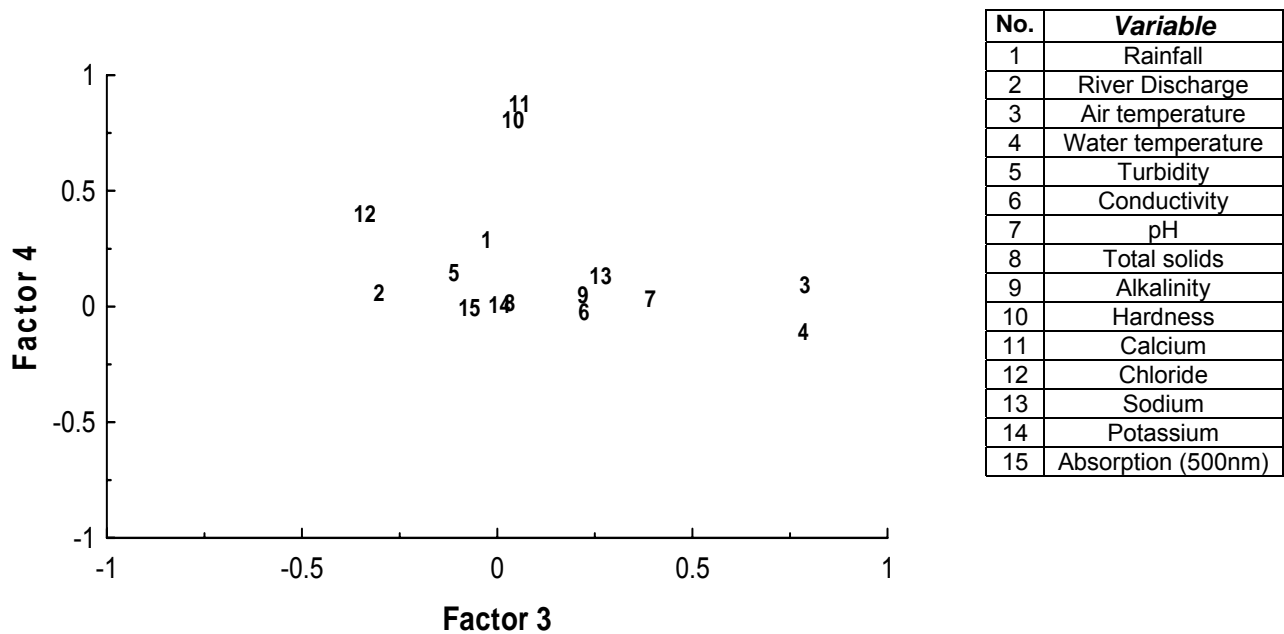


Figure 5.4.1.6 Factor Loadings for Kulfo River Factor 3 – Factor 4

5.4.2 Factors Common to Hare River

From the principal component analysis of the water quality data considered, four factors have been selected using the scree plot criteria (intersection of the lower milder slope with the upper steeper slope of the Eigen values versus principal component plot). The Eigen value plot is given in Figure 5.4.2.1.

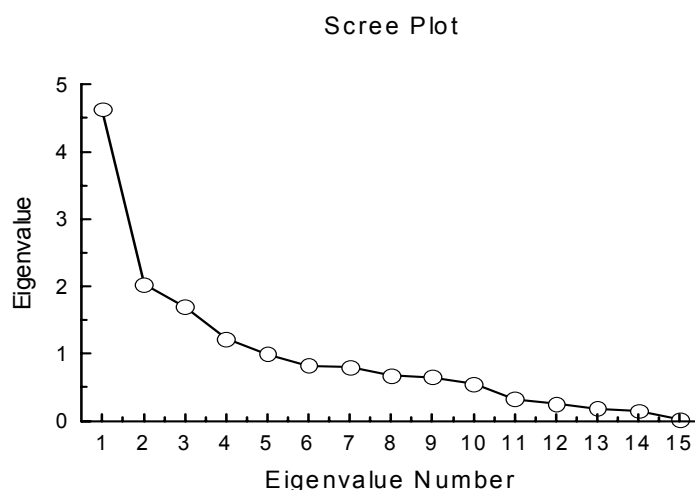


Fig. 5.4.2.1 Eigen Values Plot for Hare River Data. The plot of the Eigen values is from the principal component analysis of the water quality data. The Eigen values are obtained by orthogonal transformation of the water quality correlation matrix into a matrix of independent components (a diagonal matrix). The Eigen values are proportional to the data variance and the total variance of the data remains constant during the transformation. For example in the above figure the first Eigen value accounts for a great portion of the data variance.

Factor 1 in the figure 5.4.2.2 is, similar to river Kulfo, the long-term transition factor associated with the falling flow phase of the river discharge. That is accompanied by significant change in weather parameters: air temperature changes significantly. The change in water temperature is also noticeable. These changes occur over a longer term (see the spectrum plots of air and water temperatures for Hare River below). Other real factors are loaded negatively: river discharge decreases significantly. Rainfall has zero loading on this factor. And the river solids load (variables 8, 15, 5) all decrease significantly. Since rainfall has a positive near zero loading it indicates the wet part of the long-term seasonal variation (also evidenced by negative high loading on water and air temperature).

Sodium is loaded highly on this factor followed by conductivity and alkalinity. The change in conductivity is largely due to Sodium. Calcium and magnesium change very little with this factor. Comparing the retention of Sodium and hydrogen ions between the two rivers Hare and Kulfo, it is possible to see the difference in terms of the loading on factor 1. For Kulfo river pH has a higher loading while sodium is less loaded than pH. Both indicate higher retention of positive ions (H^+ , Na^+ , NH_4^+ , etc). Whereas for Hare River the Sodium level loading is maximum and the pH-loading minimum, these conditions indicate similar characteristics: less retention of positive ions for Hare river catchment [65].

The other contrasting comparison between these two rivers is made with respect to hardness loading on factor 1. Kulfo River exchanges more hardness and less Sodium while the opposite is true for Hare River, i.e., the hardness loading is low on factor one while the Sodium loading is high. These conditions can be correlated with the low Sodium dominance of Kulfo River and the high Sodium dominance ratio of Hare River.

Chloride changes little may be due to the lack of evaporative storage at the lower subsurface flow. The buffering potential of the soil is seen through the high bicarbonate exchange-giving rise to increased alkalinity during the transition to the drier season.

Factor 2 is related with the rising phase of the river flow. Rainfall is positively loaded with this factor, which indicates the period of increased precipitation. At the same time river flow has the maximum loading on it. Solids loads increase rapidly (variables 8, 15, 5). Since air and water temperature are negatively loaded with it but only slightly, this factor represents some average period and not a spontaneous high frequency variation. Chloride level increases almost the same as rainfall, which indicates a near surface input from the catchments due to evaporative storage. This increase cannot be considered to be part of atmospheric input as the discharge loading is much higher than chloride loading on the same factor. Potassium increases and in relative terms it indicates the surface-near surface storage input that overshadows any decrease due to dilution. This is because the potassium levels are low during dry seasons. Conductivity decreases the most because it represents the aggregate of ions in solution. All the other ions (except Calcium) decrease due to dilution effects and little surface input.

Factor 2 represents the rising portion of the flow curve as the river discharge considerably increases with this factor so also the rainfall. Unlike river Kulfo rainfall is the more representative parameter for the water quality variations. This factor also shows a relatively greater change in absorption. Since weather parameters are poorly loaded on this factor (air and water temperatures), it indicates the within season short-term high frequency change in water quality variation largely induced by surface flow processes. The loading on pH is greater than that of alkalinity for Hare River indicating pH changes more rapidly for river Hare rather than river Kulfo.

Total solids has greater loading on this factor than on any other which, however, is due to its mixed source (surface suspended and sub surface dissolved solids).

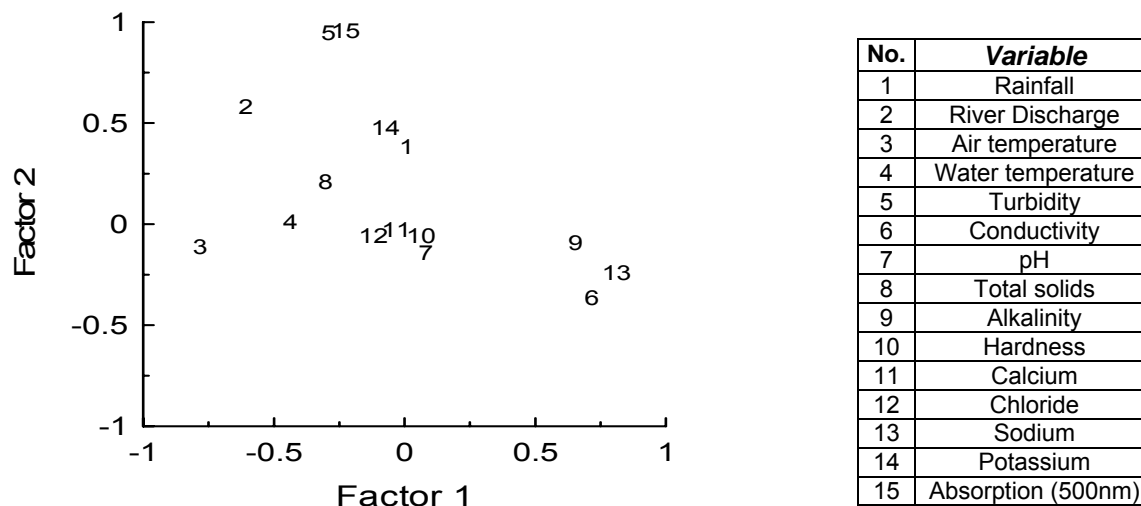


Figure 5.4.2.2 Factor Loadings for Hare River Factor 1 – Factor 2. Less retention of positive ion is exhibited on Hare River by the lower loading of pH on this factor compared to the loading of pH on factor 1 on Kulfo River. Factor 1 is the long term transition factor. Factor 2 is the short term rain induced surface flow factor.

Factor 3 may represent the short term leaching effect as chloride, calcium and hardness increase. Rainfall and discharge have almost zero loading on this factor. The fact that the loading of hardness, calcium and chloride are greater than that of Sodium on factor 3 may indicate the evaporative concentration of chemicals introduced by rainfall events. Chemical analysis of precipitation samples showed that the relative magnitudes of calcium, chloride and hardness were greater than that of Sodium. This factor is represented by the Fourth factor in River Kulfo's factor analysis. It might be useful to compare the relative loadings of the chemical variables on this factor. For Kulfo river factor 4 that might indicate the leaching flow regime is accompanied by a slight increase in river discharge and greater association with rainfall (precipitation). In contrast to these Hare river has low precipitation association slightly decreasing discharge and decreasing turbidity (negative loading on turbidity). This is made further clearer by the relative slopes of the catchments: Kulfo river has an average of 8% slope while Hare's slope is 20% (Seleshi Bekele, 2000) and greater than that of Kulfo. In steeper slope catchments the runoff is high and the infiltration low and the reverse is true in milder slope catchments. Kulfo's leaching flow follows a more porous and shorter horizontal flow

path and is directly proportional to precipitation events. Hare River follows a longer leaching path, a less horizontal flow and more linked to low precipitation events. If chloride, turbidity and by implication nitrates coliforms and phosphates are considered leachable pollutants [66], it would appear that river Kulfo leaches more of these pollutants than river Hare. It is noted earlier that the reverse was true of positive ions that were slowly released with factor 1 (such as hydrogen and Sodium ion) and with factor 2 (ammonium ions). For Hare River this factor represents the phase where there has been rain of low magnitude and intensity in the station considered but the discharge is decreasing slightly. The solids loads are reducing (see Figure 5.4.2.3). The net effect of low intensity rainfall is to increase the water hardness and calcium as well as Chloride. This variation is considered as short term variation because long term weather effects (air temperature and water temperature are poorly loaded on this factor. Air temperature is positively loaded while water temperature is negatively loaded on this factor. Considering the low Eigen value of this factor compared with the first three factors, it is obvious to see that this factor explains only few of the data variation among the set considered. The low communality of Calcium, hardness and chloride as well as rainfall is explained by their association with this factor.

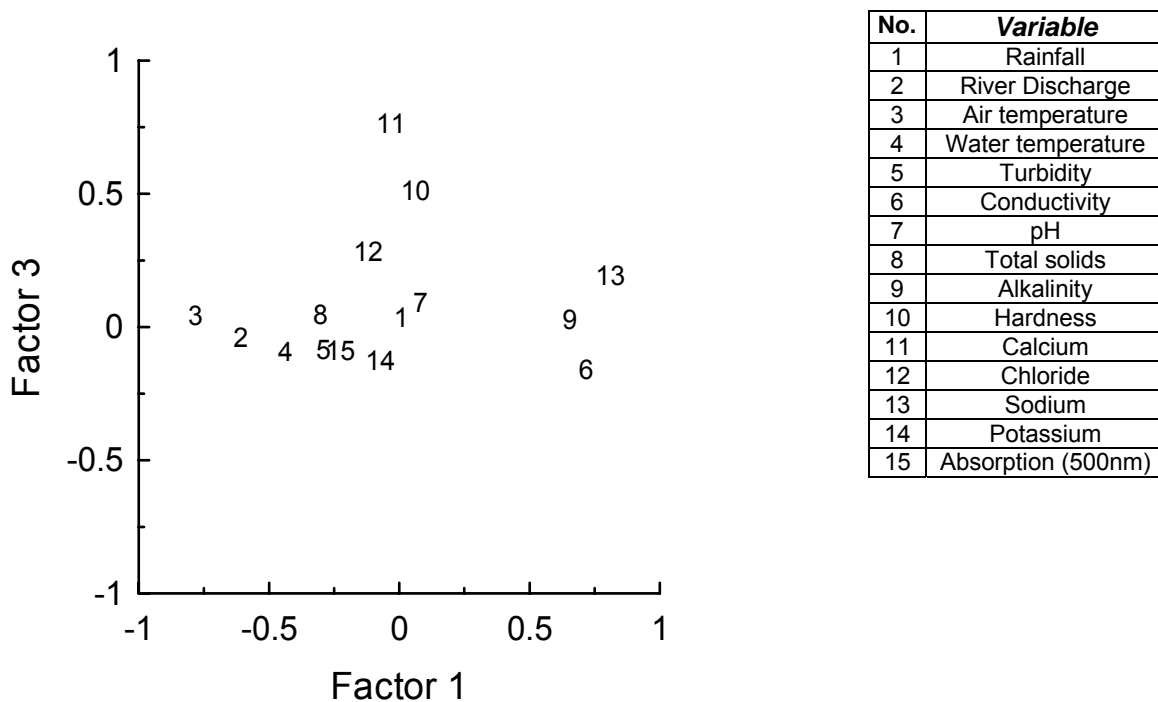


Figure 5.4.2.3 Factor Loadings for Hare River Factor 1 – Factor 3. Factor 3 represents the short term leaching flow effects. The fact that calcium and chloride significantly on this factor may indicate evaporative concentration effects on near surface flow.

Factor 4 for Hare River may indicate the end of the leaching phase as shown by the increase in conductivity and higher loading on water temperature and also to a milder extent on air temperature. Rainfall is absent as expected and the solids loading is zero showing no differential change. This factor is represented by factor 3 for Kulfo River. There is a difference between these two rivers in terms of this particular common factor loading on pH. In general the pH variation on river Kulfo is associated very much with the bicarbonate alkalinity present. On the other hand for Hare River, pH shares less communality with alkalinity (bicarbonate alkalinity) and is loaded highly on factor 4. This high loading may be associated with the release of Carbon dioxide at periods of higher temperature due to increased bacterial activity within the river stream and within the soil layer. Such carbon dioxide release increases the pH and has less effect on the alkalinity. Figures 5.4.2.4 and 5.4.2.5 below show the variation carbon dioxide with the season for the two rivers Hare and Kulfo (See appendix 4-1 for calculation of carbon dioxide from the water quality data).

The average pressure of CO₂ in the river Hare is about seven times higher than the atmospheric value, i.e., 2042 ppm as against 317 ppm. Highest pCO₂ (11000 ppm) was observed in August during the rainy season. This might coincide with the period of strong erosion. Data on plankton primary production and respiration would be needed to evaluate the extent of metabolic input of CO₂ in the river. For Kulfo River the average CO₂ in the river is 994 ppm as against 317 ppm of present day CO₂ in the atmosphere. Kulfo has less carbon dioxide, which is also confirmed by the strong association bicarbonate alkalinity with the pH.

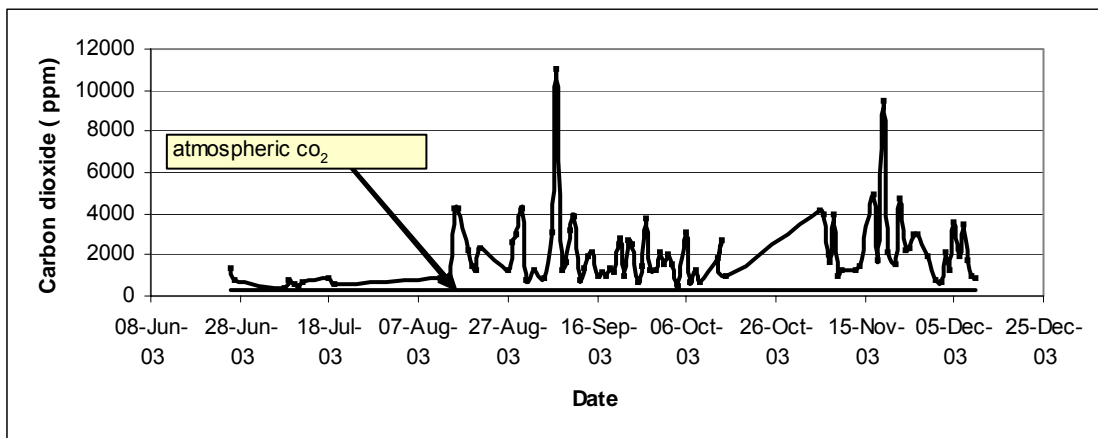


Fig. 5.4.2.4 Variation of Carbon dioxide in ppm with season (Hare River)

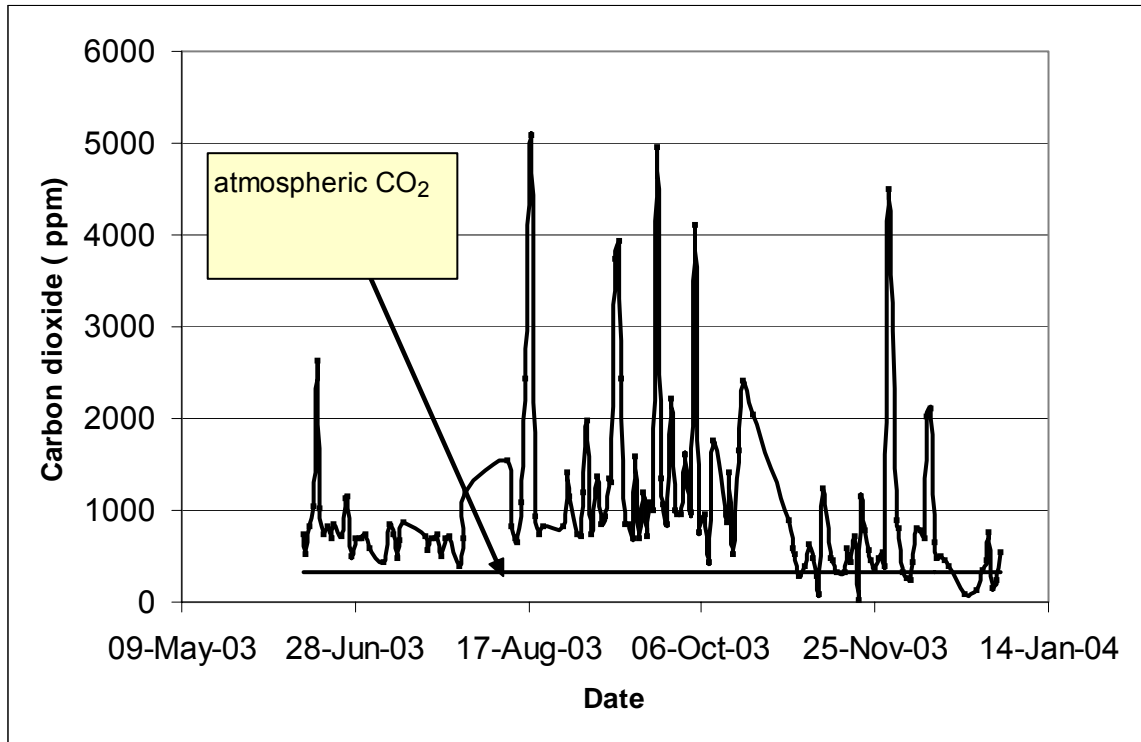
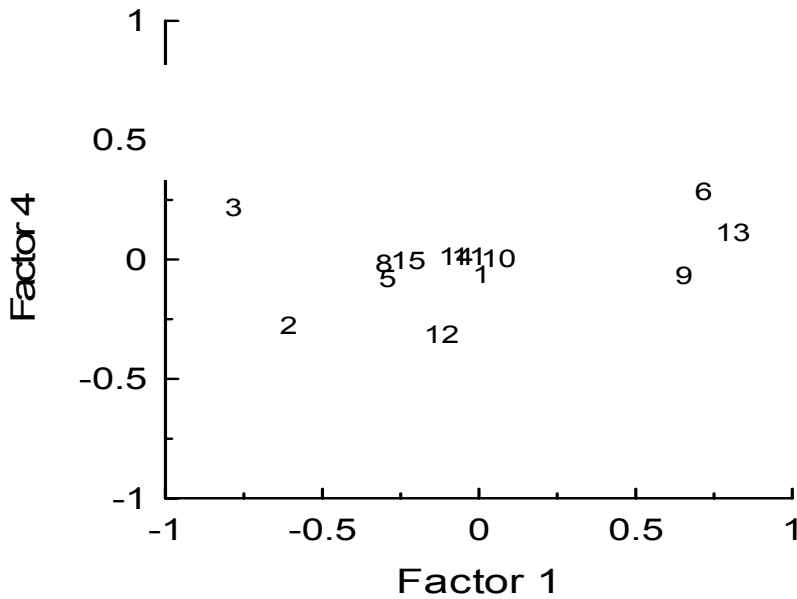


Fig. 5.4.2.5 Variation of Carbon dioxide in ppm with season (Kulfo River)

Factor 4 shows almost zero loading on rainfall, which indicates a drier part of the season. Flow continues to decrease while there is a slow reduction in turbidity. Air and water temperature are equally and highly loaded on this factor. The pH change, which is greater than that of alkalinity, might be due to sodium exchange and the release of more carbon dioxide. Hardness and calcium have almost zero loading, which indicates poor exchange of divalent ions in the drier season subsurface flow. Chloride has a negative loading which partly indicates the absence of any groundwater intrusion, evaporative storage release or any salt contamination.

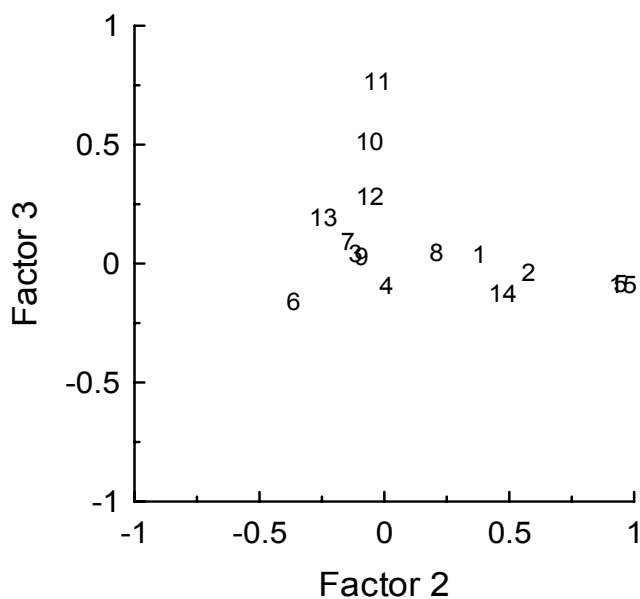
Factor Loadings: Factor 1 - Factor 4



No.	Variable
1	Rainfall
2	River Discharge
3	Air temperature
4	Water temperature
5	Turbidity
6	Conductivity
7	pH
8	Total solids
9	Alkalinity
10	Hardness
11	Calcium
12	Chloride
13	Sodium
14	Potassium
15	Absorption (500nm)

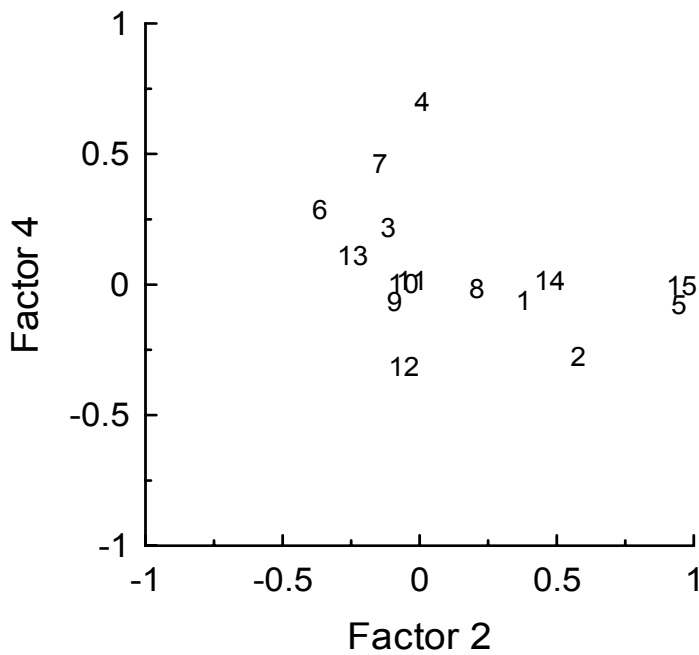
Figure 5.4.2.6 Factor Loadings for Hare River Factor 1 – Factor 4. The high loading of pH but not alkalinity on factor four may indicate the release of carbon dioxide and due to sodium exchange.

The rest of the plot of factors combination for Kulfo River is given in Figures 5.4.2.7 – 5.4.2.9.



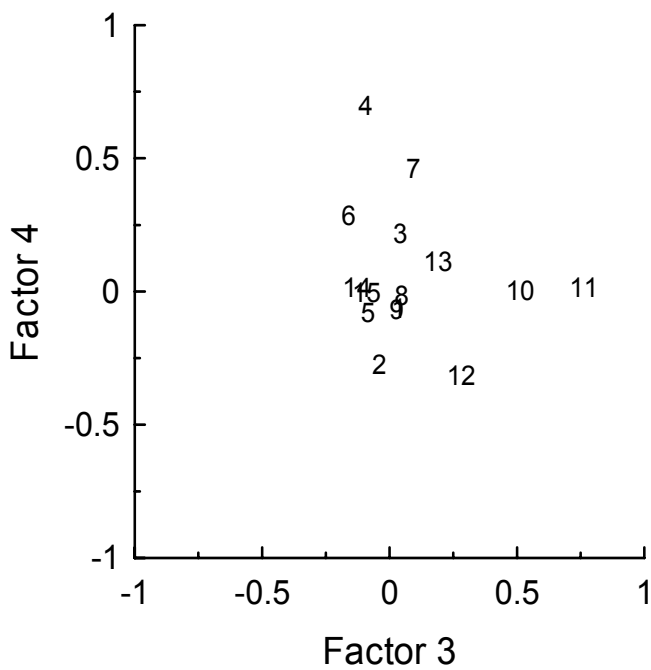
No.	Variable
1	Rainfall
2	River Discharge
3	Air temperature
4	Water temperature
5	Turbidity
6	Conductivity
7	pH
8	Total solids
9	Alkalinity
10	Hardness
11	Calcium
12	Chloride
13	Sodium
14	Potassium
15	Absorption (500nm)

Figure 5.4.2.7 Factor Loadings for Hare River Factor 2 – Factor 3



No.	Variable
1	Rainfall
2	River Discharge
3	Air temperature
4	Water temperature
5	Turbidity
6	Conductivity
7	pH
8	Total solids
9	Alkalinity
10	Hardness
11	Calcium
12	Chloride
13	Sodium
14	Potassium
15	Absorption (500nm)

Figure 5.4.2.8 Factor Loadings for Hare River Factor 2 – Factor 4



No.	Variable
1	Rainfall
2	River Discharge
3	Air temperature
4	Water temperature
5	Turbidity
6	Conductivity
7	pH
8	Total solids
9	Alkalinity
10	Hardness
11	Calcium
12	Chloride
13	Sodium
14	Potassium
15	Absorption (500nm)

Figure 5.4.2.9 Factor Loadings for Hare River Factor 3 – Factor 4

5.4.3 Factor Score Plots

A plot of factor scores for the first two major factors for river Kulfo shown in Figure 5.4.3.1 below indicates that factor two score samples show few high score scatters which are the result of high storm events.

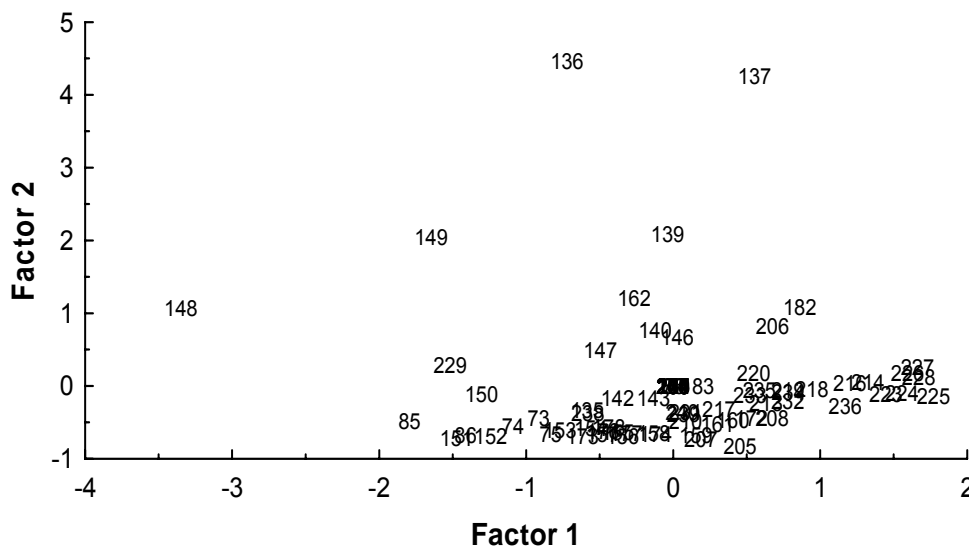


Figure 5.4.3.1 Factor Score Plot for Kulfo River Factor 1 - Factor 2

5.4.4 Importance of Data Integrity and Continuity

Insufficient and discontinuous mode of data acquisition, careless and inaccurate entry of data for storage and analysis, errors in measurement reading and standardisation and inaccurate instrument performance can make the interpretation of factor and principal component analysis above at best difficult and at worst an erroneous and a worthless effort. Working with factor analysis in this research showed that factor analysis of water quality data is not recommended if the error variance is too large. The important finding of this research was sparse monitoring combined with little attention to data integrity and accuracy stands helplessly midway between making realistic interpretation and that of providing accurate water quality information and reaches neither of these desirable ends.

A typical example to the above was provided by total solids data where few of which were entered incorrectly and made this variable share little communality with all of the factors considered and appear as a standalone variable. Subsequent examination of the data entered corrected the mistakes and factor analysis gave the expected results.

It can also be concluded that variables with high short-term variation (i.e., solids, turbidity, discharge, ammonia, etc) need care in measurement and data handling.

5.5 Design of River Water Quality Monitoring System

The design of monitoring system for the various water quality parameters considered can be sub-classified in accordance with the results of factor and principal component analysis which groups data in to independent classes. Variables falling in to common factors tend to be influenced by the same physico-chemical and biological processes and hence tend to appear as groups together. Such variables can also be related with each other (refer to chapter 7: Water Quality Modelling).

Even though the analysis of factor and principal components is not all-inclusive it can be considered as indicative of the tendency for the variation of water quality parameters as affected by common factors. Based on this hypothesis the following four classification groups can be formed.

5.5.1 Design Group 1

Monitoring in this interval associated with factor 1 variation gives the long-term seasonal maximum and minimum. Values are affected by the seasonal cumulative rainfall and river discharge, base flow. Area wide distributed pollution occurrences also show up in this long term seasonal monitoring as they persist throughout the seasons. Long term changes because of drought, water use changes and changes in the soil-chemical exchange processes will also be detected by this level of monitoring. Long-term atmospheric pollution effects also show up in this interval of monitoring.

5.5.2 Design Group 2

Monitoring in this group is associated with surface derived pollutants transported by increased runoff over catchments. River discharge is the dominant variable so also rainfall (magnitude as well as intensity). Variation of water quality parameters is associated with factor 2 variation. Turbidity, suspended solids as well as pollutants associated with particulate matters (bacteria, organic matter, nutrients such as particulate phosphorous and particulate organic compounds, etc) are loaded highly in this phase of monitoring. Variation of monthly loads is largely a function of discharge and extent of surface retention of pollutants (refer chapter 7: particulate pollutant modelling). Direct pollution from the atmosphere is loaded highly in this group of monitoring since the larger component of flow is rain-induced. Concurrent monitoring atmospheric precipitation chemistry should be part of this group of monitoring.

5.5.3 Design Group 3

Variables that are loaded highly in this group include evaporite concentration of atmospheric pollutants (chloride, nitrate, sulphate, etc). Pollutants leached from the infiltration-inflow phase of the flow, which may be concentrated by evaporation within the catchment subsurface. Such pollutants from distributed sources such as fertilizer, human and animal wastes including pollutants such as bacteria, nitrates, nitrite, soluble reactive phosphorous, sulphates, organic matter are all highly loaded on this group of monitoring.

5.5.4 Design Group 4

Water quality parameters that load highly on this group are those that occur during the long dry spell of the season and that have to do less with the catchment and more with in-stream processes. Water and air temperature are highly loaded in this group. Point source pollutants such as direct in to stream effluents of wastewater from human settlements and industrial facilities as well as direct in-stream pollution by human activities are loaded highly in this group of monitoring. Comparison of Pollutants loaded in this group to a certain extent show the sensitivity of the parameters to in stream pollution. As an example, stream pH in Kulfo River is buffered more by the catchment soil chemical exchange process than it is in Hare River. Monitoring of point sources of pollution should be included as part of this group of monitoring. However, the pH changes more than any of the other conservative parameters that include possibly also the effect of in-stream pollution.

5.5.5 Determination of Monitoring Intervals

The monitoring interval for variables within each group of monitoring is determined from spectral analysis of the time series data after trends have been detected and removed. Since such analysis requires that the data entered be continuous, any omitted data are filled before the analysis is begun.

5.5.6 Trend Detection and Elimination

Since the river water quality data mostly do not appear to have long-term trend, except seasonal variation (which is part of the low frequency spectrum), de-trending has not been applied for the analysis of the river water quality data. On the other hand Lake Abaya's conductivity and Chloride contained a linear trend, which was removed by fitting a straight line to the data. This is explained further below under Design of Lake Monitoring System.

5.5.7 Monitoring Design through Spectral Analysis

5.5.7.1 Group I monitoring variables

The variable which is most varying and is highly loaded in Group I is conductivity. The power spectral density $f_x(\lambda)$ is an infinite Fourier series representation of the data auto covariance function (The Fourier Transform). The plot of this spectral density against frequency is referred here as the spectrum plot. The spectrum plot of this variable for Kulfo River is given in figure 5.5.7.1.1. Table 5.5.7.1.1 summarises the design variables for Group 1 parameters.

Spectrum of Conductivity – Group 1 Monitoring

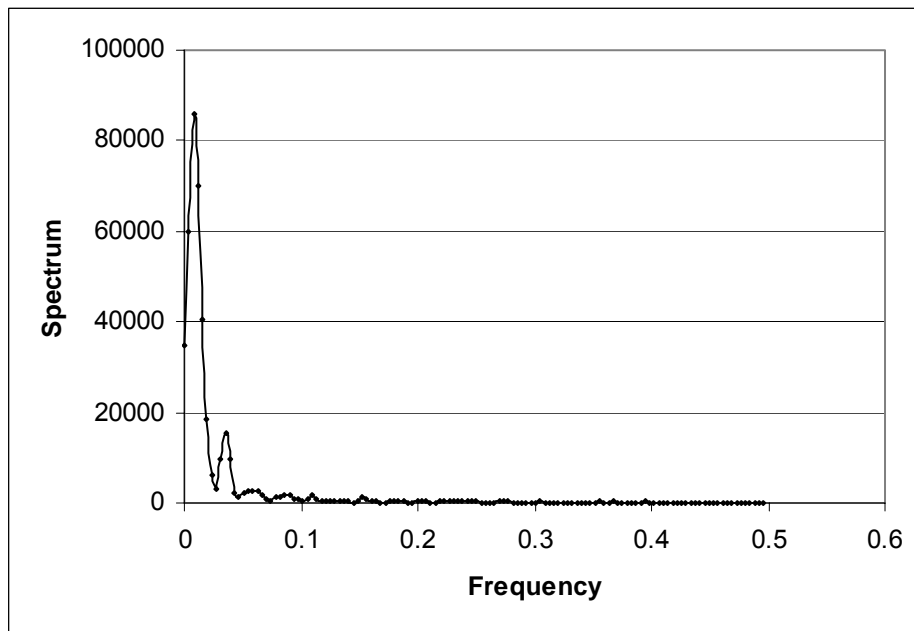


Fig. 5.5.7.1.1 Spectrum of Conductivity - Kulfo River. The spectrum plot shows the proportion of the data variance accounted by the different frequency of occurrence. In the above plot, the first peak corresponds to the long term seasonal change events. The second peak is the rainfall period occurrence. The rest of the peaks appear as noises.

The percentage of information obtained in the form of cumulative variance was calculated and the plot of the cumulative percentage information versus frequency of monitoring is shown below for conductivity. The optimum frequency of monitoring is found by projecting from the intersection of the steep and mild slopes perpendicularly to the cumulative information curve.

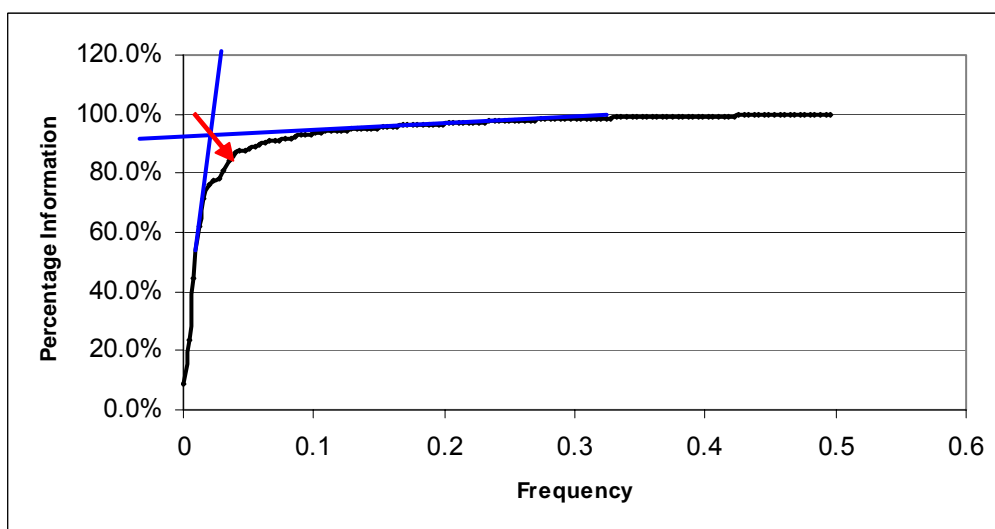


Fig. 5.5.7.1.2 Percentage Information against Frequency - Kulfo Conductivity. The graph shows the percentage of information that is derived against a given frequency of monitoring. The optimum monitoring frequency is indicated by the extension of the intersection of the slopes of fast and slow change at right angle to the curve.

The design information for the rest of the variables in group 1 monitoring is provided in the table 5.5.7.1.1. Since the spectrum curves for the other water quality parameters are similar they have not been repeated here.

Table 5.5.7.1.1 Design of monitoring Interval for Group I parameters. The percentage of information against the frequency of monitoring is derived from the spectral analysis results whose curves were shown in the above figures.

	Conductivity	Alkalinity	pH	Sodium	Air Temp	Hardness	Water Temp
First Peak - Frequency	0.0078125	0.00781	0.00781	0.00391	0.00781	0.00781	0.00781
Second Peak Frequency	0.03515625	0.03516	0.03516	0.00781	0.03906	0.03906	0.03906
Third Peak frequency	0.0585	0.06250	0.06250	0.03125	0.07031	0.05850	0.07030
Fourth Peak Frequency	0.0898	0.08594	0.08594	0.07813	0.09766	0.08590	0.09375
First Peak Monitoring Interval	64	64	64	128	64	64	64
Second Peak Monitoring Interval	14	14	14	64	13	13	13
Third Peak Monitoring Interval	9	8	8	16	7	9	7
Fourth Peak Monitoring Interval	6	6	6	6	5	6	5
Percentage Information 1st Peak	45%	45%	60%	47%	47%	55%	43%
Percentage Information 2nd Peak	85%	80%	92%	69%	85%	86%	83%
Percentage Information 3rd Peak	90%	86%	95%	88%	89%	88%	88%
Percentage Information 4th Peak	93%	89%	96%	93%	91%	91%	91%
Optimum Frequency	0.03515	0.03515	0.03515	0.03515	0.03515	0.03515	0.03515
Optimum Monitoring length (Days)	14	14	14	14	14	14	14
Optimum Percentage Information	85%	80%	92%	88%	84%	84%	81%
1 week Percentage Information	91%	87%	95%	92%	89%	89%	88%
2 weeks Percentage information	85%	80%	92%	88%	84%	84%	81%
1 month percentage information	70%	68%	84%	80%	75%	75%	72%
2 months percentage information	45%	45%	59%	68%	46%	55%	43%
3 months percentage information	20%	20%	30%	40%	18%	30%	15%

5.5.7.2 Group II Monitoring Variables

One of the variables which is most varying and is highly loaded in Group II is river discharge. The spectrum plots of this variable for Kulfo River is given in the figures 5.5.7.2.1 and 5.5.7.2.2. Table 5.5.7.2.1 below indicates the percentage of variance accounted for by the monitoring intervals.

Spectrum of the Discharge Variation

The spectral data plot for the discharge is given below for both Hare and Kulfo rivers. As table 5.5.7.2.1 below demonstrates the frequencies of peaks of discharge for both rivers are very close as expected since both rivers are in close proximity with each other and lie in the same hydrological regime.

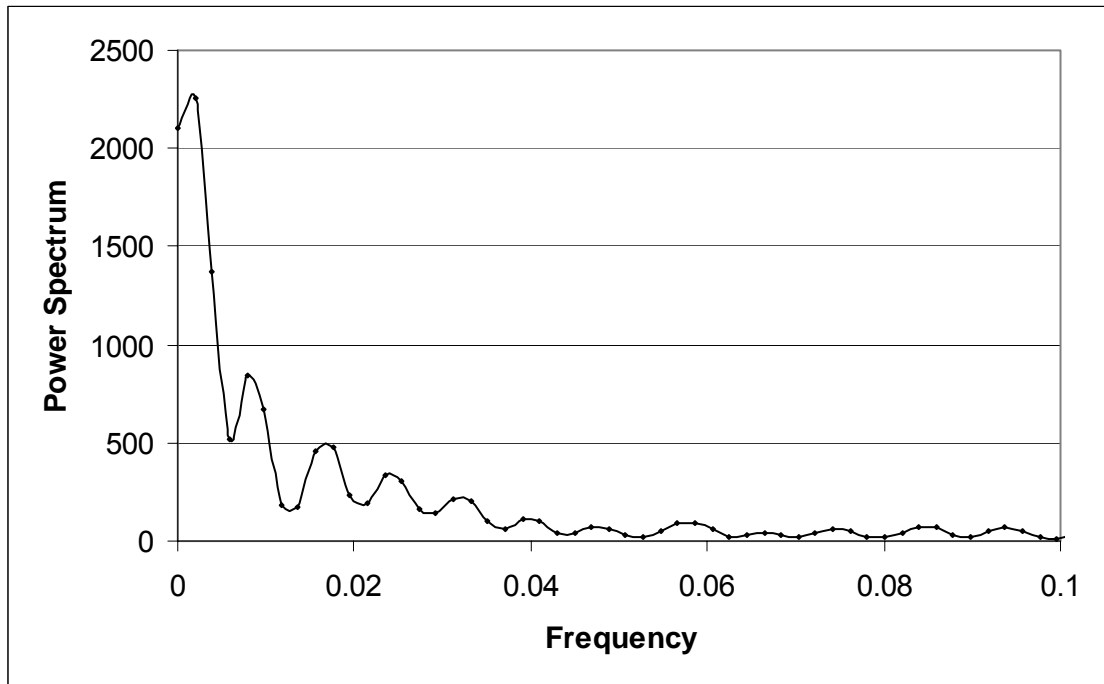


Fig. 5.5.7.2.1 Spectrum of Kulfo River Discharge. Kulfo river discharge shows several peaks of varying frequencies. Such variables need more frequent monitoring as the data contain many periodic components.

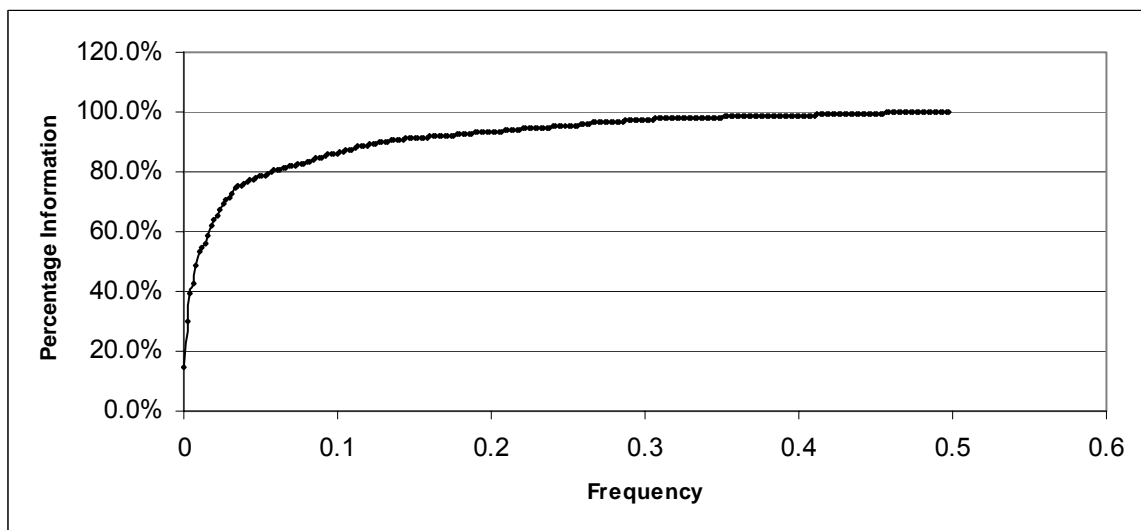


Fig. 5.5.7.2.2 Percentage Information against Frequency of Monitoring - Kulfo River Discharge.

Spectrum of Turbidity

The fact that Group II variables are largely short frequency variation parameters is seen best through the spectrum plot of turbidity which contains multiple peaks at several high frequency observation as shown in the graph below. The percentage information curve does not show a steep slope, which suggests that high frequency monitoring or continuous is desirable to get sizable percentage information about the turbidity [67].

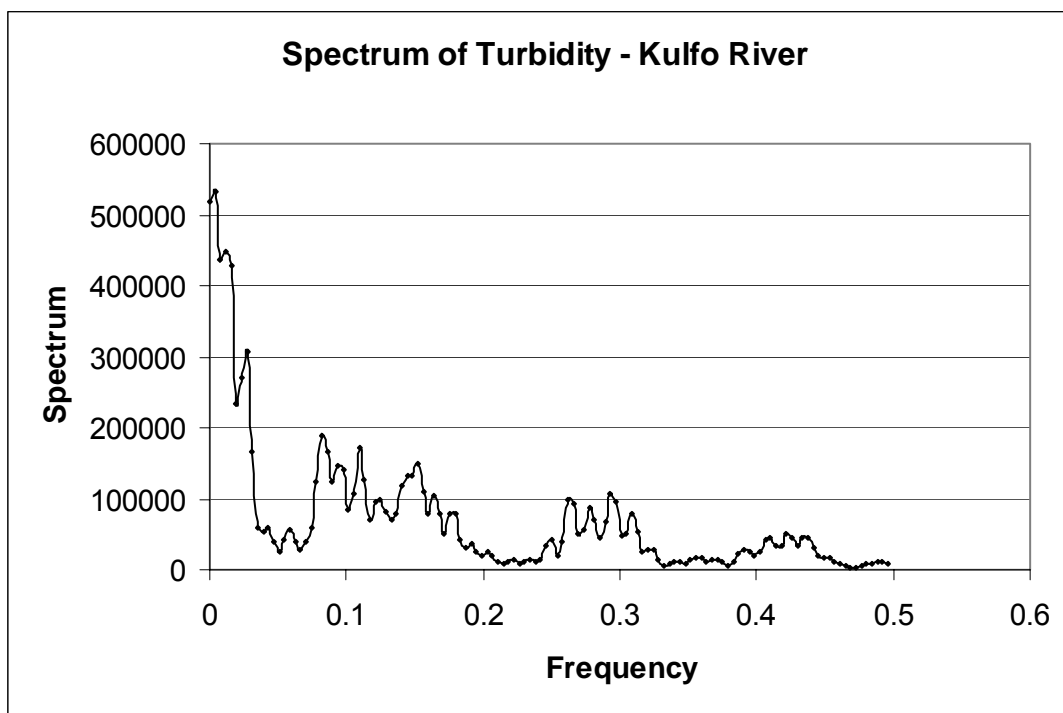


Fig. 5.5.7.2.3 Spectrum of Turbidity - Kulfo River

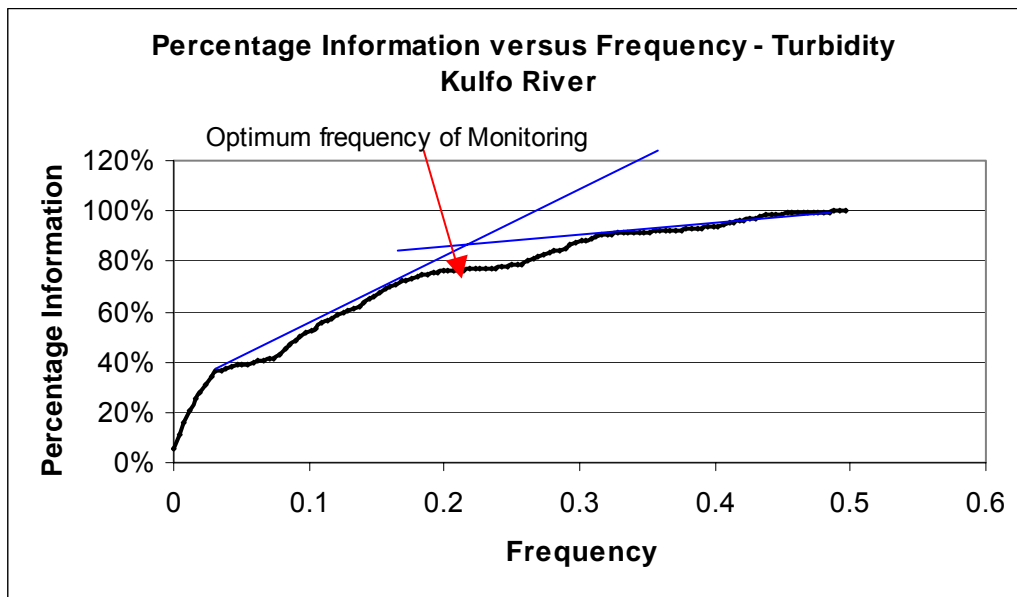


Fig. 5.5.7.2.4 Percentage Information versus Frequency - Turbidity Kulfo River

Spectrum of Rainfall

Rainfall also displays multiple spectrums of both short term and long term frequencies. The cumulative percentage of information graph (Figure 5.5.7.2.6) is also characterized by milder slopes.

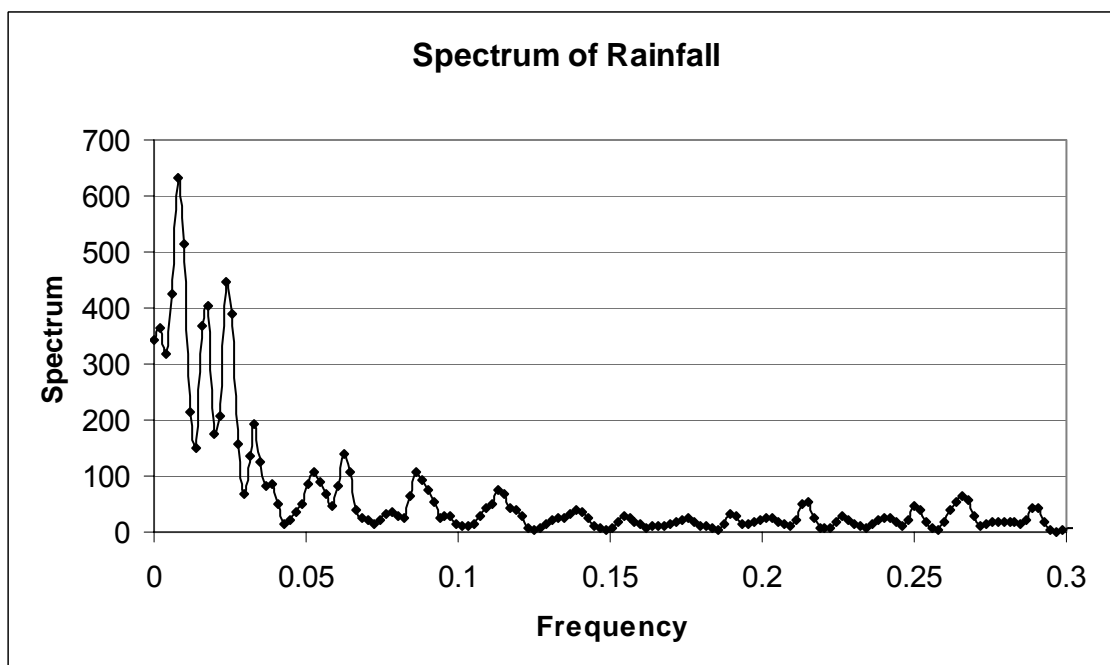


Fig. 5.5.7.2.5 Spectrum of Rainfall

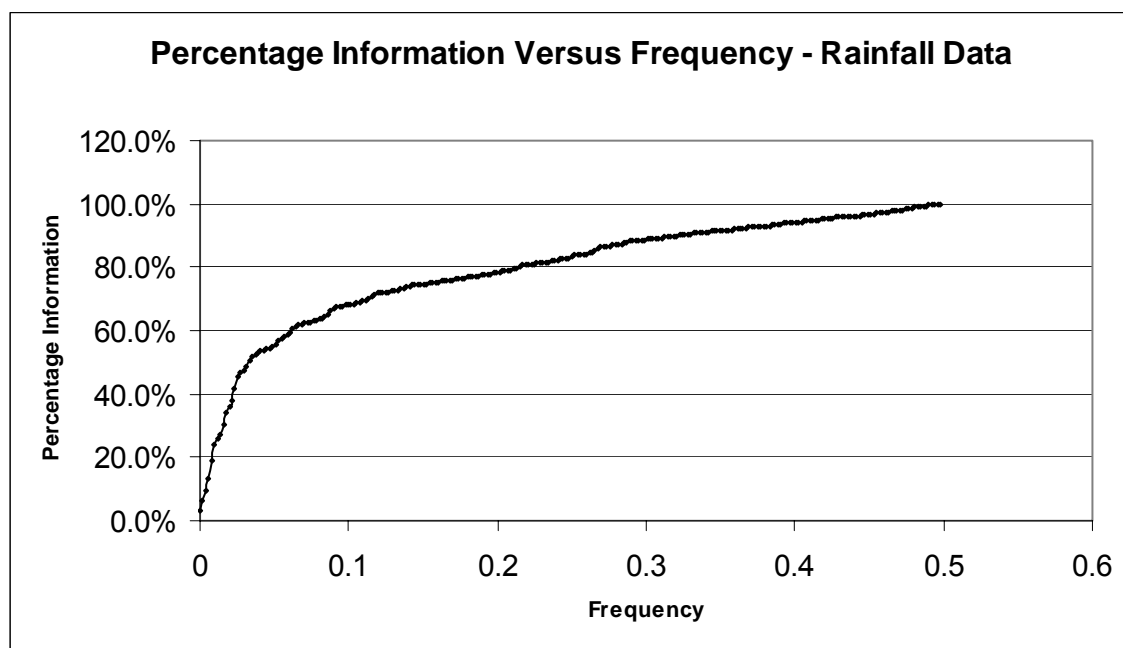


Fig. 5.5.7.2.6 Percentage Information versus Frequency - Rainfall Data

Table 5.5.7.2.1 shows the peaks, frequencies and percentage of information accounted for in each of the monitoring interval. It is noted that for discharge, turbidity, total solids and rainfall less than one week monitoring interval is required to obtain at least more than 66% of the information to enable interpretation with respect to the principal components and common factors. Potassium and Chloride show slightly more frequent monitoring interval than say conductivity, which is due to the added correlation of this variable with this group.

Table 5.5.7.2.1 Design of Monitoring Interval for Group II Variables - Kulfo River

	Turbidity	River Discharge	Total Solids	Potassium	Rainfall	Chloride
First Peak – Frequency (cycle/day)	0.00391	0.00195	0.01172	0.00391	0.00781	0.00781
Second Peak Frequency	0.01170	0.00781	0.05469	0.03516	0.02344	0.03125
Third Peak frequency	0.02734	0.01758	0.08984	0.05859	0.03320	0.05468
Fourth Peak Frequency	0.08200	0.02344	0.17578	0.09375	0.06250	0.08984
Fifth Peak Frequency	0.15230	0.03320	0.25780	0.10938	0.08789	0.13280
Sixth Peak frequency	0.29290	0.03906	0.31250	0.31250	0.11328	0.19530
First Peak Monitoring Interval(days)	128	256	43	128	64	64
Second Peak Monitoring Interval	43	64	9	14	21	16
Third Peak Monitoring Interval	18	28	6	9	15	9
Fourth Peak Monitoring Interval	6	21	3	5	8	6
Fifth Peak Monitoring Interval	3	15	2	5	6	4

	Turbidity	River Discharge	Total Solids	Potassium	Rainfall	Chloride
Sixth Peak Monitoring Interval	2	13	2	2	4	3
Percentage Information 1st Peak	11%	30%	20%	48%	19%	23%
Percentage Information 2nd Peak	21%	49%	36%	82%	42%	69%
Percentage Information 3rd Peak	35%	62%	47%	86%	51%	80%
Percentage Information 4th Peak	45%	67%	67%	89%	61%	84%
Percentage Information 5th Peak	68%	74%	81%	91%	66%	87%
Percentage Information 6th Peak	86%	76%	85%	97%	70%	91%
Optimum Frequency	0.18359	0.18940	0.17968	0.05859	0.17578	0.06250
Optimum Monitoring length (Days)	3	3	3	9	3	8
Optimum Percentage Information	75%	93%	68%	86%	77%	81%
1 Day Percentage Information	100%	100%	100%	100%	100%	100%
2 Day Percentage Information	79%	96%	80%	95%	83%	92%
1 week Percentage Information	41%	82%	37%	87%	62%	82%
2 weeks Percentage information	37%	75%	33%	82%	52%	74%
1 month percentage information	25%	59%	26%	73%	29%	44%
2 months percentage information	16%	49%	14%	65%	20%	23%
3 months percentage information	8%	42%	9%	50%	10%	15%

5.5.7.3 Group III Monitoring Variables

Of the variables, which are highly loaded on this group, include air temperature, water temperature and pH. The spectrums of air temperature and pH are plotted in the figures 5.5.7.3.1 and 5.5.7.3.2.

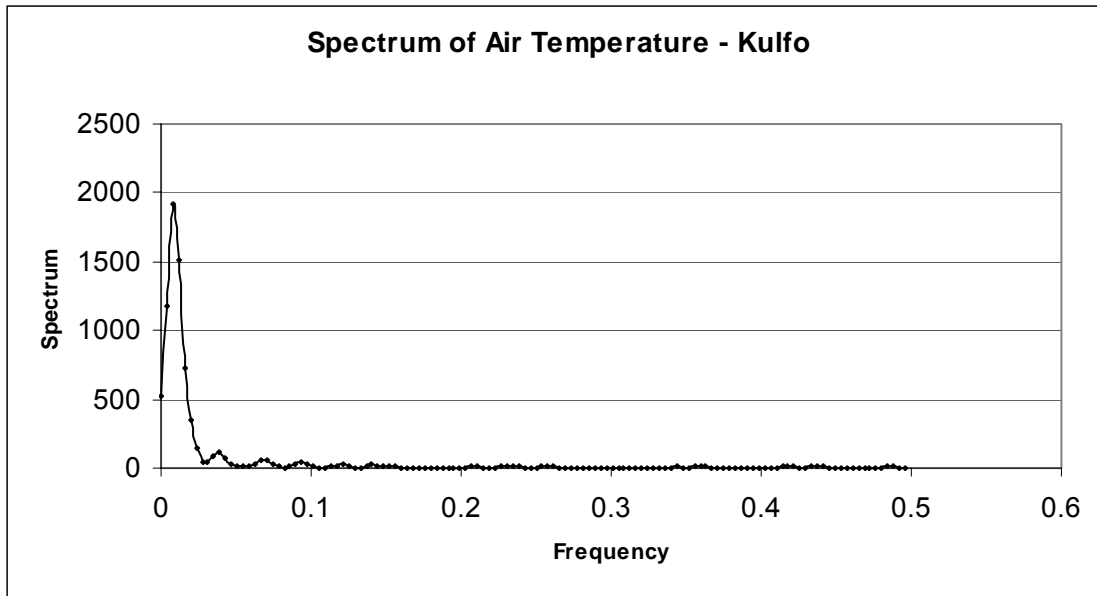


Fig. 5.5.7.3.1 Spectrum of Air Temperature – Kulfo

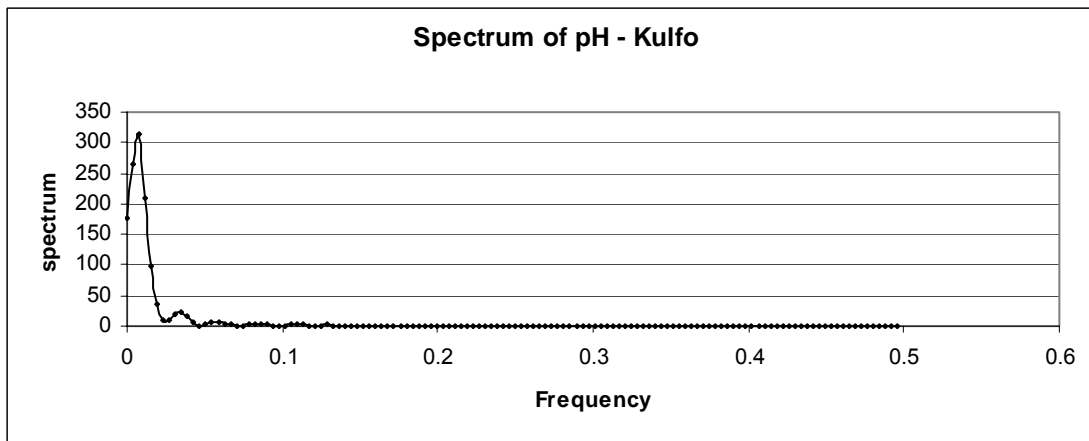


Fig. 5.5.7.3.2 Spectrum of pH – Kulfo

The design of monitoring interval for group three variables is given in table 5.5.7.3.1. It is to be noted that the interval corresponding to the dry part of the season and of higher monitoring frequency than group 1 and 2 shall be selected as this group accounts for variance after group 1 and 2.

Table 5.5.7.3.1 Design of Monitoring Interval for Group III Variables - Kulfo River

	Air Temperature	Water Temperature	pH	Sodium	Alkalinity	Conductivity
First Peak - Frequency	0.00781	0.00781	0.00781	0.00391	0.00781	0.0078125
Second Peak Frequency	0.03906	0.03906	0.03516	0.00781	0.03516	0.0351563
Third Peak frequency	0.07031	0.07030	0.06250	0.03125	0.06250	0.0585
Fourth Peak Frequency	0.09766	0.09375	0.08594	0.07813	0.08594	0.0898
First Peak Monitoring Interval	64	64	64	128	64	64
Second Peak Monitoring Interval	13	13	14	64	14	14
Third Peak Monitoring Interval	7	7	8	16	8	9
Fourth Peak Monitoring Interval	5	5	6	6	6	6
Percentage Information 1st Peak	47%	43%	60%	47%	45%	45%
Percentage Information 2nd Peak	85%	83%	92%	69%	80%	85%
Percentage Information 3rd Peak	89%	88%	95%	88%	86%	90%
Percentage Information 4th Peak	91%	91%	96%	93%	89%	93%
Optimum Frequency	0.03515	0.03515	0.03515	0.03515	0.03515	0.03515
Optimum Monitoring length (Days)	14	14	14	14	14	14
Optimum Percentage Information	84%	81%	92%	88%	80%	85%
1 week Percentage Information	89%	88%	95%	92%	87%	91%
2 weeks Percentage information	84%	81%	92%	88%	80%	85%
1 month percentage information	75%	72%	84%	80%	68%	70%
2 months percentage information	46%	43%	59%	68%	45%	45%
3 months percentage information	18%	15%	30%	40%	20%	20%

5.5.7.4 Group IV Monitoring Variables

Of the variables, which are highly loaded on this group, include hardness, chloride. Calcium and rainfall. The spectrums of hardness and calcium as well as chloride are plotted in figures 5.5.7.4.1 – 5.5.7.4.3. The spectrum of rainfall was explained earlier under group II monitoring variables.

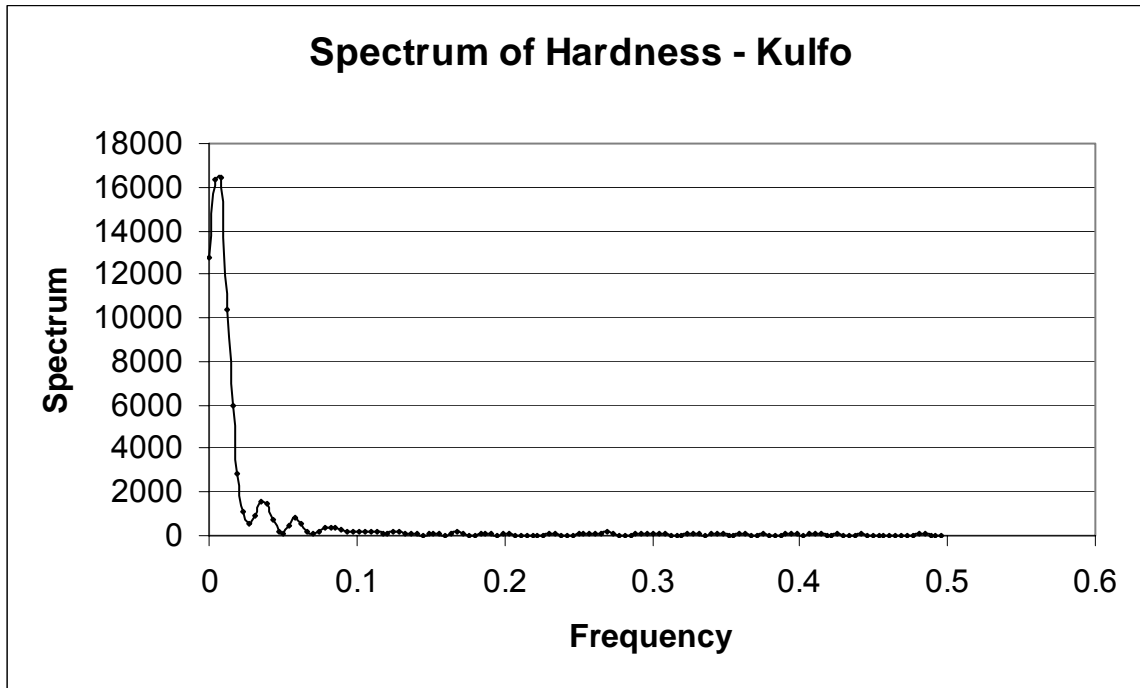


Fig. 5.5.7.4.1 Spectrum of Hardness - Kulfo

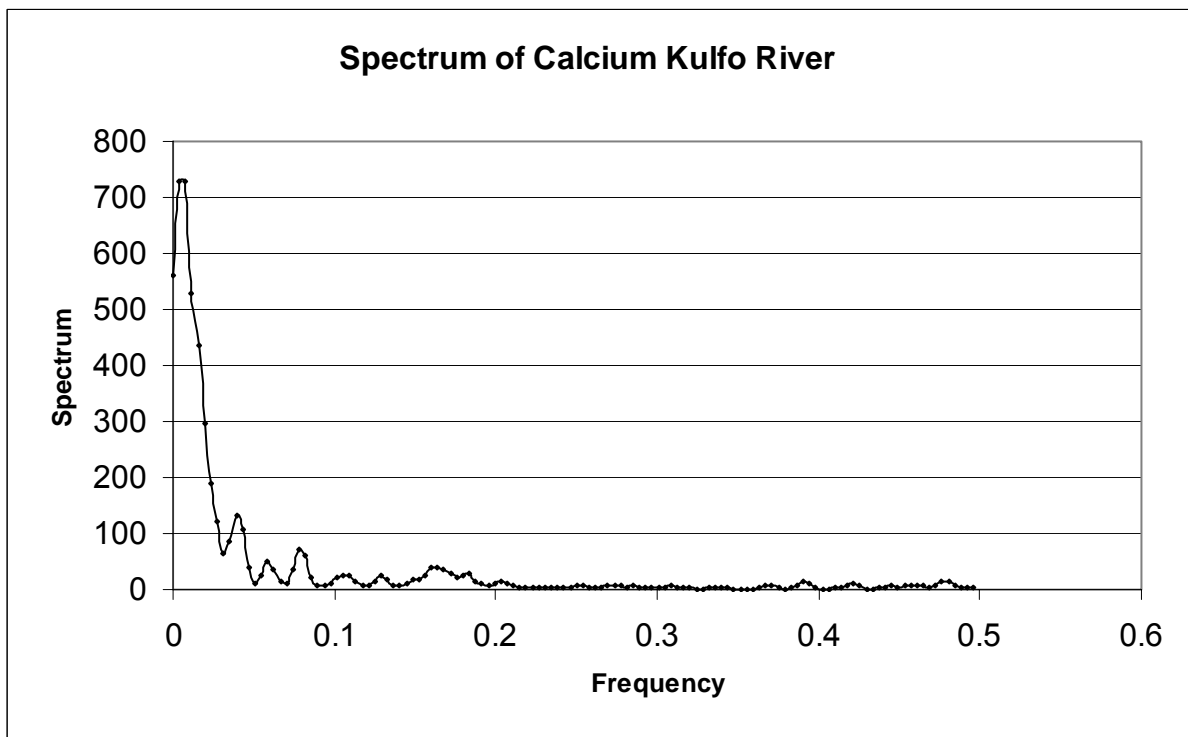


Fig. 5.5.7.4.2 Spectrum of Calcium Kulfo Rive

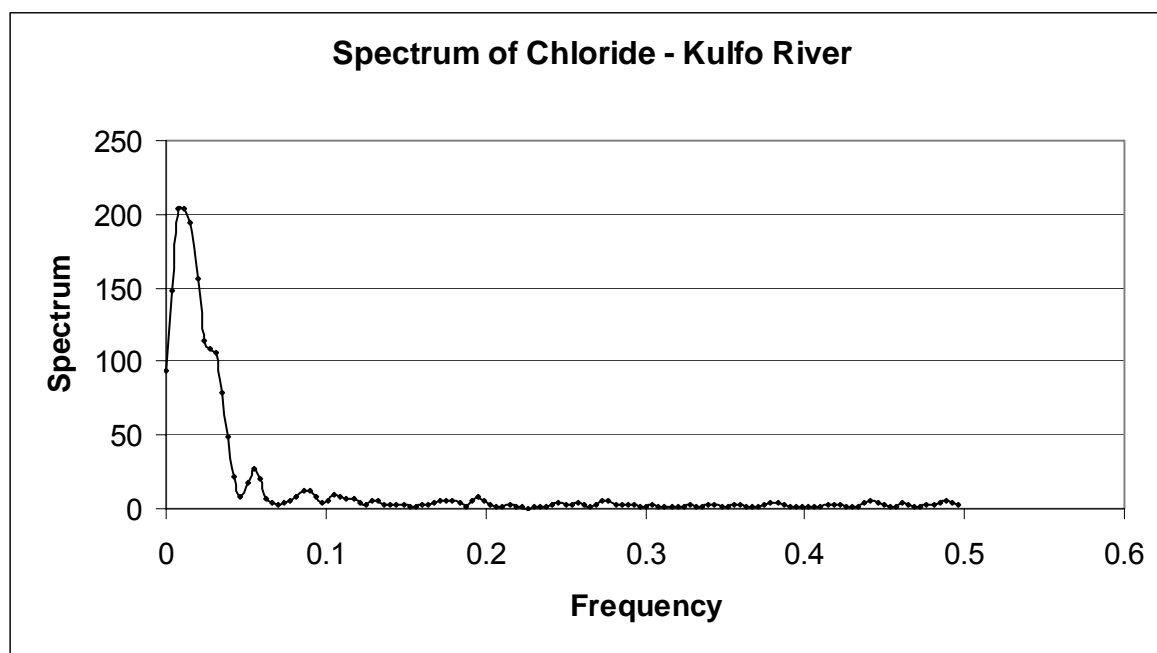


Fig. 5.5.7.4.3 Spectrum of Chloride - Kulfo River

The design of Monitoring interval for this group of variables is summarized in table 5.5.7.4.1. This group has a high frequency monitoring during rainfall period when the rainfall intensity is low and the river discharge varies little.

Table 5.5.7.4.1 Design of Monitoring Interval for Group IV Variables - Kulfo River

	Hardness	Calcium	Chloride	Rainfall
First Peak - Frequency	0.00781	0.00781	0.00781	0.00781
Second Peak Frequency	0.03906	0.03906	0.03125	0.02344
Third Peak frequency	0.05850	0.05850	0.05468	0.03320
Fourth Peak Frequency	0.08590	0.08203	0.08984	0.06250
First Peak Monitoring Interval	64	64	64	64
Second Peak Monitoring Interval	13	13	16	21
Third Peak Monitoring Interval	9	9	9	15
Fourth Peak Monitoring Interval	6	6	6	8
Percentage Information 1st Peak	55%	38%	23%	19%
Percentage Information 2nd Peak	86%	73%	69%	42%
Percentage Information 3rd Peak	88%	78%	80%	51%
Percentage Information 4th Peak	91%	82%	84%	61%
Optimum Frequency	0.03515	0.13280	0.06250	0.17578
Optimum Monitoring length (Days)	14	4	8	3
Optimum Percentage Information	84%	86%	81%	77%

	Hardness	Calcium	Chloride	Rainfall
1 week Percentage Information	89%	79%	82%	62%
2 weeks Percentage information	84%	71%	74%	52%
1 month percentage information	75%	57%	44%	29%
2 months percentage information	55%	40%	23%	20%
3 months percentage information	30%	26%	15%	10%

5.6 DESIGN OF LAKE WATER QUALITY MONITORING SYSTEM

5.6.1 Temporal Monitoring Interval Design- Lake Abaya

The determination of monitoring interval follows the same spectral analysis as the river water quality design after trends have been removed. For Lake Abaya's chloride and conductivity data, de-trending has been applied since the data contained a linear trend. The spectra of some of the parameters analysed are shown in figures 5.6.1.1 – 5.6.1.4 below.

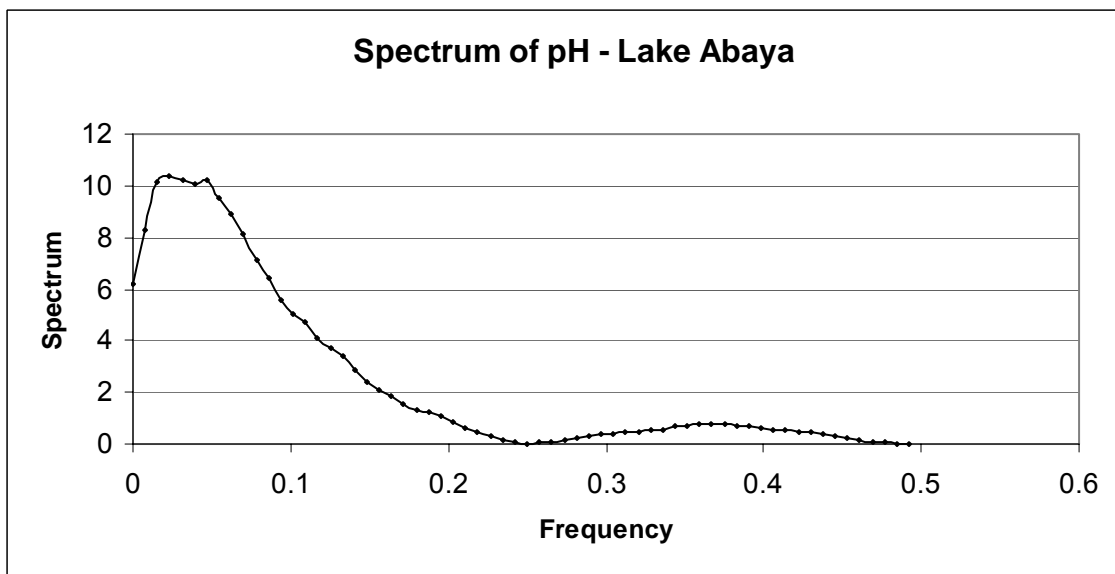


Fig. 5.6.1.1 Spectrum of pH - Lake Abaya

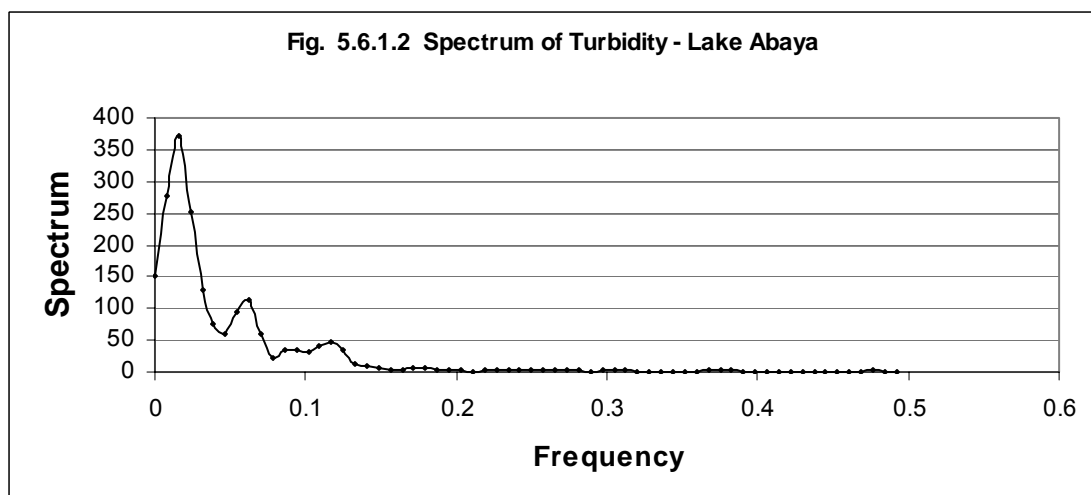


Fig. 5.6.1.2 Spectrum of Turbidity - Lake Abaya

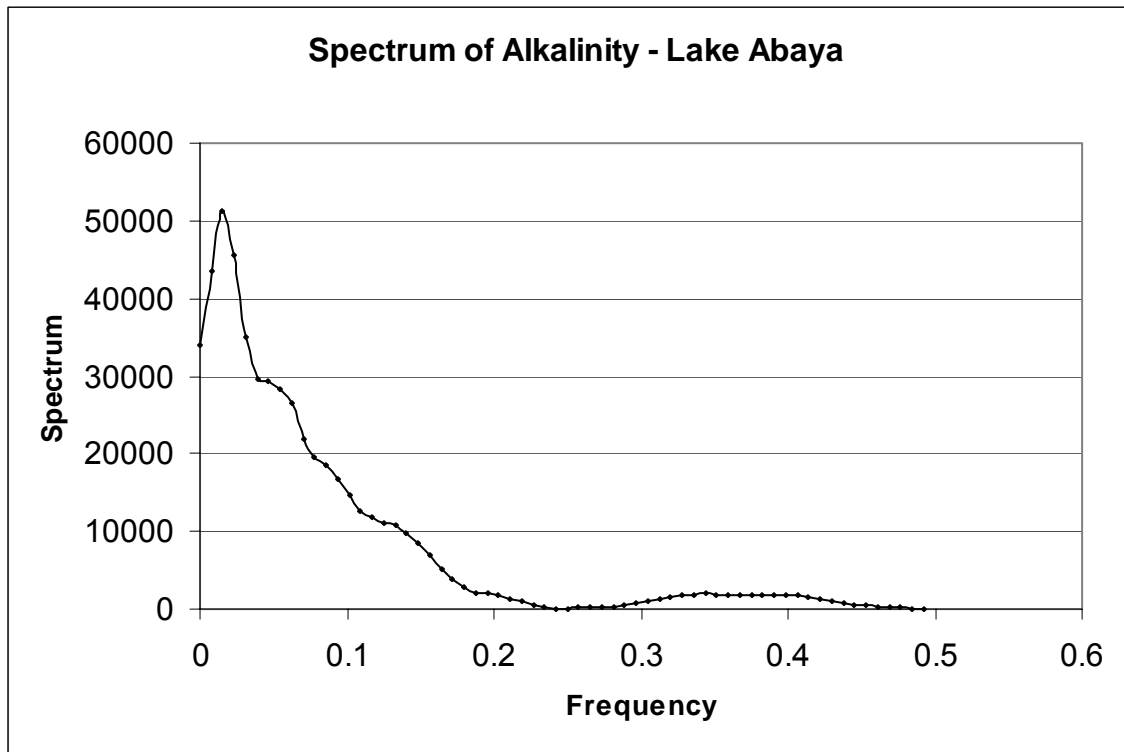


Fig. 5.6.1.3 Spectrum of Alkalinity - Lake Abaya

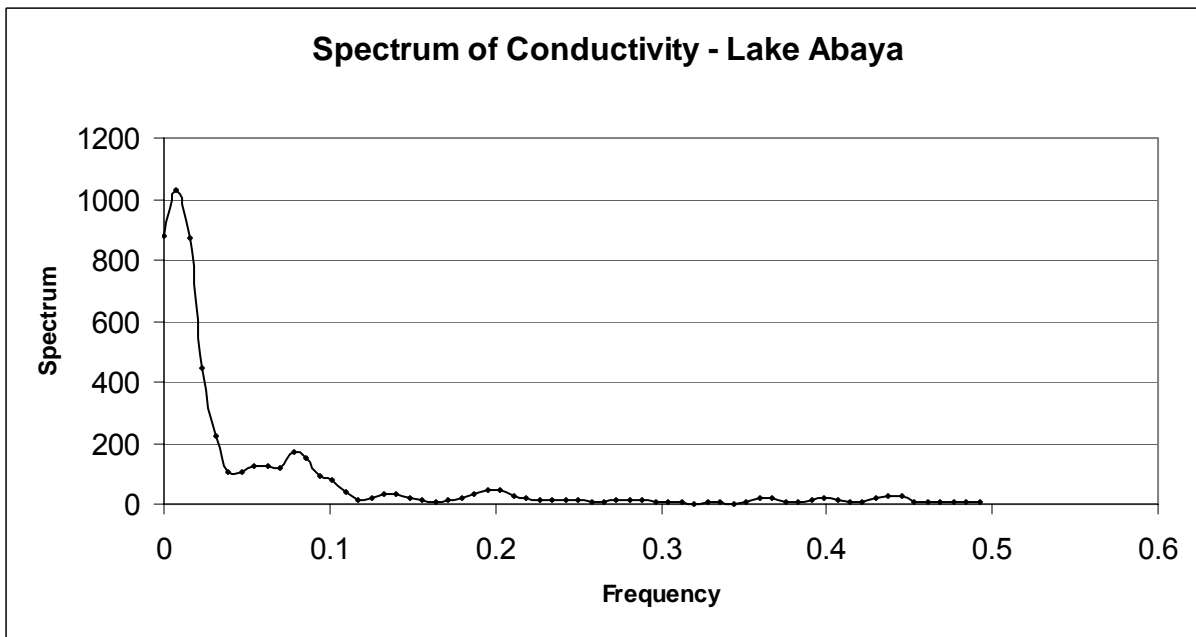


Fig. 5.6.1.4 Spectrum of Conductivity - Lake Abaya

Table 5.6.1.1 below shows the summary of design intervals for Lake Abaya after the spectral analysis. PH requires frequent monitoring. Except pH the rest of the parameters will supply more than 50% of the information with a monitoring interval of 1 month. The average optimum-monitoring interval is around 2 weeks.

Table 5.6.1.1 Lake Abaya Design of Temporal Monitoring Interval

	pH	Turbidity	Conductivity	Alkalinity
First Peak - Frequency	0.02343	0.01563	0.00781	0.01563
Second Peak Frequency	0.04698	0.06250	0.07813	0.04688
Third Peak frequency	0.36710	0.11718	0.14063	0.14063
Fourth Peak Frequency	NA	0.17968	0.19530	0.34375
First Peak Monitoring Interval	64	96	192	96
Second Peak Monitoring Interval	32	24	19	32
Third Peak Monitoring Interval	4	13	11	11
Fourth Peak Monitoring Interval	NA	8	8	4
Percentage Information 1st Peak	22%	42%	36%	24%
Percentage Information 2nd Peak	41%	79%	80%	50%
Percentage Information 3rd Peak	96%	93%	88%	87%
Percentage Information 4th Peak	NA	97%	91%	96%
Optimum Frequency	0.13280	0.11710	0.08590	0.14840
Optimum Monitoring length (Days)	11	13	17	10
Optimum Percentage Information	82%	93%	83%	89%
1 week Percentage Information	92%	97%	93%	94%
2 weeks Percentage information	75%	88%	87%	79%
1 month percentage information	43%	73%	72%	55%
2 months percentage information	22%	54%	61%	33%
3 months percentage information	15%	42%	53%	24%

5.6.2 Temporal Monitoring Interval Design- Lake Chamo

The determination of monitoring interval follows the same spectral analysis as the river water quality design. For Lake Chamo, de-trending has not been applied since the data contained no apparent linear trend. The spectrum of some of the parameters analysed is shown in the figures 5.6.2.1 – 5.6.2.4.

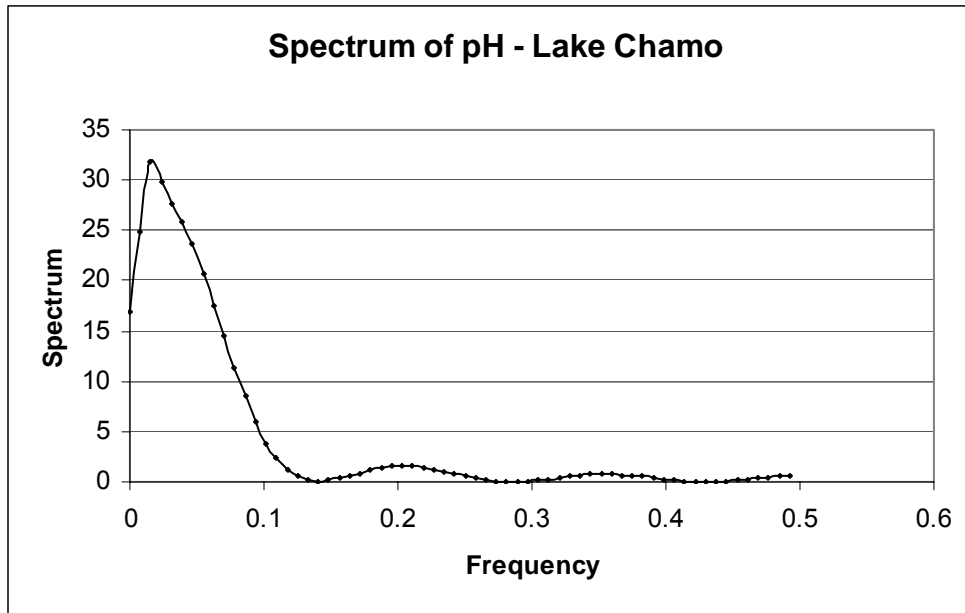


Fig. 5.6.2.1 Spectrum of pH - Lake Chamo

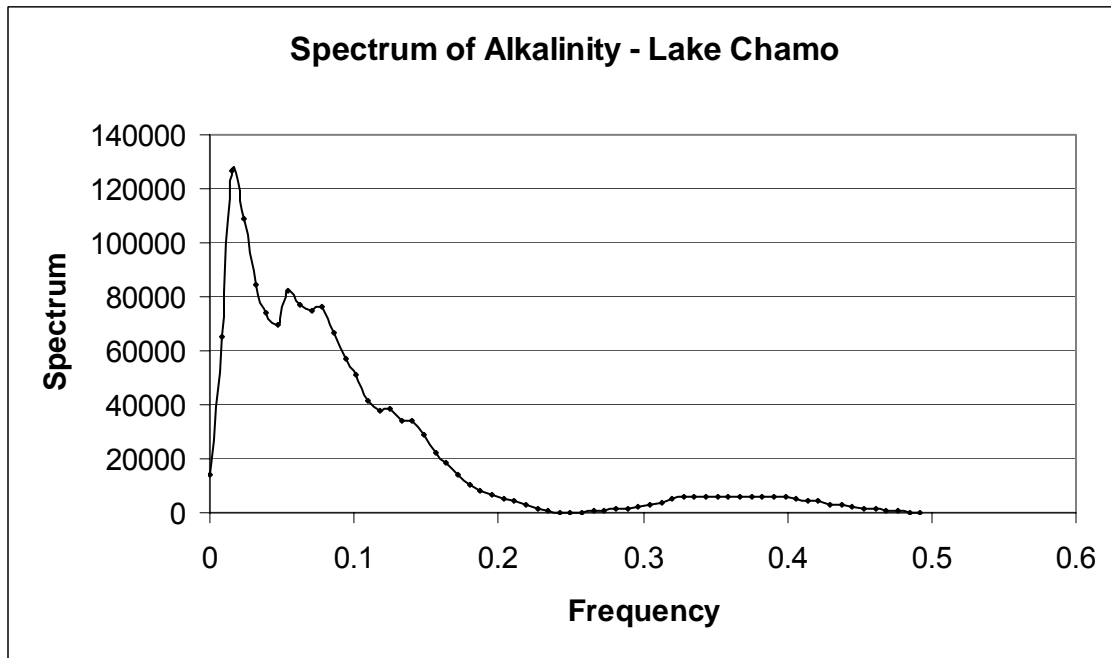


Fig. 5.6.2.2 Spectrum of Alkalinity - Lake Chamo

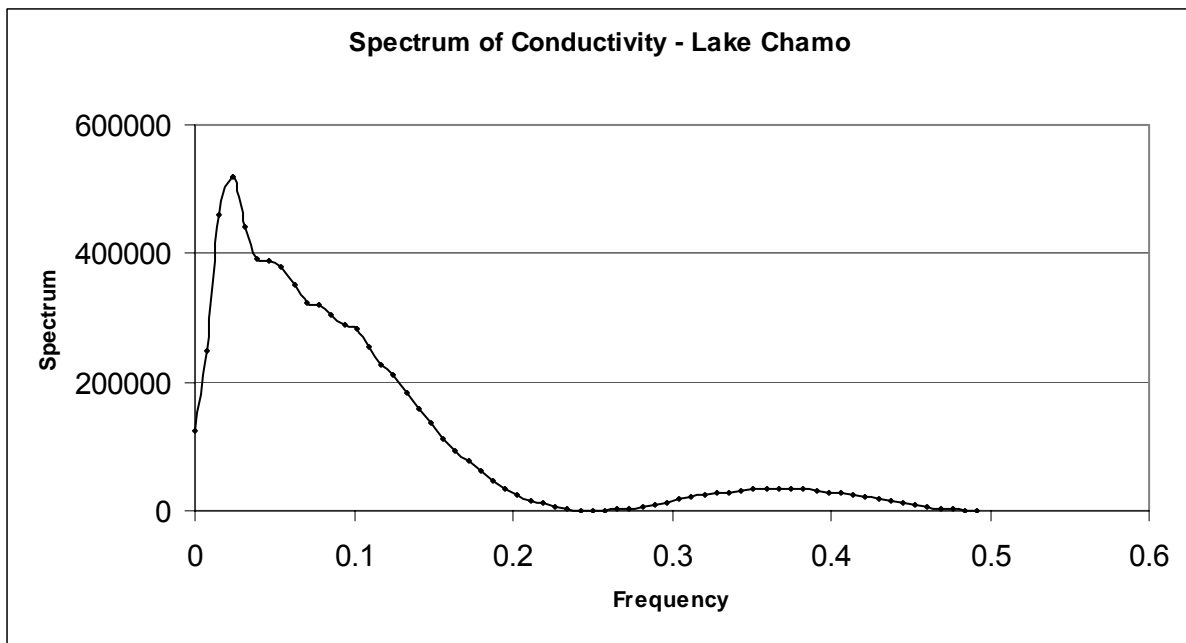


Fig. 5.6.2.3 Spectrum of Conductivity - Lake Chamo

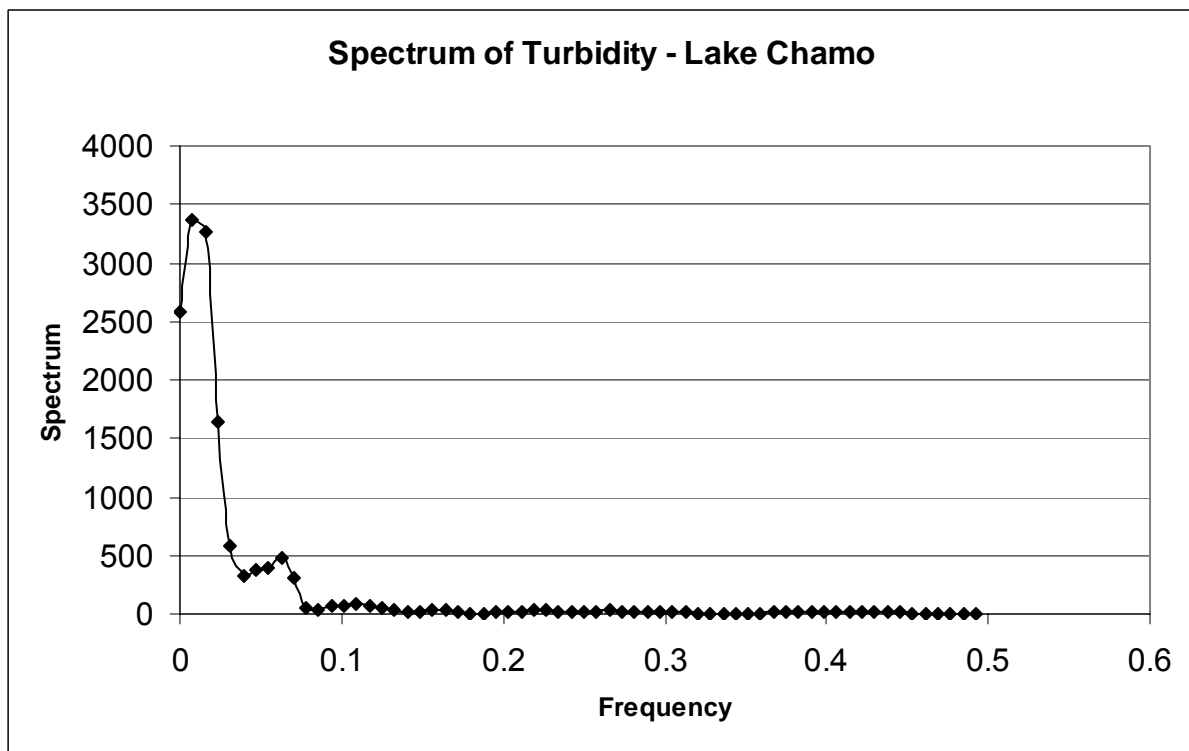


Fig. 5.6.2.4 Spectrum of Turbidity - Lake Chamo

Table 5.6.2.1 below shows the summary of design intervals for Lake Chamo after the spectral analysis. Again here 2 weeks monitoring interval is the average optimum. More than 2/3 of the information can only be provided through this length of monitoring interval.

Table 5.6.2.1 Lake Chamo Design of Temporal Monitoring Interval

	pH	Turbidity	Conductivity	Alkalinity
First Peak - Frequency	0.01563	0.00781	0.02344	0.01563
Second Peak Frequency	0.19530	0.015625	0.04688	0.05468
Third Peak frequency	0.35160	0.06250	0.07812	0.07812
Fourth Peak Frequency	NA*	0.10938	0.10156	0.12500
First Peak Monitoring Interval	96	192	64	96
Second Peak Monitoring Interval	8	24	32	27
Third Peak Monitoring Interval	4	14	19	19
Fourth Peak Monitoring Interval	NA*	14	15	12
Percentage Information 1st Peak	25%	41%	19%	14%
Percentage Information 2nd Peak	93%	64%	37%	43%
Percentage Information 3rd Peak	98%	90%	56%	59%
Percentage Information 4th Peak	NA*	94%	68%	79%
Optimum Frequency	0.09375	0.07030	0.15625	0.14840
Optimum Monitoring length (Days)	16	21	10	10
Optimum Percentage Information	89%	87%	87%	84%
1 week Percentage Information	94%	97%	92%	92%
2 weeks Percentage information	91%	94%	72%	74%
1 month percentage information	69%	86%	37%	43%
2 months percentage information	35%	75%	19%	22%
3 months percentage information	25%	64%	12%	14%
* Not Available				

5.6.3 Spatial Monitoring Interval Design

Spatial water quality variations have been mapped by means of cluster analysis in some research studies [68]. The spatial monitoring interval design was carried out using the cluster

analysis of field water quality data of Lake Abaya. The significance of the clusters was tested statistically. The procedure is summarised below.

The detail of the hierarchal cluster analyses for the water quality data of Lake Abaya is presented in Appendix 5-3. The variables included in the cluster analyses are: air pressure, Air temperature, water temperature, dissolved oxygen, TDS, conductivity, redox potential, and pH. 44 sampling points have been considered in the cluster analyses. Figure 5.6.3.1 below shows the layout view of the Cluster Analysis Results when superimposed on the Lake view. The analysis result was plotted with GIS Arcview software version 3.1.

5.6.3.1 Comparison of Variable Values among the Different Clusters.

Table 5.6.3.1.1 below shows the average values of the water quality variables within each cluster. It can be seen that the difference amongst these average values is small in comparison with magnitude of the variables. Cluster 2 probably represents an outlier.

Table 5.6.3.1.1 the Average Value of Water Quality Data within Cluster Groups

Water Temperature.	PH	TDS	Conductivity	Redox Potential	Dissolved Oxygen	Cluster
(^o C)	(pH Units)	(mg.L ⁻¹)	μS.Cm ⁻¹	mV	mg.L ⁻¹	
26.24	9.26	669.29	1026.00	-92.00	4.91	1
23.40	9.52	673.00	950.00	-114.00	4.50	2
24.00	9.14	677.20	1044.40	-90.90	4.64	3
22.93	9.14	689.53	1040.53	-87.67	4.06	4
23.78	9.12	775.50	1026.75	-90.50	4.45	5
23.70	9.04	643.86	1029.29	-85.14	3.80	6

5.6.3.2 Significance of the Clustering Differences within Lake Abaya

5.6.3.2.1 Variation of pH among the clusters

In order to test for the significance of the differences in pH among the clusters, a statistical test was carried out on the data to test for the hypothesis that the mean values of the clusters are equal. The result of the statistical test done on an Excel spreadsheet is provided in tables 5.6.3.2.1.1 – 5.6.3.2.1.3 given below.

Result of Cluster Analysis for Lake Abaya

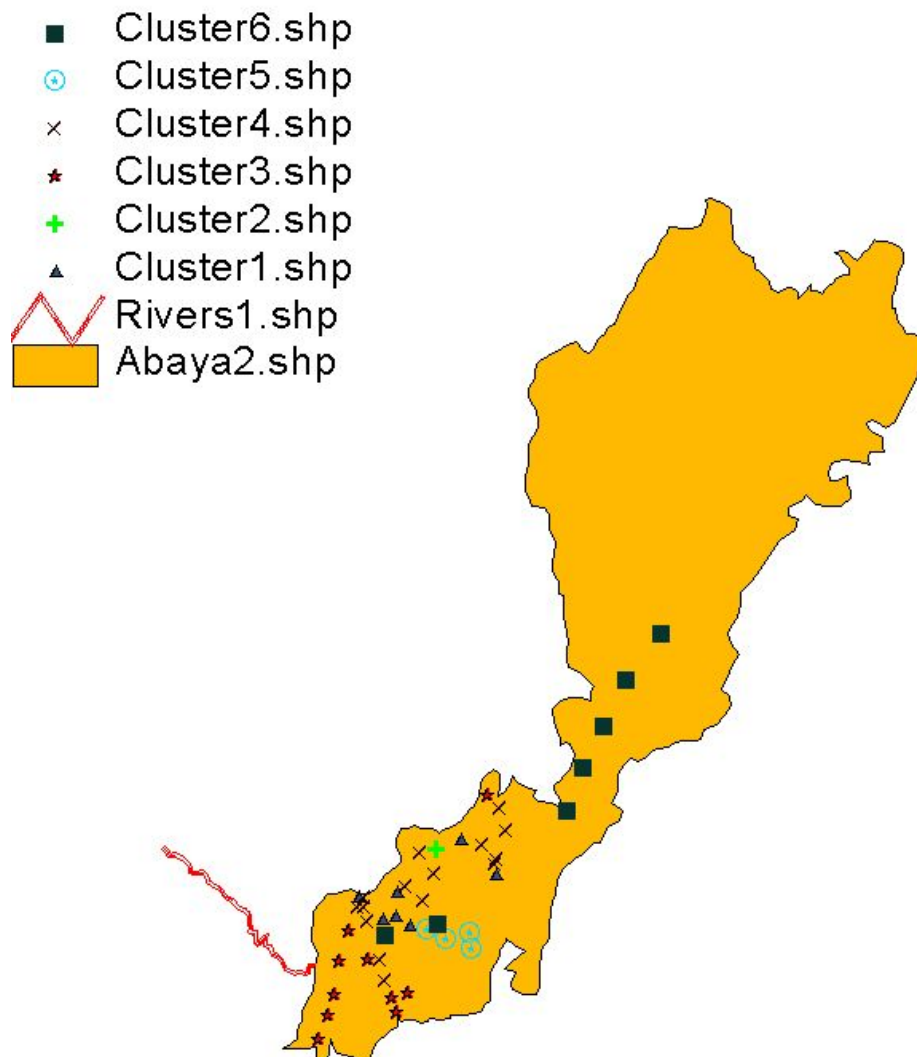


Fig 5.6.3.1 Plot of the Cluster Analyses Results on the Layout of Lake Abaya using GIS.

Table 5.6.3.2.1.1 Statistical Significance Test for pH Difference within Clusters

PH Difference Test	Cluster 1/1	Cluster3/1	Cluster 4/1	Cluster 5/1	Cluster 6/1
Mean Value	9.2629	9.1440	9.1447	9.1225	9.0429
Variance	0.0037	0.0004	0.0032	0.0009	0.0008
Number of Observations	7.0000	10.0000	15.0000	4.0000	7.0000
Hypothetical Mean Difference		0.0000	0.0000	0.0000	0.0000
Degree of Freedom		7.0000	11.0000	9.0000	8.0000
t - Statistics		-4.9873	4.3241	5.1085	8.6953
P (T<=t) one - sided		0.0008	0.0006	0.0003	0.0000
Critical t - value with one sided t-test		1.8946	1.7959	1.8331	1.8595
P (T<=t) two - sided		0.0016	0.0012	0.0006	0.0000
Critical t - value with two sided t-test		2.3646	2.2010	2.2622	2.3060

Table 5.6.3.2.1.2 Statistical Significance Test for pH Difference within Clusters

PH Difference Test	Cluster 3/3	Cluster 4/3	Cluster 5/3	Cluster 6/3
Mean Value	9.1440	9.1447	9.1225	9.0429
Variance	0.0004	0.0032	0.0009	0.0008
Number of Observations	10.0000	15.0000	4.0000	7.0000
Hypothetical Mean Difference		0.0000	0.0000	0.0000
Degree of Freedom		18.0000	4.0000	10.0000
t - Statistics		-0.0421	1.3362	8.4238
P (T<=t) one - sided		0.4835	0.1262	0.0000
Critical t - value with one sided t-test		1.7341	2.1318	1.8125
P (T<=t) two - sided		0.9669	0.2524	0.0000
Critical t - value with two sided t-test		2.1009	2.7765	2.2281

Table 5.6.3.2.1.3 Statistical Significance Test for pH Difference within Clusters

PH Difference Test	Cluster 4/4	Cluster 5/4	Cluster 6/4
Mean Value	9.1447	9.1225	9.0429
Variance	0.0032	0.0009	0.0008
Number of Observations	15.0000	4.0000	7.0000
Hypothetical Mean Difference		0.0000	0.0000
Degree of Freedom		10.0000	20.0000

PH Difference Test	Cluster 4/4	Cluster 5/4	Cluster 6/4
t - Statistics		1.0591	5.6624
P (T<=t) one - sided		0.1572	0.0000
Critical t - value with one sided t-test		1.8125	1.7247
P (T<=t) two - sided		0.3145	0.0000
Critical t - value with two sided t-test		2.2281	2.0860

It is seen from the above tables that the following re-clustering is made with respect to the pH value:

Group	Cluster Member
1	1
2	2
3	3, 4, 5
4	6

5.6.3.2.2 Variation of Other Water Quality variables among the clusters

Similar to the pH analyses demonstrated above, statistical test were carried out for the other water quality variables included in the cluster analysis. Table 5.6.3.2.2.1 below summarizes the re-clustering of the original clusters in to groups. This table also differentiates the clustering with respect to the water quality variables.

Table 5.6.3.2.2.1 Regrouping of Clusters by Statistical tests

Variable	Group 1 Cluster	Group 2 Cluster	Group 3 Cluster	Group 4 Cluster
Dissolved Oxygen	1,3	4	6	5
PH	1	3,4,5	6	
Redox Potential	1,3,5,	4	6	
Water temperature	1,3,6	4	5	
TDS	1,3,4,6	5		
Conductivity	1,3,4,5,6			

5.6.3.2.3 Interpretation of Re-Clustering of Lake Area

The one variable that varied across the clusters the most is dissolved oxygen. This is to be expected, as the dissolved oxygen is a dynamic variable. Clusters 1 and 3 are grouped together by all variables except the pH. This is to be expected as the clusters are close together and can as well be taken as one. The next most dynamic variables are the pH, redox potential and Water Temperature. Conductivity was found to be the least dynamic of all.

The average longitudinal cluster distance is 10 Kilometers while the lateral distance of 5 kilometers seems to define the cluster. Based on this analysis a 5 Km lateral by 10 km longitudinal grid sampling can be adopted for lake Abaya that takes account of the spatial water quality variation. Thus grid sampling spacing is dictated by the most dynamic variables such as pH, dissolved oxygen, redox potential.

Determination of Number of Sampling Points using the above sampling grid (5 km width by 10 km length) and taking in to account the fetch and total area of Lake Abaya (1085 Sq. Km) gives a total of 32 sampling points. For lake Chamo, the number of points is about 12 using the same grid spacing for the total area of lake Chamo (329 Sq. Km).

CHAPTER SIX**INTEGRATING WATER QUALITY MONITORING WITH MANAGEMENT**

S.No.	CONTENTS	PAGE
6.1	Introduction – Ammonia Case study	241
6.2	Source of Ammonia	241
6.3	Occurrence	241
6.4	Health Implication	242
6.5	Lake Ammonia Dynamics	242
6.6	Lake Environmental Implication of Ammonia	243
6.7	Ammonia Variation with Seasonal Flows	245
6.8	Implication on Water Quality management of the Rivers	246
6.9	Improvement of Water Quality with respect to Ammonia Removal	247
6.10	Ammonia in the Lakes Abaya and Chamo	248
6.11	Analysis – Ammonia Speciation	249
	6.11.1 Calculation of Safe Ammonia Speciation for the Rivers and Lakes under study	249
	6.11.2. Temperature and Ionic Strength Correction	250
	6.11.2.1 Temperature Correction	250
	6.11.2.2 Adjustment for Ionic strength	252
	6.11.3 Calculation of the Percentage of Ammonia for a Given Determined total ammonium Value	253
6.12	Implication on the Lakes Water Quality	255
6.13	Extent of Nitrification	256
6.14	Energy of Nitrification for Lakes Abaya and Chamo	256
6.15	Influence of Dissolved Oxygen and Temperature	258
6.16	Proposed Catchment Level Remedies	259
	6.16.1 Waste Diversion	259
	6.16.2 Agricultural Best management Practices	259
6.17	Proposed Onsite (Lake Level) Remedies	259
	6.17.1 Artificial Aeration System Application	259
	6.17.2 Application of Biotechnology	260
6.18.	Ammonia in Drinking Water Supply and aquaculture Ponds	260
	6.18.1 Catchment Level remedial and Protection Measures	260
	6.18.2 Possible Onsite Remedies to be Applied to Drinking Water Ponds and Lakes	260

S.NO.	LIST OF FIGURES	PAGE
Fig. 6.7.1	Ammonia Increase with River Flow (Hare River)	245
Fig. 6.7.2	Ammonia Increase with River Flow (Kulfo River)	246
Fig. 6.11.3.1	Variation of Percentage of Ammonia with pH and Temperature (Applicable to all water Sources in the Basin)	254
Fig. 6.14.1	Theoretical Percentage Increase in Nitrification with pH	258

S.NO.	LIST OF TABLES	PAGE
Table 6.11.2.1.1	Thermodynamic Data - Enthalpy and Free Energy	250
Table 6.11.2.1.2	Temperature Correction for Ammonia Equilibrium Constant	252
Table 6.11.3.1	Percentage of Ammonia (NH ₃) present for given values of pH and Temperature	254
Table 6.11.3.2	Ammonia values at ranges of Temperature and pH variation of the Water Sources Considered	255

6.1 INTRODUCTION - AMMONIA CASE STUDY

The approach of integrating water quality management with monitoring is described in this section below with respect to one of the parameters monitored: ammonia. Ammonia Monitoring, Determination and Management of Water Sources in the Abaya Chamo basin are presented below as demonstration of an integrated approach.

6.2 SOURCES OF AMMONIA

Ammonia is present in the environment as a result of natural processes and industrial activity, including certain types of intensive farming. Atmospheric ammonia is volatilized from the earth's surface in quantities of about 10^8 tones.year⁻¹, mostly from natural biological activity [34]. Industrial activity may cause local and regional elevations in emission and atmospheric concentrations. Surface waters receive ammonia from point sources, such as effluent from sewage treatment and industrial plants. Much more significant quantities arise from non-point sources, such as atmospheric deposition, the breakdown of vegetation and animal wastes, applied artificial fertilizers and urban runoff, and these are significant, even in industrial areas [34].

6.3 OCCURRENCE

Surface waters contain concentrations of total ammonia that vary both regionally and seasonally. In Unpolluted areas, most surface waters contain less concentration of ammonia, though those near large metropolitan areas may contain higher, as total ammonia. In hydrologically isolated acidified small lakes, concentrations may reach 3 mg NH₄+N.litre⁻¹, and values near intensive farms of 12 mg NH₄+N.litre⁻¹ have been recorded. Ground water usually contains low concentrations of ammonia, because of ammonium adsorption and/or nitrification; this, and the conversion of ammonia to chloramines on chlorination, results in low levels of ammonia in most treated drinking water [34].

Ammonia in soil is largely fixed; that in solution is in dynamic equilibrium with nitrate and is not directly available to plants. Ammonia occurs in unprocessed foods,

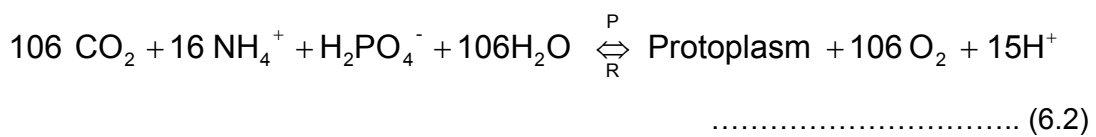
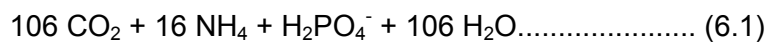
but ammonium salts are added to processed foods. Acceptable Daily Intakes (ADIs), where specified, relate to the anion. Cigarette smoking and certain medicines may contribute to intake, in some cases, but the intake from all sources is small in comparison with endogenous intestinal ammonia production [34].

6.4 HEALTH IMPLICATION

Ammonia does not present a direct threat to man except as a result of accidental exposure, particularly in industry. Farm animals may be adversely affected when reared intensively in closed conditions. Localized effects of point-source emissions of ammonia and of deposition in sensitive environments is a cause of concern.

6.5 LAKE AMMONIA DYNAMICS

The ammonia concentration in lake affects lake productivity as well as providing possible toxicity to fish. It is known that in the absence of nitrate and nitrite or at low concentrations of these compounds the ammonia can be substituted for the photosynthetic reaction described by the following equation [36]:



The uptake of ammonia by photosynthesis results in a decrease in alkalinity of 15/106 or about 0.14 equivalents per mole of carbon fixed. The ammonia content in this way also influences the pH resulting in a decrease in pH by the release of the H⁺ ions. At higher pH, the contribution of ammonia to a pH in relation to the Lakes Abaya and Chamo, which have major bicarbonate alkalinities, appears to be small.

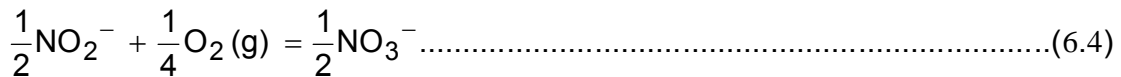
In addition, depending on the redox condition of the lakes, ammonia can be decreased due to oxidation by autotrophic Nitrosomonas bacteria resulting in the formation of nitrite and nitrate there by providing an autochthonous nutrient input for

photosynthesis. Ammonia is expected under oxic conditions to be rapidly oxidized to nitrite and nitrate due to oxidation by bacteria [36].

Nitrification by Chemolithotrophs (Authotrophs, Nitrosomonas)



Nitrification by Chemolithotrophs (Authotrophs, Nitrobacter) $\Delta G^\circ_W = -37.6\text{Kj.mol}^{-1}$



The free energies of formations above show favorable oxidation of ammonia to nitrate. They are calculated assuming average pH and ignoring the effects of concentrations. For oxidized (Oxic) lakes the ammonia concentration should show a gradual decrease with depth. Under anoxic conditions bottom sediments in the lake can provide ammonia to the upper water layer.

6.6 LAKE ENVIRONMENTAL IMPLICATION OF AMMONIA

Ammonia in the form of NH₃ rather than NH₄⁺ can provide toxicity to fish and be a cause of fish kill. The relative concentrations of these is determined with respect to the redox potential(pe) – pH equilibrium of the lake, ammonia being dominant at a higher pH such as that encountered in Lakes Abaya and Chamo and at higher temperature. The toxicity of ammonia is apparently species-specific for invertebrates and fish. Macro invertebrates are reportedly less sensitive to ammonia than fish species [69, 70]. Flow-through tests determined that ammonia was acutely toxic to 19 freshwater macro invertebrate species at concentrations ranging from 0.53 to 22.8 mg L⁻¹, whereas ammonia toxicity to 29 fish species ranges from 0.083 to 4.60 mg L⁻¹. Studies reported 96-h LC50s for ammonia ranging from 0.71 to 2.95 mg L⁻¹ for 11 macro invertebrate species. The crustacean species were less sensitive to un-ionized ammonia than non-crustacean species. They reported a 96-h LC50 of 2.05 mg L⁻¹ for *G. pulex* exposed to ammonia in moderately hard water (hardness 98-106 mg L⁻¹ as CaCO₃). In contrast, others reported a 96-h LC50 for *Chironomus riparius* of 9.4 mg L⁻¹ [69, 70].

Toxicity levels for un-ionized ammonia depend on the individual species; however, levels below 0.02 ppm are considered safe.

Ammonia nitrogen that enters ponds or lakes behaves in one of three ways. It may act as a prime nutrient that is used to support phytoplankton and aquatic plants. Some of the ammonia will be lost as ammonium to the atmosphere as a gas, and third is by conversion by biological activity. "Nitrogen is a nutrient (that is) essential for the growth of plants and microorganisms." There are three forms of nitrogen found in the water; ammonia, nitrites and nitrates. Ammonia concentrations that are left unchecked can become high enough to kill fish. "Under aerobic conditions (with oxygen), the ammonia form of nitrogen is oxidized to nitrite (NO_2^-) by the *Nitrosomonas* genera of bacteria. The nitrite nitrogen is an unstable compound that is rapidly oxidized (oxygen required) by *Nitrobacter* bacteria to nitrate nitrogen (NO_3^-). The oxidation of ammonia to nitrite and then to nitrate is called nitrification and is the basis of ammonia removal. To elaborate on this point, the bacteria associated with the conversion of ammonia to nitrate is so energy and oxygen intensive that their biological activity could consume all the free oxygen in a pond or lake water column leaving no oxygen for higher forms of life, such as fish. Without enough oxygen present in the water column, this reaction would cease [69, 70, and 71].

Fish excrete ammonia and lesser amounts of urea into the water as wastes. Two forms of ammonia occur in aquatic systems, ionized and un-ionized. The un-ionized form of ammonia (NH_3) is extremely toxic while the ionized form (NH_4^+) is not. Both forms are grouped together as "total ammonia." Through biological processes, toxic ammonia can be degraded to harmless nitrates. Un-ionized ammonia levels rise as temperature and pH increase. Toxicity levels for un-ionized ammonia depend on the individual species; however, levels below 0.06 ppm are considered safe.

However, the intermediate form of ammonia, known as nitrite has been known to occur at toxic levels (brown-blood disease) in fishponds [71].

The danger ammonia poses for fish depends on the water's temperature and pH, along with the dissolved oxygen and carbon dioxide levels.

The higher the pH and the warmer the temperature, the more toxic the ammonia. Also, ammonia is much more toxic to fish and aquatic life when water contains very little dissolved oxygen and carbon dioxide. Ammonia is toxic to fish and aquatic

organisms, even in very low concentrations. When levels reach 0.06 mg L^{-1} , fish can suffer gill damage. When levels reach 0.2 mg L^{-1} , sensitive fish like trout and salmon begin to die. As levels near 2.0 mg L^{-1} , even ammonia-tolerant fish like carp begin to die. Ammonia levels greater than approximately 0.1 mg L^{-1} can indicate polluted waters [71].

6.7 AMMONIA VARIATION WITH SEASONAL FLOWS

There is an apparent increase in ammonia loading on the rivers with increased flow. Hare river catchment release more ammonia per unit of flow than Kulfo catchment. The predominantly sandy soils have extremely low binding capacities for many nutrients. As a result sandy soil catchments have much better water quality than clay soil catchments, as the soils have a low affinity for binding with nutrients, which pass straight through the sandy substrates. The difference in ammonia binding capacity between these two rivers may therefore be explained in terms of the soil characteristics with respect to the clay content of the soil. In general the upper highland catchment has a slightly higher binding capacity due to the higher clay content than the lower land catchments such as Kulfo and Sile catchments.

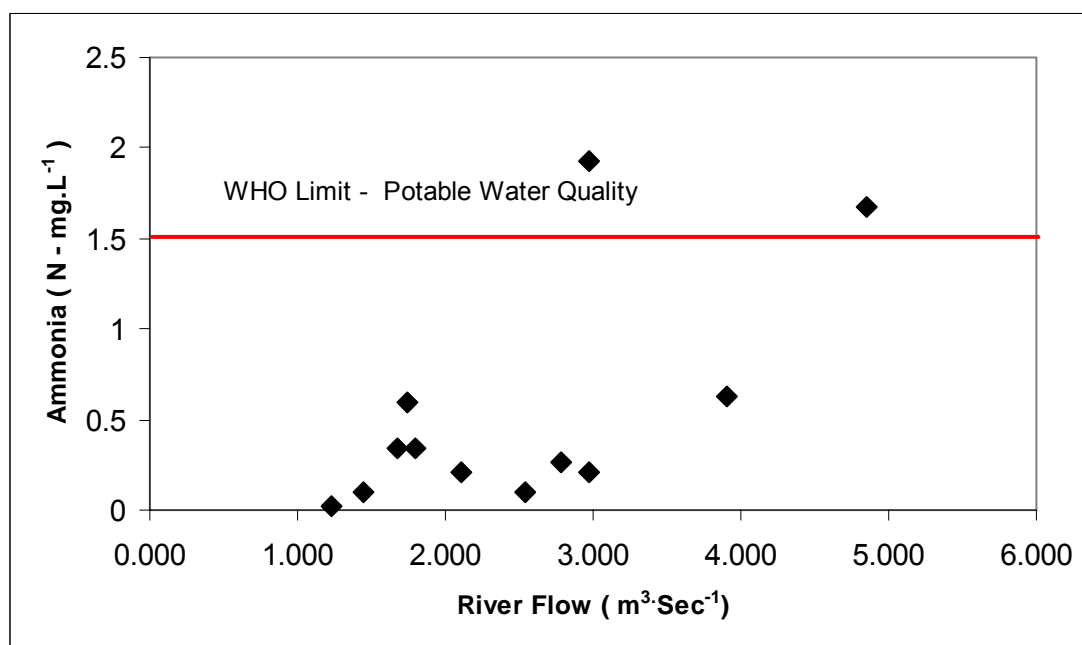


Fig. 6.7.1 Ammonia Increase with River Flow (Hare River) shown in Chapter 3 is reproduced here again for discussion.

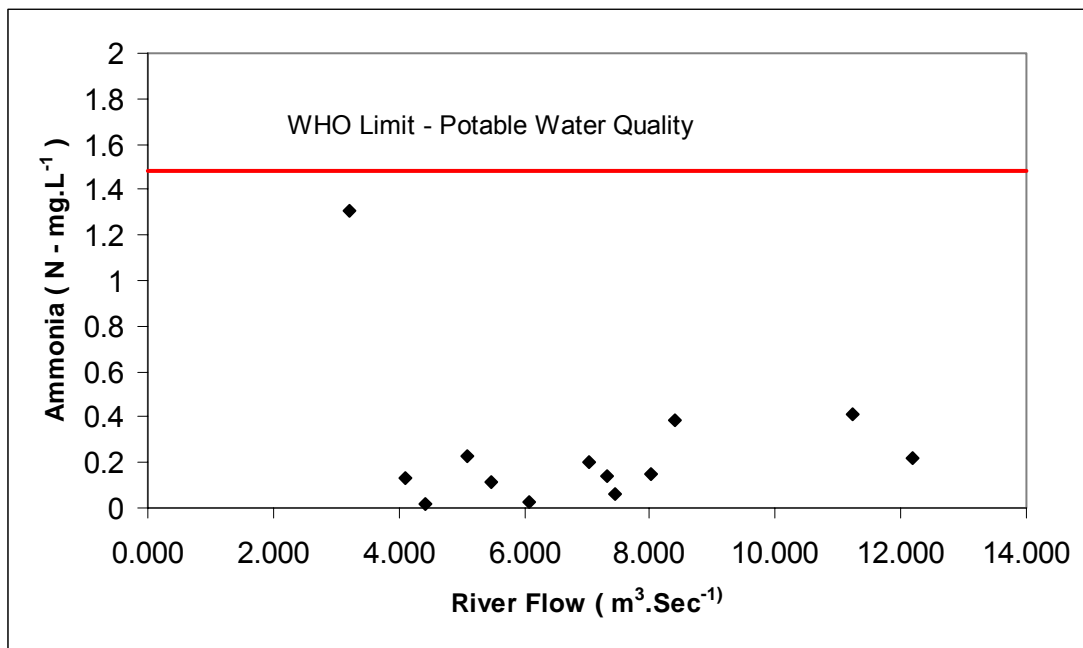


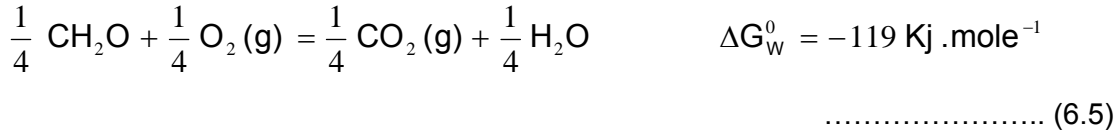
Fig. 6.7.2 Ammonia variation with River Flow (Kulfo River) shown in chapter three is reproduced here for discussion.

6.8 IMPLICATION ON WATER QUALITY MANAGEMENT OF THE RIVERS

The World Health organization guideline states mainly an aesthetic limit on the ammonia level for potable purposes. The WHO guideline value that states an aesthetic water quality limit of Ammonia is 1.5 mg L^{-1} measured as Nitrogen. With the measurement undertaken here above it is possible to identify if and when this limit is exceeded. However, since ammonia exerts an oxygen demand as well as chlorine demand its presence may not be desirable from the water quality point of view. This is particularly true during the rainy season when the ammonia level tends to increase.

Under normal conditions and anticipating that the organic loading of the rivers is low, it is possible to achieve nitrification of ammonia more or less rapidly under natural oxidizing conditions. The redox of nitrification may, however, be dominated by carbonaceous oxidation under high organic loading. Considering the redox reactions of the two processes under aerobic conditions:

Aerobic Respiration:

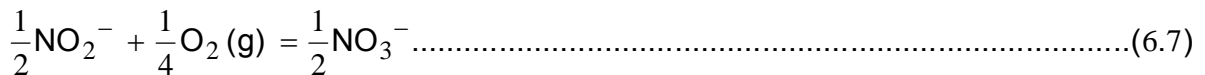


For Nitrification the reaction is:

Nitrification by Chemolithotrophs (Authotrophs, Nitrosomonas)



Nitrification by Chemolithotrophs (Authotrophs, Nitrobacter) $\Delta G^0_{\text{W}} = -37.6 \text{ Kj} \cdot \text{mole}^{-1}$



Comparison of the free energies suggests that carbonaceous oxidation is dominant. The presence or absence of ammonia is therefore dependent on the ultimate oxidation of organic matter.

6.9 IMPROVEMENT OF WATER QUALITY WITH RESPECT TO AMMONIA REMOVAL

Slow sand filters that are properly matured and with adequate depth of sand should be able to achieve nitrification under all conditions of flow for both the rivers Hare and Kulfo. These treatments are cost effective and adaptable to the rural conditions of living of the population in the rivers catchment.

Ponds protected from sanitary pollution and designed for longer period should be able to reduce the ammonia load both by dilution and nitrification. Considering the aggregate nitrification reaction



The oxygen demand of ammonia for a maximum concentration of 2 mg L⁻¹ of ammonia (assuming the dominant form is NH₄⁺ at low pH in rainy season) the ammonia oxygen demand will be:

$$\frac{2 * 32}{14 + 4} * 2 \text{ mg/L} = 7 \text{ mg .L}^{-1}$$

For a well-aerated pond, this value will be replenished from the atmosphere given that nitrification is a slow reaction. Slow sand filters may need aeration before and after the slow sand filter treatment in order to replace the lost dissolved oxygen.

6.10 AMMONIA IN THE LAKES ABAYA AND CHAMO

The ammonia in Lake Abaya varies between 0.5 – 1.5 mg L⁻¹ whereas for Lake Chamo the variation is between 0 – 1 mg L⁻¹. The ammonia in Lake Chamo is measured to be somewhat less due to the balance between photosynthesis and bacterial oxidation shifting more to the photosynthetic reaction. Apart from nitrification, ammonia in the lakes is expected to be taken by algal photosynthesis. As the dry season continues and in the absence of flows in to the lakes, the depletion of these nutrients might result in the net oxygen depletion due to dark respiration by algae and death and decay of algae at the bottom lake followed by release of noxious gases including ammonia at the bottom.

Lake Abaya's algal productivity (Chlorophyll a < 5 µg L⁻¹) is limited by the absorption of light by clay colloids suspension and therefore the photosynthetic dynamics is subdued and unless the lake is grossly polluted due to organic nitrogen input by domestic wastewater the ammonia increase due to internal recycling may not be significant. The ammonia level in Lake Abaya is higher than that of Lake Chamo due to lack of photosynthesis and perhaps also due to greater level of external input of pollution.

6.11 ANALYSIS – AMMONIA SPECIATION

6.11.1 Calculation of Safe Ammonia Speciation for the Rivers and Lakes under study

The ammonia determination gives the total sum of unionized ammonia (NH₃) and the ionized part (NH₄⁺). Since it is the unionized part (NH₃) that displays toxicity and presents odor problem (from aesthetic point of view) [72], it is necessary to determine this component out of the experimentally determined total ammonia.

Expressing the concentration in Molarity (M) with respect to the nitrogen atom, the total determined ammonia is expressed in terms of the two components [36]:

$$[\text{NH}_4^+] + [\text{NH}_3] (\text{aq}) = \text{Total Ammonia (N)} \dots\dots\dots (6.9)$$

From the Equilibrium concentration relationship



$$K_e = \frac{[\text{NH}_3][\text{H}^+]}{\text{NH}_4^+} \dots\dots\dots (6.11)$$

$$[\text{NH}_4^+] = [\text{NH}_3] + K_e^{-1} [\text{NH}_3] [\text{H}^+] \dots\dots\dots (6.12)$$

$$\text{TAN} = [\text{NH}_3] (1 + K_e^{-1} [\text{H}^+]) \dots\dots\dots (6.13)$$

From which the two ammonia species are calculated as:

$$\text{NH}_3 = \frac{\text{TAN}}{1 + K_e^{-1} [\text{H}^+]} \dots\dots\dots (6.14)$$

$$[\text{NH}_4^+] = (K_e^{-1}) [\text{NH}_3] [\text{H}^+] \dots\dots\dots (6.15)$$

6.11.2. Temperature and Ionic Strength Correction

The equilibrium constant needs temperature and ionic strength correction. The temperatures of the various sources of water considered differ from each other as well as auto variability during the various months of the year depending on meteorological factors.

6.11.2.1 Temperature Correction

The temperature correction is obtained through the Van't Hoff equation [36]:

$$\ln\left[\frac{K_T}{K_{T_0}}\right] = -\frac{\Delta H^0}{R} \left[\frac{1}{T} - \frac{1}{T_0}\right] \dots\dots\dots (6.16)$$

Where ΔH^0 is the change in enthalpy of the reaction (the heat absorbed by a chemical reaction as it proceeds to the right).

The following values tabulated in Table 6.11.2.1.1 were taken from thermodynamic data (Source. Aquatische Chemie by Laura Siegg and Werner Stumm – Second edition. 1991. Pages 185 - 191) [73].

Table 6.11.2.1.1 Thermodynamic Data - Enthalpy and Free Energy [73]

Chemical	H ⁰	G ⁰	Temperature (°C)
Hydrogen Ion (H ⁺)	0	0	25
Ammonia (NH ₃)	-80.29	-26.57	25
Ammonium Ion (NH ₄ ⁺)	-132.5	-79.37	25

The equilibrium constant at 25 Degree Celsius (298 K^o) is calculated from

$$\Delta G^0 = G^0(\text{NH}_3) + G^0(\text{NH}_3) - G^0(\text{NH}_4^+)$$

$$\Delta G^0 = -26.57 - (-79.37) = 52.80$$

$$\text{Log}(K_{T_0}) = \frac{-\Delta G^0}{RT} = \frac{-52.80}{2.3(5.7066)} = -9.2524$$

$$K_{T_0} = 10^{-9.249}$$

Similarly the change in enthalpy due to the reaction is calculated as:

$$\Delta H^0 = H^0(\text{NH}_3) + H^0(\text{NH}_3) - H^0(\text{NH}_4^+)$$

$$\Delta H^0 \text{ (KJ.Mole}^{-1}\text{)} = 0 + -80.29 - (-132.50) = 52.21$$

The value of R (the universal Gas constant) is given as $R = 8.314 \times 10^{-3} \text{ KJ.Mole}^{-1}$

Using this value in the Van't Hoff equation, the change in equilibrium constant is given through:

$$\text{Ln}\left(\frac{K_T}{K_{T_0}}\right) = \frac{-\Delta H^0}{R} \left[\frac{1}{T} - \frac{1}{T_0} \right]$$

$$\frac{K_T}{K_0} = e^{\left[\frac{-52.21 \text{ KJ.Mole}^{-1}}{8.314 \times 10^{-3} \text{ KJ.Mole}^{-1} \cdot \text{K}^0} \right] \left[\frac{1}{T} - \frac{1}{298} \right]}$$

Linearising of the equation by taking the (y-x) variables as $\text{Log}(K_e)$ and $1/T$ respectively gives:

$$\text{Log}(K_e) = -0.09709 - \frac{-2727.27}{T_{K^0}}$$

Table 6.11.2.1.2. shows the adjustment for the equilibrium constant formed through the application of the above equation:

Table 6.11.2.1.2 Temperature Correction for Ammonia Equilibrium Constant

Temperature (°C)	Log (Ke)	Temperature	Log (Ke)	Temperature	Log (Ke)
10	-9.7341	20	-9.4052	30	-9.0980
11	-9.7002	21	-9.3735	31	-9.0684
12	-9.6665	22	-9.3421	32	-9.0390
13	-9.6330	23	-9.3108	33	-9.0097
14	-9.5998	24	-9.2798	34	-8.9807
15	-9.5668	25	-9.2490	35	-8.9519
16	-9.5340	26	-9.2184	36	-8.9232
17	-9.5015	27	-9.1880	37	-8.8947
18	-9.4691	28	-9.1578	38	-8.8664
19	-9.4371	29	-9.1278	39	-8.8383

6.11.2.2 Adjustment for Ionic strength

The ionic strength of the different water sources are variable Lake Abaya and Chamo in particular possess higher ionic strength for which the equilibrium condition differs appreciable from the one calculated above assuming infinite dilution. This applies partly to the rivers Hare and Kulfo in particular at dry season flow when the soil/ground water contribution to the ions is higher. At higher ionic strength it requires less work to charge ions and as a result the activities of the ions (for formation of a compound) decrease. This means the ΔG^0 values of the individual charges become more negative (more favorable to form). For infinite dilution these activities are conventionally taken as one. The activity coefficient of an ion of radius R_0 and charge Z is given by [73]:

$$\begin{aligned} \ln(\gamma_Z) &= \Delta G_{(\text{elec})} - \Delta G_{0(\text{elec})} \\ &= -AZ^2 \frac{I^{1/2}}{1 + BR_0I^{1/2}} \end{aligned}$$

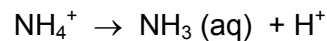
Where the constants A and B depend on the dielectric constant ($\epsilon\epsilon_0$) and absolute temperature T of the system. For the ranges of ionic strength encountered in this study ($I < 0.5$), the empirical formula given by Davis that eliminates the ionic radius term by incorporating a linear term ($0.3 \cdot I$) is given as follows:

$$\ln(\gamma_i) = -0.5Z^2 \left[\frac{I^{1/2}}{1+I^{1/2}} - 0.3I \right]$$

The detail calculation of the ionic strength of the water sources under study is given in Appendix 6-1.

6.11.2.2.1 Adjustment of Ionic Strength for the Ammonia Reaction

From the chemical balance:



The equilibrium constant is defined as:

$$K_a = \frac{[\text{NH}_3][\text{H}^+]}{[\text{NH}_4^+]} * \frac{\gamma_{\text{NH}_4^+}}{\gamma_{\text{NH}_3} * \gamma_{\text{H}^+}}$$

Or in terms of the logarithms:

$$\text{Log}(K_a) = \text{Log}(K_e) + \text{Log} \gamma(\text{NH}_4^+) - \text{Log} \gamma(\text{NH}_3) - \text{Log} \gamma(\text{H}^+)$$

Since $\text{Log} \gamma(\text{NH}_3) = 0$ and $\text{Log} \gamma(\text{NH}_4^+) = \text{Log} \gamma(\text{H}^+)$ under all ionic conditions, it turns out that the equilibrium constant is not affected by ionic strength.

Therefore, $\text{Log}(K_a) = \text{Log}(K_e)$

6.11.3 Calculation of the Percentage of Ammonia for a given Determined Total ammonium Value

Using the chemical speciation equations for the ionized and unionized part of the measured ammonia, the component in terms of percentage for a range of temperatures has been worked out and the results are included in the table 6.11.3.1 and Figure 6.11.3.1.

Table 6.11.3.1 Percentage of Ammonia (NH₃) present for given values of pH and Temperature

pH	10°c	15°c	20°c	25°c	30°c	35°c	pH	10°c	15°c	20°c	25°c	30°c	35°c
5.0	0	0	0	0.01	0.01	0.01	8.6	7	10	14	18	24	31
5.2	0	0	0.01	0.01	0.01	0.02	8.8	10	15	20	26	33	41
5.4	0	0.01	0.01	0.01	0.02	0.03	9.0	16	21	28	36	44	53
5.6	0.01	0.01	0.02	0.02	0.03	0.04	9.2	23	30	38	47	56	64
5.8	0.01	0.02	0.02	0.04	0.05	0.07	9.4	32	41	50	59	67	74
6.0	0.02	0.03	0.04	0.06	0.08	0.11	9.6	42	52	61	69	76	82
6.2	0.03	0.04	0.06	0.09	0.13	0.18	9.8	54	63	71	78	83	88
6.4	0.05	0.07	0.1	0.14	0.2	0.28	10.0	65	73	80	85	89	92
6.6	0.07	0.11	0.16	0.22	0.32	0.44	10.2	75	81	86	90	93	95
6.8	0.12	0.17	0.25	0.35	0.5	0.7	10.4	82	87	91	93	95	97
7.0	0.18	0.27	0.39	0.56	0.79	1.1	10.6	88	92	94	96	97	98
7.2	0.29	0.43	0.62	0.89	1.25	1.74	10.8	92	94	96	97	98	99
7.4	0.46	0.68	0.98	1.4	1.97	2.73	11.0	95	96	98	98	99	99
7.6	0.73	1.07	1.54	2.19	3.08	4.26	11.2	97	98	98	99	99	99
7.8	1.15	1.68	2.42	3.43	4.79	6.59	11.4	98	99	99	99	100	100
8.0	1.81	2.64	3.79	5.34	7.39	10.05	11.6	99	99	99	100	100	100
8.2	2.84	4.12	5.87	8.2	11.23	15.04	11.8	99	99	100	100	100	100
8.4	4.43	6.38	8.99	12.4	16.7	21.91	12.0	99	100	100	100	100	100

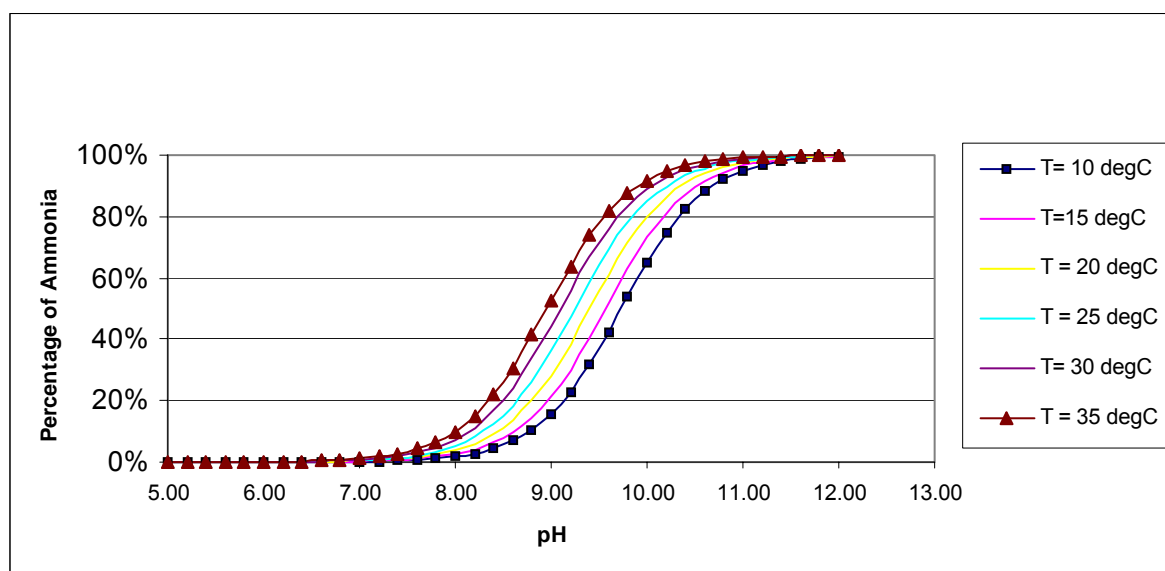


Fig. 6.11.3.1 Variation of Percentage of Ammonia with pH and Temperature (Applicable to all water Sources in the Basin). Since the ammonia formation from ammonium is an endothermic reaction, the ammonia percentage increases with increase in temperature.

Table 6.11.3.2 Ammonia values at ranges of Temperature and pH variation of the Water Sources Considered

Water source	PH Range (pH Units)	Temperature Range (Degree C)	Total measured Ammonia (mg L ⁻¹ of N)	Percentage Of Ammonia (%)	Ammonia (N) Range of Variation (mg L ⁻¹)
Lake Abaya	8.9 – 9.2	18-26	0.9 - 1.21	18-48	0.16-0.58
Lake Chamo	9.1-9.4	19-27	0.1 - 0.75	28-60	0.03-0.45
River Hare	6.9 –8.31	9-24	0.0 – 1.93	0.12-10	0-0.19
River Kulfo	7.2 - 8.7	10-28	0.02 – 1.3	0.29-27	0.006-0.35
River Sile	7.4 - 8.5	15-27	0.01 – 1.1	0.68-21	0.006-0.23

6.12 IMPLICATION ON THE LAKES WATER QUALITY

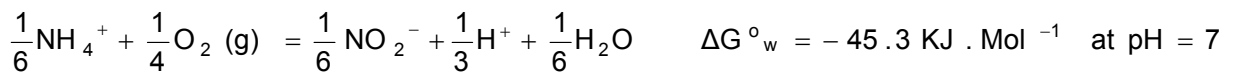
The calculated concentration for the lakes shows the presence of ammonia, which might show some form of toxicity to certain species in the eco system including fish. Since the lakes pH remains high most of the time, it is likely that ammonia remains in the unionized form. Temperature increase favor ammonia formation as the change from ammonium ion to ammonia is an endothermic reaction. The following areas and times therefore need particular monitoring:

1. Parts of the lakes receiving immediate discharge of nitrogen wastes. Rivers draining agricultural areas where organic nitrogen has been applied as fertilizer and where best agricultural management practices have not been employed. As the water flows further in to the lake it is anticipated that nitrification under normal circumstances in addition to uptake by plants will reduce ammonia levels.
2. Rivers draining areas where domestic waste is inappropriately disposed and there is high population density, urban runoff is draining in to rivers.
3. Ammonia uplift from the lake bottom after a prolonged dry period under hot, still conditions. Possible stratification and the formation of hypolimnion. Reduced redox conditions favors formation of ammonia from anaerobic bacterial action and during turn over these may diffuse in to the epilimnion layer causing high level of ammonia. Fertilizer release from bottom sediments may cause high ammonia concentrations [75].

4. Under oxic condition, reduced redox might encourage the reduction of nitrate to ammonia by blue green algae (cyano bacteria).

6.13 EXTENT OF NITRIFICATION

The nitrosomonas bacteria that oxidize ammonia to nitrite have an optimum pH range of 8.0 - 8.8. The lower limit for reasonable growth for nitrosomonas bacteria is given as pH 7.0 - 7.6. While the upper limit is 9.4. Around pH 6 - 6.2 nitrosomonas bacteria cease to function. For both lakes Abaya and Chamo nitrification is possible under areas with prevailing aerobic conditions. Polluted parts of the lakes may have inhibited oxygen supply and the redox atmosphere may not favor nitrification. The effect of nitrification on pH is to decrease the pH of the water (acidification).



Since Abaya and Chamo lakes have higher alkalinity (Discussed under section alkalinity), the higher buffering capacity of the lakes counter acts the decrease in pH due to ammonia nitrification. From the above reaction it is apparent that the energy available for nitrification increases at increase in pH:

6.14 ENERGY OF NITRIFICATION FOR LAKES ABAYA AND CHAMO

For the pH ranges of the lakes Abaya and Chamo, the above energy (pH = 7) can be modified as follows:

Considering the first half-redox reaction:

$$\frac{1}{4}\text{O}_2 + \text{H}^+ + \text{e}^- = \frac{1}{2}\text{H}_2\text{O} \quad \Delta G^\circ = -118.3 \text{ KJ Mole}^{-1}$$

$$P_e^\circ = \frac{-0.175}{n} \Delta G^\circ = \frac{-0.175}{1} (-118.3) = +20.70$$

$$P_e = P_e^\circ - \text{Log} \left[\frac{1}{(\text{P}_{\text{O}_2})^{1/4} [\text{H}^+]} \right] = 20.70 - \text{pH} - \frac{1}{4} \text{Log}(\text{P}_{\text{O}_2})$$

Similarly for the other half redox reaction:

$$\frac{1}{6}\text{NH}_4^+ + \frac{1}{3}\text{H}_2\text{O} = \frac{1}{6}\text{NO}_2^- + \frac{4}{3}\text{H}^+ + \text{e}^-$$

$$P_e^\circ = -15.2$$

$$P_e = -15.2 - \text{Log} \left[\frac{(\text{NO}_2^-)^{1/6} (\text{H}^+)^{4/3}}{(\text{NH}_4^+)^{1/6}} \right] = -15.2 - \frac{1}{6} \text{Log}(\text{NH}_4^+) + \frac{1}{6} \text{Log}(\text{NO}_2^-) + \frac{4}{3} \text{pH}$$

Adding the two potentials and neglecting the concentration terms, the redox potential becomes:

$$P_e = 20.70 - 15.2 + (4/3) \text{pH} - \text{pH} = 5.5 + (1/3)\text{pH}$$

For pH = 7 this energy becomes $p_e = 5.5 + (1/3)(7) = 7.833$

The energy of formation for pH = 7 will be:

$$\Delta G_w = -\frac{n P_e}{0.175} = \frac{-(1)(7.833)}{0.175} = -44.8 \text{ kJ. mole}^{-1}$$

Figure 6.1.4.1 shows the increase or decrease in percentage of the energy available for other pH conditions:

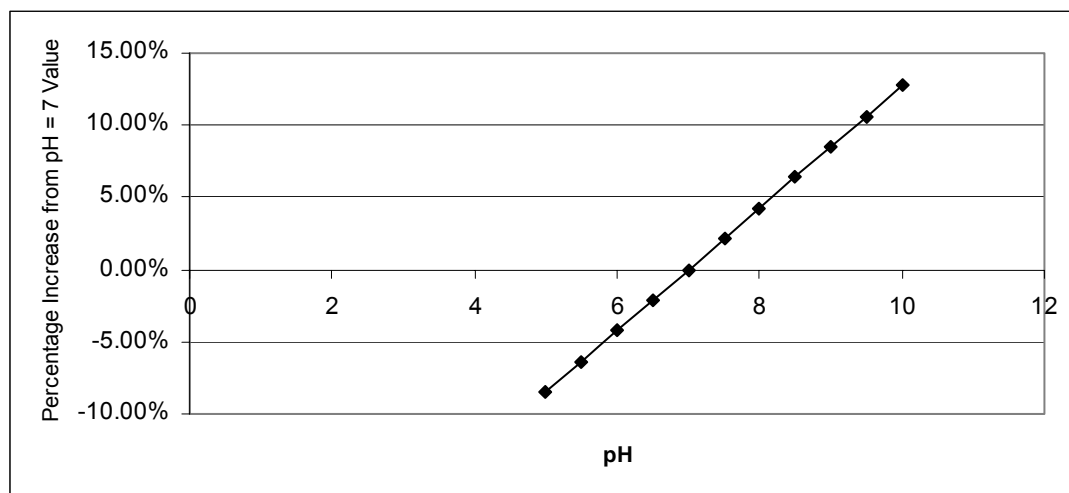


Fig. 6.14.1 Theoretical Percentage Increase in Nitrification with pH. Although nitrification increases with increase in pH the efficiency decreases outside the optimum range.

It is anticipated that there will be an increase (10%) in the rate of nitrification hence conversion of ammonia at the prevailing pH values for the two lakes. However, this is not the case as nitrification efficiency falls outside the optimum range of 6.5 -8.5 pH values.

6.15 INFLUENCE OF OXYGEN AND TEMPERATURE

The lakes Dissolved oxygen varies between 2 and 6 mg L⁻¹ of O₂. Nitrification is limited by the range 2-2.5 mg L⁻¹. Competition by heterotrophe / nitrifier and diffusion limitation set this limit to the dissolved oxygen. Only areas of the lakes that become anoxic or reduced in their dissolved oxygen state might have limited rate of ammonia conversion. However since the retention times of water in both lakes are high this effect might be compensated for. In addition the low BOD of the lakes reduces competition by heterotrophes [76].

The temperatures prevailing on both lakes favor higher rate as far as nitrification rate increase due to temperature are concerned.

6.16 PROPOSED CATCHMENT LEVEL REMEDIES

6.16.1 Waste Diversion

Wastes from the textile industry, effluent of the AWTI waste water and lack of onsite system of sanitation as well as washing, bathing in the rivers are some of the common sources of organic nitrogen pollution entering above the level that the eco system can sustain. Controlled sanitary disposal, treatment of factory and institutional wastes and modification of the habits of riverside usage of water by providing appropriate treatment and increase water supply provision can reduce the ammonia transport in to the lake systems.

6.16.2 Agricultural Best Management Practices

Under limited pH conditions, ammonia in the soil may not be converted to nitrate and may be readily dissolved in the rain and transported in to the rivers and lakes. Appropriate and timely application of fertilizers as well as avoidance of slope farming, soil conservation and constructed wetlands for agricultural runoff pollutant removals are some of the measures that will reduce the incidence of organic nitrogen and ammonia pollution of rivers and lakes.

1. Soil Conservation: Forestation reduces soil erosion. Soil conservation measures generally reduce the incidence of N-load in to the water systems.
2. Preservation of Wet Lands: Clearing of the wetlands for agricultural uses may have deprived the natural ecosystem potential for pollutant removals. An appropriate action to preserve these natural wetlands is necessary.

6.17. Proposed Onsite (Lake Level) Remedies

6.17.1 Artificial Aeration System Application

Parts of the lakes that are polluted with organic loading may become anoxic due to limited oxygen conditions. In addition eutrophication under stratified condition as happens during the hot summer season; the lakes bottom can become anoxic

releasing ammonia and other anoxic gases into the water body [74]. Increased ammonia and the decline in oxygen cause fish death. By application of aeration through a system consisting of compressor, plastic tubes and ceramic diffusers, ammonia, hydrogen sulfide, methane, and carbon dioxide are diffused into the atmosphere. Acid-producing anaerobic bacteria are destroyed by exposure to ultraviolet light on the surface film, and by oxygen toxicity when the bottom water becomes oxygenated.

6.17.2 Application of Biotechnology

Nitrosomonas and nitrobacter are autotrophic chemolith bacteria. Grown under appropriate conditions can be applied to the water bodies for initiating the ammonia conversion to nitrite and nitrates.

6.18. AMMONIA IN DRINKING WATER SUPPLY AND AQUACULTURE PONDS

The concern of ammonia in drinking water supply ponds is associated with aesthetic concerns as well as the added oxygen and chlorination demand the water places. As the rivers (Hare Kulfo and Sile) show increased level only during the rainy season, the problem arises during this period. Moreover the pH of the rivers reduced to below 7 during these seasons in addition to increase in organic pollution. All these factors may lead to reduced level of nitrification in the pond.

6.18.1 Catchment Level remedial and Protection Measures

As was explained with respect to the lakes, the measures also simultaneously apply to the man-made ponds. Restated again: waste diversion, agricultural best management practices, forestation and soil conservation practices are important.

6.18.2 Possible Onsite Remedies to be applied to Drinking Water Ponds And Lakes

1. Appropriate design of ponds to facilitate aeration such provision of shallow depth.

2. Provision of longer retention time hence increased level of nitrification. Large pond provides dilution and increased alkalinity.
3. Application of biological filter
4. Slow sand filter with greater depth allows nitrification to take place.
5. Bioremediation (Biotechnology) can be applied to stressed aquaculture pond to reduce ammonia.
6. Prevention of direct pollution of pond by domestic waste.
7. Pond Catchment grassing to provide natural treatment and reduce ammonia load.

CHAPTER 7**WATER QUALITY MODELLING**

S.No.	CONTENTS	PAGE
7.1	Introduction	264
7.2	Interpolation of Missing Data	264
7.3	Time Domain Auto Regressive Modeling	266
7.4	Time Domain Cross Regression between Variables from ARIMA Models	267
7.5	Forecasting Future Changes from ARIMA Models	268
7.6	Auto-regressive Model fitted to Conductivity Data	268
7.7	Frequency Domain Regression	269
	7.7.1 Application of Frequency Domain Regression between TDS and Conductivity – Kulfo River	272
	7.7.2 Spectral Model of Total Solids and Rainfall	274
7.8	Modelling Using the State – Space Methodology	276
	7.8.1 Application of State – Space Model between Sodium and TDS – Kulfo River	278
	7.8.2 Estimation of Water Quality of River Hare from Kulfo Data using State – Space Method	280
7.9	Discharge Based Contaminant Modeling	281
	7.9.1 Application of Discharge Based Contaminant Modeling to Kulfo River	283
	7.9.1.1 The Rating Curve Equation (Kulfo River)	283
	7.9.1.2 Conversion of Turbidity Load to Suspended Solids Load	284
	7.9.1.3 Calculation of the moments in Taylor Series and of Bias	284
	7.9.1.4 Transfer Function for Solids Loading Calculation	284
	7.9.1.5 Mean Daily Solids Loading Flow from River Kulfo	285
7.10	Modeling Solids with Turbidity and Absorption Measurements	287
	7.10.1 Problem with Measurement of High Turbidity	287
	7.10.1.1 Modes of solution to the Problem of measuring high Turbidity	288
	7.10.2 Modeling Solids with Absorption Measurements	289
7.11	Modeling Settling Characteristics of Solids	291
	7.11.1 Settlement Characteristics of Rivers that are Tributaries to The Abaya – Chamo Lake System	293

S.NO.	LIST OF FIGURES	PAGE
Fig. 7.2.1	Smoothing Spline Regression Fit to Hardness Data	265
Fig. 7.2.2	Comparison of Cubic Spline with State Space Methodology for Conductivity Missing Data	265
Fig. 7.2.3	Daily Flow variation (Kulfo River) after Interpolation Using Smoothing Spline Regression	266
Fig. 7.6.1	Conductivity Data Fitted with ARIMA (3,1) Model	269
Fig.7.7.1.1	Estimate of TDS From Spectral Relation with Conductivity (ARIMA)	273
Fig.7.7.1.2	Actual and Estimated Spectral Density TDS from ARIMA model	273
Fig. 7.7.2.1	Actual and Simulated Total Solids Curve	274
Fig. 7.7.2.2	Factor Loadings from principal Component Analysis	275
Fig. 7.7.2.3	Estimated Spectrum of Total Solids from Rainfall	275
Fig. 7.8.1.1	State - Space Model of Sodium Data from Conductivity data	279
Fig. 7.8.2.1	Prediction of Conductivity of Kulfo River from that of Hare River by State Space methodology	280
Fig. 7.9.1.1.1	Regression of Turbidity on Discharge - Kulfo River	283
Fig. 7.9.1.4.1	Solids Load Transfer Function Simulated Arithmetic Mean Flow and Turbidity - Kulfo River	285
Fig. 7.9.1.4.2	Simulation of Mean Daily Solids Flow River Kulfo (Based on Arithmetic Mean)	286
Fig. 7.10.1.1	Box Plot of Turbidity determined by Several levels of Dilution	287
Fig. 7.10.1.1.2	Turbidity Versus Concentration Graph- Kulfo River	288
Fig. 7.10.1.2.1	Turbidity Reading Chart - River Kulfo	289
Fig. 7.10.2.1	Polynomial Regression of Suspended Solids on Absorption with 95% Confidence Limits - Kulfo River	290
Fig. 7.10.2.2	Linearity Fit of Absorption Measurement	291
Fig. 7.11.1	Settling Characteristics of Solids in River Hare	292
Fig. 7.11.1.1	Settling Characteristics of Rivers in Abaya - Chamo Basin	294

S.NO.	LIST OF TABLES	PAGE
Table 7.9.1.5.1	Solids Load Calculation Figures using Arithmetic Mean Flow and Turbidity Data	286
Table 7.10.1.2.1	Turbidity Optimum Sample Concentration Level for Measurement by Dilution	289
Table 7.11.1	Regression Models of Settling Characteristics of Solids in Hare and Kulfo Rivers	293

7.1 INTRODUCTION

The objective of water quality modelling in general is to mathematically model the pattern of water quality variation in time and space and for pollutant load estimation [77]. In addition relating water quality variables so as to enable prediction of one variable that is monitored in terms of the other which may not have been frequently monitored could be a useful modelling effort. Some model types such as auto correlation of observation of a single variable time series water quality data enable a time series model development that, for example can be used to forecast future changes. Regionally related water quality data, such as by using state-space method described below provide a means of interpolating regional water quality data. The techniques used for modelling are listed below and the results of applying these models to the water quality data collected for this research are described in detail in the topics that follow.

1. Time Domain Auto Regressive Modeling
2. Frequency Domain Regression:
3. Modeling using the State – Space Methodology
4. Discharge Based Contaminant Modeling
5. Modelling Solids with Turbidity and Absorption Measurements
6. Modelling Settling Characteristics of Solids.

7.2 INTERPOLATION OF MISSING DATA

For time series modelling as well as spectral analysis, data must be continuous within the interval of analysis chosen. If there are long gaps in the data, the analysis will give erroneous results even if the Interpolation of missing data has been accomplished. Two approaches have been used here to fill the small gaps in the data missed in the analysis, which is listed below.

1. Curve fitting technique such using smoothing spline regression (degree one – three often used)
2. Advanced modelling between using expectation maximization algorithm. The expectation maximization is an auto regressive modelling where the error between the actual data variance and the model variance is minimized to

determine the missing values. This approach here is presented only as an illustrative rather than normative one.

An example of data interpolation using these two techniques is provided in figures 7.2.1, 7.2.2 and 7.2.3.

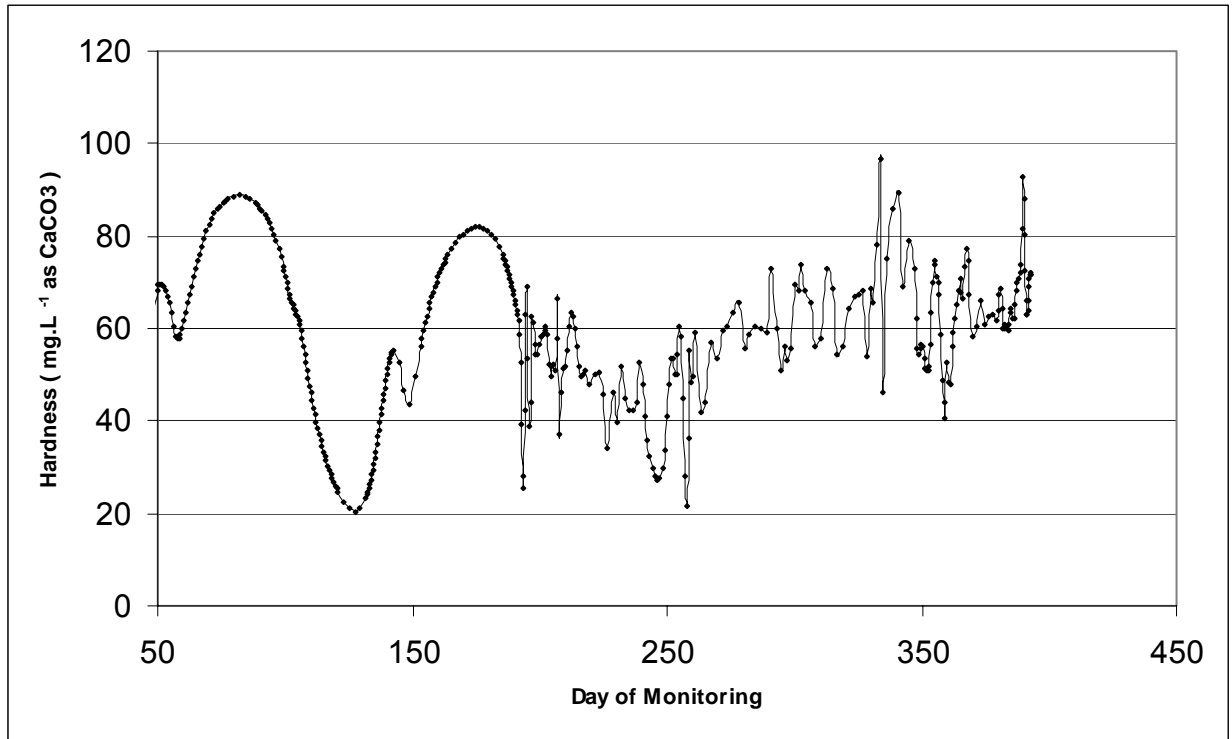


Fig. 7.2.1 Smoothing Spline Regression Fit to Hardness Data. A lower degree polynomial is suitable for filling the missing data.

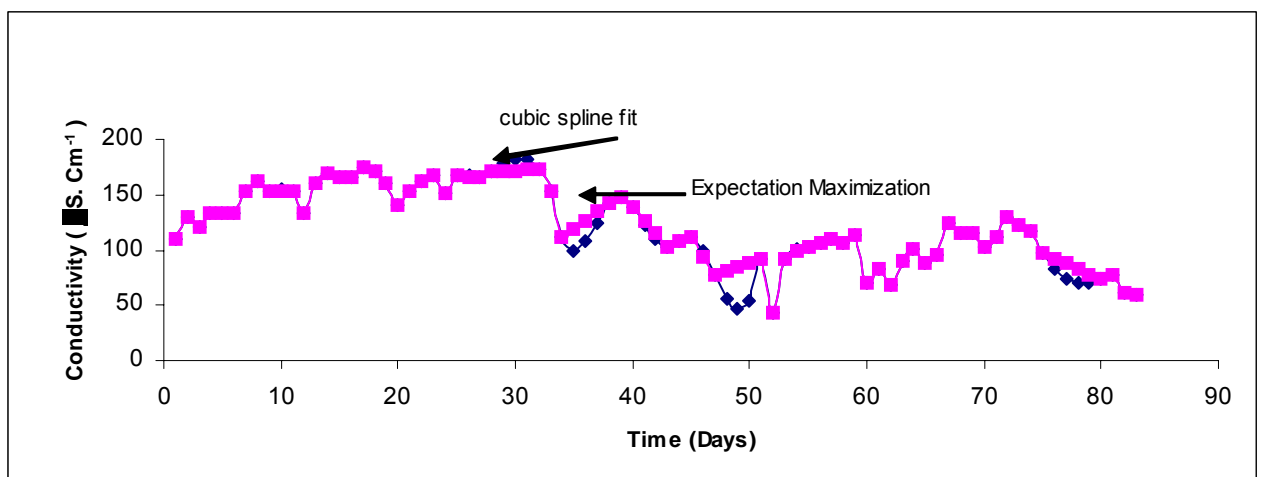


Fig. 7.2.2 Comparison of Cubic Spline with expectation maximization for Conductivity Missing Data. The two curves are close to each other. The expectation maximization algorithm gives a closer fit to the data than the cubic spline procedure.

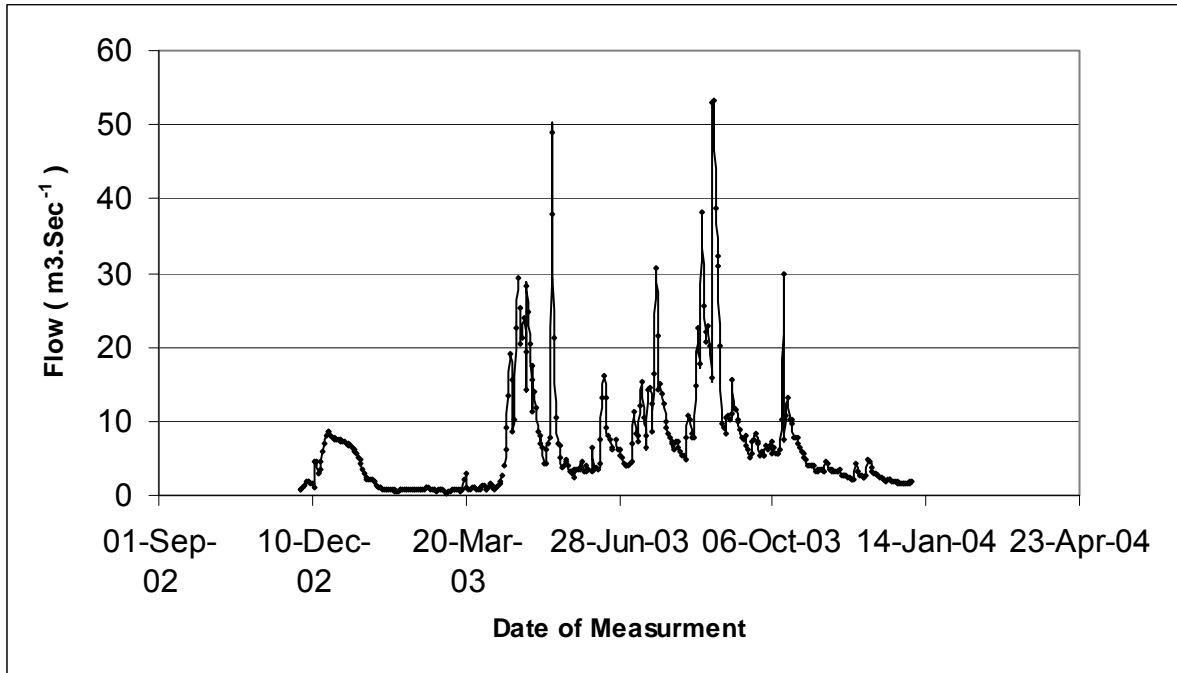


Fig. 7.2.3 Daily Flow variation (Kulfo River) after Interpolation Using Smoothing Spline Regression. Smoothing spline regression also gives an acceptably close fit to the data while filling the missing values.

7.3 TIME DOMAIN AUTO REGRESSIVE MODELLING

The auto Regressive Integrated with Moving Average Model (ARIMA) models a time series data by combining the auto covariance of the data and the noise component. The auto covariance is accounted by the auto regression equation involving past observation. The noise part is accounted for by a moving average model. The general Autoregressive moving average model (ARMA) of order p and q for a stationary water quality series is expressed by writing [78, 79, 80, and 81]:

$$\phi(B) X(t) = \theta(B)W(t) \dots \dots \dots (7.1)$$

$$x(t) - \sum_{k=1}^p \phi_k x_{t-k} = \sum_{k=1}^q \theta_k w_{t-k} \dots \dots \dots (7.2)$$

If the operators $\phi(B)$ and $\theta(B)$ are determined the equation can be solved for $x(t)$ by introducing the variable $\psi(B)$ so that

$$X(t) = \psi(B) w(t) \dots \dots \dots (7.3)$$

The values of $\psi(B)$ are determined from the convolution equation:

$$\phi(B) \psi(B) = \theta(B) \dots \dots \dots (7.4)$$

The full seasonal Auto regressive integrated moving average model multiplies the various seasonal and non-seasonal components together with their non- seasonal counterparts to develop a representation of the form:

$$\phi_p(B^s) \phi(B) \Delta_S^D \Delta^d x_t = \alpha + \theta_Q(B^s) \theta(B) w(t) \dots \dots \dots (7.5)$$

The parameters $\phi(B)$, $\theta(B)$ and σ_w^2 above are determined by minimizing the Log likelihood function. The Box_Jenkins model is a familiar and pioneering method for solving the above equation.

7.4 TIME DOMAIN CROSS REGRESSION BETWEEN VARIABLES FROM ARIMA MODELS

The regression between two water quality stationary time series in the time domain can be estimated from the equation [78, 79, 80, and 81]:

$$Y(t) = h(B) X(t) + N(t) \dots \dots \dots (7.6)$$

$$\text{Where } h(t) = h_0 + h_1 B + h_2 B^2 + \dots \dots \dots (7.7)$$

Where also B is the backward operator, i.e., $BX(t) = X(t-1)$

The values of h in $h(t)$ are estimated from the ratio between the covariance and variance of the residuals of the two stationary time series. The two residuals are calculated from the ARIMA models as:

$$\phi(B)\theta^{-1}(B)X_t = \alpha_t \dots\dots\dots(7.8)$$

$$\phi(B)\theta^{-1}(B)Y_t = \beta_t \dots\dots\dots(7.9)$$

The values of h (m) are then calculated from:

$$h(m) = \frac{C_{\alpha\beta}(m)}{S_{\alpha}^2} \dots\dots\dots(7.10)$$

7.5 Forecasting Future Changes from Auto Regressive Integrated with Moving Average (ARIMA) Models

The following expectation identities for the ARMA (p, q) process are useful for constructing the forecasts.

$$E(X_t | X_s, X_{s-1}, \dots) = \begin{cases} X_t & t \leq s \\ X_t^s & t > s \end{cases}$$

$$E(w_t | X_s, X_{s-1}, \dots) = \begin{cases} w_t & t \leq s \\ 0 & t > s \end{cases} \dots\dots\dots(7.11)$$

$$X_{t+1} - X_{t+1}^t = \sum_{K=0}^{1-1} \psi_k W_{t+1-k}$$

Since the forecast includes the w (t) term this is determined for an ARIMA (P, 0, q) process by assuming w (t) = 0 for t ≤ p and for solving for w (p+1) recursively for t = p+1, p+2, etc.

7.6 Auto-regressive Model fitted to Conductivity Data

Figure 7.6.1 shows the application of autoregressive modeling using ARIMA (3, 1) model after high frequency variation was filtered with a one lag (three points) moving average. It is seen that water quality variables such as conductivity and others classified in group I that display major variation during longer season are best modeled with autoregressive modeling. This condition is not available for water quality variables influenced by surface derived short frequency events such as turbidity, suspended solids and other contaminants.

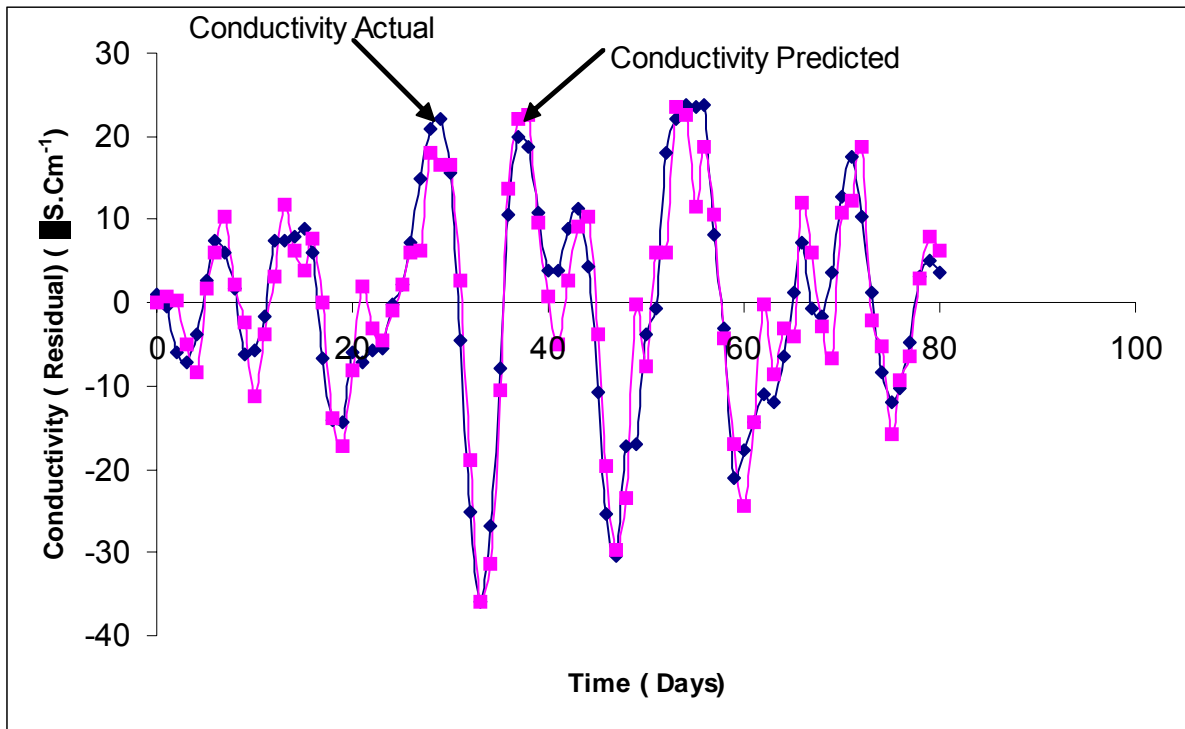


Fig. 7.6.1 Conductivity Data Fitted with ARIMA (3, 1) Model. Conductivity data is adequately modeled with ARIMA model.

7.7 Frequency Domain Regression

The frequency domain regression between two water quality variables is based on spectral transformation of the data. The periodic properties of water quality data may be analyzed using the principles and methods of spectral analysis. A manual transformation of a given periodic data (stationary data) is done by a discrete Fourier Transform (DFT) [78, 79, 80, and 81].

$$X(K) = T^{-1/2} \sum_{t=0}^{T-1} x_t e^{-2\pi i v_k t} \dots\dots\dots (7.12)$$

The sample periodogram $P_x (V_k)$ is given by:

$$P_x (V_k) = X(K) * \overline{X(K)} = |X(K)|^2 \dots\dots\dots (7.13)$$

Where V_k is the frequency, $X(t)$ is the water quality data at time t and T is the total time period.

The power spectral density $f_x(\lambda)$ is an infinite Fourier series representation of the auto covariance function (The Fourier Transform)

$$f_x(v) = \sum_{m=-\infty}^{\infty} R_x(m) e^{-2\pi i v m} \dots\dots\dots (7.14)$$

The auto-covariance function is then given as the inverse transform of the spectral density function:

$$R_x(m) = \int_{-1/2}^{1/2} f_x(v) e^{2\pi i v m} \dots\dots\dots (7.15)$$

The spectral density is therefore a measure of the auto covariance function. The area under the spectral density curve represents the total auto covariance of the data. The periodogram as defined earlier is the sample approximation of the spectral density function at a given frequency:

$$E(P_x(v_k)) = f_x(v_k) \dots\dots\dots (7.16)$$

The **Cross Spectral density function** is defined similarly:

$$f_{xy}(v) = \sum_{m=-\infty}^{\infty} R_{xy}(m) e^{-2\pi i v m} \dots\dots\dots (7.17)$$

Where, as before, the cross covariance function is given as the inverse transform of the cross-spectral density function.

Filtering

A water quality series may be transformed to achieve a certain spectral properties. For example high frequency variation may be removed from the data. This is generally (but not exclusively) achieved by applying a linear filter of the form:

$$Y(t) = \sum_{s=-\infty}^{\infty} a_s x_{t-s} \dots\dots\dots (7.18)$$

Where a_s is generally referred to as the impulse response function. The spectral properties of the transformed series $Y(t)$ is easily obtained through the convolution equation:

$$f_y(v) = |A(v)|^2 f_x(v) \dots\dots\dots (7.19)$$

Filter Design:

Since the impulse response function is difficult to obtain by integration using the inverse transform, the following approximation is employed.

$$a_t^M = M^{-1} \sum_{K=0}^{M-1} A(\omega_k) e^{2\pi i \omega_k t} \dots\dots\dots (7.20)$$

$$\omega_k = \frac{k}{M}, k = 0, 1, \dots \dots M-1$$

Where the value of t varies from $-M/2, \dots 0, \dots M/2$.

Tapering of the Impulse response Function:

The rippling effect of the impulse response function can be reduced by applying a cosine bell. This is done by replacing the impulse response function by:

$$a_t^M = h_t a_t^M \dots\dots\dots (7.21)$$

$$h_t = \frac{1}{2} \left[1 + \cos\left(\frac{2\pi t}{M}\right) \right]$$

Working out the Frequency Domain Regression:

For the relation $Y(t) = \sum_{s=-\infty}^{\infty} a_s X_{t-s}$ the solution for the frequency response function $A(v)$ which is the Fourier transform of the impulse response function is given by:

$$A(V) = \frac{f_{xy}(v)}{f_x(v)} \dots\dots\dots (7.22)$$

The impulse response function is then given as the inverse Fourier transform of the frequency response function:

$$a(t) = \int_{-1/2}^{1/2} A(v) e^{2\pi i v t} dv \dots\dots\dots (7.23)$$

Again since the above integral is difficult to evaluate, the discrete Fourier transform approximation described earlier is normally used.

The squared coherence function which is the measure of the correlation between $Y(t)$ and $x(t)$ is given by:

$$\gamma_{xy}(v) = \frac{|f_{xy}(v)|^2}{f_x(v)f_y(v)} \dots\dots\dots (7.24)$$

The squared coherence varies between 0 and 1.

7.7.1 Application of Spectral Regression between TDS and Conductivity – Kulfo River

Spectral analysis of TDS and conductivity was carried out on this modified data where a 1-lag moving average was employed as a suitable high pass filter. The resulting estimate of TDS from conductivity is shown in Figure 7.7.1.1 below. As is evident the graphs closely follow each other except at some points (low peaks) where the spectral relation appears to be weak.

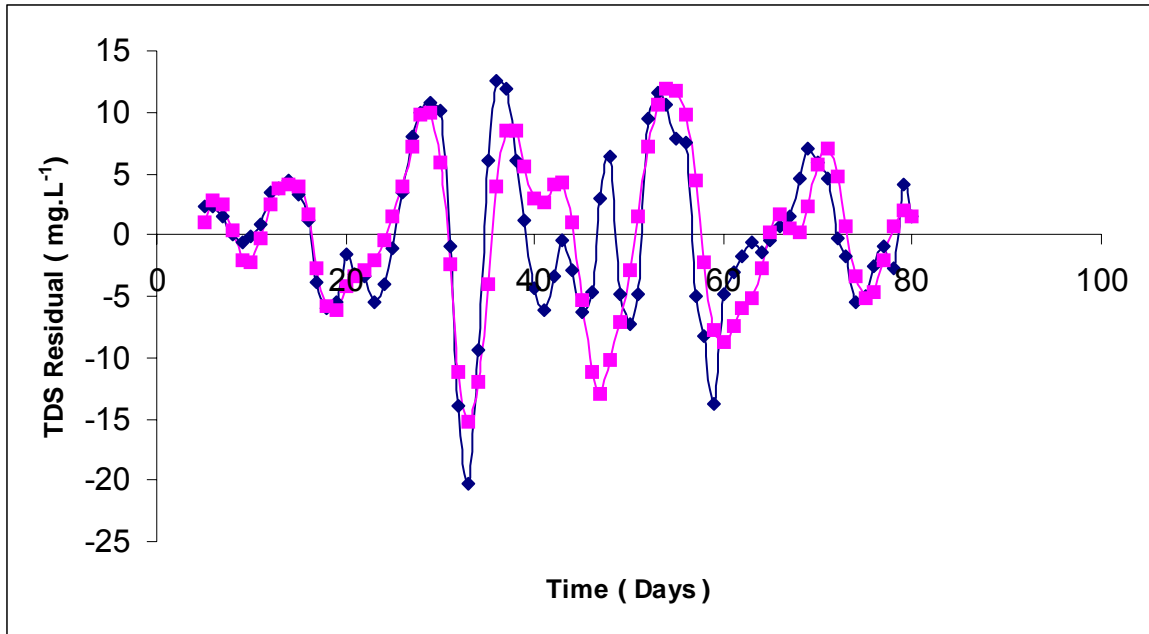


Fig.7.7.1.1 Estimate of TDS from Spectral Relation with Conductivity (ARIMA). TDS and conductivity are closely related by the ARIMA model.

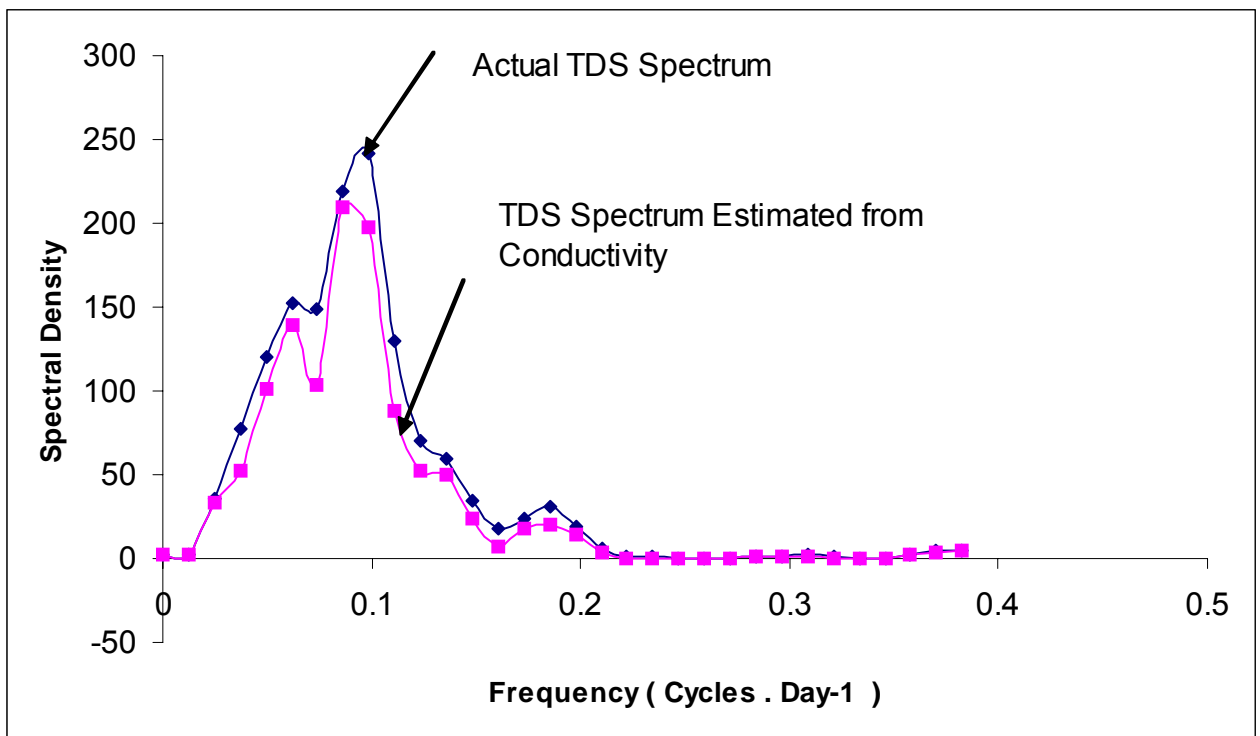


Fig.7.7.1.2 Actual and Estimated Spectral Density TDS from ARIMA model

7.7.2 Spectral Model of Total Solids and Rainfall

Figure 7.7.2.1 below shows comparison of the actual total solids data and that estimated from rainfall data. The two curves are related but not well matched. Three reasons are suspected. First the rainfall data is not sufficiently representative the data being collected from the station at AWTI. Second the total solids laboratory test results have higher standard deviation. Third the length of the data record may not be adequate.

Therefore for want of a better relationship between these two variables it is essential:

1. To select representative rainfall station data
2. To include discharge measurement data
3. To take longer length of data record

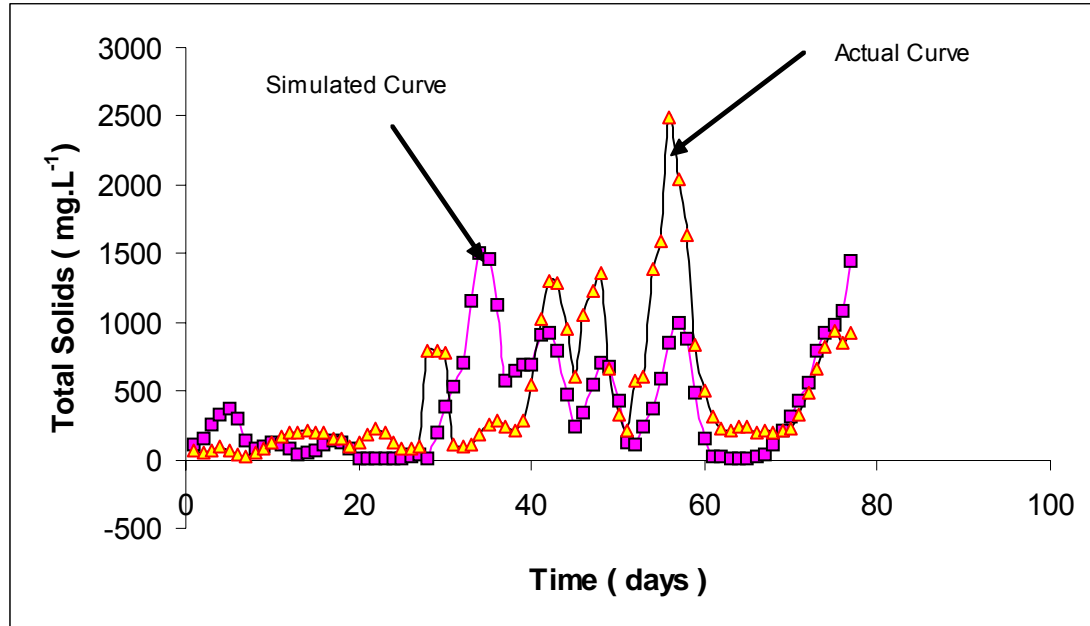


Fig. 7.7.2.1 Actual and Simulated Total Solids Curve

The principal component analysis carried out among the water quality data indicated that the total solids and rainfall were related but only slightly (Numbers 16 and 17 of figure 7.7.2.2).

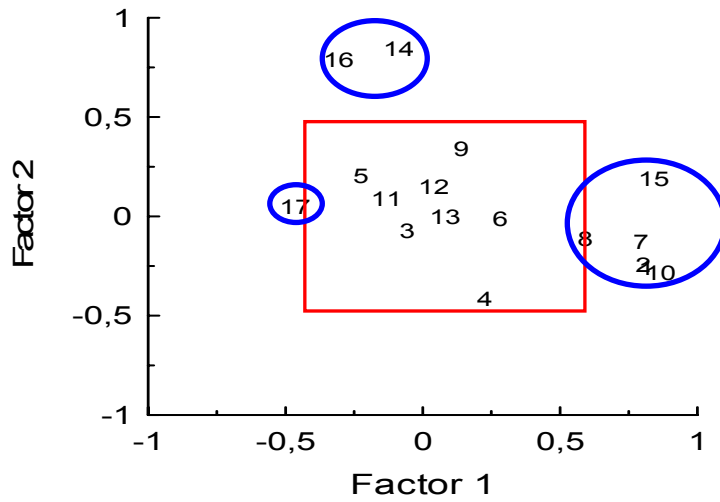


Fig. 7.7.2.2 Factor Loadings from principal Component Analysis

If all the four factors mentioned above are taken in to account in data analysis better relationship might be obtained in terms of the factor scores of these two variables.

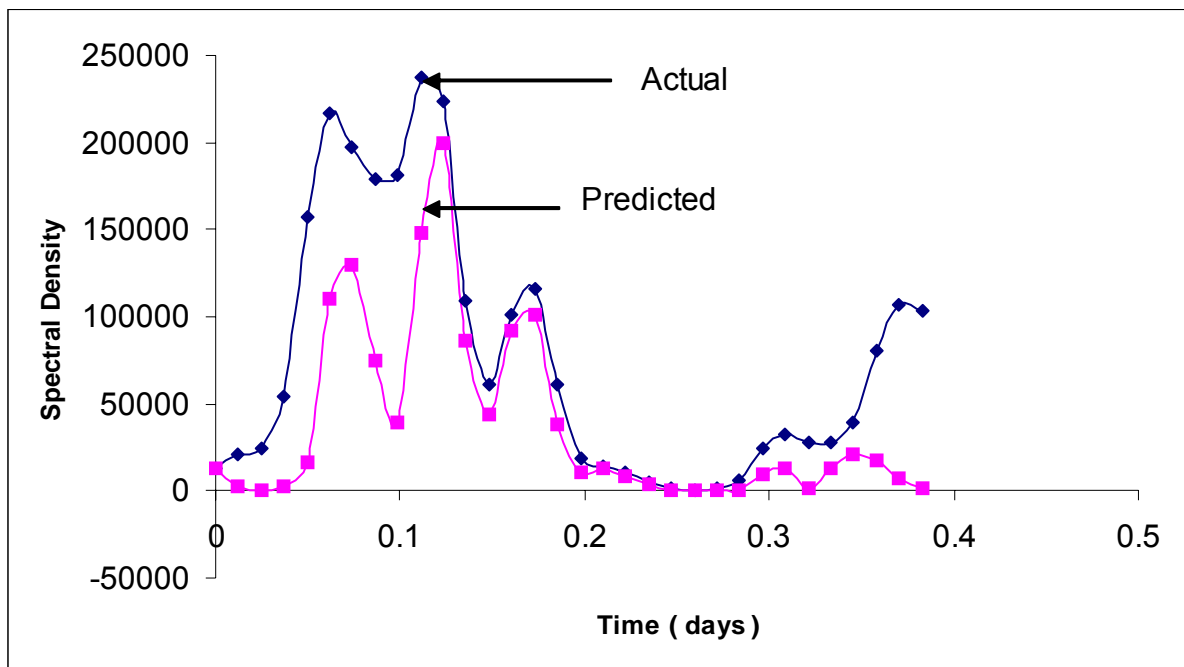


Fig. 7.7.2.3 Estimated Spectrum of Total Solids from Rainfall

7.8 MODELLING USING THE STATE – SPACE METHOD

The general form of the multivariate state – space model involves assuming that the $r \times 1$ observation vector (y_{t1}, \dots, Y_{tr}) can be written in the form of the observation equation [81]

$$Y_t = A_t X_t + V_t \dots \dots \dots (7.25)$$

The state equation, which is not observed, is given by

$$X_t = \phi X_{t-1} + W_t \dots \dots \dots (7.26)$$

The general mean- squared covariance matrix of the estimator is denoted by

$$P_{tt}^S = E[(x_t - X_t^s) (X_u - X_u^s)' | Y_1, \dots, Y_s] \dots \dots \dots (7.27)$$

The Kalman Filter Recursion

The calculation of the kalman filter estimator proceeds by forward recursion

$$X_t^{t-1} = \Phi X_{t-1}^{t-1}$$

$$X_t^t = X_t^{t-1} + K_t (Y_t - A_t X_t^{t-1})$$

The weight or gain matrix K_t is defined as:

$$K_t = P_{tt}^{t-1} A_t' (A_t P_{tt}^{t-1} A_t' + R)^{-1}$$

Where the covariances are updated recursively using the recursions

$$P_{tt}^{t-1} = \phi P_{t-1, t-1}^{t-1} \phi' + Q$$

$$P_{tt}^t = P_{tt}^{t-1} - K_t A_t P_{tt}^{t-1} \quad \text{with } P_{00}^0 = \Sigma$$

If the estimator is to be based on all the data Y_1, \dots, Y_T we need the Kalman smoother estimators. These can be developed solving successively the backward recursions for $t = T, T-1, \dots, 1$ using the equations:

$$X_{t-1}^T = X_{t-1}^{t-1} + J_{t-1} (X_t^T - X_t^{t-1}),$$

$$J_{t-1} = P_{t-1,t-1}^{t-1} \phi'(P_{tt}^{t-1})^{-1}$$

The mean square error covariance for the smoothed estimator satisfies the recursions

$$P_{t-1,t-1}^T = P_{t-1,t-1}^{t-1} + J_{t-1} (P_{tt}^T - P_{tt}^{t-1}) J_{t-1}'$$

The regression estimators are given by:

$$\phi(i+1) = S_t(1) [S_{t-1}(0)]^{-1}$$

$$Q(i+1) = T^{-1} \left\{ S_t(0) - S_t(1) [S_{t-1}(0)]^{-1} S_t'(1) \right\} \dots\dots\dots (7.28)$$

$$R(i+1) = T^{-1} \sum_{t=1}^T \left[(Y_t - A_t X_t^T) (Y_t - A_t X_t^T)' + A_t P_{tt}^T A_t' \right]$$

Where $S_t(J) = \sum_{t=1}^T (P_{t,t-j}^T + X_t^T X_{t-j}^T)$

The overall procedure can be regarded as simply alternating between the Kalman filtering and smoothing recursions and the multivariate normal maximum likelihood equations. The iterative procedure is summarized as follows:

1. Initialize μ_0, ϕ_0, Q_0, R_0 and fix Σ
2. Use the Kalman recursions to calculate X_t^T, P_{tt}^T and $P_{t,t-1}^T$
3. Evaluate the log likelihood
4. Update parameters to μ_1, ϕ_1, Q_1, R_1
5. Return to step 2.

7.8.1 Application of State – Space Model between Sodium and TDS – Kulfo River

The relationship between sodium and TDS was found to be approximately linear with squared correlation coefficient of around 0.7. This approximate linear relationship is not adequate to explain local variation and periodicity of the data. A more accurate estimate of the sodium data from conductivity data was attempted by the application of the method of state-space modeling.

First the conductivity and sodium data were regressed and the linear relationship was established:

$$C(t) = 16.796329 * S(t) - 5.537829 + V(t) \quad \text{and} \quad R^2 = 0.62 \quad (\text{squared coefficient of regression})$$

Where C (t) is the conductivity and S (t) is the sodium concentration.

The variance s_v^2 was recorded to be 518.322

Next the variable C (t) of conductivity was transformed to $C'(t)$ so that

$$C'(t) = S(t) + V(t) \dots\dots\dots \text{The observation equation}$$

$$C'(t) = \frac{C(t) + 5.537829}{16.796329}$$

The transformed variance will be

$$S_v'^2 = \frac{518.322}{(16.796329)^2} = 1.83726$$

The sodium data was modeled with auto Regressive model of order 3 (AR (3)) with the resulting equation:

$$S(t) = 0.89376 C(t-1) - 0.536256 S(t-2) + 0.216 S(t-3)$$

With variance of $S_w^2 = 0.9545403$ and $AIC = 240.549$

The variance ratio $\frac{S_w^2}{S_v^2} = \frac{0.95454}{1.83726} = 0.5195$ is used for constraining the state – space solution.

The state space model then will be:

$$C'(t) = [1, 0, 0] \begin{bmatrix} S(t) \\ S(t-1) \\ S(t-2) \end{bmatrix} + [V(t)] \dots \text{The observation equation}$$

$$\begin{bmatrix} S(t) \\ S(t-1) \\ S(t-2) \end{bmatrix} = \begin{bmatrix} \phi_1 & \phi_2 & \phi_3 \\ 1 & 0 & 0 \\ 0 & 1 & 0 \end{bmatrix} \begin{bmatrix} S(t-1) \\ S(t-2) \\ S(t-3) \end{bmatrix} \dots \text{The state equation.}$$

The state – space model resulted in virtually the same model as the previous AR (3) model of sodium. Since the starting value in the state space model is a random variable the curves were adjusted by a median coefficient. Figure 7.8.1.1 shows a comparison between the actual data and the state – space estimate of the sodium – conductivity model.

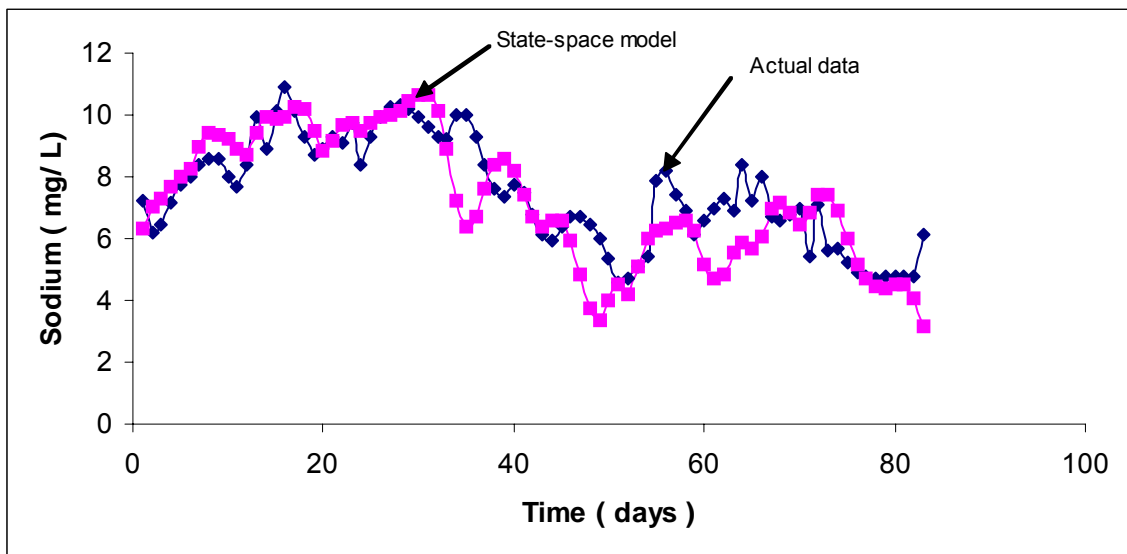


Fig. 7.8.1.1 State - Space Model of Sodium Data from Conductivity data. The conductivity is

taken as the space data and Sodium is represented by the state-space equation developed from previous data. Since both variables display long term variation, the model gives close fit to the actual data.

7.8.2 Estimation of Water Quality of River Hare from Kulfo Data using State – Space Method

The procedure of estimation of the water quality between these two rivers is the same as that used above in the intra- river water quality estimation. Here the water quality of Kulfo River is taken as the observed data and the Hare river water quality data is represented as a state variable. The variance ratio between the state variable and the observed variable is established beforehand using existing data and estimate of the Hare river water quality of future data is obtained by the state space relationship constrained further by variance ratio established in advance.

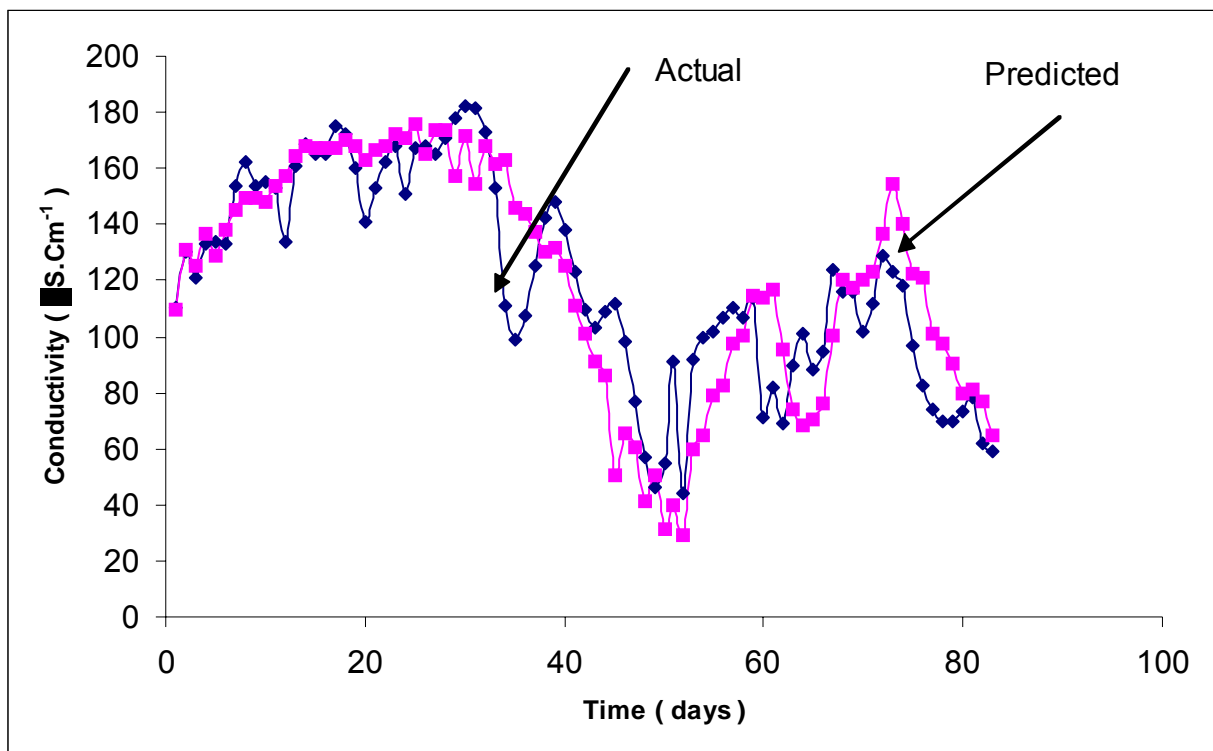


Fig. 7.8.2.1 Prediction of Conductivity of Kulfo River from that of Hare River by State Space methodology

Figure 7.8.2.1 shows a comparison of the conductivity of Kulfo River as obtained from that of The Hare River using the state-Space modeling and the actual data. As can be seen the estimate is closer to the actual data. The state – space model is a

suitable model for integrating regional water quality information. Similar model can be used for transferring information of intra as well as inter-river water quality information.

7.9 DISCHARGE BASED CONTAMINANT MODELING

The discharge-based contaminant modelling approach employs the contaminant-rating curve, in which the correlation between discharge and contaminant concentration is directly considered. In this case the sparse concentration data are first used to estimate the contaminant-rating curve. The contaminant-rating curve is then used to extrapolate concentrations for periods of observed flow when concentration data are not available [82, 83, 84, 85, 86].

The rating curve generally takes the power (log-log) form.

$$C(t) = a Q^b \quad (7.29)$$

Where a and b are regression coefficients dependent upon stream conditions. The flow weighted mean concentration determined using the rating curve approach can now be determined using:

$$\bar{C}_Q = C_o \int_0^\infty Q^{*(i)b+1} f(t) dt \quad (7.30)$$

Where $C_o = C(\bar{Q})$, or, for a finite number of discharges, $m \gg n$:

$$\bar{C}_Q = \frac{C_o}{m} \sum_{i=1}^m [Q^{*(i)}]^{b+1} \quad (7.31)$$

Method of Moments

The method of moments can be used in conjunction with the rating curve to determine the flow-weighted mean concentration. The use of discharge moments is preferred due to the greater availability of discharge observations. One notes that [82, 83, 84, 85, 86]:

$$\bar{C}_Q = C_o \int_0^{\infty} [Q^*(t)]^{b+1} f(t) dt = C_o E\left[[Q^*(t)]^{b+1}\right] \quad (7.32)$$

so that the objective reduces to the determination of the expected value of normalized discharge raised to an arbitrary power. Appendix 7.5 - 7.8 show how a Taylor series expansion can be used to determine the expected value:

$$E\left[[Q^*(t)]^{b+1}\right] = 1 + \frac{b^2 + b}{2!} M_2 [Q^*(t)] + \dots + \binom{b+1}{n} M_n [Q^*(t)] + \dots \quad (7.33)$$

Where

$$\binom{u}{v} = \frac{u!}{(u-v)! v!} \quad (7.34)$$

And $M_n [x]$ is the nth moment of x about the mean. It is clear that:

$$E \left[\left(Q^*(t)^{b+1} \right) \right] = 1 \text{ if } b = [-1, 0] \quad (7.35)$$

Which implies that an unbiased estimate only results if there no - or an inverse – relationship between discharge and concentration. This formulation does not converge rapidly for values of $b \gg 1$ and for random variables whose higher moments do not approach zero. The method of moments is commonly employed using only the first two moments (Gilroy et al., 1990), but this ignores the influence of non-zero higher-order moments.

7.9.1 Application of Discharge Based Contaminant Modelling to Kulfo River

7.9.1.1 The Rating Curve Equation (Kulfo River)

Linear regression analysis was done on the log-transformed discharge – Turbidity data of Kulfo River using SPSS statistical software version 12.0. The outliers from the data were removed by case wise diagnostics using studentised residuals. The power equation relating turbidity with discharge for Kulfo River becomes:

$$T = 2.780 Q^{1.489}$$

The coefficient of determination (R^2) after outliers have been removed comes to 0.74. The cumulative normal probability plot shows the residual falling approximately on the normal line. The plot of residuals against predicted value also shows no systematic variation of the residuals with respect to the predicted values.

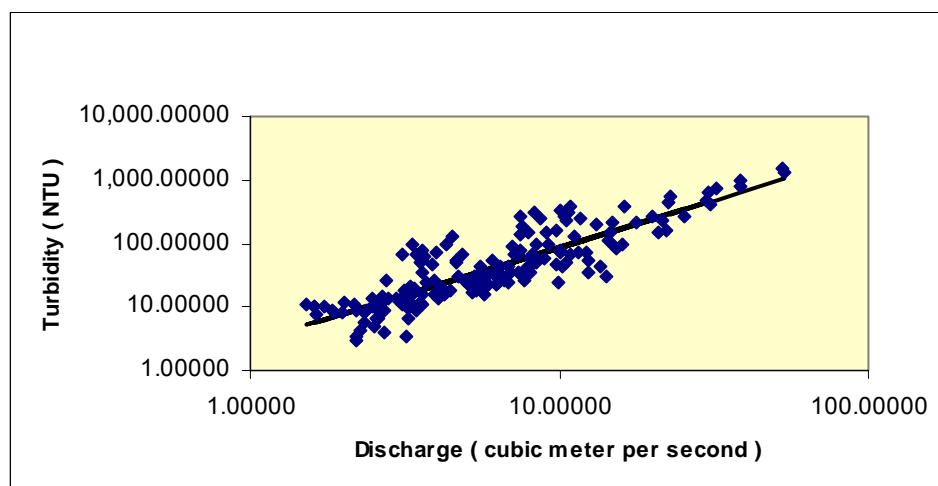


Fig. 7.9.1.1.1 Regression of Turbidity on Discharge - Kulfo River

7.9.1.2 Conversion of Turbidity Load to Suspended Solids Load

Turbidity is approximately related to suspended solids [87]. There is a statistically significant relationship between Turbidity and Suspended solids data for river Kulfo (with coefficient of determination, R^2 of 0.97). The equation for Converting turbidity data to suspended solids data is given by:

$$SS = -12.0694 + 2.2634 * T + 0.00273 * T^2$$

Where SS is the suspended solid in mg L^{-1} and T is the turbidity in NTU.

Using the above equation, the turbidity data have been converted to the corresponding suspended solids in order to calculate the solids loading.

7.9.1.3 Calculation of the moments in Taylor Series and of Bias

The moments about mean of the normalized discharge were calculated for the total data ($N = 219$) as well as for each of the one-month data. It is seen that there is a convergence problem for the total data. This problem almost disappears for the one-month data. The calculation for the first one-month data is given in the Appendix 7.6.

7.9.1.4 Transfer Function for Solids Loading Calculation

As a result of the extremes of discharge and turbidity occurrences and the failure of the rating curve function to include these values, there is a deviation of the calculated solids load from the actual [88]. However, the plot of the calculated versus actual solids load follows a definite pattern. This implies that it is possible to estimate the actual solids load from the calculated one obtained solely from discharge data. The availability of longer periods of discharge data makes this approach useful, as it is possible to simulate the solids load from the discharge data alone.

Figure 7.9.1.4.1 shows the transfer functions obtained by regression analysis for the arithmetic mean flow approaches. A simple parabola suffices to obtain the regression curve. S_a is the actual load while S_c is the calculated theoretical load in the transfer function given in figure 7.9.1.4.1.

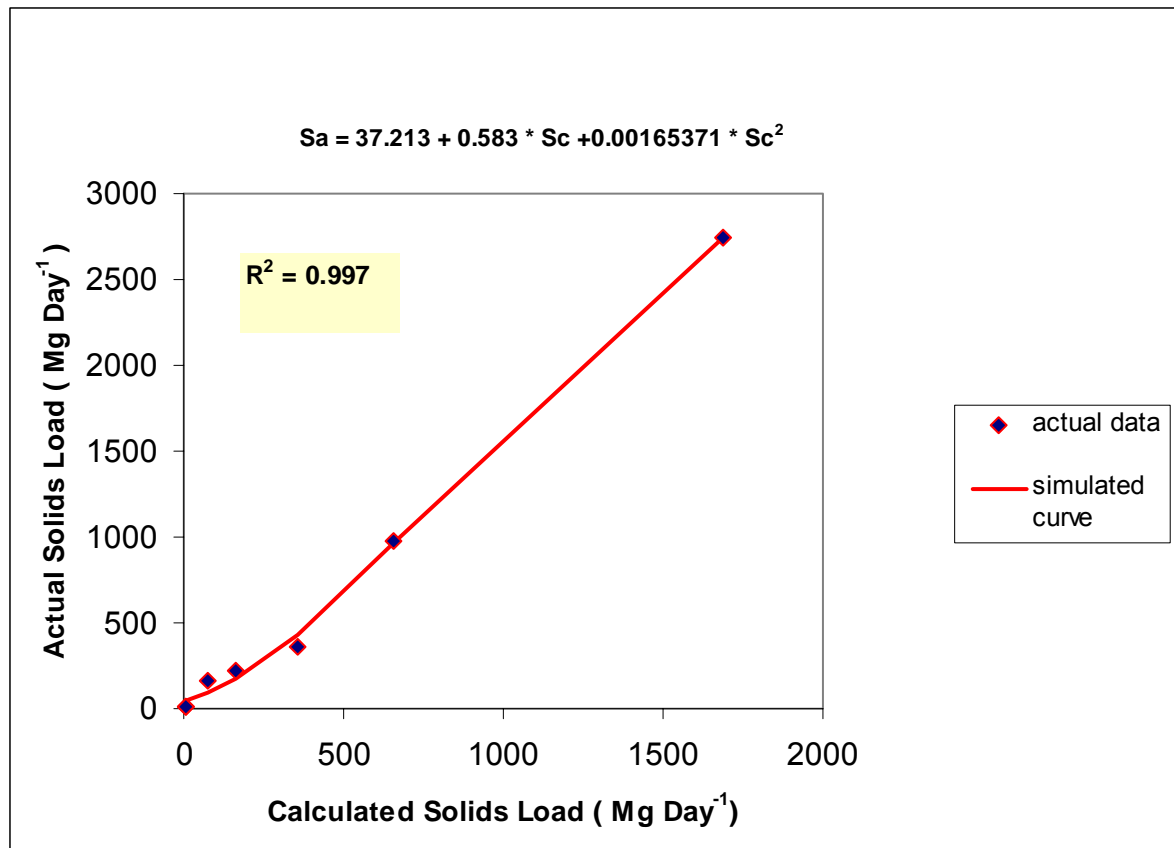


Fig. 7.9.1.4.1 Solids Load Transfer Function Simulated. Arithmetic Mean Flow and Turbidity - Kulfo River. Despite the data variance there is a good correlation between observed data and the values estimated by the model.

7.9.1.5 Mean Daily Solids Loading Flow from River Kulfo

Based on the transfer function generated, the simulated mean daily solids load are plotted in figure 7.9.1.4.2 for each month. Similar calculation and simulation can be done for weekly and other periods from discharge data alone based on established rating curve calculation. Table 7.9.1.5.1 summarizes the load calculation - actual versus theoretical.

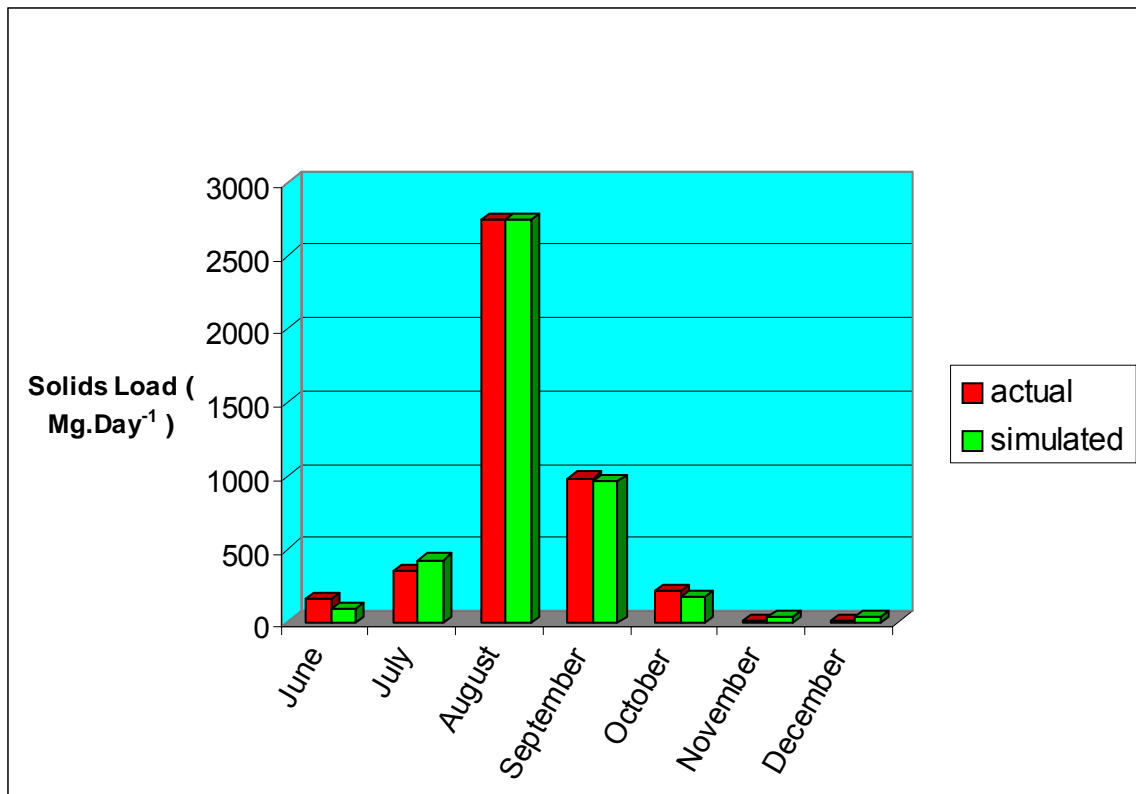


Fig. 7.91.4.2 Simulation of Mean Daily Solids Flow River Kulfo (based on Arithmetic Mean)

Table 7.9.1.5.1 Solids Load Calculation Figures using Arithmetic Mean Flow and Turbidity Data

Month	Arithmetic Mean Flow (m ³ .Day ⁻¹)	\overline{CQ} (NTU)	Theoretical Solids Load (Mg Day ⁻¹)	Actual Solids Load Mg Day ⁻¹	Simulated Solids Load (Mg Day ⁻¹)	Theoretical Bias	Actual Bias
June	6.09	64.12	75.91	162.09	90.72	1.57	1.65
July	10.69	148.46	354.84	355.36	424.54	1.57	1.54
August	15.54	383.15	1685.69	2742.00	2742.63	2.32	2.06
September	11.68	230.05	659.09	982.54	961.92	2.13	1.55
October	7.95	98.09	162.33	216.17	172.77	1.61	1.66
November	3.32	17.65	8.24	7.72	42.13	1.06	1.08
December	2.70	14.30	4.86	8.94	40.09	1.17	1.35

7.10 MODELLING SOLIDS WITH TURBIDITY AND ABSORPTION MEASUREMENTS

7.10.1 Problem with Measurement of High Turbidity

The box plot in figure 7.10.1.1 shows how the scaled up value of turbidity resulted in a wide scatter when the dilution level is varied. Different samplers working at different dilution may then report turbidity values that show such extremes of variations.

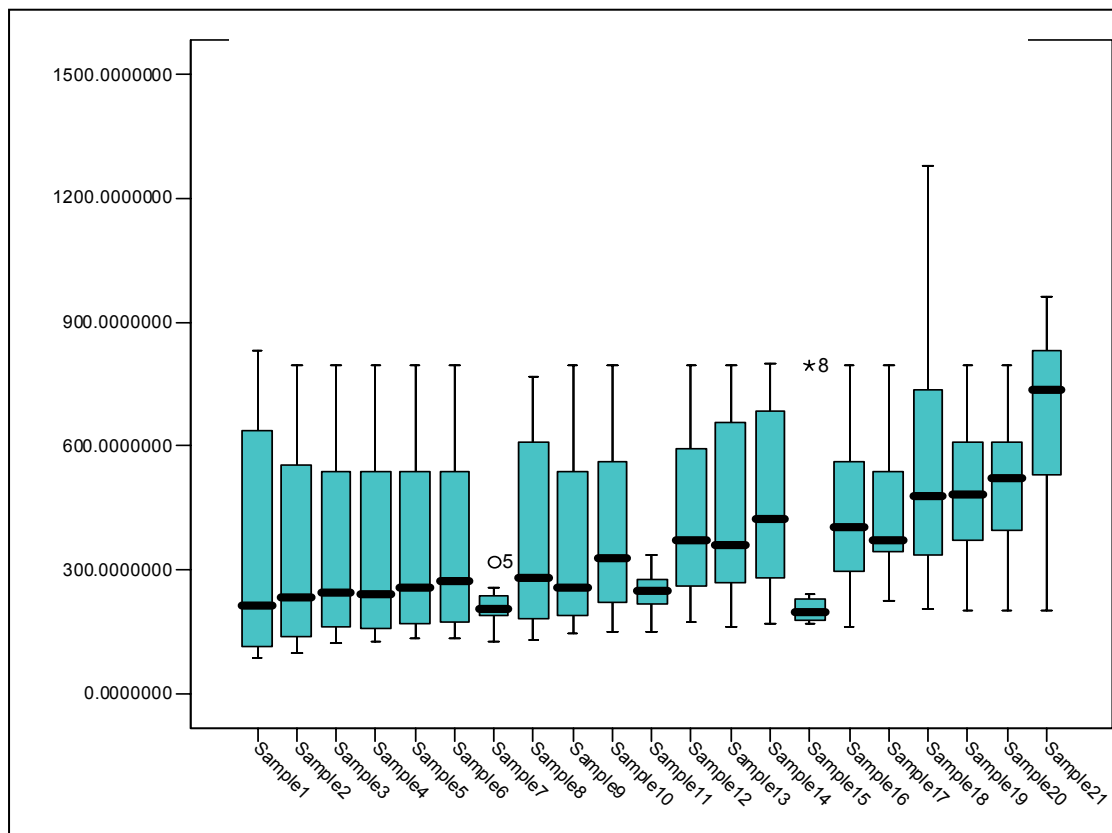


Fig. 7.10.1.1 Box Plot of Turbidity determined by several levels of Dilution

7.10.1.1 Linearity Check for Turbidity

When one looks at the plot of the turbidity at several levels of dilution, such plots contain curvature. Figure 7.10.1.2 below displays the erratic deviation of the values of turbidity from the supposed assumption of a liner variation. Furthermore, higher concentration readings grossly understate the turbidity values. Readings below 80-100 NTU approximately fall on straight line most of the times. Reading beyond this limit underestimated the turbidity reading.

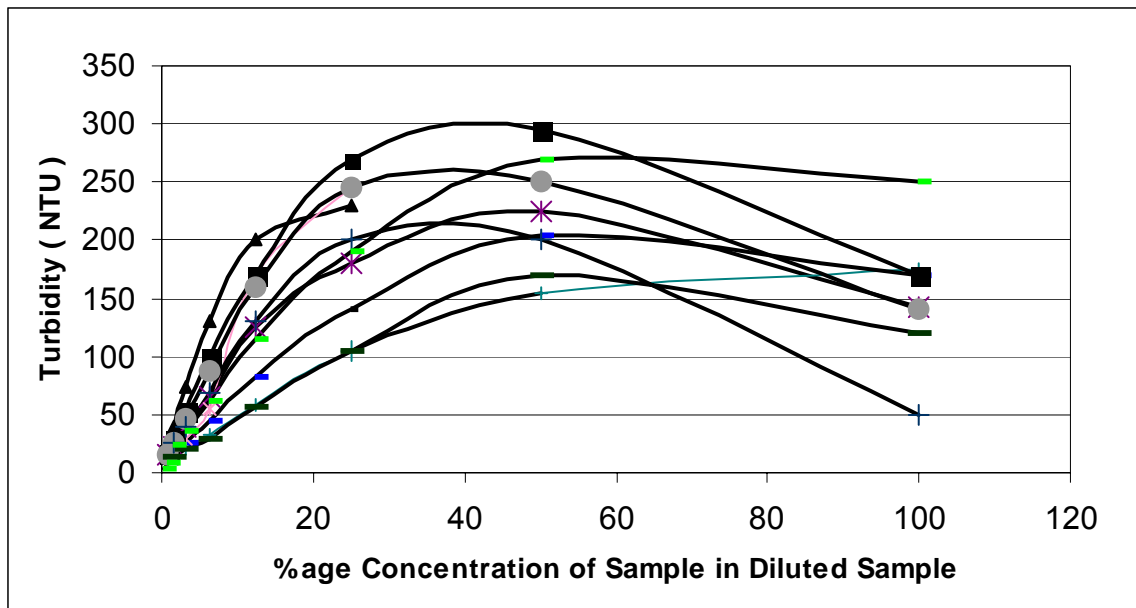


Fig. 7.10.1.1.2 Turbidity versus Concentration Graph- Kulfo River. The Measurement of Turbidity by dilution shows non-linear behaviour when the reading exceeds 80-100 NTU. Dilution of Sample must be sufficient to bring the Turbidity reading of the diluted sample to below 100.

7.10.1.1 Modes of solution to the Problem of Measuring High Turbidity

1. Regression Analysis using multiple dilution
2. Preparation of Concentration Charts and Reading Values from the charts for a specific water source.
3. Determination from a best Dilution level known from previous data to give values close to the actual value determined by method 1 above.

For both sources of samples from rivers Hare and Kulfo, the optimum concentration level was found to lie in the ranges given in table7.10.1.2.1

Table 7.10.1.2.1 Turbidity Optimum Sample Concentration Level for Measurement by dilution

Turbidity	0-100	100-300	300-600	>600
Concentration of Sample	100%	50%	25%	12.50%

Therefore, a dilution that corresponds with the anticipated turbidity given in table 7.10.1.2.1 can be chosen and the measurement be scaled up afterwards. A dilution reading that falls between 50 and 100 is the optimum range for scaling up.

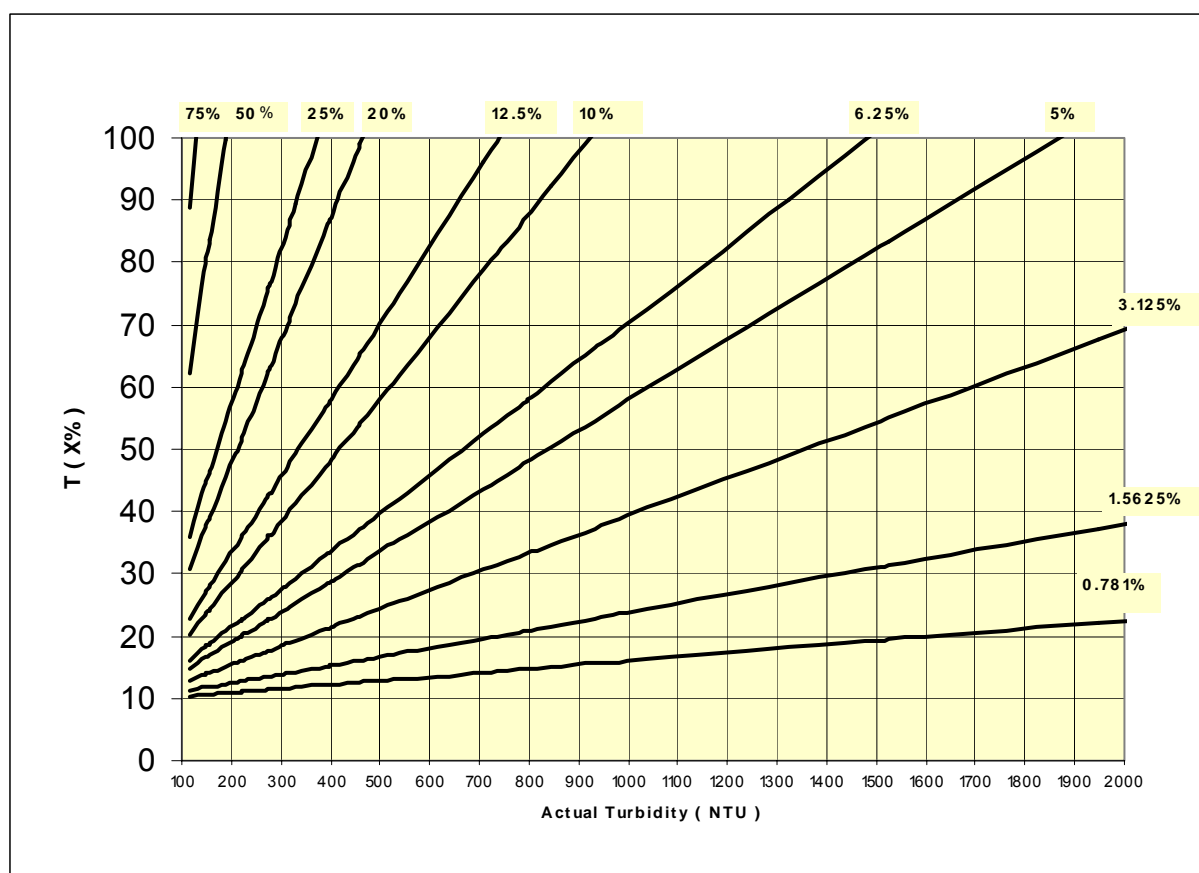


Fig. 7.10.1.2.1 Turbidity Reading Chart - River Kulfo

7.10.2 Modelling Solids with Absorption Measurements

Spectrophotometric absorption measurements due to suspended solids were carried out on rivers Hare and Kulfo water samples at different times. These measurements were compared with simultaneous measurements of turbidity and suspended solids. The results show that there is a good correlation between absorption measurements and that of turbidity and suspended solids. Absorption and turbidity measurements

show closer fit with coefficient of determination of 0.99 ($R^2 = 0.99$). Absorption and suspended solids measurement show a good fit with coefficient of determination of 0.97 ($R^2 = 0.97$). The curve relating absorption (as the x-variable) with suspended solids (as the y-variable) is a parabola where the slope increases at higher suspended solids. The relationship shows tight cluster of stream data near the origin and wider spread higher on the axes. This relationship that shows scatter at high-suspended solids is, however, probably due to natural variability in suspended solids size, shape, and composition as well as watercolor. Moreover, due to the low precision of measurement of suspended solids at low values of suspended solids (i.e. 60 mg L^{-1}) in this study, prediction of lower values of suspended solids from absorption measurements also had had higher margins of error. Such errors, however, could be reduced with the availability of better precision equipment for suspended solids measurement.

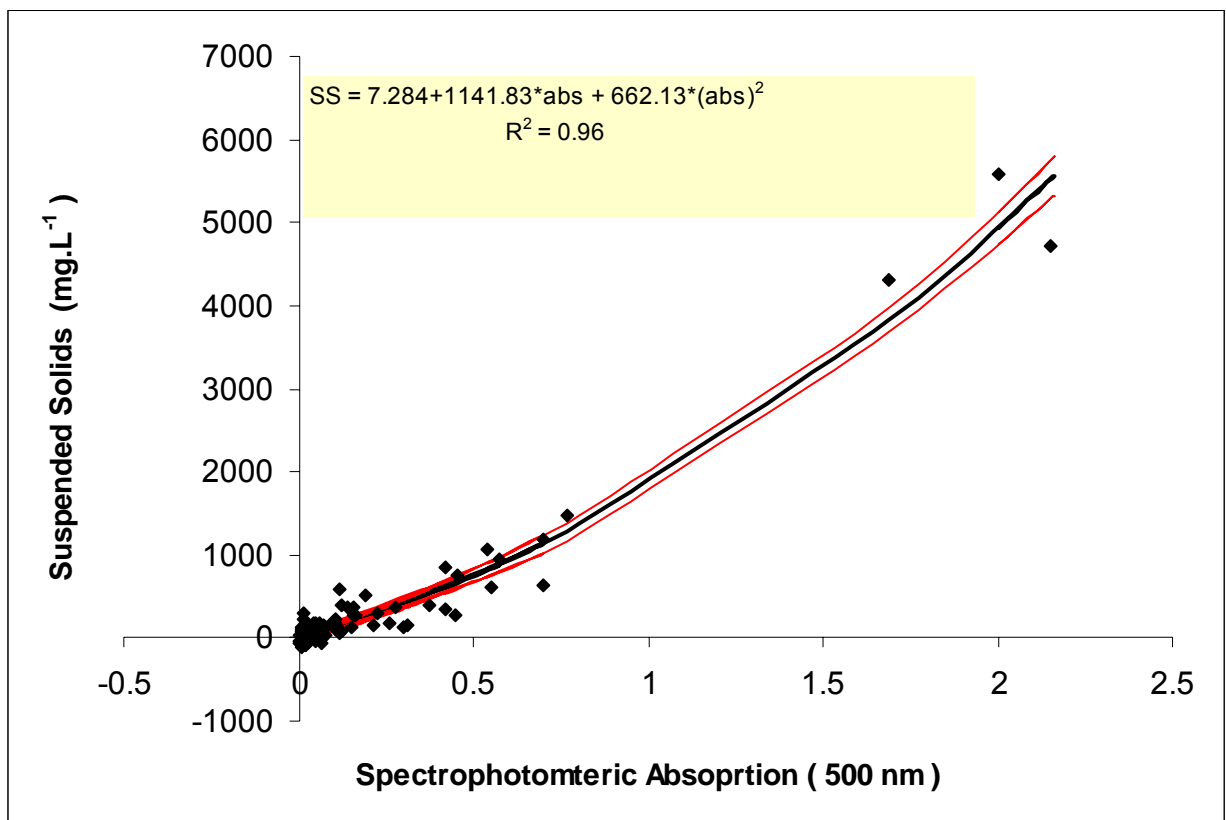


Fig. 7.10.2.1 Polynomial Regression of Suspended Solids on Absorption with 95% Confidence Limits - Kulfo River

The advantages of Absorption Measurement over turbidity for Solids Modelling lies in the fact that higher solids load absorption measurements display linearity at several levels of dilution (figure 7.10.2.2). Therefore, determination can be done with a single

dilution unlike turbidity, which requires several dilutions whose results should fall on straight line. The disadvantage of absorption measurement lies in the fact that it is less sensitive to low solid concentration.

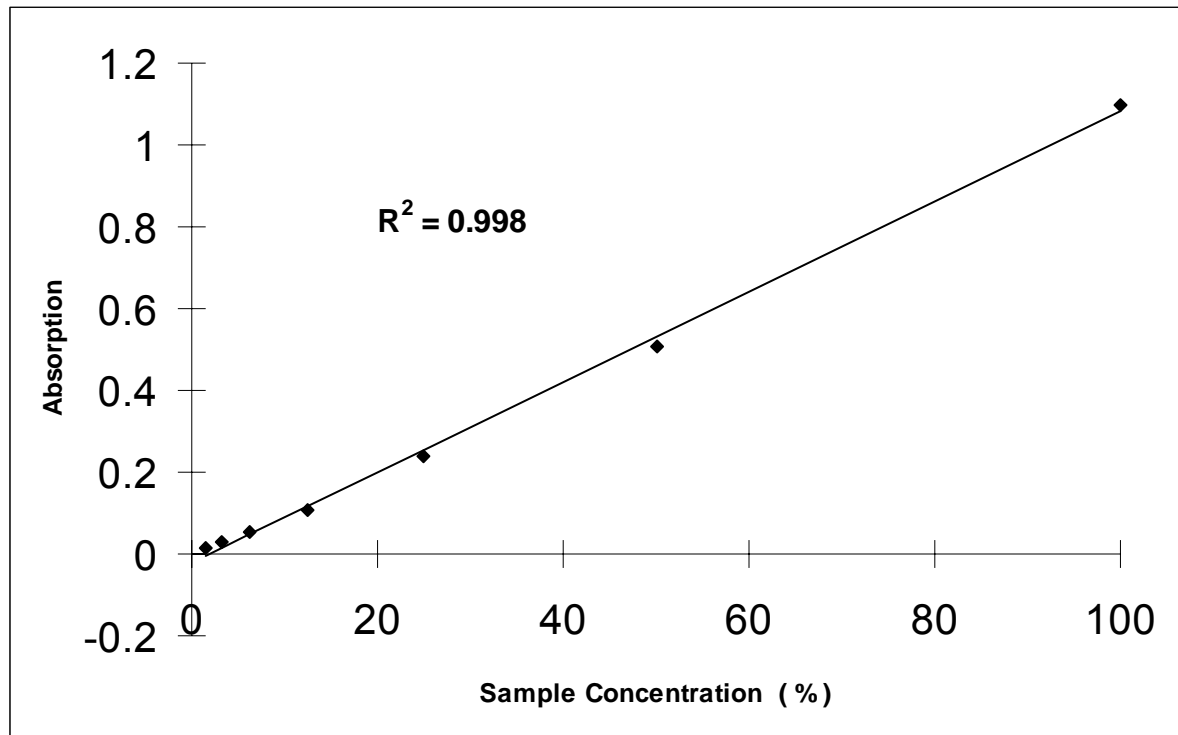


Fig. 7.10.2.2 Linearity of Absorption Measurement by Dilution

7.11 Modelling Settling Characteristics of Solids

Suspended Solids are present in varying quantities in the Rivers Hare and Kulfo throughout the year. The settling characteristics of the solids depend on the proportions of the different particle sizes present both organic and inorganic in the rivers. The two rivers being tributaries to the lakes Abaya and Chamo, their solids size gradation influence the physical properties of the lakes: lake turbidity, lake volume (through sedimentation) as well as biological properties such as growth of plants limited by lack of light penetration in turbulent parts of the lakes. The fate of suspended load includes deposition that causes siltation problems in rivers or channels, which may require dredging. A precise modeling of the time series of settlement characteristics of solids enables better design of water treatment facilities such as ponds, sedimentation tanks and filters.

This study showed how by a simple laboratory procedure of depth measurement of absorption with time, it was possible to determine the settling characteristics of

suspended solids in rivers. Multiple regression analysis of settling data showed the settling rate was dependent not only on time but also on the initial suspended solids at the log-log scale.

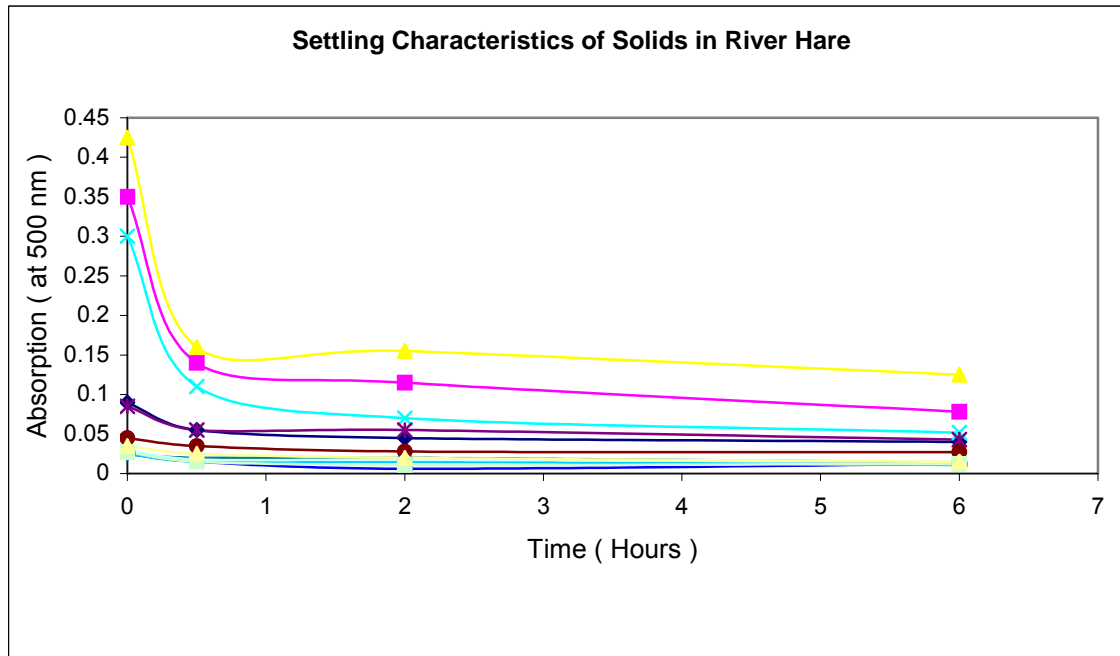


Fig. 7.11.1 Settling Characteristics of Solids in River Hare

Using this data and applying Stokes Law for discrete settlement it was possible to determine the percentage of clay and clay-silt present in the river suspended load. It was observed from the analysis of data that the percentage of fine actually decreases with an increased load of suspended load. This is due to the dilution effect of suspended solids that is in the form of fines. This also means that increased runoff does not result in the proportional increase of clay fines. The increment follows a decreasing trend. The result of the modeling the data of settlement suggests that the velocity of settlement of particles increases logarithmically with particle size.

Table 7.11.1 Regression Models of Settling Characteristics of Solids in Hare And Kulfo Rivers

River Name	Linear Logarithmic relation	Power Relation	R ²
Kulfo	$\log(C(t)) = -0.38115 + 0.848553 \cdot \log(C(0)) - 0.34088 \cdot \log(t)$	$C(t) = 0.4157 C_0^{(0.849)} \cdot t^{(-0.341)}$	0.89
Hare	$\log C(t) = -0.3258 + 0.933 \log(C_0) - 0.30059 \log(t)$	$C(t) = 0.4723 C_0^{(0.933)} \cdot t^{(-0.301)}$	0.92

Comparison of the settling characteristics of the two rivers Hare and Kulfo discloses that at very high loads, Kulfo has faster rate of removal of solids. At lower loads River Hare has a faster rate of settlement. However, the cutoff point at absorption value of 0.3 is so high that its cumulative probability of occurrence (the range from 0 to 0.3) is very wide. This implies the lower side of the cut-off point for which river Hare has a greater rate of settlement has a much greater rate of occurrence. On a wider scale both rivers appear to have similar percentage of fines at a given load of suspended solids. The results of settling study using absorption measurement cannot be, however, explicitly related to the corresponding solids removal. The reason lies on the change in particles size distribution during settlement, which changes the absorption characteristics. Therefore, a further study of the effect of size on absorption is required if the end results need to be stated in terms of suspended solids.

7.11.1 Settlement Characteristics of Rivers that are Tributaries to the Abaya – Chamo Lake System

Settling column test applied to samples taken from rivers tributaries to the two lakes Abaya and Chamo produced the settling characteristics curves below (after solids retained was converted to percentage). The upper four curves that had lower percentage remove are for the rivers: North Hamesa, Hamesa, Basa and Bishan Guracha. These are the rivers that drain from the high lands of the basin on the northern side and they contribute more to the appearance of Lake Abaya because of their low settling characteristics.

On the other hand, the curves on the lower side of figure 7.11.1.1 are for the rivers in the low lands. They have faster rates of settlement similar to the rivers Hare and Kulfo discussed in detail above.

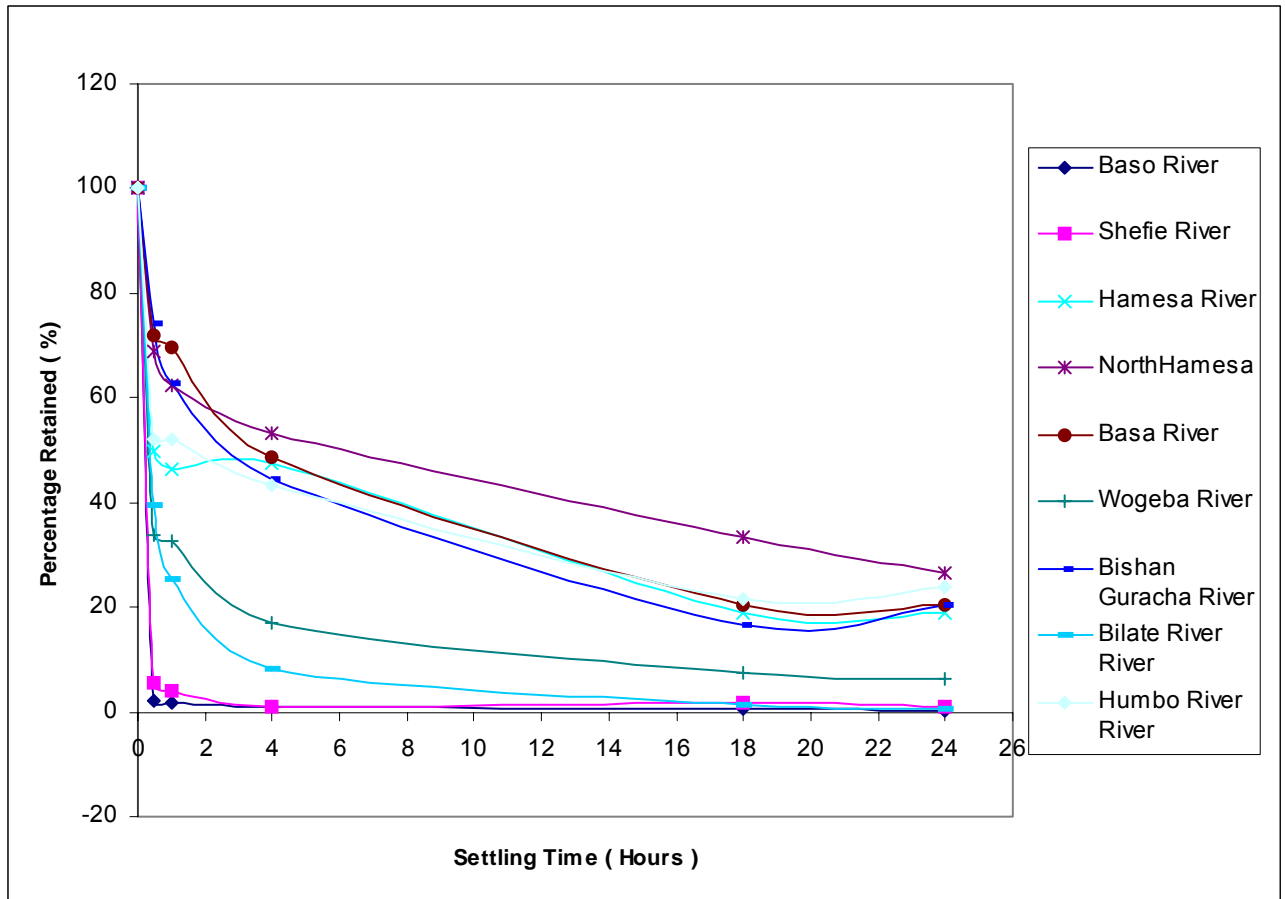


Fig. 7.11.1.1 Settling Characteristics of Rivers in Abaya - Chamo basin

Analysis of samples taken from rivers that are tributaries to the Abaya-Chamo lakes system showed that the rivers draining from the high lands that have a surface soil mostly composed of clay minerals have a lower rate of settlement. These rivers (Hamesa, Bishan Guracha, and Basa) contribute more to the reddish - brown appearance of Lake Abaya.

CHAPTER EIGHT**SUMMARY DISCUSSION**

S.No.	CONTENTS	PAGE
8.1	River Water Quality Assessment	296
8.2	Lake Water Quality Assessment	297
8.3	Ground Water Quality assessment	297
8.4	Water Quality Monitoring Design	299
	8.4.1 Development of Partial Orthogonal Physical Vector Model	299
	8.4.2 Monitoring Intervals (River Water Quality)	301
	8.4.3 Design of Lake Water Quality Monitoring System	302
	8.4.4 Ground Water Quality Monitoring	303
8.5	Water Quality Modeling	303
8.6	Management of Monitoring	305
8.7	Proposal for Future Improvements	307

8.1 RIVER WATER QUALITY ASSESSMENT

Water quality monitoring data for rivers Hare, Kulfo and Sile - which are part of the tributaries of the Abaya - Chamo Lake Basin in Southern Ethiopia, has been presented and the variability discussed. The water quality parameters are a function of the geo-chemistry of the catchments, hydrological events including atmospheric inputs and the catchment morphology where land use is a factor. The lower lying Sile River is characterised by increased alkalinity and salinity than the upper lying Hare and Kulfo rivers. The seasonal variation of the water quality parameters can be classified as mainly long-term seasonal variability or short-term rain induces surface flow based variability. Alkalinity and conductivity display distinct long term seasonal variation and low short frequency runoff induced variation. This similar variability is followed by calcium and hardness and to a lesser degree sodium and potassium. On the other hand Chloride, Solids, turbidity all display short-term variation mainly caused by surface flow runoff episodes.

The buffering capacity of the rivers and their alkalinity is negatively correlated with the sodium dominance ratio. Catchments with fewer ratios of Sodium ion release in to rivers retain more H^+ ion and nutrients such as NH_4^+ than catchments with lower ratio. The weathering rates for Rivers Hare and Kulfo were computed by normalizing the river discharges and solids load to their respective catchment areas. A plot of this normalized solids load against normalized discharge shows Hare river has greater rate of weathering than Kulfo River. Regional similarity between the water quality variables was tested by applying principal component analysis to the aggregate data of all rivers. It was found out that the principal components stay the same, which implies no new information has been added. Therefore, variables belonging to the same principal components were related. For example Chloride of Kulfo River belongs to the same principal component as Hare River and they are linearly related. Therefore, regional correlation among water quality variables is strongly suggested as part of monitoring optimization. This time series monitoring of water quality can serve as a basis of sampling and monitoring design as shown in this thesis in Chapter 5.

8.2 LAKE WATER QUALITY ASSESSMENT

Monitoring of the variation of water quality of the lakes Abaya and Chamo over the short term follows the seasonal precipitation pattern with Lake Chamo displaying significant variation in response to seasonal changes. Lake Abaya has a more stable concentration with limited response to the seasons. Due to the fact that Lake Chamo has been subject to flow reduction and decrease in water level the impact of seasonal water quality changes has become significant and may affect the lake ecology as such. Comparison of seasonal variation with longer-term data records show that both lakes are being subject to increased salinity although Lake Abaya shows only a moderate increase. Examination of the different contributing factors points to decreased flow and the global climate regime change as being the probable cause of the salinity increase followed by increase upper catchment use of the tributary rivers' water. Since Lake Chamo depends on the outflow from Lake Abaya for its water level as well as chemical balance and since this overflow has ceased to exist, Lake Chamo has been subjected to decrease in water level and increase in salinity for a longer period. Some observations have pointed to sediment deposits at the mouth of Lake Abaya's overflow acting as barrier and inhibiting the overflow [96].

The nutrient and chlorophyll measurements characterise both lakes as eutrophic. Dissolved oxygen measurement fall below 3 mg L^{-1} in Lake Chamo in the dry season with simultaneous loss of phosphorous. This condition may have been caused by algal death and respiration and may lead to increased concentration of ammonia and nutrients through internal recycling. Cynobacteria, species normally abundant in Lake Chamo may find this condition suitable. The increase in nitrogen and sulphate as well as ammonia in both lakes over recent years might be due to pollution from the catchment rather than internal recycling and this cannot be conclusively stated, as past measurements of inflow river water quality measurements are not available. Pollution assessment of the tributary catchment shall be undertaken as part of a water quality-monitoring program for the lakes.

8.3 GROUND WATER QUALITY

8.3.1 Ground Water Chemical Characteristics

In general the chemical composition is largely of the bicarbonate-calcium-magnesium type, which is typical of the basaltic parent rock formation of the area. There is a general inverse correlation of the dissolved constituents with elevation in the area. The increase in chloride concentration observed in some of the ground water samples is attributable to surface sources and evaporative conditions since aquifers are believed to contain little chloride material in them. On the other hand the increase in Sodium and potassium as well as Calcium at the lower lying deeper wells is expected since base cations generally increase with increase in the extent of ground water dissolution. For samples such as from Arbaminch university ground water, Korga and Ola-Mulato boreholes the alkalinity is greater than the hardness. Since these boreholes are located lowland the cation exchange process resulting in loss of calcium and Magnesium for sodium may be the cause. This argument goes well for Korga and Ola-Mulato wells, as they are located in clay rich regions of the upper catchment.

A piper trilinear plot of the ground water quality threw some light on the flow characteristic and the extent of evolvement of the dissolved chemical species in the samples. Some samples plot near surface sources such as rain with low Total dissolved solids indicating near surface flow conditions. Others such as Arbaminch springs plot near to the rivers Kulfo, Sile and Hare. This spring water has its source in the upland catchment and its chemical characteristics resemble that of the base flow river conditions. Therefore, there is a possibility that pollution from the sources may travel in much the same way as such pollution travel as subsurface flow and appear with the rivers base flow.

Many of the samples plot in the high calcium-Magnesium-Bicarbonate areas of the piper trilinear diagram. Few samples plot in the high sodium, potassium area indicating different recharge conditions as well as ion exchange processes resulting in the loss of hardness and gain of sodium and potassium.

8.3.2 Extent of Pollution of Ground Water Sources

The ground water sources investigated show direct pollution from human and animal wastes because of lack of appropriate protection (unprotected wells, open sources, rivers and springs) therefore posing immediate health dangers from water borne illnesses and nitrate interference in blood hemoglobin activity in infants. Such sources are identified by very high coliform counts as well as relatively high values of

nitrite. The aquifer characteristics in some ground water favored leaching of wastes from animal and human origins as well as possibly agricultural fertilizers showing high nitrate and phosphate as well as nitrite. Well protection measures must be taken including walling and capping of open wells, removal of toilets from near wells, fencing of wells and excluding animals and human wastes from around water sources, treatment of river water and even spring water sources with slow sand filters and management of application of fertilizers as well as locating wells away from areas of agricultural activities.

8.4 WATER QUALITY MONITORING DESIGN

8.4.1 Development of Partial Orthogonal Physical Vector Model

The application of principal component analysis to fifteen of the water quality data of river Kulfo show the first few components account for the majority of the data variation. 75% of the data variation can be accounted for by the first five principal components. The remaining principal components have Eigen values less than 1 indicating redundancy or dependent Eigen vectors. Subsequent Factor analysis with four factor accounts for about 2/3 of the data variance with many water quality variables sharing high communalities with the common factors and a few having greater uniqueness perhaps indicating the fact that they are being influenced by factors different from the main ones affecting most of the data variation.

The common factor with which most samples variables show larger change is factor I for both Hare and Kulfo rivers. Alignment of high loading of real factors, such air and water temperature indicates long term changes and reflects sufficient retention time in the sub-layer of the catchment for the interaction of flow within the sub soil. Depletion of small charged ions (H^+ , NH_4^+ , etc) is observed which is part of the cation exchange process with the soil matrix depending on the catchment's capacity for the exchange of these ions. The increase in alkalinity (largely HCO_3^-) and Sodium are part of these exchange processes. The relative dynamics between alkalinity and relative sodium dominance Index (SDI) of the river water during this time is a reflection of the catchment's buffering capacity and catchment sensitivity to release of nutrients and heavy metals, etc. Low lying rivers such as Sile River, display low sodium dominance and high buffering capacity than Kulfo which in turn shows more compared to river Hare that is located upland.

The other compounds showing variable association with this factor simply reflect the order of retention/release within the soil matrix. It is known that the soil matrix has an affinity for highly charged ions and more electro positive ions the order of retention $\text{Ca}^{++} > \text{Mg}^{++} > \text{K}^+ > \text{Na}^+$. This is reflected in the reverse order of their loading on factor

Factor 2 represents the rising portion of the flow curve as the river discharge considerably increases with this factor so also the rainfall. The extent of communality of rainfall is associated with its representativeness. This is not the case for river Kulfo as the record at AWTI weather station is less adequate to be strong factor for Kulfo River. Real weather parameters load poorly indicating short-term conditions associated with surface runoff and rain as well as high discharge conditions. Highly variant with factor is solid load and all particulate contaminants.

Factor 3 may represent the short term leaching effect as chloride, calcium and hardness increase. Rainfall and discharge have almost zero loading on this factor. On the other hand weather parameters are poorly loaded on this factor with water temperature showing negative loading indicating cold weather conditions. The fact that the loading of hardness, calcium and chloride are greater than that of Sodium on factor 3 may indicate the evaporative concentration of chemical introduced by rainfall events. Other compounds with short residence time in the soil upper layer are transported and show high loading with this factor. Low rainfall intensity on milder sloped catchments may have greater loading on this factor as both facilitate leaching flow as shown by high rainfall loading and low discharge loading on this factor for Kulfo River.

Factor 4 for Hare River may indicate the end of the leaching phase as shown by the increase in conductivity and higher loading on water temperature and also to a milder extent on air temperature. Rainfall is absent as expected and the solids loading is zero showing no differential change. This factor is represented by factor 3 for Kulfo River. There is a difference between these two rivers in terms of this particular common factor loading on pH. In general the pH variation on river Kulfo is associated very much with the bicarbonate alkalinity present. On the other hand for Hare River, pH shares less communality with alkalinity (bicarbonate alkalinity) and is loaded highly on factor 4. This high loading may be associated with the release of Carbon dioxide at periods of higher temperature due to increased bacterial activity within the

river stream and within the soil layer. Such carbon dioxide release increases the pH and has less effect on the alkalinity. In addition higher pH may be associated with other unspecified in stream pollution events and may require separate monitoring tasks.

In conclusion factor analysis with overlapping of real factors enabled a Partial Physical Orthogonal Vectors Model for the water quality variation and helped assess the response and sensitivity of the catchment to pollutant overload (i.e., how the catchment behaves to atmospheric and land deposition of pollutants, ex. Fertilizer, forest burning, acid rain, etc).

This model in future can be expanded by including greater number of variables, greater number of real factors thought to be relevant causes to water quality variation, (ex., fertilizer, forest cover, slope catchment, population settlements, sanitation, land uses and mal-practices such as forest burning,, etc), and by including greater number of monitoring sites at the same time. In addition point effluents, Precipitation chemistry analysis results can be incorporated in the model in order to integrate the atmosphere, anthropogenic influences to the water quality variation. This model can also be extended to lakes, springs, and ground water and even to piped water supply sources.

8.4.2. Monitoring Intervals (River Water Quality)

For group 1 variables, including conductivity, alkalinity, sodium, pH and Hardness there are two major peaks corresponding to monitoring frequencies of 2 months and 2 weeks. The optimum monitoring length is 2 weeks giving on average 85% of the variance information. A monitoring length of 1 month on average gives 75% of the information, which is more than adequate for the physical factor model interpretation, described earlier.

For group II variables, characterized by a high frequency peak events monitoring length needs to be much shorter or continuous monitoring approach needs to be adopted that will also allow auto correlative and cross correlative modeling. Turbidity monitoring, for example, with 2 days interval will only give 80% of the information. The optimum monitoring of 3 days interval will on average give only 75% of the information. Since particulate pollutants and pollutants adsorbed on to the soil

surface vary directly with solids content, at least, some of these variables need to be monitored continuously. This requirement goes well for discharge, turbidity (solids) and rainfall as well. Rainfall measurement location will have to be investigated so as to give a representative real common factor.

Group III monitoring is focused on dry season monitoring and when in-stream processes and pollution such as from point effluent sources will have major impact. PH is the prime loaded factor while air and water temperature are positively loaded, increasing their values with time. Since the first two peaks of variables in this group are related to factor I and II, the monitoring for this group will be at week interval during the dry season with occasional within a week monitoring on a daily basis. Longitudinal Stream pollution survey is essential during this period.

Group IV variable monitoring is focused on wet season monitoring but when the effect of rainfall and discharge peak is low. In effect this monitoring takes place within the rainy season for a series involving the whole days of the week knowing that precipitation intensity is low and the discharge is therefore unchanged. Pollutants that are accumulated as evaporative storage within the leached layer of the subsoil show up during this period of monitoring.

8.4.3 Design of Lake Water Quality Monitoring System

Despite the location proximity, lakes Abaya and Chamo display different temporal water quality variability influenced by their respective lake morphology, influence of tributary rivers, climatic effects and in-lake bio chemical processes. The design of lake water quality monitoring system has to be considered within its own boundary. Spectral analysis of the water quality data of both lakes indicates 2 weeks monitoring interval as an average optimum. Lake Chamo turbidity and pH are less variable than that of Abaya. 69% of the pH variability and 86% of the turbidity for Lake Chamo is covered with 1 month monitoring length. For Lake Abaya these percentages are only 43% (pH) and 73% (turbidity) respectively. The reverse is true for conductivity and alkalinity; whereas only 37% of the conductivity and 43% of the alkalinity is covered with one month monitoring for Lake Chamo, for Lake Abaya this percentage is 72% (conductivity) and 55% (alkalinity). A generalized proposal for lake water quality monitoring is 2 weeks monitoring interval offers more than 75% of the information in

almost all case while greater interval of monitoring has to be considered separately for each individual variable.

Spatial monitoring design by means of Hierarchical cluster analysis carried out for Lake Abaya indicated a cluster length of 10 km along the fetch and about 5 km across the width. Considering the total area of the lake (1085 Km²) this gives a total of about 32 sampling points. Following the same analogy for Lake Chamo gives a spatial monitoring set of 12 points. This sampling interval is dictated by the more dynamic variables such as pH and dissolved oxygen, which have greater number of clusters spatially.

8.4.4 Ground water Quality Monitoring

The seasonal variations of ground water quality depend on the hydro-geological conditions. The classification based on the piper trilinear plot shows many ground water sources as being affected by surface flow inputs and possibly variation of the ground water quality according to the influence of these surface influxes in to the aquifer. Other sources showed a more subdued seasonal variation. The design procedure for ground water quality is basically similar to those of lakes and rivers described above.

Because of the flow characteristics, lack of protection and the hydrogeology of the aquifer formation some of the ground water sources investigated showed direct pollution by faecal coliforms and organic matter including nitrite/ammonia/nitrate.

Monitoring therefore has to take account the aquifer characteristics, the nature of flow in the ground water, the surface pollutant influx effects and the use of the ground water such as for drinking and the extent of ground water source protection afforded to the supply.

8.5 Water Quality Modeling

Water quality variables, which reflect average changes over the seasons such as variables classed within group I described above, are adequately modeled with ARIMA models both for auto variance and covariance since they display strong auto covariance. This has been demonstrated and shown for conductivity and TDS time

series data. Discharge data is also fairly adequately represented by auto regressive model.

Water quality variables affected by surface runoff processes such as solids, turbidity and particulate-bound contaminant (such as NH_4^+) displayed high noise variance and AIC value indicating poor auto regression. Spectral level regression models showed only partial fits due to the length of the data record. Only the latest stages appear to fit the data well. It is suggested that longer water quality data be made available in order to adequately fit the group II variable data with spectral level regression.

It has been shown that simple missing data could be interpolated using smoothing spline regression (of degree 0-3). Auto regressive models fitted the missing data well when such models were adequate. State-space relation has been shown also to offer good interpolation between variables within a sampling point as well as interpolating between points with in same or different variables. Forecast models work well for water quality variables, which are adequately fitted by ARIMA models.

Discharge based contaminant mean load estimation has been carried out using a model that supposedly compensates for bias of mean estimate error. However, bias was not completely eliminated due to the inadequacy of the lognormal distribution assumption as well as the inadequacy of the rating curve equation particularly for the rivers studied in this research. However, after discovering that the relation between the estimated load and the actual measured load follow a definite pattern, a transfer function has been developed to relate these discrepancies.

It has been shown that the water quality data display "order" in the regional sense. This regional covariance has been used to transfer water quality information between measured and unmeasured sites once a relationship is established using state-space method as was shown for water quality data between Hare and Kulfo River. This approach of regionalization allows interpolation to be made between regions of measurement and reduces the cost of water quality monitoring work.

8.6 MANAGEMENT OF MONITORING

8.6.1 Methods of Determination

Wide variety of methods has been used in the past for analyzing the water qualities of the water resources in the Abaya - Chamo Lakes Basin. In several cases the detail procedures of the methods of determinations have not been reported. Some of the results obtained are way out of the expected range and are of doubtful accuracy. The lack of standardization of methods and procedures makes interpretation of data and information difficult or possibly wrong conclusion would be drawn on such data [89]. The methods of determination employed in this research mostly produce the desired accuracy while being low cost and hence replicable for use in sub regions and local laboratories with appropriate training. For river water quality monitoring BOD does not seem to give an acceptable accuracy. Instead for organic matter assessment COD is better employed although it is far too expensive than a BOD test in terms of the reagents and running costs. For assessing suspended solids use of spectrophotometer absorption difference between filtered and unfiltered portion of sample gives a better assessment and accuracy than the use of turbidity for high suspended solids sample.

8.6.2 Variables to be Monitored

For the various water resources of the region, the following variables are necessary.

Basic variables (eg. water temperature, pH, conductivity, dissolved oxygen, and discharge) used for a general characterization of water quality. Suspended particulate matter (eg. suspended solids, turbidity and organic matter (TOC, BOD and COD)). Organic pollution indicators (eg. dissolved oxygen, Biochemical Oxygen Demand (BOD), Chemical Oxygen Demand (COD), ammonium). Indicators of eutrophication: nutrients (eg. nitrogen and phosphorus), and various biological effect variables (eg. chlorophyll a, Secchi disc transparency, phytoplankton, zoobenthos). Indicators of acidification (eg. pH, alkalinity, conductivity, sulphate, nitrate, aluminum, phytoplankton and diatom sampling) Specific major ions (eg. chloride, sulphate, sodium, potassium, calcium and magnesium) as essential factors in determining the suitability of water for most uses (eg. public water supply, livestock watering and crop irrigation) Metals (eg. cadmium, mercury, copper and zinc) Organic micro pollutants such as pesticides and the numerous chemical substances used in industrial processes (eg. PCB,

HCH, PAH). Indicators of radioactivity (eg. total alpha and beta activity, ^{137}Cs , ^{90}Sr) Microbiological indicator organism (eg. total coliforms, faecal coliforms and faecal streptococci bacteria) Biological indicators of the environmental state of the ecosystem (eg. phytoplankton, zooplankton, zoobenthos, fish, macrophytes and birds and animals related to surface waters) [90, 91, 92].

8.6.3 Data storage Data Analysis and Data Quality Control

As mentioned above, past water quality analysis records in some cases indicated doubtful results. Methods and detection limits and standard deviations are not specified. Therefore, it is not possible to evaluate the extent of method validation. Future reports should include method validations such as blank run results, recoveries and standardization.

The detection limits, mean values and 95% confidence limits worked out and demonstrated in this research can serve as controls for detecting mistakes and errors in the data quality assurance and control.

For lake water analysis such as that of Lakes Chamo and Abaya, spectrophotometric determination have been seen to be influenced by matrix effect due to salinity and other constituents of the lakes. It is essential, therefore, to employ standard addition test results and verify matrix effects have been accounted for.

It is essential and expedient that local authorities are responsible for data acquisition. However, the information has to be organized at the national level. In order to make comparison of results uniform, standards and procedures as well as data reporting formats must be followed [93].

8.6.4 Alternative to Use of Field monitoring equipment and Reagents

Comparison of field measurement of Silica using field reagents and the result obtained using laboratory prepared standards show that these reagents under estimated low silica determination. The use of such field equipment and reagents, therefore, requires care if scientific interpretation and accurate assessment is the end

objective. At least these reagents' performance should be calibrated against laboratory prepared certified standards.

It is proposed that as an alternative, reference and standards can be prepared by a central laboratory and common measurement equipments safely transported to strategically locate intermediate regional laboratories as per the schedule of water quality monitoring task so that the use of equipments is optimised. This is a semi-mobile monitoring scheme. A fully mobile monitoring is impractical due to possibility of equipment damage and the impracticality of providing technical facilities and the personal and environmental risk associated with carrying out analysis on mobile cars.

A central laboratory can provide chemicals and common instruments, assure standards are met and serve as an external quality control body.

8.7 PROPOSAL FOR FUTURE IMPROVEMENTS

- 1 Incorporation of Land use information
- 2 Lake water monitoring to be integrated with sediment quality information. The spatial monitoring proposal is not based on exhaustive study and requires further detailed proposal.
- 3 Data quality Control – Proposal for a method validation format to be followed by agencies carrying water quality analysis. Analysis done with field equipment and reagents imported for field use need to be validated by calibration of the water quality results obtained with this reagents against results obtained for same sample by reference laboratory prepared certified chemicals.
- 4 Precipitation Chemistry Data:
- 5 Need for continuous and long data record. Modeling and forecasting necessitate long period of record and there should be an effort in future to make these data available [94].
- 6 Regionalization. As was shown in this research, regional state-space relationship can be used to transfer water quality information within the Abaya - Chamo region and in order to establish good regional model, an extensive regional water quality data set must be established in space and time within the region to allow interpolation and relative evaluation of water quality changes.

CONCLUSION

Water quality monitoring work was done on the water resources within the Abaya-Chamo basin. The methods, method validation and analysis results have been presented and discussed. Seasonal variation and trends as well as associated water quality management issues have been discussed. Recommendations have been made for effective water quality monitoring based on observations in this study.

There is a general increase in salinity and alkalinity of surface water sources from higher to lower elevation within the Abaya-Chamo basin. The seasonal variation of the surface water quality parameters can be classified as mainly long-term seasonal variability or short-term rain induces surface flow based variability. The release of nutrients into rivers from the catchments was related to high Sodium dominance ratio of the upper lying rivers and the catchments buffering capacity. The weathering rates of Hare and Kulfo rivers were found to be transported limited and were correlated with the catchment steepness. There is a regional similarity in the water quality seasonal variation among the rivers in the regions. This similarity suggests the need for establishing regional relationship in water quality.

The Lake Waters are of the Sodium-bicarbonate and chloride types and their seasonal variation generally follows the precipitation pattern. Both Lake Abaya and Chamo have in the past 40 years been subjected to increased salinity. The increase on Lake Chamo is quite high. Reduction of inflow to the lakes and periodic drought are the possible explanation for this increase in salinity. The nutrient and chlorophyll measurements characterise both lakes as eutrophic. Dissolved oxygen measurement fall below 3 mg L^{-1} in Lake Chamo in the dry season with simultaneous loss of phosphorous. This condition may have been caused by algal death and respiration and may lead to increased concentration of ammonia and nutrients through internal recycling. Cyanobacteria, species normally abundant in Lake Chamo may find this condition suitable. The increase in nitrogen and sulphate as well as ammonia in both lakes over recent years might be due to pollution from the catchment rather than internal recycling and this cannot be conclusively stated, as past measurements of inflow river water quality

measurements are not available. Pollution assessment of the tributary catchment shall be undertaken as part of a water quality-monitoring program for the lakes.

In general the chemical composition of the ground water in the area is largely of the bicarbonate-calcium-magnesium type, which is typical of the basaltic parent rock formation of the area. There is a general inverse correlation of the dissolved constituents with elevation in the area. Other researchers also found similar behaviour in the region [60]. The similarity in flow characteristics and chemical behaviour of surface water samples and ground water samples was revealed by means of the piper tri linear diagram. For example Arbaminch spring Source plots on the diagram near the river water indicating less evolved water with near surface flow conditions.

The ground water sources investigated show direct pollution from human and animal wastes because of lack of appropriate protection. Well protection measures must be taken including walling and capping of open wells, removal of toilets from near wells, fencing of wells and excluding animals and human wastes from around water sources, treatment of river water and even spring water sources with slow sand filters and management of application of fertilizers as well as locating wells away from areas of agricultural activities.

A water quality monitoring system based on an integrated partial physical orthogonal model has been designed based on data generated within the water resources of the Abaya – Chamo drainage basin. Abstract common factors were extracted by the application of principal component and factor analysis. By overlaying real factors with abstract common factors the underlying causes for the water quality variations have been explained. Surface flow factors, sub surface flow factors, leaching flow factors, effects of soil matrix, rainfall magnitude and intensity, discharge, catchment area and slope, in stream pollution and point sources of pollution, evaporative storage and precipitation chemistry all showed up in such integrated model. This model can be extended by including further physical factors as well as natural and anthropogenic pollution sources and factors. This model can be extended to lakes and ground water sources as well.

Design of water quality monitoring intervals was accomplished with the help of spectral analysis of the data after trends were diagnosed and removed and within groups of

monitoring as defined by the factor model described above. The percentage information for a given frequency of monitoring was derived from the integral of the spectral density plot, which is equivalent to the auto-covariance of the data. Optimum monitoring intervals are indicated in the plot of such integrals. For example for river water the major variables to be monitored from four independent groups were: Conductivity (Group I), Turbidity (Group II), Chloride or Nutrients (Group III) and pH (Group IV). Spatial monitoring spacing for lake water quality was determined after hierarchical cluster analysis. Smaller grid size is suggested by dynamic variable (i.e., pH, Dissolved Oxygen, redox potential...) giving 10 km length by 5 km width monitoring grid. Statistical tests were applied on the cluster groups of samples.

The possibility of modelling the various water quality parameters was investigated. Auto regressive modelling fits well variables that have seasonally evened variation. Variables with short-term fluctuation were modelled with spectral level regression. State-space method was satisfactorily applied for relating the time series between two sampling points located on different rivers. Discharge- base contaminant modelling was modified to compensate for error by establishing a pattern of relationship between calculated and observed contaminant loads.

LITERATURE

- 1 Ogg C W, Keith G A. New federal support for priority watershed management needs”, JAWRA, (2001) 38(2): 577-586.
- 2 Novotny V. Integrated Water Quality Management, Water Science and Technology, (1996) 33(4-5): 1-7.
- 3 UNEP/WHO. Water Quality Monitoring - A Practical Guide to the Design and Implementation of Freshwater Quality Studies and Monitoring Programmes. © UNEP/WHO (1996).
- 4 Robert McCormick, Brian K. Miller. Non- point Source Pollution: A Threat to Our Waters. <http://www.agcom.purdue.edu/AgCom/Pubs/menu.htm>(2004)
- 5 Wang X. Integrating Water Quality management and Land Use Planning in a Watershed Context. Journal of Environmental management. 61, pp25 – 36. 2000.
- 6 European Fresh Water Monitoring Design. Representativeness Of Current Monitoring Programmes Topic Report No 10/1996.
- 7 Welch K A and W B Lyons, McMurdo L. Comparative limnology of the Taylor Valley lakes: The major solutes. Antarctic Journal of the United States--Review (1995), 292-293.
- 8 Harmancioglu N B, Fistikoglu O, Ozkul S D, Singh V P, and M N Alpasian. Water Quality Monitoring Network Design. Kluwer academic Publishers, London (1999).
- 9 Berthouex and Brown. *Statistics for Environmental Engineers*. (1994) p.71-79.
- 10 Chatfield C and Collins A J Introduction to Multivariate Analysis. Chapman and Hill (1980).
- 11 Karpuzcu M, Senes S, and Akkoyunlu A. Design of a Monitoring System for Water Quality by Principal component Analyses, a case study. Proceedings of the International symposium on Environmental management: Environment (1987) 87, pp. 673 – 690.
- 12 Hair J F, Anderson R E and Black W C . Multivariate Data Analyses With Readings Macmillan Publishing Company New York (1992).
- 13 CSA (Central Statistical Authority, Office of Housing and Census Commission, FDRE) the 1994 Population and Housing Census of Ethiopia. Results for Southern Nations Nationalities and People’s Region, (1996, 1). Volumes I – Parts I – V, Addis Ababa.

-
- 14 CSA (Central Statistical Authority, Office of Housing and Census Commission, FDRE) the 1994 Population and Housing Census of Ethiopia. Results for Oromyia Region, (1996, 1). Volumes II – Parts I – V, Addis Ababa.
- 15 Zinabu G M, Elizabeth Kebede and Zerihun Desta. Long Term Changes in the Chemical Features of Waters of Seven Ethiopian Rift-Valley Lakes. *Hydrobiologia* 477: 81-91 (2002).
- 16 Zinabu G M, J Nicolas and G Pierce. Concentrations of Heavy metals and Related Trace elements in Some Ethiopian Rift-valley lakes and their in-flows. *Hydrobiologia*. 429. 171-178 (2003).
- 17 Downing J A, McClain M T, Willey R and 10 others The impact of accelerating land use change on the N-cycle of tropical aquatic ecosystems: current conditions and projected changes. *Biogeochemistry* (1999). 46, 109-148.
- 18 American Public Health Association. Standard Methods for the Examination of Water and Wastewater. 18th ed. Method 2540. American Public Health Association, American Water Works Association, and Water Environment Federation, Washington DC, (1992). 2-53.
- 19 DIN 38405 Teil 10: Deutsche Einheitsverfahren zur Wasser-, Abwasser- und Schlamm –Untersuchung, (Gruppe D, Anionen) Bestimmung des Nitrit Ions (Februar 1981.
- 20 Bd. I. Jena: VEB Gustav Fischer Ausgewählte Methoden der Wasser Untersuchung. Verlag 1976. pp 58-59
- 21 Robertson D M, Roerish E D, Influence of various water quality sampling strategies on load estimates for small streams. *Water Resources Research*, (1999). 35(12): 3747-3759.
- 22 Youden W J Statistical Method for Chemists. National Bureau of Standards, Washington, D.C. (1951).
- 23 United States Environmental Protection Agency. Methods for Chemical Analysis of Water and Wastes. Method #160.4 and #160.3. Environmental Monitoring and Support Laboratory United States Environmental Protection Agency, Cincinnati, Ohio (1992).
- 24 DIN 32 645 Deutsche Norm Nachweis, Erfassungs und Bestimmungsgrenze, Mai 1994.

- 25 U S Geological Survey Office of Water Quality. Changes in field treatment protocols and bottle types for whole-water samples collected for total ammonium plus organic nitrogen and total phosphorus determinations Office of Water Quality Technical Memorandum No. 99.04 accessed July 29, 2002, at URL:
- 26 Williams G P. Bank-full discharge of rivers“, *Water Resources Research* (1978) 14(6): 1141- 1154.
- 27 Simon A. Energy, time, and channel evolution in catastrophically disturbed fluvial systems“, *Geomorphology*, (1992) 5(3-5): 345-372.
- 28 B.J. Cosby, R.C. Ferrier, A. Jenkins and R.F. Wright. Modelling the effects of acid deposition: refinements, adjustments and inclusion *Hydrology and Earth System Sciences*, 5(3), 499–517 (2001).
- 29 Kao S J, Liu K, Estimating the suspended sediment load by using the historical hydrometric record from the Lanyang-Hsi Watershed. *Terrestrial Atmospheric and Oceanic Sciences*, (2001) 12(2): 401-414.
- 30 Robert Kent *And* Kenneth Belitz. Concentrations of Dissolved Solids and Nutrients in Water Sources and Selected Streams of the Santa Ana Basin, California, October 1998–September 2001. U.S. Geological Survey.
- 31 Turner M G and R.H. Gardner (eds.), *Quantitative Methods in Landscape Ecology*. Springer-Verlag, New York (1989).
- 32 V Straškrabová, C Callieri and J Fott (Guest Editors). The MOLAR Project: atmospheric deposition and lake water chemistry. Pelagic food web in mountain lakes. Mountain Lakes Research Program. *J. Limnol.* (1999)58(2): 88-106
- 33 Moore I D, Burch G J, Sediment transport capacity of sheet and rill flow: Application of unit stream power theory, *Water Resources Research*, (1986) 22(8): 1350-1360.
- 34 WHO Guidelines for Drinking-Water Quality. Volume 2. Health Criteria and Other Supporting Information. World Health Organization, Geneva (1984) 335 pp.
- 35 Hicks D M, Gomez B, Trustrum N A. Erosion Thresholds and Suspended sediment 24 yields, Waipaoa River Basin, New Zealand, *Water Resources Research*, (2000) 36(4): 1129- 1142.

- 36 Morel M M and Janet G H Principles and Applications of Aquatic Chemistry. John Wiley and Sons (1993) USA.
- 37 Nearing M A, Norton L D, Bulgakov D A, Larionov, G A, West L T, Dontsova K M. "Hydraulics and erosion in eroding soils", *Water Resources Research*, (1997) 33(4): 865-876.
- 38 Preston S D, Bierman V J, Silliman S E., "An evaluation of methods for the estimation of tributary mass loads", *Water Resources Research*, (1989), 25(6): 1379-1389.
- 39 Granat L, Areskaug H, Hovmand M, Devenish M, Schneider B, Bieber E, Marquardt W, Reissell A, Järvinen O, Hanssen J E and Sjöberg K. Inter-comparison of precipitation collectors for chemical analysis, HELCOM inter-calibration -second stage. (*Baltic Sea Environment Proceedings*, 41). (1992). pp. 15-88.
- 40 Robertson D M. Regionalized loads of sediment and phosphorus to Lakes Michigan and Superior - High flow and long-term average. *Journal of Great Lakes Research*, (1997) 23(4): 416-439.
- 41 Bulgarian Academy of Sciences Central Laboratory of General Ecology. Management Plan of the Srebarna Biosphere Reserve. Sofia, (2000).
- 42 Charlson R J and Rodhe H. Factors controlling the acidity of natural rainwater. *Nature*, (1982) 295, 683-685.
- 43 Sanders T G, Ward, R C, Loftis, J C, Steel, T D, Adrian, D D, Yevjevich, V. Design of Networks for Monitoring Water Quality. Water Resources Publications, Littleton, Colorado (1983).
- 44 Garn H S, Olson D L, Seidel T L and Rose W J. Hydrology and water quality of Lauderdale Lakes, Walworth County, Wisconsin, 1993-94: U.S. Geological Survey Water-Resources Investigations Report (1996) 96-4235, 29 p.
- 45 David W C and James O Sickman. Changes In The Chemistry Of Lakes And Precipitation In High-Elevation National Parks In The Western United States, 1985–1999. *Water Resources Research*, (2003). Vol. 39, No. 6, 1171, Doi: 10.1029/2002wr001533,
- 46 Kebede E, Zinabu Gebremariam, and others. The Ethiopian Rift Valley lakes Chemical Characteristics of a Salinity Alkalinity series. *Hydrobiologica* (1994) 288. Page 1-12 Kluwer Academic Publishers, Belgium.

- 47 Otterbach L. Water Resources Quality and Potential Assessment for Irrigation Agriculture in the Abaya / Chamo Basin south Ethiopia. University of Siegen. Germany (1995).
- 48 Zinabu G M, Elizabeth Kebede and Zerihun Desta. Long Term Changes in the Chemical Features of Waters of Seven Ethiopian Rift-Valley Lakes. *Hydrobiologia* 477: 81-91 (2002).
- 49 Davit K J, Freon J Creed, I F, Pollard B, Foote L and Bailey S. Climate, hydrogeology, and water chemistry relationships in wetland-pond complexes of the Western Boreal Forest: Preliminary results. Annual Scientific Meeting, Canadian Geophysical Union, Banff, Alberta, May 23-27, (2000).
- 50 Seleshi Bekele Awulachew. Investigation of Water Resources Aimed at Multi – Objective Development with Respect to Limited Data Situation. The Case of the Abaya - Chamo Basin. Ph. D. Dissertation. Dresden University of Technology. December (2000).
- 51 Dillon P J and Molot L A Effect of landscape forms on export of dissolved organic carbon, iron and phosphorus from forested stream catchments. *Water Resources Research* (1997) 33, 2591-2600.
- 52 Thiemann S. Personal Communication, Siegen, Germany (2004).
- 53 Schutt B. Gerd Foerch, Stefan Thiemann and Bernd Wenclawiak. Modern Water Level Changes of Lake Abaya, Southern Ethiopia as Response to Changes in Sediment Basin. University of Siegen, Germany (2002).
- 54 Lathrop R C, S R Carpenter, C A Stow, P A Soranno and J C Panuska. Phosphorus loading reductions needed to control blue-green algal blooms in Lake Mendota. *Can. J. Fish. Aquat. Sci.* (1998) 55:1169-1178.
- 55 Loizeau J L, Dominik J, Evolution of the Upper Rhone River discharge and suspended sediment load during the last 80 years and some implications for Lake Geneva. *Aquatic Sciences* (2000) 62(1): 54- 67.
- 56 Carpenter S R, Ludwig D and W A Brock. Management of Eutrophication for lakes subject to potentially irreversible change. *Ecol. Appl.* (1999) 9:751-771.
- 57 Richards R P, Baker D B. Trends in nutrient and suspended sediment concentrations in Lake Erie tributaries, 1975-1990, *Journal of Great Lakes Research*, (1993) 19(2): 200-211.

- 58 V Straškrabová, C Callieri and J Fott (Guest Editors). Limnological survey in eight high mountain lakes located in Lago Maggiore watershed (Switzerland). Pelagic food web in mountain lakes. Mountain Lakes Research Program J. Limnol (1999) 58(2). 179-192.
- 59 M S Swaminathan Research Foundation, Chennai, India. Biogeochemistry of Small Catchments (1998).
- 60 Jeffrey M McKenzie, Donald I Siegel, William Patterson and D. Jonathan Mckenzie. A geochemical survey of spring water from the main Ethiopian Rift valley, Southern Ethiopia: Implications for Well-Head Protection. Hydrogeology Journal (2001) 9.265 – 272.
- 61 Shaver, G R, K J Nadelhoffer and A E Giblin.. Biogeochemical diversity and element transport in a heterogeneous landscape, the North Slope of Alaska, (1990) pp.105-126.
- 62 Gibbons Statistical Methods for Groundwater Monitoring (1994). p.95-121.
Gilbert R O. Statistical Methods for Environmental Pollution Monitoring, Van Nostrand Reinhold Company, New York (1987).
- 63 Vidal M, Melgar J, Lopez A, and Santoalla M C. Spatial and Temporal Hydro chemical Changes in Groundwater under the Contaminating Effects of Fertilizers and Waste Water. Journal of Environmental management (2000) pp215 – 225.
- 64 Schillinger J E, Gannon J J,. Bacterial adsorption and suspended particles in urban storm water. Journal of the Water Pollution Control Federation, (1985) 57(5): 384-389.
- 65 McDiffett W F, A W Beidler, T F Dominick, and K D McCrea. Nutrient concentration-stream discharge relationships during storm events in a first-order stream, Hydrobiologia, (1989) 179, 97– 102.
- 66 Behrendt H and Opitz D Retention of nutrients in river systems: dependence on specific runoff and hydraulic load. *Hydrobiologia* (2000) 410, 111-122.
- 67 Wagner R J, Mattraw H C, Ritz G F, and Smith B A. Guidelines and standard procedures for continuous water-quality monitors: site selection, field operation, calibration, record computation, and reporting: U.S. Geological Survey Water-Resources Investigations (2000) Report 00-4252, 53 p.

- 68 Natusch F S and Hopke P K. Analytical Aspects of Environmental Chemistry. John Wiley and Sons (1983).
- 69 Ruth Francis-Floyd and Craig Watson. Ammonia. University of Florida. IFAS extension. (2000).
- 70 Stoddard J L. Long-term changes in watershed retention of nitrogen, in Environmental Chemistry of Lakes and Reservoirs, edited by L. A. Baker, (1994) pp. 223–284, Am. Chem. Soc., Washington, D. C.
- 71 Commission on Geosciences, Environment and Resources (CGER). Restoration of Aquatic Ecosystems: Science, Technology, and Public Policy (1992).
- 72 U S Geological Survey. Water Chemistry in a Nutrient and Sediment Control. System near Owasco, New York. Open-File Report 99-xxxx (1999).
- 73 Laura Siegg and Werner Stumm. Aquatische Chemie – Second edition (1991).
- 227 Stumm W & J Morgan. Aquatic Chemistry. 2nd ed., Wiley Interscience, New York (1981).
- 74 Fast A W The effects of artificial aeration on lake ecology. PhD Thesis Michigan State University, East Lansing. (1971) 566 p.
- 75 H S Garn, J F Elder and D M Robertson. Lake Studies Team, U.S. Geological Survey, Wisconsin District. Why Study Lakes? An Overview of USGS Lake Studies in Wisconsin. July 2003.
- 76 Understanding Pond & Lakes. Aquatic Biologists Inc. (2004)
- 235 Bennett G W Management of Lakes and Ponds. Van Nostrand Reinhold Co., N. Y. (1970). pp. 22-222.
- 77 Richards R Peter. Estimation of pollutant loads in rivers and streams: A guidance document for NPS Programs. Water quality laboratory, Heidelberg College. 310. East market street tiffin, oh 44883. USA (1995).
- 78 Chatfield C The Analysis of Time Series: Theory and Practice. Chapman and Hall. London. (1975).
- 79 Brockwell J P and Richard A Davis Introduction to Time Series and Forecasting. Springer – Verlag. Newyork (1996).
- 80 Shumway H R and David S. Stoffer. Time Series Analysis and Its Applications. Springer – Verlag. Newyork (2000).

-
- 81 Shumway H.R. Applied Statistical Time Series Analysis. Prentice-Hall Series in Statistics (1988).
- 82 Rasmussen C T. Characterizing Sediment Loads on the North Oconee river, Northeast Georgia, Using Geometric Mean Concentration, Warnell School of Forest Resources, University of Georgia, Athens (2002).
- 83 Ferguson R I River loads underestimated by rating curves. *Water Resources Research*, (1986) 22(1): 74-76.
- 84 McCuen R H, Leahy R B, Johnson P A,. Problems with logarithmic transformations in regression, *Journal of Hydraulic Engineering - ASCE*, (1990) 116(3): 414-428.
- 85 Schwartz S S, Naiman D Q. Bias and variance of planning level estimates of pollutant loads, *Water Resources Research*, (1999) 35(11): 3475-3487.
- 86 Crawford C G Estimation of suspended-sediment rating curves and mean suspended sediment loads, *Journal of Hydrology*, (1991) 129(1-4): 331-348.
- 87 Lewis J. Turbidity-controlled suspended sediment sampling for runoff event load estimation. *Water Resources Research*, (1996) 32(7): 2299-2310.
- 88 Makililo F. An inquiry into suspended matter in the Luiche and Malagarasi Rivers: Provenance and pathways to Lake Tanganyika, East Africa (2000).
- 89 A A V V Guidelines for data acquisition and data quality evaluation in environmental chemistry (1980). *Anal. Chem.*, 52: 2242-2249.
- 90 UNESO/WHO/UNEP. *Water Quality Assessments - A Guide to Use of Biota, Sediments and Water in Environmental Monitoring – Second Edition* (1992).
- 91 WHO *Guidelines for Drinking-Water Quality. Volume1. Recommendations. Second edition*, World Health Organization, Geneva, (1993) 188 pp.
- 92 WHO. *Toxic Cyanobacteria in Water: A guide to their public health consequences, monitoring and management* (1999).
- 93 National Parke Service Crater Lake Limnological Studies Final Report Executive Summary * Abstract * Long-term. Monitoring Program Technical Information Center. Denver Service Center. P.O. Box 25287. Denver, Colorado 80225-0287(303) (1999) 969-2130.
- 94 *Water-Resources Investigations Report 03-4326. National Water-Quality Assessment Program* (2001).

- 95 Wood R B and Talling J.F. Chemical and Algal Relationships in a Salinity Series of Ethiopian Inland Waters. *Hydrobiologia*. (1988) 15: 29-67
- 96 Stefan Thiemann, Personal Communication. University of Siegen (2004).

APPENDIX

S.No.	CONTENTS	PAGE
Appendix 4 – 1.	Calculation of Carbon dioxide, total Inorganic carbon and Buffering capacity for the rivers and lakes with in the Abaya – Chamo Water Resources Basin.	320
Appendix 5 – 1	Factor and Principal Component Analysis of Kulfo River Water Quality Data	331
Appendix 5-2	Spectral Analysis of Kulfo pH Data Using Fast Fourier Transform	335
Appendix 5-3	Cluster Analysis of Lake Abaya’s Water Quality Data	338
Appendix 6	Ionic Strength Adjustment for Water Sources Under Study	344
Appendix 7-1	One – lag MA model of TDS and conductivity	349
Appendix 7-2	Water Quality Data for River Kulfo. Missing values filled in by Cubic Spline Interpolation.	350
Appendix 7- 3	Spectral Analysis Result Using Fast Fourier Transform.	355
Appendix 7- 4	Arithmetic Moments of Normalised Discharge	357
Appendix 7- 5.	Geometric Moments of Normalised Discharge	357
Appendix 7-6:	Moment calculation using the first 10 terms of the Taylor series for the first month data	358
Appendix 7-7:	Moments for total data (N = 219) worked from natural log flows.	358
Appendix 7-8 :	Bias Calculation	359

APPENDIX 4 – 1. CALCULATION OF CARBON DIOXIDE, TOTAL INORGANIC CARBON AND BUFFERING CAPACITY FOR THE RIVERS AND LAKES WITH IN THE ABAYA – CHAMO WATER RESOURCES BASIN.

Calculation of Alkalinity equilibrium Constants for the Different Water Sources
(adjustment for ionic Strength of Solutions)

Equilibrium Equation:



The ionic strength adjustment is written as:

$$\text{Log } K_{1a} = \text{Log } k_1 - \gamma_{\text{H}^+} - \gamma_{\text{HCO}_3^-}$$

$$\text{Log } K_{2a} = \text{Log } K_2 - \gamma_{\text{H}^+} + \gamma_{\text{HCO}_3^-} - \gamma_{\text{CO}_3^{2-}}$$

Table Appendix 4-1-1 below shows the calculated equilibrium constants after adjustment for ionic strength of sample sources.

Table Appendix 4-1-1 Calculated ionic Strength and Equilibrium Constants

Source	Ionic Strength	LogK1	LogK2	γ_{H^+}	$\gamma_{\text{HCO}_3^-}$	$\gamma_{\text{CO}_3^{2-}}$	K1a	K2a
Abaya	0.0136	-6.35	-10.33	-0.051	-0.051	-0.203	-6.248	-10.127
Chamo	0.0237	-6.35	-10.33	-0.064	-0.064	-0.257	-6.221	-10.073
Hare	0.0014	-6.35	-10.33	-0.018	-0.018	-0.071	-6.315	-10.259
Kulfo	0.0027	-6.35	-10.33	-0.024	-0.024	-0.098	-6.301	-10.232
Sile	0.0086	-6.35	-10.33	-0.041	-0.041	-0.166	-6.267	-10.164

Appendix 4-1-2 Total Inorganic carbon Contents

The plot of total inorganic carbon content for Hare River is shown in Figure Appendix 4-1-1. The open to atmosphere conditions is shown in the graph as a line. It is seen that most of the plots fall above this line. This implies that the base flow conditions (greater carbon content) dominates and provides buffering to pH changes during rain times.

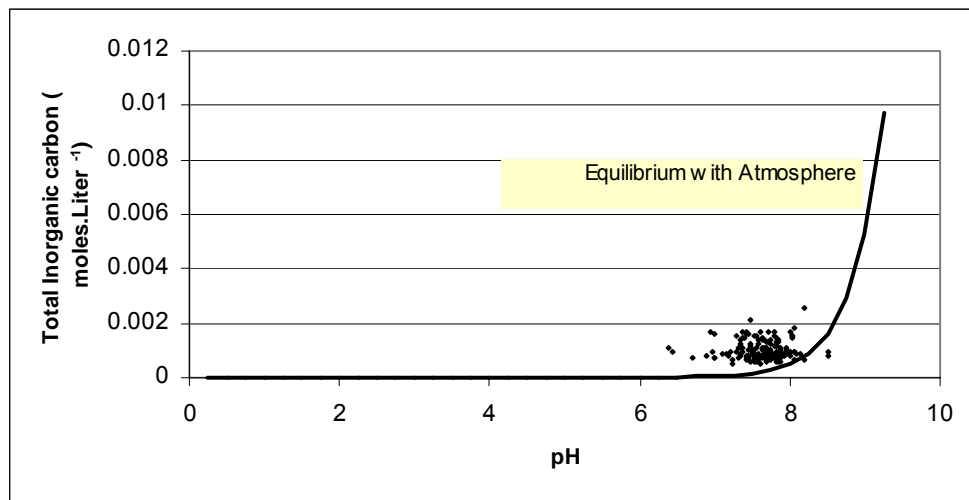


Fig. Appendix 4-1-1 Total Inorganic Carbon Under Closed and Open Conditions (Hare River)

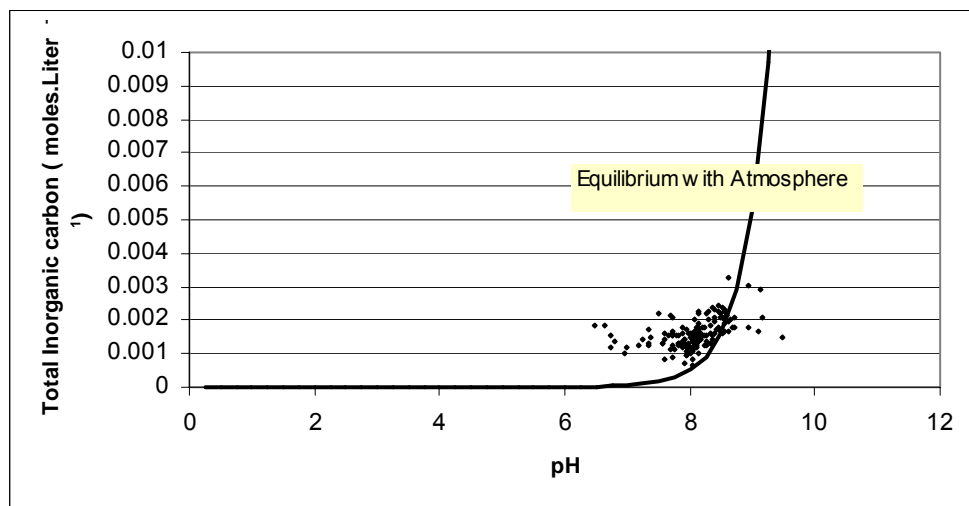


Fig. Appendix 4-1-2 Total Inorganic Carbon Under Closed and Open Conditions (Kulfo River)

The total inorganic carbon (TOTC) is defined as:

$$\text{TOTC} = [\text{H}_2\text{CO}_3] + [\text{HCO}_3^-] + [\text{CO}_3^{2-}]$$

Further the relationship of each component to the TOTC is given by the equations:

$$\begin{aligned} [\text{H}_2\text{CO}_3] &= \alpha_0 * C_T \\ [\text{HCO}_3^-] &= \alpha_1 * C_T \\ [\text{CO}_3^{2-}] &= \alpha_2 * C_T \end{aligned}$$

Where the α values are given through:

$$\begin{aligned} \frac{1}{\alpha_0} &= 1 + \frac{K_1}{[\text{H}^+]} + \frac{K_1 * K_2}{[\text{H}^+]^2} \\ \frac{1}{\alpha_1} &= \frac{[\text{H}^+]}{K_1} + 1 + \frac{K_2}{[\text{H}^+]} \\ \frac{1}{\alpha_2} &= \frac{[\text{H}^+]^2}{K_1 K_2} + \frac{[\text{H}^+]}{K_2} + 1 \end{aligned}$$

The value of C_T is determined from the alkalinity and pH as:

$$C_T = \frac{\text{Alkalinity} + [\text{H}^+] - [\text{OH}^-]}{\alpha_1 + 2\alpha_2}$$

Appendix 4-1-3 CARBON DIOXIDE CONTENT

The concentration of Carbon dioxide is given through the equation.

$$P_{CO_2} = \frac{[H_2CO_3^*]}{K_{H(CO_2)}} = \frac{[H_2CO_3^*]}{10^{-3.5}} \text{ (atm)}$$

The concentration in ppm of CO₂ is given as

$$P_{CO_2} \text{ (ppm)} = \frac{P_{CO_2} \text{ (atm)} * 10^6}{1 \text{ atm}}$$

Based on the above calculation the carbon dioxide contents of the samples for Rivers Hare and Kulfo were plotted and are shown in Figures Appendix 4.1.3 and 4.1.4 below. Comparison with atmospheric Carbon dioxide is shown with a horizontal line (317 ppm equivalent to 10^{-3.5} atm). The carbon dioxide content is many times higher than the atmospheric content. It is generally observed that irrespective of lithology, climate or latitude, rivers have a higher partial pressure of CO₂ than ambient atmosphere (Kempe 1982). An explanation is offered by in-situ oxidation of organic matter within the riverine environment. However, results obtained from the other research observations seem to indicate that terrestrial (soil) CO₂ is prevalent during at least part of the seasonal cycle.

The average pressure of CO₂ in the river Hare is about seven times higher than the atmospheric value, i.e., 2042 ppm as against 317 ppm. Highest pCO₂ (11000 ppm) was observed in August during the rainy season. This might coincide with the period of strong erosion. Data on plankton primary production and respiration would be needed to evaluate the extent of metabolic input of CO₂ in the river. For Kulfo River the average CO₂ in the river is 994 ppm as against 317 ppm of present day CO₂ in the atmosphere. Kulfo has less carbon dioxide, which is also confirmed by the strong association bicarbonate alkalinity with the pH.

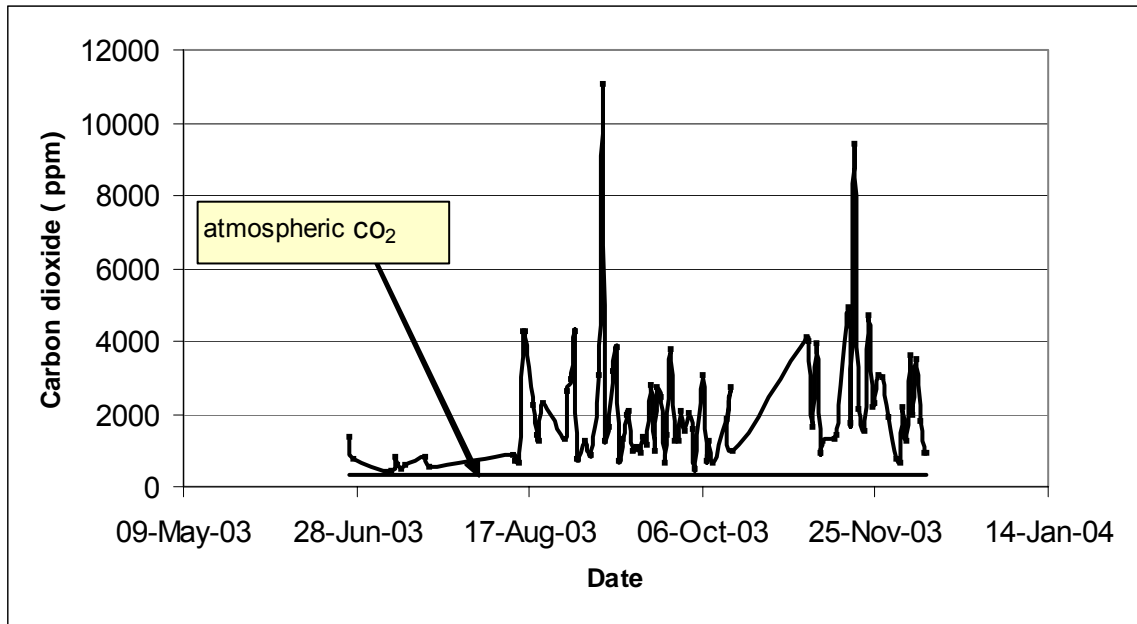


Fig. Appendix 4-1-3 Variation of Carbon dioxide in ppm with season (Hare River)

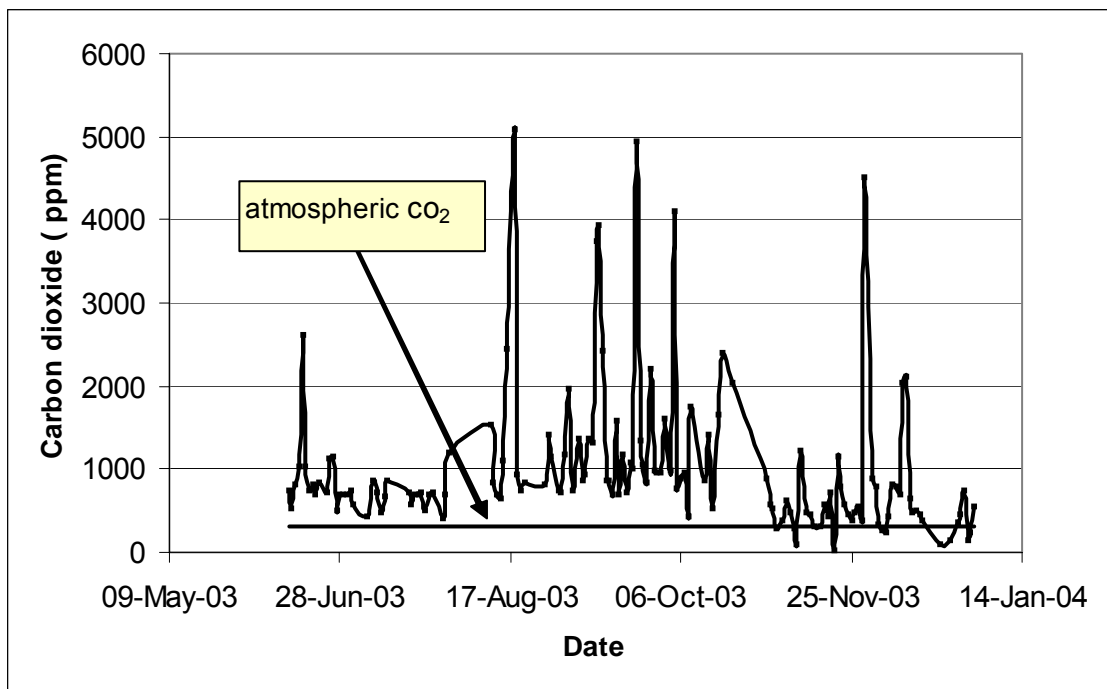


Fig. Appendix 4-1-4 Variation of Carbon dioxide in ppm with season
(Kulfo River)

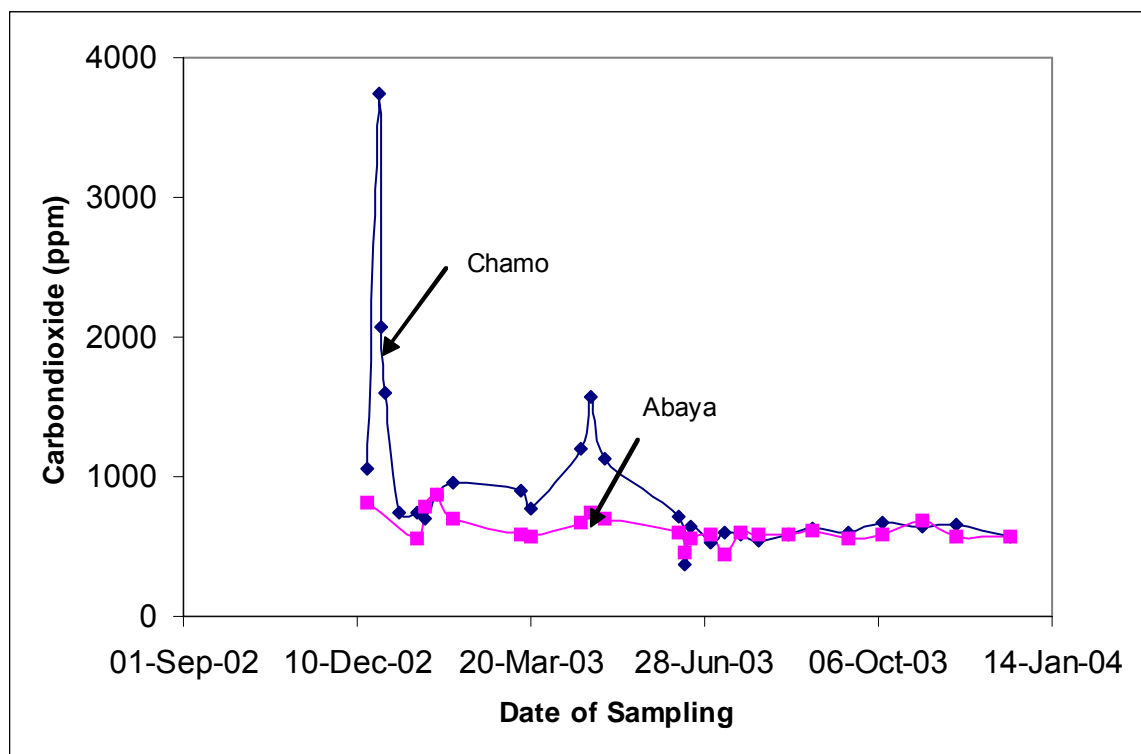


Fig. Appendix 4-1-5 Seasonal variation of Carbon Dioxide for the Lake

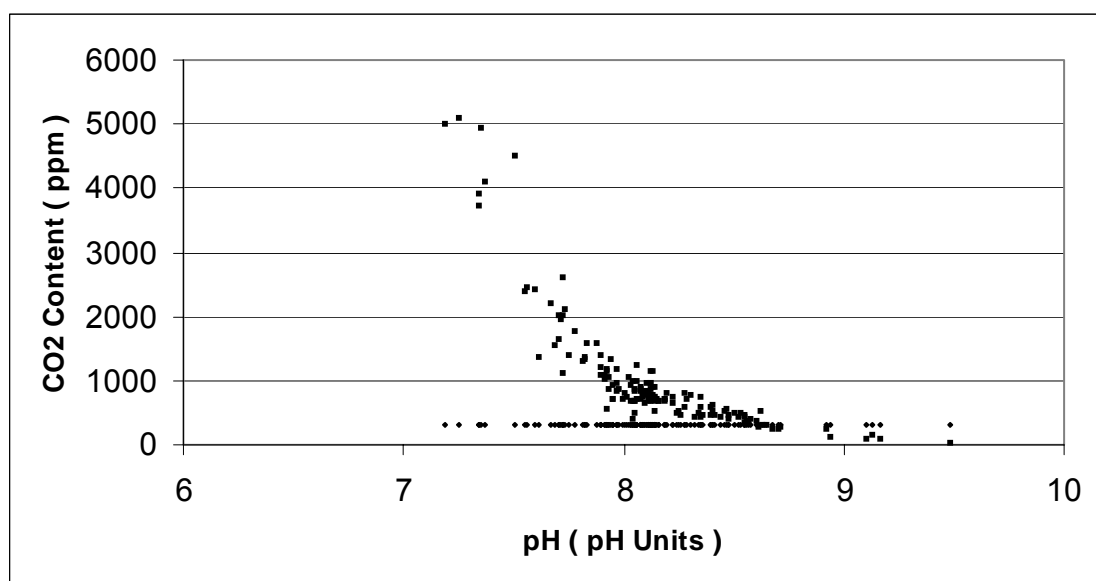


Fig. Appendix 4-1-6 Variation of CO₂ Content with pH (Kulfo River)

APPENDIX 4-1-4 BUFFERING CAPACITY

Assuming the buffering capacity is supplied mainly through the carbonate system, the buffering capacity is calculated through:

$$\beta_{\text{pH}} = 2.3 * \left([\text{H}^+] + [\text{OH}^-] + \frac{[\text{H}_2\text{CO}_3^*][\text{HCO}_3^-]}{[\text{H}_2\text{CO}_3^*] + [\text{HCO}_3^-]} + \frac{[\text{CO}_3^{2-}][\text{HCO}_3^-]}{[\text{CO}_3^{2-}] + [\text{HCO}_3^-]} \right)$$

A simplified formula also exists for calculating the buffering capacity (Minor species Formula):

$$\beta_{\text{pH}} = 2.3 \sum_i \lambda_i^2 [\text{S}_i]$$

Where λ_i is the coefficient of species S_i in the TOTH equation, when the components are the principal components. Assuming for both the rivers and lakes bicarbonate is the principal component, the principal components table can be constructed (H^+ and HCO_3^- as components):

Table Appendix 4-1-2 Chemical Principal Component Table

	H^+	HCO_3^-
H^+	1	0
OH^-	-1	0
H_2CO_3^*	1	1
HCO_3^-	0	1
CO_3^{2-}	-1	1
C_T	1	1
Alkalinity	-1	0

Therefore, the Minor Species formula gives the buffering capacity as.

$$\beta_{pH} = 2.3 \sum_i \lambda_i^2 [S_i] = 2.3 * \left([H^+] + [OH^-] + [H_2CO_3^*] + [CO_3^{2-}] \right)$$

There is a large discrepancy between these two formulas near the K- values of the equilibrium, where the Minor species formula should not be used. Figure Appendix 4-1-7 shows the discrepancy.

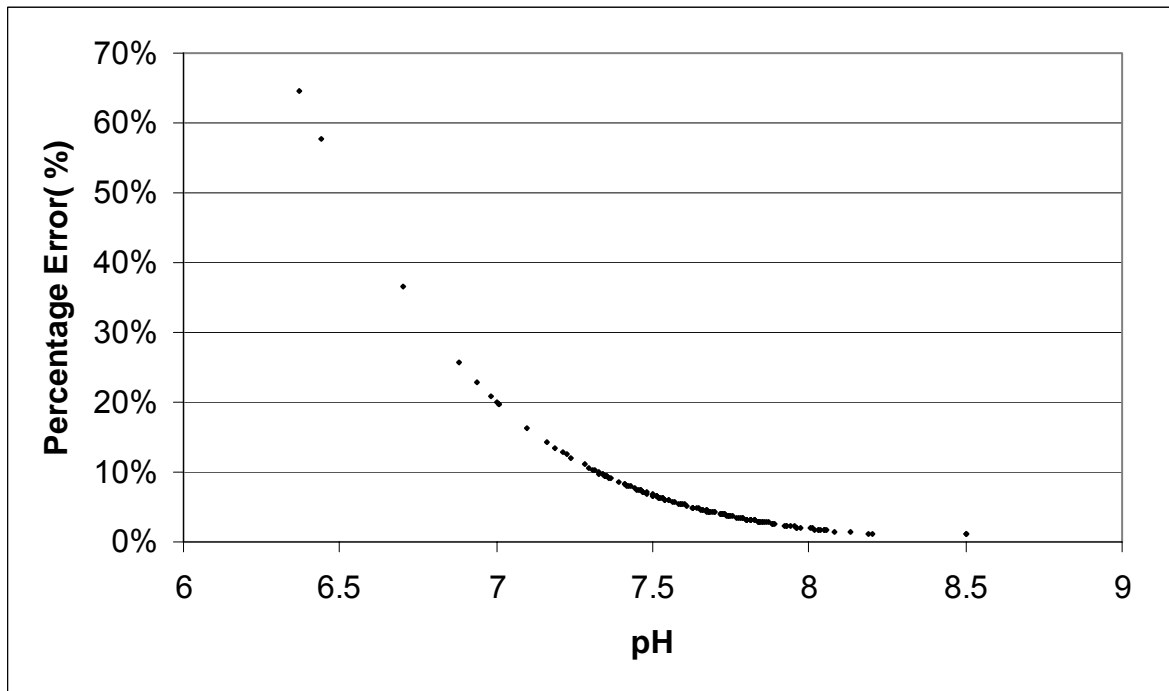


Fig. Appendix 4-1-7 Percentage Difference Buffering Capacity Approximate Formula

The plot of variation of buffering capacity for the various sources is given in the figures Appendix 4-1-8 up to 4-1-10. There is a large variation of pH to acid input at higher pH. Therefore, pH variation is expected at higher pH value.

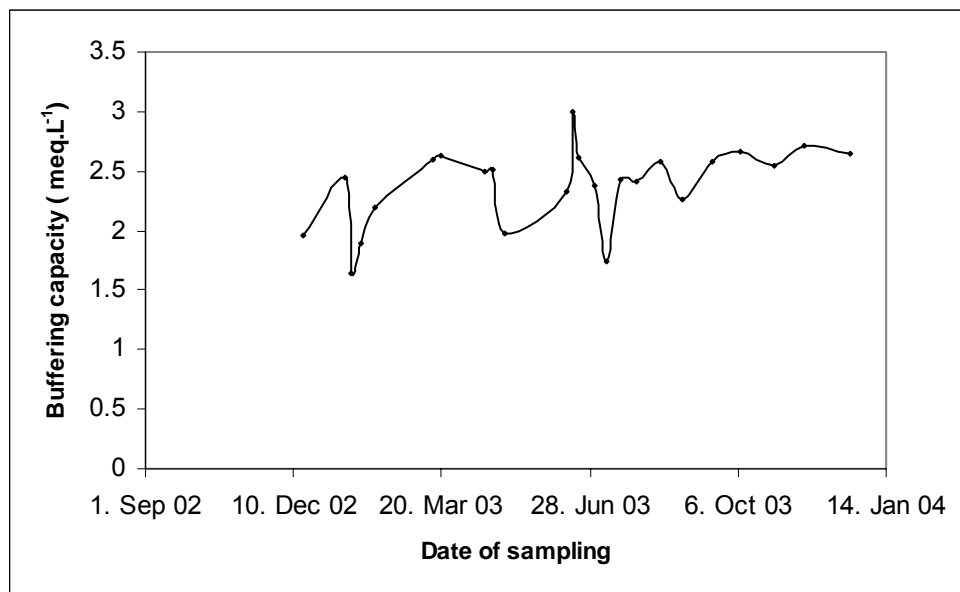


Fig. Appendix 4-1-8 Buffering Capacity of Chamo Lake

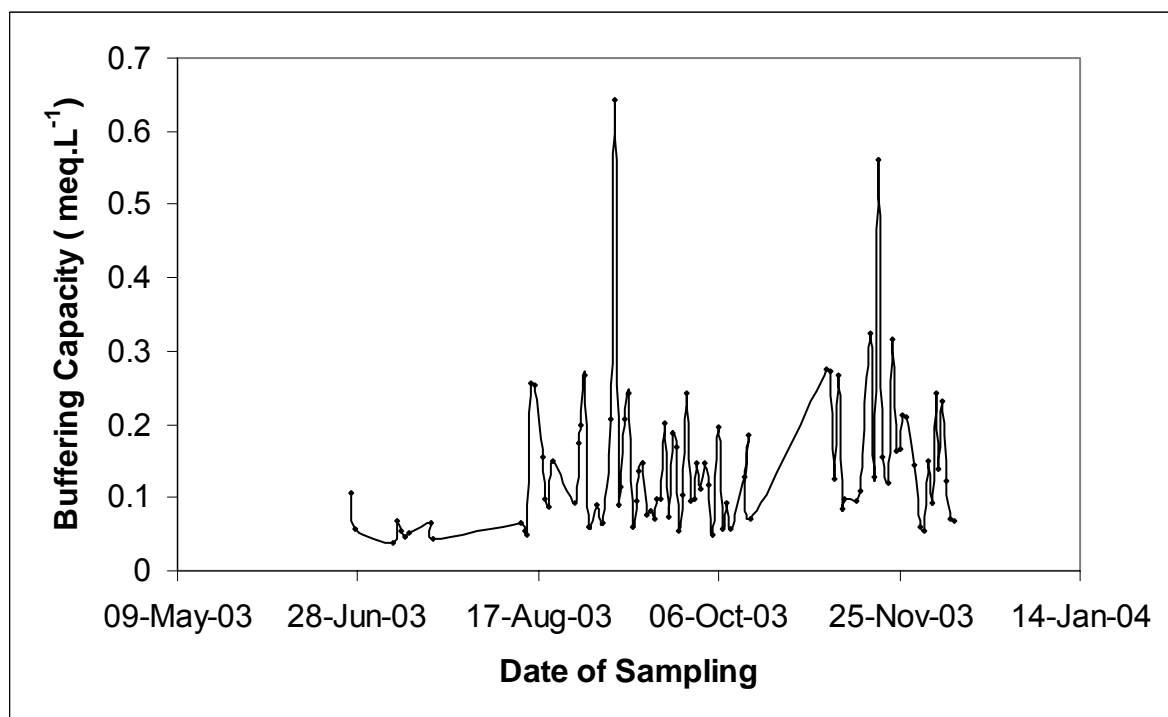


Fig. Appendix 4-1-9 Buffering capacity (Hare River)

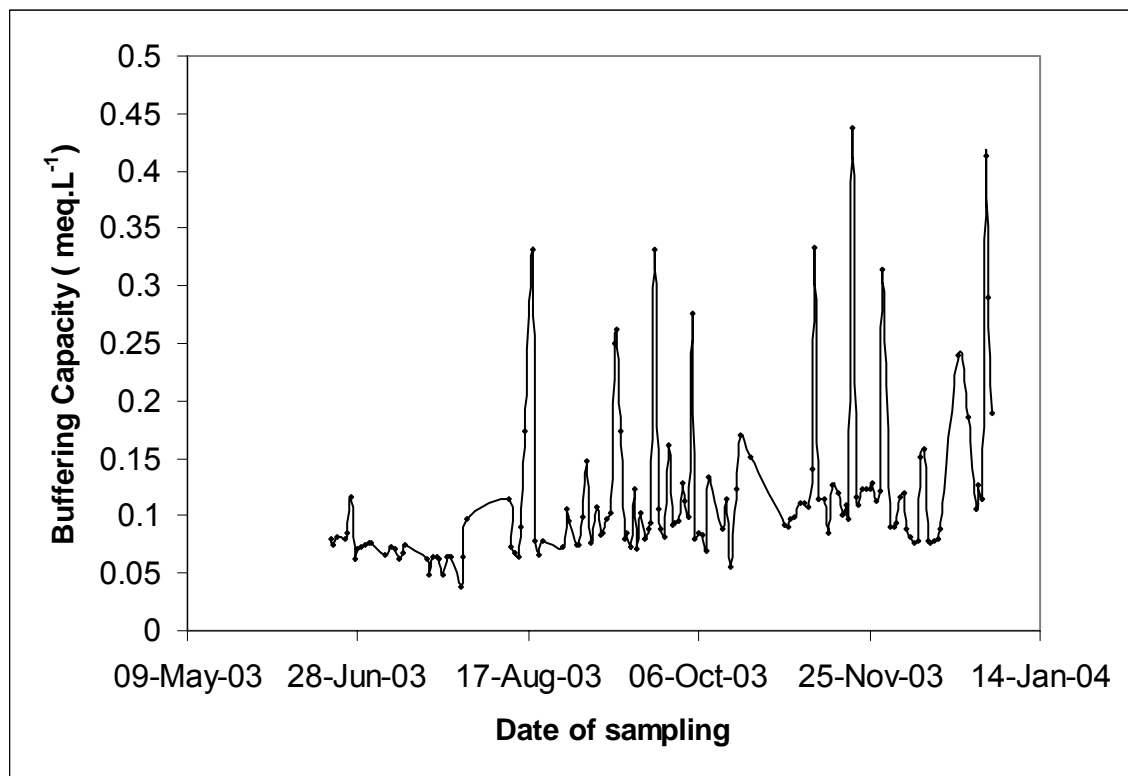


Fig. Appendix 4-1-10 Buffering Capacity (Kulfo River

Appendix 5 – 1 Factor and Principal Component Analysis of Kulfo River Water Quality Data

	Rainfall	River Discharge	Air Temp	Water temp	Turbidity	Conductivity	PH	Total Solids	Alkalinity	Hardness	Calcium	Chloride	Sodium	Potassium	Spectral Absorption
	X1	X2	X3	X4	X5	X6	X7	X8	X9	X10	X11	X12	X13	X14	X15
Mean	1.36	8.61	20.04	15.37	157.59	135.05	8.15	479.46	82.27	62.38	13.47	6.08	6.98	0.93	0.45
S.D.	2.57	10.14	3.95	2.91	296.26	27.31	0.39	913.83	19.04	10.52	6.52	2.06	1.73	0.27	1.45
Variance	6.61	102.79	15.61	8.45	87767.04	745.65	0.15	835077.85	362.51	110.57	42.47	4.24	2.98	0.07	2.11

Correlation Matrix

	Rainfall	River Discharge	Air Temp	Water temp	Turbidity	Conductivity	PH	Total Solids	Alkalinity	Hardness	Calcium	Chloride	Sodium	Potassium	Spectral Absorption
Rainfall	1.00														
River Discharge	0.14	1.00													
Airtemp	-0.04	-0.48	1.00												
Watertemp	-0.10	-0.35	0.74	1.00											
Turbidity	0.17	0.87	-0.34	-0.31	1.00										
Conductivity	-0.10	-0.51	0.63	0.44	-0.57	1.00									
pH	-0.02	-0.32	0.59	0.58	-0.34	0.73	1.00								
Total Solids	0.01	0.41	-0.28	-0.24	0.65	-0.59	-0.34	1.00							
Alkalinity	-0.10	-0.43	0.57	0.25	-0.36	0.77	0.60	-0.40	1.00						
Hardness	0.15	-0.13	0.26	0.04	-0.09	0.31	0.28	-0.18	0.30	1.00					
Calcium	0.32	0.01	0.14	-0.04	0.09	0.01	0.06	-0.03	0.05	0.71	1.00				
Chloride	-0.01	0.22	-0.23	-0.35	0.18	-0.12	-0.06	0.02	-0.06	0.34	0.30	1.00			
Sodium	-0.04	-0.38	0.46	0.32	-0.34	0.58	0.46	-0.30	0.49	0.29	0.16	-0.10	1.00		
Potassium	0.09	0.24	-0.30	-0.09	0.34	-0.47	-0.22	0.57	-0.44	-0.13	-0.03	0.09	-0.02	1.00	
Spectrop.	0.13	0.34	-0.20	-0.17	0.53	-0.28	-0.35	0.29	-0.15	-0.16	-0.01	0.11	-0.13	0.20	1.00

Eigenvalues of Correlation Matrix

#1	#2	#3	#4	#5	#6	#7	#8	#9	#10	#11	#12	#13	#14	#15
5.37	2.14	1.53	1.13	1.04	0.86	0.73	0.63	0.52	0.32	0.24	0.21	0.14	0.10	0.04

Maximum Likelihood Method

# of Factors	4.00
Iteration	30.00
Log(Likelihood)	-213.87
AIC	565.75
Chi^2 with Bartlett's Correction	103.23
Df	51.00
P-Value	0.00 *** (P<=0.001)

Factor Loadings Results before Rotation

	Factor1	Factor2	Factor3	Factor4	Uniqueness	Communality	Initial Communality Estimate
Rainfall	0.17	0.02	0.27	-0.01	0.90	0.10	0.33
River Discharge	0.87	-0.07	-0.06	-0.20	0.20	0.80	0.90
Airtemp	-0.34	0.63	0.05	0.58	0.15	0.85	0.82
Watertemp	-0.31	0.42	-0.13	0.65	0.29	0.71	0.79
Turbidity	1.00	0.00	0.00	0.00	0.00	1.00	0.94
Conductivity	-0.57	0.80	-0.07	-0.12	0.03	0.97	0.86
pH	-0.34	0.69	-0.02	0.13	0.39	0.61	0.76
Total Solids	0.65	-0.26	-0.04	0.20	0.47	0.53	0.76
Alkalinity	-0.36	0.70	-0.01	-0.06	0.37	0.63	0.75
Hardness	-0.09	0.38	0.78	-0.07	0.24	0.76	0.69
Calcium	0.09	0.16	0.86	0.05	0.23	0.77	0.67

Factor Loadings Results before Rotation							
	Factor1	Factor2	Factor3	Factor4	Uniqueness	Communality	Initial Communality Estimate
Chloride	0.18	-0.03	0.39	-0.32	0.72	0.28	0.46
Sodium	-0.34	0.49	0.11	0.07	0.62	0.38	0.55
Potassium	0.34	-0.32	0.01	0.16	0.75	0.25	0.60
Spectrop.	0.53	0.00	-0.09	-0.02	0.71	0.29	0.59
Proportion	0.24	0.18	0.11	0.07			
Cumulative Proportion	0.24	0.42	0.53	0.60			
Caution: One or more of the communalities are close to one.							

Results after Varimax Rotation (Orthomax with Weight=1)						
Factor Pattern Matrix (Factor Loadings)						
	Factor1	Factor2	Factor3	Factor4	Uniqueness	Communality
Rainfall	-0.06	0.11	-0.03	0.29	0.90	0.10
River Discharge	-0.22	0.81	-0.30	0.06	0.20	0.80
Airtemp	0.45	-0.15	0.79	0.09	0.15	0.85
Watertemp	0.24	-0.15	0.78	-0.11	0.29	0.71
Turbidity	-0.28	0.94	-0.11	0.15	0.00	1.00
Conductivity	0.91	-0.30	0.22	-0.02	0.03	0.97
pH	0.66	-0.13	0.39	0.04	0.39	0.61
Total Solids	-0.48	0.55	0.03	0.02	0.47	0.53
Alkalinity	0.75	-0.14	0.22	0.05	0.37	0.63
Hardness	0.30	-0.12	0.04	0.81	0.24	0.76
Calcium	0.01	-0.03	0.06	0.88	0.23	0.77
Chloride	0.00	0.09	-0.34	0.40	0.72	0.28
Sodium	0.50	-0.21	0.26	0.13	0.62	0.38
Potassium	-0.44	0.23	0.01	0.01	0.75	0.25

Results after Varimax Rotation (Orthomax with Weight=1)						
Factor Pattern Matrix (Factor Loadings)						
	Factor1	Factor2	Factor3	Factor4	Uniqueness	Communality
Spectrop.	-0.13	0.52	-0.07	-0.01	0.71	0.29
Proportion	0.20	0.16	0.12	0.12		
Cumulative Proportion	0.20	0.36	0.48	0.60		
Caution: One or more of the communalities are close to one.						

Standardized Scoring Coefficients				
	Factor1	Factor2	Factor3	Factor4
Rainfall	0.00	0.00	0.00	0.02
River Discharge	0.01	0.00	-0.02	0.00
Airtemp	-0.03	0.01	0.17	0.02
Watertemp	-0.03	0.01	0.13	-0.02
Turbidity	0.00	0.00	0.00	0.00
Conductivity	0.04	0.01	-0.01	-0.01
pH	0.08	0.05	0.19	0.00
Total Solids	0.00	0.00	0.00	0.00
Alkalinity	0.00	0.00	0.00	0.00
Hardness	0.00	-0.01	0.00	0.04
Calcium	-0.01	-0.01	0.00	0.08
Chloride	0.01	-0.01	-0.04	0.04
Sodium	0.01	0.00	0.01	0.02
Potassium	-0.10	-0.01	0.11	0.00
Spectrop.	0.00	0.00	0.00	-0.01
Constant for Centering	-5.57	-2.26	-4.84	-3.24

APPENDIX 5-2 SPECTRAL ANALYSIS OF KULFO PH DATA USING FAST FOURIER TRANSFORM

Tau (Time)	Autocovariance	Autocorrelation	Tau (Time)	Auto covariance	Autocorrelation
0	9.942	1.000	62	-0.403	-0.041
2	9.324	0.938	64	-0.365	-0.037
4	8.716	0.877	66	-0.304	-0.031
6	8.149	0.820	68	-0.237	-0.024
8	7.549	0.759	70	-0.141	-0.014
10	6.921	0.696	72	-0.063	-0.006
12	6.308	0.635	74	-0.005	0.000
14	5.703	0.574	76	0.054	0.005
16	5.129	0.516	78	0.125	0.013
18	4.591	0.462	80	0.184	0.018
20	4.043	0.407	82	0.228	0.023
22	3.543	0.356	84	0.281	0.028
24	3.030	0.305	86	0.318	0.032
26	2.531	0.255	88	0.359	0.036
28	1.999	0.201	90	0.403	0.041
30	1.505	0.151	92	0.436	0.044
32	1.054	0.106	94	0.462	0.046
34	0.612	0.062	96	0.499	0.050
36	0.162	0.016	98	0.526	0.053
38	-0.258	-0.026	100	0.552	0.056
40	-0.652	-0.066	102	0.577	0.058
42	-1.041	-0.105	104	0.600	0.060
44	-0.964	-0.097	106	0.616	0.062
46	-0.895	-0.090	108	0.629	0.063
48	-0.847	-0.085	110	0.642	0.065
50	-0.771	-0.078	112	0.653	0.066
52	-0.671	-0.067	114	0.663	0.067
54	-0.618	-0.062	116	0.672	0.068
56	-0.549	-0.055	118	0.679	0.068
58	-0.495	-0.050	120	0.686	0.069
60	-0.455	-0.046	122	0.691	0.069
			124	0.694	0.070
			126	0.697	0.070

Frequency	Spectrum (two-sided)	Spectrum Integral	Percentage Information	Frequency	Spectrum (two-sided)	Spectrum Integral	Percentage Information
0	178.066	178.066	14%	0.128906	1.767	1237.115	98%
0.003906	264.958	443.024	35%	0.132813	1.482	1238.597	98%
0.007813	314.062	757.086	60%	0.136719	0.856	1239.454	98%
0.011719	209.717	966.803	76%	0.140625	0.332	1239.786	98%
0.015625	98.729	1065.532	84%	0.144531	0.206	1239.992	98%
0.019531	34.375	1099.907	87%	0.148438	0.741	1240.732	98%
0.023438	10.336	1110.243	88%	0.152344	1.586	1242.318	98%
0.027344	10.621	1120.864	88%	0.15625	1.538	1243.856	98%
0.03125	18.929	1139.792	90%	0.160156	0.754	1244.610	98%
0.035156	22.647	1162.440	92%	0.164063	0.267	1244.877	98%
0.039063	16.788	1179.227	93%	0.167969	0.222	1245.099	98%
0.042969	6.512	1185.739	94%	0.171875	0.600	1245.699	98%
0.046875	1.505	1187.244	94%	0.175781	1.121	1246.820	98%
0.050781	2.870	1190.114	94%	0.179688	1.062	1247.881	98%
0.054688	5.946	1196.060	94%	0.183594	0.513	1248.394	98%
0.058594	6.629	1202.689	95%	0.1875	0.187	1248.581	98%
0.0625	4.768	1207.457	95%	0.191406	0.185	1248.766	99%
0.066406	2.422	1209.879	95%	0.195313	0.411	1249.177	99%
0.070313	0.757	1210.635	96%	0.199219	0.660	1249.837	99%
0.074219	0.852	1211.487	96%	0.203125	0.582	1250.419	99%
0.078125	2.452	1213.939	96%	0.207031	0.345	1250.763	99%
0.082031	3.898	1217.837	96%	0.210938	0.165	1250.928	99%
0.085938	3.749	1221.586	96%	0.214844	0.098	1251.026	99%
0.089844	1.999	1223.585	97%	0.21875	0.213	1251.239	99%
0.09375	0.652	1224.236	97%	0.222656	0.490	1251.729	99%
0.097656	0.735	1224.971	97%	0.226563	0.677	1252.406	99%
0.101563	1.401	1226.372	97%	0.230469	0.485	1252.891	99%
0.105469	1.997	1228.369	97%	0.234375	0.168	1253.059	99%
0.109375	2.350	1230.719	97%	0.238281	0.090	1253.149	99%
0.113281	1.859	1232.578	97%	0.242188	0.232	1253.381	99%
0.117188	0.767	1233.345	97%	0.246094	0.431	1253.812	99%
0.121094	0.623	1233.968	97%	0.25	0.457	1254.269	99%
0.125	1.381	1235.348	97%	0.253906	0.257	1254.526	99%

Frequency	Spectrum (two-sided)	Spectrum Integral	Percentage Information	Frequency	Spectrum (two-sided)	Spectrum Integral	Percentage Information
0.257813	0.102	1254.628	99%	0.386719	0.086	1261.387	100%
0.261719	0.062	1254.690	99%	0.390625	0.245	1261.632	100%
0.265625	0.189	1254.879	99%	0.394531	0.295	1261.927	100%
0.269531	0.497	1255.376	99%	0.398438	0.177	1262.104	100%
0.273438	0.603	1255.979	99%	0.402344	0.075	1262.179	100%
0.277344	0.390	1256.369	99%	0.40625	0.032	1262.211	100%
0.28125	0.150	1256.519	99%	0.410156	0.053	1262.264	100%
0.285156	0.075	1256.594	99%	0.414063	0.193	1262.457	100%
0.289063	0.179	1256.773	99%	0.417969	0.301	1262.757	100%
0.292969	0.310	1257.083	99%	0.421875	0.252	1263.009	100%
0.296875	0.314	1257.397	99%	0.425781	0.150	1263.159	100%
0.300781	0.258	1257.656	99%	0.429688	0.068	1263.227	100%
0.304688	0.162	1257.817	99%	0.433594	0.076	1263.303	100%
0.308594	0.065	1257.883	99%	0.4375	0.236	1263.539	100%
0.3125	0.119	1258.002	99%	0.441406	0.382	1263.920	100%
0.316406	0.254	1258.256	99%	0.445313	0.308	1264.228	100%
0.320313	0.347	1258.603	99%	0.449219	0.142	1264.370	100%
0.324219	0.330	1258.932	99%	0.453125	0.053	1264.423	100%
0.328125	0.159	1259.091	99%	0.457031	0.127	1264.551	100%
0.332031	0.029	1259.121	99%	0.460938	0.362	1264.913	100%
0.335938	0.058	1259.179	99%	0.464844	0.475	1265.388	100%
0.339844	0.175	1259.354	99%	0.46875	0.324	1265.712	100%
0.34375	0.305	1259.659	99%	0.472656	0.142	1265.855	100%
0.347656	0.279	1259.938	99%	0.476563	0.096	1265.950	100%
0.351563	0.150	1260.088	99%	0.480469	0.196	1266.147	100%
0.355469	0.098	1260.186	99%	0.484375	0.417	1266.564	100%
0.359375	0.092	1260.279	99%	0.488281	0.494	1267.058	100%
0.363281	0.230	1260.509	99%	0.492188	0.334	1267.392	100%
0.367188	0.383	1260.893	99%	0.496094	0.223	1267.615	100%
0.371094	0.253	1261.146	99%				
0.375	0.080	1261.226	99%				
0.378906	0.046	1261.272	99%				
0.382813	0.029	1261.301	100%				

Appendix 5-3 Cluster Analysis of Lake Abaya's Water Quality Data

The spatial monitoring interval design was carried out using the cluster analysis of field water quality data of Lake Abaya. The significance of the clusters was tested statistically. The procedure is summarised below.

The variables included in the cluster analyses are: air pressure. Air temperature, water temperature, dissolved oxygen, TDS, conductivity, redox potential, and pH. 44 sampling points have been considered in the cluster analyses.

The vertical dendrogram of the cluster agglomeration is presented in figure appendix 5-3-4 below. The change in dissimilarity has been plotted against agglomeration step and the resulting graph is shown in figure appendix 5.3.1 below:

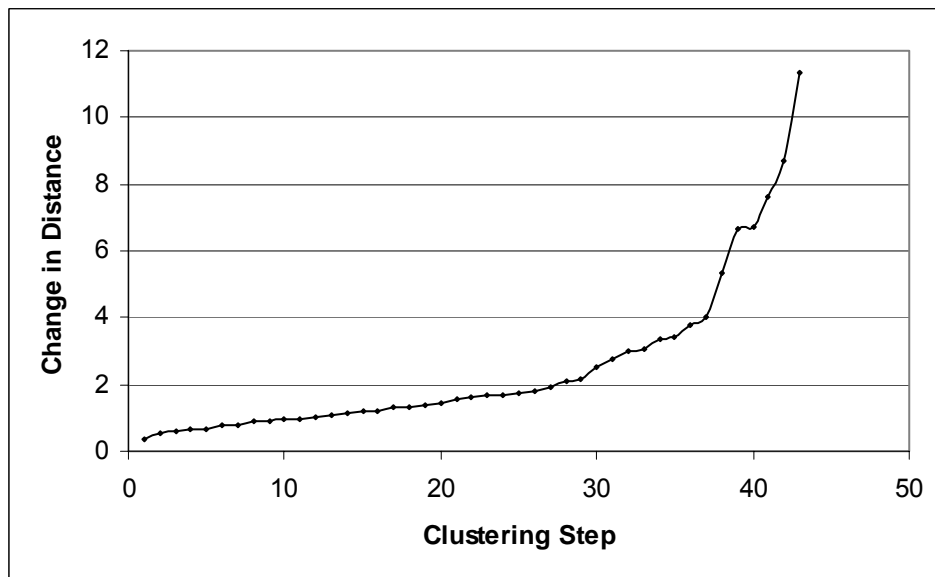


Fig. Appendix 5.3.1 Graph of Cluster Agglomeration Steps.

As can be seen from figure 5.3.1 above, the biggest change in the dissimilarity of cluster occurs when changing from agglomeration step from a distance of 4 to 5.3. This corresponds to change in agglomeration of 5 –13 to 4-5.

Table appendix 5.3.1 below shows the sequence of cluster agglomeration of the sampling points.

Table Appendix 5.3.1 Cluster Agglomeration Sequence

1	3	38	35	36	37	39	2	4	32	27	29	33	43	28	30	31	34	5	41	40	42
44	13	16	14	15	17	18	19	20	26	25	21	22	23	24	6	12	7	8	10	9	11

Table appendix 5.3.2 below shows summary of the cluster of sampling points at several level of agglomeration

Table Appendix 5.3.2 Summary of Sample Clustering at Several levels of Agglomeration.

Agglomeration Distance	Cluster 1	Cluster 2	Cluster 3	Cluster 4	Cluster 5	Cluster 6
4	1-39	2	4-34	5 – 25	21 – 24	6 – 11
6	1 – 36	37 – 39	2	4 – 24	6 – 11	
8	1 – 39	2	4 – 11			
10	1 – 2	4 – 11				

APPENDIX 5.3.2 CLUSTERING OF WATER QUALITY VARIABLES

Figure appendix 5-3-2 below shows the cluster agglomeration steps for water quality variables. It is seen that the biggest jump occurs when agglomerating from step 4 to step 5.

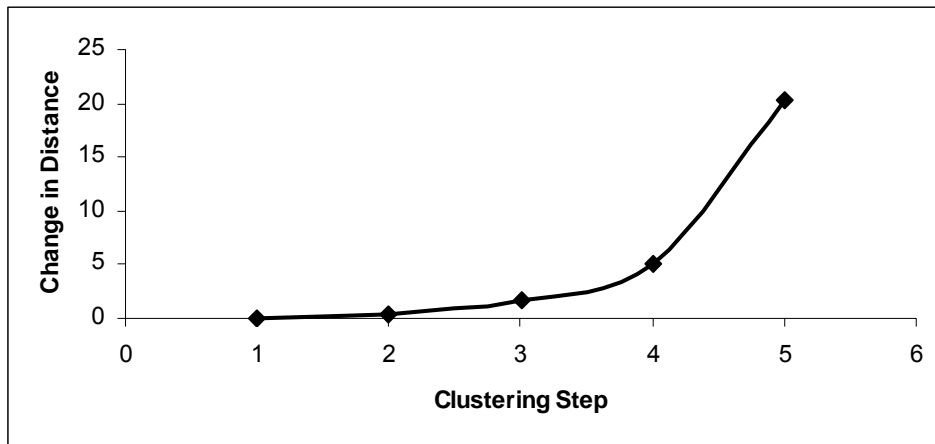


Fig. Appendix 5.3.2 Variable Cluster Agglomeration Steps

Table appendix 5.3.3 below shows the agglomeration schedule of the water quality variables.

Table Appendix 5.3.3 Agglomeration Schedule for Water Quality Variables

Agglomeration Schedule			
Step	Object1	Object2	Distance
1	2	6	0.069
2	1	2	0.284
3	1	5	1.784
4	3	4	5.036
5	1	3	20.282

Table appendix 5.3.4 below shows the dissimilarity matrix by the standard Euclidian distance.

Table Appendix 5.3.4 Dissimilarity Matrix by Euclidian Distance

Variable	Object1	Object2	Object3	Object4	Object5	Object6
	Water Temperature	PH	TDS	Conductivity	Redox Potential	Dissolved Oxygen
Water Temperature	0					
PH	0.21	0.00				
TDS	9.40	9.61	0.00			
Conductivity	14.39	14.60	5.04	0.00		
Redox Potential	1.62	1.41	11.02	16.01	0.00	
Dissolved Oxygen	0.28	0.07	9.68	14.67	1.34	0.00

Figure appendix 5.3.3 below shows the vertical dendrogram of the agglomeration schedule.

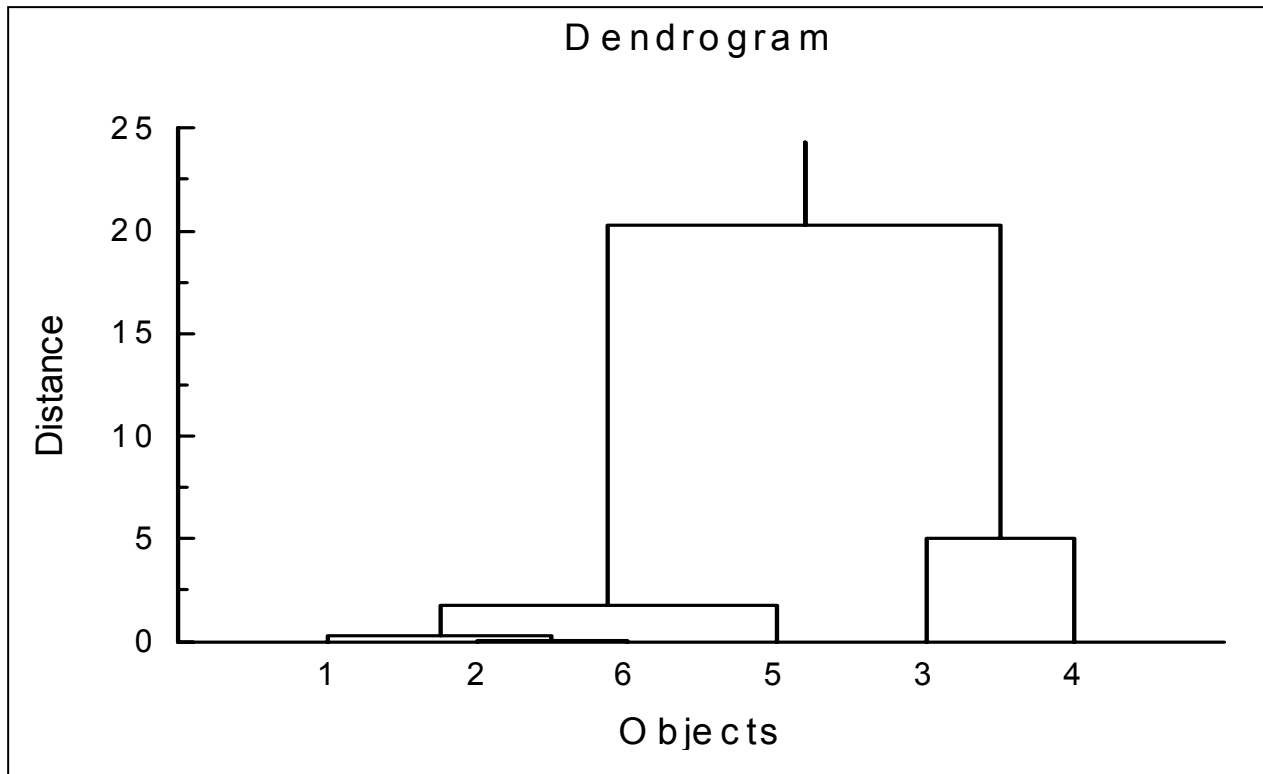


Fig. Appendix 5.3.3 Vertical Dendrogram of Cluster variables

It is seen from the cluster agglomeration that, variables 1, 2, 5 and 6 are considered as homogenous. Their clustering may have been caused by temporary variability factors. On the other hand variables 3 and 4 (TDS and conductivity) are clustered together and separately from the others. This may have been due to the fact that these variables measure long-term effects of water quality. However, the higher cluster distance of 5 between these variables (3 and 4) is unexpected as the two variables measure more or less the same thing. It may point to errors in the instrumentation used to measure these variables.

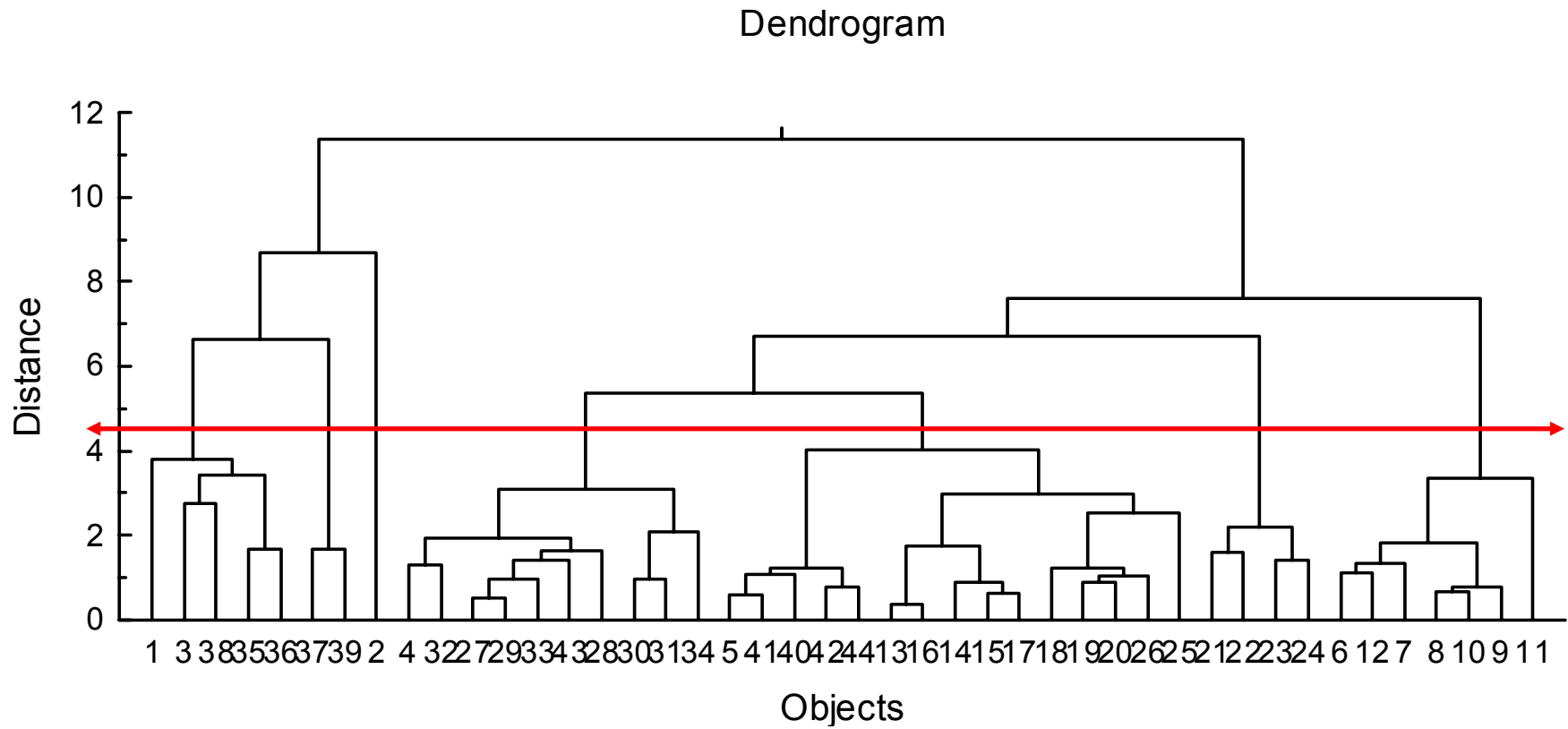


Fig. Appendix 5.3.4 Vertical Dendrogram of Sample Clusters

Table appendix 5.3.5 shows the agglomeration schedule of the cluster composed of the sampling points.

Table Appendix 5.3.5 Cluster Agglomeration of Sampling Points

Agglomeration Schedule			
Step	Object1	Object2	Distance
1	13	16	0.353
2	27	29	0.516
3	5	41	0.580
4	15	17	0.631
5	8	10	0.662
6	8	9	0.777
7	42	44	0.780
8	19	20	0.872
9	14	15	0.891
10	30	31	0.946
11	27	33	0.958
12	19	26	1.031
13	5	40	1.065
14	6	12	1.125
15	18	19	1.217
16	5	42	1.219
17	4	32	1.301
18	6	7	1.334
19	23	24	1.399
20	27	43	1.424
21	21	22	1.589
22	27	28	1.644
23	35	36	1.652
24	37	39	1.681
25	13	14	1.732
26	6	8	1.812
27	4	27	1.918
28	30	34	2.086
29	21	23	2.186
30	18	25	2.542
31	3	38	2.732
32	13	18	2.987
33	4	30	3.078
34	6	11	3.348
35	3	35	3.428
36	1	3	3.785
37	5	13	4.011
38	4	5	5.368
39	1	37	6.638
40	4	21	6.699
41	4	6	7.607
42	1	2	8.696
43	1	4	11.365

Appendix 6. Ionic Strength Adjustment for Water Sources under Study

The ionic strength I is given by the formula:

$$I = \frac{1}{2} \sum Z_i^2 [S_i]_0$$

Where Z_i are the charges of the ion and $[S_i]_0$ the Molar concentration of the respective ion. Taking the average dry condition of each water sources in this study, the ionic strengths are calculated as shown in Table Appendix 6.4 below.

Appendix 6.1 Chemical Information

The chemical formula. Atomic weight charge and equivalent weights for the major ions encountered are given in table appendix 6.1 below.

Table Appendix 6.1 Chemical Formulas and atomic weights

Ion	Chemical Formula	Molecular Weight	Charge	Equivalent Weight
Calcium	Ca ²⁺	40.08	+2	20.04
Magnesium	Mg ²⁺	24.305	+2	12.1525
Sodium	Na ⁺	22.9898	+1	22.9898
Potassium	K ⁺	39.0983	+1	39.0983
Carbonate	CO ₃ ²⁻	60.0092	-2	30.0046
Bicarbonate	HCO ₃ ⁻	61.0171	-1	61.0171
Chloride	Cl ⁻	35.453	-1	35.453
Sulphate	SO ₄ ²⁻	96.0576	-2	48.0288
Nitrate	NO ₃ ⁻	62.0049	-1	62.0049
Nitrite	NO ₂ ⁻	46.0055	-1	46.0055
Ammonium	NH ₄ ⁺	18.0383	+1	18.0383
Phosphate	PO ₄ ³⁻	94.9714	-3	31.65713
H-Silica	HsiO ₃ ⁻	77.0916	-1	77.0916
siliciumion	SiO ₃ ²⁻	76.0837	-2	38.04185

Appendix 6.2 Concentrations and Molarity

The concentrations and molarities for average dry high ionic concentrations conditions are taken for each water source. The concentrations and molarities are given in table appendix 6.2 below.

Table Appendix 6.2 Concentrations and Molarity of Lakes and rivers. Abaya Chamo Basin.

Ion	Unit	Concentration(mg L ⁻¹)					Molarity				
		Abaya	Chamo	Hare	Kulfo	Sile	Abaya	Chamo	Hare	Kulfo	Sile
pH	pH Units	8.9	9.24	7.6	8.6	8.4					
Calcium	mg L ⁻¹	18.0	14	8	17	12	0.00045	0.000366	0.000216	0.000445	0.000315
Magnesium	mg L ⁻¹	3.2	10	2	5	5	0.000134	0.000421	8.77E-05	0.000207	0.002107
Sodium	mg L ⁻¹	239.6	420	4	8	20	0.010423	0.018295	0.000204	0.000365	0.000896
Potassium	mg L ⁻¹	17.3	22	1	0.9	3	0.000445	0.000576	2.56E-05	2.3E-05	8.18E-05
Carbonate	mg L ⁻¹	55.2	117	0	0	3	0.000921	0.00196	0	0	5.53E-05
Bicarbonate	mg L ⁻¹	421	765	5	110	337	0.006903	0.012544	0.00085	0.001804	0.005525
Chloride	mg L ⁻¹	77	140	4	5	19	0.002173	0.003967	0.000113	0.000149	0.000542
Sulphate	mg L ⁻¹	25	24	7	9	1.1	0.000264	0.000259	7.29E-05	9.58E-05	1.18E-05
Nitrate	mg L ⁻¹	1.8	1	0.3	1.2	1.2	2.9E-05	1.61E-05	5.27E-06	2.06E-05	2.08E-05
Nitrite	mg L ⁻¹	0.05	0.02	0.03	0.05	0.06	1.09E-06	4.35E-07	6.52E-07	1.09E-06	1.3E-06
Ammonium	mg L ⁻¹	0.91	0.5	0.26	0.53	1.1	5.04E-05	2.77E-05	1.44E-05	2.94E-05	6.18E-05
Phosphate	mg L ⁻¹	0.18	0.02	0.06	0.06	0.07	1.97E-06	2.95E-07	6.42E-07	6.42E-07	7.37E-07
H-Silica	mg L ⁻¹	38	2.3	17	18	1.2	0.000495	3.06E-05	0.000227	0.000236	1.62E-05
Siliciumion	mg L ⁻¹	0.00	0.00	2.3	0	0	9.99E-09	1.39E-09	3.13E-12	3.01E-10	4.07E-10

Appendix 6.3 Ions Balance Check

Table appendix 6.3 below gives the milli-equivalent per liter of ions and the anion/cation balance. As it can be seen the percentage error for the river water is higher due to the low concentration of ions in solution.

Table Appendix 6.3 Ionic Balance Check

Ion	Chemical Formula	Milli – Equivalent per Liter					Sum of Cations / Anions					
		Abaya	Chamo	Hare	Kulfo	Sile		Abaya	Chamo	Hare	Kulfo	Sile
Calcium	Ca ²⁺	0.9003	0.7322	0.4322	0.8897	0.630402	Cations(me.L ⁻¹)	12.08	20.47	0.96	1.76	5.883323
Magnesium	Mg ²⁺	0.2681	0.8420	0.1755	0.4147	4.21327	Anions(me.L ⁻¹)	11.56	20.98	0.99	2.01	6.242223
Sodium	Na ⁺	10.4229	18.2953	0.2044	0.3654	0.89605	%Difference	4.31%	2.49%	2.81%	14.10%	6.10%
Potassium	K ⁺	0.4449	0.5760	0.0256	0.0230	0.081845						
Carbonate	CO ₃ ²⁻	1.8411	3.9201	0.0000	0.0000	0.110508						
Bicarbonate	HCO ₃ ⁻	6.9033	12.5439	0.8502	1.8044	5.525386						
Chloride	Cl ⁻	2.1731	3.9670	0.1128	0.1495	0.542289						
Sulphate	SO ₄ ²⁻	0.5288	0.5181	0.1457	0.1916	0.023528						
Nitrate	NO ₃ ⁻	0.0290	0.0161	0.0053	0.0206	0.020805						
Nitrite	NO ₂ ²⁻	0.0011	0.0004	0.0007	0.0011	0.001304						
Ammonium	NH ₄ ⁺	0.0504	0.0277	0.0144	0.0294	0.061757						
Phosphate	PO ₄ ³⁻	0.0059	0.0009	0.0019	0.0019	0.002211						
H-Silica	HSiO ₃ ⁻	0.4946	0.0306	0.2269	0.2359	0.016192						
siliciumion	SiO ₃ ²⁻	0.0000	0.0000	0.0000	0.0000	8.13E-07						

Appendix 6. 4. Calculation of Ionic Strength

The ionic strength contribution of each ion and the total ionic strength are given in the table appendix 6.4 below.

Table Appendix 6.4 Calculation of Ionic Strength

Ion	Chemical Formula	Individual Ionic Strength					Total Ionic Strength			
		Abaya	Chamo	Hare	Kulfo	Sile	Abaya	Chamo	Hare	Kulfo
Calcium	Ca ²⁺	0.0009	0.000732	0.000432	0.00089	0.00063	0.013551	0.023726	0.00136	0.002693
Hardness	CaCO ₃ (s)	0	0	0	0	0				Sile

Ion	Chemical Formula	Individual Ionic Strength					Total Ionic Strength			
		Abaya	Chamo	Hare	Kulfo	Sile	Abaya	Chamo	Hare	Kulfo
Magnesium	Mg ²⁺	0.000268	0.000842	0.000175	0.000415	0.004213				0.008554
Sodium	Na ⁺	0.005211	0.009148	0.000102	0.000183	0.000448				
Potassium	K ⁺	0.000222	0.000288	1.28E-05	1.15E-05	4.09E-05				
Carbonate	CO ₃ ²⁻	0.001841	0.00392	0	0	0.000111				
Bicarbonate	HCO ₃ ⁻	0.003452	0.006272	0.000425	0.000902	0.002763				
Chloride	Cl ⁻	0.001087	0.001983	5.64E-05	7.47E-05	0.000271				
Sulphate	SO ₄ ²⁻	0.000529	0.000518	0.000146	0.000192	2.35E-05				
Nitrate	NO ₃ ⁻	1.45E-05	8.06E-06	2.63E-06	1.03E-05	1.04E-05				
Nitrite	NO ₂ ⁻	5.43E-07	2.17E-07	3.26E-07	5.43E-07	6.52E-07				
Ammonia	NH ₃ (g)	0	0	0	0	0				
Ammonium	NH ₄ ⁺	2.52E-05	1.39E-05	7.21E-06	1.47E-05	3.09E-05				
Phosphate	PO ₄ ³⁻	0.002179	0.000464	0.000232	0.000256	3.32E-06				
Silica	SiO ₂ (s)	0	0	0	0	0				
H-Silica	HSiO ₃ ⁻	0.000247	1.53E-05	0.000113	0.000118	8.1E-06				
siliciumion	SiO ₃ ²⁻	2E-08	2.79E-09	6.25E-12	6.02E-10	8.13E-10				

Appendix 6.5 Activity Coefficients of Individual ions (Log (γ))

The activity coefficient for common ions is calculated and is given in table appendix 6.5.

Table Appendix 6.5 Activity Coefficients for common ions

Ion			Activity Coefficient (Log (γ))				
			Abaya	Chamo	Hare	Kulfo	Sile
	Formula	Charge					
	Ionic Strength		0.0136	0.0237	0.0014	0.0027	0.0086
Hydrogen	H ⁺	1	-0.051	-0.064	-0.018	-0.024	-0.041
Hydroxide	OH ⁻	-1	-0.051	-0.064	-0.018	-0.024	-0.041
Calcium	Ca ²⁺	2	-0.203	-0.257	-0.071	-0.098	-0.166
Hardness	CaCO ₃ (s)	0	0.000	0.000	0.000	0.000	0.000

Ion			Activity Coefficient (Log (γ))				
			Abaya	Chamo	Hare	Kulfo	Sile
	Formula	Charge					
	Ionic Strength		0.0136	0.0237	0.0014	0.0027	0.0086
Magnesium	Mg ²⁺	2	-0.203	-0.257	-0.071	-0.098	-0.166
Sodium	Na ⁺	1	-0.051	-0.064	-0.018	-0.024	-0.041
Potassium	K ⁺	1	-0.051	-0.064	-0.018	-0.024	-0.041
Carbonate	CO ₃ ²⁻	2	-0.203	-0.257	-0.071	-0.098	-0.166
Bicarbonate	HCO ₃ ⁻	1	-0.051	-0.064	-0.018	-0.024	-0.041
Chloride	Cl ⁻	1	-0.051	-0.064	-0.018	-0.024	-0.041
Sulphate	SO ₄ ²⁻	2	-0.203	-0.257	-0.071	-0.098	-0.166
Nitrate	NO ₃ ⁻	1	-0.051	-0.064	-0.018	-0.024	-0.041
Nitrite	NO ₂ ⁻	1	-0.051	-0.064	-0.018	-0.024	-0.041
Ammonia	NH ₃ (g)	0	0.000	0.000	0.000	0.000	0.000
Ammonium	NH ₄ ⁺	1	-0.051	-0.064	-0.018	-0.024	-0.041
Phosphate	PO ₄ ³⁻	3	-0.457	-0.579	-0.159	-0.220	-0.373
Silica	SiO ₂ (s)	0	0.000	0.000	0.000	0.000	0.000
H-Silica	HSiO ₃ ⁻	1	-0.051	-0.064	-0.018	-0.024	-0.041
siliciumion	SiO ₃ ²⁻	2	-0.203	-0.257	-0.071	-0.098	-0.166

Appendix 7-1 One – lag MA model of TDS and conductivity

1lagMA model of TDS and conductivity									
Spectrum Frequency	Coherency (1,2)	Spectrum Frequency	S (1,1)	S (2,2)	Re {S (1,2)}	Im {S (1,2)}	Amplitude (1,2)	Phase (1,2)	Coherency (1,2)
0.0	1.0	0.0	9.1	2.7	4.9	0.6	4.9	0.1	1.0
0.0	0.8	0.0	10.8	2.7	4.5	1.8	4.8	0.4	0.8
0.0	1.0	0.0	92.5	35.2	49.3	26.5	56.0	0.5	1.0
0.0	0.7	0.0	529.6	77.6	153.5	64.2	166.3	0.4	0.7
0.0	0.8	0.0	1501.1	120.7	364.6	136.5	389.3	0.4	0.8
0.1	0.9	0.1	1757.5	152.6	460.2	183.5	495.4	0.4	0.9
0.1	0.7	0.1	766.9	148.4	268.4	84.6	281.4	0.3	0.7
0.1	1.0	0.1	262.7	219.0	234.6	-8.6	234.7	0.0	1.0
0.1	0.8	0.1	482.1	241.7	308.7	15.8	309.1	0.1	0.8
0.1	0.7	0.1	486.0	129.7	192.5	74.0	206.3	0.4	0.7
0.1	0.7	0.1	255.1	70.2	78.5	84.3	115.2	0.8	0.7
0.1	0.8	0.1	69.6	59.8	39.8	43.5	58.9	0.8	0.8
0.1	0.7	0.1	19.2	34.8	15.8	14.6	21.5	0.7	0.7
0.2	0.4	0.2	22.7	17.8	13.0	2.1	13.2	0.2	0.4
0.2	0.7	0.2	34.1	23.9	24.3	-1.4	24.4	-0.1	0.7
0.2	0.6	0.2	26.4	31.2	21.6	7.5	22.8	0.3	0.6
0.2	0.7	0.2	20.8	19.2	11.9	12.2	17.0	0.8	0.7
0.2	0.7	0.2	15.0	5.5	5.0	5.8	7.7	0.9	0.7
0.2	0.2	0.2	4.4	1.2	0.9	0.4	1.0	0.4	0.2
0.2	0.1	0.2	1.6	0.6	0.2	0.3	0.3	0.9	0.1
0.2	0.9	0.2	2.4	0.2	0.3	0.7	0.7	1.2	0.9
0.3	0.9	0.3	2.8	0.2	0.5	0.6	0.8	0.8	0.9
0.3	0.9	0.3	2.8	0.5	0.9	0.7	1.1	0.7	0.9
0.3	0.9	0.3	2.7	0.9	1.3	0.8	1.6	0.6	0.9
0.3	0.9	0.3	2.6	1.7	1.8	0.8	2.0	0.4	0.9
0.3	0.9	0.3	2.4	1.9	1.9	0.6	2.0	0.3	0.9
0.3	0.5	0.3	3.2	1.1	1.4	-0.2	1.4	-0.1	0.5
0.3	0.8	0.3	3.9	0.4	0.8	-0.8	1.2	-0.8	0.8
0.3	0.3	0.3	2.4	0.6	0.6	-0.3	0.7	-0.5	0.3
0.4	0.8	0.4	2.8	2.4	2.2	0.8	2.4	0.3	0.8
0.4	0.9	0.4	6.3	4.4	4.9	1.1	5.0	0.2	0.9
0.4	0.9	0.4	8.0	4.7	5.8	0.9	5.9	0.1	0.9

Appendix 7-2: Water Quality Data for River Kulfo. Missing values filled in by Cubic Spline Interpolation.

Date	S.No.	Conduct.	TDS	Redox	Dissolved Oxygen	Turbidity	pH	water temp	Calcium	Magnesium	Hardness	Alkalinity	Chloride	Air Temp	Pota.	Sodium	Total Solids	Rain Fall
		$\mu\text{S.Cm}^{-1}$	mg L^{-1}	mV	mg L^{-1}	NTU	pH	$^{\circ}\text{C}$	mg L^{-1}	mg L^{-1}	mg L^{-1} (CaCO_3)	mg L^{-1} (CaCO_3)	mg L^{-1}	$^{\circ}\text{C}$	mg L^{-1}	mg L^{-1}	mg L^{-1}	mm.D^{-1}
18-Jun	1.00	110.00	67.00	-55.00	4.80	68.00	8.40	17.60	13.00	2.00	76.00	57.00	3.00	28.00	0.97	7.25	148.00	0.40
19-Jun	2.00	130.00	71.00	-54.00	3.90	34.00	8.10	19.60	13.00	1.00	66.00	59.00	3.00	26.00	0.87	6.21	140.00	0.00
20-Jun	3.00	121.00	75.00	-53.00	3.40	25.00	8.70	19.40	13.00	1.00	78.00	65.00	3.00	27.00	0.77	6.42	36.00	0.00
21-Jun	4.00	133.00	83.00	-53.00	2.60	27.00	8.60	18.00	14.00	1.00	68.00	68.00	2.00	25.00	0.97	7.15	44.00	0.00
22-Jun	5.00	134.00	89.00	-37.00	2.50	38.00	8.40	18.00	15.00	1.00	60.00	67.00	3.00	26.50	0.87	7.77	82.00	0.00
23-Jun	6.00	133.00	97.00	-56.00	4.20	20.00	8.30	18.70	15.00	1.00	84.00	72.00	2.00	27.00	0.87	7.98	88.00	0.00
24-Jun	7.00	154.00	100.00	-50.00	3.30	17.00	8.50	18.70	16.00	1.00	106.00	79.00	2.00	27.00	0.87	8.39	14.00	3.90
25-Jun	8.00	162.00	106.00	-37.00	4.30	17.00	8.30	17.60	16.00	2.00	92.00	78.00	2.00	21.00	1.17	8.60	64.80	1.60
26-Jun	9.00	154.00	103.00	-63.00	4.50	15.00	8.60	22.90	16.00	1.00	172.00	78.00	2.00	29.00	1.07	8.60	126.00	0.80
27-Jun	10.00	155.33	102.00	-81.18	4.91	14.83	9.02	22.71	16.49	1.31	171.33	79.76	2.00	29.27	1.33	8.00	76.30	0.00
28-Jun	11.00	153.00	104.00	-88.71	4.90	14.00	9.25	21.40	17.00	2.00	150.00	82.00	2.00	28.00	1.67	7.66	6.00	0.00
29-Jun	12.00	134.00	103.00	-84.00	3.90	10.00	9.00	23.80	17.00	2.00	176.00	83.00	2.00	32.00	1.77	8.39	14.00	0.00
30-Jun	13.00	161.00	105.00	-67.00	4.20	14.00	8.90	19.00	18.00	2.00	154.00	87.00	2.50	25.00	2.46	9.94	44.71	2.00
1-Jul	14.00	169.00	108.00	-95.00	3.50	10.00	9.30	25.10	18.00	2.00	184.00	87.00	2.00	30.00	1.87	8.91	80.04	0.00
2-Jul	15.00	165.00	112.00	-64.00	3.90	5.00	8.90	19.30	18.00	2.00	130.00	87.00	2.50	24.00	2.36	10.15	120.82	0.00
3-Jul	16.00	165.00	107.00	-78.00	3.10	8.00	9.00	19.20	19.00	2.00	160.00	88.00	2.50	26.50	2.06	10.88	167.86	0.00

Date	S.No.	Conduct.	TDS	Redox	Dissolved Oxygen	Turbidity	pH	water temp	Calcium	Magnesium	Hardness	Alkalinity	Chloride	Air Temp	Pota.	Sodium	Total Solids	Rain Fall
4-Jul	17.00	175.00	111.00	-75.00	3.80	7.00	9.00	18.90	19.00	1.00	150.00	85.00	2.50	27.00	2.76	10.15	222.00	0.00
5-Jul	18.00	172.00	110.00	-70.00	4.30	10.00	8.80	19.10	20.00	2.00	166.00	90.00	2.50	26.50	2.06	9.32	193.16	0.05
6-Jul	19.00	160.00	102.00	-63.00	4.50	10.00	8.70	19.70	17.00	1.00	152.00	80.00	2.50	27.50	2.46	8.70	186.00	0.00
7-Jul	20.00	141.00	97.00	-49.00	4.30	30.00	8.50	18.70	17.00	1.00	168.00	75.00	2.50	26.50	2.73	8.91	248.00	2.20
8-Jul	21.00	153.00	105.00	-70.00	3.00	14.00	8.80	19.10	18.00	2.00	173.00	87.00	3.00	26.50	1.82	9.32	139.00	0.00
9-Jul	22.00	162.00	105.00	-64.00	3.50	8.00	8.80	18.60	18.00	2.00	119.00	89.00	2.50	24.50	1.92	9.12	211.00	0.00
10-Jul	23.00	168.00	110.00	-39.00	4.70	6.00	8.30	17.90	19.00	2.00	177.00	90.00	2.50	23.00	1.82	9.72	112.00	0.00
11-Jul	24.00	151.00	101.00	-53.00	4.30	9.00	8.60	19.00	17.00	1.00	199.00	79.00	2.00	26.00	1.72	8.41	121.00	0.00
12-Jul	25.00	167.00	105.00	-75.00	4.00	7.00	8.50	20.50	18.00	2.00	210.00	86.00	2.00	28.50	1.72	9.32	51.00	0.00
13-Jul	26.00	167.67	104.27	-53.72	3.73	65.99	8.22	18.25	16.82	2.37	202.67	76.88	2.93	26.17	1.82	9.92	190.96	0.00
14-Jul	27.00	165.00	105.00	-37.00	3.60	95.00	8.20	16.80	16.00	2.00	185.00	71.00	3.50	24.00	2.03	10.24	319.00	0.00
15-Jul	28.00	171.00	113.00	-72.00	3.70	11.00	8.80	20.50	18.00	1.00	168.00	87.00	2.50	27.00	2.25	10.31	182.00	0.00
16-Jul	29.00	177.80	116.72	-81.93	4.03	30.93	8.97	21.77	19.08	0.74	167.73	94.14	2.05	27.20	2.41	10.20	102.15	0.00
17-Jul	30.00	182.40	117.02	-72.39	4.43	42.69	8.81	21.12	19.35	1.07	179.76	93.84	2.07	25.52	2.44	9.96	75.24	0.00
18-Jul	31.00	181.80	116.06	-56.65	4.64	38.11	8.55	19.79	19.20	1.62	194.42	90.13	2.30	23.83	2.26	9.64	81.71	0.05
19-Jul	32.00	173.00	116.00	-48.00	4.40	9.00	8.40	19.00	19.00	2.00	202.00	87.00	2.50	24.00	1.78	9.31	102.00	0.00
20-Jul	33.00	153.00	111.00	-49.00	3.70	8.00	8.50	19.50	19.00	2.00	197.00	87.00	2.50	27.00	1.88	9.21	121.00	1.70
21-Jul	34.00	111.00	78.00	-33.00	3.20	190.00	8.10	19.20	13.00	1.00	178.00	56.00	4.00	24.00	5.31	10.00	2134.00	0.00
22-Jul	35.00	99.20	71.96	-33.08	3.11	244.17	8.09	20.25	10.69	1.00	167.97	45.16	4.58	25.05	6.20	9.97	116.17	0.00
23-Jul	36.00	107.30	85.82	-43.81	3.30	194.73	8.35	21.87	11.42	1.00	166.29	50.54	4.35	28.30	5.05	9.28	104.24	0.70

Date	S.No.	Cond uct.	TDS	Redox	Dissolved Oxygen	Turbidity	pH	water temp	Calcium	Magne sium	Hardness	Alkalinity	Chlor ide	Air Temp	Pota.	Sodium	Total Solids	Rain Fall
24-Jul	37.00	125.00	104.02	-54.38	3.52	103.92	8.60	22.72	13.44	1.00	169.97	62.14	3.70	30.39	3.12	8.37	97.07	21.20
25-Jul	38.00	142.00	111.00	-54.00	3.50	34.00	8.60	21.50	15.00	1.00	176.00	70.00	3.00	28.00	1.68	7.64	103.00	1.70
26-Jul	39.00	148.00	98.00	-37.00	3.10	23.00	8.20	17.60	15.00	1.00	182.00	68.00	2.50	19.50	1.48	7.34	149.00	0.00
27-Jul	40.00	138.00	94.00	-72.00	2.90	30.00	8.80	21.40	16.00	1.00	183.00	69.00	2.50	28.00	1.88	7.74	293.00	5.00
28-Jul	41.00	123.30	85.01	-67.09	3.02	34.54	8.72	22.33	14.49	1.00	182.45	63.16	2.75	30.73	1.92	7.46	307.16	0.70
29-Jul	42.00	109.70	74.73	-41.67	3.36	35.96	8.29	21.01	11.98	1.00	178.21	54.31	3.02	28.79	1.75	6.76	239.85	1.70
30-Jul	43.00	103.00	69.00	-30.00	3.70	34.00	8.10	18.90	11.00	1.00	168.00	49.00	3.00	25.00	1.58	6.16	184.00	0.60
31-Jul	44.00	109.00	71.00	-53.00	3.90	29.00	8.50	17.10	13.00	1.00	151.00	51.00	2.50	21.50	1.58	5.96	200.00	6.00
1-Aug	45.00	112.00	75.00	-61.00	2.80	125.00	8.60	17.80	12.00	1.00	167.00	45.00	3.00	21.00	1.31	6.40	464.00	9.50
2-Aug	46.00	98.38	69.32	-47.64	2.64	184.30	8.35	17.94	10.81	1.00	163.67	40.72	3.38	22.88	1.02	6.71	973.44	0.05
3-Aug	47.00	77.00	56.00	-21.00	3.40	200.00	7.90	17.20	10.00	1.00	140.00	39.00	3.50	26.00	0.85	6.71	1631.00	0.10
4-Aug	48.00	56.71	57.59	-22.87	3.93	171.29	7.95	19.07	9.55	1.00	128.81	38.46	3.22	29.98	0.76	6.44	1288.25	0.00
5-Aug	49.00	46.38	67.27	-42.53	4.15	115.52	8.30	22.17	9.45	1.00	128.77	38.84	2.68	33.40	0.74	5.97	945.50	0.00
6-Aug	50.00	54.86	72.82	-59.42	3.99	65.49	8.61	24.17	9.63	1.00	135.09	39.56	2.18	34.24	0.76	5.34	602.75	1.10
7-Aug	51.00	91.00	62.00	-53.00	3.40	54.00	8.50	22.70	10.00	1.00	143.00	40.00	2.00	30.50	0.80	4.60	260.00	8.30
8-Aug	52.00	44.00	29.00	-13.00	2.40	1250.00	7.80	16.70	10.47	1.00	148.78	39.74	2.34	21.50	0.90	4.70	2299.00	2.90
9-Aug	53.00	92.00	62.00	-47.00	2.50	190.00	8.30	17.00	11.00	1.00	153.00	39.00	3.00	20.00	1.00	5.10	1128.00	0.00
10-Aug	54.00	100.00	66.00	-52.00	3.00	130.00	8.40	16.80	11.00	1.00	152.00	42.00	2.50	24.50	1.00	5.40	637.00	0.00
11-Aug	55.00	102.00	70.00	-10.00	4.00	73.00	7.30	16.80	11.00	1.00	153.00	47.00	2.50	22.00	5.54	7.90	226.00	0.00
12-Aug	56.00	106.83	67.44	-31.29	4.07	51.83	7.14	18.07	11.69	1.00	151.31	49.49	2.56	23.03	6.80	8.21	125.97	0.00

Date	S.No.	Cond uct.	TDS	Redox	Dissolved Oxygen	Turbidity	pH	water temp	Calcium	Magne sium	Hardness	Alkalinity	Chlor ide	Air Temp	Pota.	Sodium	Total Solids	Rain Fall
13-Aug	57.00	110.00	63.00	-55.00	3.40	107.00	7.50	19.00	12.00	1.00	150.00	49.00	3.00	25.00	5.15	7.40	290.00	0.00
14-Aug	58.00	107.00	62.00	-19.00	2.40	255.00	7.80	18.10	11.00	1.00	152.00	46.00	4.00	25.00	1.92	6.90	1310.00	0.00
15-Aug	59.00	114.00	68.00	-38.00	3.20	74.00	8.20	16.90	13.00	1.00	149.00	50.00	2.50	22.50	1.00	6.10	232.00	6.60
16-Aug	60.00	71.00	28.00	-54.00	2.20	150.00	8.40	23.00	11.00	1.00	151.00	31.00	2.00	30.00	10.74	6.60	2627.00	7.40
17-Aug	61.00	82.00	55.00	-54.00	2.80	1700.00	8.50	17.90	11.00	1.00	151.00	35.00	2.00	22.00	3.88	7.00	1915.00	3.90
18-Aug	62.00	69.00	55.00	-65.00	2.60	170.00	8.60	20.90	11.00	1.00	168.00	32.00	3.00	30.00	13.58	7.30	2913.00	0.00
19-Aug	63.00	90.00	59.00	-84.00	2.80	180.00	9.00	18.20	11.00		161.00	39.00	2.50	27.50	5.74	6.90	1318.00	0.00
20-Aug	64.00	101.00	65.00	-71.00	2.70	230.00	8.70	17.80	12.00	1.00	158.00	42.00	3.00	23.00	2.60	8.40	687.00	0.30
21-Aug	65.00	88.00	63.00	-67.00	3.20	120.00	8.40	17.60	11.00	1.00	157.00	44.00	3.50	25.00	2.21	7.20	520.00	0.00
22-Aug	66.00	95.00	67.00	-54.00	3.40	78.00	8.00	18.10	11.00	1.00	155.00	44.00	3.00	23.00	2.11	8.00	318.00	0.00
23-Aug	67.00	124.00	67.00	-67.00	3.60	47.00	8.30	17.00	12.00	1.00	155.00	48.00	3.00	23.00	1.43	6.70	113.00	0.00
24-Aug	68.00	116.00	70.00	-22.00	3.40	37.00	7.90	17.70	12.00	1.00	147.00	50.00	2.50	25.50	1.43	6.60	242.00	0.00
25-Aug	69.00	116.00	74.00	-53.00	3.50	31.00	8.50	18.20	13.00	1.00	161.00	56.00	2.00	23.50	1.53	6.80	265.23	0.00
26-Aug	70.00	102.00	72.00	-47.00	3.40	80.00	8.40	18.60	13.00	1.00	156.00	50.00	2.50	24.00	1.62	7.00	233.00	0.00
27-Aug	71.00	112.00	81.00	-21.00	3.20	72.00	7.90	18.20	14.00	1.00	161.00	60.00	4.00	25.00	1.53	5.40	214.00	0.00
28-Aug	72.00	129.00	82.00	-25.00	3.90	18.00	8.00	17.80	14.00	1.00	158.00	58.00	3.00	22.00	1.53	7.10	157.00	0.05
29-Aug	73.00	123.00	68.00	-55.00	3.70	65.00	8.50	17.40	11.00	1.00	167.00	48.00	3.00	20.50	1.43	5.60	246.00	1.10
30-Aug	74.00	118.00	75.00	-45.00	3.70	35.00	8.40	17.80	12.00	1.00	144.00	54.00	2.50	21.50	1.55	5.70	178.00	1.10
31-Aug	75.00	97.00	64.00	-63.00	3.80	33.00	8.70	18.00	11.00	1.00	142.00	56.00	2.50	22.00	1.65	5.20	203.15	2.80
1-Sep	76.00	82.61	58.37	-64.90	4.43	46.34	8.58	17.92	10.21	1.00	135.47	54.11	2.97	23.10	1.77	4.89	313.79	4.20

Date	S.No.	Conduct.	TDS	Redox	Dissolved Oxygen	Turbidity	pH	water temp	Calcium	Magnesium	Hardness	Alkalinity	Chloride	Air Temp	Pota.	Sodium	Total Solids	Rain Fall
2-Sep	77.00	73.94	56.96	-53.90	5.35	73.04	8.14	17.68	9.65	1.00	127.11	49.11	3.71	24.58	1.90	4.75	477.06	2.70
3-Sep	78.00	70.05	56.96	-38.00	6.15	106.77	7.64	17.48	9.29	1.00	121.42	42.96	4.37	26.00	2.00	4.72	660.09	0.50
4-Sep	79.00	70.05	55.57	-25.21	6.41	141.20	7.31	17.51	9.08	1.00	122.88	37.60	4.58	26.95	2.02	4.76	830.03	2.60
5-Sep	80.00	73.00	50.00	-23.54	5.70	170.00	7.40	18.00	9.00	1.00	136.00	35.00	4.00	27.00	1.94	4.80	954.00	5.60
6-Sep	81.00	78.00	39.00	-41.00	3.90	190.00	8.00	19.00	9.00	1.00	162.00	36.00	2.50	26.00	1.74	4.80	1018.00	18.50
7-Sep	82.00	62.00	62.00	-80.00	4.50	170.00	8.70	18.60	10.00	1.00	162.00	42.00	2.50	25.00	1.55	4.80	580.00	2.40
8-Sep	83.00	59.00	28.00	-57.00	3.80	200.00	8.20	18.40	9.00	1.00	146.00	38.00	5.00	28.00	2.23	6.10	1158.00	0.00
9-Sep															1.65	5.20		

Appendix 7- 3: Spectral Analysis Result Using Fast Fourier Transform.

S (l, l) = autospectral density. S (l, j) = cross spectral density

1 = Conductivity. 2 = TDS .

Spectrum Frequency	S(1,1)	S(2,2)	S(3,3)	S(4,4)	Re{S(1,2)}=K	Im{S(1,2)}=-Q	Amplitude(1,2)	Phase(1,2)	Coherency(1,2)
0.0000	0.0000	0.0000	6.4445	0.2577	0.0000	0.0000	0.0000	-0.0443	1.0000
0.0078	0.0000	0.0002	15.2758	0.3933	0.0001	0.0000	0.0001	-0.1777	1.0000
0.0156	0.0055	0.0234	29.1194	0.5330	0.0085	-0.0075	0.0113	-0.7214	0.9955
0.0234	0.3792	0.2352	31.0125	0.5608	0.0839	-0.2699	0.2827	-1.2694	0.8960
0.0313	9.4933	1.6886	21.4671	0.5288	3.4853	-0.8284	3.5824	-0.2334	0.8006
0.0391	51.697	16.7004	21.7162	0.4358	26.2291	8.7181	27.6400	0.3209	0.8849
0.0469	101.58	44.6294	44.9595	0.4326	45.5446	38.3471	59.5383	0.6998	0.7819
0.0547	310.92	53.3381	97.9485	0.5313	62.5126	72.6924	95.8750	0.8605	0.5543
0.0625	1076.5	93.3991	120.2049	0.5855	257.7802	127.3319	287.5135	0.4588	0.8222
0.0703	1819.1	169.580	96.0987	0.4779	519.3282	177.0826	548.6893	0.3286	0.9759
0.0781	1464.0	143.946	98.4681	0.3178	435.9174	138.4931	457.3885	0.3076	0.9927
0.0859	562.41	66.5079	110.7438	0.3115	165.1181	67.0782	178.2231	0.3859	0.8492
0.0938	125.24	59.4751	110.2994	0.5697	59.7592	25.9341	65.1440	0.4094	0.5697
0.1016	96.793	87.4357	109.9285	0.7298	81.0787	-16.6705	82.7748	-0.2028	0.8096
0.1094	224.53	155.504	118.5376	0.6035	177.4633	-18.7120	178.4471	-0.1051	0.9120
0.1172	395.85	261.780	111.4317	0.5150	314.4127	38.7330	316.7895	0.1226	0.9684
0.1250	455.66	254.632	109.1740	0.6061	320.5681	38.7480	322.9014	0.1203	0.8986
0.1328	536.70	127.037	139.7616	0.8629	208.0636	19.6186	208.9865	0.0940	0.6406
0.1406	597.68	59.7478	163.5117	0.9431	131.9034	81.5475	155.0758	0.5537	0.6734
0.1484	349.80	68.7898	257.2724	0.8847	71.7345	107.7706	129.4618	0.9835	0.6965
0.1563	141.59	88.5175	353.3005	1.0028	58.8828	77.1947	97.0886	0.9192	0.7521
0.1641	169.55	88.8437	292.5690	1.0601	94.8349	63.9198	114.3652	0.5931	0.8683
0.1719	146.29	66.2173	178.6634	0.9523	63.5997	56.9680	85.3831	0.7304	0.7526
0.1797	60.712	61.4412	131.6237	0.7826	4.7944	40.3947	40.6782	1.4527	0.4436
0.1875	26.527	57.8664	203.4802	0.5976	0.2496	15.4766	15.4786	1.5547	0.1561
0.1953	37.820	30.4661	242.8818	0.4954	18.6325	0.7263	18.6466	0.0390	0.3018
0.2031	39.671	11.2209	254.7982	0.6535	19.6653	1.1443	19.6986	0.0581	0.8717
0.2109	88.886	32.1616	325.8134	0.9977	50.8197	-5.3633	51.1019	-0.1051	0.9135
0.2188	178.15	82.3556	254.5579	1.0001	116.9798	-17.5258	118.2854	-0.1487	0.9536
0.2266	163.66	107.645	171.3003	0.6221	112.7633	6.0704	112.9265	0.0538	0.7238

Spectrum Frequency	S(1,1)	S(2,2)	S(3,3)	S(4,4)	Re{S(1,2)}=K	Im{S(1,2)}=-Q	Amplitude(1,2)	Phase(1,2)	Coherency(1,2)
	65	1							
0.2344	102.11	106.792	405.4038	0.6975	36.8067	65.0802	74.7674	1.0561	0.5126
0.2422	83.173	111.202	871.6067	1.0555	5.5167	88.8058	88.9769	1.5088	0.8560
0.2500	49.895	82.2224	962.8943	0.7919	17.7499	47.4388	50.6507	1.2128	0.6253
0.2578	21.250	27.2404	656.0154	0.4893	13.0872	5.2101	14.0862	0.3789	0.3428
0.2656	30.166	4.2484	441.2149	0.5543	8.3977	-2.6595	8.8087	-0.3067	0.6055
0.2734	51.927	18.2254	352.6147	0.5972	24.4537	-4.7005	24.9014	-0.1899	0.6552
0.2813	58.509	37.5458	302.0521	0.6385	39.4332	-14.0960	41.8769	-0.3433	0.7983
0.2891	43.741	32.6930	194.5765	0.5149	25.9339	-21.9785	33.9944	-0.7030	0.8081
0.2969	33.299	18.3060	315.9953	0.5523	2.2391	-19.6790	19.8059	-1.4575	0.6435
0.3047	27.548	14.1842	947.6053	0.9954	-9.2333	-10.9191	14.2997	-2.2727	0.5233
0.3125	29.751	13.1743	1426.117	1.0744	-9.8935	-3.1333	10.3778	-2.8349	0.2748
0.3203	56.333	7.0586	1031.728	0.7033	-1.1654	4.4805	4.6296	1.8253	0.0539
0.3281	59.037	6.7968	314.8404	0.4072	6.3291	5.5665	8.4287	0.7214	0.1770
0.3359	29.885	22.1903	53.1690	0.3387	1.0474	9.4348	9.4928	1.4602	0.1359
0.3438	40.738	33.2607	91.9264	0.4024	4.7828	14.5830	15.3473	1.2539	0.1738
0.3516	67.320	24.4604	143.2888	0.3844	20.2939	-1.0748	20.3223	-0.0529	0.2508
0.3594	67.381	13.7900	126.8487	0.3207	17.6207	-3.7310	18.0114	-0.2087	0.3491
0.3672	77.161	20.3190	243.0014	0.5185	21.5209	20.3558	29.6227	0.7576	0.5597
0.3750	87.603	55.6576	553.4498	0.8030	52.0442	34.9347	62.6820	0.5912	0.8058
0.3828	98.669	102.214	540.4125	0.7296	90.5297	25.8435	94.1463	0.2781	0.8788
0.3906	110.94	98.1829	237.1133	0.5119	99.3433	1.1698	99.3502	0.0118	0.9061
0.3984	77.307	46.9227	137.7533	0.4683	53.2358	-9.1850	54.0223	-0.1709	0.8045
0.4063	27.344	11.0831	188.8486	0.4802	6.6585	-2.0248	6.9595	-0.2952	0.1598
0.4141	8.9650	5.7698	211.9820	0.4505	1.3227	0.3502	1.3682	0.2588	0.0362
0.4219	19.464	11.4879	194.8500	0.4020	3.4572	-5.7901	6.7437	-1.0325	0.2034
0.4297	30.472	11.4593	159.5337	0.4462	-5.3497	-10.0168	11.3559	-2.0613	0.3693
0.4375	19.972	11.0309	133.9958	0.6110	-7.6013	-0.4401	7.6140	-3.0838	0.2631
0.4453	10.027	14.0634	105.6726	0.5673	-1.7944	7.5142	7.7255	1.8052	0.4232
0.4531	8.8146	8.4259	80.3119	0.4359	2.5958	2.7147	3.7560	0.8078	0.1899
0.4609	19.041	11.7074	72.9801	0.3853	8.5925	9.5210	12.8250	0.8366	0.7378
0.4688	48.555	39.3098	120.3106	0.2973	31.7911	22.4571	38.9229	0.6150	0.7937
0.4766	57.645	58.0434	177.9693	0.3506	50.5695	11.6287	51.8894	0.2260	0.8047
0.4844	55.321	49.3763	282.9516	0.5243	44.3334	-13.4525	46.3295	-0.2946	0.7858

Spectrum Frequency	S(1,1)	S(2,2)	S(3,3)	S(4,4)	Re{S(1,2)}=K	Im{S(1,2)}=-Q	Amplitude(1,2)	Phase(1,2)	Coherency(1,2)
0.4922	62.037	40.3971	375.2010	0.6082	37.8557	-25.4411	45.6103	-0.5917	0.8301

Appendix 7- 4 Arithmetic Moments of Normalised Discharge

$Q^* = \frac{Q}{Q}$	
$x = \frac{Q(t)}{Q} = Q^*(t)$	$\bar{x} = E[x] = 1$
$f(x) = x^{b+1}$	$f(\bar{x}) = (\bar{x})^{b+1} = 1$
$f'(x) = (b+1)x^b$	$f'(\bar{x}) = b+1$
$f''(x) = b(b+1)x^{b-1}$	$f''(\bar{x}) = b(b+1)$
$f^k(x) = \frac{(b+1)!}{(b-k+1)!} x^{b-k+1}$	$f^k(\bar{x}) = \frac{(b+1)!}{(b-k+1)!}$

Appendix 7- 5. Geometric Moments of Normalised Discharge

$Q^* = \frac{Q}{Q}$	
$x = \ln\left[\frac{Q(t)}{Q}\right] = \ln[Q^*(t)]$	$\bar{x} = E[x] = \ln\left(\frac{Q_g}{Q}\right)$
$f(x) = e^{(b+1)x}$	$f(\bar{x}) = \left(\frac{Q_g}{Q}\right)^{b+1}$
$f'(x) = (b+1)e^{(b+1)x}$	$f'(\bar{x}) = b+1\left(\frac{Q_g}{Q}\right)^{b+1}$

$f''(x) = (b+1)^2 e^{(b+1)x}$	$f''(\bar{x}) = (b+1)^2 \left(\frac{Q_g}{Q}\right)^{b+1}$
$f^k(x) = (b+1)^k e^{(b+1)x}$	$f^k(x) = (b+1)^k \left(\frac{Q_g}{Q}\right)^{b+1}$

Appendix 7-6: Moment calculation using the first 10 terms of the Taylor series for the First month data

b	Number	(b+1)-(N-1)	Moment	Factorial	b factor	Product	Resultant
1.489	1.000	2.489	0.000	1	2.489	0.000	1.000
1.489	2.000	1.489	0.274	2	3.706	0.507	1.507
1.489	3.000	0.489	0.234	6	1.812	0.071	1.578
1.489	4.000	-0.511	0.390	24	-0.926	-0.015	1.563
1.489	5.000	-1.511	0.555	120	1.399	0.006	1.570
1.489	6.000	-2.511	0.858	720	-3.514	-0.004	1.565
1.489	7.000	-3.511	1.333	5040	12.336	0.003	1.569
1.489	8.000	-4.511	2.113	40320	-55.650	-0.003	1.566
1.489	9.000	-5.511	3.386	362880	306.686	0.003	1.569
1.489	10.000	-6.511	5.476	3628800	-1996.836	-0.003	1.566

Appendix 7-7: Moments for total data (N = 219) worked from natural log flows.

b	Number	(b+1) ^N	Moment	Factorial	Resultant	1+Resultant
1.489	1.000	2.489	0.000	1.000	0.000	1.000
1.489	2.000	6.195	0.546	2.000	1.690	2.690
1.489	3.000	15.420	0.169	6.000	0.434	3.124
1.489	4.000	38.380	0.884	24.000	1.414	4.538
1.489	5.000	95.527	0.822	120.000	0.654	5.192
1.489	6.000	237.766	2.343	720.000	0.774	5.966
1.489	7.000	591.799	3.482	5040.000	0.409	6.375
1.489	8.000	1472.988	8.114	40320.000	0.296	6.671
1.489	9.000	3666.267	14.823	362880.000	0.150	6.821
1.489	10.000	9125.338	32.384	3628800.000	0.081	6.903

Appendix 7-8: Bias Calculation

The arithmetic biases were calculated for different periods using the available contemporaneous discharge and turbidity data. The table below shows the result of the calculation.

Number of Days	Period	Bias
1	Daily	1.00
7	Weekly	1.14
14	Biweekly	1.25
30	Monthly	1.45
60	Bimonthly	1.64
120	Quarterly	2.16
180	Semiannual	2.26
219	Total Data	2.28

Curriculum Vitae

Family Name Teklemariam
First Name: Ababu
Gender: Male
Nationality: Ethiopian
Date of Birth May 1, 1966
Place of Birth: Addis Ababa, Ethiopia.
Marital Status: Married with one Daughter.

Education:

1. Elementary school (Grade 1- 6) (1971 – 1976): Berhanena Selam School, Addis Ababa. Ethiopia.
2. Junior School (Grade 7-8) (1977-1978): Edget Behibret School, Addis Ababa, Ethiopia.
3. High School (Grade 9-12) (1979-1982): Addis Ketema School. Addis Ababa, Ethiopia.
4. B.Sc. Degree: Civil Engineering (1983 – 1987): Addis Ababa University, Addis Ababa, Ethiopia.
5. M.Sc. Degree: Water and Waste Engineering: (1990-1991). Loughborough University, United Kingdom.
6. Ph.D. Degree Student since 2001- University of Siegen Germany. (Submitted the PhD thesis to be defended by December 2004).

Job Experience:

1. Graduate assistant: Arbaminch University (1988-1989), Arbaminch, Ethiopia. Course tutor for Hydraulics, Engineering mechanics, Water supply and treatment, waste disposal and related topics.
2. Lecturer: Arbaminch University (1992- 1999): Offered courses to B.Sc. degree students in the Department of water supply and environmental engineering. Advised final year students in their project works in the same department. Courses taught include: Water supply and treatment, waste water disposal, solid waste disposal, computer application in

water and environmental engineering, Numerical analysis, environmental hydraulics and dynamics, construction management.

Faculty Position:

1. Academic Dean: 1992-1995: Arbaminch University. Responsible for planning and executing all the academic programs. Management of the academic staff and vice-chairperson of the academic position.
2. Acting Dean: 1996: Arbaminch University. Responsible for the overall management. Chairperson of the academic commission.

Publications:

1. Inlet zones of Sedimentation tanks: Unpublished M.Sc. Thesis. Loughborough University, United Kingdom. Developed an improved numerical technique and computer program (BASIC) for analyzing inlet flow distribution earlier proposed by Kawamura. In addition the research work included laboratory analysis of inlet flow distribution.
2. Roughing Filtration of Water using contact-floating media and seeds of the Moringa Tree. Proceedings of the third symposium on sustainable water resources development, Arbaminch University, 1999.
3. Analysis of water Quality data in the time and Spectral Domain for Water Quality Monitoring. Paper presented to the 6th symposium on sustainable water resources development, Arbaminch University, 2003.
4. Design of Integrated Water Quality Monitoring and Management Networks for Water Resources within the Abaya –Chamo Drainage Basin. December 2004. Ph.D. Thesis Submitted to the University of Siegen to be defended in May 2005.

Research Experience:

1. Developed a new previously untested technique for improving the cleaning of roughing filters using a floating plastic media and weight pressing mechanism. The media is pressed with weight during filtration to prevent it from floating and later released during cleaning. No backwashing needed.
2. Extensive water quality monitoring of rivers, ground waters and lakes as part of my PhD research work within the Abaya-Chamo drainage network. Applied cluster analysis,

principal component analysis and time series analysis to classify and provide a monitoring basis for water quality of rivers, ground water and lakes. Assessed the seasonal and long-term interaction in the water quality of lakes Abaya and Chamo and proposed - based on the assessment - the probable causes of the lakes long-term salinity increases.

Computer Experience:

Includes programming in FORTRAN, VISUAL BASIC. GIS experience with Arcview. Data base experience with Visual Basic. Microsoft Office Experience with. MS Access, Word, EXCEL and Power Point presentation.

References:

1. Professor Pande B.B. Lal. Department of Hydraulic Engineering. Arbaminch University. P.O.Box 21. Arbaminch Ethiopia. Tel. 251-6-810771. Fax. 251-6-810279.
2. Dr. Adrian Coad. Swiss Center for Appropriate Technology (SKAT). Vadianstrasse 42, CH – 9000 St Gallen, Switzerland. (E-mail: adrian.coad@skat.ch.)
3. Dr. Bayu Chane. Department of Civil Engineering. Faculty of Technology. Addis Ababa University. P. O. Box 385. Addis Ababa, Ethiopia. Tel. 251-1-551022. Fax 251-1-552601